

# BIOSAFETY AND BIOSECURITY APPROACHES TO COUNTER SARS-COV-2: FROM DETECTION TO BEST PRACTICES AND RISK ASSESSMENTS

EDITED BY: Stephen Allen Morse, Segaran P. Pillai, Jianming Qiu  
and Yao-Wei Huang

PUBLISHED IN: Frontiers in Bioengineering and Biotechnology,  
Frontiers in Medicine and Frontiers in Public Health





# frontiers

## Frontiers eBook Copyright Statement

The copyright in the text of individual articles in this eBook is the property of their respective authors or their respective institutions or funders. The copyright in graphics and images within each article may be subject to copyright of other parties. In both cases this is subject to a license granted to Frontiers.

The compilation of articles constituting this eBook is the property of Frontiers.

Each article within this eBook, and the eBook itself, are published under the most recent version of the Creative Commons CC-BY licence.

The version current at the date of publication of this eBook is CC-BY 4.0. If the CC-BY licence is updated, the licence granted by Frontiers is automatically updated to the new version.

When exercising any right under the CC-BY licence, Frontiers must be attributed as the original publisher of the article or eBook, as applicable.

Authors have the responsibility of ensuring that any graphics or other materials which are the property of others may be included in the CC-BY licence, but this should be checked before relying on the CC-BY licence to reproduce those materials. Any copyright notices relating to those materials must be complied with.

Copyright and source acknowledgement notices may not be removed and must be displayed in any copy, derivative work or partial copy which includes the elements in question.

All copyright, and all rights therein, are protected by national and international copyright laws. The above represents a summary only. For further information please read Frontiers' Conditions for Website Use and Copyright Statement, and the applicable CC-BY licence.

ISSN 1664-8714

ISBN 978-2-88971-483-4

DOI 10.3389/978-2-88971-483-4

## About Frontiers

Frontiers is more than just an open-access publisher of scholarly articles: it is a pioneering approach to the world of academia, radically improving the way scholarly research is managed. The grand vision of Frontiers is a world where all people have an equal opportunity to seek, share and generate knowledge. Frontiers provides immediate and permanent online open access to all its publications, but this alone is not enough to realize our grand goals.

## Frontiers Journal Series

The Frontiers Journal Series is a multi-tier and interdisciplinary set of open-access, online journals, promising a paradigm shift from the current review, selection and dissemination processes in academic publishing. All Frontiers journals are driven by researchers for researchers; therefore, they constitute a service to the scholarly community. At the same time, the Frontiers Journal Series operates on a revolutionary invention, the tiered publishing system, initially addressing specific communities of scholars, and gradually climbing up to broader public understanding, thus serving the interests of the lay society, too.

## Dedication to Quality

Each Frontiers article is a landmark of the highest quality, thanks to genuinely collaborative interactions between authors and review editors, who include some of the world's best academicians. Research must be certified by peers before entering a stream of knowledge that may eventually reach the public - and shape society; therefore, Frontiers only applies the most rigorous and unbiased reviews.

Frontiers revolutionizes research publishing by freely delivering the most outstanding research, evaluated with no bias from both the academic and social point of view. By applying the most advanced information technologies, Frontiers is catapulting scholarly publishing into a new generation.

## What are Frontiers Research Topics?

Frontiers Research Topics are very popular trademarks of the Frontiers Journals Series: they are collections of at least ten articles, all centered on a particular subject. With their unique mix of varied contributions from Original Research to Review Articles, Frontiers Research Topics unify the most influential researchers, the latest key findings and historical advances in a hot research area! Find out more on how to host your own Frontiers Research Topic or contribute to one as an author by contacting the Frontiers Editorial Office: [frontiersin.org/about/contact](https://frontiersin.org/about/contact)

# BIOSAFETY AND BIOSECURITY APPROACHES TO COUNTER SARS-COV-2: FROM DETECTION TO BEST PRACTICES AND RISK ASSESSMENTS

Topic Editors:

**Stephen Allen Morse**, IHRC, Inc

**Segaran P. Pillai**, United States Department of Health and Human Services,  
United States

**Jianming Qiu**, University of Kansas Medical Center, United States

**Yao-Wei Huang**, Zhejiang University, China

**Citation:** Morse, S. A., Pillai, S. P., Qiu, J., Huang, Y.-W., eds. (2021). Biosafety and Biosecurity Approaches to Counter SARS-CoV-2: From Detection to Best Practices and Risk Assessments. Lausanne: Frontiers Media SA.  
doi: 10.3389/978-2-88971-483-4

# Table of Contents

- 06 Editorial: Biosafety and Biosecurity Approaches to Counter SARS-CoV-2: From Detection to Best Practices and Risk Assessments**  
Segaran P. Pillai, Jianming Qiu and Stephen A. Morse
- 09 Individual-Level Fatality Prediction of COVID-19 Patients Using AI Methods**  
Yun Li, Melanie Alfonzo Horowitz, Jiakang Liu, Aaron Chew, Hai Lan, Qian Liu, Dexuan Sha and Chaowei Yang
- 21 Controlled Heat and Humidity-Based Treatment for the Reuse of Personal Protective Equipment: A Pragmatic Proof-of-Concept to Address the Mass Shortage of Surgical Masks and N95/FFP2 Respirators and to Prevent the SARS-CoV2 Transmission**  
Louis Bernard, Guillaume Desoubeaux, Elsa Bodier-Montagutelli, Geoffrey Pardessus, Déborah Brea, Laurine Allimonier, Sébastien Eymieux, Pierre-Ivan Raynal, Virginie Vasseur, Laurent Vecellio, Ludovic Mathé, Antoine Guillon, Philippe Lanotte, Jérémie Pourchez, Paul O. Verhoeven, Stéphane Esnouf, Muriel Ferry, Nicolas Eterradosi, Yannick Blanchard, Paul Brown, Philippe Roingeard, Jean-Pierre Alcaraz, Philippe Cinquin, Mustapha Si-Tahar and Nathalie Heuzé-Vourc'h
- 30 Hot, Humid Air Decontamination of Aircraft Confirmed That High Temperature and High Humidity are Critical for Inactivation of Infectious, Enveloped Ribonucleic Acid (RNA) Virus**  
Tony L. Buhr, Alice A. Young, Erica Borgers-Klonkowski, Neil L. Kennihan, Harold K. Barnette, Zachary A. Minter, Matthew D. Bohmke, Emily B. Osborn, Shelia M. Hamilton, Monique B. Kimani, Mark W. Hammon, Charles T. Miller, Ryan S. Mackie, Jennifer M. Innocenti, Misty D. Bensman, Bradford W. Gutting, Samuel D. Lilly, Emlyn E. Hammer, Vanessa L. Yates and Brooke B. Luck
- 44 Combinations of PCR and Isothermal Amplification Techniques are Suitable for Fast and Sensitive Detection of SARS-CoV-2 Viral RNA**  
Dmitriy A. Varlamov, Konstantin A. Blagodatskikh, Evgenia V. Smirnova, Vladimir M. Kramarov and Konstantin B. Ignatov
- 50 Genetic Information Insecurity as State of the Art**  
Garrett J. Schumacher, Sterling Sawaya, Demetrius Nelson and Aaron J. Hansen
- 59 Potential False-Positive and False-Negative Results for COVID-19 IgG/IgM Antibody Testing After Heat-Inactivation**  
Jie Lin, Wei Dai, Weiwei Li, Li Xiao, Tao Luo, Yanju Guo, Yang Yang, Ying Han, Peiran Zhu, Qiuyue Wu, Bangshun He, Jian Wu and Xinyi Xia
- 68 COVID-19 in-vitro Diagnostics: State-of-the-Art and Challenges for Rapid, Scalable, and High-Accuracy Screening**  
Zeina Habli, Sahera Saleh, Hassan Zaraket and Massoud L. Khraiche
- 82 Air Curtains Equipped With Hydroalcoholic Aerosol Sprayers for Massive COVID-19 Disinfection**  
Judit Raventós and Raimon Sabate



- 85 Performance of a Point of Care Test for Detecting IgM and IgG Antibodies Against SARS-CoV-2 and Seroprevalence in Blood Donors and Health Care Workers in Panama**  
Alcibiades Villarreal, Giselle Rangel, Xu Zhang, Digna Wong, Gabrielle Britton, Patricia L. Fernandez, Ambar Pérez, Diana Oviedo, Carlos Restrepo, María B. Carreira, Dilcia Sambrano, Gilberto A. Eskildsen, Carolina De La Guardia, Julio Flores-Cuadra, Jean-Paul Carrera, Yamitzel Zaldivar, Danilo Franco, Sandra López-Vergès, Dexi Zhang, Fangjing Fan, Baojun Wang, Xavier Sáez-Llorens, Rodrigo DeAntonio, Ivonne Torres-Atencio, Isabel Blanco, Fernando Diaz Subía, Laiss Mudarra, Aron Benzadon, Walter Valverde, Lineth López, Nicolás Hurtado, Neyla Rivas, Julio Jurado, Aixa Carvallo, Juan Rodriguez, Yaseikiry Perez, Johanna Morris, Odemaris Luque, David Cortez, Eduardo Ortega-Barria, Rao Kosagisharaf, Ricardo Leonart, Chong Li and Amador Goodridge
- 95 Time Till Viral Clearance of Severe Acute Respiratory Syndrome Coronavirus 2 is Similar for Asymptomatic and Non-critically Symptomatic Individuals**  
Nitya Kumar, AbdulKarim AbdulRahman, Salman AlAli, Sameer Otoom, Stephen L. Atkin and Manaf AlQahtani
- 98 Comparison Between a Standard and SalivaDirect RNA Extraction Protocol for Molecular Diagnosis of SARS-CoV-2 Using Nasopharyngeal Swab and Saliva Clinical Samples**  
Sofía N. Rodríguez Flores, Luis Mario Rodríguez-Martínez, Bernardita L. Reyes-Berrones, Nadia A. Fernández-Santos, Elthon J. Sierra-Moncada and Mario A. Rodríguez-Pérez
- 104 Management of SARS-CoV-2 Infection: Key Focus in Macrolides Efficacy for COVID-19**  
Gaber El-Saber Batiha, Marwa A. Zayed, Aya A. Awad, Hazem M. Shaheen, Suleiman Mustapha, Oscar Herrera-Calderon, Jorge Pamplona Pagnossa, Abdelazeem M. Algammal, Muhammad Zahoor, Achyut Adhikari, Ishan Pandey, Sara T. Elazab, Kannan R. R. Rengasamy, Natália Cruz-Martins and Helal F. Hetta
- 115 Advances in Synthetic Biology and Biosafety Governance**  
Jing Li, Huimiao Zhao, Lanxin Zheng and Wenlin An
- 129 Early Warning Information for Severe and Critical Patients With COVID-19 Based on Quantitative CT Analysis of Lung Segments**  
Xu Yuyun, Yu Lexi, Wang Haochu, Shu Zhenyu and Gong Xiangyang
- 140 COVID-19 Score for Testing Symptomatic Low Risk Children: "STUDY SAFE"**  
Gavriela Feketea and Vasiliki Vlacha
- 144 Oropharyngeal Probiotic ENT-K12 Prevents Respiratory Tract Infections Among Frontline Medical Staff Fighting Against COVID-19: A Pilot Study**  
Qiang Wang, Xuan Lin, Xiaochen Xiang, Wanxin Liu, Ying Fang, Haiping Chen, Fang Tang, Hongyan Guo, Di Chen, Xiafen Hu, Qingming Wu, Baoli Zhu and Junbo Xia

**153 *De Novo Powered Air-Purifying Respirator Design and Fabrication for Pandemic Response***

Akshay Kothakonda, Lyla Atta, Deborah Plana, Ferrous Ward, Chris Davis, Avilash Cramer, Robert Moran, Jacob Freake, Enze Tian, Ofer Mazor, Pavel Gorelik, Christopher Van, Christopher Hansen, Helen Yang, Yao Li, Michael S. Sinha, Ju Li, Sherry H. Yu, Nicole R. LeBoeuf and Peter K. Sorger

**167 *Critical Capability Needs for Reduction of Transmission of SARS-CoV-2 Indoors***

Jayne B. Morrow, Aaron I. Packman, Kenneth F. Martinez, Kevin Van Den Wymelenberg, Darla Goeres, Delphine K. Farmer, Jade Mitchell, Lisa Ng, Yair Hazi, Monica Schoch-Spana, Sandra Quinn, William Bahnfleth and Paula Olsiewski



# Editorial: Biosafety and Biosecurity Approaches to Counter SARS-CoV-2: From Detection to Best Practices and Risk Assessments

Segaran P. Pillai<sup>1\*</sup>, Jianming Qiu<sup>2</sup> and Stephen A. Morse<sup>3</sup>

<sup>1</sup>Office of the Commissioner, United States Food and Drug Administration, Silver Spring, MD, United States, <sup>2</sup>Department of Microbiology, University of Kansas Medical Center, Kansas City, KS, United States, <sup>3</sup>IHRC, Inc, Atlanta, GA, United States

**Keywords:** biosafety and biosecurity, SARS-CoV2, detection, best practices, risk assessments, diagnostics, PPE

## Editorial on the Research Topic

### Biosafety and Biosecurity Approaches to Counter SARS-CoV-2: From Detection to Best Practices and Risk Assessment

Scientific communications are important for addressing technical issues that can impact the COVID-19 pandemic. To this end, Frontiers developed a Research Topic entitled “Biosafety and Biosecurity Approaches to Counter SARS-CoV-2: From Detection to Best Practices and Risk Assessment.” Thirty-four manuscripts from 14 countries were originally submitted for this Research Topic. Of these, 18 (53%) were accepted. The 18 accepted papers that comprise this Research Topic were originally submitted to three Frontiers journals: Bioengineering and Biotechnology ( $N = 9$ ), Medicine ( $N = 6$ ), and Public Health ( $N = 3$ ). The types of papers consist of original research articles ( $N = 7$ ), brief research reports ( $N = 4$ ), methods articles ( $N = 1$ ), opinions ( $N = 2$ ), and review articles ( $N = 4$ ). The ten countries from which the accepted manuscripts were submitted truly represents the scope of the pandemic: United States ( $N = 5$ ), China ( $N = 4$ ), and 1 each from France, Lebanon, Panama, Russia, Mexico, Bahrain, Spain, Portugal, and Greece.

When this Research Topic began, there were many unanswered questions including the origin of the novel SARS-CoV-2, its pathogenicity, transmissibility, efficacy of existing medical countermeasures and supportive therapies, and its survival in the environment. An et al. reviewed recent progress in the field of synthetic biology and the laws and regulations governing its use to avoid potential risks associated with this technology. As with other infectious agents, the environment can play an important role in the transmission of SARS-CoV-2. In an innovative on-line forum, Morrow et al. reviewed the challenges that industries from around the globe experienced in reducing the transmission of this virus in an indoor environment. Based on the results, the authors called for significant investments in research to understand virus persistence and transport in the built environment.

Buhr et al. used the enveloped RNA bacteriophage  $\phi 6$  as a surrogate for SARS-CoV-2 virus to study its inactivation in an aircraft environment. The surrogate was dried on wiring insulation, aircraft performance coating, polypropylene and nylon at  $>8 \log_{10}$  PFU/test coupon. Modeling showed that a 1-h treatment of a C-130 aircraft with hot ( $\geq 63^\circ\text{C}$ ) humid (90% RH) air had a 90% probability of inactivating the virus by  $>7 \log_{10}$ .

The extent of the pandemic has exacerbated the availability of critical supplies such as PPE. Two papers proposed strategies to overcome the shortage of PPE. Bernard et al. described a proof-of-concept study to address the shortage of surgical masks and N95 filtering face-piece (FFP) two respirators. They demonstrated that treating used surgical masks and FFP2 respirators in a chamber

## OPEN ACCESS

### Edited and reviewed by:

Alan Raybould,  
University of Edinburgh,  
United Kingdom

### \*Correspondence:

Segaran P. Pillai  
Segaran.Pillai@FDA.HHS.GOV

### Specialty section:

This article was submitted to  
Biosafety and Biosecurity, a section of  
Frontiers in Bioengineering and  
Biotechnology

**Received:** 03 August 2021

**Accepted:** 11 August 2021

**Published:** 24 August 2021

### Citation:

Pillai SP, Qiu J and Morse SA (2021)  
Editorial: Biosafety and Biosecurity  
Approaches to Counter SARS-CoV-2:  
From Detection to Best Practices and  
Risk Assessments.  
Front. Bioeng. Biotechnol. 9:752909.  
doi: 10.3389/fbioe.2021.752909

for 1 h at 70°C and 75% RH was sufficient to kill surrogate bacteria and viruses while maintaining the filtering capacity of the PPE. Thus, reusing used PPE during mass shortfalls is possible. In the other paper, Kothakonda et al. applied open-source product development to develop locally manufactured, modular, powered air-purifying respirator (PAPR) components, including filter cartridges and blower units. Two designs, one with a fully custom-made filter and blower unit housing, and the other with commercially available variants were developed. Engineering testing and clinical feedback demonstrated that the designs represented favorable alternative PAPRs for use during shortfalls that may occur during pandemics.

Hospitals can be a source of new infections. To reduce this possibility, Raventos and Sabata suggested that air curtains equipped with sprayers to nebulize an alcoholic solution could be used in hospitals to disinfect clothing, exposed body parts and objects that passed through to rapidly and economically reduce the propagation of the virus. Hospital workers caring for COVID-19 patients are of increased risk of acquiring SARS-CoV-2. In a study, Wang et al. reported that the use of an oropharyngeal probiotic *Streptococcus thermophilus* ENT-K-12, in a slow-dissolving lozenge form, twice a day, to create a stable upper respiratory tract microbiota, significantly reduced the incidence of certain respiratory tract infections [22/95 (23.2%) control group vs 8/98 (8.2%) probiotic group,  $p = 0.004$ ] among front-line physicians and nurses attending COVID-19 patients in a hospital setting.

In today's world, the requirement for genetic information security is an ever-growing need. The very information that allows us to understand the properties of a pathogen can also be misused through genetic manipulation for potential harm. Schumacher et al. characterized a general genetic information system from biological material collection through long-term data sharing, storage, and application in the context of security. They also discussed the challenges associated with wet and dry laboratories due to distributed devices and systems that are not designed to address the security of genetic information systems and the need for an extensive laboratory system to realize the potential of this emerging field and to protect the bioeconomy of all stakeholders.

Habli et al. reviewed the current state-of-the-art of point-of-care diagnostic platforms for the rapid detection of COVID-19 and its seroprevalence throughout the cycle of infection. The review analyzed their performance characteristics and discussed limitations with respect to COVID-19. Because of the infectiousness of SARS-CoV-2, package inserts from antibody detection kits recommended that serum samples be heat inactivated before analysis. However, Lin et al. observed that heat-inactivation significantly increased values for SARS-CoV-2 IgG antibody while values for SARS-CoV-2 IgM antibody decreased with increasing temperature of heat inactivation. This effect was dependent upon the method used for antibody detection, which pointed out the necessity for laboratories to evaluate the kits to ensure accurate COVID-19 detection results.

Villarreal et al. evaluated a lateral flow assay (LFA) that detects both IgG and IgM in serum samples from: 1) COVID-19 patients with a confirmed positive RT-PCR; 2) potentially exposed

healthcare workers; and 3) healthy blood donors. The LFA had a positive percent agreement of 97.2%. The evaluation of serum samples from hospitalized COVID-19 patients indicated a correlation between test sensitivity and the number of days since onset of symptoms. The seroprevalence among healthcare workers who reported close contact with confirmed COVID-19 patients was 12.9% versus 1.8% among those who did not report close contact.

Varlamov et al. evaluated a combination of polymerase chain reaction (PCR) and isothermal nucleic acid amplification techniques, which included conventional PCR and loop-mediated isothermal amplification (LAMP) methods, with hybrid techniques such as polymerase chain displacement reaction (PCDR) and a newly developed PCR-LAMP method. Based on their evaluation, they concluded that hybrid methods exhibited higher sensitivity and assay reaction rates than the classic LAMP- and PCR-based methods.

To ascertain early warning signs for severe and critical patients with COVID-19, Xu et al. performed a quantitative analysis of chest CT images at the lung segment level. Their analysis showed that lung involvement in the ordinary and severe/critical groups reached a peak on the 18th and 14th day, respectively. In the first stage, the percentage of lung involvement (PLI) in the right middle lobe and the left superior lobe were significantly different between the two groups. In the second stage and the fourth stage, there were statistically significant differences in PLI between the two groups in the whole lung, right superior lobe, right inferior lobe and left superior lobe. They observed that the rapid progress of the lateral segment of the right middle lobe on the second day and the anterior segment of the right upper lobe on the 13th day may be an early warning sign for severe/critical patients.

Sample type and sample processing are critical for the rapid, sensitive, and accurate diagnosis of infections such as COVID-19. Rodriguez-Flores et al. compared results of nasopharyngeal swabs and saliva samples from the same COVID-19 patients using a standard nucleic acid extraction protocol including protein lysis with proteinase K followed by binding to a column, washing, and elution, with the SalivaDirect protocol based on protein lysis and skipping the other steps to reduce processing time and cost. They noted that with the SalivaDirect protocol, saliva samples had a diagnostic sensitivity of 88.2% whereas nasopharyngeal swab samples had a diagnostic sensitivity of 93.6%.

An understanding of viral clearance in asymptomatic SARS CoV-2-infected individuals is critical for the development of interventions to minimize transmission and for public health messaging. Kumar et al. studied the timeline for viral clearance in 145 asymptomatic and 39 non-clinical symptomatic individuals. Based on their analysis, the median time till viral negativity for subclinical and for overt infections was 11 days after controlling for age and sex.

Batiha et al. have written a review article on macrolides such as azithromycin, as well as chloroquine/hydroxychloroquine, and proposals that have been made regarding their potential for consideration in COVID-19. Readers should be aware that the COVID-19 Treatment Guidelines on the United States NIH website recommend against use of chloroquine or

hydroxychloroquine and/or azithromycin for treatment of COVID-19 (<https://www.covid19treatmentguidelines.nih.gov/therapies/antiviral-therapy/chloroquine-or-hydroxychloroquine-and-or-azithromycin/>).

Li et al. adopted a deep learning model to predict fatality of individuals that tested positive given the patient's underlying health conditions, age, sex, and other factors. As the allocation of resources towards a vulnerable patient could mean the difference between life and death, a fatality prediction model may serve as a valuable tool in prioritizing resources and hospital space.

While most children infected with SARS-CoV-2 are asymptomatic or develop mild symptoms, some have been hospitalized and some have died. Feketea and Vlach developed an algorithm called "STUDY SAFE" that when used together with telemedicine can help parents decide when to test a symptomatic low risk child, and if positive, when the child can return to school.

In addition to the contribution of these scientists toward our understanding of COVID-19 response, scientists from around the world are working to enhance our knowledge and understanding about this virus and trying to identify ways to counter and eradicate this disease. Even with all of our current understanding, many unanswered questions remain that will be worth exploring. The editors of this Research Topic would like to thank the many scientists for their contribution to our knowledge about this disease and their dedication to public health.

## AUTHOR CONTRIBUTIONS

All authors listed have made a substantial, direct, and intellectual contribution to the work and approved it for publication.

## ACKNOWLEDGMENTS

The editors would like to thank the contributors to Biosafety and Biosecurity Approaches to Counter SARS-CoV-2: From Detection to Best Practices and Risk Assessment

**Conflict of Interest:** SM was employed by the company IHRC, Inc.

The remaining authors declare that the research was conducted in the absence of any commercial or financial relationships that could be construed as a potential conflict of interest.

**Publisher's Note:** All claims expressed in this article are solely those of the authors and do not necessarily represent those of their affiliated organizations, or those of the publisher, the editors and the reviewers. Any product that may be evaluated in this article, or claim that may be made by its manufacturer, is not guaranteed or endorsed by the publisher.

*Copyright © 2021 Pillai, Qiu and Morse. This is an open-access article distributed under the terms of the Creative Commons Attribution License (CC BY). The use, distribution or reproduction in other forums is permitted, provided the original author(s) and the copyright owner(s) are credited and that the original publication in this journal is cited, in accordance with accepted academic practice. No use, distribution or reproduction is permitted which does not comply with these terms.*



# Individual-Level Fatality Prediction of COVID-19 Patients Using AI Methods

Yun Li<sup>1,2</sup>, Melanie Alfonzo Horowitz<sup>3</sup>, Jiakang Liu<sup>4</sup>, Aaron Chew<sup>5</sup>, Hai Lan<sup>2,6</sup>, Qian Liu<sup>1,2</sup>, Dexuan Sha<sup>1,2</sup> and Chaowei Yang<sup>1,2\*</sup>

<sup>1</sup> Department of Geography and Geoinformation Science, George Mason University, Fairfax, VA, United States, <sup>2</sup> National Science Foundation (NSF) Spatiotemporal Innovation Center, George Mason University, Fairfax, VA, United States,

<sup>3</sup> Department of Biophysics, Johns Hopkins University, Baltimore, MD, United States, <sup>4</sup> Marian and Rosemary Bourns College of Engineering, University of California, Riverside, Riverside, CA, United States, <sup>5</sup> Valencia High School, Yorba Linda, CA, United States, <sup>6</sup> Department of Geographical Sciences, University of Maryland, College Park, MD, United States

## OPEN ACCESS

### Edited by:

Jianming Qiu,  
University of Kansas Medical Center,  
United States

### Reviewed by:

Xinjian Zhang,  
Centers for Disease Control and  
Prevention (CDC), United States  
Junxiang Wang,  
Emory University, United States

### \*Correspondence:

Chaowei Yang  
cyang3@gmu.edu

### Specialty section:

This article was submitted to  
Infectious Diseases – Surveillance,  
Prevention and Treatment,  
a section of the journal  
Frontiers in Public Health

**Received:** 27 July 2020

**Accepted:** 24 August 2020

**Published:** 30 September 2020

### Citation:

Li Y, Horowitz MA, Liu J, Chew A,  
Lan H, Liu Q, Sha D and Yang C  
(2020) Individual-Level Fatality  
Prediction of COVID-19 Patients  
Using AI Methods.  
Front. Public Health 8:587937.  
doi: 10.3389/fpubh.2020.587937

The global covid-19 pandemic puts great pressure on medical resources worldwide and leads healthcare professionals to question which individuals are in imminent need of care. With appropriate data of each patient, hospitals can heuristically predict whether or not a patient requires immediate care. We adopted a deep learning model to predict fatality of individuals tested positive given the patient's underlying health conditions, age, sex, and other factors. As the allocation of resources toward a vulnerable patient could mean the difference between life and death, a fatality prediction model serves as a valuable tool to healthcare workers in prioritizing resources and hospital space. The models adopted were evaluated and refined using the metrics of accuracy, specificity, and sensitivity. After data preprocessing and training, our model is able to predict whether a covid-19 confirmed patient is likely to be dead or not, given their information and disposition. The metrics between the different models are compared. Results indicate that the deep learning model outperforms other machine learning models to solve this rare event prediction problem.

**Keywords:** COVID-19, machine learning, deep learning, pandemic, rare event, fatality prediction

## INTRODUCTION

The Coronavirus (SARS-CoV-2 virus) has caused detrimental effects since its inception in late 2019. In the months since, the virus has progressed to become a widespread global pandemic. Over two hundred countries (tracked by Worldometer<sup>1</sup>) have been plagued by the virus, leading to almost a total of 530,000 deaths worldwide, as of July 5th, 2020 (1). Not only has this virus gravely affected individuals who have contracted the infection, but also healthcare employees and even patients with illnesses unrelated to COVID-19.

Due to the severity that some COVID-19 cases progress to, hospitalization is required, and these cases may progress to ICU admission. This inflicts enormous stress on healthcare workers as hospitals are working at full capacity and at times lack of sufficient equipment. The occurrence of hospitals frequently reaching high or full capacity is becoming an overwhelming and alarming issue, as noted by the CDC's COVID-19 Module Data Dashboard (2). This results in extensive physician burnout (3) which can be detrimental to physician-patient interaction.

<sup>1</sup> "Coronavirus Cases." Worldometer. Available online at: [www.worldometers.info/coronavirus/?utm\\_campaign=\\$homeAdvegas1](http://www.worldometers.info/coronavirus/?utm_campaign=$homeAdvegas1).



This stress can be alleviated with a more succinct understanding of which individuals are at an increased risk of fatality caused by COVID-19. Therefore, it would be beneficial to identify patients who merit priority and order treatment accordingly to these high-risk cases. Priority treatment would be given to patients who have a high likelihood of a fatal outcome, given their present state when tested positive for the virus. The limited resources housed by hospitals can be more appropriately allocated and there would be a decrease in the number of hospitalized patients under the care of overworked hospital employees.

Deaths that are caused directly by COVID-19 infection are not the only ones that should be discussed. There is an abundance of evidence suggesting intrahospital transmission of the virus. This transmission has occurred to both hospital patients, who may already be immunocompromised, and staff working tirelessly to save lives. Gold et al. noted more than 5,000 cases of this type of transmission occurring between May 14 and June 21 (4). With an increased number of COVID-19 patients admitted to a hospital, there is a higher probability of COVID-19 becoming a nosocomial disease for some inpatients. Moreover, patients with chronic or acute illnesses may have had to delay or cancel their hospital treatment appointments, due to hospitals reaching their capacity (5). As a result, their non-covid disease may have progressed to a severe point, or even death. With increased consideration taken into account when admitting patients, the persistence of these avoidable deaths will decrease.

However, it is difficult to predict the high fatality risk of a patient who should be admitted to a hospital with high priority since there are a myriad of different factors that contribute to an individual's infection progression once they test positive for covid-19. All of these metrics may be diverse, leading physicians to a disruptive confusion as to which factors to rely on, especially when each patient is unique. Complete knowledge into how this virus manifests itself in the body is lacking. Each case of COVID-19 contains distinct epidemiological features that have the power to dictate the progression of the disease and whether the outcome will result in death. There is a vital need to be able to identify these factors in order to prioritize care to those who are at greatest risk and prevent future death with this increased and proactive care. A single algorithm, like the one produced in this study, that combines all of an individual's dispositions to make a prediction would therefore be useful. This solution to improve and prioritize hospitalization with our fatality prediction approach will be able to alleviate the burden of hospitals reaching capacity, reduce medical worker burnout, and minimize the unintentional spread of the virus. Furthermore, the ability to identify and prioritize serious cases which may result in death might be life-saving for critical patients. All of these factors will benefit the COVID-19 infected individual, the healthcare employees, and hospital inpatients.

It is imperative to be able to predict which individuals tested positive for COVID-19 should be hospitalized for immediate care. This study aims to create a prediction model to be able to correctly identify patients who are at an increased risk of death, following a COVID-19 diagnosis. Utilizing informed decisions with our predictor, alongside medical expertise from medical

professionals at the scene, physicians can determine with greater certainty which individuals should receive hospitalization.

## MATERIALS AND METHODS

### Data Source

In this study, two publicly available epidemiological datasets were obtained, processed, and used for analysis. To monitor and anticipate spread of virus during the COVID-19 outbreak, a real-time database of individual-level epidemiological data is collected and published on GitHub (<https://github.com/beoutbreakprepared/nCoV2019>) (6). The dataset is supplied from an open working group repository to promote and enable the sharing of public health data to advance the field of public health. It incorporates data from a number of different sources to provide individual-level data instead of aggregate data provided by most data repositories.

Each case in the database represents an individual tested positive for COVID-19, gathered from different sources. This dataset originally contains 2,310,111 cases. To protect the privacy of patients, each case is deindividualized and anonymized. The cases are labeled with an "ID" noted in the dataset, which is only used to keep track of cases and has no relation to the actual individual. This file contains the variables including ID, age, sex, city, province, country, latitude, longitude, date onset, date admission, date confirmation, etc. Each variable is described below and this dataset will be referred to throughout the paper as the GitHub dataset.

**ID**—unique label for each deindividualized case

**Age**—age at time of positive covid-19 test

**Sex**—sex of the case

**City**—geographic location of case

**Province**—first administrative division where the case is reported

**Latitude**—latitude where case is reported

**Longitude**—longitude where case is reported

**Date onset symptoms**—date when the case began exhibiting symptoms, if symptomatic

**Date admission**—date when the case is reported to have been hospitalized

**Date confirmation**—date when the case is reported to have been tested positive for COVID-19, by a rt-PCR test

**Symptoms**—symptoms recorded for the case

**Lives in Wuhan**—"yes" if case is resident of Wuhan, "no" if case is not resident of Wuhan

**Travel history**—travel dates to and from Wuhan that were recorded for the case

**Reported market exposure**—"yes" if market exposure was recorded, "no" if it was not

**Additional information**—extra information that is informative about the case

**Chronic disease binary**—0 entered for a case without chronic disease, 1 entered for a case with chronic disease

**Chronic disease**—listed specific chronic disease per case

**Source**—URL of origin of information for each case

**Outcome**—"died" or "discharged" from hospital



**Date of death or discharge**—date of death or discharge that was reported

A smaller dataset that contains additional and extensive detailed information on the predisposition of the patient was then used. This dataset was obtained from <https://datarepository.wolframcloud.com/resources/Patient-Medical-Data-for-Novel-Coronavirus-COVID-19>. It includes patient medical data for those tested positive for coronavirus that was made to be computable. Here, a larger ratio of records contain specific symptoms and chronic diseases of applicable cases are included in a detailed account, compared to the previous GitHub dataset. As of June 30, this dataset contained 217,192 cases. This dataset will be referred to throughout the paper as the Wolfram data set. Wolfram data set includes variables as below:

**Age**—age of case at time of positive covid-19 test result

**Sex**—reported gender of case

**Date of onset symptoms**—initial date of reported symptoms

**Symptoms**—specific symptoms exhibited by case

**Travel history**—travel locations of case

**Chronic diseases**—specific chronic diseases of case

**Date of discharge or death**—recorded date of death or discharge of patient

**City**—city of residence for positive case

**Administrative division**—City, country for positive case test administration

**Country**—country of residence for case

**GeoPosition**—geographical location of case

**DateOfAdmissionHospital**—Date case was admitted to hospital, if applicable

**DateOfConfirmation**—Date case was confirmed to be positive for covid-19

**LivesInWuhan**—“True” if individual lives in Wuhan

**TravelHistoryDates**—Dates of travel history for the case, if applicable

**TravelHistoryLocation**—If applicable, lists location infected individual traveled

**ReportedMarketExposure**—Reported as “Missing,” “True,” or “False”

**ReportedMarketExposureComment**—Details where public market exposure to the virus occurred for the case

**ChronicDiseaseQ**—“True” if individual has chronic disease, “False” if no

**SequenceAvailable**—“True” is available

**DischargedQ**—if individual was discharged from hospital

**DeathQ**—if outcome was death for individual

**DateOfDeath**—date of death in DD.MM.YYYY format if individual died

**DateOfDischarge**—date of discharge in DD.MM.YYYY format if individual was discharged from hospital

There is a tradeoff between the quality of these two datasets and by using them both, we hoped to reconcile this circumstance. The GitHub based dataset used was advantageous due to its large size. Unfortunately, it lacked precise information on the specific symptoms and chronic diseases each case faced. The Wolfram dataset was beneficial due to its multiple attributes that include

specific symptoms and chronic diseases. Both datasets were used separately to train the machine learning models in order to reflect the prediction capability of datasets of different qualities.

## Methodology

### Data Processing

The GitHub data was preprocessed to keep the variables age, sex, latitude, longitude, symptoms, chronic disease, outcome, and travel history. Other variables included in the original dataset that were removed for analysis consisted of additional written information relating to the case and its report. Much of this was left empty and did not pertain to the information valuable to predicting death. Symptoms and chronic diseases are converted to a binary variable, indicating a patient has COVID-19 symptom/chronic disease or not. A new column was created, titled “combined symptoms.” If the individual had at least one symptom of any kind, there was a 1. The same is true for chronic diseases. The binary converter was utilized due to the lack of specific information regarding the symptoms and chronic diseases each case possessed. Data was limited to merely knowing if an individual harbored symptoms and/or chronic diseases, but not which ones. Outcome was either “death” as a 1 or “alive” as a 0 in the new “death” column. The GitHub data originally had over 3 million records. Cases with missing data were removed from the set and 28,958 cases were left. There were 530 deaths in the data after pre-processing, indicating a 1.83% death rate.

The Wolfram dataset included specific information on the clinical history of some patients and the symptoms exhibited. Unlike the Github dataset where we merely used the variables of “presence of symptoms” and “history of chronic illnesses” for analysis, we were able to specify and categorize the symptoms and comorbidities included. This is advantageous as it allows for detailed information to be geared toward unique individuals and cases with differing medical histories and symptoms present. Missing values were removed from the dataset and the final dataset resulted in 1,448 records with 123 deaths cases, indicating a 8.5% death rate. Symptoms and chronic diseases were then grouped into categories. We found 114 unique symptoms listed in the original dataset, which were divided into the following categories: “respiratory,” “weakness/pain,” “fever,” “high fever,” “gastrointestinal,” “nausea,” “cardiac,” “kidney,” and “asymptomatic” and “other.” High fever was noted if the fever temperature recorded is above 39 degrees Celsius. Forty-seven unique chronic diseases were categorized into “diabetes,” “neuro,” “hypertension,” “cancer,” “ortho,” “respiratory,” “cardiac,” “gastrointestinal,” “kidney,” “blood,” “prostate,” “thyroid,” and “none.” If a patient exhibited a symptom or chronic disease, a 1 was inputted in the corresponding column. This dataset was filtered to create one that only includes these unique symptoms and chronic diseases, age, gender, and death. Age was put into age ranges of intervals of 10 years from 0 to 99 years old.

For both datasets (Table 1), data was split into train, validation, and test groups. Thirty percent of the data was included in the test group. From the remaining data, 70% was assigned as the training data and 30% was included as the validation data. Once the data was properly separated, machine

**TABLE 1** | Comparison of the attributes included in the two filtered datasets.

Attribute	Description	G	W	Attribute	Description	G	W
ID	ID issued to each deindividualized case in the dataset	✓	✓	High fever	0—individual did not have a high fever (>39°C) 1—individual had a high fever	✓	
Age range	Age range individual's age falls into during time of positive COVID-19 test	✓	✓	Kidney S	0—individual did not display kidney related symptoms 1—individual displayed kidney related symptoms		✓
Gender	Reported gender of individual	✓	✓	Asymptomatic	0—individual is displaying symptoms 1—individual does not show an symptoms		✓
Latitude	Latitude where case is reported	✓		Diabetes	0—individual does not have diabetes 1—individual does have diabetes		✓
Longitude	Longitude where case is reported	✓		Neuro	0—individual does not have neurological chronic disease. 1—individual does have neurological chronic disease		✓
Symptoms	0—individual displayed no signs of symptoms 1—individual displayed signs of symptoms	✓		No chronic Disease	0—individual has chronic disease history 1—individual has no history of chronic disease		✓
Chronic Disease	0—individual had no reported chronic disease history 1—individual had history of chronic disease	✓	✓	Hypertension	0—individual does not have hypertension 1—individual does have hypertension		✓
Outcome	0—alive 1—dead	✓	✓	Cancer	0—individual does not have cancer 1—individual does have cancer		✓
Respiratory S	0—individual did not display respiratory symptoms 1—individual displayed respiratory symptoms		✓	Orthopedic CD	0—individual does not have orthopedic related chronic disease 1—individual does have orthopedic related chronic disease		✓
weakness/pain	0—individual had no weakness or pain 1—individual felt weakness or pain		✓	Respiratory related CD	0—individual does not have respiratory related chronic disease 1—individual does have respiratory related chronic disease		✓
Low fever	0—individual did not have a low fever (<39°C) 1—individual had a low fever		✓	Cardiac related CD	0—individual does not have cardiac related chronic disease 1—individual does have cardiac related chronic disease		✓
Gastrointestinal S	0—individual did not display gastrointestinal symptoms 1—individual displayed gastrointestinal symptoms		✓	Kidney related CD	0—individual does not have kidney related chronic disease 1—individual does have kidney related chronic disease		✓
Other symptoms	0—individual did not display other 1—individual displayed other symptoms		✓	Blood related CD	0—individual does not have blood related chronic disease 1—individual does have blood related chronic disease		✓
Nausea	0—individual did not experience nausea 1—individual experienced nausea		✓	Prostate related CD	0—individual does not have prostate related chronic disease 1—individual does have prostate related chronic disease		✓
Cardiac S	0—individual did not display cardiac related symptoms 1—individual displayed cardiac related symptoms		✓	Thyroid related CD	0—individual does not have thyroid related chronic disease 1—individual does have thyroid related chronic disease		✓

learning models discussed below were applied to do prediction, and the validity and prediction power of these algorithms were assessed with various metrics.

### Autoencoder for Rare Event Detection

Typically, an autoencoder is a neural network that learns representative codes from input and maps these codes back to the

input (7). This model is generally used to encode input variables and output a compressed version of that input. It consists of two main parts: the encoder and the decoder (**Figure 1**). The encoder is the part that learns about the deep features of input data. The decoder relies on learnt features to recreate the original data provided. There are three layers to the autoencoder model used: input, output, and hidden. In our research, the input layer of the network is a vector recording patient information. Hidden layers in the encoder learn a small vector representing input data. The decoder then maps hidden layers to a vector with the same dimension as the original input vector. The goal of training an autoencoder is to minimize the mean square error between the input vector and the reconstructed output vector, while also avoiding overfitting the data.

With the capability of learning representative features for input dataset and reconstructing data from extracted features, the autoencoder model can offer a solution for anomaly detection when it is trained on normal dataset (8). During the training process, the model ingests a series of normal data and learns latent common features of all normal dataset. When the trained model encodes and decodes an anomaly dataset, the reconstruction error is usually large since the model only learns how to reconstruct normal data. This means that an input data can be considered as an anomaly when the model reconstructs it with a high reconstruction error if the model is pre-trained with normal data. Similarly, the autoencoder can serve as a rare event prediction solution, in which the autoencoder is initially trained on majority events related data, the data that is considered to be normal.

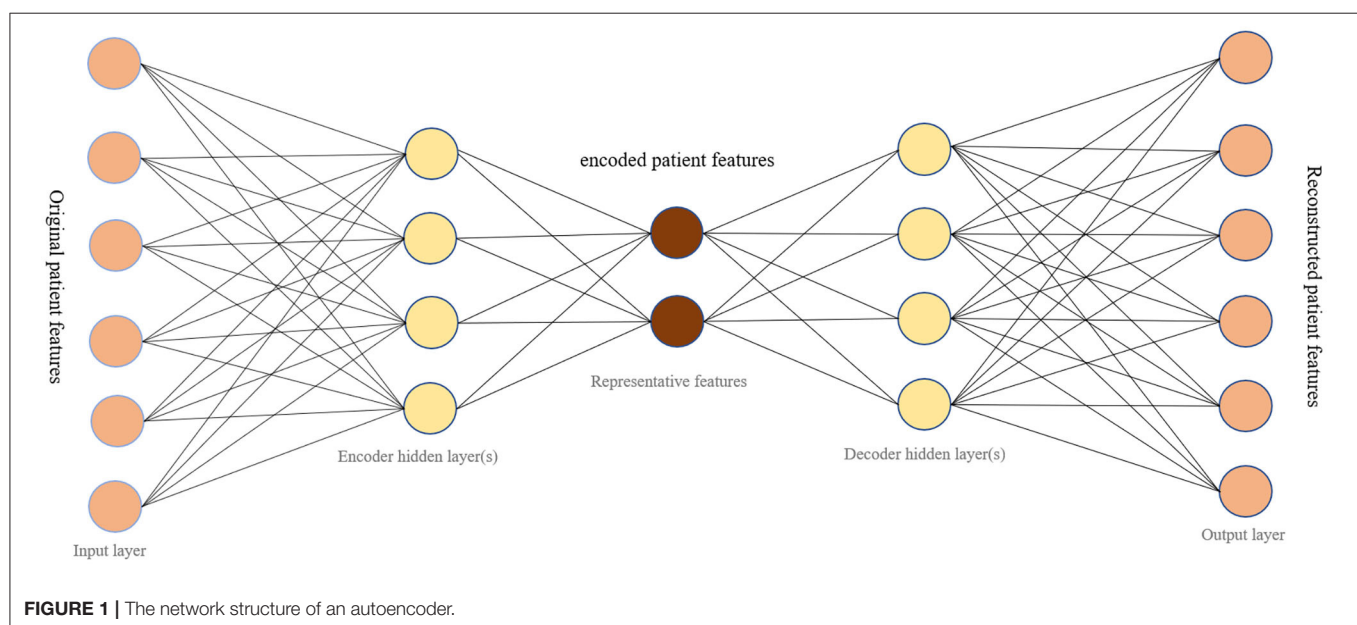
Our study relied on the latent function of autoencoders, anomaly detection, to create a model that would predict fatality upon one's COVID-19 diagnosis. Death from COVID-19 constitutes an anomaly because of how infrequently it occurs in our dataset. The autoencoder has been transformed from a data compression algorithm, to a rare event prediction model with the

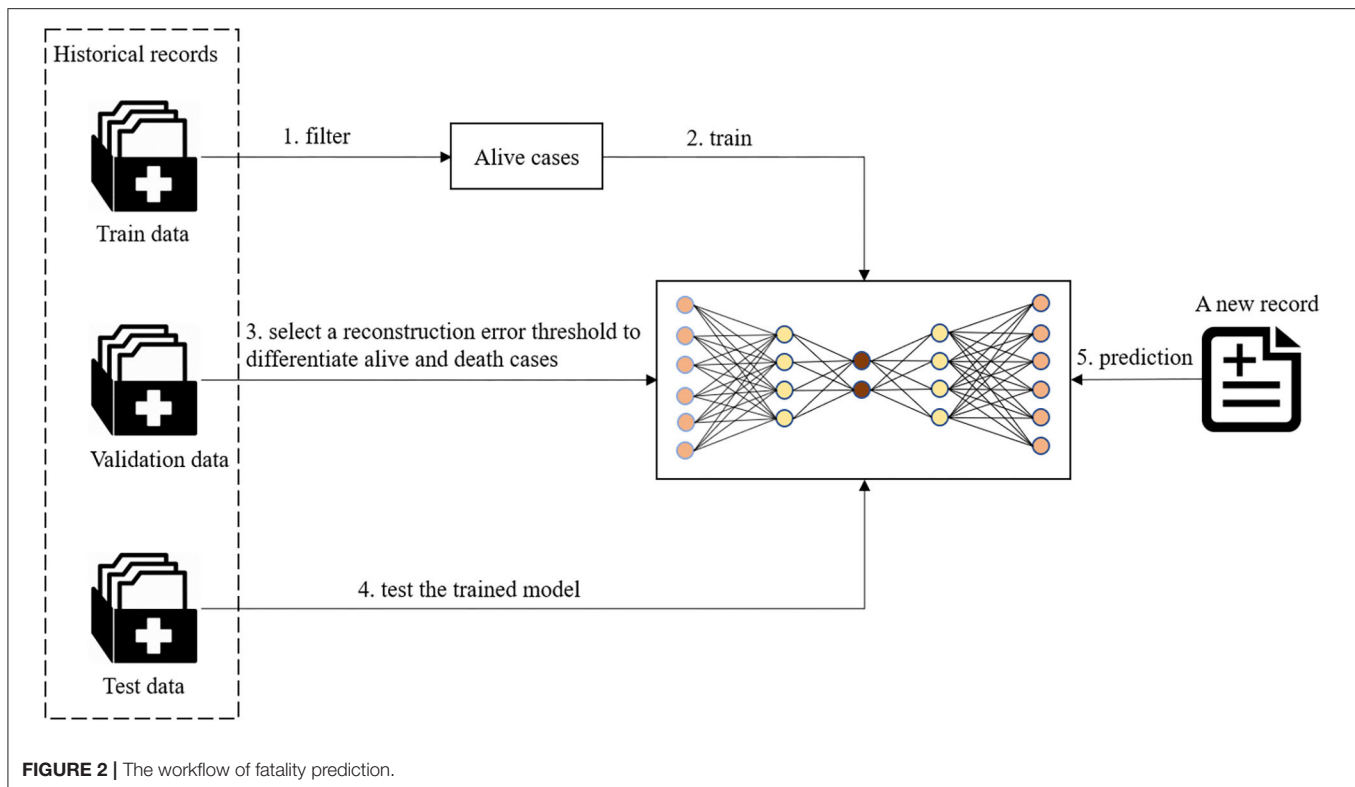
ability to distinguish between life and death. In other words, the original classification problem in our study was transformed into an anomaly detection problem.

As shown in **Figure 2**, the preprocessed data was split into train, validation, and test groups. For training the autoencoder model, a subset of data in the train group was used that solely contained non-death cases. The data was transformed to fit a standardized Gaussian curve before being input into the autoencoder model. The autoencoder model learns representative features of alive patients from their demographic information, symptoms, and chronic disease illnesses. After an autoencoder model was trained on individuals who tested positive for COVID-19 and survived in the train dataset, a series of reconstruction errors was populated by applying the trained model on validation data with different thresholds. The reconstruction error which performed best at differentiating the living and dead patients was selected as the threshold to determine a death prediction for a patient. Different thresholds were tested to find which would allow for the most optimal trade-off between recall and precision. Classification followed suit, where high construction errors were noted as a rare event. In this study, this would pertain to death.

## Evaluation

For each of the datasets we used, the Github dataset and the Wolfram dataset, an autoencoder model was trained to predict fatality in the test dataset. For comparison, the train data set was also trained with logistic regression, random forest, support vector machine (SVM), SVM one class models, isolation forest, and local outlier factor. Logistic regression, SVM, and Random forest are three widely used classification methods. A logistic regression model predicts the probability of a categorical dependent variable occurring. The SVM model seeks to find the hyperplane that has a maximal distance between two classes. Random forest is a tree-based learning algorithm which utilizes





**FIGURE 2 |** The workflow of fatality prediction.

decision trees rising from the training subset which are selected randomly to solve a classification problem. The One-class SVM algorithm is usually adopted for Novelty Detection, determining whether or not a new data record is similar to the training set, which only contains “normal” data. Both isolation forest model and local outlier factor model are outlier detection algorithms; the former works by explicitly isolating points that deviate in the dataset and the latter uses the density surrounding data points to determine whether or not they are outliers.

In order to detect which model has the best predictive power, these models were evaluated with multiple metrics, including accuracy, specificity, sensitivity and the area under the curve (AUC) score.

### Accuracy

Accuracy presents how many predictions the model has gotten correct. For this project, this would equate to the number of correctly predicted deaths and survivals over the total predictions made by the model. Unfortunately, since our data is highly imbalanced, accuracy is not a reliable metric. Our dataset contains a large amount of survival cases, causing a skew in that our models would predict “alive” a lot more often than “death,” which leads to a high accuracy regardless if the “death” predictions are accurate, since there are so few. It is the fraction of correct predictions:

$$\text{Accuracy} = \frac{\text{True Positive} + \text{True Negative}}{\text{True Positive} + \text{False Negative} + \text{False Positive} + \text{True Negative}}$$

### Specificity

Specificity is the rate of true negatives. It measures the proportion of true negatives that the model accurately predicts as negative. In this study, a true negative would be a prediction of “no death,” when the individual did not die. Specificity is less important of a metric than sensitivity, in our study, because it is more important to identify those individuals who have a greater likelihood of death, rather those who do not. Therefore, in order to ensure that we do not forget to account for any individual who can potentially encounter death, we can risk having some false positives of individuals who will receive care regardless if their prediction of death is accurate or not. It is measured by:

$$\text{Specificity} = \frac{\text{True Negative}}{\text{False Positive} + \text{True Negative}}$$

### Sensitivity

Sensitivity is the rate of true positives. It measures the proportion of true positives that the model predicts accurately as positive. A model with high sensitivity when dealing with an outcome of fatality is ideal. For this study, a true positive would be a prediction of death that is accurate. It is calculated by:

$$\text{Sensitivity} = \frac{\text{True Positive}}{\text{True Positive} + \text{False Negative}}$$

### AUC

AUC stands for “area under the curve.” In order to detect which model had the best predictive power, we calculated their AUC

value. The curve being referred to is the ROC curve, which contains the sensitivity metric on the y-axis and specificity on the x-axis. Since there is always a trade off between these two metrics, an ROC curve best displays their interaction in the model used. A curve which depicts a model that has a high value for both will be close to a 90° angle. An AUC value for a desired curve like this is 1, the maximum. An ROC curve that is no better than a random guess will be a line with a slope of one and have an AUC of 0.5.

## RESULTS

### Results on the Github Dataset

A comparison of the different models using the GitHub database is shown in **Figure 3**. All the models shown resulted in specificity and accuracy values above 0.9. Logistic regression, SVM, and random forest all have sensitivities below 0.4. Autoencoder scores above a sensitivity value of 0.4, leading it to have the best sensitivity. AUC scores, which are dependent on both the sensitivity and specificity of the models, are highest for the autoencoder model. The AUC scores for the remaining three models are almost identical, due to their similar specificities and lower sensitivities. The overall best results were obtained from the autoencoder model. The low metric values are results of the very few instances where health related attributes are included in the Github dataset, leading to a generalized analysis.

### Results on the Wolfram Dataset

For the Wolfram dataset, a correlation matrix depicts the relationships between all variables analyzed in our models. The correlation matrix is shown in **Figure 4**. A deeper red color indicates a more positive linear correlation and a deeper green color indicates a more negative linear correlation between the

two variables in question. It can be seen that the square at the intersection between “no chronic diseases” and “death” represents the strongest negative correlation. The matrix displays a strong correlation between fatality and COVID-19 patients with chronic diseases.

To train an anomaly detection model on the Wolfram dataset, the autoencoder model learned high-level features from all survival cases from the train data set, and all cases in the validation dataset aid the selection of a threshold to differentiate survival and death cases. **Figure 5A** is a plot of the various precision, recall, and F1 scores across different thresholds when predicting fatality on the validation dataset using the trained autoencoder model. The plot supported determining which threshold would be an optimal choice. It was decided, upon examining this plot, that a threshold of 2.5 could be used for our dataset. **Figure 5B** graphs the reconstruction error of all cases in the validation dataset at the chosen threshold. The dots above the threshold line show the true positives and false positive prediction cases. Orange dots represent death outcome and blue dots represent survival outcome. Only orange dots appear above the threshold line, signaling that there are only true positives present above the threshold.

When calculating the results of the autoencoder model using our selected threshold value, 36 out of 37 deaths in the test dataset were correctly predicted by the model, resulting in a 97% sensitivity rate. Lastly, the metrics across the various models for the Wolfram dataset were compared, which can be visualized in **Figure 6**. As shown in the figure, autoencoder is the optimal model as its results are highest in every metric depicted. There is vast improvement in these models when fed the Wolfram data vs. the GitHub data because the wolfram dataset contains detailed health related information. One-class SVM, isolation forest, local outlier factor, and autoencoder account for anomalies in the data, leading to their high sensitivity values. However, there is a tradeoff between one-class SVM's high AUC and sensitivity with its lower accuracy and specificity.

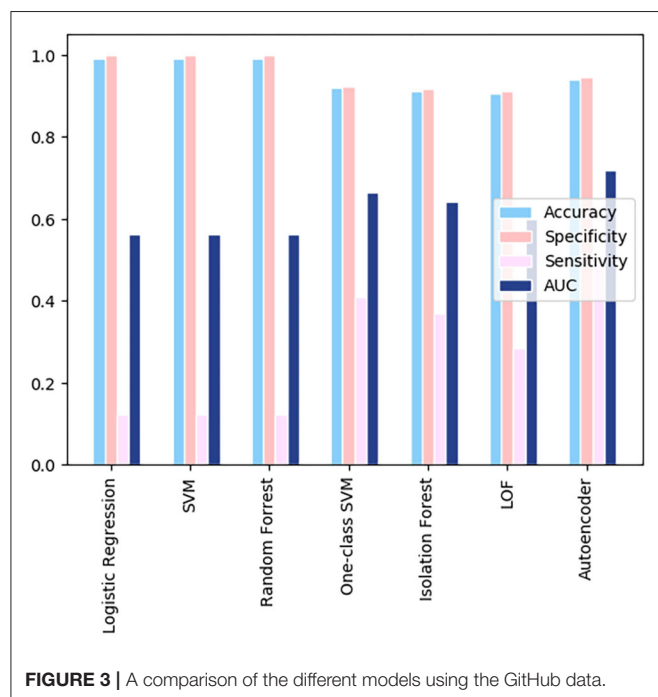
## DISCUSSION

### Related Works

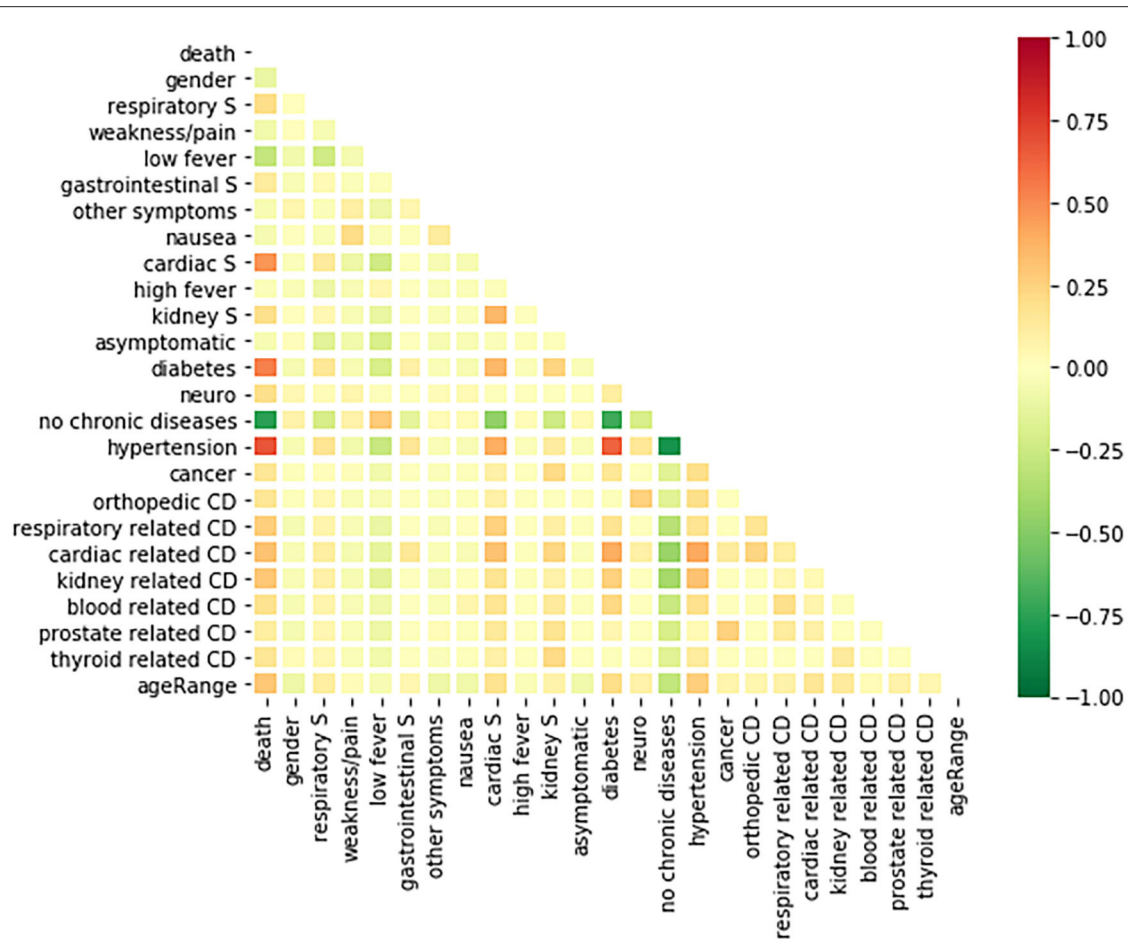
#### Machine Learning in Studying COVID-19

Machine learning has found its niche in the medical field. With the emergence of new medical data constantly created, these algorithms can serve as classification for the purpose of diagnosing a slew of diseases. One particular instance of this was done by researchers at Harvard Medical School (9). Using data from a cancer registry, they were able to make a super learner prediction function to classify the current stage of lung cancer progression in a patient.

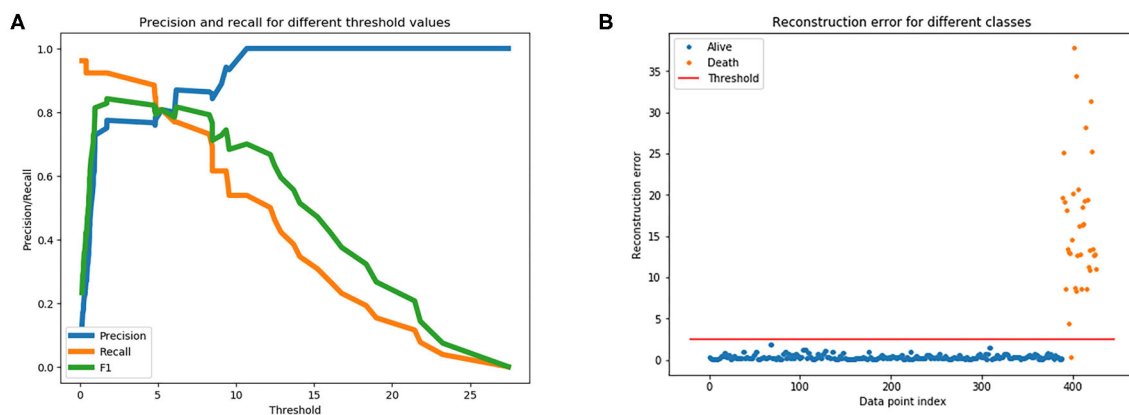
Machine learning algorithms have been a prominent force in studying COVID-19. One piece of information researchers are sure about is the fact that it is beneficial to diagnose a COVID-19 infection earlier than later. Since it is primarily a respiratory infection, a study (10) looked at CT scans for COVID-19 classification. Using an SVM model, they were able to find features of these images that are specific to COVID-19 infections







**FIGURE 4 |** A correlation matrix of the variables used in the analysis of the Wolfram database.

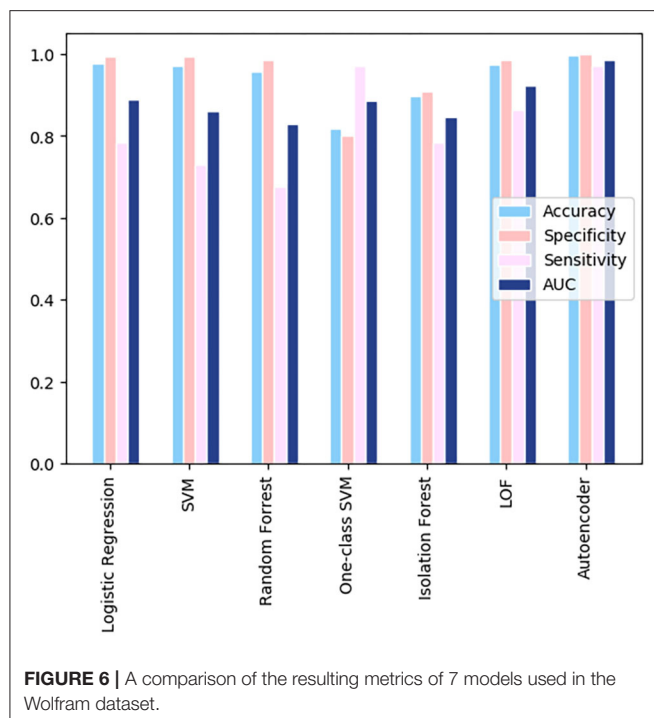


**FIGURE 5 |** (A) Is used to gather a threshold for the autoencoder model. (B) The reconstruction error at the chosen threshold of 2.5 on validation dataset.

in order to classify the disease. This method achieved a 98% accuracy score at classification.

Transitioning from diagnosing COVID-19, some studies focused on identifying regional death patterns relating to the

pandemic. One specific study predicted short term (7 days) fatality at the county level (11). In the study, they collected 23 different datasets, ranging from overall country level deaths to hospital data, and used five different predictors to determine



COVID-19 death count for county wide visualizations. These predicted models can be used to determine which hospitals should be prioritized to receive supply and how limited resources should be distributed nationwide. Attempting to study factors outside of an individual's control, a study looked at temperature (12) and COVID-19 death patterns in different areas, aiding hospitals in deciphering disease patterns. However, with the minor association between death and temperature, more variables should be included into the fatality risk model.

Currently, many studies are emerging that utilize machine learning algorithms to predict the death risk of a patient who has tested positive for COVID-19. Most of these studies have access to hospital medical records of the patients and analyze all corresponding information including demographic, symptoms, comorbidities, lab results, medical images. One such study utilized five machine learning approaches (logistic regression, partial least squares regression, elastic net, random forest, and bagged flexible discriminant analysis) to determine which factors are most associated with an individual's prognosis (13). These factors were combined to create a mortality risk score to estimate the mortality risk for 183 individual patients. Age, high-sensitivity C-reactive protein level, lymphocyte count, and d-dimer level of COVID-19 patients at admission are the factors concluded to be associated with increased mortality risk in the study. Another similar study attempted to create a clinical score to identify patients who had an increased risk of serious disease progression (14). Medical chart information of admitted patients were collected and variables correlated to critical illness with  $p < 0.02$  selected to create an online calculator for the likelihood (with 95% CIs) that a hospitalized patient with COVID-19 will develop critical illness. Logistic

regression and separately LASSO regression were used to determine 10 variables that served as a significant predictor of a severe and critical COVID-19 infection. Nemati et al. analyze survival characteristics of a group of 1,182 patients to test different variables of a patient and their overall survival to aid public health officials in their decisions regarding COVID-19 outbreaks (15). They discovered that gender and age were the two largest contributing factors to fatality, e.g., men had a higher fatality rate than women, agreeing with an original sample found in China early on (16). They also had looked for correlations underlying a patient's discharge time under COVID-19. By evaluating discharge times of individual patients with different machine learning methods, the researchers found that the gradient boosting survival analysis model was superior to other methods.

These individual level fatality studies are limited in predicting hospitalization due to their efforts to identify severe risk in patients after they are already admitted to a hospital. Most of the variables found to have a correlation with COVID-19 related deaths requiring intensive care is based on inpatient hospital lab results. These patients are already in the hospital, taking up capacity and resources. However, if fatality prediction can be developed that relies primarily on outside information, this could prove beneficial in allowing full hospitals to make informed and rational decisions on who to admit when the disease is not currently life threatening (e.g., when the patient is only experiencing minor symptoms). This will alleviate physician stress, reduce risk of virus spreading throughout the hospital, and conserve hospital resources. The proposed study will focus on the individual level detailing of the fatality risk based on their unique demographics, symptoms, and comorbidities using machine learning methods.

### Rare Event Prediction

The mortality rate for COVID-19 is a difficult calculation due to the number of people who may be infected but show no symptoms, and therefore proceed undetected, and the lag time between infection and death. Following extensive discussion from epidemiologists and scientists, the current consensus is that the fatality rate ranges between 0.5 and 1% (17). However, this percentage is dependent upon location, patient demographics, and physician experience in treating COVID-19. In a machine learning perspective, this rate constitutes a death event as a rare event.

Rare events are events that occur infrequently, such as major earthquakes, hurricanes, floods, asteroid impacts, forest fires, financial market crashes, epidemic disease spread. "Rare events are often interesting events" (18) since these events can have extensive effects that have the potential to rupture the equilibrium of systems such as the stock market and society in general. Rare event detection/prediction would be beneficial for the community to be able to better prepare for events which occur at low frequency, but lead to huge loss. However, rare event detection/prediction is a difficult task because the occurrence of a rare event is usually  $<5\%$  of all events, comprising a small percentage of data. In most instances dealing with rare events, insufficient data is gathered for a thorough analysis.



Researchers are becoming increasingly interested in using machine learning methods to detect/predict rare events using classification models or anomaly detection models. For classification models, a majority of machine learning models assume that the dataset is balanced and make predictions based upon those assumptions. A significant issue with rare events classification is that accuracy is not a reliable metric to evaluate the model because the desired event occurs too infrequently. A very high accuracy can be achieved when all events are classified as non-rare events. In medical fields, Luca et al. used a model based on Extreme Value Theory (EVT) to predict epileptic seizures for people using electroencephalogram (EEG) devices (19). They focused on hypermotor seizures that are located in the tails of a normal, standardized curve for normal movement behavior. The percent of epileptic movements per patient has a mean of 2%. This rarity of events does not allow for sufficient training data and results in an imbalanced dataset. It was noted that the datasets with the greatest amount of rare events have the EVT model result in higher sensitivity than the standard SVM machine learning model. Additionally, Sarker et al. used data from social media and search engines to predict and monitor adverse drug reactions (ADR) (20). They find the use of social media in monitoring ADRs are increasing as methods are becoming increasingly accurate and the detection time is significantly lower compared to traditional detection methods. Conner et al. similarly uses a Twitter corpus of symptom-related Tweets to detect and predict ADRs (21). By using keywords, they eliminate many irrelevant Tweets and categorically find tweets that strictly relate to the discussion of a drug and its symptoms. This study was further improved in the detection of adverse effects from vaccines (22). Using Multi-instance Domain Adaptation (MIDA) model on Twitter data, they were able to identify symptoms and align them with formal reports of symptoms to identify adverse effects in the use of a vaccine. Yates and Goharian also attempted to detect expected and unexpected ADRs by mining drug review sites for symptoms contained in the Unified Medical Language System (UMLS) (23). These methods could be applied across the world, as (24) shows that the same methods work in Spanish. His team scanned Twitter, Facebook, and Spanish medical forums using symptom related keywords and were able to detect symptoms.

Deep learning, overall, utilizes multiple layers neuronal networks to withdraw higher level features from the simpler input, emerging as an innovative way to improve the performance of data-driven applications recently. Many researchers have begun to use deep learning to solve rare event detection and prediction issues. A previous study used deep learning methods to predict the rapid intensification of a tropical cyclone (TC), a rare event in natural disasters, using a plethora of factors that contribute to a TC's intensity (25). This can prove critical in saving lives from disastrous situations. A study compared traditional machine learning models to recurrent neural network (RNN) to predict early signs of heart failure and delay one's progression to receiving that diagnosis (26). This was complicated in the past with classical machine learning models because of the intricacy of electronic health records and all of the information involved to make these predictions. This paper conveys the revolutionary pathway being carved

out by deep learning methods in medicine. Not only can deep learning solve the issue of rare event detections, but it can also be applied to more discrete problems that medical researchers face. Wang et al. (27) was able to identify potential adversarial effects through a multi-instance logistic regression model (MILR) by scanning Tweets and using VAERS information. Wang et al. (22) also uses deep learning with sSSM and nSSM models to classify the discussion of symptoms within tweets that relate to the flu. Symptoms such as arm pain and headaches could be identified in tweets related to the flu accurately under their model. In our research, we will use deep learning methods to do the fatality prediction and compare their performance with traditional machine learning methods.

## Findings of Our Study

A series of machine learning models were compared to validate which one worked best in this scenario of death prediction. Two different datasets were used: one that specified symptoms and comorbidities and one that generalized across them. Fatality related to COVID-19 is caused by a multitude of different, confounding factors. Therefore, introducing a model that can predict whether an individual's diagnosis of COVID-19 is likely to be fatal will serve as a reliable and advantageous tool. Every case of COVID-19 is unique, and this predictor model accounts for the significant features present in a COVID-19 diagnosis and relies on information that does not require any hospitalization. It focuses on demographic information, symptoms, and patient chronic disease illness. Therefore, it can be used to make a fatality prediction prior to hospitalization of the infected individual. This will provide guidance for employees at hospitals that are reaching or at capacity to make educated decisions upon whether or not to admit a patient. Cases of COVID-19 continue to rapidly rise at alarming rates, reported by CNN (28), and it is projected that the virus will persist for a continued amount of time. It is crucial that patients who are at an increased risk, where death is imminent, receive care in hospitals to prevent this outcome.

The GitHub dataset was largely generalized; it did not include specifics on symptoms or chronic diseases that individuals harvested. Moreover, death made up a very small percentage of the cases in our dataset. The results of different machine learning models indicated that the autoencoder, a deep learning model, produced the best prediction results. However, no model produced a sensitivity metric above 0.5, showing limitations of the model. The sensitivity metric is the most important as we want to minimize the number of false positives in order to avoid missing a patient who is in danger of a death outcome.

The Wolfram dataset incorporated specific symptoms and chronic diseases that plagued the individuals in the data. This allows for models based on this data to be a better fit and cater to the unique characteristics of the individuals who have the virus. Similarly, the autoencoder proved to have the most optimal results upon comparison with all of its metrics being the highest.

COVID-19 has an average fatality rate between 0.5 and 1% (17). Although this is a high fatality rate for a virus, death is still considered as a rare event for machine learning algorithms to learn. Autoencoder serves as the best prediction model for COVID-19 death in our experiments when it converts the

prediction problem to an anomaly detection problem. The results demonstrate that it will serve as the most representative model for physicians to be able to make an educated decision as to whether or not to admit a patient to a hospital and decide how extensive treatment should be a valuable tool in making decisions for the best course of action of care. However, it should not be the only resource used to make this decision. The healthcare worker will also take into account additional knowledge on the patient and use their best judgement, along with the information provided by the model.

The correlation matrix produced by the Wolfram dataset provides insight into which factors are most notable in their association with a patient's fatality. There is a high correlation between death and having a chronic disease. This is displayed by the result that having no chronic disease history and death occurring share a strong negative correlation based on the matrix. More specifically, if the individual has a chronic disease of hypertension or diabetes, they have a higher chance of death than other comorbidities in the study. Turning our attention toward symptoms, gastrointestinal, kidney related, and respiratory symptoms are shown to be positively correlated with death. Cardiac related symptoms seem to be the symptoms, out of the ones studied here, that are most correlated with COVID-19 death (29). The *r* value between having cardiac symptoms and death occurring is between 0.5 and 0.75, displaying a moderate positive correlation. The CDC similarly reports that individuals who have underlying chronic diseases report greater chances of hospitalization and death (30). This information shows that individuals who have chronic diseases should take greater precaution toward both reducing their risk of contracting the disease and receiving care if infected. Interestingly, having a low fever (below  $<39^{\circ}\text{C}$ ) has a weak negative correlation with death. This agrees with current data knowledge that states a low fever is a common symptom for a mild COVID-19 case (31).

## Limitations

There are limitations embedded in this study. The most profound limitation is the lack of abundant quality data used to train the models created. The Wolfram dataset used to train the prediction model only consisted of 1,448 cases in a centralized area. The larger GitHub dataset used contained an increased number of datapoints, but with less specific information on each case, limiting the potential prediction capability of models. We were limited by our access to data and relied solely on datasets that were publicly available, yet still based on medical records. Our study and models would improve with direct access to electronic health records, or larger datasets based on them, that contain extensive and detailed accounts of individual COVID-19 cases. Since COVID-19 fatality rates are heterogeneous depending on the region, indicated by the Center for Evidence Based Medicine, additional studies with more representative data would be beneficial. Additionally, the study did not take into account whether patients had received hospital care for COVID-19 treatment prior to their final outcome.

## CONCLUSION AND FUTURE WORK

A deep learning model was developed to predict the fatality outcome of an individual who tested positive for COVID-19. In this instance, death is dictated as a rare event and requires a model that accounts for this. Autoencoder proved to be the optimal method to serve as a death prediction model. Additionally, the correlation matrix revealed individuals were at greatest risk of fatality from COVID-19 if they showed respiratory or cardiac based symptoms and were previously diagnosed with a chronic disease.

The model solely predicted death relating to a COVID-19 diagnosis and will be able to provide some guidance to physicians who need to make a decision as to whether or not to admit a person who has tested positive for COVID-19. However, this virus is still capable of having a profound impact on quality of life on infected individuals. In the future, a model should be created that not only predicts death, but also can predict the severity of the progression of the disease. This will prompt individuals to expeditiously seek care, which will prevent the debilitating future dispositions that the disease might induce on the infected individual. This can prevent a large number of people admitted to the ICU if they were to seek care beforehand. Moreover, with increased testing availability in regions, the number of people testing positive for COVID-19 is known for a given region. By incorporating demographic information, health habit (physical exercise), or psychology factors, occupation, symptoms and chronic disease of the confirmed case, predictions can be made for the number of required hospitalizations in a given area with the trained model. If this information is combined with the current availability of medical resources deficiencies information (32) in a given area, then proper preparation can be obtained for the amount of medical resources required.

## DATA AVAILABILITY STATEMENT

The datasets presented in this study can be found in an online repository: <https://github.com/stccenter/COVID-19/tree/master/prediction/patient-level%20fatality>.

## AUTHOR CONTRIBUTIONS

YL and HL came up with the original idea. CY advised on the research idea and methods. YL designed the study. YL, MH, JL, and AC conducted the experiments. YL and MH performed the analysis. CY supervised the research and secured the funding source. MH and YL wrote a draft of the manuscript, which was improved by all other authors of the manuscript. All authors contributed to the article and approved the submitted version.

## FUNDING

This research presented in this paper was funded by NSF 1841520, 1835507, and 2027521.

## REFERENCES

- Yang C, Sha D, Liu Q, Li Y, Lan H, Guan WW, et al. Taking the pulse of COVID-19: a spatiotemporal perspective. *Int J Digital Earth*. (2020). doi: 10.1080/17538947.2020.1809723
- COVID-19 Module Data Dashboard. *Patient Impact and Hospital Capacity Pathway*. Centers for Disease Control and Prevention. (2020). Available online at: [www.cdc.gov/nhsn/covid19/report-patient-impact.html](http://www.cdc.gov/nhsn/covid19/report-patient-impact.html) (accessed June 29, 2020).
- Shah K, Chaudhari G, Kamrai D, Lail A, Patel RS. How essential is to focus on physician's health and burnout in coronavirus (COVID-19) pandemic? *Cureus*. (2020) 12:e7538. doi: 10.7759/cureus.7538
- Gold, R., and Evans, M. *Hospitals Struggle to Contain Covid-19 Spread Inside Their Walls*. The Wall Street Journal, Dow Jones and Company. (2020). Available online at: [www.wsj.com/articles/hospitals-treat-covid-19-they-spread-it-too-11594046342](http://www.wsj.com/articles/hospitals-treat-covid-19-they-spread-it-too-11594046342) (accessed July 6, 2020).
- Woolf SH, Chapman DA, Sabo RT, Weinberger DM, Hill L. Excess deaths from COVID-19 and other causes, March-April. *JAMA*. (2020) 324:510–13. doi: 10.1001/jama.2020.11787
- Xu B, Gutierrez B, Mekaru S, Sewalk K, Goodwin L, Loskill A, et al. Epidemiological data from the COVID-19 outbreak, real-time case information. *Sci Data*. (2020) 7:1–6. doi: 10.1038/s41597-020-0448-0
- Schmidhuber J. Deep learning in neural networks: an overview. *Neural Netw*. (2015) 61:85–117. doi: 10.1016/j.neunet.2014.09.003
- Ranjan C. *Extreme Rare Event Classification Using Autoencoders in Keras*. Towards Data Science (2019). Available online at: <https://towardsdatascience.com/extreme-rare-event-classification-using-autoencoders-in-keras-a565b386f098>
- Bergquist SL, Brooks GA, Keating NL, Landrum MB, Rose S. Classifying lung cancer severity with ensemble machine learning in health care claims data. *Proc Mach Learn Res*. (2017) 68:25–38.
- Barstugan M, Ozkaya U, Ozturk S. *Coronavirus (COVID-19) Classification Using CT Images by Machine Learning Methods*. (2020). Available online at: [ArXiv.org: arxiv.org/abs/2003.09424](https://arxiv.org/abs/2003.09424) (accessed Mar 20, 2020).
- Altieri N, Barter R, Duncan J, Dwivedi, R., Kumbier, K., Li, X., et al. (2020). *Berkeley Statistics*. Available online at: [arXiv.org](https://arxiv.org) (accessed May 16, 2020).
- Siddiqui MK, Morales-Menendez R, Gupta PK, Hafiz MNI, Fida H, Khudeja K, et al. Correlation between temperature and COVID-19 (suspected, confirmed and death) cases based on machine learning analysis. *J Pure Appl Microbiol*. (2020) 14(Suppl. 1):1017–24. doi: 10.22207/JPAM.14.SPL.1.40
- Chen X, Liu Z. Early prediction of mortality risk among severe COVID-19 patients using machine learning. *medRxiv*. (2020). doi: 10.1101/2020.04.13.20064329
- Liang W, Liang H, Ou L, Chen B, Chen A, Li C, et al. Development and validation of a clinical risk score to predict the occurrence of critical illness in hospitalized patients with COVID-19. *JAMA Intern Med*. (2020) 180:1–9. doi: 10.1001/jamainternmed.2020.2033
- Nemati M, Ansary J, Nemati N. Machine-learning approaches in COVID-19 survival analysis and discharge-time likelihood prediction using clinical data. *Patterns*. (2020) 1:100074. doi: 10.1016/j.patter.2020.100074
- Jin JM, Bai P, He W, Wu F, Liu XF, Han DM, et al. Gender differences in patients with COVID-19: focus on severity and mortality. *Front Pub Health*. (2020) 8:52. doi: 10.3389/fpubh.2020.00152
- Mallapaty S. How deadly is the coronavirus? Scientists are close to an answer. *Nature*. (2020) 582:467–8. doi: 10.1038/d41586-020-01738-2
- Weiss GM, Hirsh H. Learning to predict extremely rare events. In: *AAAI Workshop on Learning from Imbalanced Data Sets*. Austin: AAAI Press (2000). p. 64–8.
- Luca S, Karsmakers P, Cuppens K, Croonenborghs T, Van de Vel, A, Ceulemans B, et al. Detecting rare events using extreme value statistics applied to epileptic convulsions in children. *Artif Intell Med*. (2014) 60:89–96. doi: 10.1016/j.artmed.2013.11.007
- Sarker A, Ginn R, Nikfarjam A, O'Connor K, Smith K, Jayaraman S, et al. Utilizing social media data for pharmacovigilance: a review. *J Biomed Inform*. (2015) 54:202–12. doi: 10.1016/j.jbi.2015.02.004
- Conner-Kerr T, Duggan C, Walker K, Kute T. Effects of low frequency ultrasound on Adriamycin (ADR) uptake and cell growth in breast cancer cells. *Rehabil Oncol*. 32:39. doi: 10.21037/atm.2020.02.155
- Wang J, Zhao L. Multi-instance domain adaptation for vaccine adverse event detection. In: *Proceedings of the 2018 World Wide Web Conference*. Lyon (2018). p. 97–106.
- Yates A, Goharian N. ADRTTrace: detecting expected and unexpected adverse drug reactions from user reviews on social media sites. In: *European Conference on Information Retrieval*. Berlin: Springer (2013). p. 816–9.
- Segura-Bedmar I, Revert R, Martínez P. Detecting drugs and adverse events from Spanish social media streams. In: *Proceedings of the 5th International Workshop on Health Text Mining and Information Analysis (LOUHI)*. Gothenburg (2014). p. 106–15.
- Li Y, Yang R, Yang C, Yu M, Hu F, Jiang Y. Leveraging LSTM for rapid intensifications prediction of tropical cyclones. *ISPRS Ann Photogram Remote Sens Spatial Inform Sci*. (2017) 4:101–5. doi: 10.5194/isprs-annals-IV-4-W2-101-2017
- Choi E, Schuetz A, Stewart WF, Sun J. Using recurrent neural network models for early detection of heart failure onset. *J Am Med Inform Assoc*. (2017) 24:361–70. doi: 10.1093/jamia/ocw112
- Wang J, Zhao L, Ye Y. Semi-supervised multi-instance interpretable models for flu shot adverse event detection. In: *2018 IEEE International Conference on Big Data (Big Data)*. Seattle, WA: IEEE (2018). p. 851–60.
- Maxouris C. *Hospitals Face 'an Explosion of Covid' and Signs of Another Surge as Coronavirus Case Numbers Climb*. CNN (2020). Available online at: [www.cnn.com/2020/07/02/health/coronavirus-hospitalizations-rates-rise/index.html](http://www.cnn.com/2020/07/02/health/coronavirus-hospitalizations-rates-rise/index.html) (accessed September 15, 2020).
- Jordan Rachel E, Peymane A, Cheng KK. Covid-19: risk factors for severe disease and death. *BMJ*. (2020) 368:m1198. doi: 10.1136/bmj.m1198
- Stokes EK, Zambrano LD, Anderson KN, Marder EP, Raz KM, El Burai Felix S, et al. Coronavirus disease 2019 case surveillance - United States, January 22–May 30, 2020. *Centers Dis Control Prevent*. (2020) 69:759–65. doi: 10.15585/mmwr.mm6924e2
- Carlino MV, Valenti N, Cesaro F, Costanzo A, Cristiano G, Guarino M, et al. Predictors of intensive care unit admission in patients with coronavirus disease 2019 (COVID-19). *Monaldi Arch Chest Dis*. (2020) 90. doi: 10.4081/monaldi.2020.1410
- Sha D, Miao X, Lan H, Stewart K, Ruan S, Tian Y, et al. Spatiotemporal analysis of medical resource deficiencies in the US under COVID-19 pandemic. *medRxiv*. (2020). doi: 10.1101/2020.05.24.20112136

**Conflict of Interest:** The authors declare that the research was conducted in the absence of any commercial or financial relationships that could be construed as a potential conflict of interest.

Copyright © 2020 Li, Horowitz, Liu, Chew, Lan, Liu, Sha and Yang. This is an open-access article distributed under the terms of the Creative Commons Attribution License (CC BY). The use, distribution or reproduction in other forums is permitted, provided the original author(s) and the copyright owner(s) are credited and that the original publication in this journal is cited, in accordance with accepted academic practice. No use, distribution or reproduction is permitted which does not comply with these terms.



## OPEN ACCESS

## Edited by:

Stephen Allen Morse,  
Centers for Disease Control and  
Prevention (CDC), United States

## Reviewed by:

Pedro Xavier-Elsas,  
Federal University of Rio de  
Janeiro, Brazil  
Segaran P. Pillai,  
United States Department of  
Homeland Security, United States

## \*Correspondence:

Louis Bernard  
l.bernard@chu-tours.fr  
Nathalie Heuzé-Vourc'h  
nathalie.vourc'h@med.univ-tours.fr

†These authors have contributed  
equally to this work

## Specialty section:

This article was submitted to  
Infectious Diseases - Surveillance,  
Prevention and Treatment,  
a section of the journal  
Frontiers in Medicine

Received: 16 July 2020

Accepted: 03 September 2020

Published: 20 October 2020

## Citation:

Bernard L, Desoubeaux G,  
Bodier-Montagutelli E, Pardessus J,  
Brea D, Allimonier L, Eymieux S,  
Raynal P-I, Vasseur V, Vecellio L,  
Mathé L, Guillon A, Lanotte P,  
Pourchez J, Verhoeven PO, Esnouf S,  
Ferry M, Eterradosi N, Blanchard Y,  
Brown P, Roingard P, Alcaraz J-P,  
Cinquin P, Si-Tahar M and  
Heuzé-Vourc'h N (2020) Controlled  
Heat and Humidity-Based Treatment  
for the Reuse of Personal Protective  
Equipment: A Pragmatic  
Proof-of-Concept to Address the  
Mass Shortage of Surgical Masks and  
N95/FFP2 Respirators and to Prevent  
the SARS-CoV2 Transmission.  
Front. Med. 7:584036.  
doi: 10.3389/fmed.2020.584036

# Controlled Heat and Humidity-Based Treatment for the Reuse of Personal Protective Equipment: A Pragmatic Proof-of-Concept to Address the Mass Shortage of Surgical Masks and N95/FFP2 Respirators and to Prevent the SARS-CoV2 Transmission

Louis Bernard<sup>1,2\*</sup>, Guillaume Desoubeaux<sup>2,3,4†</sup>, Elsa Bodier-Montagutelli<sup>2,4,5†</sup>,  
Jeffrey Pardessus<sup>2,4</sup>, Déborah Brea<sup>2,4</sup>, Laurine Allimonier<sup>2,4</sup>, Sébastien Eymieux<sup>2,6,7</sup>,  
Pierre-Ivan Raynal<sup>2,6</sup>, Virginie Vasseur<sup>2,4</sup>, Laurent Vecellio<sup>2,4</sup>, Ludovic Mathé<sup>8</sup>,  
Antoine Guillon<sup>2,4,9</sup>, Philippe Lanotte<sup>2,10,11</sup>, Jérémie Pourchez<sup>12</sup>, Paul O. Verhoeven<sup>13,14</sup>,  
Stéphane Esnouf<sup>15</sup>, Muriel Ferry<sup>15</sup>, Nicolas Eterradosi<sup>16</sup>, Yannick Blanchard<sup>16</sup>,  
Paul Brown<sup>16</sup>, Philippe Roingard<sup>2,6,7</sup>, Jean-Pierre Alcaraz<sup>17</sup>, Philippe Cinquin<sup>17,18</sup>,  
Mustapha Si-Tahar<sup>2,4†</sup> and Nathalie Heuzé-Vourc'h<sup>2,4\*</sup>

<sup>1</sup> Médecine interne et maladies infectieuses, CHU de Tours, Tours, France, <sup>2</sup> Université de Tours, Tours, France, <sup>3</sup> Parasitologie-mycologie-médecine tropicale, CHU de Tours, Tours, France, <sup>4</sup> Inserm U1100, Centre d'étude des pathologies respiratoires (CEPR), Tours, France, <sup>5</sup> Pharmacie à usage intérieur, CHU de Tours, Tours, France, <sup>6</sup> Biologie cellulaire-Microscopie électronique, CHU de Tours, Tours, France, <sup>7</sup> UMR Inserm U1259-Morphogénèse et antigénicité du VIH et des virus des hépatites, Tours, France, <sup>8</sup> Blanchisserie centrale GCS NOT, CHU de Tours, Tours, France, <sup>9</sup> Médecine intensive-Réanimation, CHU de Tours et Université de Tours, Tours, France, <sup>10</sup> Bactériologie-Virologie-Hygiène hospitalière, CHU de Tours, Tours, France, <sup>11</sup> ISP Equipe 5-Bactéries et Risque Materno-fœtal, INRAE, Nouzilly, France, <sup>12</sup> Mines Saint-Etienne, Université Jean Monnet, INSERM, U 1059 Sainbiose, Centre CIS, Saint-Etienne, France, <sup>13</sup> GIMAP, EA 3064, Université Jean Monnet, Université de Lyon, Saint-Etienne, France, <sup>14</sup> Service des Agents Infectieux et d'Hygiène, CHU de Saint-Etienne, Saint-Etienne, France, <sup>15</sup> Service d'Étude du Comportement des Radionucléides (SECR), CEA, Université Paris Saclay, Gif-sur-Yvette, France, <sup>16</sup> French Agency for Food Environmental and Occupational Health Safety (Anses), Ploufragan, France, <sup>17</sup> TIMC-IMAG, UMR5525 Univ. Grenoble Alpes-CNRS, La Tronche, France, <sup>18</sup> CIC-IT1406 INSERM/CHU Grenoble Alpes/Univ. Grenoble Alpes, La Tronche, France

**Background:** The coronavirus infectious disease-2019 (COVID-19) pandemic has led to an unprecedented shortage of healthcare resources, primarily personal protective equipment like surgical masks, and N95/filtering face piece type 2 (FFP2) respirators.

**Objective:** Reuse of surgical masks and N95/FFP2 respirators may circumvent the supply chain constraints and thus overcome mass shortage. Methods, design, setting, and measurement: Herein, we tested the effects of dry- and moist-air controlled heating treatment on structure and chemical integrity, decontamination yield, and filtration performance of surgical masks and FFP2 respirators.

**Results:** We found that treatment in a climate chamber at 70°C during 1 h with 75% humidity rate was adequate for enabling substantial decontamination of both respiratory



viruses, oropharyngeal bacteria, and model animal coronaviruses, while maintaining a satisfying filtering capacity.

**Limitations:** Further studies are now required to confirm the feasibility of the whole process during routine practice.

**Conclusion:** Our findings provide compelling evidence for the recycling of pre-used surgical masks and N95/FFP2 respirators in case of imminent mass shortfall.

**Keywords:** SARS-CoV-2, facemask, recyclability, surgical face masks, COVID-19, heating, FFP2/N95, coronavirus

## HIGHLIGHTS

- A worldwide mass shortage of surgical masks and N95/FFP2 respirators has been observed during the coronavirus infectious disease-2019 (COVID-19) pandemic;
- Alternative means for recycling pre-used face masks are warranted in such a context of sanitary crisis;
- A moist heating treatment results in a satisfactory decontamination of critical respiratory pathogens while preserving the structural integrity and filtration efficiency of protective masks.

## INTRODUCTION

Severe acute respiratory syndrome coronavirus 2 (also referred to as SARS-CoV-2) is responsible for the coronavirus infectious disease-2019 (COVID-19) pandemic. SARS-CoV-2 remains viable over several hours on different inert surfaces and up to 3 h in the air (1). During previous other epidemics, the airborne route of transmission was already associated with nosocomial super-spreading events (2). Although not fully elucidated so far, transmission of SARS-CoV-2 may occur partly by aerosol droplets and contaminated postillions of aerodynamic diameter ranging from 0.25 to 3.0  $\mu\text{m}$  (3). Accordingly, any face-to-face contact closer than  $\leq 6$  feet to a symptomatic patient should be considered significant exposure, if sustained for at least a few minutes (4).

In order to reduce the risk of interindividual contamination (5), most governments, medical societies, and health associations agreed to recommend to healthcare workers and caregivers systematic wearing of protective face masks, like surgical masks and N95/filtering face piece (FFP) respirators to cover the mouth and nose during the COVID-19 pandemic (to be complemented by meticulous hand hygiene, eye protection, gloves, and gown wearing). Approved protective masks are composed of several layers of nanofibers made with polypropylene (6). Surgical masks are primarily designed to prevent transmission of pathogens from infected patients wearing them to others and from contaminating their surroundings and direct environment (5). Additionally, FFP respirators protect noninfected healthy people wearing them from inhalation of aerosol particles. According to European standards, FFPs are sorted in three distinct subclasses depending on their aerosol filtration efficiency and leakage percentages. During the COVID-19 pandemic, caregivers are encouraged

to wear at least FFP2-grade respirators (specifications close to N95 respirators in the USA), coming in contact with patients infected with SARS-CoV-2 or suspected of being so. Both surgical masks and N95/FFP2 respirators are single-use disposable devices, and most industrial manufacturers are currently overwhelmed by massive orders. Thus, several countries and health facilities are now suffering from in- and out-hospital mass shortage of protective surgical masks and N95/FFP2 respirators.

Therefore, in the present context of world sanitary emergency, alternative processes allowing to extend the existing on-hand supplies are critically required to offer satisfying respiratory protective means for all healthcare workers (7). Production of fabric masks (e.g., with non-cellulose synthetic fibers based on nonwoven polypropylene [Spunbond, Meltblown, Spunbond (SMS)]) (5) or application of different decontamination means to pre-used protective masks has been urgently assessed. Many strategies are unsatisfactory (8, 9), insufficiently documented, or leading to poor decontamination yields and loss of filtration performances. Moreover, both the practical transposition of all these treatment procedures to each hospital service, attendant care, and nursing department and the wearers' comfort have often been neglected. Thanks to an incredible international multidisciplinary effort, promising disinfecting processes are emerging and some are already in application in "real-life conditions."

Herein, we demonstrate the benefits of an easy-to-use recycling solution that will reduce the overall burden on mass shortage in healthcare facilities using a heating stage at 70°C, a temperature known to inactivate the SARS-CoV-2 (10). Hence, we provide a simple procedure that efficiently decontaminates surgical masks and FFP2 respirators from respiratory pathogens while preserving filtration performances.

## MATERIALS AND METHODS

### Protective Masks

All assays on oropharyngeal bacteria, influenza virus, and filtration performances were carried out using conventional elastic surgical masks (different brands including THF type II R 3 Plis<sup>®</sup>, CA Diffusion, Halluin, France) and FFP type 2 (FFP2) respirators (RP2\_M<sup>®</sup>, CA Diffusion). Inactivation assays on surrogate animal coronaviruses were performed using surgical (THF type IIR CA1960<sup>®</sup>, CA Diffusion) and FFP2 (FFP2 NRD type IIR 2192S-WH<sup>®</sup>, Medicom, Saint Barthélemy d'Anjou,

France). All were certified by EN 149:2001+A1:2009 NF or EN 14683+AC standards.

## Model Strains of Oropharyngeal Bacteria

*Streptococcus pyogenes* (isolate 19-103100), *Staphylococcus aureus* (strains ATCC 29213 and ATCC 6538), and *Haemophilus influenzae* strains (isolate CIP776) were grown in heart-brain liquid medium (BD Brain Heart infusion broth<sup>®</sup>, Beckton Dickinson, Rungis, France) or in Muller-Hinton<sup>®</sup> agar (bioMérieux, Craponne, France).

For titration, bacteria were diluted 10-fold up to 1:10,000, and 50  $\mu$ l of each dilution were then deposited onto agar plates, trypticase soy agar TSH<sup>®</sup> (bioMérieux) for *S. aureus* and *S. pyogenes* or onto Chocolate agar PolyViteX<sup>®</sup> agar (bioMérieux) for *H. influenzae*, before incubation at 37°C and subsequent counting of the number of colony-forming units (CFU/ml).

## Model Strains of Respiratory Viruses

The influenza A H3N2/Scotland/20/74 strain was prepared as previously described (11) and cultured onto canine kidney epithelial mycoplasma-free Madin-Darby canine kidney (MDCK) cells (ATCC CCL-34) with minimum essential medium-Eagle (MEM) supplemented with 10% fetal bovine serum (FBS) and 1% penicillin/streptomycin.

Two animal coronaviruses were used as surrogates for SARS-CoV-2. Porcine epidemic diarrhea virus (PEDV) strain CV777 (12) was grown on Vero cells (ATCC<sup>®</sup> CCL-81) in MEM (Thermo Fisher Scientific, Waltham, MA, USA) supplemented with 0.3% tryptone phosphate broth, 0.02% yeast extract (12) (adjuvants to culture media cells), 1% penicillin/streptomycin, and 10  $\mu$ g/ml trypsin (13). Infectious bronchitis virus of chicken (IBV) strain Mass 41 (14) was propagated on primary cultures of kidney cells prepared from specific pathogen-free chicken embryos of 19 days of age (14), maintained in BHK-21 medium (Gibco, Cergy-Pontoise, France), supplemented with 0.15% tryptone phosphate broth, 1% penicillin/streptomycin, 1.5% of FBS, and the pH was adjusted to 7.2 with NaHCO<sub>3</sub> (15). Suspensions of IBV and PEDV were prepared in culture medium containing 20% FBS before inoculation onto masks.

Influenza virus titration was performed using the plaque-forming unit (PFU) method adapted from Matrosovich et al. (16). Briefly, six-well cell culture plates were seeded at  $1.0 \times 10^6$  MDCK cells/well. One day later, cells were washed with MEM buffer and infected at 37°C with 400  $\mu$ l of serial dilutions of the sample. Plates were gently shaken every 10 min for 1 h. Then, each well was covered with 3 ml of a mixture of MEM buffer, 1.2% Avicel<sup>®</sup> (Dupont, Copenhagen, Denmark), 1% penicillin/streptomycin, and 1  $\mu$ g/ml of TPCK-Trypsin<sup>®</sup> (Thermo Fisher Scientific). Plates were further incubated at 37°C for 72 h. After two washings in PBS buffer, cell layers were stained with a solution containing 10% crystal violet oxalate, 10% formaldehyde, and 20% ethanol, and plaques were counted. Viral titers were finally expressed as PFU/ml. Animal PEDV and IBV coronaviruses were titrated according to Reed and Muench (17), and virus titers were expressed as TCID<sub>50</sub>/ml (50% tissue culture infective dose per milliliter), as calculated based on immunoperoxidase monolayer assay on Vero cells (PEDV) or

immunofluorescent assay on primary chicken kidney cells (IBV) (18), using pathogen-specific pig and chicken anti-sera.

## Dry- and Moist-Air Heating Treatment Procedures

The surgical masks and FFP2 respirators were inserted into ISO11607-certified sterilization bags (NF EN 868-5, Amcor, Zürich, Switzerland) and submitted to different heat treatments based on either single usual runs (70°C–15 min, 70°C–60 min, 90°C–3 h, 100°C for 60 min, or 120°C–10 min) in the tumble-drying machine (Kannegiesser<sup>®</sup>, Nanterre, France) with rotation but without detergent or single transit [70°C–1 h no humidity or 70°C–1 h with 75% humidity rate (HR)] in an HPP260<sup>®</sup> constant climate chamber (Mettler GmbH, Schwabach, Germany). For the coronavirus experiments, the experimentally contaminated protective masks were inserted into a Binder KBF115<sup>®</sup> climate chamber (Binder GmbH, Tuttlingen, Germany) and submitted to a single heat treatment of 70°C–1 h—with 75% HR.

## Assessment of the Structural and Chemical Integrity

After the heating treatment, surgical masks and FFP2 respirators underwent successive evaluations that were carried out as GO/NO GO steps in order to ensure the preservation of their integrity and their function (**Supplementary Figure 1**). For GO/NO GO Step 1, unused surgical masks, and FFP2 respirators were thoroughly observed for obvious changes in physical appearance (color, shape, and size), and their ultrastructure was compared to untreated masks using scanning electron microscopy [(SEM) Ultra Plus<sup>®</sup> FEG, Zeiss, Oberkochen, Germany]. For such a purpose, mask layers were first coated with 40-Å platinum using a PECS 682<sup>®</sup> apparatus (Gatan, Pleasanton, CA, USA).

At the molecular level, modifications of the treated (unused) surgical masks and FFP2 respirators were evaluated by Fourier-transform infrared spectroscopy equipped with single-reflection diamond attenuated total reflectance (ATR) accessory (i.e., Vertex 70v FT-IR<sup>®</sup> spectrometer, Bruker, Billerica, MA, USA) with a Golden Gate<sup>®</sup> (Specac, Orpington, United Kingdom): acquisition was recorded between 4,000 and 600  $\text{cm}^{-1}$ , with a resolution of 4  $\text{cm}^{-1}$  and 64 scan repetitions. Volatile molecules trapped in the film were identified by thermal desorption (TD) through a TD 350<sup>®</sup> thermo-desorber (PerkinElmer, Courtaboeuf, France) coupled to a GC-6890<sup>®</sup> gas chromatography (GC) associated with a MS5973N<sup>®</sup> mass spectrometer [(MS) Agilent, Les Ulis, France] under TD conditions at 140°C and under helium for 10 min (19). Only the treatment conditions that allowed correct preservation of the masks integrity were kept for further assessments described below.

## Assessment of the Decontamination Yield

For GO/NO GO Step 2 (**Supplementary Figure 1**), 50  $\mu$ l of each pathogen suspension were deposited onto a delimited area of protective surgical masks and FFP2 respirators on either the inner or the outer lining. Then, the masks were incubated at 37°C

for 1 h to dry the pathogen suspension and further submitted to dry-air or moist-air heating treatments, as described above. Control masks (with deposition of bacteria or virus suspension, but no heating treatment) were stored at 4–6°C for the same duration. Thereafter, all the afore-delimited areas were cut out, placed into 2-ml sterile water or culture medium (when loaded with either bacteria or viruses, respectively, in order to resuspend the residual pathogens), and then mixed. Next, the suspensions were diluted and analyzed as described above for titration. Since the relative extraction rates from the FFP2 respirator fibers were estimated at 22 and 15% for bacteria (*S. aureus*) and virus (influenza A H3N2/Scotland/20/74), respectively, the lower limit of detection (LOD) was thus established at <100 CFU/ml for bacteria and <17 PFU/ml for influenza virus. The extraction rate was 0.06 and 10% for the IBV and PEDV (a 10-fold dilution was necessary to dilute the residual FBS, which interfered with viral isolation). The extraction rates (ratio between infectious titers of initial viral inoculum and virus eluted from masks) were 16.6 and 3% for the PEDV and IBV, respectively. The LOD for the PEDV and IBV re-isolation procedures was determined by 10-fold serial dilutions and was  $10^{1.5}$  TCID<sub>50</sub>/ml for both viruses. The TCID<sub>50</sub> reduction after moist-air heating treatment was calculated to be at least the difference between the infectious titer of eluted virus and the LOD. Only the treatment condition that allowed correct achievement of decontamination yield were kept for further assessments described below.

### Assessment of the Bacterial Filtration

For GO/NO GO Step 3, the evaluation of the filtration efficacy of the surgical masks was performed following the EN 14683:2019 standard (20) (**Supplementary Figure 1**). Briefly, a specimen of the inside surgical mask material was clamped between a six-stage viable Andersen cascade impactor and an aerosol chamber (glass, 445 mm long and 60 mm in external diameter; **Supplementary Figure 2**, left panel). Aerosolization of  $3.0 \pm 0.3$  µm droplets from a 3-ml suspension of *S. aureus* (ATCC 6538) was achieved by the E-Flow® mesh nebulizer (Pari GmbH, Starnberg, Germany) to maintain a bacterial challenge ( $2,200 \pm 500$  CFU per test) during a 1-min nebulization. Each test specimen was conditioned at  $21 \pm 5^\circ\text{C}$  and  $85 \pm 5\%$  HR for the time required to bring them into equilibrium with atmosphere prior to testing. Finally, the filtration efficiency of the masks was expressed as a percentage of the CFU initially present in the challenge aerosol that passed through the material.

### Assessment of the Viral Filtration

For the rest of GO/NO GO Step 3 (**Supplementary Figure 1**), aerosolization of a suspension at  $3.5 \times 10^7$  PFU/ml influenza A H3N2/Scotland/20/74 virus strain was achieved by the Aerogen Solo® mesh nebulizer (Aerogen, Galway, Ireland) (21) and using the experimental setup described in **Supplementary Figure 2** (right panel). The size of the droplets ( $3.6 \pm 0.1$  µm) was similar to the EN 14683:2019 standard that is dedicated to the assessment of medical devices for usage against respiratory pathogens. After nebulization, the virus was collected in a BioSampler® device (SKC, Eighty Four, PA, USA) filled with 5 ml of MEM buffer, and the percentage of viral particles passing through the masks was

determined by virus titration as aforementioned. Considering the experimental setting, the LOD for filtration was estimated at 2.5 PFU/ml.

### Measurement of the Inspiratory Resistance

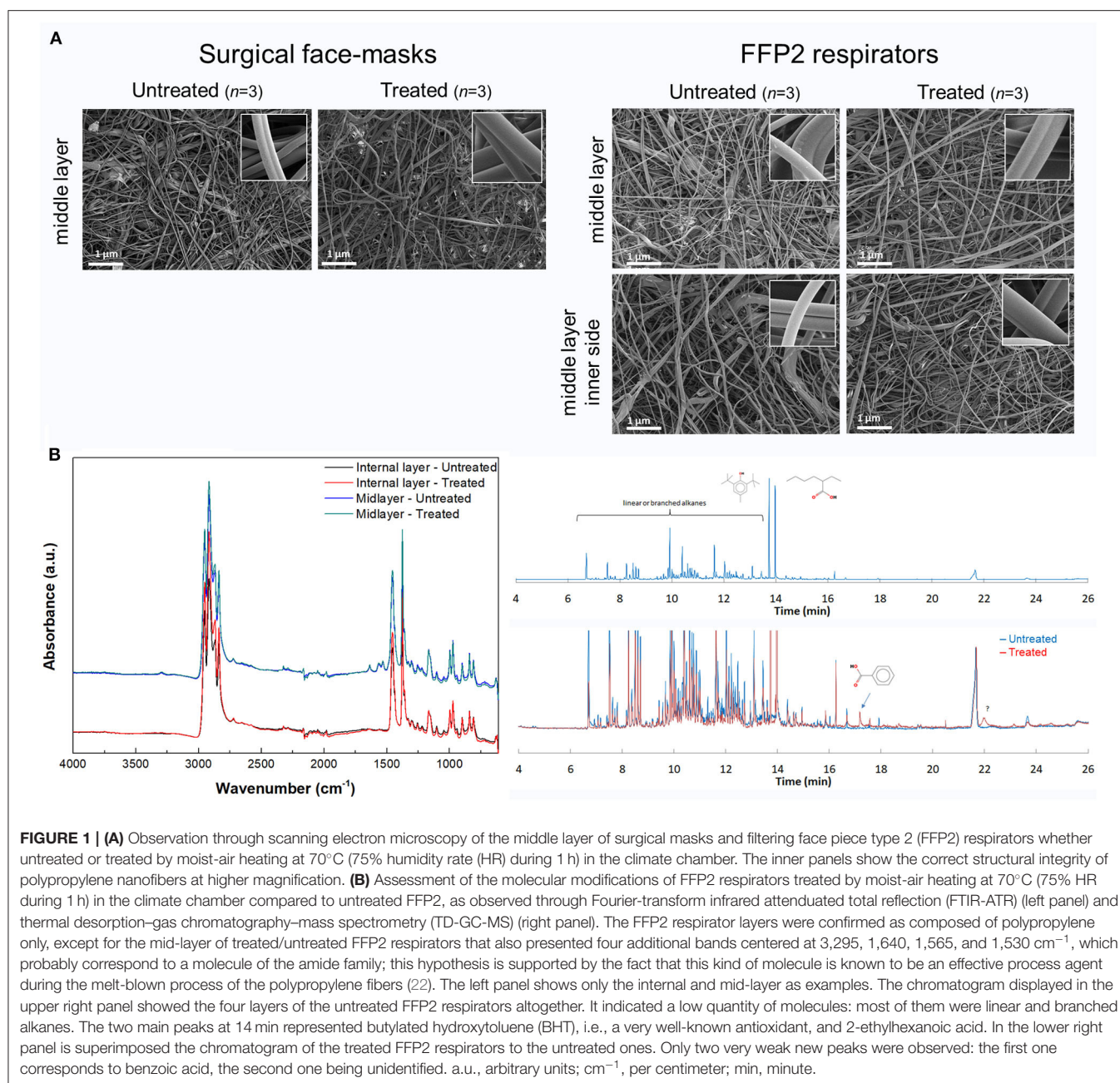
For GO/NO GO Step 3 bis., an original mounting using a 4000 series® digital flow meter (TSI, Marseille, France) was exploited for measuring the inspiratory resistance of the surgical masks and FFP2 respirators before and after treatments (**Supplementary Figure 3**). Two pressure gauges (Magnehelic 2000-0®, Dwyer Instruments, Suresnes, France) continuously controlled the pressure differential between the flow meter and the pump. Different inspiratory flow rates were tested from 15 to 60 L/min. The difference in inspiratory resistance of heat-treated masks compared to control masks was expressed in Pascal (Pa) per square centimeter.

## RESULTS

The global design of the study is summarized in **Supplementary Figure 1**. Following the runs in the tumble-drying machine, only the treatment condition at 70°C during 15 or 60 min allowed complete preservation of the global structure and the integrity of the surgical masks and FFP2 respirator nanofibers. In contrast, longer or hotter processes were deleterious for the quality, with slight or rough obvious destruction. After one 60-min cycle in the climate chamber at 70°C and 75% HR, no macro- or micro-alterations were observed (**Figure 1A**). Contrary to the autoclaving process, the surgical masks and FFP2 respirators were not wet in such a condition (GO/NO GO Step 1, positively checked). The same finding was observed after 3–5 iterative cycles of moist heating (data not shown). After moist-air heating treatment, there was no proof of (oxidization-based or chemical) alteration at the molecular level (**Figure 1B**) of any layer of the surgical masks and FFP2 respirators. This was also the case for the elastic rubber band (not shown). Besides, the mask layers were confirmed as composed of polypropylene only, except for the mid-layer of treated/untreated surgical masks and FFP2 respirators that also presented four additional bands centered at 3,300, 1,642, 1,564, and 723 cm<sup>-1</sup> and 3,295, 1,640, 1,565, and 1,530 cm<sup>-1</sup>, respectively, which probably correspond to a molecule of the amide family. TD-GC-MS chromatogram indicated that two new molecules were trapped in the treated FFP2 respirators (in comparison with untreated respirators): they actually corresponded to benzoic acid and an unidentified compound (**Figure 1B**). Nevertheless, their respective signal intensities were so weak that no one could conclude to significant modification of any of the four layers of the FFP2 respirators. The same comment applied to the elastic rubber bands (not shown). Altogether, only the treatment conditions with dry-air heating at 70°C for 15–60 min and moist-air heating at 70°C for 1 h were thus kept for further investigations (**Supplementary Figure 1**).

Decontamination assay showed the inability of dry-air heating (70°C, 15 or 60 min) to drastically reduce the number of bacteria and the virus titers (by 0 to  $-1.0 \log_{10}$  only; data not shown). In

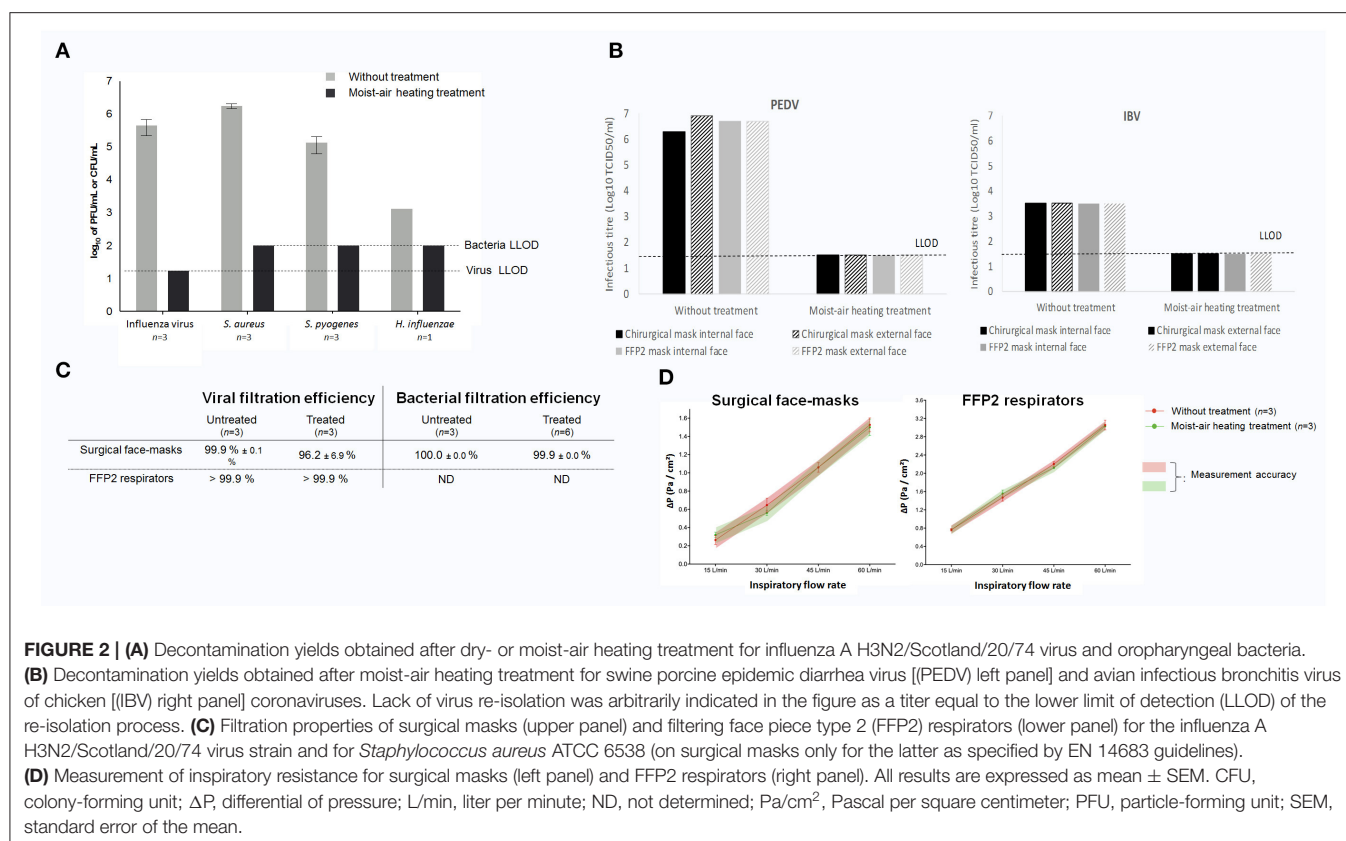




contrast, moist-air heating in climate chamber (70°C, 75% HR for 60 min) resulted in a remarkable decrease of oropharyngeal pathogens and influenza virus (GO/NO GO Step 2, positively checked):  $-6.0 \log_{10}$  for *S. aureus*,  $-5.0 \log_{10}$  for *S. pyogenes*,  $-3.0 \log_{10}$  for *H. influenza*, and  $-5.5 \log_{10}$  for the influenza A H3N2/Scotland/20/74 virus strain ( $P < 0.05$ ) (Figure 2A), which corresponds to the maximum based on the limit of detection of each assay. The moist heating treatment also allowed inactivation of the two surrogate animal coronaviruses, as evidenced by TCID<sub>50</sub> reductions of at least  $-5 \log_{10}$  and  $-2 \log_{10}$  for PEDV or IBV, respectively, irrespective of the kind of protective masks and mask side (inside/outside linings) tested (Figure 2B). Therefore,

only the moist-air treatment condition (70°C for 60 min with 75% HR) was kept for further analyses.

After treatment in the climate chamber at 70°C during 60 min with 75% HR, the bacterial filtration efficiency of surgical masks for *S. aureus* was assessed at  $100.0 \pm 0.0\%$  for the moist-heated treatment (vs.  $99.9 \pm 0.0\%$  for untreated masks; right panel of Figure 2C, GO/NO GO Step 3, positively checked), following the EN 14683 standard. The viral filtration performances for the influenza virus were  $96.2 \pm 6.9\%$  with the surgical masks and  $>99.9\%$  with the FFP2 respirators (left panel of Figure 2C, GO/NO GO Step 3, positively checked). Noteworthy, filtration of fluorescein, using the same experimental setup, resulted



in 98.9 and 99.9% filtration for surgical masks ( $n = 2$ ) and FFP2 respirators ( $n = 2$ ), respectively (data not shown). The discrepancy between the virus and fluorescein filtration rate for surgical masks was due to the heterogeneous and low viability of the influenza A H3N2/Scotland/20/74 virus during nebulization/collection (data not shown).

Whatever the inspiratory flow, no difference was observed regarding the resistance parameters of control masks and treated ones for both surgical masks and FFP2 respirators (Figure 2D, GO/NO GO Step 3 bis., positively checked).

## DISCUSSION

SARS-CoV-2 is a virus with an outer envelope, which means that it is theoretically very sensitive to conventional decontamination methods. Few years ago during the H1N1 influenza pandemic, the National Academy of Medicine (formerly known as Institute of Medicine, USA) already suggested that simple decontamination techniques [e.g., bleach, ethylene oxide, ultraviolet (UV) germicidal irradiation, hydrogen peroxide gas, microwave oven irradiation, etc. (8, 23)] should be deeply investigated in an effort to extend the service life of protective masks (24). Unfortunately, many processes showed that either the structural integrity or the filtration performance of such treated mask could be drastically altered following multiple exposure to aerosols, chemicals, and extreme temperature (25). Furthermore, inappropriate decontamination may be a

potential risk of infection since recycled surgical masks and N95/FFP2 respirators may become a reservoir for pathogens (26). For instance, UV treatment was found to destroy the outer polypropylene nanofibers. Likewise, dry heating  $\geq 160^\circ\text{C}$ , as well as 70% isopropyl alcohol spraying, caused significant filter degradation (8). Gamma irradiation with 20 kGy (2 Mrad) was demonstrated as sufficient for inactivating the viruses, but studies showed possible deformation of the masks, compromising the inner filtering layer of N95/FFP2 respirators and also the correct mask fitting on the face (9). However, in light of the current sanitary emergency, the Atlanta Centers for Disease Control and Prevention (CDC) recently provided guidelines for “crisis alternate strategies,” including the use of improvised homemade or treated masks (27). Thanks to several national task forces, comprising both academic laboratories and private companies, evaluating the reuse of surgical masks and N95/FFP2 respirators, promising decontamination processes have emerged during the COVID-19 sanitary crisis. One of the most advanced is hydrogen peroxide vapor, already applied in a clinical setting in the USA, and showing decontamination and maintenance of post-decontamination performances on N95 respirators (28). Hopefully, wearers will not suffer discomfort due to residual hydrogen peroxide odor, as previously described (29).

Tumble-drying machines are cosmopolitan equipment, which is commonly used at home or in the hospital for laundry. They offer the possibility to heat at  $70^\circ\text{C}$ —a temperature

reported to *in vitro* inactivate the SARS-CoV-2 by decreasing its TCID<sub>50</sub> titer in Vero-E6 cells from 6.8 log<sub>10</sub> to undetectable level after 5 min of exposure—or higher temperatures (10). In the past, such hot-air drying processes already showed good decontamination performance for reducing the bacteria and virus burden (30, 31), but only at  $\geq 92^{\circ}\text{C}$  (32). Unfortunately, in the present study, we evidenced that dry-air heating in the tumble machine failed to reach satisfying decontamination yields and even generated sometimes degradation of the material with exposure to moderate to extreme hot temperatures  $>70^{\circ}\text{C}$  and/or the mechanical frictions inside the machine. In contrast, and as suggested by preliminary studies (33, 34), we showed herein that a unique step of moist-air heating at  $70^{\circ}\text{C}$  during 1 h in climate chamber, with 75% HR, was efficient on relevant surrogate viruses of SARS-CoV-2. Overall, our findings showed that this treatment did not generate an alteration of the surgical masks and FFP2 respirators at the structural and molecular levels, while it ensured effective bacterial/viral decontamination and allowed conservation of their filtration efficiency and resistance performances. Interestingly, the masks were not wet after climate chamber decontamination (contrary to autoclaving), avoiding an additional drying step that may be deleterious.

To date, climate chambers are mostly reserved to hospital pharmacies or pharmaceutical companies. They enable traceable control of the temperatures, and they can provide 3–80% HR inside. One could easily imagine the feasibility of implementing and defining a logical circuit for recycling the protective surgical masks and N95/FFP2 respirators and then ensuring their return to their first user—a critical item to be considered to ensure acceptability of reuse.

Through the aforementioned method, one can say that we have totally fulfilled the conditions recommended by The Center for Infectious Disease Research and Policy of Minnesota University, which states that, in the case of a pandemic, an acceptable decontamination method must render the organism (or a closely related surrogate) nonviable and not diminish filter and fit performance, respirator integrity and structure, or comfort, odor, and wears. Moreover, the moist heating treatment has also been recently included in pandemic crisis standards of care decontamination recommendations by the Atlanta CDC based on previous studies showing efficient decontamination of closely related virus surrogates (H1N1 virus) (33). One limitation of our study lies in the fact that only one brand of FFP2 respirators has been tested for the preservation of its filtration properties through recycling treatment. Moreover, our experimental procedures deviated slightly from the standards NF EN 149+A1 (FFP2)/NF EN 14683+AC recommendations for assessing the filtering performance and the inspiratory resistance of untreated and treated protective masks (35). Therefore, further investigations in line with the standard guidelines are required, in addition to ones using the actual SARS-CoV-2 instead of animal surrogate viruses. Another limitation lies in the approach of our demonstration that was carried out on the bench only: most surgical masks and FFP2 respirators tested herein had never been worn by nursing staff [noteworthy, a few pre-used masks were nonetheless moist heating treated and then tested; they exhibited

neither difference in the SEM morphology nor in resistance at inspiratory flow (data not shown)]. In practice, further assessment in real life seems necessary to specifically address the saturation of filters with saliva/expectoration. Moreover, an evaluation of the impact of multiple treatment cycles seems required. However, other previous assays showed sustainment of all the face mask properties at the sealing surface up to 10 iterative treatment cycles based on moist-air heating (36), and our preliminary data herein did not show any negative impact for three to five cycles on structural integrity, altogether supporting the rationale for our approach.

## CONCLUSIONS

### Major Finding

Overall, our findings may pave the way in healthcare facilities for the reutilization of decontaminated, intact protective masks. Our study supports this straightforward strategy to circumvent surgical masks and N95/FFP2 respirators mass shortage, especially during the current COVID-19 pandemic.

### Perspectives

Should our recycling process be extended to other brands of surgical masks and N95/FFP2 respirators and thus be validated in the future by (inter-)national and sanitary authorities, mask decontamination could be recommended in hospital laundries and laboratories equipped with the adequate heat equipment.

## DATA AVAILABILITY STATEMENT

The raw data supporting the conclusions of this article will be made available by the authors, without undue reservation.

## AUTHOR CONTRIBUTIONS

All authors have seen and approved the manuscript. They all contributed significantly to the work. LB, GD, LV, AG, PL, PR, MS-T, and NH-V conceived the ideas. EB-M, JPa, LA, DB, SEy, P-IR, VV, JPo, PV, LM, SEs, MF, NE, YB, LB, PB, PR, and NH-V collected the data. SEs, JPo, NE, NH-V, MS-T, GD, J-PA, and PC contributed to the organization of the tests. GD, LB, EB-M, MF, JPo, PR, MS-T, and NH-V led the writing. The manuscript has not been previously published nor being considered for publication elsewhere.

## ACKNOWLEDGMENTS

The authors are thankful to all the staff for their technical/scientific contribution in the study: Véronique Dennion-Delattre for Tours University Hospital, Yoann Montigaud, Lara Leclerc, Coralie Laurent, and Gwendoline Sarry for Les Mines Saint-Etienne, Estelle Audoux and Amelie Prier for Saint-Etienne university, Béatrice Grasland, Lionel Bigault, Hélène Quenault, Evelyne Lemaître, and Chantal Allée for Anses, Floriane Carpentier for the CEA. The Anses team thanks Prof. J.L. Lanoisellé (Institut de Recherche Dupuy De



Lôme, Pontivy, France) for kindly allowing access to the Institute climatic chamber. The authors thank the REACTing consortium and the APAVE. This work is part of a French task force initiated by CNRS and CEA, involving several research organisms and industrial partners.

## REFERENCES

- van Doremalen N, Bushmaker T, Morris DH, Holbrook MG, Gamble A, Williamson BN, et al. Aerosol and surface stability of SARS-CoV-2 as compared with SARS-CoV-1. *N Engl J Med.* (2020) 382:1564–7. doi: 10.1101/2020.03.09.20033217
- Chen Y-C, Huang L-M, Chan C-C, Su C-P, Chang S-C, Chang Y-Y, et al. SARS in hospital emergency room. *Emerg Infect Dis.* (2004) 10:782–8. doi: 10.3201/eid1005.030579
- Liu Y, Ning Z, Chen Y, Guo M, Liu Y, Gali NK, et al. Aerodynamic analysis of SARS-CoV-2 in two Wuhan hospitals. *Nature.* (2020) 582:557–60. doi: 10.1101/2020.03.08.982637
- Klompas M, Morris CA, Sinclair J, Pearson M, Shenoy ES. Universal masking in hospitals in the Covid-19 era. *N Engl J Med.* (2020) 382:e63. doi: 10.1056/NEJMp2006372
- Rodriguez-Palacios A, Cominelli F, Basson AR, Pizarro TT, Illic S. Textile masks and surface covers-A spray simulation method and a “universal droplet reduction model” against respiratory pandemics. *Front Med.* (2020) 7:260. doi: 10.3389/fmed.2020.00260
- Fang J, Zhang L, Sutton D, Wang X, Lin T. Needleless melt-electrospinning of polypropylene nanofibres. *J Nanomater.* (2012) 2012:e382639. doi: 10.1155/2012/382639
- CAB\_Solidarites, CAB\_Solidarites. *COVID-19 : Stratégie de Gestion et D'utilisation des Masques de Protection.* Ministère des Solidarités et de la Santé (2020). Available online at: <http://solidarites-sante.gouv.fr/actualites/presse/communiqués-de-presse/article/covid-19-strategie-de-gestion-et-d-utilisation-des-masques-de-protection> (Accessed March 23, 2020).
- Viscusi D, King W, Shaffer R. Effect of decontamination on the filtration efficiency of two filtering facepiece respirator models. *J Int Soc Respir Prot.* (2007) 24:93–107.
- Feldmann F, Shupert WL, Haddock E, Twardoski B, Feldmann H. Gamma irradiation as an effective method for inactivation of emerging viral pathogens. *Am J Trop Med Hyg.* (2019) 100:1275–7. doi: 10.4269/ajtmh.18-0937
- Chin A, Chu J, Perera M, Hui K, Yen H-L, Chan M, et al. Stability of SARS-CoV-2 in different environmental conditions. *Lancet Microbe.* (2020) 1:e10. doi: 10.1101/2020.03.15.20036673
- Guillot L, Le Goffic R, Bloch S, Escriviou N, Akira S, Chignard M, et al. Involvement of toll-like receptor 3 in the immune response of lung epithelial cells to double-stranded RNA and influenza A virus. *J Biol Chem.* (2005) 280:5571–80. doi: 10.1074/jbc.M410592200
- Pensaert MB, de Bouck P. A new coronavirus-like particle associated with diarrhea in swine. *Arch Virol.* (1978) 58:243–7. doi: 10.1007/BF01317606
- Strandbygaard B, Lavazza A, Lelli D, Blanchard Y, Grasland B, Poder SL, et al. Inter-laboratory study to characterize the detection of serum antibodies against porcine epidemic diarrhoea virus. *Vet Microbiol.* (2016) 197:151–60. doi: 10.1016/j.vetmic.2016.11.020
- Picault JP, Drouin P, Guittet M, Bennejean G, Protas J, L'Hospitalier R, et al. Isolation, characterisation and preliminary cross-protection studies with a new pathogenic avian infectious bronchitis virus (Strain PL-84084). *Avian Pathol.* (1986) 15:367–83. doi: 10.1080/03079458608436300
- Hopkins SR. Serological comparisons of strains of infectious bronchitis virus using plaque-purified isolants. *Avian Dis.* (1974) 18:231–9. doi: 10.2307/1589131
- Matrosovich M, Matrosovich T, Garten W, Klenk H-D. New low-viscosity overlay medium for viral plaque assays. *Virol J.* (2006) 3:63. doi: 10.1186/1743-422X-3-63
- Reed LJ, Muench H. A simple method of estimating fifty per cent endpoints. *Am J Epidemiol.* (1938) 27:493–7. doi: 10.1093/oxfordjournals.aje.a118408
- Grasland B, Loizel C, Blanchard P, Oger A, Nignol A-C, Bigarré L, et al. Reproduction of PMWS in immunostimulated SPF piglets transfected with infectious cloned genomic DNA of type 2 porcine circovirus. *Vet Res.* (2005) 36:685–97. doi: 10.1051/vetres:2005024
- Buchalla R, Boess C, Bögl KW. Characterization of volatile radiolysis products in radiation-sterilized plastics by thermal desorption-gas chromatography-mass spectrometry: screening of six medical polymers. *Radiat Phys Chem.* (1999) 56:353–67. doi: 10.1016/S0969-806X(99)00311-4
- Allegra S, Riffard S, Leclerc L, Girardot F, Stauffert M, Forest V, et al. A valuable experimental setup to model exposure to Legionella's aerosols generated by shower-like systems. *Water Res.* (2020) 172:115496. doi: 10.1016/j.watres.2020.115496
- Bowling JD, O'Malley KJ, Klimstra WB, Hartman AL, Reed DS. A vibrating mesh nebulizer as an alternative to the collision three-jet nebulizer for infectious disease aerobiology. *Appl Environ Microbiol.* (2019) 85:e00747–19. doi: 10.1128/AEM.00747-19
- US Patent for Charge Stabilized Electret Filter Media Patent (Patent # 5,645,627 issued July 8, 1997) - Justia Patents Search. Available online at: <https://patents.justia.com/patent/5645627> (Accessed April 22, 2020).
- Vo E, Rengasamy S, Shaffer R. Development of a test system to evaluate procedures for decontamination of respirators containing viral droplets. *Appl Environ Microbiol.* (2009) 75:7303–9. doi: 10.1128/AEM.0799-09
- Institute of Medicine. *Reusability of Facemasks during an Influenza Pandemic: Facing the Flu.* Washington, DC: The National Academies Press (2006).
- Martin SB, Moyer ES. Electrostatic respirator filter media: filter efficiency and most penetrating particle size effects. *Appl Occup Environ Hyg.* (2000) 15:609–17. doi: 10.1080/10473220050075617
- Coulliette AD, Perry KA, Edwards JR, Noble-Wang JA. Persistence of the 2009 pandemic influenza A (H1N1) virus on N95 respirators. *Appl Environ Microbiol.* (2013) 79:2148–55. doi: 10.1128/AEM.03850-12
- CDC. *Coronavirus Disease 2019 (COVID-19).* Centers for Disease Control and Prevention (2020). Available online at: <https://www.cdc.gov/coronavirus/2019-ncov/hcp/ppe-strategy/face-masks.html> (Accessed April 3, 2020).
- Staff RT. *Duke: How to Decontaminate N95 Masks for Reuse* | RT. RT: For Decision Makers in Respiratory Care (2020) Available online at: <https://www.rtmagazine.com/public-health/healthcare-policy/occupational-health/duke-how-to-decontaminate-n95-respirators-for-reuse/> (Accessed May 19, 2020).
- Viscusi DJ, Bergman MS, Novak DA, Faulkner KA, Palmiero A, Powell J, et al. Impact of three biological decontamination methods on filtering facepiece respirator fit, odor, comfort, and donning ease. *J Occup Environ Hyg.* (2011) 8:426–36. doi: 10.1080/15459624.2011.585927
- Ansari SA, Springthorpe VS, Sattar SA, Tostowaryk W, Wells GA. Comparison of cloth, paper, and warm air drying in eliminating viruses and bacteria from washed hands. *Am J Infect Control.* (1991) 19:243–9. doi: 10.1016/S0196-6553(05)80256-1
- Tano E, Melhus A. Level of decontamination after washing textiles at 60°C or 70°C followed by tumble drying. *Infect Ecol Epidemiol.* (2014) 4:24314. doi: 10.3402/iee.v4.24314
- Pastorino B, Touret F, Gilles M, Lamballerie X de, Charrel RN. Prolonged infectivity of SARS-CoV-2 in fomites. *Emerg Infect Dis.* (2020) 26:2256–7. doi: 10.1101/2020.04.11.036855
- Heimbuch BK, Wallace WH, Kinney K, Lumley AE, Wu C-Y, Woo M-H, et al. A pandemic influenza preparedness study: use of energetic methods to decontaminate filtering facepiece respirators contaminated

## SUPPLEMENTARY MATERIAL

The Supplementary Material for this article can be found online at: <https://www.frontiersin.org/articles/10.3389/fmed.2020.584036/full#supplementary-material>

- with H1N1 aerosols and droplets. *Am J Infect Control*. (2011) 39:e1–9. doi: 10.1016/j.ajic.2010.07.004
34. Lore MB, Heimbuch BK, Brown TL, Wander JD, Hinrichs SH. Effectiveness of three decontamination treatments against influenza virus applied to filtering facepiece respirators. *Ann Occup Hyg*. (2012) 56:92–101. doi: 10.1093/annhyg/mer054
  35. BS EN 149:2001+A1:2009 - Juin 2001. Available online at: [https://www.boutique.afnor.org/norme/bs-en-1492001a12009/appareils-de-protection-respiratoire-demi-masques-filtrants-contre-les-particules-exigences-essais-marquage/article/668354/eu089165?gclid=EAIaIQobChMivJW69-Sw6AIVDtTeCh3aLwBYEAAAYASAAEgIT3vD\\_BwE](https://www.boutique.afnor.org/norme/bs-en-1492001a12009/appareils-de-protection-respiratoire-demi-masques-filtrants-contre-les-particules-exigences-essais-marquage/article/668354/eu089165?gclid=EAIaIQobChMivJW69-Sw6AIVDtTeCh3aLwBYEAAAYASAAEgIT3vD_BwE) (Accessed March 23, 2020).
  36. Fischer R, Morris DH, Doremalen N van, Sarchette S, Matson J, Bushmaker T, et al. Effectiveness of N95 Respirator Decontamination and Reuse against SARS-CoV-2 Virus. *Emerg Infect Dis*. (2020) 26:2253–5. doi: 10.31219/osf.io/phcsb

**Conflict of Interest:** NH-V has previously had a research contract with Aerogen.

The remaining authors declare that the research was conducted in the absence of any commercial or financial relationships that could be construed as a potential conflict of interest.

Copyright © 2020 Bernard, Desoubeaux, Bodier-Montagutelli, Pardessus, Brea, Allimonier, Eymieux, Raynal, Vasseur, Vecellio, Mathé, Guillon, Lanotte, Pourchez, Verhoeven, Esnouf, Ferry, Etteradossi, Blanchard, Brown, Roingeard, Alcaraz, Cinquin, Si-Tahar and Heuzé-Vourc'h. This is an open-access article distributed under the terms of the Creative Commons Attribution License (CC BY). The use, distribution or reproduction in other forums is permitted, provided the original author(s) and the copyright owner(s) are credited and that the original publication in this journal is cited, in accordance with accepted academic practice. No use, distribution or reproduction is permitted which does not comply with these terms.



## OPEN ACCESS

### Edited by:

Stephen Allen Morse,  
Centers for Disease Control and  
Prevention (CDC), United States

### Reviewed by:

Raymond Whiting Nims,  
RMC Pharmaceutical Solutions, Inc.,  
United States  
Dana Mitzel,  
Agricultural Research Service,  
United States

### \*Correspondence:

Tony L. Buhr  
tony.buhr@navy.mil

### Specialty section:

This article was submitted to  
Biosafety and Biosecurity,  
a section of the journal  
Frontiers in Bioengineering and  
Biotechnology

**Received:** 07 August 2020

**Accepted:** 17 September 2020

**Published:** 23 October 2020

### Citation:

Buhr TL, Young AA,  
Borgers-Klonkowski E, Kennihan NL,  
Barnette HK, Minter ZA, Bohmke MD,  
Osborn EB, Hamilton SM, Kimani MB,  
Hammon MW, Miller CT, Mackie RS,  
Innocenti JM, Bensman MD,  
Gutting BW, Lilly SD, Hammer EE,  
Yates VL and Luck BB (2020) Hot,  
Humid Air Decontamination of Aircraft  
Confirmed That High Temperature and  
High Humidity Are Critical for  
Inactivation of Infectious, Enveloped  
Ribonucleic Acid (RNA) Virus.  
Front. Bioeng. Biotechnol. 8:592621.  
doi: 10.3389/fbioe.2020.592621

# Hot, Humid Air Decontamination of Aircraft Confirmed That High Temperature and High Humidity Are Critical for Inactivation of Infectious, Enveloped Ribonucleic Acid (RNA) Virus

Tony L. Buhr\*, Alice A. Young, Erica Borgers-Klonkowski, Neil L. Kennihan, Harold K. Barnette, Zachary A. Minter, Matthew D. Bohmke, Emily B. Osborn, Shelia M. Hamilton, Monique B. Kimani, Mark W. Hammon, Charles T. Miller, Ryan S. Mackie, Jennifer M. Innocenti, Misty D. Bensman, Bradford W. Gutting, Samuel D. Lilly, Emllyn E. Hammer, Vanessa L. Yates and Brooke B. Luck

Naval Surface Warfare Center-Dahlgren Division, Concepts and Experimentation Branch (B64), Dahlgren, VA, United States

**Aims:** To develop infectious (live/dead) enveloped virus test indicators and response surface methodology (RSM) models that evaluate survival of an enveloped ribonucleic acid (RNA) virus on contaminated aircraft materials after exposure to hot, humid air (HHA).

**Methods and Results:** Enveloped RNA bacteriophage Phi6 ( $\Phi 6$ ) was dried on wiring insulation, aircraft performance coating (APC), polypropylene, and nylon at  $\geq 8 \log_{10}$  plaque-forming units (PFU) test coupon<sup>-1</sup>. Only 2.4  $\log_{10}$  inactivation was measured on APC at 70°Celsius (°C), 5% relative humidity (RH) after 24 h. In contrast, HHA RSM models showed a 90% probability of a 7  $\log_{10}$  inactivation at  $\geq 63^\circ\text{C}$ , 90% RH after 1 h, and decontamination kinetics were similar across different materials. HHA decontamination of C-130 and C-17 aircraft showed  $>7 \log_{10}$  and  $\geq 5.9 \log_{10}$  inactivation of enveloped virus on 100 and 110 test indicators, respectively, with a 1-h treatment, excluding ramp-up and ramp-down times.

**Conclusions:** Enveloped RNA virus test indicators were successfully developed, lab tested for HHA decontamination, analyzed for RSM, and field-tested in aircraft demonstrations.

**Significance and Impact of the Study:** The utility of HHA decontamination was demonstrated after inactivating enveloped RNA virus on aircraft with a 1-h HHA treatment within aircraft temperature and RH limits.

**Keywords:**  $\Phi 6$ , enveloped virus, decontamination, hot humid air, aircraft

## INTRODUCTION

There is a need to develop aircraft decontamination procedures for enveloped RNA viruses ranging from hemorrhagic fever viruses to coronaviruses (Centers for Disease Control Prevention, 2019; National Business Aviation Association, 2020). A candidate procedure for aircraft decontamination is hot, humid air (HHA), which has been tested for *Bacillus* spore decontamination (Buhr et al., 2012, 2015, 2016). HHA decontamination is highly feasible for enveloped virus decontamination since enveloped viruses are considered much easier to kill than spores (Spaulding, 1957). In order to develop HHA decontamination profiles and test in aircraft field demonstrations, a biosafety level 1 (BSL-1) enveloped RNA virus was needed as a test indicator to meet the requirements imposed by biosafety and environmental reviews for field testing. Field test approval is a lengthy process that can require decades of compiled research to approve BSL-1 organisms for field testing, regardless of whether the organism is contained or released during the test (Bishop and Robinson, 2014; Buhr et al., 2016). It is particularly challenging to justify and approve enveloped virus strains for rapid field testing (2 months for biosafety approval at different facilities, enveloped virus test indicator preparation, and 2 aircraft field tests including results) during a pandemic such as the SARS-CoV-2/COVID-19 pandemic. Furthermore, active, infectious virus was needed for a live/dead (infectious/non-infectious for viruses) assay since live/dead assays are the hallmark of decontamination testing.

Φ6 is a BSL-1 enveloped RNA virus originally isolated in a bean field as a lytic virus that infected the plant pathogenic bacterium *Pseudomonas syringae* pathovar *phaseolicola* (Vidaver et al., 1973; Van Etten et al., 1976; Mindich, 2004). Early hopes to produce the virus in large quantities to spray on bean fields as an environmentally friendly biocontrol agent were never commercially realized. However, due to its rare combination as a BSL-1, enveloped RNA virus it has been proposed as a general surrogate for a number of different enveloped RNA viruses particularly for field testing (Gallandat and Lantagne, 2017). The Φ6 envelope structure is similar to many other enveloped viruses as the envelope consists of a glycoprotein/protein-embedded lipid membrane, and the host cell has similar temperature sensitivity to mammalian cells at around 40°C. This is important since the envelope components are considered a primary target for inactivation by many different decontaminants (McDonnell and Burke, 2011; Wiggington et al., 2012). Here Φ6 was prepared to develop BSL-1 enveloped virus test indicators at  $\geq 7.6 \log_{10}$  coupon<sup>-1</sup>, test HHA decontamination parameters, develop response surface models for HHA decontamination, and measure enveloped virus inactivation during C-130 and C-17 aircraft field tests.

**Abbreviations:** RSM, response surface methodology; HHA, hot humid air; APC, aircraft performance coating; PFU, plaque-forming units; RH, relative humidity; HB010Y, *P. syringae* pathovar *phaseolicola*; TSA, tryptic soy agar; TSB, tryptic soy broth; HEPES, 4-(2-hydroxyethyl)-1-piperazineethanesulfonic acid; DOE, design of experiment; NTC, naval topcoat; SF, survival fraction; GMSE, geometric mean survival fraction; GSD, geometric standard deviation; TPP®, Techno plastic products.

## MATERIALS AND METHODS

### Φ6 and Host Cell Preparations

Φ6 and its host organism *P. syringae* pathovar *phaseolicola* HB10Y (HB10Y), causal agent of halo blight of the common bean, *Phaseolus vulgaris*, were isolated in Spain. Both were a kind gift from Dr. Leonard Mindich at Rutgers University, New Jersey Medical School. HB10Y was prepared by inoculating 100–200 ml of 3% tryptic soy broth (TSB; Fluka PN#T8907-1KG) in a 1-liter (l) smooth-bottom Erlenmeyer flask with a high efficiency particulate air filter cap. Cultures were incubated at  $26 \pm 2^\circ\text{C}$ , 200 revolutions (rev) minute (min)<sup>-1</sup> for  $20 \pm 2$  hours (h). 11.1 ml of 100% glycerol (Sigma PN #G7757-500ML) was added per 100 ml of host culture. The final concentration of glycerol was 10%. One-ml aliquots of HB10Y were pipetted into screw-cap microfuge tubes with O-rings and stored at  $-80^\circ\text{C}$ . HB10Y samples were titered prior to freezing by serially diluting samples in 10 millimolar (mM) of 4-(2-hydroxyethyl)-1-piperazineethanesulfonic acid (HEPES, Sigma PN#H4034-100G) + 10% Sucrose (Sigma PN #S7903-250G), pH 7.0, and plating on Tryptic Soy Agar (TSA; Hardy Diagnostics, Santa Maria, CA). Plates were inverted and incubated at  $26 \pm 2^\circ\text{C}$  for  $48 \pm 2$  h to show titers of  $\sim 10^9$  cells ml<sup>-1</sup>. After freezing, tubes were thawed at room temperature (RT,  $22 \pm 3^\circ\text{C}$ ), serially diluted, and plated to show sustained viability after long-term storage at  $-80^\circ\text{C}$ .

Φ6 was prepared after inoculating broth cultures of HB10Y. A frozen stock prep of HB10Y was thawed at  $22 \pm 3^\circ\text{C}$ . HB10Y was added either directly from a frozen stock or by transferring a single colony from a streaked TSA plate to 100–200 ml of 3% TSB in a 1-l smooth-bottom Erlenmeyer flask with a HEPA cap and incubated at  $26 \pm 2^\circ\text{C}$ , 200 rev min<sup>-1</sup> overnight. Cells were then diluted and grown to mid-log phase. The host flask was inoculated with 0.5–1 ml of Φ6 at a concentration of  $\sim 1\text{--}2 \times 10^{11}$  plaque-forming units (PFU) ml<sup>-1</sup> at the time of inoculation. The culture was incubated at  $26 \pm 2^\circ\text{C}$ , 200 rev min<sup>-1</sup> for  $24 \pm 2$  h. The Φ6 preparation was stored at  $4^\circ\text{C}$  until after titering was completed. After titer determination was completed, typically around  $1\text{--}2 \times 10^{11}$  PFU ml<sup>-1</sup>, then 1–1.3 ml volumes were aliquoted into 1.5-ml screw-cap tubes with O-rings, inverted, and stored at  $-80^\circ\text{C}$ .

### Environmental Test Chamber Setup and Validation

Thermotron SM-8-8200 (Thermotron Industries, Holland, MI, USA) environmental chambers were used to control temperature and RH as described (Buhr et al., 2015).

### Coupon Materials and Sterilization

Square 2 centimeter (cm) × 2 cm coupons of different test materials or the inside surface of 50-ml Techno Plastic Products AG, Switzerland (TPP®), polypropylene conical tubes were inoculated with  $>8 \log_{10}$  Φ6 virus inoculum. The inoculated 2 cm × 2 cm coupons were set inside sterile TPP® tubes during testing (Buhr et al., 2012, 2015, 2016). Materials for inoculation included aluminum 2024-T3 coupons painted with water-based aircraft performance coating (APC), stainless-steel 304 coupons painted with Navy Top Coat (NTC) [Coatings Group at the



University of Dayton Research Institute (Dayton, OH, USA)], wiring insulation (Kapton Film Type HN, 1 mil, Reference No. 6197844-00 from Cole Parmer, Vernon Hills, IL, USA), and nylon webbing (nylon) (US Netting, Erie, PA, USA) with the ends of each coupon cauterized to prevent fraying. Polypropylene plastic and wiring insulation represent non-porous materials found on commercial and military aircraft. APC and NTC represent semi-porous surfaces found on military aircraft and ships, with APC the primary focus for this testing. Nylon webbing represents porous materials found on military and commercial aircraft since nylon is used to manufacture various carpets and fabrics. Prior to inoculating and testing, coupons were rinsed with 18 mega-Ohm-cm, de-ionized water, placed on absorbent paper in an autoclave-safe container, and autoclaved for 30 min at 121°C, 100 kilopascals. Autoclaved coupons were stored in sterile containers until used. Microbial recovery from autoclaved APC coupons was variable. There was no visible damage, changes in contact angle measurements, or evidence of surface variability on autoclaved APC coupons after inspection with a scanning electron microscope (data not shown). In order to clean and remove interferents such as dried, residual paint solvent, APC coupons were soaked in 70% ethanol for 20 min, rinsed at least 3 times with sterile 18 mega-ohm-cm water, and dried.

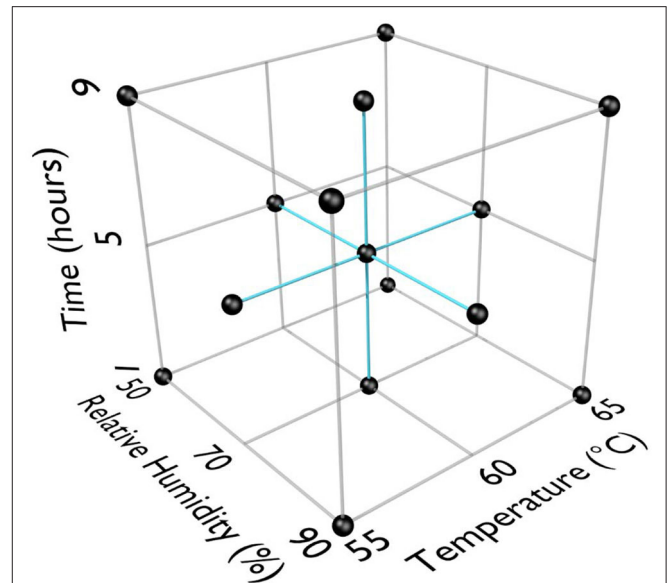
## Response Surface Methodology (RSM)

RSM was used for previous work with HHA decontamination of materials contaminated with spores because the RSM Design of Experiments (DOE) was requested by the funding agencies as an industry-accepted method to describe HHA points of failure (Beauregard et al., 1992; Lenth, 2009; Myers et al., 2009; Buhr et al., 2012, 2015). RSM required three equally spaced test parameters for each variable; time, temperature, and humidity. An extensive amount of trial-and-error testing showed a very rapid and dramatic impact of temperature and RH on virus decontamination. Test temperatures were 55, 60, and 65°C. Test RH was 50, 70, and 90%. Test times were 1, 5, and 9 h to provide a practical timeframe for decontamination of  $\leq 24$  h. RSM DOE test parameters are displayed in **Figure 1**. The first 13 test runs (first iteration) included the center and corners of the experimental test box. The latter 6 test runs (second iteration) included the face-points at the center of each side of the test box.

## Virus Test Method and Design

An overlay procedure used for  $\Phi 6$  was adapted from procedures used for *Escherichia coli* and its bacteriophages using TSA and TSB media instead of Luria-Bertani agar and broth. Plates were incubated at  $26 \pm 2^\circ\text{C}$  for  $20 \pm 2$  h before quantifying plaques. Plates were then incubated another  $24 \pm 2$  h at RT and scored a final time.

$\Phi 6$  stock preps were removed from  $-80^\circ\text{C}$  storage and thawed at RT prior to preparing inoculum by transferring stock  $\Phi 6$  into 50-ml conical tubes containing 10 mM HEPES + 10% sucrose pH 7.0 for a final concentration of  $1\text{--}2 \times 10^9$  PFU  $\text{ml}^{-1}$ . The infectious virus concentration was confirmed by titrating. Test coupons and conical tubes were inoculated with 0.1 ml of  $\Phi 6$  inoculum, held at RT for  $24 \pm 2$  h to dry allowing virus to adhere to the test material, then transferred to TPP<sup>®</sup> tubes. Following



**FIGURE 1** | Response surface methodology (RSM) design of experiments (DOE) for three test factors ( $^\circ\text{C}$ , % relative humidity, time in h).

exposure of  $\Phi 6$  to various hot humid air decontamination testing parameters, samples were extracted and plated.

For  $\Phi 6$  extraction, 5 ml of 10 mM HEPES + 10% sucrose pH 7 were added to each conical tube with a virus-inoculated coupon and vortexed for 2 min. After vortexing, 5 ml of HB10Y log-phase culture was added and allowed to infect at RT for 15 min, followed by 2 min of vortexing. Each sample was serially diluted in 900  $\mu\text{l}$  of 10 mM HEPES + 10% sucrose pH 7 out to the  $-6$  dilution. For each  $\Phi 6$  dilution, 1,000  $\mu\text{l}$  for the first dilution and 200  $\mu\text{l}$  for subsequent dilutions were transferred into individual tubes containing 200  $\mu\text{l}$  log-phase HB10Y. Then, 1,200 or 200  $\mu\text{l}$  of those  $\Phi 6$ /HB10Y mixtures was added to individual TSB overlay tubes, poured onto individual TSA plates, and allowed to solidify for  $\geq 30$  min. Solidified plates were then inverted, incubated for  $20 \pm 2$  h at  $26^\circ\text{C}$ , and quantified. Plates were incubated another 24 h at RT and quantified a final time. Quantitation and calculations of survival were performed as previously described (Buhr et al., 2012, 2014). The maximum (100%) recoverable virus reference, the inoculum titer, was used to calculate extraction efficiency. Extraction efficiency was the number of PFU removed from non-treated control coupons divided by the number of PFU in the inoculum.

## Response Surface Methodology (RSM) Performance Envelopes—Mathematical Model Development

RSM to represent survivability of  $\Phi 6$  bacteriophage were developed. For a given DOE point, sample data varied with respect to initial  $\Phi 6$  bacteriophage population and a final surviving  $\Phi 6$  bacteriophage population. To facilitate model development, the results of the samples were normalized into a Survival Fraction (SF). A SF is simply the surviving population

divided by the initial population. SF is assumed to never be greater than one or less than zero.

The smallest non-zero SF that may be observed is limited due to the initial population being a finite number. Specifically, the smallest observable SF is 1 divided by the initial population. However, if the results reflect that of a 1-ml sample taken from a 10-ml sample (as is true for this data), then the smallest observable SF is 10 divided by the initial population. If extraction efficiency is <100%, then the smallest observable SF becomes 10 divided by the initial population divided by the extraction efficiency. If test data shows a surviving population of zero, it is likely because the theoretical SF is smaller than the smallest observable SF. Because of the limitation imposed by a finite initial population, any test result showing a survival population of zero was treated as a SF that is less than or equal to the smallest observable SF.

The geometric mean survival fraction (GMSF) equation below shows how GMSF was calculated for each DOE point. In Equation 1, “N” represents the number of samples for a given DOE point.

$$GMSF = \left( \prod_{i=1}^N \frac{\text{survival\_count}_i}{\text{initial\_population}_i} \right)^{\frac{1}{N}} \quad (1)$$

All GMSF values from the experiments lie between “0” and “1,” and they differ from each other by orders of magnitude, which can make it difficult to find a good fit to the data. To avoid this problem and to facilitate the data fitting process, it is desirable to transform the widely varying GMSF values such that the transformed values are distributed in a linear fashion. To achieve this, the natural log of the GMSF values was computed. However, this transform still resulted in a very non-linear distribution. A second transform was performed, using Equation 2 below, that flipped the sign of the first transform and then took its natural log. This yielded a more linear distribution of data.

$$GMSF_i^T = \ln(-1 \cdot \ln(GMSF_i)) \quad (2)$$

One benefit of this transform is that it constrains all model predictions to a value between “0” and “1” and thereby prevents a result that contradicts the definition of SF. Data fit exploration focused on obtaining a good fit to the data set of transformed GMSF values. During the data fitting process, a constraint was imposed on the fit such that as temperature and/or RH and/or time increase, SF decreases consistently without exception. The final functional form for predicting GMSF is shown in the system of equations below (Equation 3).

$$f = c_0 + c_1 T + c_2 R + c_3 H + c_4 TR + c_5 TH + c_6 HR + c_7 (T - T_0)^{n_1} (R - R_0)^{n_2} (H - H_0)^{n_3} \\ GMSF = e^{-e^f} \quad (3)$$

Where:

$T$  = temperature (°C),  $R$  = relative humidity (%),  $H$  = time (hours)

$c_0$  to  $c_7$  = addition and multiplication coefficients

$n_1$  to  $n_3$  = power coefficients

$T_0$  = temperature offset coefficient

$R_0$  = relative humidity offset coefficient

$H_0$  = time offset coefficient

$GMSF$  = geometric mean survival fraction.

As is evident in the data, a given exposure condition will result in a distribution of various SF values that can vary geometrically. Because of this geometric variation, it is appropriate to assume the natural log of the survival fractions for a given sample follow a normal distribution for a given exposure condition. An estimate of the expected distribution of results is important because it helps a user identify a probability that an expected total kill will occur for a given exposure condition. For example, a user can utilize the expected distribution to identify the exposure condition required to achieve at least a 7 log<sub>10</sub> kill with a 95% probability.

Most of the exposure DOE points consist of only 5 samples, and this small sample size increases the uncertainty in determining the population geometric standard deviation (GSD) from the sample geometric standard deviation. There was no clear and consistent pattern in the sample geometric standard deviations that would allow for the development of a reasonable equation to predict geometric standard deviation as a function of exposure conditions. However, the DOE center point (Temp = 60, RH = 70, H = 5) consists of 25 samples for each medium and consists of enough data to reasonably estimate a geometric standard deviation that is assumed to be representative for the entire DOE factor space. Using the test results from the DOE center point for each medium, the geometric standard deviation was computed using Equation 4 below.

$$f = \sqrt{\frac{\sum_{i=1}^n (\ln(SF_i) - \ln(GMSF))^2}{n-1}} \\ GSD = e^f \quad (4)$$

Where:

$n$  = number of samples

$i$  = indexed reference to a particular sample

$SF_i$  = survival fraction for sample “i”

$GMSF$  = geometric mean survival fraction

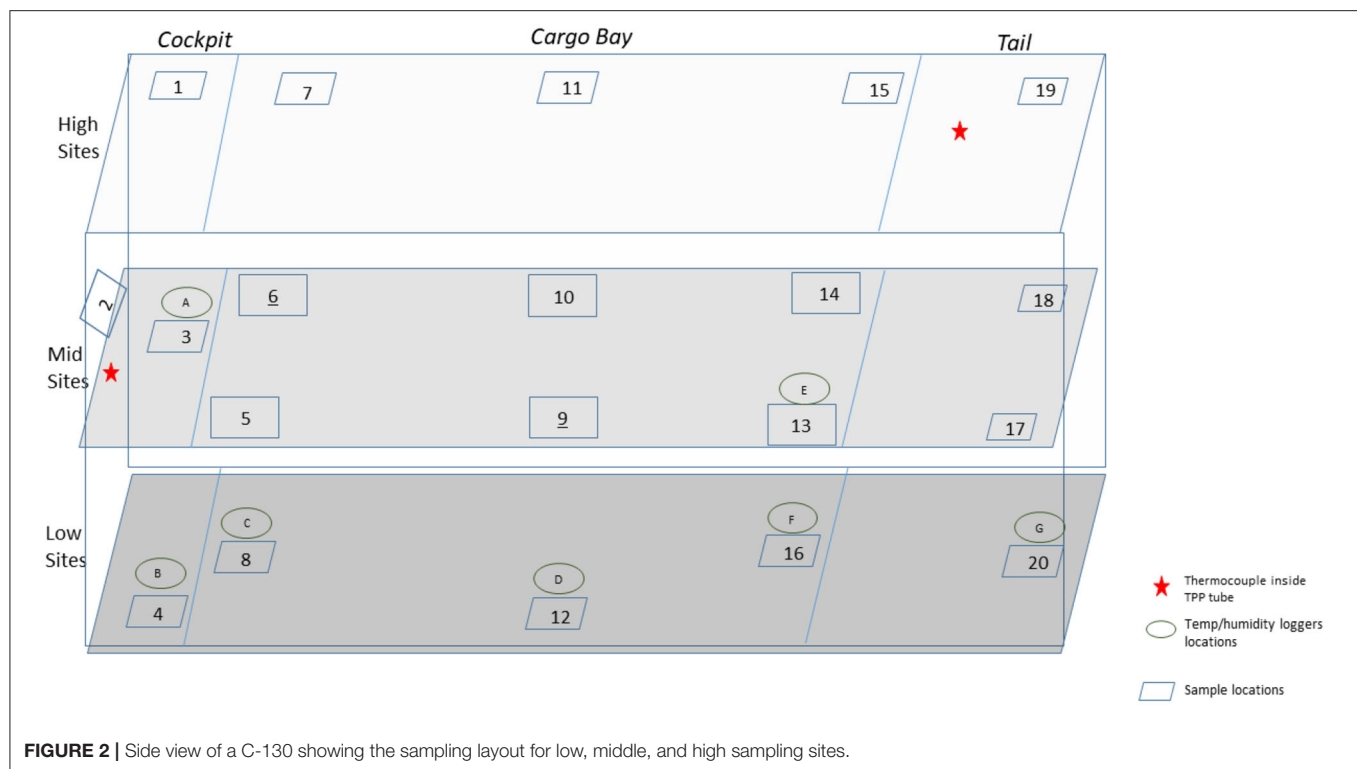
$GSD$  = geometric standard deviation.

The normal distribution of possible Survival Fraction logs for a given exposure condition is described by the natural log of the GMSF predicted using Equation 3 and the natural log of the GSD computed using Equation 4. The GMSF will vary based on exposure conditions and medium, but the GSD will only vary by medium. The equations for the Normal distribution are provided in Equations 5 and 6 below.

$$PDF = \frac{1}{\sqrt{2\pi\sigma^2}} e^{-\frac{(\ln(x)-\mu)^2}{2\sigma^2}} \quad (5)$$

$$CDF = \frac{1}{2} + \frac{1}{2} \operatorname{erf} \left[ \frac{\ln(x) - \mu}{\sqrt{2\sigma^2}} \right] \quad (6)$$

Where:



*PDF = probability distribution function. Characterizes the relative frequency of occurrence.*

*CDF = cumulative distribution function. The integral of the PDF with results ranging from 0 to 1.*

*$x$  = horizontal axis of possible Survival Fractions*

*$\mu$  = natural log of geometric mean survival fraction (GMSF)*

*$\sigma$  = natural log of geometric standard deviation (GSD)*

*erf = the error function.*

The cumulative distribution function equation returns the area for a region under the Probability Distribution Function curve by integrating from  $-\infty$  to a specified SF. A CDF result of “0.95” indicates that 95% of the SF values observed will be less than the specified SF.

The Solver add-in for Microsoft Excel 2016 was used to explore various fits to the transformed survival fractions. The Solver add-in has the added benefit of allowing fit constraints which was crucial to obtaining a good and reasonable fit. The “Evolutionary” method in Solver proved a valuable tool in optimizing the coefficients shown in Equation 3. Excel was also used to produce the various plots in this report and assess model performance.

## C-130 and C-17 Aircraft Test Demonstrations

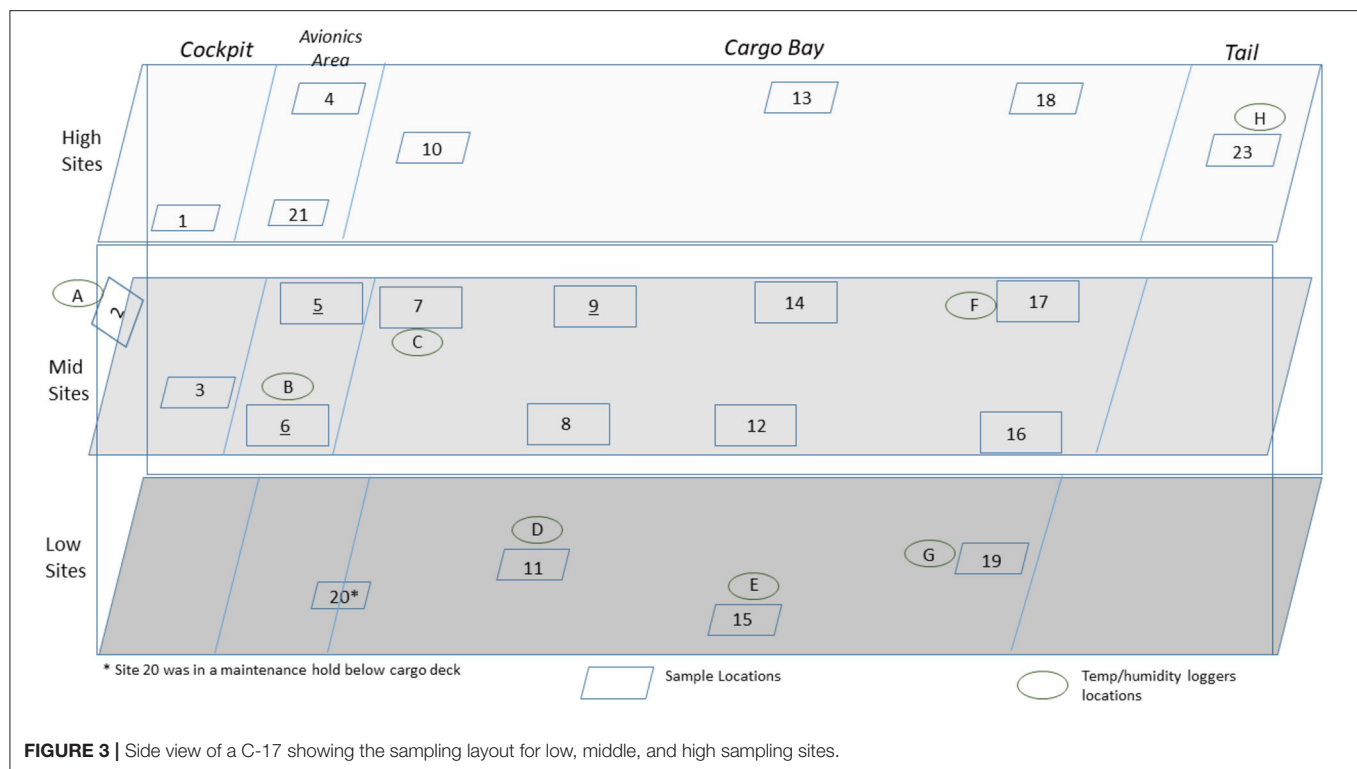
Enveloped virus test indicators consisted of APC coupons inoculated with 1 of 5 independent virus preparations at  $>8 \log_{10}$  coupon $^{-1}$ , and the test coupons were placed inside TPP<sup>®</sup> tubes prior to storage, shipping, and testing. Test indicators were placed in 20–22 locations with 5 test indicators per location within

the aircraft. Each of the 5 test indicators was inoculated with an independent virus preparation. HHA tests were conducted inside a C-130 fuselage located at Army Combat Capabilities Developmental Command, Edgewood, MD, USA (**Figure 2**), or in a C-17 located at Dover Air Force Base, Dover, DE, USA (**Figure 3**), using a previously tested HHA system (Buhr et al., 2016) ran and managed/monitored by a consortium listed in the acknowledgments. After HHA exposure, the test indicators were shipped to a laboratory for virus extraction. Shipping controls were shipped, but not treated with HHA. Laboratory controls were not shipped. Both control sets were prepared, extracted, and quantified alongside the test indicators. Shipping and laboratory controls were maintained inside 50-ml conical tubes with 0.2- $\mu$ m filter caps that allowed equilibration of temperature and humidity exactly the same as the test samples. The controls were maintained at ambient temperature and humidity and measured using data loggers, while test samples were exposed to HHA.

## RESULTS

### HHA Inactivation of Enveloped RNA Virus

In order to develop RSM performance envelopes, partial inactivation data was needed especially at the DOE mid-point. A small test at 50, 60, 70, and 80°C, RH at 5 or 90% for 1 and 24 h, produced critical data showing that high RH was critical for enveloped virus inactivation (**Table 1**). The virus inoculum was held at RT while test samples were exposed to temp/RH. There was only 2.4  $\log_{10}$  enveloped virus inactivation at 70°C, 5% RH, for 24 h compared to complete inactivation at 70°C, 90% RH,



**TABLE 1 |** Log<sub>10</sub> PFU recovered (survival) and reduction (L.R.) after drying Φ6 on APC coupons (enveloped virus test indicator) and then hot air exposure at 5 or 90% RH for 1 or 24 h.

Parameters	Survival	L.R.	Parameters	Survival	L.R.
50°C, 5%, 1 h	7.5 ± 0.2	0.8 ± 0.1	50°C, 90%, 1 h	7.3 ± 0.4	0.9 ± 0.2
60°C, 5%, 1 h	7.0 ± 0.3	1.3 ± 0.2	60°C, 90%, 1 h	1.4 ± 0.3	6.8 ± 0.1
70°C, 5%, 1 h	6.3 ± 0.2	2.0 ± 0.1	70°C, 90%, 1 h	0.0 ± 0.0	8.2 ± 0.0
80°C, 5%, 1 h	6.1 ± 0.2	2.2 ± 0.1	80°C, 90%, 1 h	0.0 ± 0.0	8.2 ± 0.0
Inoculum–1 h	8.3 ± 0.0	NA	Inoculum–1 h	8.2 ± 0.1	NA
50°C, 5%, 24 h	6.8 ± 0.4	1.4 ± 0.2	50°C, 90%, 24 h	1.1 ± 1.6	6.9 ± 0.7
60°C, 5%, 24 h	6.2 ± 0.2	2.0 ± 0.1	60°C, 90%, 24 h	0.0 ± 0.0	8.0 ± 0.0
70°C, 5%, 24 h	5.8 ± 0.5	2.4 ± 0.2	70°C, 90%, 24 h	0.0 ± 0.0	8.0 ± 0.0
80°C, 5%, 24 h	1.4 ± 1.3	6.8 ± 0.6	80°C, 90%, 24 h	0.0 ± 0.0	8.0 ± 0.0
Inoculum–24 h	8.2 ± 0.1	NA	Inoculum–24 h	8.0 ± 0.1	NA

Five test indicators per test. Not applicable (NA).

for 1 h. In addition, there was no enveloped virus inactivation after drying enveloped virus on NTC and treating at 26.7°C at 5, 30, 55, and 80% RH for up to 10 d (data not shown). These data drove the test parameters shown in **Figure 1**. Although 65°C was greater than the original 60°C temperature goal, 65°C was selected for the experimental design because inactivation at <60°C was too slow to generate RSM that met the <24 h objective. Therefore, 65°C was incorporated in the DOE and 60°C, 70% RH, 5 h, was set as the mid-point for the final DOE in order to obtain sufficient partial kill data to develop the RSM performance envelopes.

Overall, there were several thousand trial-and-error data points leading to the HHA decontamination DOE data set in **Table 2**, which shows data from nineteen test runs with five independent virus preparations per coupon type. There were 475 Φ6 virus test samples and 475 corresponding controls, plus non-inoculated coupon controls. Each test variable (temperature, RH, and time) had an impact on decontamination. Importantly, high RH, high temperature, and longer times increased inactivation rates as expected. Inactivation of enveloped virus dried on to materials was found to be  $\geq 7 \log_{10}$  at 60°C, 90%, for 9 h. This surpassed the original goal of  $\geq 7 \log_{10}$  at  $\leq 60^\circ\text{C}$ , 24 h. Furthermore, the enveloped virus inoculum held in aqueous solution (solution controls) was shown to be much more sensitive to the rise in temperature than virus dried on to materials and subjected to hot, humid air. Therefore, water and/or high humidity were significant parameters for inactivating enveloped virus.

There was one statistical outlier for APC at 60°C, 50% RH for 5 h (**Table 2**). The subsequent RSM modeling showed that decontamination kinetics of all materials was essentially the same so long as this data point was treated as an outlier. A full set of tests was not repeated for 60°C, 50% RH, for 5 h because there was no information advantage to update this outlier for this large data set. Much trial and error indicated that APC coupons required 70% ethanol cleaning to remove residue that interfered with microbe recovery and ethanol cleaning was specific to APC; hence, the source of this outlier was likely due to insufficiently cleaned APC coupons.



**TABLE 2** | Log<sub>10</sub> virus survival of Φ6 after drying on to different materials and then exposure to different temperatures, RH, and time according to the DOE in **Figure 1**.

Material	°C	50% RH			70% RH			90% RH		
		1 h		5 h	1 h		5 h	1 h		5 h
		Survival	L.R.	Survival	L.R.	Survival	L.R.	Survival	L.R.	Survival
Nylon	55	8.2 ± 0.2	0.2 ± 0.1	NA	7.0 ± 0.2	1.4 ± 0.1	NA	5.5 ± 0.1	2.8 ± 0.1	NA
	60	NA	NA	7.0 ± 0.4	1.3 ± 0.2	NA	6.7 ± 0.2	1.6 ± 0.1	NA	7.2 ± 0.1
Polypropylene	65	73 ± 0.2	1.1 ± 0.1	NA	5.6 ± 0.1	2.8 ± 0.1	NA	0.7 ± 0.9	7.6 ± 0.4	NA
	55	83 ± 0.3	0.1 ± 0.1	NA	7.6 ± 0.2	0.8 ± 0.1	NA	7.8 ± 0.3	0.5 ± 0.1	NA
Wiring	60	NA	NA	6.9 ± 0.2	1.4 ± 0.1	NA	8.1 ± 0.1	0.2 ± 0.1	NA	7.7 ± 0.2
	65	72 ± 0.2	1.2 ± 0.1	NA	2.4 ± 0.4	6.0 ± 0.2	NA	6.5 ± 0.7	1.9 ± 0.2	NA
APC	55	83 ± 0.1	0.1 ± 0.0	NA	7.9 ± 0.3	0.5 ± 0.1	NA	2.0 ± 0.8	6.3 ± 0.2	NA
	60	NA	NA	6.9 ± 0.6	1.4 ± 0.3	NA	7.9 ± 0.1	0.4 ± 0.1	NA	7.5 ± 0.1
Solution Control	65	7.0 ± 0.4	1.4 ± 0.2	NA	4.1 ± 0.6	4.3 ± 0.3	NA	2.0 ± 1.4	6.3 ± 0.6	NA
	55	83 ± 0.1	0.1 ± 0.0	NA	6.8 ± 0.5	1.6 ± 0.2	NA	7.0 ± 0.6	1.3 ± 0.3	NA
APC—aircraft	60	NA	NA	3.8 ± 0.9	4.5 ± 0.4	NA	7.8 ± 0.2	0.5 ± 0.1	NA	0.0 ± 0.0
	65	53 ± 0.7	3.1 ± 0.3	NA	2.9 ± 1.6	5.5 ± 0.7	NA	0.8 ± 0.8	7.5 ± 0.3	NA
APC—aircraft	55	0.0 ± 0.0	8.4 ± 0.0	NA	0.3 ± 0.6	8.1 ± 0.3	NA	0.0 ± 0.0	8.3 ± 0.0	NA
	60	NA	NA	0.0 ± 0.0	8.3 ± 0.0	NA	0.0 ± 0.0	8.3 ± 0.0	0.0 ± 0.0	8.3 ± 0.0
APC—aircraft	65	0.0 ± 0.0	8.4 ± 0.0	NA	0.0 ± 0.0	8.4 ± 0.0	NA	0.0 ± 0.0	8.3 ± 0.0	NA
	60	0.0 ± 0.0	8.4 ± 0.0	NA	0.0 ± 0.0	8.4 ± 0.0	NA	0.0 ± 0.0	8.4 ± 0.0	NA

The DOE consisted of 13 independent runs—8.4 ± 0.0 log<sub>10</sub>; six independent runs—8.3 ± 0.1 log<sub>10</sub>; five independent tests per material per test run. Survival data with 0 survival was below the limit of detection of 1.0 log<sub>10</sub>. APC—aircraft performance coating; solution control—wet virus inoculum—not dried on a material; NA—not tested for DOE. Hours (h). Polypropylene material from the TPP® tubes was the material. \*An outlier was removed.

## HHA RSM for Enveloped RNA Virus Inactivation

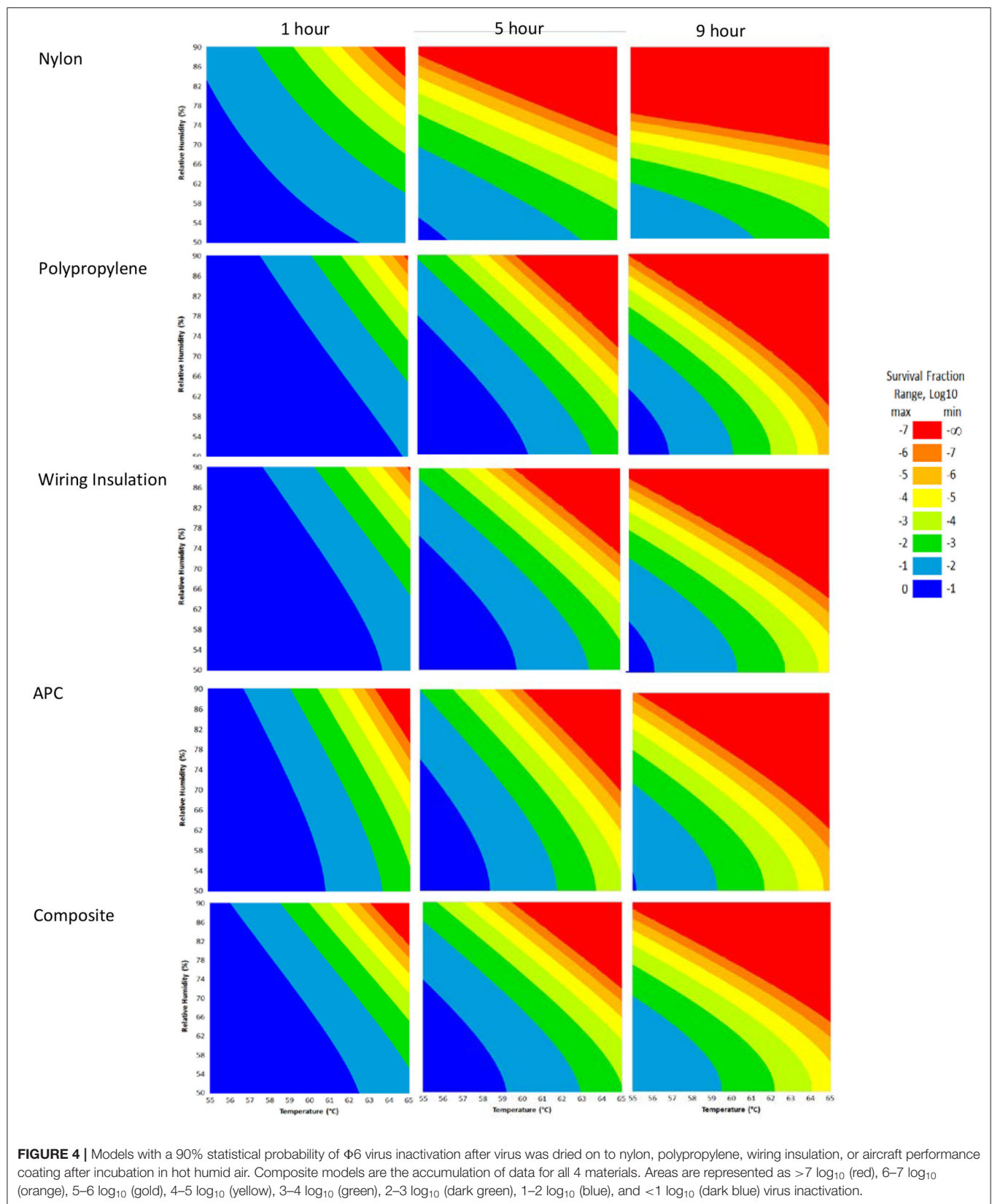
RSM for each material (**Figure 4**) were constructed from the DOE Φ6 inactivation data in **Table 2**. Inactivation of Φ6 virus was similar on all coupon types indicating that material type had little impact on inactivation kinetics. Since virus inactivation was similar across each material, an additional composite RSM was generated (**Figure 4**). The models more clearly showed virus inactivation kinetics compared to the table data. At 1 h, there was a 90% probability of at least a 7 log<sub>10</sub> virus inactivation at 65°C, 90% RH, after virus-contaminated materials were treated with HHA.

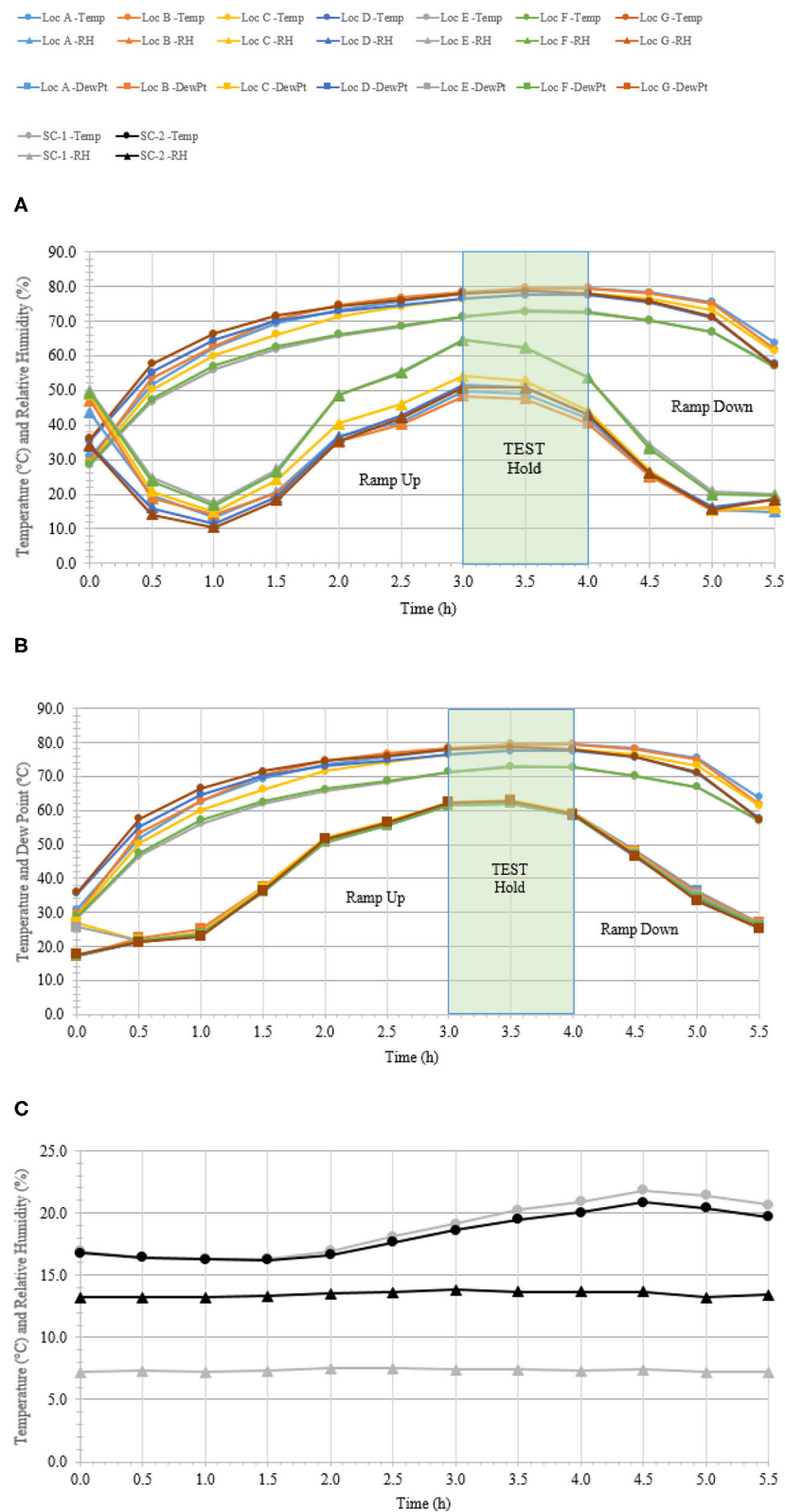
The composite model after 1 h of virus inactivation was critical for directing HHA parameters during the aircraft field testing. The RSM models were calculated using relative humidity because the laboratory environmental chambers controlled humidity using relative humidity. After extensive testing to develop methods and results to develop the RSM models using relative humidity, the sponsoring agencies then requested that relative humidity be converted to dew points for large aircraft testing. Based on a 4 log<sub>10</sub> objective and the 4 log<sub>10</sub> inactivation parameters in the RSM composite model (**Figure 4**), relative humidity was converted to dew points. This conversion showed that 4 log<sub>10</sub> inactivation occurred at a dew point humidity of ≥59.4°C for 1 h, excluding ramp-up and ramp-down times, so long as the temperature was above the dew point. Therefore, the translation made it apparent that absolute humidity or dew point strongly correlated with inactivation. For example, there was a 90% probability of a 4 log<sub>10</sub> kill at ≥61.7°C and a dew point humidity ≥59.4°C. The temperature could go up or down with the same inactivation kinetics so long as the absolute humidity/dew point was maintained. Hence, the inactivation kinetics correlated with the total amount of water in the air. Models with dew points and/or absolute humidity are in the queue for future development.

## C-130 Aircraft Field Test

A total of 100 enveloped virus test indicators were distributed at 20 sites throughout a C-130 fuselage as depicted in **Figure 2**. Based on the RSM in **Figure 4** and with a >4 log<sub>10</sub> inactivation goal, the HHA goals for the C-130 were ≥61.7°C and a dew point humidity of ≥59.4°C for 1 h, excluding ramp-up and ramp-down times. The measured HHA parameters for the C-130 are shown in **Figure 5**. For clarity, both RH and dew points are shown in **Figure 5** so that the parameters can be compared to both the RSM expressed in RH and the large-scale aircraft objective expressed as a dew point. As shown, the temperature and humidity goals were exceeded. In addition, the ramp-up time was 2.5–3 h, which was longer than lab testing with a ramp-up of 1 h; hence, ramp-up conditions on the aircraft likely contributed to enveloped virus inactivation. Ramp-down time was nearly 2 h, which was also much longer than lab conditions. The total HHA time including ramp-up and ramp-down for the C-130 was 5.5 h compared to 2 h in the lab-based RSM. The C-130 temperatures were always above the dew points so there was no condensation on the virus-inoculated APC samples (**Figure 5**). Samples were shipped to







**FIGURE 5 |** Temperature and humidity profiles during HHA decontamination of a C-130. **(A)** Temperature (°C) and RH (%) from seven locations (A–G) throughout the C-130. **(B)** Temperature and dew point (°C) from seven locations (A–G) throughout the C-130. **(C)** Temperature (°C) and RH (%) logged within two sets of shipping controls (SC).

**TABLE 3** | Log<sub>10</sub> PFU recovered (survival) and reduction (L.R.) after drying  $8.3 \pm 0.1$  log<sub>10</sub> of Φ6 per APC coupon (enveloped virus test indicator) and then HHA exposure in a C-130 aircraft.

Test indicators	Survival	L.R.
Non-shipped controls (10)	$8.1 \pm 0.1$	NA
Shipped controls (25)	$8.1 \pm 0.1$	NA
Test indicators (100)	$0.0 \pm 0.0$	$8.1 \pm 0.1$

The detection range was 1.0–8.1 log<sub>10</sub> where the upper limit was the amount extracted from the controls. Since there was no enveloped virus recovery on any test indicator, there was practical confidence of a complete virus kill. The number of test indicators are in parentheses. Not applicable (NA).

a lab for extraction. **Table 3** shows  $8.1 \pm 0.1$  log<sub>10</sub> PFU were recovered on 10 non-shipped control samples and 25 ground-shipped control samples out of  $8.3 \pm 0.1$  log<sub>10</sub> PFU dried on to the APC coupons. The loss of 0.2 log<sub>10</sub> PFU on the control coupons could have been due to extraction efficiency and/or a small drop in virus viability. In either case, the 8.1 log<sub>10</sub> PFU recovery on the control coupons was high, and if validated there was no significant loss of viability during transportation to and from the field site. The detection range was 1.0–8.1 log<sub>10</sub>. Since the temperature and RH limits were exceeded for a 7 log<sub>10</sub> kill and there was no viable virus recovered from any test indicator, there is practical confidence that a complete >8 log<sub>10</sub> kill was achieved.

### C-17 Aircraft Field Test

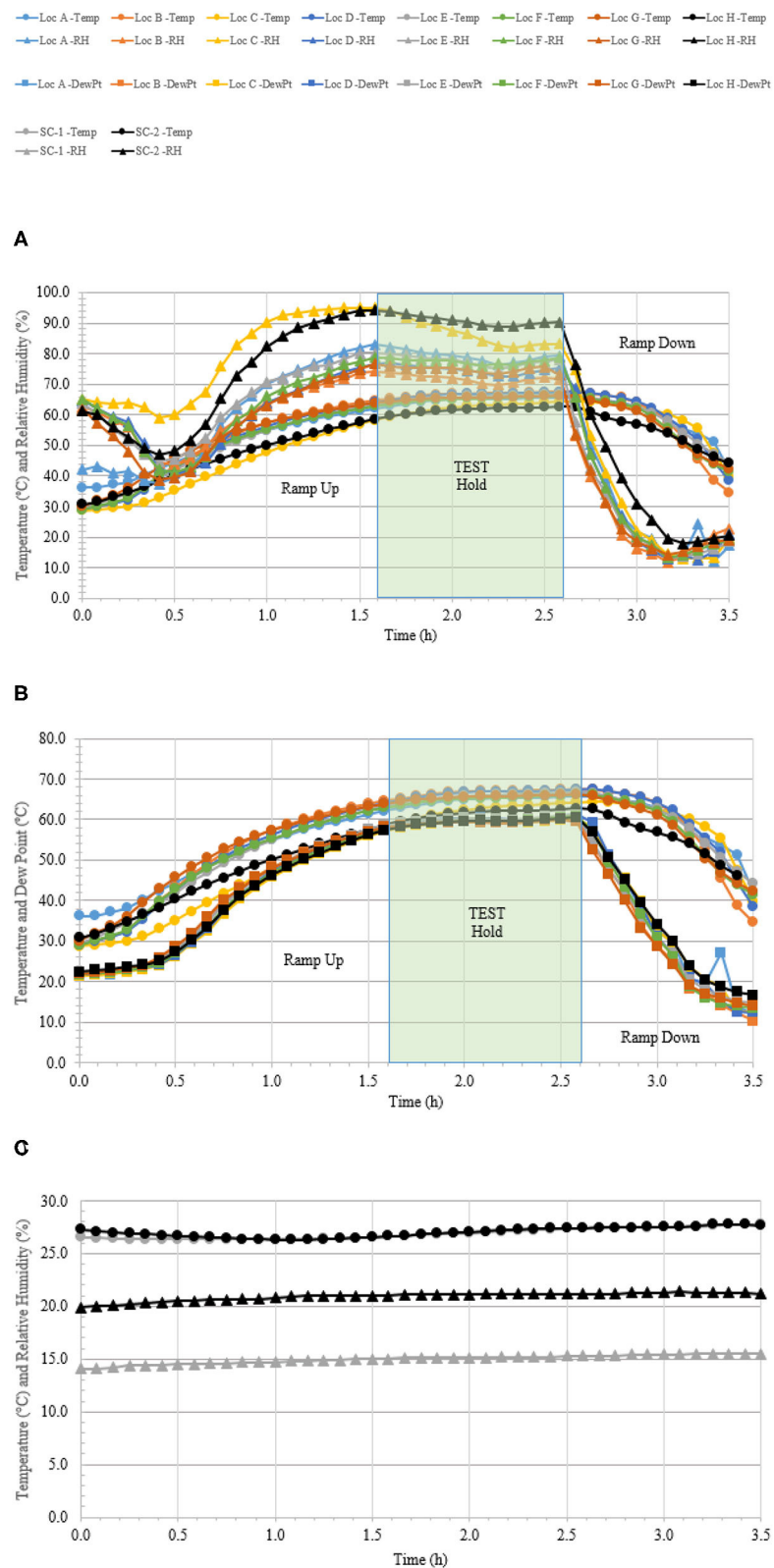
A total of 110 enveloped virus test indicators were distributed throughout the C-17 as depicted in **Figure 3**. Based on the RSM in **Figure 4**, results from the C-130 test, and with a >4 log<sub>10</sub> inactivation goal, the HHA parameters were set to  $\geq 61.7^\circ\text{C}$  and a dew point humidity of  $\geq 57.2^\circ\text{C}$  for the C-17, at which point a 1-h “hold time” was started. Another goal was to increase the temperature and humidity during the 1 h “hold time” to  $61.7^\circ\text{C}$  and a dew point humidity of  $\geq 59.4^\circ\text{C}$ . The measured HHA parameters for the C-17 are shown in **Figure 6**. For clarity, both RH and dew points are shown in **Figure 6** so that the parameters can be compared to both the RSM expressed in RH and the large-scale aircraft objective expressed as a dew point. The temperature reached  $65.0^\circ\text{C}$  and humidity reached a  $60.6^\circ\text{C}$  dew point, surpassing the temperature and humidity goals during the 1 h hold time. In addition, the ramp-up time was 1.5 h, which saved >1 h compared to the C-130 test, but was 0.5 h longer than lab tests. Ramp-down time was 45 min compared to 2 h for the C-130 and only one min for lab tests. The total HHA time for the C-17 was <3.5 h compared to 5.5 h for the C-130 and 2 h for lab tests. The C-17 temperatures were always above the dew points so there was no condensation on the virus-inoculated APC samples (**Figure 6**). Samples were ground-shipped to a lab for extraction. **Table 4** shows  $7.6 \pm 0.1$  log<sub>10</sub> PFU on 10 non-shipped control samples and 25 ground-shipped control samples out of  $8.2 \pm 0.1$  log<sub>10</sub> PFU dried on to the APC coupons. The loss of 0.6 log<sub>10</sub> PFU on the control coupons could have been due to extraction efficiency and/or a drop in virus viability. In either case, the 7.6 log<sub>10</sub> PFU recovery on the control coupons was high and it showed no practical significant loss of virus

viability during transportation to and from the field site. The limit of detection was 1.0 log<sub>10</sub>. Since there was viable PFU from at least one of the 110 test indicators, all samples with no viable PFU were assigned 1.0 log<sub>10</sub>. Site 15 on the C-17 showed the lowest log reduction of  $5.9 \pm 0.6$  log<sub>10</sub> PFU. This site had the most air movement. Although there were no TPP<sup>®</sup> tubes with temperature and RH readings at Site 15, we speculate that the rapid air movement slowed the penetration of moist air across the 0.2 μm membrane of the TPP<sup>®</sup> tubes, hence the lowest level of inactivation. Every other C-17 location had at least a 6 log<sub>10</sub> reduction. Ramp-up/ramp-down times were longer than the lab tests used for RSM, and raising the heat and humidity during the 1 h hold time contributed to the virus inactivation. Hence the goal of >4 log<sub>10</sub> reduction was surpassed as predicted by RSM.

### DISCUSSION

Φ6 was selected as a BSL-1, enveloped RNA virus test indicator for both lab and field tests. Φ6 has been widely used as an enveloped virus surrogate (de Carvalho et al., 2017). The structural similarity of Φ6 to many other enveloped viruses including coronaviruses suggest that the Φ6 structure should be similarly susceptible to general decontaminants. Furthermore, the structural molecules of the virus are produced by host cells with similar temperature sensitivity at around  $40^\circ\text{C}$ , further suggesting that Φ6 should be similarly susceptible to general decontaminants.

For this study, virus was dried  $\geq 24$  h before exposing to the environmental test conditions because (1) the level of virus drying/level of free water was an important consideration for standardizing these tests and  $\geq 24$  h drying mitigated drying variability and (2)  $\geq 24$  h drying was done in attempt to mimic environments where free water is limited, especially for virus bound in debris. There was no Φ6 inactivation after the virus was dried on different surfaces for at least 24 h at RT followed by a 10-d exposure to  $26.7^\circ\text{C}$  at 80% RH, and there was only 2.4 log<sub>10</sub> inactivation at  $70^\circ\text{C}$ , 5% RH, for 24 h. This is a higher level of temperature and humidity stability than reported in other enveloped virus studies, but none of the articles we reviewed tested virus that was dried for at least 24 h. A review of articles describing enveloped virus stability to temperature and/or humidity, including coronavirus, showed that most stability tests were with wet virus or virus that was only dried for an hour. Sizun et al. (2000), Rabenau et al. (2005), and Chan et al. (2011) tested similar coronaviruses including dried SARS-CoV, CoV-229E, and CoV-OC-43 at different virus concentrations, virus purities, additives such as fetal calf serum, and fomites, but all the tests were at ambient environmental conditions of  $21\text{--}25^\circ\text{C}$ , which contrasts with no virus inactivation at  $26.7^\circ\text{C}$ , 80% RH, 10 d in this study. Complete virus inactivation ranged from 3 h up to 13 d across these reports. Numerous published reports for enveloped virus stability have tested wet virus preparations (e.g., Anonymous—Department of Homeland Security, 2020; Biryukov et al., 2020; Castaño et al., 2020; Harbourn et al., 2020; Matson et al., 2020; Ren et al., 2020) and also showed much higher sensitivity to temperature and RH than reported in the current



**FIGURE 6 |** Temperature and humidity profiles during HHA decontamination of a C-17. **(A)** Temperature (°C) and RH (%) from eight locations (A–H) throughout the C-17. **(B)** Temperature and dew point (°C) from eight locations (A–H) throughout the C-17. **(C)** Temperature (°C) and RH (%) logged within two sets of shipping controls (SC).

**TABLE 4 |** Log<sub>10</sub> PFU recovered (survival) and reduction (L.R.) after drying  $8.2 \pm 0.1$  log<sub>10</sub> of  $\Phi 6$  per APC coupon (enveloped virus test indicator) and then HHA exposure in a C-17 aircraft.

Test indicator locations	Survival	L.R.
Non-shipped controls (10)	$7.6 \pm 0.1$	NA
Shipped controls (25)	$7.6 \pm 0.1$	NA
22—Repurposed as a control on-site (5)	$7.6 \pm 0.2$	NA
1—Flight deck (FD)—ceiling (5)	$1.4 \pm 0.8$	$6.2 \pm 0.3$
2—FD—glare shield (5)	$1.3 \pm 0.6$	$6.3 \pm 0.3$
3—FD—crew rest area (5)	$1.0 \pm 0.0$	$6.6 \pm 0.1$
4—Avionics—rack doghouse (5)	$1.0 \pm 0.0$	$6.6 \pm 0.1$
5—Lower avionics rack (5)	$1.0 \pm 0.0$	$6.6 \pm 0.1$
6—Lavatory (5)	$1.5 \pm 0.9$	$6.1 \pm 0.4$
7—Load master station (5)	$1.3 \pm 0.5$	$6.3 \pm 0.2$
8—Forward Cargo Bay (FCB)—left (5)	$1.5 \pm 0.9$	$6.1 \pm 0.4$
9—FCB—right (5)	$1.4 \pm 0.7$	$6.2 \pm 0.3$
10—FCB—ceiling (5)	$1.3 \pm 0.6$	$6.3 \pm 0.3$
11—FCB—floor (5)	$1.4 \pm 0.9$	$6.2 \pm 0.4$
12—Mid Cargo Bay (MCB)—left (5)	$1.5 \pm 0.9$	$6.1 \pm 0.4$
13—MCB—right (5)	$1.0 \pm 0.0$	$6.6 \pm 0.1$
14—MCB—ceiling (5)	$1.3 \pm 0.7$	$6.3 \pm 0.3$
15—MCB—floor (5)	$1.7 \pm 1.3$	$5.9 \pm 0.6$
16—Aft Cargo Bay (ACB)—left (5)	$1.0 \pm 0.0$	$6.6 \pm 0.1$
17—ACB—right (5)	$1.4 \pm 0.8$	$6.2 \pm 0.4$
18—ACB—ceiling (5)	$1.4 \pm 0.2$	$6.2 \pm 0.1$
19—ACB—floor (5)	$1.0 \pm 0.0$	$6.6 \pm 0.1$
20—Mx tunnel—skin heat exchanger (5)	$1.0 \pm 0.0$	$6.6 \pm 0.1$
21—Mx tunnel—middle (5)	$1.4 \pm 0.7$	$6.2 \pm 0.3$
23—Ramp area (5)	$1.1 \pm 0.1$	$6.5 \pm 0.1$

The detection range was  $1.0$ – $7.6$  log<sub>10</sub> where the upper limit was the amount extracted from the controls. Since there was enveloped virus recovery on some test indicators, the lowest recorded kill level was  $1.0$  log<sub>10</sub> even if there were no viable PFU measured from a test indicator. The number of test indicators are in parentheses. Not applicable (NA).

study. While there are numerous differences in methods and results described across these studies, a key difference in the testing described herein was that virus was dried at least 24 h before exposing to the environmental test conditions and that may be a key variable for virus stability.

There is general agreement in the literature that higher temperature and humidity will increase the inactivation rates for enveloped virus. However, a direct side-by-side study would eliminate the impact of methods to define temperature and humidity profiles. This would also highlight physiochemical similarities/differences inherent to a specific virus or common to virus families (Nims and Plavsic, 2013; Castaño et al., 2020). Side-by-side testing comparing dried  $\Phi 6$  to several dried coronaviruses, including  $\Phi 6$  SARS-CoV-2, are moving forward in our lab. Once these data are collected, a more standardized comparison can be made between the temperature and humidity susceptibility among these enveloped viruses.

There are numerous mathematical tools that can be used to analyze decontamination data. RSM models were very useful here since they provided simplified graphical data to rapidly

adjust to changing goals for log reduction, time, temperature, and humidity. This became very important since the HHA goals (requirements) were frequently redefined by end users (aircraft maintenance authorities at Aircraft Mobility Command) over the past 20 years, and numerous goal changes were directed during the COVID-19 pandemic. The original goals were to show enveloped virus inactivation of  $\geq 7$  log<sub>10</sub> out of a  $\geq 8$  log<sub>10</sub> challenge. This challenge level was set because measurements with high concentrations of microbes greatly increased the confidence in inactivation and it mitigated the risk of incomplete decontamination (Hamilton et al., 2013), an important consideration for decision makers that assess contamination/decontamination. High challenge levels are important since exposure limits (infectious dosages) are not well-defined for many viruses such as SARS-CoV and SARS-CoV-2. Although HHA does not fall under the EPA's regulatory jurisdiction because it is not classified as a chemical disinfectant, the inactivation goal was reduced from 7 log<sub>10</sub> to 3 log<sub>10</sub> inactivation by the funding agencies during the COVID-19 pandemic to match the EPA N-list for decontaminants and provide decontaminant options to end users. The HHA RSM showed 90% probability levels of inactivation for log reductions of 0 through 7 log<sub>10</sub>, which allowed for rapid adjustments during the aircraft testing.

There were originally no time limitations set for aircraft sterilization (spore decontamination). The HHA time goal was reduced to  $\leq 24$  h for enveloped virus to increase HHA throughput and user acceptance. The time goal was further reduced by the end users and funding agencies to "1 h hold time; <6 h total time" after the COVID-19 pandemic had begun.

The HHA temperature goal was originally capped at the accepted temperature limit of C-130 aircraft (80°C), but that was for sterilization (spore decontamination). The HHA temperature goal was reduced to 60°C for the enveloped virus to increase HHA acceptance over a range of aircraft since 60°C is a standard, accepted test temperature for most aircraft materials. The time goal of  $\leq 24$  h provided the rationale for measuring HHA over several hours to develop RSM models. However, the end users and funding agencies raised the accepted temperature limit to 68.3°C during COVID-19 to reduce decontamination time.

Although there was a strong preference to reduce/eliminate humidity from HHA to reduce cost and complexity, all of the experimental data here showed that  $\Phi 6$  was stable after drying. Virus was quickly inactivated after it was diluted in aqueous solutions and heated (solution control data). For HHA, the combination of high heat and high humidity, i.e., a high dew point, was critical to virus inactivation on materials in hour-long timeframes. This is consistent with long-known observations that enveloped virus is stabilized after drying on fomites. As an example, the enveloped virus smallpox was stabilized after it peeled/sloughed along with host cells and then dried on porous materials including clothes and blankets. Furthermore, historic data shows that enveloped viruses were stabilized in cold, dry climates (Fenn, 2001).

The end goal of the RSM was simplistic graphs where all decontamination test variables could be compared, understood, and utilized for field testing and field application. This was



particularly useful for large hot, humid air decontamination systems with fluctuating temperature and RH, potential power disruptions, and decontamination goals that have fluctuated widely over time. Since the RSM models showed little difference in inactivation kinetics among the different materials, a composite RSM was developed as a primary reference guide. This reference guide served the purpose of guiding HHA field testing in aircraft. The RSM models translated to field demonstrations because there was a  $\geq 5.9 \log_{10}$  enveloped virus inactivation after both aircraft field tests, as predicted. The RSM models were also used as a guide for a number of iterative improvements between the first and second aircraft demonstration that shortened the overall HHA decontamination time from 5.5 to  $<3.5$  h.

There were numerous conclusions. The  $\Phi 6$  test indicators were useful measurements of inactivation for both lab and field testing. HHA successfully inactivated enveloped virus at high temperature and high humidity. The RSM models were adaptable to changes in user requirements and successfully utilized to predict HHA results for field applications. Much methods development and testing remains to confirm HHA inactivation kinetics across virus species, and to develop HHA models that include HHA ramp-up and ramp-down times. Lastly, HHA decontamination of aircraft was successful because the enveloped virus on the C-17 aircraft was inactivated, the aircraft was flown after the HHA field test, and then the C-17 was certified as an operational aircraft.

## DATA AVAILABILITY STATEMENT

All datasets generated for this study are included in the article/supplementary material.

## REFERENCES

- Anonymous—Department of Homeland Security (2020). *Estimated Natural Decay of SARS-CoV-2 (Virus That Causes COVID-19) on Surfaces Under a Range of Temperatures and Relative Humidity*. Available online at: <https://www.dhs.gov/science-and-technology/sars-calculator#:~:sim:text=COVID%20Stability%3A&text=Relative%20Humidity%20and%20Temperature%20can,Humidity%20between%2020%2D60%25> (accessed June 1, 2020).
- Beauregard, M. R., Mikulak, R. J., and Olson, B. A. (1992). *A Practical Guide to Statistical Quality Improvement, Opening up the Statistical Toolbox*. New York, NY: Van Nostrand Reinhold, 351–360.
- Biryukov, J., Boydston, J. A., Dunning, R. A., Yeager, J. J., Wood, S., Reese, A. L., et al. (2020). Increasing temperature and relative humidity accelerates inactivation of SARS-CoV-2 on surfaces. *mSphere* 5:e00441-20. doi: 10.1128/mSphere.00441-20
- Bishop, A. H., and Robinson, C. V. (2014). *Bacillus thuringiensis* HD-1 cry-: development of a safe non-insecticidal simulant for bacillus anthracis. *J. Appl. Microbiol.* 117, 654–662. doi: 10.1111/jam.12560
- Buhr, T., Young, A., Bensman, M., Minter, Z., Kennihan, N., Johnson, C., et al. (2016). Hot, humid air decontamination of a C-130 aircraft contaminated with spores of two acrystalliferous *Bacillus thuringiensis* strains, surrogates for *Bacillus anthracis*. *J. Appl. Microbiol.* 120, 1074–1084. doi: 10.1111/jam.13055
- Buhr, T., Young, A. A., Barnette, H., Minter, Z. A., Kennihan, N., McPherson, D. C., et al. (2015). Test methods and response surface models for hot, humid air decontamination of materials contaminated with dirty spores of *Bacillus anthracis*  $\Delta$ Sterne and *B. thuringiensis* Al Hakam. *J. Appl. Microbiol.* 119, 1263–1277. doi: 10.1111/jam.12928

## AUTHOR CONTRIBUTIONS

TB was the principal investigator and the principal for methods development, test design, execution analysis, and writing. AY was a lead tester and contributed to methods development test design, execution, and data assembly. EB-K, NK, ZM, MBo, and EO participated in methods development, test design, test execution, and data assembly. SH, MK, MH, CM, RM, JI, MBe, BG, VY, SL, EH, and BL contributed to test execution and data assembly. HB was the math modeler. All team members participated or contributed to writing, figures, tables, and/or editing.

## FUNDING

This work was supported through funding provided by the Defense Threat Reduction Agency (DTRA), Hazard Mitigation Capability Area (BA2 and 3 funds, Project Number CB10141), and Joint Program Executive Office CBRND/Joint Program Manager-CBRN Protection/Joint Biological Agent Decontamination System Program (JBADS).

## ACKNOWLEDGMENTS

Thanks are due to Dr. Tabitha Newman for technical support. The aircraft demonstration events involved a consortium of supporters including DTRA, JPEO-CBRND, Aeroclave, LLC, Air Force, Air Mobility Command, United States Transportation Command, Naval Surface Warfare Center—Dahlgren Division, Air Force Research Lab, METSS Corporation, CCDC, and Dover Air Force Base. This manuscript has been released as a pre-print at bioRxiv (Buhr et al., 2020).

- Buhr, T., Young, A. A., Johnson, C. A., Minter, Z., and Wells, C. (2014). Decontamination of materials contaminated with *Francisella philomiragia* or MS2 bacteriophage using PES-Solid, a solid source of peracetic acid. *J. Appl. Microbiol.* 117, 397–404. doi: 10.1111/jam.12540
- Buhr, T. L., Young, A. A., Borgers-Klonkowski, E., Kennihan, N. L., Barnette, H. K., Minter, Z. A., et al. (2020). Hot, humid air decontamination of aircraft confirmed that high temperature and high humidity are critical for inactivation of infectious, enveloped ribonucleic acid (RNA) virus. *bioRxiv [Preprint]*. 1–29. doi: 10.1101/2020.07.20.212365
- Buhr, T. L., Young, A. A., Minter, Z. A., and Wells, C. M. (2012). Test method development to evaluate hot, humid air decontamination of materials contaminated with *Bacillus anthracis*  $\Delta$ Sterne and *B. thuringiensis* Al Hakam spores. *J. Appl. Microbiol.* 113, 1037–1051. doi: 10.1111/j.1365-2672.2012.05423.x
- Castano, N., Cordts, S., Jalil, M. K., Zhang, K., Koppaka, S., Bick, A. (2020). Fomite transmission and disinfection strategies for SARS-CoV-2 and related viruses. *arXiv.2005.11443 [q-bio.OT]*. 1–24.
- Centers for Disease Control and Prevention (2019). *Interim Guidance for Ebola Virus Cleaning, Disinfection and Waste Disposal in Commercial Passenger Aircraft*. Available online at: <https://www.cdc.gov/vhf/ebola/prevention/cleaning-commercial-passenger-aircraft.html> (accessed May 15, 2020).
- Chan, K. H., Malik Peiris, J. S., Lam, S. Y., Poon, L. L. M., Yuen, K. Y., Seto, W. H., et al. (2011). The effects of temperature and relative humidity on the viability of the SARS coronavirus. *Adv. Virol.* 2011:734690. doi: 10.1155/2011/734690
- de Carvalho, N. A., Stachler, E. N., Cimabue, N., and Bibby, K. (2017). Evaluation of Phi6 persistence and suitability as an enveloped virus surrogate. *Environ. Sci. Technol.* 51, 8692–8700. doi: 10.1021/acs.est.7b01296

- Fenn, E. A. (2001). *Pox Americana: The Great Smallpox Epidemic of 1775-82*. New York, NY: Hill and Wang.
- Gallandat, K., and Lantagne, D. (2017). Selection of a biosafety level 1 (BSL-1) surrogate to evaluate surface disinfection efficacy in ebola outbreaks: comparison of four bacteriophages. *PLoS ONE* 12:e0177943. doi: 10.1371/journal.pone.0177943
- Hamilton, M., Hamilton, G., Goeres, D., and Parker, A. (2013). Guidelines for the statistical analysis of a collaborative study of a laboratory disinfectant product performance test method. *JAOAC Int.* 96, 1138–1151. doi: 10.5740/jaoacint.12-217
- Harbourt, D., Haddow, A., Piper, A., Bloomfield, H., Kearney, B., Gibson, K., et al. (2020). Modelling the stability of severe acute respiratory syndrome coronavirus 2 (SARS-CoV-2) on skin, currency, and clothing. *medRxiv [Preprint]*. 1–18. doi: 10.1101/2020.07.01.20144253
- Lenth, R. V. (2009). Response-surface methods in R, using rsm. *J. Stat. Softw.* 32, 1–17. doi: 10.18637/jss.v032.i07
- Matson, M. J., Yinda, C. K., Seifert, S. N., Bushmaker, T., Fischer, R., van Doremalen, N., et al. (2020). Effect of environmental conditions on SARS-CoV-2 stability in human nasal mucus and sputum. *Emer. Infect. Dis.* 26, 2276–2278. doi: 10.3201/eid2609.202267
- McDonnell, G., and Burke, P. (2011). Disinfection: is it time to reconsider Spaulding? *J. Hosp. Inf.* 78, 163–170. doi: 10.1016/j.jhin.2011.05.002
- Mindich, L. (2004). Packaging, replication and recombination of the segmented genomes of bacteriophage  $\Phi 6$  and its relatives. *Virus Res.* 101, 83–92. doi: 10.1016/j.virusres.2003.12.008
- Myers, R. H., Montgomery, D. C., and Anderson-Cook, C. M. (2009). *Response Surface Methodology*. Hoboken, NJ: John Wiley & Sons, Inc.
- National Business Aviation Association (2020). *Aircraft Disinfection for the Coronavirus*. Available online at: <https://nbaa.org/aircraft-operations/safety/coronavirus/aircraft-disinfection-coronavirus/> (accessed May 15, 2020).
- Nims, R. W., and Plavsic, M. (2013). Intra-family and inter-family comparisons for viral susceptibility to heat inactivation. *J. Microbial biochem. Tech.* 5, 136–141. doi: 10.4172/1948-5948.1000112
- Rabenau, H. F., Cinatl, J., Morgenstern, B., Bauer, G., Preiser, W., and Doerr, H. W. (2005). Stability and inactivation of SARS coronavirus. *Med. Microbiol. Immunol.* 194, 1–6. doi: 10.1007/s00430-004-0219-0
- Ren, S.-Y., Wang, W.-B., Hao, Y.-G., Zhang, H.-R., Wang, Z.-C., Chen, Y.-L., et al. (2020). Stability and infectivity of coronaviruses in inanimate environments. *World J Clin Cases.* (2020) 8:1391–9. doi: 10.12998/wjcc.v8.i8.1391
- Sizun, J., Yu, M. W., and Talbot, P. J. (2000). Survival of human coronaviruses 229E and OC43 in suspension and after drying on surfaces: a possible source of hospital-acquired infections. *J. Hosp. Infect.* 46, 55–60. doi: 10.1053/jhin.2000.0795
- Spaulding, E. H. (1957). Chemical disinfection and antisepsis in the hospital. *J. Hosp. Res.* 9, 5–31.
- Van Etten, J., Lane, L., Gonzalez, C., Partridge, J., and Vidaver, A. (1976). Comparative properties of bacteriophage  $\phi 6$  and  $\phi 6$  nucleocapsid. *J. Virol.* 18, 652–658. doi: 10.1128/JVI.18.2.652-658.1976
- Vidaver, A. K., Roski, R. K., and Van Etten, J. L. (1973). Bacteriophage  $\phi 6$ : a lipid-containing virus of *Pseudomonas phaseolicola*. *J. Virol.* 11, 799–805. doi: 10.1128/JVI.11.5.799-805.1973
- Wiggington, K. R., Pecson, B. M., Sigstam, T., Bosshard, F., and Kohn, T. (2012). Virus inactivation mechanisms: impact of disinfectants on virus function and structural integrity. *Environ. Sci. Technol.* 46, 12069–12078. doi: 10.1021/es3029473

**Conflict of Interest:** The authors declare that the research was conducted in the absence of any commercial or financial relationships that could be construed as a potential conflict of interest.

Copyright © 2020 Buhr, Young, Borgers-Klonkowski, Kennihan, Barnette, Minter, Bohmke, Osborn, Hamilton, Kimani, Hammon, Miller, Mackie, Innocenti, Bensman, Gutting, Lilly, Hammer, Yates and Luck. This is an open-access article distributed under the terms of the Creative Commons Attribution License (CC BY). The use, distribution or reproduction in other forums is permitted, provided the original author(s) and the copyright owner(s) are credited and that the original publication in this journal is cited, in accordance with accepted academic practice. No use, distribution or reproduction is permitted which does not comply with these terms.



# Combinations of PCR and Isothermal Amplification Techniques Are Suitable for Fast and Sensitive Detection of SARS-CoV-2 Viral RNA

Dmitriy A. Varlamov<sup>1</sup>, Konstantin A. Blagodatskikh<sup>2</sup>, Evgenia V. Smirnova<sup>3\*</sup>, Vladimir M. Kramarov<sup>4</sup> and Konstantin B. Ignatov<sup>3,4\*</sup>

<sup>1</sup> Syntol JSC, Moscow, Russia, <sup>2</sup> Laboratory of Molecular Oncology, Pirogov Russian National Research Medical University, Moscow, Russia, <sup>3</sup> Shemyakin-Ovchinnikov Institute of Bioorganic Chemistry, Russian Academy of Sciences, Moscow, Russia, <sup>4</sup> Vavilov Institute of General Genetics, Russian Academy of Sciences, Moscow, Russia

## OPEN ACCESS

### Edited by:

Stephen Allen Morse,  
Centers for Disease Control  
and Prevention (CDC), United States

### Reviewed by:

Segaran P. Pillai,  
United States Department  
of Homeland Security, United States  
Wei Zou,  
University of Michigan, United States

### \*Correspondence:

Konstantin B. Ignatov  
ignatovkb@bk.ru  
Evgeniya V. Smirnova  
smirnova.evgeniya@gmail.com

### Specialty section:

This article was submitted to  
Biosafety and Biosecurity,  
a section of the journal  
Frontiers in Bioengineering and  
Biotechnology

**Received:** 10 September 2020

**Accepted:** 15 October 2020

**Published:** 04 November 2020

### Citation:

Varlamov DA, Blagodatskikh KA,  
Smirnova EV, Kramarov VM and  
Ignatov KB (2020) Combinations  
of PCR and Isothermal Amplification  
Techniques Are Suitable for Fast  
and Sensitive Detection  
of SARS-CoV-2 Viral RNA.  
*Front. Bioeng. Biotechnol.* 8:604793.  
doi: 10.3389/fbioe.2020.604793

The newly identified coronavirus, severe acute respiratory syndrome coronavirus 2 (SARS-CoV-2), causes coronavirus disease 2019 (COVID-19) and has affected over 25 million people worldwide as of August 31, 2020. To aid in the development of diagnostic kits for rapid and sensitive detection of the virus, we evaluated a combination of polymerase chain reaction (PCR) and isothermal nucleic acid amplification techniques. Here, we compared conventional PCR and loop-mediated isothermal amplification (LAMP) methods with hybrid techniques such as polymerase chain displacement reaction (PCDR) and a newly developed PCR-LAMP method. We found that the hybrid methods demonstrated higher sensitivity and assay reaction rates than those of the classic LAMP and PCR techniques and can be used to for SARS-CoV-2 detection. The proposed methods based on the modern hybrid amplification techniques markedly improve virus detection and, therefore, can be extremely useful in the development of new diagnostic kits.

**Keywords:** SARS-CoV-2, COVID-19, loop-mediated isothermal amplification, polymerase chain displacement reaction, PCR-LAMP, hybrid virus detection technique

## INTRODUCTION

The SARS-CoV-2 pandemic started in late December 2019, in Wuhan, China (Jiang and Shi, 2020; Wu et al., 2020; Zhou et al., 2020). By August 31, 2020, over 25 million cases of SARS-CoV-2 infection have been confirmed worldwide, with a death toll over 0.8 million. One key aspect of a safe transition from lockdown is the ability to continuously test the population for the presence of SARS-CoV-2 and hence, COVID-19 infected individuals. Nucleic acid testing is the primary method for COVID-19 diagnosis. The SARS-CoV-2 virion contains a single-stranded positive-sense RNA genome, 30,000 nucleotides in length (Zhou et al., 2020). Thus, testing involves the reverse transcription (RT) of SARS-CoV-2 RNA into complementary DNA (cDNA), followed by amplification of targeted regions of the cDNA. Currently, standard molecular techniques for the detection of the virus are quantitative RT polymerase chain reaction (RT-qPCR) (Bruce et al., 2020; Chu et al., 2020; Corman et al., 2020; Garafutdinov et al., 2020; Gray et al., 2020; Yip et al., 2020; Zhu et al., 2020) and RT loop-mediated isothermal amplification (RT-LAMP) (Ben-Assa et al., 2020;

Butler et al., 2020; Garafutdinov et al., 2020; Gray et al., 2020; Lu et al., 2020; Zhang et al., 2020). RT-LAMP and RT-qPCR can be performed in either a one-step or two-step assay. In the one-step assay, RT and cDNA amplification processes are consolidated into one reaction. This assay format can provide rapid and reproducible results for high-throughput analysis. The challenge of the combined reaction process is the difficulty in optimizing the RT and amplification steps as they occur simultaneously, thereby leading to lower target amplicon generation. In the two-step assay, the reaction is carried out sequentially in separate tubes. This assay format is more sensitive than the one-step assay, but it is more time- and labor-consuming and requires optimization of additional parameters. Since the release of the SARS-CoV-2 genomic sequence, many RT-qPCR and RT-LAMP assays have been developed and used for the confirmation of many cases of SARS-CoV-2 infection during the course of the pandemic (Garafutdinov et al., 2020; Udugama et al., 2020).

RT-qPCR is the “gold standard” for molecular diagnostic assays and the method predominantly employed for diagnosing COVID-19 using respiratory tract samples (Garafutdinov et al., 2020; Udugama et al., 2020). It is a robust technique that reliably detects 30–50 copies of SARS-CoV-2 RNA molecules (Bruce et al., 2020; Gray et al., 2020) or less (Corman et al., 2020). However, RT-qPCR is a relatively time-consuming technique, requiring approximately 1.5–2 h.

RT-LAMP is an isothermal technique that provides a good alternative to PCR-based amplification assays. LAMP was first described in 2000 (Notomi et al., 2000). It uses a strand-displacing DNA polymerase, four or six primers, and provides a very fast and specific amplification of target DNA or cDNA at a constant temperature. One of the key advantages of using LAMP-based tests to detect infectious agents is the short duration of the assay (about 30–45 min for the DNA amplification stage). During the COVID-19 pandemic, rapid diagnostic assays such as RT-LAMP have become extremely important for high-throughput screening of patients. However, in several studies describing experiments on the detection of SARS-CoV-2 RNA molecules, RT-LAMP assays demonstrated less sensitivity than corresponding RT-qPCR tests, consistently detecting only 400–500 copies of RNA, with sporadic detection of as little as 120 copies (Gray et al., 2020; Zhang et al., 2020). Furthermore, RT-LAMP can generate false negative results up to 20% for patients with low viral loads testing positive by RT-qPCR (Ben-Assa et al., 2020; Butler et al., 2020).

Polymerase chain displacement reaction (PCDR) (Harris et al., 2013; Ignatov et al., 2014) and the newly developed PCR-LAMP technique (described below) are hybrid methods combining PCR-based thermocycling nucleic acid amplification with isothermal amplification. PCDR is a hybrid technique of PCR with strand displacement amplification (SDA). PCR-LAMP combines a PCR-like thermocycling mode at the initial stage of amplification with an isothermal LAMP mode during the following stage. The hybrid methods combine both the high sensitivity of PCR and the fast assay rate of isothermal amplification. In this work, we demonstrate the feasibility of applying the hybrid techniques of PCR thermocycling with SDA and LAMP isothermal amplification in the detection of SARS-CoV-2 viral RNA.

## MATERIALS AND METHODS

### Enzymes and Reagents

Moloney Murine Leukemia Virus (M-MLV) reverse transcriptase was supplied by Thermo Fisher Scientific (Carlsbad, CA, United States). Reverse (reverse transcriptase enzyme), SD HotStart DNA polymerase (10 U/ $\mu$ L), SD DNA polymerase (100 U/ $\mu$ L), and 10 $\times$  SD polymerase reaction buffer were supplied by Bioron GmbH (Römerberg, Germany). dNTPs were obtained from Bioline Limited (London, United Kingdom). Oligonucleotide primers were synthesized by Syntol JSC (Moscow, Russia). SARS-CoV-2 viral RNA (isolate—SARS-CoV-2/human/RUS/20200417\_10/2020; GenBank accession number MT890462) (25,000 copies/ $\mu$ L) was supplied by Syntol JSC. The concentration of the RNA was verified by RT-qPCR with positive synthetic SARS-CoV-2 RNA Control 2 (SKU: 102024) from Twist Bioscience (San Francisco, CA, United States) and SARS-CoV-2 RT-qPCR Detection Kit from Syntol JSC. The real-time amplification reactions were performed using a CFX96 Touch Real-Time Detection System (Bio-Rad Laboratories, Inc., Hercules, CA, United States).

### Two-Step RT-qPCR and RT-qPCR Assays

Reverse transcription (RT) reactions were performed using M-MLV reverse transcriptase according to the manufacturer's (Thermo Fisher Scientific) instructions. Briefly, the RT reaction mixtures (20  $\mu$ L each) were prepared as follows: RNA template solution (12  $\mu$ L) containing 20, 200, 2000, or 20,000 copies of SARS-CoV-2 viral RNA, or 50 ng of human total RNA as a negative control, were mixed with 4  $\mu$ L of 5 $\times$  first-strand buffer, 2  $\mu$ L of 0.1 M DTT, 1  $\mu$ L of 10 mM dNTP mix, 1  $\mu$ L of 10  $\mu$ M FP1 Primer (Supplementary Table S1) and 50 U of M-MLV reverse transcriptase. The RT mixtures were incubated for 50 min at 37°C and then 15 min at 70°C to inactivate the reaction.

For qPCDR and qPCR amplification of cDNA, 5  $\mu$ L of the RT mixtures (containing 25% of the cDNA generated) was added to 20  $\mu$ L of the respective qPCDR and qPCR master mixes that contained 1 $\times$  SD polymerase reaction buffer, 0.5 U/ $\mu$ L SD HotStart DNA polymerase, 3 mM MgCl<sub>2</sub>, 0.35 mM dNTPs (each), and 0.4 $\times$  SYBR Green I intercalating dye. The qPCR master mix contained two primers: FP2 and RP2 (0.4  $\mu$ M each). The qPCDR master mix contained four primers: two inner primers FP2 and RP2 (0.4  $\mu$ M each), and two outer primers FP1 and RP1 (0.2  $\mu$ M each). The primers are described in Supplementary Table S1. Amplifications were carried out using a Bio-Rad CFX96 PCR machine and the following protocol: initial preheating at 92°C for 3 min, followed by 50 cycles: 92°C (10 s), and 68°C (30 s).

### One-Step RT-q(PCR-LAMP) and RT-qLAMP Assays

RT-q(PCR-LAMP) and RT-qLAMP assay reactions (25  $\mu$ L) contained either 5, 50, 500, or 5000 copies of SARS-CoV-2 viral RNA or 50 ng of human total RNA as a negative control, 1 $\times$  SD polymerase reaction buffer, 10 mM DTT, 3.5 mM MgCl<sub>2</sub>, 0.5 mM



dNTPs (each), 0.275× SYBR Green I intercalating dye, 0.4 U/μL Reverse reverse transcriptase, 4 U/μL SD DNA polymerase, and six primers (**Supplementary Table S1**): outer primers (F3 and B3; 0.16 μM each), inner primers (FIP and BIP; 1.6 μM each), and loop primers (LF and LB; 1.2 μM each).

The RT step of the assays was carried out as follows: 30 s at 58°C and then 7 min at 50°C, followed by qLAMP or q(PCR-LAMP) reactions. qLAMP was performed at 66°C for 40 min. q(PCR-LAMP) was carried out with an initial preheating at 92°C for 15 s, followed by 1, 2, 4, or 6 PCR cycles: 92°C (5 s) and 66°C (15 s), followed by isothermal amplification at 66°C for 35 min.

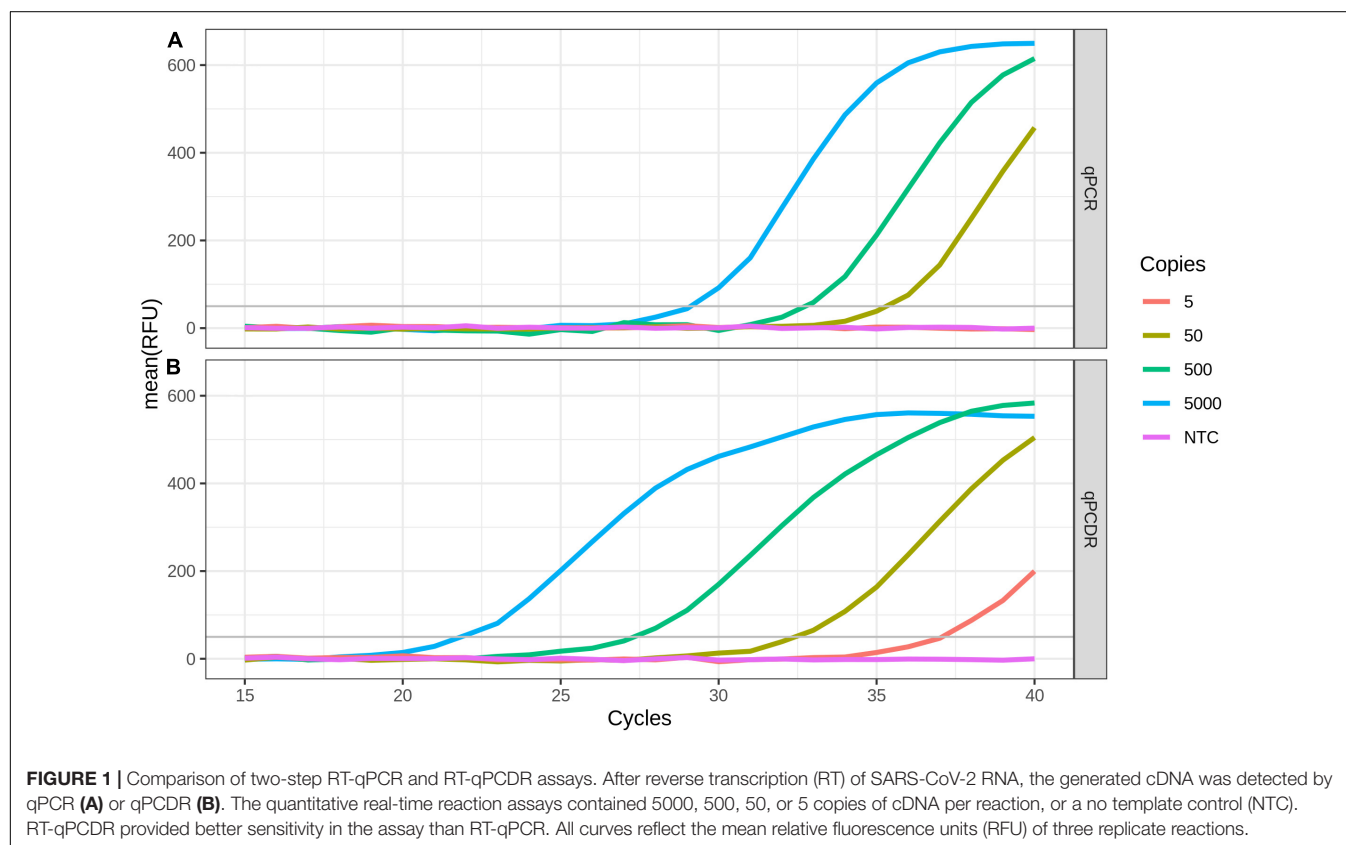
## Data Analysis

All calculations were conducted with R language usage (R Core Team, 2019). Besides standard functions, several packages were used including RDML for raw amplification data manipulation (Rödiger et al., 2017), chipPCR for Cq calculation (Rödiger et al., 2015), and ggplot2 for generation of plots (Wickham, 2016).

## RESULTS

### RT-qPCDR Versus RT-qPCR

The sensitivity of the RT-qPCDR and RT-qPCR techniques in detecting SARS-CoV-2 RNA was evaluated using the two-step assay in which the RT and cDNA amplification steps were performed in two separate reactions. SD DNA polymerase used to amplify the cDNA is a thermostable Taq DNA polymerase mutant that has strong 5′–3′ strand displacement and 5′–3′ polymerase activities. This polymerase is suitable for PCR, PCDR, and isothermal DNA amplifications (Ignatov et al., 2014; Shchit et al., 2017; Smith, 2017; Alyethodi et al., 2018; Lou et al., 2018; Wang et al., 2018). The mixes for performing either qPCR or qPCDR were identical, except for two extra outer primers added in case of qPCDR. RT-qPCDR yielded better Cq values (−ΔCq approximately 5–7 cycles) and at least a ten-fold improvement in sensitivity than that of RT-qPCR (**Figure 1** and **Table 1**). Under the experimental conditions, the qPCDR-based test detected as



**TABLE 1 |** qPCR and qPCDR amplification of SARS-CoV-2 cDNA.

SARS-CoV-2 cDNA copies per reaction	5000	500	50	5	NTC
Cq of qPCR	29.61 ± 0.04	33.25 ± 0.07	35.94 ± 0.04	NA	NA
Cq of qPCDR	22.72 ± 0.06	28.09 ± 0.05	33.20 ± 0.09	37.66 ± 1.36	NA
ΔCq	6.89	5.16	2.74	–	–

The mean quantification cycles (Cq) ± standard deviation of three replicates for the indicated cDNA copy numbers are provided. The amplifications were carried out with SD HotStart DNA polymerase using a series of SARS-CoV-2 cDNA templates with 10-fold dilutions from 5000 to 5 copies per reaction (NTC, no template control). ΔCq is the difference between the Cq of the qPCR and qPCDR for each template dilution.



few as 5 copies of SARS-CoV-2 cDNA in less than 40 cycles. In contrast, the qPCR-based test provided consistent detection only at 50 copies of viral cDNA per reaction in 38–40 cycles.

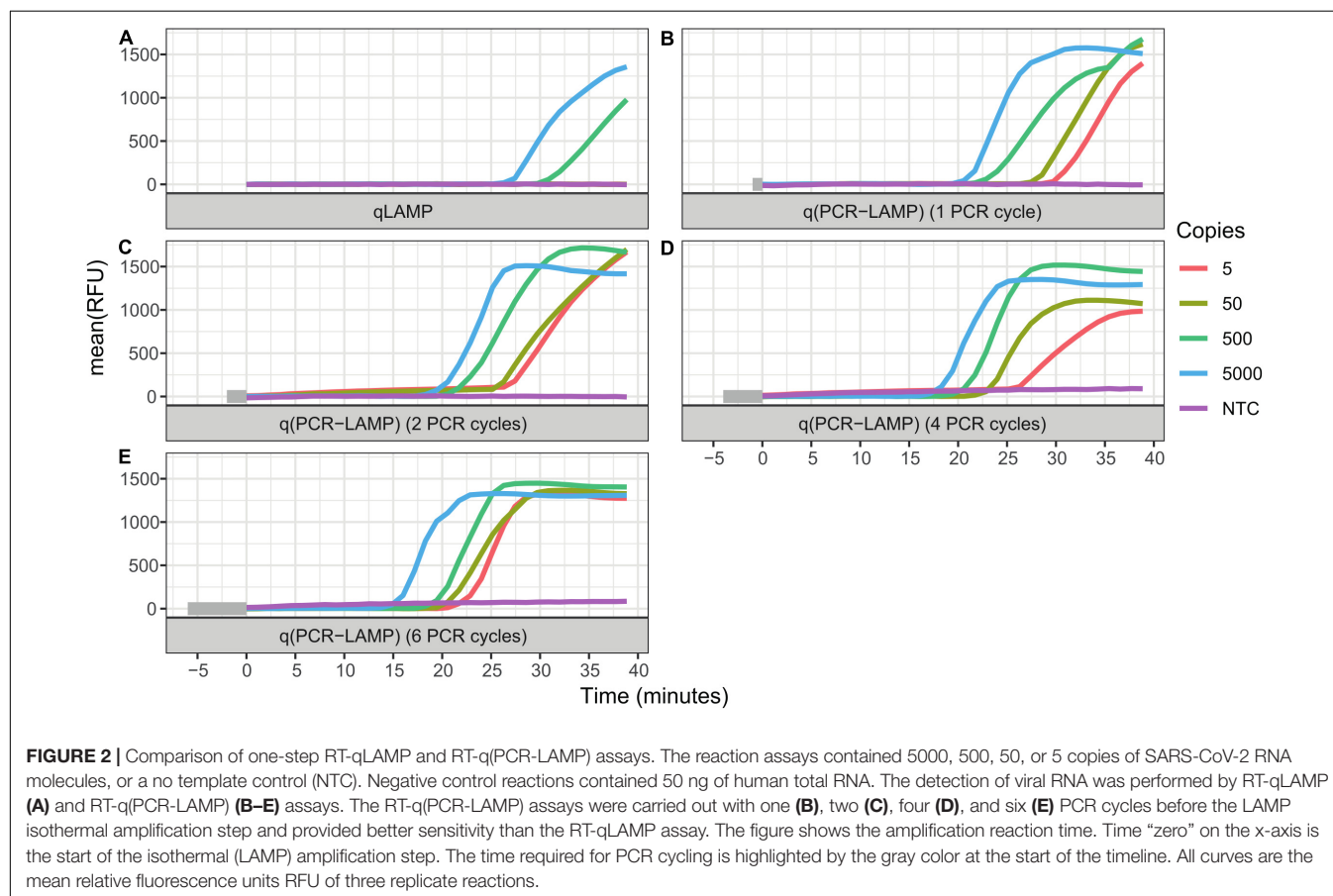
## RT-q(PCR-LAMP) Versus RT-qLAMP

The standard RT-qLAMP and hybrid RT-q(PCR-LAMP) reactions were performed in a one-step assay, where RT and cDNA amplification were carried out in the reaction mixture containing both Reverse reverse-transcriptase and SD DNA polymerase. The standard RT-qLAMP assay was able to detect only 500 copies of SARS-CoV-2 RNA per reaction (**Figure 2** and **Table 2**). In contrast, the RT-q(PCR-LAMP) test provided consistent detection at levels as low as 5 copies per reaction

(lower titers were not tested). Increasing the number of PCR cycles up to six before LAMP improved the assay results, but additional cycles beyond six did not provide any additional benefit (data not shown).

## DISCUSSION

During the COVID-19 pandemic, the availability of rapid diagnostic assays is extremely important for high-throughput screening of individuals. For the fast and sensitive detection of a target nucleic acid, we offer a new approach for DNA amplification, combining PCR and isothermal amplification techniques in one assay.



**TABLE 2 |** Comparison of RT-qLAMP and RT-q(PCR-LAMP) assays.

SARS-CoV-2 RNA copies per reaction	5000	500	50	5	NTC
Tq (min) of qLAMP	27.51 ± 0.24	31.47 ± 3.72	NA	NA	NA
Tq (min) of q(PCR-LAMP); 1 cycle of PCR	21.30 ± 0.98	23.44 ± 4.27	28.44 ± 5.03	30.40 ± 3.39	NA
Tq (min) of q(PCR-LAMP); 2 cycles of PCR	19.88 ± 0.85	21.69 ± 1.72	25.83 ± 5.44	26.86 ± 6.17	NA
Tq (min) of q(PCR-LAMP); 4 cycles of PCR	18.10 ± 0.29	20.70 ± 0.89	23.31 ± 4.18	26.24 ± 5.06	NA
Tq (min) of q(PCR-LAMP); 6 cycles of PCR	15.56 ± 0.90	19.54 ± 0.67	20.81 ± 0.76	22.23 ± 0.93	NA

SARS-CoV-2 RNA was detected by RT-qLAMP and RT-q(PCR-LAMP) assays. The q(PCR-LAMP) amplifications were performed with 1, 2, 4, and 6 cycles of PCR. The table lists the mean quantification times (Tq) ± standard deviation of three replicates of the qLAMP and q(PCR-LAMP) reactions for the indicated RNA copy numbers. The assays were carried out with Reverse reverse-transcriptase and SD DNA polymerase using a series of SARS-CoV-2 RNA 10-fold dilutions from 5000 to 5 copies per reaction (NTC, no template control).

PCDR is the first method of DNA amplification, which combines PCR and isothermal amplification technique, was described in 2013. It is a hybrid of PCR and isothermal SDA. The technique requires heat denaturation of dsDNA, as in conventional PCR, as well as the strand displacement activity of DNA polymerase, as in SDA. In PCDR, at least four primers are employed and amplification is initiated simultaneously from the outer primers and the inner primers. By using a DNA polymerase with the strand displacement activity, the inner DNA strands are displaced during DNA synthesis from the outer primers and can be used as additional template strands for DNA amplification. As a result, PCDR enhances DNA amplification more than two-times per cycle as compared with the standard two-primer PCR. The schematic, mechanism and kinetics of PCDR amplification have been described previously (Harris et al., 2013; Ignatov et al., 2014). We used RT-qPCDR for the detection of SARS-CoV-2. The use of qPCDR allowed us to detect as few as 5 copies of SARS-CoV-2 cDNA in the reaction in less than 40 cycles, which took about 45–50 min. Under similar conditions, conventional qPCR was able to detect only 50 copies of cDNA. Thus, in agreement with earlier described findings (Harris et al., 2013; Ignatov et al., 2014; Lou et al., 2018; Wang et al., 2018), the PCDR-based assay demonstrated higher efficiency and at least a ten-fold increased sensitivity than that of the PCR-based assay (**Figure 1** and **Table 1**).

LAMP is a fast and specific isothermal method for DNA amplification. Unfortunately, the use of LAMP for SARS-CoV-2 detection provides robust detection of the virus only if a few hundred (or more) copies of viral RNA are present in the reaction assay (Gray et al., 2020; Zhang et al., 2020). Lower amounts of viral RNA generate a large proportion of false negative results (Ben-Assa et al., 2020); thus, the improvement of assay sensitivity is very important. In an attempt to improve sensitivity, we combined LAMP and PCR and added several PCR cycles before the isothermal amplification. Our hypothesis was that in the case of a low amount of cDNA, the additional PCR cycles would provide amplification of the starting material to the level of DNA copies, which would be sufficient to ensure the start of LAMP. For example, 6 PCR cycles can amplify 5 copies of a target DNA up to 320 copies, which is sufficient for the fast and specific initiation of LAMP. Also, an increase in the number of PCR cycles before LAMP leads to a decrease in the time ( $T_q$ ) of the LAMP stage in the qPCR-LAMP assays.

The results of the RT-qLAMP and RT-q(PCR-LAMP) assays (**Figure 2** and **Table 2**) demonstrated that RT-q(PCR-LAMP) was approximately 100-fold more sensitive than conventional RT-qLAMP. The use of RT-q(PCR-LAMP) allowed us to detect as few as 5 copies of SARS-CoV-2 RNA per reaction and required only 35 min for the amplification step, including 6 cycles of PCR.

## CONCLUSION

In conclusion, the hybrid methods of DNA amplification combined with PCR and isothermal amplification, such as PCDR and PCR-LAMP, allowed us to markedly improve the results of

SARS-CoV-2 detection in comparison with conventional PCR and LAMP assays. The hybrid methods reduced the testing time and/or increased the sensitivity against standard amplification methods. The described RT-qPCDR and RT-q(PCR-LAMP) methods are fast and very sensitive and can be used for SARS-CoV-2 RNA detection.

## DATA AVAILABILITY STATEMENT

The original contributions presented in the study are included in the article/**Supplementary Material**, further inquiries can be directed to the corresponding authors.

## AUTHOR CONTRIBUTIONS

VK and KI were responsible for obtaining funding for the research. DV, KB, VK, and KI contributed to conception and design of the study and data curation. DV, KB, and KI were involved in the investigation and methodology development. KB, VK, and KI carried out the formal analysis. ES, VK, and KI validated the results. ES and KI supervised the research and contributed to the manuscript review and revision. KB, ES, and KI wrote the first draft of the manuscript. KI was responsible for obtaining the necessary resources and preparing visuals. All authors contributed to the article and approved the submitted version.

## FUNDING

The authors declare that this study received funding from the Russian State Budget (Grant number 0112-2019-0001). The funder had no role in the study design, data collection and analysis, decision to publish, or preparation of the manuscript. Syntol JSC provided support in the form of salary for DV, but did not have any additional role in the study design, data collection and analysis, decision to publish, or preparation of the manuscript.

## ACKNOWLEDGMENTS

We thank Dr. Mikhail Chanyshv from Pirogov Medical University (Moscow, Russia) who helped us in our experiments and Syntol JSC (Moscow, Russia) for support of this project. We would also like to thank Editage ([www.editage.com](http://www.editage.com)) for English language editing.

## SUPPLEMENTARY MATERIAL

The Supplementary Material for this article can be found online at: <https://www.frontiersin.org/articles/10.3389/fbioe.2020.604793/full#supplementary-material>

## REFERENCES

- Alyethodi, R. R., Singh, U., Kumar, S., Alex, R., Deb, R., Sengar, G. S., et al. (2018). T-ARMS PCR genotyping of SNP rs445709131 using thermostable strand displacement polymerase. *BMC Res. Notes* 11:132. doi: 10.1186/s13104-018-3236-6
- Ben-Assa, N., Naddaf, R., Gefen, T., Capucha, T., Hajjo, H., Mandelbaum, N., et al. (2020). SARS-CoV-2 on-the-spot virus detection directly from patients. *medRxiv* [Preprint]. doi: 10.1101/2020.04.22.20072389
- Bruce, E. A., Tighe, S., Hoffman, J. J., Laaguib, P., Gerrard, D. L., Diehl, S. A., et al. (2020). RT-qPCR Detection of SARS-CoV-2 RNA from patient nasopharyngeal swab using qiagen rneasy kits or directly via omission of an rna extraction step. *bioRxiv* [Preprint]. doi: 10.1101/2020.03.20.001008
- Butler, D. J., Mozsary, C., Meydan, C., Danko, D., Foox, J., Rosiene, J., et al. (2020). Shotgun transcriptome and isothermal profiling of SARS-CoV-2 infection reveals unique host responses, viral diversification, and drug interactions. *bioRxiv* [Preprint]. doi: 10.1101/2020.04.20.048066
- Chu, D. K. W., Pan, Y., Cheng, S. M. S., Hui, K. P. Y., Krishnan, P., Liu, Y., et al. (2020). Molecular diagnosis of a novel coronavirus (2019-nCoV) causing an outbreak of pneumonia. *Clin. Chem.* 66, 549–555. doi: 10.1093/clinchem/hvaa029
- Corman, V. M., Landt, O., Kaiser, M., Molenkamp, R., Meijer, A., Chu, D. K., et al. (2020). Detection of 2019 novel coronavirus (2019-nCoV) by real-time RT-PCR. *Eurosurveillance* 25:2000045. doi: 10.2807/1560-7917.ES.2020.25.3.2000045
- Garafutdinov, R. R., Mavzyutov, A. R., Alekseev, Y. I., Vorobev, A. A., Nikonov, Y. M., Chubukova, O. V., et al. (2020). Human betacoronaviruses and their highly sensitive detection by PCR and other amplification methods. *Biomics* 12, 121–179. doi: 10.31301/2221-6197.bmcs.2020-7
- Gray, A. N., Ren, G., Zhang, Y., Tanner, N., and Nichols, N. M. (2020). *Facilitating Detection of SARS-CoV-2 Directly From Patient Samples: Precursor Studies with RT-qPCR and Colorimetric RT-LAMP Reagents*. Ipswich, MA: New England Biolabs. Application Note.
- Harris, C., Sanchez-Vargas, I., Olson, K., Alphe, L., and Fu, G. (2013). Polymerase chain displacement reaction. *BioTechniques* 54, 93–97. doi: 10.2144/000113951
- Ignatov, K. B., Barsova, E. V., Fradkov, A. F., Blagodatskikh, K. A., Kramarova, T. V., and Kramarov, V. M. (2014). A strong strand displacement activity of thermostable DNA polymerase markedly improves the results of DNA amplification. *BioTechniques* 57, 81–87. doi: 10.2144/000114198
- Jiang, S., and Shi, Z.-L. (2020). The first disease X is caused by a highly transmissible acute respiratory syndrome coronavirus. *Viol. Sin.* 35, 263–265. doi: 10.1007/s12250-020-00206-5
- Lou, B., Song, Y., RoyChowdhury, M., Deng, C., Niu, Y., Fan, Q., et al. (2018). Development of a tandem repeat-based polymerase chain displacement reaction method for highly sensitive detection of 'Candidatus Liberibacter asiaticus'. *Phytopathology* 108, 292–298. doi: 10.1094/PHYTO-06-17-0210-R
- Lu, R., Wu, X., Wan, Z., Li, Y., Zuo, L., Qin, J., et al. (2020). Development of a novel reverse transcription loop-mediated isothermal amplification method for rapid detection of SARS-CoV-2. *Viol. Sin.* 35, 344–347. doi: 10.1007/s12250-020-00218-1
- Notomi, T., Okayama, H., Masubuchi, H., Yonekawa, T., Watanabe, K., Amino, N., et al. (2000). Loop-mediated isothermal amplification of DNA. *Nucleic Acids Res.* 28, e63–e63. doi: 10.1093/nar/28.12.e63
- R Core Team (2019). *R: A Language and Environment for Statistical Computing*. Vienna: R Foundation for Statistical Computing.
- Rödiger, S., Burdukiewicz, M., and Schierack, P. (2015). chipPCR: an R package to pre-process raw data of amplification curves. *Bioinformatics* 31, 2900–2902. doi: 10.1093/bioinformatics/btv205
- Rödiger, S., Burdukiewicz, M., Spiess, A.-N., and Blagodatskikh, K. (2017). Enabling reproducible real-time quantitative PCR research: the RDML package. *Oxford Bioinform.* 33, 4012–4014. doi: 10.1093/bioinformatics/btx528
- Shchit, I. Y., Ignatov, K. B., Kudryavtseva, T. Y., Shishkova, N. A., Mironova, R. I., Marinin, L. I., et al. (2017). The use of loop-mediated isothermal DNA amplification for the detection and identification of the anthrax pathogen. *Mol. Genet. Microbiol. Virol.* 32, 100–108. doi: 10.3103/S0891416817020094
- Smith, O. (2017). Rapid, field-based screening for chital (*Axis axis*) DNA in illegal meat markets. *Conserv. Genet. Resour.* 9, 523–525. doi: 10.1007/s12686-017-0714-4
- Udugama, B., Kadhiresan, P., Kozłowski, H. N., Malekjahani, A., Osborne, M., Li, V. Y. C., et al. (2020). Diagnosing COVID-19: the disease and tools for detection. *ACS Nano* 14, 3822–3835. doi: 10.1021/acsnano.0c02624
- Wang, J., Li, H., Li, T., Zhang, J., and Ling, L. (2018). An efficient template-independent polymerase chain displacement reaction for the detection of *Salmonella typhimurium*. *Anal. Methods* 10, 4229–4232. doi: 10.1039/C8AY01625A
- Wickham, H. (2016). *ggplot2: Elegant Graphics for Data Analysis*. New York, NY: Springer-Verlag.
- Wu, F., Zhao, S., Yu, B., Chen, Y.-M., Wang, W., Song, Z.-G., et al. (2020). A new coronavirus associated with human respiratory disease in China. *Nature* 579, 265–269. doi: 10.1038/s41586-020-2008-3
- Yip, C. C.-Y., Ho, C.-C., Chan, J. F.-W., To, K. K.-W., Chan, H. S.-Y., Wong, S. C.-Y., et al. (2020). Development of a novel, genome subtraction-derived, SARS-CoV-2-Specific COVID-19-nsp2 real-time RT-PCR assay and its evaluation using clinical specimens. *Int. J. Mol. Sci.* 21:2574. doi: 10.3390/ijms21072574
- Zhang, Y., Odiwuor, N., Xiong, J., Sun, L., Nyaruaba, R. O., Wei, H., et al. (2020). Rapid molecular detection of SARS-CoV-2 (COVID-19) Virus RNA using colorimetric LAMP. *medRxiv* [Preprint]. doi: 10.1101/2020.02.26.20028373
- Zhou, P., Yang, X.-L., Wang, X.-G., Hu, B., Zhang, L., Zhang, W., et al. (2020). A pneumonia outbreak associated with a new coronavirus of probable bat origin. *Nature* 579, 270–273. doi: 10.1038/s41586-020-2012-7
- Zhu, N., Zhang, D., Wang, W., Li, X., Yang, B., Song, J., et al. (2020). A novel coronavirus from patients with pneumonia in China, 2019. *N. Engl. J. Med.* 382, 727–733. doi: 10.1056/NEJMoa2001017

**Conflict of Interest:** DV is employed by Syntol JSC. The SD polymerase used in this study is the subject of a patent application (US20160145588, EP2981609). This does not alter the authors' adherence to the *Frontiers'* policies on sharing data and materials.

The remaining authors declare that the research was conducted in the absence of any commercial or financial relationships that could be construed as a potential conflict of interest.

Copyright © 2020 Varlamov, Blagodatskikh, Smirnova, Kramarov and Ignatov. This is an open-access article distributed under the terms of the Creative Commons Attribution License (CC BY). The use, distribution or reproduction in other forums is permitted, provided the original author(s) and the copyright owner(s) are credited and that the original publication in this journal is cited, in accordance with accepted academic practice. No use, distribution or reproduction is permitted which does not comply with these terms.



# Genetic Information Insecurity as State of the Art

Garrett J. Schumacher<sup>1,2,3\*</sup>, Sterling Sawaya<sup>1</sup>, Demetrius Nelson<sup>1</sup> and Aaron J. Hansen<sup>2,3</sup>

<sup>1</sup> GeneInfoSec Inc., Boulder, CO, United States, <sup>2</sup> Technology, Cybersecurity and Policy Program, College of Engineering and Applied Science, University of Colorado Boulder, Boulder, CO, United States, <sup>3</sup> Department of Computer Science, College of Engineering and Applied Science, University of Colorado Boulder, Boulder, CO, United States

## OPEN ACCESS

### Edited by:

Segaran P. Pillai,  
United States Department  
of Homeland Security, United States

### Reviewed by:

Gerald Epstein,  
National Defense University,  
United States  
Siguna Mueller,  
Independent Researcher, Kaernten,  
Austria

### \*Correspondence:

Garrett J. Schumacher  
g@geneinfosec.com

### Specialty section:

This article was submitted to  
Biosafety and Biosecurity,  
a section of the journal  
Frontiers in Bioengineering and  
Biotechnology

**Received:** 05 August 2020

**Accepted:** 16 November 2020

**Published:** 08 December 2020

### Citation:

Schumacher GJ, Sawaya S,  
Nelson D and Hansen AJ (2020)  
Genetic Information Insecurity as  
State of the Art.  
Front. Bioeng. Biotechnol. 8:591980.  
doi: 10.3389/fbioe.2020.591980

Genetic information is being generated at an increasingly rapid pace, offering advances in science and medicine that are paralleled only by the threats and risk present within the responsible systems. Human genetic information is identifiable and contains sensitive information, but genetic information security is only recently gaining attention. Genetic data is generated in an evolving and distributed cyber-physical system, with multiple subsystems that handle information and multiple partners that rely and influence the whole ecosystem. This paper characterizes a general genetic information system from the point of biological material collection through long-term data sharing, storage and application in the security context. While all biotechnology stakeholders and ecosystems are valuable assets to the bioeconomy, genetic information systems are particularly vulnerable with great potential for harm and misuse. The security of post-analysis phases of data dissemination and storage have been focused on by others, but the security of wet and dry laboratories is also challenging due to distributed devices and systems that are not designed nor implemented with security in mind. Consequently, industry standards and best operational practices threaten the security of genetic information systems. Extensive development of laboratory security will be required to realize the potential of this emerging field while protecting the bioeconomy and all of its stakeholders.

**Keywords:** biotechnology, cyberbiosecurity, cybersecurity, genomics, laboratory, cloud services, databases, privacy

## INTRODUCTION

Genetic information contained in nucleic acids, such as deoxyribonucleic acid (DNA), has become ubiquitous in society, enabled primarily by rapid biotechnological development and drastic decreases in DNA sequencing and DNA synthesis costs (Naveed et al., 2015; Berger and Schneck, 2019). Innovation in these industries has far outpaced regulatory capacity and remained somewhat isolated from the information security and privacy domains. Human genetic data contains a wealth of sensitive information. It can be used to identify an individual (Lin et al., 2004; Lowrance and Collins, 2007; Erlich et al., 2018) and predict their physical characteristics (Lippert et al., 2017; Li et al., 2019). The identifiability of genetic information is a critical challenge leading to growing consumer privacy concerns (Baig et al., 2020). Yet, genetic data is not always defined as protected health information or personally identifiable data by law. Once digital genetic data is stolen or disclosed, it cannot be reissued or changed in the same manner as other information types. A single human whole genome sequence can cost hundreds to thousands of dollars per sample, and when



amassed, genetic information of large cohorts can be worth millions of dollars<sup>1,2,3</sup>. This positions human genetic information systems as likely targets for cyber and physical attacks, both of which could lead to global-scale impact.

It is also well known that biotechnology has a dual use nature leading to positive and negative applications, and genetic data of non-human sources is also valuable and can be considered sensitive. Synthetic biology has great potential to revolutionize many industries, but designer microbes can also be generated with CRISPR-Cas and other techniques that present global health and national security concerns (Salerno and Koelm, 2002; Chosewood and Wilson, 2009; Berger and Roderick, 2014; Werner, 2019). Microbiological genetic information systems are considered critical public health infrastructure (Fayans et al., 2020), plants can be manipulated to create potential health hazards (Mueller, 2019a), and methods for tracking genetically modified organisms can be exploited if appropriate techniques are not used (Mueller, 2019b). Sensitive genetic data of humans and other entities and their respective systems must be secured to prevent private to global risks (Jordan et al., 2020; Sawaya et al., 2020).

Security incidents surrounding genetic information systems are on the rise, and many relevant incidents have been documented by news sources<sup>4,5,6,7</sup> and breach notifications<sup>8,9,10,11,12,13,14,15</sup>. The most common reasons have been misconfigurations in cloud security settings, email phishing attacks, and the compromise of connected third-party systems. As a result, these groups may face legal action<sup>16</sup>, penalties, reputational loss, and many other risks and consequences. The National Health Service's Genomics England database in the United Kingdom has been targeted by nation-state

threat actors<sup>17</sup>, and 23andMe's Chief Security Officer said their database of around 10 million individuals is of extreme value and therefore "certainly is of interest to nation states."<sup>18</sup> Despite this recognition, proper measures to protect genetic information are often lacking under current practices in relevant industries and stakeholders.

Extensive work has been published surrounding the security of genetic information, highlighting that, as a newly developing field, cyberbiosecurity will require continuous assessment of risks as they emerge (Peccoud et al., 2018). Genetic information security is considered a critical aspect to comprehensive cyberbiosecurity and the bioeconomy (Institute of Medicine and National Research Council, 2006; Murch et al., 2018; Berger and Schneck, 2019; Murch and DiEuliis, 2019; Reed and Dunaway, 2019; Fayans et al., 2020; Jordan et al., 2020; National Academies of Sciences, Engineering, and Medicine, 2020; Sawaya et al., 2020). Multi-stakeholder and interdisciplinary collaboration, improved understanding of the security risks to biotechnology, characterization of biotechnology ecosystems, and assessment frameworks specific to biotechnology sectors and facility types will all be required in order to develop appropriate cyberbiosecurity countermeasures (Peccoud et al., 2018; Millett et al., 2019; Schabacker et al., 2019).

Toward the above issues and goals, this paper expands upon a previous microbiological genetic information system assessment (Fayans et al., 2020) by including a broader range of genetic information and system components, as well as novel concepts and additional vulnerabilities and threats to the ecosystem. Herein, genetic information systems are characterized from a security perspective, and the foundation for future assessments of these ecosystems has been established for which improvement and further development will be needed.

## METHODOLOGY

Confidential communications and interviews with leaders and technical personnel from eighteen relevant stakeholders occurred over the course of 9 months. These organizations can be broadly categorized as manufacturers and vendors, insurance and healthcare providers, research institutions, government and military groups, third-party service providers, and diagnostic laboratories. A third of these organizations contained one or more sequencing laboratories, and the remainder covered critical components of the system before or after sequencing laboratory stages. Several of the organizations allowed on-premise observation of, and interaction within, their environments, as well as in-depth uncredentialed and credentialed assessments of their property, people, processes, and technology. Specifically, DNA sequencing instruments as the point of raw data generation and other laboratory equipment and their networked data communications were focused on. Standard security tools and techniques were

<sup>1</sup><https://www.bloomberg.com/news/articles/2020-08-05/blackstone-said-to-reach-4-7-billion-deal-to-buy-ancestry-com>

<sup>2</sup><https://www.gsk.com/en-gb/media/press-releases/gsk-and-23andme-sign-agreement-to-leverage-genetic-insights-for-the-development-of-novel-medicines/>

<sup>3</sup><https://www.ancestry.com/corporate/newsroom/press-releases/ancestrydna-and-calico-to-research-the-genetics-of-human-lifespan>

<sup>4</sup><https://www.bloomberg.com/news/articles/2019-11-06/breach-at-dna-test-firm-veritas-exposed-customer-information>

<sup>5</sup><https://www.bostonherald.com/2019/08/22/mgh-data-breach-exposes-10000-patients/>

<sup>6</sup><https://www.latimes.com/business/la-fi-vitagene-dna-privacy-exposed-20190709-story.html>

<sup>7</sup><https://www.komando.com/security-privacy/ancestry-com-suffers-big-data-leak-300000-user-credentials-exposed/435921/>

<sup>8</sup><https://www.wizcase.com/blog/mackiev-leak-research/>

<sup>9</sup><https://blog.myheritage.com/2020/07/security-alert-malicious-phishing-attempt-detected-possibly-connected-to-gedmatch-breach/>

<sup>10</sup><https://www.ambrygen.com/legal/substitute-notice>

<sup>11</sup><https://media.dojmt.gov/wp-content/uploads/Data-Breach-NotificationDetails11.pdf>

<sup>12</sup><https://media.dojmt.gov/wp-content/uploads/Consumer-Notice-73.pdf>

<sup>13</sup><https://privacyrights.org/data-breaches/myriad-genetic-laboratories-inc>

<sup>14</sup><https://blog.myheritage.com/2018/06/myheritage-statement-about-a-cybersecurity-incident/>

<sup>15</sup><https://media.dojmt.gov/wp-content/uploads/Shire-Human-Genetic-Therapies-Inc.pdf>

<sup>16</sup><https://www.classaction.org/news/ambry-genetics-corp-hit-with-class-action-over-jan-2020-data-breach-affecting-230000>

<sup>17</sup><https://www.telegraph.co.uk/news/2018/12/05/nhs-storing-patients-genetic-data-high-security-army-base-due/>

<sup>18</sup><https://www.telegraph.co.uk/technology/2020/03/09/dna-testing-firms-risk-state-sponsored-hacks-says-23andme-security/>



applied, such as vulnerability scanning, packet monitoring, threat modeling, configuration assessment, digital forensics, and full-stack assessments, including hardware teardowns and dynamic and static analysis of various software components. Organizational policies, external regulations, and other relevant items were also examined. Specific details and results have been omitted for confidentiality purposes. Such activities provided insight into the stakeholders' perceptions, external requirements, implementations, concerns, and weaknesses regarding the security of their genetic information systems and organizations overall. This manuscript is primarily a summary of the researchers' practical experience and direct observation of laboratory infrastructure backed by literature and industry input. Observed vulnerabilities and threats uncovered in the research have been reported to the appropriate agencies and stakeholders; this information will be made public once ethical disclosure and mitigation processes have concluded.

## THE GENETIC INFORMATION THREAT LANDSCAPE

Confidentiality, integrity, and availability are the core principles governing the security of sensitive systems and information (International Organization for Standardization [ISO], 2012). Confidentiality is the principle of ensuring access to assets is restricted based upon the assets' sensitivity. Integrity is the concept of protecting assets from unauthorized modification or deletion, while availability ensures assets are accessible to authorized parties at all times. Genetic information, which includes both biological material and digital genetic data, is the primary asset of concern, and associated assets, such as metadata, electronic health records and intellectual property, are also vulnerable within these systems. Genetic information systems are centered around one or more genetic sequencing devices, and include all inputs and outputs of these sequencing devices, as well as all upstream or downstream components that handle those data or materials.

Genetic information systems are distributed cyber-physical systems containing numerous stakeholders (**Supplementary Appendix 1**), personnel, and devices with extensive computing and networking capabilities (Reed and Dunaway, 2019; **Figure 1**). Software, hardware, and many other components introduce attack vectors that can be used to compromise these systems (**Figure 1**), including through purposefully adversarial activity and human error. Organizations take steps to monitor and prevent error, and molecular biologists are skilled in laboratory techniques; however, they were found to commonly not have the expertise and resources to securely configure and operate these environments, nor are stakeholders always enabled to do so by third-party service contracts that we examined. Basic security features and tools, such as antivirus software, are usually recommended with little support given, and they can also easily be subverted. Advanced and comprehensive controls and policies are not commonly implemented. On-premise or adjacent network attacks could lead to certain devices, stakeholders, and individuals being affected, while supply chain and remote attacks

could lead to global-scale impact. Depending on the type and scale of a threat or exploit, hundreds to millions of people's data could be compromised.

## Personnel and Physical Access

Unauthorized physical access or insider threats could allow for theft of assets or the use of other attack vectors on any phase of the ecosystem. Small independent laboratories do not often have resources to implement strong physical security. Large institutions are usually enabled to maintain strong physical security, but the relatively large number of personnel and devices that need to be secured creates a complex attack surface. Ultimately, the strongest cybersecurity can be easily circumvented by weak physical security.

Insider threats are a problem for information security because personnel possess deeper knowledge of an organization and its systems. Many countries rely on foreign nationals working in biotechnological fields that may be susceptible to foreign influence<sup>19</sup>, and citizens can also be susceptible<sup>20</sup>. Personnel could introduce many exploits on-site if coerced or threatened (Reed and Dunaway, 2019; Walsh and Streilein, 2020). Even when not acting in a purposefully malicious manner, personnel can unintentionally compromise the integrity and availability of genetic information through error (US Office of the Inspector General, 2004). Appropriate safeguards should be in place to ensure that privileged individuals are empowered to do their work correctly and efficiently, but all activities should be documented and monitored when working with sensitive genetic information.

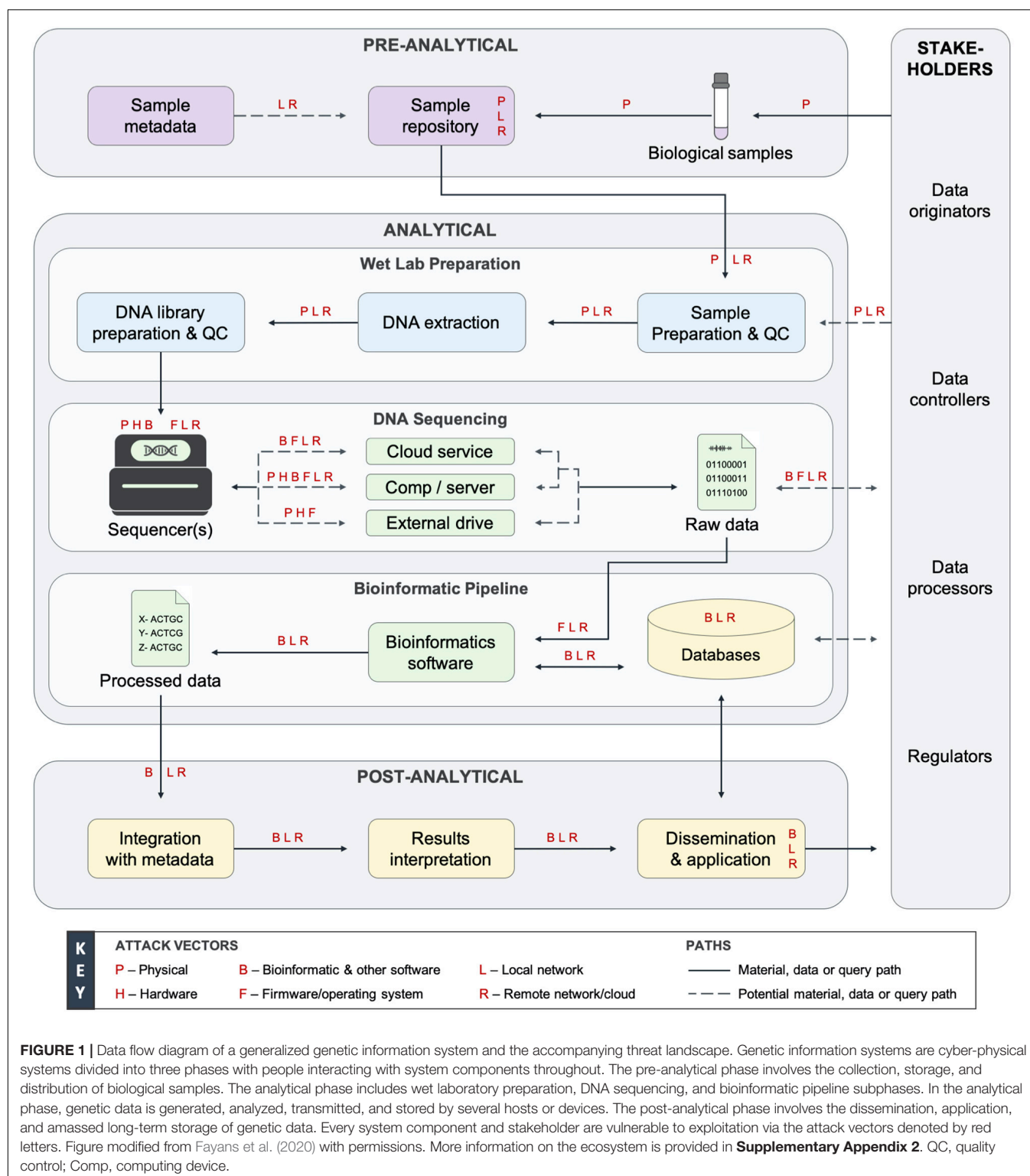
## Biological Samples, Metadata, and Repositories

Sample collection, storage, and distribution processes have received little recognition as legitimate points for the compromise of genetic information. Biological samples as inputs into this ecosystem can be modified maliciously to contain encoded malware, although this has to date only been demonstrated in a system in which the sequencing software was artificially engineered to include a vulnerability that would be triggered by the encoded malware (Ney et al., 2017). Biological samples could also be degraded, modified, or destroyed to compromise the materials, and resulting data's, integrity and availability. We found sample repository and storage equipment to often be connected to networks for monitoring purposes, making them vulnerable to adjacent network and remote attacks. Biorepositories and the collection and distribution of samples could be targeted to steal numerous biological samples, such as in known genetic testing scams<sup>21</sup>, and targeted exfiltration of small numbers of samples may be difficult to detect. The storage, transit, and destruction of sensitive biological material should be considered by stakeholders to be an important facet of overall genetic information security and cyberbiosecurity.

<sup>19</sup><https://www.fbi.gov/investigate/counterintelligence/foreign-influence>

<sup>20</sup><https://www.sciencemag.org/news/2020/06/fifty-four-scientists-have-lost-their-jobs-result-nih-probe-foreign-ties>

<sup>21</sup><https://oig.hhs.gov/fraud/consumer-alerts/alerts/geneticcam.asp>



Though potentially unlikely, other organizations within the ecosystem could be targeted for the theft of samples and processed DNA libraries, as well. The wet laboratory preparation and DNA sequencing subphases last several weeks and produce unused waste and stored material. At the

conclusion of sequencing runs, the consumables that contain DNA molecules are not always considered sensitive and can be found unwittingly maintained in many laboratories. Several cases have been documented of DNA being recovered and successfully sequenced while aged for years in non-controlled

environments (Colotte et al., 2011). Limited attention is paid to the secure destruction of consumables or other potential sources of biological material as there is little concern for such targeted attacks.

## Laboratories and Equipment

DNA sequencing systems and laboratories were found to be multifaceted in their design and threat profile. DNA sequencing instruments have varying scalability of throughput, cost, and unique considerations for secure operation (Table 1). They have built-in computers and commonly have connected computers and servers for data storage, networking, and analytics. Sequencing system devices contain a number of different hardware components, firmware, software, and operating systems, including insecure legacy versions (National Academies of Sciences, Engineering, and Medicine, 2020). Wireless or wired local network and remote Internet connections are required for maintenance, data transmission, and analytics in most operations. Wireless capabilities and Bluetooth technology were commonly found within laboratories, presenting unnecessary access vectors and threats to these systems.

Device vendors obtain various internal hardware components from several sources and integrate them into laboratory devices that contain vendor-specific intellectual property and software. Generic hardware components are often produced in various countries, which is cost effective but leads to insecurities and a lack of hardening for specific end-use purposes. Hardware vulnerabilities could be exploited on-site, or they can be implanted during manufacturing and supply-chain processes for widespread and unknown security issues (Anderson and Kuhn, 1997; Schwartz et al., 2017; Ender et al., 2020; Fayans et al., 2020). Such hardware issues are unpatchable and will remain with devices forever until newer devices can be manufactured to replace older versions. Unfortunately, adversaries can always shift their techniques to create novel vulnerabilities within new hardware in a continual vicious cycle.

Third-party manufacturers and device vendors implement firmware in these hardware components. Embedded device firmware has been shown to be more susceptible to cyberattacks than other forms of software (Schwartz et al., 2017). In-field upgrades are difficult to implement, and like hardware, firmware and operating systems can be maliciously altered within the supply chain (Fayans et al., 2020). A firmware-level exploit would allow for the evasion of operating system and software-level security features. Firmware exploits can remain hidden for long periods, even after hardware replacements or wiping and restoring to default factory settings. For example, operating systems have specific disclosed Common Vulnerabilities and Exposures (CVEs)<sup>22</sup>. Additionally, researchers have confirmed the possibility of index hopping, or index misassignment, by sequencing device software, resulting in customers receiving confidential data from other customers (Ney et al., 2017) or downstream data processors inputting incorrect data into their analyses. Some software vulnerabilities can be partially mitigated by frequent updates. However, operating systems and

firmware are typically updated every 6–12 months by a field agent accessing a sequencing device on site. Device operators are not allowed to modify the device in any way, yet they are responsible for security aspects of this equipment. With ubiquitous implementation throughout the ecosystem, software issues are especially concerning (National Academies of Sciences, Engineering, and Medicine, 2020).

DNA sequencing infrastructure is proliferating, and sequencing services are becoming more affordable. In 2020, technology developed by Beijing Genomics Institute has finally resulted in the \$100 human genome (Drmanac, 2020) while US prices remain around \$1,000 per sample. Stakeholders often take advantage of cheaper services by third-party sequencing providers that reside across national borders (Office of the US Trade Representative, 2018), indicating that genetic data could be aggregated globally by nation-states<sup>23</sup> and other actors during the analysis phase.

## Storage and Compute Infrastructure

Raw signal sequencing data are stored on a sequencing system's memory and are transmitted to one or more endpoints. Transmitting data securely across a local network requires internal information technology (IT) configurations. Vendor documentation usually mentions implementing a firewall to secure sequencing systems. Doing so correctly requires deep knowledge of secure networking and vigilance of network activity. Documentation also commonly mentions disabling and enabling certain network protocols and ports and further measures that can be difficult for most small- to medium-sized organizations, while also omitting other common controls and mitigations.

Laboratories and DNA sequencing systems are connected to third-party services, and laboratories have little control over the security posture of these connections. Independent cloud platforms and DNA sequencing vendors' cloud platforms are implemented for bioinformatic processing, data storage, and device monitoring and maintenance capabilities (Table 1). Multi-factor authentication, role- and task-based access, and many other security measures are not common in these platforms. Misconfigurations to cloud services and remote communications are a primary vulnerability to genetic information, demonstrated by prior breaches. Laboratory information management systems (LIMS) are also frequently implemented within laboratories and connected to sequencing systems and laboratory networks (Roy et al., 2016), and DNA sequencing vendors provide their own LIMSs as part of their cloud offerings. Even when LIMS and cloud platforms meet all regulatory requirements for data security and privacy, they are handling data that is not truly anonymized and therefore remains identifiable and sensitive. Furthermore, specific CVEs have been disclosed for dnaTools' dnaLIMS product<sup>24</sup> that were actively exploited

<sup>22</sup><https://cve.mitre.org/>

<sup>23</sup><https://www.fbi.gov/news/pressrel/press-releases/fbi-and-cisa-warn-against-chinese-targeting-of-covid-19-research-organizations>

<sup>24</sup><https://www.shorebreaksecurity.com/blog/product-security-advisory-psa0002-dnalims/>

**TABLE 1** | Overview of popular genetic sequencing devices and systems.

Vendor	Product	Time (h)	Output (Gb)	Operating system	Computing	Network connection	Cloud service (CSP)
Illumina	iSeq	19	1	Windows 10 & Windows 7	Standalone &/or external device	Wired or wireless	BaseSpace (AWS)
	MiniSeq	24	8				
	MiSeq	24	15				
	NextSeq	30	300				
	HiSeq	84	1,500				
	NovaSeq	44	6,000				
Oxford Nanopore Technologies	SmidgION <sup>M</sup>	–	~1	Android & iOS	External device	Wired or wireless	EPI2ME (AWS)
	Flongle <sup>M</sup>	16	2	Windows, Macintosh, Linux	External device	Wired	
	MinION Mk1B <sup>M</sup>	48	30				
	MinION Mk1C <sup>M</sup>	48	30	Linux (Ubuntu)	Standalone &/or external device		
	GridION Mk1	48	150				
	PromethION	72	8,600				
Pacific Biosciences	Sequel	20	50	Linux (Ubuntu & CentOS)	Standalone	Wired	SecureLink (AWS)
	Sequel II	30	4,000				
Applied Biosystems*	SeqStudio	2	~0.45	Windows 10	Standalone & external device	Wired or wireless	Thermo Fisher Cloud (AWS)
	3500/3500xL	2	–	Windows Vista SP1			
	3730/3730xL	3	–	Windows 2000 Pro			
Ion Torrent*	GeneStudio S5	8	50	Linux (Ubuntu)	Standalone & external device	Wired	
	Genexus	48	20				

Maximum run time in hours, maximum output in gigabytes, operating system, computing capabilities, network connection type, and cloud platform provided per vendor and product. Time and output are maximum values based on one full sequencing run. Information gathered from vendors' websites (<https://www.illumina.com/systems/sequencing-platforms.html>, <https://nanoporetech.com/products/>, <https://www.pacb.com/products-and-services/>, <https://www.thermofisher.com/us/en/home/brands/applied-biosystems.html>, <https://www.thermofisher.com/us/en/home/brands/ion-torrent.html>) and technical documentation (Supplementary Appendix 3). h, hours; Gb, gigabytes; CSP, cloud service provider; AWS, Amazon Web Services. \*Thermo Fisher Scientific brands; <sup>M</sup>Mobile sequencing instrument for in-field use.

by a foreign nation-state<sup>25</sup>. Phishing attacks are another major threat, as email services add to the attack surface in many ways. Sequencing service providers often share links granting access to datasets via email. These email chains are a primary trail of transactions that could be exploited to exfiltrate data on clients, metadata of samples, or genetic data itself.

Some laboratories transmit raw data directly to an external hard drive per customer or regulatory requirements. Reducing network activity in this way can greatly minimize the threat surface of sensitive genetic information. Separating networks and devices from other networks, or air gapping, while using hard drives is possible, but even air-gapped systems have been shown to be vulnerable to compromise (Guri et al., 2019; Guri, 2020). Sequencing devices are still required to be connected to the Internet for maintenance and are often connected between offline operations. Hard drives can be physically secured and transported; however, these methods are time and resource intensive, and external drives could be compromised for the injection of modified software or malware.

## Bioinformatic Pipeline

To determine the success of a sequencing run, bioinformatics analyses are necessary, but this software has not been commonly scrutinized in security contexts or subjected to the same adversarial pressure as other more mature software (National Academies of Sciences, Engineering, and Medicine, 2020). Open-source software is widely used across genomics, acquired from several online code repositories, and heavily modified for individual purposes, but it is only secure when security researchers are incentivized to assess these products. In a specialized and niche industry like genomics and bioinformatics, this is typically not the case. Bioinformatic programs have been found to be vulnerable due to poor coding practices, insecure function usage, and buffer overflows (Ney et al., 2017), such as the Burrow Wheeler Aligner (BWA) example<sup>26, 27</sup>. This program is hosted on cloud platforms and available for on-site use within laboratories. Researchers have also uncovered that algorithms can be forced to mis-classify by intentionally modifying data inputs, breaking the integrity

<sup>25</sup><https://www.zdnet.com/article/mysterious-iranian-group-is-hacking-into-dna-sequencers/>

<sup>26</sup>[https://share-ng.sandia.gov/news/resources/news\\_releases/genomic\\_cybersecurity/](https://share-ng.sandia.gov/news/resources/news_releases/genomic_cybersecurity/)

<sup>27</sup><https://nvd.nist.gov/vuln/detail/CVE-2019-10269>



of any resulting outputs (Finlayson et al., 2019). Nearly every imaginable algorithm, model type, and use case have been shown to be vulnerable to this kind of attack across many data types (Biggio and Roli, 2018), especially those relevant to raw signal and sequencing data formats. Similar attacks could be carried out in the processing of raw signal data internal to a sequencing system or on downstream bioinformatic analyses accepting raw sequencing data or processed data as an input.

## Dissemination Practices and Database Storage

Alarming amounts of human and other sensitive genetic data are publicly available<sup>28, 29, 30, 31, 32</sup> (Vinatzer et al., 2019). Several funding and publication agencies require public dissemination, so researchers commonly contribute to open and semi-open databases (Shi and Wu, 2017). Healthcare providers either house their own internal databases or disseminate to third-party databases. Their clinical data is protected like any other healthcare information as required by regulations; however, this data can be sold and aggregated by external entities. DTC companies keep their own internal databases closely guarded and can charge steep prices for third-party access. Data sharing is prevalent when the price is right. Data originators often have access to their genetic data and test results for download in plaintext. These reports can then be uploaded to public databases, such as GEDmatch and DNALand, for further analyses, including finding distant genetic relatives with a shared ancestor (Erich et al., 2018). A well-known use of such identification tactics was the infamous Golden State Killer case (Edge and Coop, 2019). Data sharing is dependent upon the data controller's wants and needs, barring any legal or business requirements from other involved stakeholders.

Genetic database vulnerabilities have been well studied and disclosed (Gymrek et al., 2013; Erlich and Narayanan, 2014; Naveed et al., 2015; Edge et al., 2017; Ney et al., 2018; Vinatzer et al., 2019; Edge and Coop, 2020; Ney et al., 2020). For example, the contents of the entire GEDmatch database could be leaked by uploading artificial genomes (Ney et al., 2020). Such an attack would violate the confidentiality of more than a million users' and their relatives' genetic data because the information is not truly anonymized. Even social media posts can be filtered for keywords indicative of participation in genetic research studies to identify research participants in public databases (Liu et al., 2019). All told, tens of millions of research participants, consumers, and relatives may already be at risk.

## DISCUSSION

Security is a spectrum; stakeholders must do everything they can to chase security as a best practice. Securing genetic information is a major challenge in this rapidly evolving

ecosystem. Attention has primarily been placed on the post-analytical phase of genetic information systems for security and privacy, but adequate measures have yet to be universally adopted. The pre-analytical and analytical phases are also vulnerable points for data compromise that must be addressed. Adequate national regulations are needed for security and privacy enforcement, incentivization, and liability, but legal protection is dictated by regulators' responses and timelines. However, data originators, controllers, and processors can take immediate action to protect their data.

Genetic information security is a shared responsibility between sequencing laboratories and device vendors, as well as all other involved stakeholders. To protect genetic information, laboratories, biorepositories, and other data processors need to create strong organizational policies and reinvestments toward their physical and cyber infrastructure. They also need to determine the sensitivity of their data and material and take necessary precautions to safeguard sensitive genetic information. Data controllers, especially healthcare providers and DTC companies, should reevaluate how their genetic data is generated and processed, with special consideration for the identifiability of human genetic data. Device vendors need to consider security when their products are being designed, implemented, and maintained throughout their lifecycles.

Many of these recommendations go against the current paradigms in genomics and related industries and will therefore take time, motivation, and incentivization before being actualized, with regulation being a critical factor. In order to secure and protect all stakeholders of genetic information systems, sequencing instrumentation, bioinformatics software, cloud platforms, data access models, and other system components need to be analyzed, and in-depth assessments of this threat surface will be required. Unique threat models and assessment frameworks are needed for specific and niche industry sectors, and genomics is a perfect example. Novel security and privacy countermeasures will need to be developed that protect the confidentiality of genetic information while ensuring its integrity for accurate diagnoses and applications and its availability for rapid public health responses. These security requirements will need to be balanced and dependent upon the context of use cases. These items will require collaborative engagement between stakeholders to reevaluate and implement improved security controls into genetic information systems (Berger and Schneck, 2019; Schabacker et al., 2019; Moritz et al., 2020). The development and implementation of genetic information security will foster a healthy and sustainable bioeconomy without damaging privacy or security.

There can be security without privacy, but privacy requires security. These two can be at odds with one another in certain contexts. For example, personal security aligns with personal privacy, whereas public security can require encroachment on personal privacy. A similar story is unfolding within genomics. Genetic data must be shared for public good, but this can jeopardize personal privacy. However, genetic data necessitates the strongest protections possible for public security and personal security. Appropriate genetic information security will simultaneously protect everyone's safety, health, and privacy.

<sup>28</sup>[https://my.pgp-hms.org/public\\_genetic\\_data](https://my.pgp-hms.org/public_genetic_data)

<sup>29</sup><https://gnomad.broadinstitute.org/downloads>

<sup>30</sup><https://platform.stjude.cloud/data/diseases>

<sup>31</sup>[https://www.ensembl.org/Homo\\_sapiens/Info/Index](https://www.ensembl.org/Homo_sapiens/Info/Index)

<sup>32</sup><https://www.completegenomics.com/public-data/>

## DATA AVAILABILITY STATEMENT

The datasets presented in this article are not readily available because the interviewed and assessed stakeholders involved in this work have requested anonymity and confidentiality due to their service agreements with vendors and the sensitivity of the information they supplied. Ethical vulnerability disclosures are ongoing with vendors and the US Cybersecurity and Infrastructure Security Agency that will be published in future manuscripts when appropriate to do so. Therefore, limited data is available beyond the findings presented within the manuscript and accompanying **Supplementary Material**. Requests to access the datasets should be directed to GS, [g@geneinfosec.com](mailto:g@geneinfosec.com).

## AUTHOR CONTRIBUTIONS

GS: inception and drafting of manuscript. GS, SS, and DN: literature review and analysis. GS, SS, DN, and AH: stakeholder engagement, interviews, and critical review of draft. GS and AH: security assessments. All authors contributed to the article and approved the submitted version.

## FUNDING

This project was funded equally by the GeneInfoSec Inc. and the Technology, Cybersecurity, and Policy Program at the University of Colorado Boulder.

## REFERENCES

- Anderson, R., and Kuhn, M. (1997). *Low cost attacks on tamper resistant devices*. In *International Workshop on Security Protocols*. Berlin: Springer, 125–136. doi: 10.1007/BFb0028165
- Baig, K., Mohamed, R., Theus, A. L., and Chiasson, S. (2020). “I’m hoping they’re an ethical company that won’t do anything that I’ll regret” Users Perceptions of At-home DNA Testing Companies,” in *Proceedings of the 2020 CHI Conference on Human Factors in Computing Systems*, (New York: United Nation), 1–13. doi: 10.1145/3313831.3376800
- Berger, K. M., and Roderick, J. (2014). *National and transnational security implications of big data in the life sciences*. Washington, DC: American Association for the Advancement of Science.
- Berger, K. M., and Schneck, P. A. (2019). National and transnational security implications of asymmetric access to and use of biological data. *Front. Bioengin. Biotechnol.* 7:21. doi: 10.3389/fbioe.2019.00021
- Biggio, B., and Roli, F. (2018). Wild patterns: Ten years after the rise of adversarial machine learning. *Pattern Recogn.* 84, 317–331. doi: 10.1016/j.patcog.2018.07.023
- Chosewood, L. C., and Wilson, D. E. (2009). *Biosafety in microbiological and biomedical laboratories*. Maryland: National Institutes of Health.
- Colotte, M., Coudy, D., Tuffet, S., and Bonnet, J. (2011). Adverse effect of air exposure on the stability of DNA stored at room temperature. *Biopreserv. Biobank.* 9, 47–50. doi: 10.1089/bio.2010.0028
- Drmanac, R. (2020). “First \$100 genome sequencing enabled by new extreme throughput DNBSEQ platform,” in *Advances in Genome Biology and Technology (AGBT) General Meeting 2020*, (Florida: AGBT).
- Edge, M. D., Algee-Hewitt, B. F., Pemberton, T. J., Li, J. Z., and Rosenberg, N. A. (2017). Linkage disequilibrium matches forensic genetic records to disjoint genomic marker sets. *Proc. Natl. Acad. Sci.* 114, 5671–5676. doi: 10.1073/pnas.1619944114
- Edge, M. D., and Coop, G. (2019). How lucky was the genetic investigation in the Golden State Killer case?. *bioRxiv* 7:531384. doi: 10.1101/531384
- Edge, M. D., and Coop, G. (2020). Attacks on genetic privacy via uploads to genealogical databases. *Elife* 9:e51810. doi: 10.7554/eLife.51810
- Ender, M., Moradi, A., and Paar, C. (2020). “The Unpatchable Silicon: A Full Break of the Bitstream Encryption of Xilinx 7-Series FPGAs,” in *29th USENIX Security Symposium (USENIX Security 20)*, (California: USENIX).
- Erlich, Y., and Narayanan, A. (2014). Routes for breaching and protecting genetic privacy. *Nat. Rev. Genet.* 15, 409–421. doi: 10.1038/nrg3723
- Erlich, Y., Shor, T., Pe’er, I., and Carmi, S. (2018). Identity inference of genomic data using long-range familial searches. *Science* 362, 690–694. doi: 10.1126/science.aau4832
- Fayans, I., Motro, Y., Rokach, L., Oren, Y., and Moran-Gilad, J. (2020). Cyber security threats in the microbial genomics era: implications for public health. *Eurosurveillance* 25:1900574. doi: 10.2807/1560-7917.ES.2020.25.6.1900574
- Finlayson, S. G., Bowers, J. D., Ito, J., Zittrain, J. L., Beam, A. L., and Kohane, I. S. (2019). Adversarial attacks on medical machine learning. *Science* 363, 1287–1289. doi: 10.1126/science.aaw4399
- Guri, M. (2020). *POWER-SUPPLaY: Leaking Data from Air-Gapped Systems by Turning the Power-Supplies Into Speakers*. arXiv preprint, arXiv:2005.00395.
- Guri, M., Bykhovsky, D., and Elovici, Y. (2019). “Brightness: Leaking sensitive data from air-gapped workstations via screen brightness,” in *2019 12th CMI Conference on Cybersecurity and Privacy (CMI)*, (Netherlands: IEEE), 1–6. doi: 10.1109/CMI48017.2019.8962137
- Gymrek, M., McGuire, A. L., Golan, D., Halperin, E., and Erlich, Y. (2013). Identifying personal genomes by surname inference. *Science* 339, 321–324. doi: 10.1126/science.1229566

The authors declare that this study received funding from GeneInfoSec Inc. and the University of Colorado Boulder’s Technology, Cybersecurity and Policy Program. The authors affiliated with both funders were involved in study design, data collection and analysis, preparation of the manuscript, and the decision to submit it for publication.

## ACKNOWLEDGMENTS

We would like to acknowledge the confidential research participants, collaborators, vendors, and agencies on this study for their time, resources, and interest in bettering genetic information security. Thank you to Cory Cranford, Arya Thaker, Ashish Yadav, and Dr. Kevin Gifford and Dr. Daniel Massey of the Department of Computer Science (formerly of the Technology, Cybersecurity and Policy Program) at the University of Colorado Boulder, and Steve Watson and Matthew Domanic of VTO Labs, Inc. for their support of this work. Lastly, thank you to the reviewers and editorial team for their time and valuable input. This manuscript was previously released as a pre-print at *bioRxiv* (Schumacher et al., 2020).

## SUPPLEMENTARY MATERIAL

The Supplementary Material for this article can be found online at: <https://www.frontiersin.org/articles/10.3389/fbioe.2020.591980/full#supplementary-material>

- Institute of Medicine and National Research Council (2006). *Globalization, Biosecurity, and the Future of the Life Sciences*. Washington, DC: The National Academies Press.
- International Organization for Standardization [ISO] (2012). *ISO/IEC 27032:2012. Information technology – security techniques – guidelines for cybersecurity*. Geneva: ISO.
- Jordan, S. B., Fenn, S. L., and Shannon, B. B. (2020). Transparency as Threat at the Intersection of Artificial Intelligence and Cyberbiosecurity. *Computer* 53, 59–68. doi: 10.1109/MC.2020.2995578
- Li, J., Gonzalez Zarzar, T. B., White, J., Indencleef, K., Hoskens, H., Ortega Castrillon, A., et al. (2019). Robust Genome-Wide Ancestry Inference for Heterogeneous Datasets and Ancestry Facial Imaging based on the 1000 Genomes Project. *bioRxiv* 549881. doi: 10.1101/549881
- Lin, Z., Owen, A. B., and Altman, R. B. (2004). Genomic research and human subject privacy. *Science* 305:183. doi: 10.1126/science.1095019
- Lippert, C., Sabatini, R., Maher, M. C., Kang, E. Y., Lee, S., Arikan, O., et al. (2017). Identification of individuals by trait prediction using whole-genome sequencing data. *Proc. Natl. Acad. Sci.* 114, 10166–10171. doi: 10.1073/pnas.1711251114
- Liu, Y., Yan, C., Yin, Z., Wan, Z., Xia, W., Kantarcioglu, M., et al. (2019). “Biomedical Research Cohort Membership Disclosure on Social Media,” in *AMIA Annual Symposium Proceedings*, (Maryland: American Medical Informatics Association), 607.
- Lowrance, W. W., and Collins, F. S. (2007). Identifiability in genomic research. *Science* 317, 600–602. doi: 10.1126/science.1147699
- Millett, K. K., dos Santos, E., and Millett, P. D. (2019). Cyber-Biosecurity Risk Perceptions in the Biotech Sector. *Front. Bioengin. Biotechnol.* 7:136. doi: 10.3389/fbioe.2019.00136
- Moritz, R. L., Berger, K. M., Owen, B. R., and Gillum, D. R. (2020). Promoting biosecurity by professionalizing biosecurity. *Science* 367, 856–858. doi: 10.1126/science.aba0376
- Mueller, S. (2019a). Are Market GM plants an unrecognized platform for bioterrorism and biocrime? *Front. Bioengin. Biotechnol.* 7:121. doi: 10.3389/fbioe.2019.00121
- Mueller, S. (2019b). On DNA Signatures, Their Dual-Use Potential for GMO Counterfeiting, and a Cyber-Based Security Solution. *Front. Bioengin. Biotechnol.* 7:189. doi: 10.3389/fbioe.2019.00189
- Murch, R. S., and DiEuliis, D. (2019). *Mapping the cyberbiosecurity enterprise*, Lausanne: Frontiers Media SA. doi: 10.3389/978-2-88963-213-8
- Murch, R. S., So, W. K., Buchholz, W. G., Raman, S., and Peccoud, J. (2018). Cyberbiosecurity: an emerging new discipline to help safeguard the bioeconomy. *Front. Bioengin. Biotechnol.* 6:39. doi: 10.3389/fbioe.2018.00039
- National Academies of Sciences, Engineering, and Medicine (2020). *Safeguarding the Bioeconomy*. Washington, DC: The National Academies Press.
- Naveed, M., Ayday, E., Clayton, E. W., Fellay, J., Gunter, C. A., Hubaux, J. P., et al. (2015). Privacy in the genomic era. *ACM Comput. Surv.* 48, 1–44. doi: 10.1145/2767007
- Ney, P. M., Ceze, L., and Kohno, T. (2018). *Computer security risks of distant relative matching in consumer genetic databases*. arXiv preprint, arXiv:1810.02895.
- Ney, P. M., Ceze, L., and Kohno, T. (2020). “Genotype extraction and false relative attacks: security risks to third-party genetic genealogy services beyond identity inference,” in *Network and Distributed System Security Symposium (NDSS)*, (New York: NDSS) doi: 10.14722/ndss.2020.23049
- Ney, P. M., Koscher, K., Organick, L., Ceze, L., and Kohno, T. (2017). “Computer Security, Privacy, and DNA Sequencing: Compromising Computers with Synthesized DNA, Privacy Leaks, and More,” in *26th USENIX Security Symposium (USENIX Security 17)*, (Maryland: USENIX), 765–779.
- Office of the US Trade Representative (2018). *Findings of the Investigation Into China's Acts, Policies and Practices Related to Technology Transfer, Intellectual Property, and Innovation Under Section 301 of the Trade Act of 1974*. Washington: Office of the United States Trade Representative, Executive Office of the President.
- Peccoud, J., Gallegos, J. E., Murch, R., Buchholz, W. G., and Raman, S. (2018). Cyberbiosecurity: from naive trust to risk awareness. *Trends Biotechnol.* 36, 4–7. doi: 10.1016/j.tibtech.2017.10.012
- Reed, J. C., and Dunaway, N. (2019). Cyberbiosecurity Implications for the Laboratory of the Future. *Front. Bioengin. Biotechnol.* 7:182. doi: 10.3389/fbioe.2019.00182
- Roy, S., LaFramboise, W. A., Nikiforov, Y. E., Nikiforova, M. N., Routbort, M. J., Pfeifer, J., et al. (2016). Next-generation sequencing informatics: challenges and strategies for implementation in a clinical environment. *Archiv. Pathol. Lab. Med.* 140, 958–975. doi: 10.5858/arpa.2015-0507-RA
- Salerno, R. M., and Koelm, J. G. (2002). *Biological laboratory and transportation security and the biological weapons convention*. Washington: National Nuclear Security Administration.
- Sawaya, S., Kenneally, E., Nelson, D., and Schumacher, G. J. (2020). *Artificial intelligence and the weaponization of genetic data*. Available online at: <https://ssrn.com/abstract=3635050> [accessed on April 24, 2020]. doi: 10.2139/ssrn.3635050
- Schabacker, D. S., Levy, L. A., Evans, N. J., Fowler, J. M., and Dickey, E. A. (2019). Assessing cyberbiosecurity vulnerabilities and infrastructure resilience. *Front. Bioengin. Biotechnol.* 7:61. doi: 10.3389/fbioe.2019.00061
- Schumacher, G. J., Sawaya, S., Nelson, D., and Hansen, A. J. (2020). Genetic information insecurity as state of the art. *bioRxiv* 2020:192666. doi: 10.1101/2020.07.08.192666
- Shi, X., and Wu, X. (2017). An overview of human genetic privacy. *Anna. N Y Acad. Sci.* 1387:61. doi: 10.1111/nyas.13211
- Shwartz, O., Mathov, Y., Bohadana, M., Elovici, Y., and Oren, Y. (2017). *Opening Pandora's box: effective techniques for reverse engineering IoT devices*. In *International Conference on Smart Card Research and Advanced Applications*. Cham: Springer. doi: 10.1007/978-3-319-75208-2\_1
- US Office of the Inspector General (2004). *The FBI DNA laboratory: A review of protocol and practice vulnerabilities*. Office of the Inspector General, Washington: United States Department of Justice.
- Vinatzer, B. A., Heath, L. S., Almohri, H. M., Stulberg, M. J., Lowe, C., and Li, S. (2019). Cyberbiosecurity Challenges of Pathogen Genome Databases. *Front. Bioengin. Biotechnol.* 7:106. doi: 10.3389/fbioe.2019.00106
- Walsh, M., and Streilein, W. (2020). Security Measures for Safeguarding the Bioeconomy. *Health Secur.* 18, 313–317. doi: 10.1089/hs.2020.0029
- Werner, E. (2019). *The Coming CRISPR Wars: Or why genome editing can be more dangerous than nuclear weapons*. Preprint Posted.

**Conflict of Interest:** GS, SS, and DN were founders and owners of GeneInfoSec Inc. and are developing technology and services to protect genetic and other biological information systems. GeneInfoSec Inc. has not received US Federal research funding. AH when writing this manuscript and submitting it to the bioRxiv preprint server, declared that the research was conducted in the absence of any commercial or financial relationships that could be construed as a potential conflict of interest. AH now declares a potential future interest as a consultant in the area of laboratory information security.

Copyright © 2020 Schumacher, Sawaya, Nelson and Hansen. This is an open-access article distributed under the terms of the Creative Commons Attribution License (CC BY). The use, distribution or reproduction in other forums is permitted, provided the original author(s) and the copyright owner(s) are credited and that the original publication in this journal is cited, in accordance with accepted academic practice. No use, distribution or reproduction is permitted which does not comply with these terms.



# Potential False-Positive and False-Negative Results for COVID-19 IgG/IgM Antibody Testing After Heat-Inactivation

Jie Lin<sup>1,2,3†</sup>, Wei Dai<sup>1†</sup>, Weiwei Li<sup>1†</sup>, Li Xiao<sup>1,2,3†</sup>, Tao Luo<sup>1</sup>, Yanju Guo<sup>1</sup>, Yang Yang<sup>1</sup>, Ying Han<sup>1</sup>, Peiran Zhu<sup>1</sup>, Qiuyue Wu<sup>1</sup>, Bangshun He<sup>1,4</sup>, Jian Wu<sup>1\*</sup> and Xinyi Xia<sup>1,3\*</sup>

<sup>1</sup> COVID-19 Research Center, Institute of Laboratory Medicine, Jinling Hospital, Nanjing University School of Medicine, Nanjing Clinical College of Southern Medical University, Nanjing, China, <sup>2</sup> The 904th Hospital, Wuxi, China, <sup>3</sup> Joint Expert Group for COVID-19, Department of Laboratory Medicine & Blood Transfusion, Wuhan Huoshenshan Hospital, Wuhan, China, <sup>4</sup> General Clinical Research Center, Nanjing First Hospital, Nanjing Medical University, Nanjing, China

## OPEN ACCESS

### Edited by:

Stephen Allen Morse,  
Centers for Disease Control and  
Prevention (CDC), United States

### Reviewed by:

Man-Qing Liu,  
Wuhan Centre for Disease Prevention  
and Control, China  
Pedro Xavier-Elsas,  
Federal University of Rio de  
Janeiro, Brazil

### \*Correspondence:

Xinyi Xia  
xinyixia@nju.edu.cn  
Jian Wu  
wujiang2010@outlook.com

<sup>†</sup>These authors have contributed  
equally to this work

### Specialty section:

This article was submitted to  
Infectious Diseases - Surveillance,  
Prevention and Treatment,  
a section of the journal  
Frontiers in Medicine

Received: 30 July 2020

Accepted: 18 December 2020

Published: 18 January 2021

### Citation:

Lin J, Dai W, Li W, Xiao L, Luo T,  
Guo Y, Yang Y, Han Y, Zhu P, Wu Q,  
He B, Wu J and Xia X (2021) Potential  
False-Positive and False-Negative  
Results for COVID-19 IgG/IgM  
Antibody Testing After  
Heat-Inactivation.  
Front. Med. 7:589080.  
doi: 10.3389/fmed.2020.589080

**Objectives:** With the worldwide spread of coronavirus disease 2019 (COVID-19) caused by severe acute respiratory syndrome coronavirus 2 (SARS-CoV-2), various antibody detection kits have been developed to test for SARS-CoV-2-specific IgG, IgM, and total antibody. However, the use of different testing methods under various heat-inactivation conditions might affect the COVID-19 detection results.

**Methods:** Seven different antibody detection kits produced by four manufacturers for detection of SARS-CoV-2 IgG, IgM, and total antibody were tested at Wuhan Huoshenshan Hospital, China. Most of the kits used the indirect immunity, capture, and double-antigen sandwich methods. The effects of various heat-inactivation conditions on SARS-CoV-2-specific IgG, IgM, and total antibody detection were analyzed for the different test methods.

**Results:** Using the indirect immunity method, values for SARS-CoV-2 IgG antibody significantly increased and those for IgM antibody decreased with increasing temperature of heat-inactivation using indirect immunity method. However, values for SARS-CoV-2 IgM and total antibody showed no change when the capture and double-antigen sandwich methods were used. The changes in IgG and IgM antibody values with the indirect immunity method indicated that heat-inactivation could affect COVID-19 detection results obtained using this method. In particular, 18 (22.2%) SARS-CoV-2 IgM positive samples were detected as negative with heat-inactivation at 65°C for 30 min, and one (25%) IgG negative sample was detected as positive after heat-inactivation at 56°C for 60 min and 60°C for 30 min.

**Conclusions:** Heat-inactivation could increase SARS-CoV-2 IgG antibody values, and decrease IgM antibody values, causing potential false-positive or false-negative results for COVID-19 antibody detection using the indirect immunity method. Thus, before conducting antibody testing, the testing platforms should be evaluated in accordance with the relevant requirements to ensure accurate COVID-19 detection results.

**Keywords:** COVID-19, SARS-CoV-2, IgG and IgM antibody, heat-inactivation, indirect immunity method



## INTRODUCTION

Coronavirus disease 2019 (COVID-19), caused by severe acute respiratory syndrome coronavirus 2 (SARS-CoV-2), has rapidly spread worldwide, threatening human health and economic development (1). As of 1 December 2020, the World Health Organization has documented 63,691,642 confirmed cases of COVID-19, with 1,476,277 deaths (2.32%) worldwide. On January 30, 2020, the World Health Organization issued a statement announcing that COVID-19 was a Class I public health emergency of global concern (2).

In the early stages of the COVID-19 outbreak, nucleic acid detection was the main method used for the detection of this disease (3). However, this method required samples from throat swabs, which were highly infectious, and methodological limitations led to long detection periods (4). According to the Diagnosis and Treatment Protocol for Novel Coronavirus Pneumonia (7th Trial Version) in China released on March 3, 2020 (5), serological testing for SARS-CoV-2-specific IgG antibody (Ab) and IgM Ab was identified as suitable for the detection of COVID-19. On April 1, 2020, the US Food and Drug Administration authorized the first SARS-CoV-2 Ab detection kit (6).

Heat-inactivation is a common virus inactivation method used in laboratories. Owing to serious pathogenicity and infectivity of COVID-19, the Inspection Branch of the Chinese Association of Laboratory Medicine required that effective biological safety precautions were taken in laboratories when analyzing the virus; among these precautions, it was recommended that serum samples should be heat-inactivated before serological Ab detection to ensure biosecurity. However, heat-inactivation could affect the values of IgG and IgM Ab detection, with possible effects on the results of clinical tests for COVID-19. At present, at Wuhan Huoshenshan Hospital of China, seven different Ab detection kits for SARS-CoV-2-specific IgG, IgM, and total Ab, produced by four manufacturers, have been used in clinical tests. The current study investigated the effects of various heat-inactivation conditions (including 56°C for 30 min, 56°C for 45 min, 56°C for 60 min, 60°C for 30 min and 65°C for 30 min) on the SARS-CoV-2 antibody detection with the indirect immunity, capture, and double-antigen sandwich methods, using chemiluminescence microparticle immunoassay (CMIA) and up-converting phosphor technology (UPT). Potential false-positive and false-negative rates for COVID-19 detection were also analyzed.

## MATERIALS AND METHODS

### Data Collection

All serum samples used in this study were collected from patients admitted to Wuhan Huoshenshan Hospital of China between February 4 and April 12, 2020, and diagnosed with COVID-19 infection by nucleic acid testing according to the Diagnosis and Treatment Protocol for Novel Coronavirus Pneumonia (7th Trial Version). Huoshenshan Hospital was established in early February, 2020, and built within 10 days, it is one of the biggest designated hospitals for COVID-19 patients in

China, with well-trained clinicians and up-to-date laboratory equipment. This study was approved by the Medical Ethical Committee of Huoshenshan Hospital, Wuhan, China (HSSLL011 and HSSLL012), and written informed consent was obtained from the patients.

### Experimental Regents and Instruments

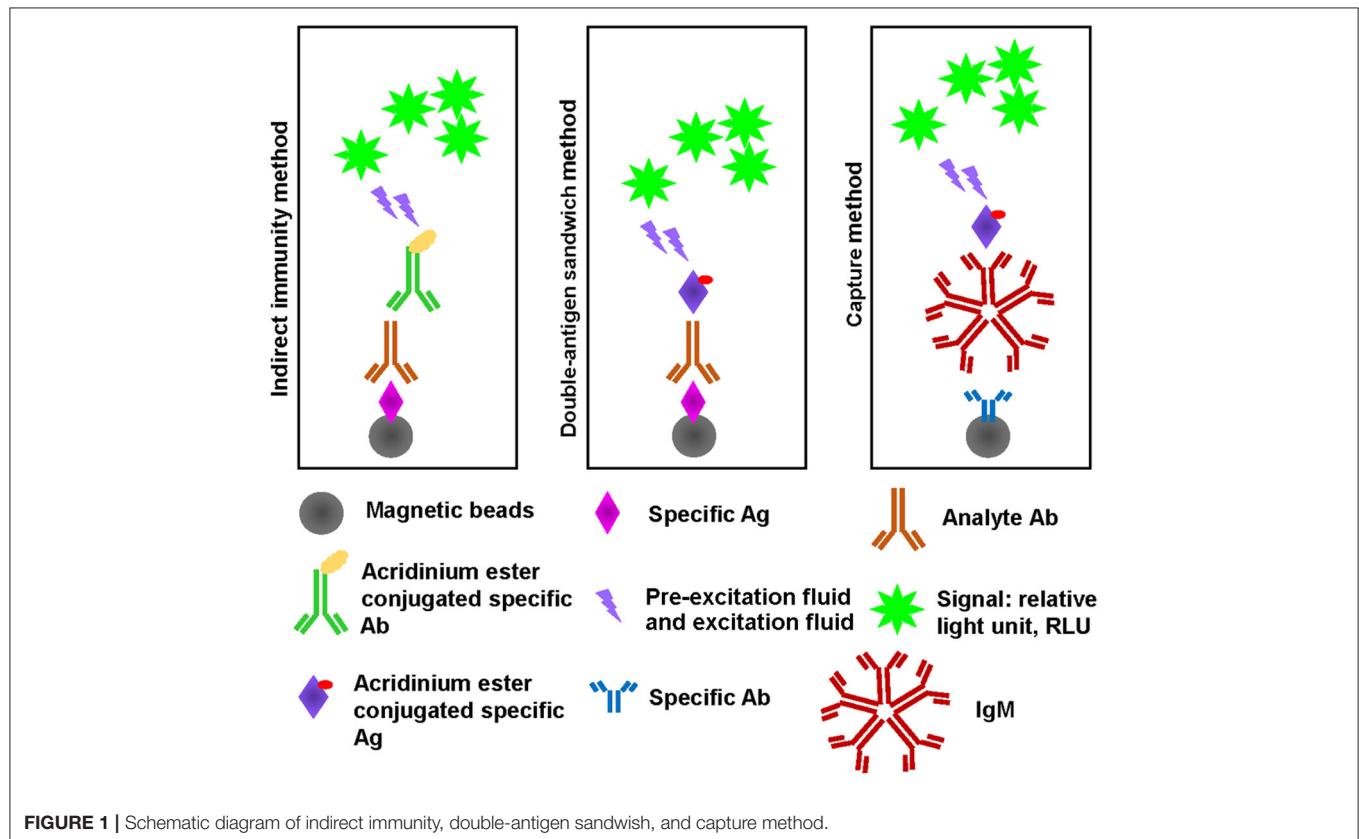
Seven different SARS-CoV-2-specific IgG, IgM, and total Ab detection kits, using the indirect immune method, capture method, or double-antigen sandwich method, based on CMIA and UPT, and produced by four different manufacturers, were tested at Wuhan Huoshenshan Hospital of China (Table 1). In which, the SARS-CoV-2-specific IgG and IgM Ab detection kits, using the indirect immune method, based on CMIA, produced by the same manufacture were under the approval process by National Medical Products Administration of China. The other five different Ab detection kits, including SARS-CoV-2-specific IgG, IgM, and total antibody detection kits, using the indirect immune method, capture method, or double-antigen sandwich method, based on CMIA and UPT, produced by three manufactures had been approved by National Medical Products Administration of China, and the corresponding approval number of National medical device products had been released online. A UPT immunoassay analyzer (UPT-3A-1200), automatic chemiluminescence immunoassay analyzer (Caris200), automatic chemiluminescence immunoassay analyzer (CL-2000i), and automatic chemiluminescence immunoassay analyzer (iFlash 3000-H) were used in this study.

### Experimental Methods

Owing to the specificity of Wuhan Huoshenshan Hospital, detection SARS-CoV-2 Ab without heat-inactivation was used as a control. Serological tests for, and total Ab were performed using the corresponding Ab detection kits, according to the manufacturers' instructions. In brief, for SARS-CoV-2-specific IgG and IgM Ab detection using indirect immunity method, magnetic beads coated with the specific IgG or IgM antigen (Ag) were mixed with analyte serum samples to form Ag/Ab complex, after washing, second Ab Mouse anti-human IgG or IgM coated with acridinium ester were mixed to form Ag/Ab/second Ab complex, after washing, pre-excitation fluid and excitation fluid was added, then the relative light unit (RLU) of signal was detected. For SARS-CoV-2 total Ab detection using double-antigen sandwich method, were mixed with analyte serum samples to form Ag/Ab complex, after washing, specific Ag coated with acridinium ester were mixed to form Ag/Ab/Ag complex, after washing, pre-excitation fluid and excitation fluid was added, then the RLU of signal was detected. For SARS-CoV-2-specific IgM Ab detection using capture method, magnetic beads coated with anti-human specific IgM Ab mixed with analyte serum samples, after washing, specific Ag coated with acridinium ester were mixed to form Ab/IgM/Ab complex, after washing, pre-excitation fluid and excitation fluid was added, then the RLU of signal was detected (Figure 1). Before testing, serum samples were heat-inactivated in a water bath at 56°C for 30 min, 56°C for 45 min, 56°C for 60 min, 60°C for 30 min, and 65°C for 30 min.

**TABLE 1** | SARS-CoV-2 antibody detection kits.

Manufacturer	A		B		C		D
	IgG Ab	IgM Ab	IgG Ab	IgM Ab	IgM Ab	Total Ab	Total Ab
Method	Indirect immunity		Indirect immunity		Capture	Double-antigen	Double-antigen
Technology	Chemiluminescence microparticle immunoassay		Chemiluminescence microparticle immunoassay		Chemiluminescence microparticle immunoassay		Up-converting phosphor technology

**FIGURE 1** | Schematic diagram of indirect immunity, double-antigen sandwich, and capture method.

## Statistical Analysis

Data are presented as mean  $\pm$  standard deviation (SD), and measured by GraphPad Prism 8.0. Statistical significance was analyzed by two-tailed paired student's *t*-test. Differences at  $p < 0.05$  were considered to statistical significance.

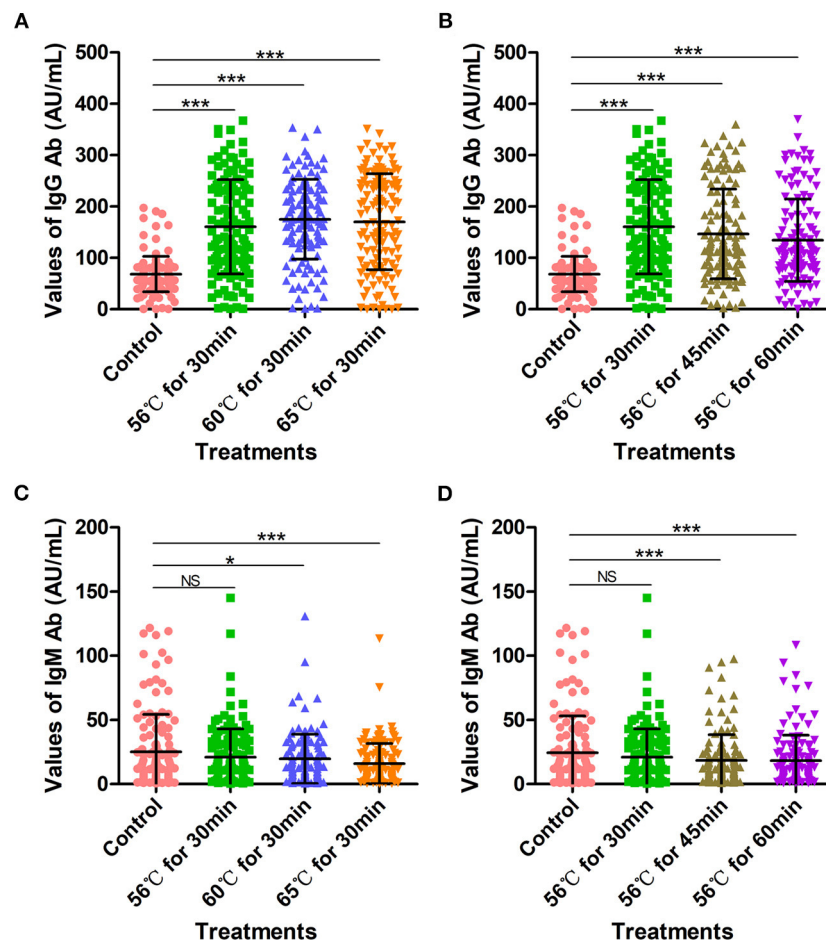
## RESULTS

### Effects of Heat-Inactivation Conditions on Indirect Immunity Method

A total of 129 serum samples collected from COVID-19 patients admitted to Wuhan Huoshenshan Hospital were tested with SARS-CoV-2 specific IgG and IgM Ab detection kits using the indirect immunity method, produced by manufacturer A. Before testing, samples were heat-inactivated in water bath at 56°C for 30 min, 56°C for 45 min, 56°C for 60 min, 60°C for 30 min, or 65°C for 30 min. The average IgG Ab value for the control group without heat-inactivation was 68.46 AU/mL, whereas those

obtained after heat-inactivation at 56°C for 30 min, 60°C for 30 min, and 65°C for 30 min were significantly higher ( $p < 0.001$ ) at 160.44, 175.21, and 170.21 AU/mL, respectively (**Figure 2A**). In addition, when serum samples were heat-inactivated at 56°C, the IgG Ab values after heat-inactivation for 30, 45, and 60 min were significantly higher ( $p < 0.001$ ) than control values, with averages of 160.44, 146.61, and 134.37 AU/mL, respectively (**Figure 2B**, **Supplementary Table 1**).

The average IgM Ab value in the control group was 24.35 AU/mL; for heat-inactivation time of 30 min, IgM Ab values decreased compared with controls as the temperature of heat-inactivation increased ( $p < 0.05$ ). In particular, for heat-inactivation at 65°C, IgM Ab levels were very significantly decreased compared with controls ( $p < 0.001$ ). The average IgM Ab values obtained after heat-inactivation at 56°C for 30 min, 60°C for 30 min, and 65°C for 30 min were 20.95 AU/mL, 19.70 AU/mL, and 15.98 AU/mL, respectively (**Figure 2C**). Notably, even at 56°C, heat-inactivation for 30 min, 45 min, and 60 min led to lower IgM Ab values compared with controls ( $p < 0.05$ ),



**FIGURE 2 |** SARS-CoV-2-specific IgG and IgM antibody detection values with indirect immunity-based kit produced by manufacturer A. **(A)** SARS-CoV-2 IgG antibody detection values after heat-inactivation for 30 min. Before testing, a total of 129 samples were heat-inactivated at 56, 60, or 65°C for 30 min. **(B)** SARS-CoV-2 IgG antibody detection values after heat-inactivation at 56°C. Before testing, a total of 129 samples were heat-inactivated at 56°C for 30, 45, or 60 min. **(C)** SARS-CoV-2 IgM antibody detection values after heat-inactivation for 30 min. Before testing, a total of 129 samples were heat-inactivated at 56, 60, or 65°C for 30 min. **(D)** SARS-CoV-2 IgM antibody values after heat-inactivation at 56°C. Before testing, a total of 129 samples were heat-inactivated at 56°C for 30, 45, or 60 min. The detection of SARS-CoV-2 antibody without heat-inactivation were used as control. NS, non-significant; \* $p \leq 0.05$ ; \*\*\* $p \leq 0.001$ .

with average values of 20.95, 18.49, and 18.22, respectively (Figure 2D, Supplementary Table 2).

These increases in SARS-CoV-2-specific IgG Ab values and decreases in IgM values obtained with the indirect immunity method after heat-inactivation could cause potential false-positive and false-negative results in COVID-19 detection. As shown in Table 2, one (25%) IgG Ab-negative sample was determined as positive owing to increased IgG values after heat-inactivation at 56°C for 60 min and 60°C for 30 min (Table 2). Correspondingly, a total of 12 (16.2%), 10 (13.5%), 18 (24.3%), 12 (16.0%) and 13 (17.6%) IgM-positive samples were detected as negative, owing to IgM values decreasing after heat-inactivation at 56°C for 30 min, 60°C for 30 min, 65°C for 30 min, 56°C for 45 min, and 56°C for 60 min, respectively (Table 2).

Another 20 serum samples collected from COVID-19 patients admitted to Wuhan Huoshenshan Hospital were tested with SARS-CoV-2 specific IgG and IgM Ab detection kits produced

by manufacturer B, also based on the indirect immunity method. Before testing, samples were heat-inactivated at 56°C for 30 min, 56°C for 45 min, or 60°C for 30 min in a water bath. The IgG Ab values obtained after heat-inactivation at 56°C for 30 min and 56°C for 45 min were significantly higher than those of the control group without heat-inactivation ( $p < 0.05$ ); the average value for the control group was 228.04 U/mL, whereas values of 244.58 U/mL and 242.59 U/mL were obtained after heat-inactivation at 56°C for 30 min and 56°C for 45 min, respectively (Figure 3A). Notably, when samples were heat-inactivated at 60°C for 30 min, the IgG Ab value was significantly decreased in comparison with the control group ( $p < 0.0001$ ), with an average IgG Ab value of 179.55 U/mL. This might have been because the IgG Ab was deactivated by heat-inactivation at a high temperature (Supplementary Table 3). In addition, whereas the control group had an average cutoff index (COI) value of 1.19, heat-inactivation at higher temperature led to lower COI

**TABLE 2 |** Potential false-positive and false-negative rates after heat-inactivation for SARS-CoV-2 IgG and IgM Ab detection with indirect immunity-based kit produced by manufacturer A.

IgG Ab	56°C for 30 min			Total	56°C for 45 min			Total	56°C for 60 min			Total	60°C for 30 min			Total	65°C for 30 min			Total
	Po	Ne			Po	Ne			Po	Ne			Po	Ne			Po	Ne		
Control	Po	125	0	125	125	0	125	125	125	0	125	125	124	1	125	125	121	4	125	125
	Ne	0	(0.0%)	4	0	(0.0%)	4	1	1	(25.0%)	3	4	1	(25.0%)	3	4	0	(0.0%)	4	4
Total		125		129		125		129		126		129		125		129		121		129
IgM Ab	Po	62	12	74	62	12	74	61	61	13	74	74	64	10	74	74	56	18	74	74
	Ne	16	(29.1%)	39	11	(21.4%)	44	12	12	(21.8%)	43	55	17	(30.9%)	38	55	16	(29.1%)	39	55
Total		78		129		73		129		73		129		81		129		72		129

blue bold, false-negative; red bold, false-positive; Po, positive; Ne, negative.

values for IgM Ab; in particular, with heat-inactivation at 60°C for 30 min, IgM Ab values were significantly decreased ( $p < 0.01$ ), with an average COI value of 0.61. For heat-inactivation at a given temperature, IgM Ab values decreased with increasing time of heat-inactivation ( $p < 0.01$ ). The average COI values for IgM Ab with heat-inactivation at 56°C for 30 min and 56°C for 45 min were 0.98 and 0.93, respectively (Figure 3B, Supplementary Table 4).

As shown in Supplementary Table 4, although SARS-CoV-2 IgG Ab values increased after heat-inactivation using the indirect immunity method, all the samples used in this experiment were initially IgG positive; thus, there was no potential for false-positives (Table 3). However, owing to the decreases in SARS-CoV-2-specific IgM Ab values after heat-inactivation, there were five (71.4%) initially IgM-positive samples were determined as negative after heat-inactivation at 60°C for 30 min (Table 3). These results show that heat-inactivation could lead to increased SARS-CoV-2 IgG Ab values and decreased IgM antibody, directly causing false-negative or false-positive results in COVID-19 detection using the indirect immunity method.

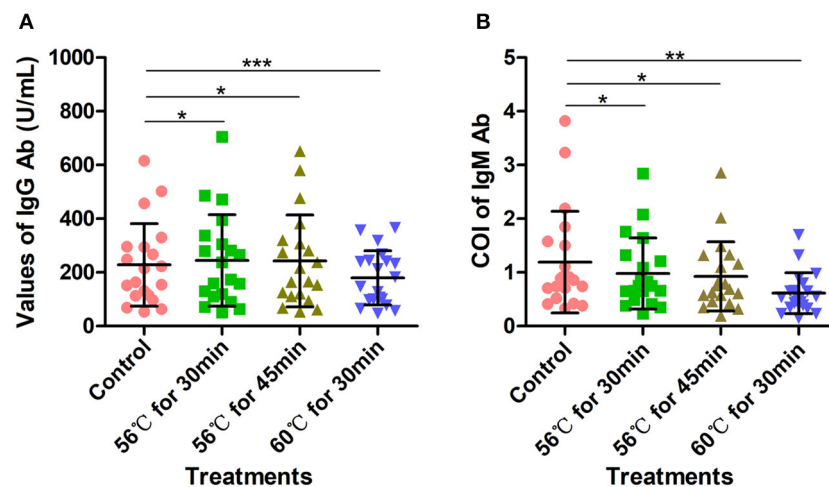
## Effects of Heat-Inactivation Conditions With Capture Method

A total of 34 serum samples collected from COVID-19 patients admitted to Wuhan Huoshenshan Hospital were tested with a SARS-CoV-2-specific IgM Ab detection kit based on the capture method, produced by manufacturer C. Before testing, serum samples were heat-inactivated at 56°C for 30 min or 60°C for 30 min in a water bath. The detection results for IgM Ab were not affected by heat-inactivation ( $p > 0.05$ ); the average IgM Ab for the control group without heat-inactivation was 2.66, compared with 2.68, and 2.57 after heat-inactivation at 56°C for 30 min and 60°C for 30 min, respectively (Figure 4, Supplementary Table 5). As the different heat-inactivation conditions had no effect on the detection results of IgM Ab with the capture method, there was no effect on COVID-19 detection.

## Effects of Heat-Inactivation Conditions With Double Antigen Sandwich Method

The above 34 serum samples were also tested with a SARS-CoV-2 total Ab detection kit based on the double-antigen sandwich method. Before testing, serum samples were heat-inactivated at 56°C for 30 min or 60°C for 30 min in a water bath. Heat-inactivation at 56°C for 30 min had no significant effect on the detection of SARS-CoV-2 total Ab, with an average value of 642.9 compared with 649.76 for the control group ( $p > 0.05$ ). However, the SARS-CoV-2 total Ab values after heat-inactivation at 60°C for 30 min were significantly lower than those of the control group ( $p < 0.0001$ ), with an average value of 584.18 (Figure 5A, Supplementary Table 6). This might have been because of the deactivation of the Ab at the higher temperature. However, although SARS-CoV-2 total Ab values decreased after heat-inactivation at 60°C for 30 min, there was no corresponding effect on COVID-19 detection.





**FIGURE 3 |** Detection of SARS-CoV-2-specific IgG and IgM antibodies with indirect immunity-based kit produced by manufacturer B. **(A)** Density of SARS-CoV-2-specific IgG antibody detection. Before testing, 20 samples were heat-inactivated at 56°C for 30 min, 56°C for 45 min, or 60°C for 30 min, respectively. **(B)** COI values for SARS-CoV-2-specific IgM antibody. Before testing, 20 samples were heat-inactivated at 56°C for 30 min, 56°C for 45 min, or 60°C for 30 min. The detection of SARS-CoV-2 antibody without heat-inactivation were used as control. \* $p \leq 0.05$ ; \*\* $p \leq 0.01$ ; \*\*\* $p \leq 0.001$ .

**TABLE 3 |** Potential false-positive and false-negative rates after heat-inactivation for SARS-CoV-2 IgG and IgM Ab detection with indirect immunity-based kit produced by manufacturer B.

IgG Ab		56°C for 30 min		Total	56°C for 45 min		Total	60°C for 30 min		Total
		Po	Ne		Po	Ne		Po	Ne	
Control	Po	20 (100.0%)	<b>0</b> (0.0%)	20	20 (100.0%)	<b>0</b> (0.0%)	20	20 (100.0%)	<b>0</b> (0.0%)	20
	Ne	<b>0</b> (0.0%)	0 (100.0%)	0	<b>0</b> (0.0%)	0 (100.0%)	0	<b>0</b> (0.0%)	0 (100.0%)	0
Total		20	0	<b>20</b>	20	0	<b>20</b>	20	0	<b>20</b>
IgM Ab		Po	Ne	Total	Po	Ne	Total	Po	Ne	Total
Control	Po	7 (100.0%)	<b>0</b> (0.0%)	7	7 (100.0%)	<b>0</b> (0.0%)	7	2 (28.6%)	<b>5</b> (71.4%)	7
	Ne	<b>0</b> (0.0%)	13 (100.0%)	13	<b>0</b> (0.0%)	13 (100.0%)	13	<b>0</b> (0.0%)	13 (100.0%)	13
Total		7	13	<b>20</b>	7	13	<b>20</b>	2	18	<b>20</b>

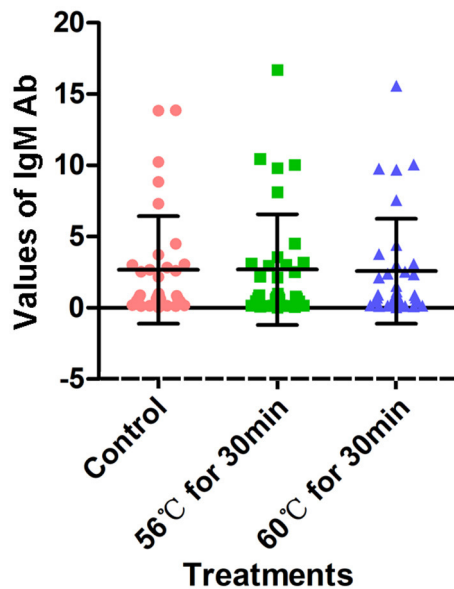
blue bold, false-negative; red bold, false-positive; Po, positive; Ne, negative.

Similarly, 10 serum samples collected from COVID-19 patients admitted to Wuhan Huoshenshan Hospital were tested using a SARS-CoV-2 total Ab detection kit based on the double-antigen sandwich method produced by manufacturer D. Before testing, samples were heat-inactivated at 56°C for 30 min or 60°C for 30 min in a water bath. The average SARS-CoV-2 total Ab value after heat-inactivation at 56°C for 30 min was 5.55, similar to average value of 5.54 for the control group ( $p < 0.05$ ). However, heat-inactivation for the same time of 30 min but at 60°C caused the average total Ab value to decrease to 4.92, which was significantly lower than the control value ( $p < 0.05$ ) (Figure 5B, Supplementary Table 7). Again, this could be attributed to deactivation of the Ab at the higher temperature. In addition, although the SARS-CoV-2 total Ab value decreased after heat-inactivation at 60°C for 30 min, there was no effect on the detection of COVID-19 with the double-antigen sandwich method.

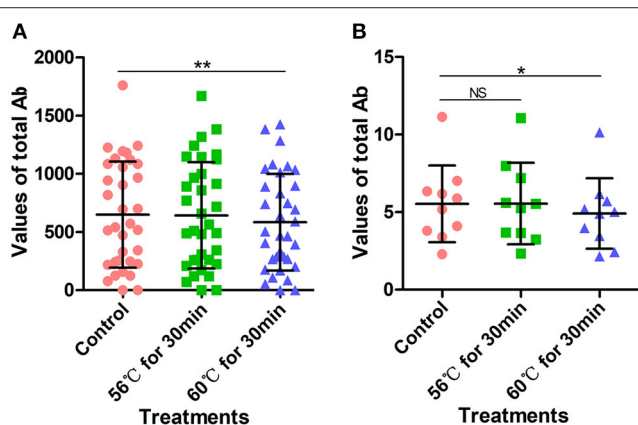
## DISCUSSION

COVID-19 is a highly infectious disease, with an  $R_0$  value of 3.0–3.5 (7). Early prevention, identification, and diagnosis are particularly important to control the spread of this disease (8). Although the nucleic acid test is the gold standard for COVID-19 detection, it has a long detection time, and the results are susceptible to various factors including the quality of the specimen, the site of viral infection, and the amount of viral expression (9). Serological Ab detection has been added to the Diagnosis and Treatment Protocol for Novel Coronavirus Pneumonia (7th Trial Version) in China, as an auxiliary method for COVID-19 detection, and can be used in conjunction with nucleic acid detection to achieve fast screening for COVID-19 (10).

CMIA is a novel analysis method, takes full advantage of the rapid automation of magnetic separation, the high sensitivity



**FIGURE 4 |** Detection results of SARS-CoV-2-specific IgM antibody with capture method. Before testing, a total of 34 samples were heat-inactivated at 56°C for 30 min or 60°C for 30 min. The detection of SARS-CoV-2 antibody without heat-inactivation were used as control.



**FIGURE 5 |** SARS-CoV-2 total antibody values tested using double-antigen sandwich method. **(A)** SARS-CoV-2 total antibody values tested using CMIA kit produced by manufacturer C. Before testing, a total of 34 samples were heat-inactivated at 56°C for 30 min or 60°C for 30 min. **(B)** SARS-CoV-2 total antibody tested using UPT-kit produced by manufacturer D. Before testing, 10 samples were heat-inactivated at 56°C for 30 min or 60°C for 30 min. The detection of SARS-CoV-2 antibody without heat-inactivation were used as control. NS, non-significant; \* $p \leq 0.05$ , \*\* $p \leq 0.01$ .

of chemiluminescence, and the specificity of immunoassays. Commonly used of CMIA methods include the indirect immunity method, capture method, solid-phase antigen competition method, and double-antibody sandwich method. The specificity of the reaction between antigen and antibody is determined by the spatial configuration of the antigenic determinant and the antigen-binding region of the Ab (11).

Notably, similar to globulins, the resistance to physical and chemical factors of IgG and IgM Ab could be destroyed by heating to 60–70°C; various enzymes and substances that cause protein coagulation and denaturation also lead to loss of function of Abs (12).

In this study, the indirect immunity, capture, and double-antigen sandwich methods were used to detect SARS-CoV-2-specific IgG, IgM, and total Ab. The indirect immunity method has high sensitivity and economical, as fewer labeled Abs are needed and more than one labeled secondary Ab can bind to the primary Ab (13). However, its disadvantages include the possibility of cross-reactivity of the secondary Ab with the adsorbed antigen, which could increase background noise. The capture method, also known as the reverse indirect method, is mainly used for the determination of certain Ab subtype components such as IgM in serum. Owing to the co-existence in serum of IgM and IgG specific to a certain antigen, the presence of IgG can interfere with the measurement of IgM. Therefore, a secondary Ab against IgM is first attached to a solid phase carrier to capture all IgM in the sample, and an antigen specific to IgM to be tested is added. This method has higher stability compared with the indirect immunity method and commonly used for IgM Ab detection. However, the disadvantages of the capture method include its relatively low sensitivity, which decreases its range of applications.

In order to improve biological safety, infectious materials and serum samples are required to be heat-inactivated by reliable methods before serological testing (14). In a previously published investigation of heat-inactivation stability of SARS (15), Rabenau et al. found that the titer of SARS virus was lower than the detection limit after being heat-inactivated at 56°C for 30 min; after heat-inactivation at 60°C for 30 min, there was no residue of SARS virus (16). Kariwa et al. also found no infectious SARS virus after heat-inactivation at 56°C for 60 min or longer (17). However, heat-inactivation of the virus might have an impact on the spatial conformation and protein structure of the antigen-Ab binding region, possibly leading false-positive and false-negative results (14).

In this study, the serological detection of SARS-CoV-2-specific IgG Ab without heat-inactivation was compared with detection after heat-inactivation at 56°C for 30 min, 45 min, and 60 min, and at 60 or 65°C for 30 min, using the indirect immunity method. As the time and temperature of heat-inactivation increased, IgG Ab values significantly increased. When different temperatures of heat-inactivation were compared, IgG Ab values increased after heat-inactivation at 56°C, and increased further after heat-inactivation at 60°C, whereas they decreased after heat-inactivation at 65°C. This phenomenon might occur because the structure of IgG is composed of two heavy and two light chains linked together, creating a large monomeric molecules with a tetrameric quaternary structure, formed by the polymerization of itself under certain temperature conditions. Under the condition of heat-inactivation treatment, the monomeric molecules of IgG antibody could be aggregated, hence the detection values of IgG antibody increase. It has been reported that the thermal polymerization conditions of IgG directly affect the structure of its products and its biological reactivity. For a polymerization

time of 30 min, thermal polymerization of IgG occurs in a narrow temperature range of 60–64°C. However, as the thermal polymerization temperature increases, its degree of polymerization and the products increase, as does its binding capacity (18). The binding capacity is strongest at a thermal polymerization temperature of 62°C, and it can react with the epitope on the Fc segment of IgG molecules (19). During thermal polymerization, the conformation of IgG changes, and the number and accessibility of active sites increase, reaching maximum values under certain conditions. As the thermal polymerization conditions are strengthened, the reaction activity of the product begins to decline. This might be because the further increase in the degree of polymerization reduces the accessibility of the reaction site, or because the severe denaturation conditions cause the destruction of the original active site. In addition, excessively high temperatures can cause protein denaturation. Although this IgG aggregation is antigen-nonspecific, and the enhanced signal has no relationship to the recognition of viral antigens, increasing IgG Ab could cause potential false-positive results in COVID-19 detection.

In this study, the serological detection of SARS-CoV-2-specific IgM Ab before heat-inactivation was compared with detection after heat-inactivation at 56°C for 30 min, 56°C for 45 min, 56°C for 60 min, 60°C for 30 min, and 60°C for 30 min. The results indicated that IgM Ab values decreased with increasing time and temperature of heat-inactivation when using the indirect immunity method, possibly because the stability of IgM Ab is much lower than that of IgG Ab (20). It was known that IgM is a symmetrical pentamer structure, where all heavy chains and all light chains are identical. Although the large size (900 kDa) of IgM, its structure could be denatured by the heat-inactivation treatment. In clinical tests, heat-inactivation is a common method to reduce the impact of IgM. The IgM pentamer is an asymmetrical pentagon with an open groove that can bind to specific proteins (21). Heat-inactivation could destroy the polygonal structure of IgM, thereby affecting the specific binding of antigen to Ab (22). There is also evidence that heating could cause false-negative results in the detection of IgM. This is consistent with some of the results of this study.

Additionally, proteins have evolved to have disulfide bonds in their natural conformations, which contribute to thermodynamic stability. These disulfide bonds are broken during heating, and the protein undergoes irreversible denaturation through the disulfide-thiol exchange reaction. Methanethiosulphonate (MTS) could specifically suppress the heat-induced disulphide-thiol exchange reaction, and improve the heat-resistance of proteins. Combining MTS reagents with glycineamide, further enhanced protein stabilization (23). This aspect was not investigated in the current study, but it should be the subject of further research. Different manufacturers select different specific binding sites of antigens, and the various methods differ in their products. The SARS-CoV-2-specific IgG antibody detection kits produced by manufacturers B were certainly added with MTS. In addition, heating changes the composition and structure of serum proteins, which affects matrix effects in serum detection results.

Currently, the testing process for COVID-19 is not standardized; there is an urgent need to reduce the development time of detection kits and test platforms, and there has not been sufficient evaluation and clinical verification using large samples. Therefore, factors that might cause inaccurate results need to be considered. Before conducting tests, the testing methods and platforms should be evaluated in accordance with the relevant requirements, in order to reduce potential false-negative and false-positive results, and provide accurate results for COVID-19 detection.

## DATA AVAILABILITY STATEMENT

The raw data supporting the conclusions of this article will be made available by the authors, without undue reservation.

## ETHICS STATEMENT

The study has been reviewed and approved by the Medical Ethical Committee of Huoshenshan Hospital, Wuhan, China (HSSL011 and HSSL012). Written informed consent was obtained from the individual(s) for the publication of any potentially identifiable images or data included in this article.

## AUTHOR CONTRIBUTIONS

XX and JW conceived the study. JL performed the experiments, collected data, and wrote the manuscript. WD, WL, and LX analyzed the data, generated the figures, and edited the manuscript. TL, YG, YY, and YH contributed to the data analysis. PZ, QW, and BH contributed to the manuscript editor. All authors contributed to the article and approved the submitted version.

## FUNDING

This work was supported by the Key Foundation of Wuhan Huoshenshan Hospital (2020[18]), the Key Research & Development Program of Jiangsu Province (BE2018713), the Medical Innovation Project of Logistics Service (18JS005), the Foundation of Jiangsu Population Association (JSPA2019017), and the Jiangsu Provincial Association for Maternal and Child Health Studies Commissioned Research Project Funding (JSFY202005).

## ACKNOWLEDGMENTS

We thank all COVID-19 patients included in this study. We are grateful to the clinical staffs who treated the patients.

## SUPPLEMENTARY MATERIAL

The Supplementary Material for this article can be found online at: <https://www.frontiersin.org/articles/10.3389/fmed.2020.589080/full#supplementary-material>

## REFERENCES

- Chinazzi M, Davis JT, Ajelli M, Gioannini C, Litvinova M, Merler S, et al. The effect of travel restrictions on the spread of the 2019 novel coronavirus (COVID-19) outbreak. *Science*. (2020) 368:395–400. doi: 10.1126/science.aba9757
- Wang C, Horby PW, Hayden FG, Gao GF. A novel coronavirus outbreak of global health concern. *Lancet*. (2020) 395:470–3. doi: 10.1016/S0140-6736(20)30185-9
- Li R, Pei S, Chen B, Song Y, Zhang T, Yang W, et al. Substantial undocumented infection facilitates the rapid dissemination of novel coronavirus (SARS-CoV-2). *Science*. (2020) 368:489–93. doi: 10.1126/science.abb3221
- Corman VM, Landt O, Kaiser M, Molenkamp R, Meijer A, Chu DK, et al. Detection of 2019 novel coronavirus (2019-nCoV) by real-time RT-PCR. *Euro Surveill*. (2020) 25:2000045. doi: 10.2807/1560-7917.ES.2020.25.3.2000045
- Diagnosis and Treatment Protocol for Novel Coronavirus Pneumonia (Trial Version 7). *Chin Med J (Engl)*. (2020) 133:1087–95. doi: 10.1097/CM9.0000000000000819
- Food U, Administration D. Policy for diagnostics testing in laboratories certified to perform high complexity testing under CLIA prior to emergency use authorization for coronavirus disease-2019 during the public health emergency. (2020).
- Munster VJ, Koopmans M, van Doremalen N, van Riel D, de Wit E. A novel coronavirus emerging in china - key questions for impact assessment. *N Engl J Med*. (2020) 382:692–4. doi: 10.1056/NEJMp2000929
- Agosti E, Giorgianni A, Locatelli D. Impact of COVID-19 outbreak on spinal pathology: single center first impression. *Spinal Cord*. (2020) 58:726–7. doi: 10.1038/s41393-020-0480-0
- Pan Y, Long L, Zhang D, Yuan T, Cui S, Yang P, et al. Potential false-negative nucleic acid testing results for severe acute respiratory syndrome coronavirus 2 from thermal inactivation of samples with low viral loads. *Clin Chem*. (2020). 66:794–801. doi: 10.1093/clinchem/hvaa091
- Chen N, Zhou M, Dong X, Qu J, Gong F, Han Y, et al. Epidemiological and clinical characteristics of 99 cases of 2019 novel coronavirus pneumonia in Wuhan, China: a descriptive study. *Lancet*. (2020) 395:507–13. doi: 10.1016/S0140-6736(20)30211-7
- Akazawa-Ogawa Y, Takashima M, Lee YH, Ikegami T, Goto Y, Uegaki K, et al. Heat-induced irreversible denaturation of the camelid single domain VHH antibody is governed by chemical modifications. *J Biol Chem*. (2014) 289:15666–79. doi: 10.1074/jbc.M113.534222
- Saerens D, Conrath K, Govaert J, Muyldermans S. Disulfide bond introduction for general stabilization of immunoglobulin heavy-chain variable domains. *J Mol Biol*. (2008) 377:478–88. doi: 10.1016/j.jmb.2008.01.022
- Bonfini B, Tittarelli M, Luciani M, Di Pancrazio C, Rodomonti D, Iannetti L, et al. Development of an indirect ELISA for the serological diagnosis of dourine. *Vet Parasitol*. (2018) 261:86–90. doi: 10.1016/j.vetpar.2018.08.014
- Xue X, Zhu C, Huang S, Pan L, Xu J, Li W. Effect of heat inactivation of blood samples on the efficacy of three detection methods of SARS-CoV-2 antibodies. *Nan Fang Yi Ke Da Xue Xue Bao*. (2020) 40:316–20. doi: 10.12122/j.issn.1673-4254.2020.03.03
- Poon LL, Guan Y, Nicholls JM, Yuen KY, Peiris JS. The aetiology, origins, and diagnosis of severe acute respiratory syndrome. *Lancet Infect Dis*. (2004) 4:663–71. doi: 10.1016/S1473-3099(04)01172-7
- Rabenau HF, Kampf G, Cinatl J, Doerr HW. Efficacy of various disinfectants against SARS coronavirus. *J Hosp Infect*. (2005) 61:107–11. doi: 10.1016/j.jhin.2004.12.023
- Kariwa H, Fujii N, Takashima I. Inactivation of SARS coronavirus by means of povidone-iodine, physical conditions and chemical reagents. *Dermatology*. (2006) 212(Suppl. 1):119–23. doi: 10.1159/000089211
- Zhao B, Liu S, Liu Y, Li G, Zhang Q. Liquid chromatography tandem mass spectrometry for therapeutic drug monitoring of voriconazole in heat-inactivated blood samples: its application during COVID-19 pandemic. *Nan Fang Yi Ke Da Xue Xue Bao*. (2020) 40:342–5. doi: 10.12122/j.issn.1673-4254.2020.03.08
- Volkin DB, Klibanov AM. Thermal destruction processes in proteins involving cystine residues. *J Biol Chem*. (1987) 262:2945–50.
- Stahl D, Lacroix-Desmazes S, Barreau C, Sibrowski W, Kazatchkine MD, Kaveri SV. Altered antibody repertoires of plasma IgM and IgG toward nonself antigens in patients with warm autoimmune hemolytic anemia. *Hum Immunol*. (2001) 62:348–61. doi: 10.1016/s0198-8859(01)00225-7
- Czajkowsky DM, Shao Z. The human IgM pentamer is a mushroom-shaped molecule with a flexural bias. *Proc Natl Acad Sci USA*. (2009) 106:14960–5. doi: 10.1073/pnas.0903805106
- Muller R, Gräwert MA, Kern T, Madl T, Peschek J, Sattler M, et al. High-resolution structures of the IgM Fc domains reveal principles of its hexamer formation. *Proc Natl Acad Sci USA*. (2013) 110:10183–8. doi: 10.1073/pnas.1300547110
- Futami J, Miyamoto A, Hagimoto A, Suzuki S, Futami M, Tada H. Evaluation of irreversible protein thermal inactivation caused by breakage of disulphide bonds using methanethiosulphonate. *Sci Rep*. (2017) 7:12471. doi: 10.1038/s41598-017-12748-y

**Conflict of Interest:** The authors declare that the research was conducted in the absence of any commercial or financial relationships that could be construed as a potential conflict of interest.

Copyright © 2021 Lin, Dai, Li, Xiao, Luo, Guo, Yang, Han, Zhu, Wu, He, Wu and Xia. This is an open-access article distributed under the terms of the Creative Commons Attribution License (CC BY). The use, distribution or reproduction in other forums is permitted, provided the original author(s) and the copyright owner(s) are credited and that the original publication in this journal is cited, in accordance with accepted academic practice. No use, distribution or reproduction is permitted which does not comply with these terms.





# COVID-19 *in-vitro* Diagnostics: State-of-the-Art and Challenges for Rapid, Scalable, and High-Accuracy Screening

Zeina Habli<sup>1</sup>, Sahera Saleh<sup>1</sup>, Hassan Zaraket<sup>2,3</sup> and Massoud L. Khraiche<sup>1\*</sup>

<sup>1</sup> Neural Engineering and Nanobiosensors Group, Biomedical Engineering Program, Maroun Semaan Faculty of Engineering and Architecture, American University of Beirut, Beirut, Lebanon, <sup>2</sup> Department of Experimental Pathology, Immunology and Microbiology, Faculty for Medicine, American University of Beirut, Beirut, Lebanon, <sup>3</sup> Center for Infectious Diseases Research, Faculty of Medicine, Beirut, Lebanon

## OPEN ACCESS

### Edited by:

Maria José Saavedra,  
Universidade de Trás os Montes e Alto  
Douro, Portugal

### Reviewed by:

Stephen Allen Morse,  
Centers for Disease Control and  
Prevention (CDC), United States  
Ramesh Goyal,  
Delhi Pharmaceutical Sciences and  
Research University, India

### \*Correspondence:

Massoud L. Khraiche  
mkhraiche@aub.edu.lb

### Specialty section:

This article was submitted to  
Biosafety and Biosecurity,  
a section of the journal  
Frontiers in Bioengineering and  
Biotechnology

**Received:** 13 September 2020

**Accepted:** 21 December 2020

**Published:** 28 January 2021

### Citation:

Habli Z, Saleh S, Zaraket H and  
Khraiche ML (2021) COVID-19 *in-vitro*  
Diagnostics: State-of-the-Art and  
Challenges for Rapid, Scalable, and  
High-Accuracy Screening.  
Front. Bioeng. Biotechnol. 8:605702.  
doi: 10.3389/fbioe.2020.605702

The world continues to grapple with the devastating effects of the current COVID-19 pandemic. The highly contagious nature of this respiratory disease challenges advanced viral diagnostic technologies for rapid, scalable, affordable, and high accuracy testing. Molecular assays have been the gold standard for direct detection of the presence of the viral RNA in suspected individuals, while immunoassays have been used in the surveillance of individuals by detecting antibodies against SARS-CoV-2. Unlike molecular testing, immunoassays are indirect testing of the viral infection. More than 140 diagnostic assays have been developed as of this date and have received the Food and Drug Administration (FDA) emergency use authorization (EUA). Given the differences in assay format and/or design as well as the lack of rigorous verification studies, the performance and accuracy of these testing modalities remain unclear. In this review, we aim to carefully examine commercialized and FDA approved molecular-based and serology-based diagnostic assays, analyze their performance characteristics and shed the light on their utility and limitations in dealing with the COVID-19 global public health crisis.

**Keywords:** SARS-CoV-2, COVID-19, pandemic, diagnostics, screening, serological immunoassays, point-of-care

## INTRODUCTION

Severe acute respiratory syndrome coronavirus 2 (SARS-CoV-2) leads to the infectious disease COVID-19, which was first reported in Wuhan, China in December 2019. The disease has since spread across the globe infecting over 215 countries. SARS-CoV-2 is highly contagious and spreads from person-to-person by the respiratory route, primarily via droplets, aerosols, and contact with contaminated surfaces and fomites (Yeasmin et al., 2020). Its reproduction number ( $R_0$ ) is estimated to be around 2.68 with a doubling time of 6.4 days. On the other hand, its incubation period from infection to first symptoms is on average 5 days with a possibility of reaching 14 days (Wu et al., 2020b). The clinical manifestations of COVID-19 include fever, cough, fatigue, and breathing difficulties, which could result in severe complications, such as severe pneumonia and respiratory distress syndrome (ARDS). To date, only a very limited number of therapeutic options have shown little effects on reducing COVID-19 associated death, such as remdesivir and dexamethasone (reviewed in Kaddoura et al., 2020).

In the absence of proven antiviral drug therapies and commercially available vaccines, the current pandemic containment and mitigation strategy is relying on the isolation of the infected individuals and their close contacts in addition to social distancing. The problem is exacerbated by the presence of many asymptomatic patients that can only be identified via molecular based disease screening methods. Due to that, mass testing has been central to the worldwide disease containment efforts which represented a challenge to cost, scalability, and speed of state-of-the-art viral screening technology.

Real-time reverse transcriptase-polymerase chain reaction (RT-PCR) is the clinical gold standard for the etiological diagnosis of COVID-19 in which viral RNA is directly detected in respiratory specimens by means of molecular biology techniques. On the other hand, serology-based immunoassays are being used in central labs or rapid testing for epidemiological surveillance to detect antibodies produced by infected individuals in response to SARS-CoV-2 exposure. So far, scientists are racing to develop novel approaches for rapid testing with high sensitivity and low cost to meet the diagnostic challenges. This goes hand in hand with the evolving effort to battle COVID-19, as many countries have opted to employ safe reopening to mitigate the economic crisis and manage health consequences. Safe reopening measures include investments in the public health infrastructure, implementing rapid and sensitive diagnostics of suspected cases, contact tracing and integrating social distancing and quarantining when needed (Gottlieb et al., 2020).

In this body of work, we carry out a deep technical analysis of the current COVID-19 diagnostic tests approved by the FDA for emergency use in Clinical Laboratory Improvement Amendments (CLIA)-certified molecular diagnostics laboratories. The work also closely probes each testing technology to identify their advantages and disadvantages and the clinical and field challenges still facing mass testing for COVID-19.

## SARS-COV-2 VIROLOGY AND PATHOPHYSIOLOGY

### SARS-CoV-2 Viral Structure and Genome

SARS-CoV-2 is an enveloped large positive-sense single-stranded RNA virus with a genome of ~30 kb (**Figure 1**). The virus belongs to the genus *betacoronavirus* and has a diameter of 50–200 nm. SARS-CoV-2 is characterized by the spike glycoproteins protruding from its surface giving it the characteristic crown-like appearance under the electron microscope (Casella et al., 2020; Zhou et al., 2020). The SARS-CoV-2 genome encodes for four major structural and functional proteins: the spike (S), membrane (M), envelope (E), and nucleocapsid (N) proteins (Zou et al., 2020). The S protein consists of two functional subunits, S1 and S2; S1 is responsible for recognizing and binding the host cell receptor, angiotensin-converting enzyme 2 (ACE2), while S2 mediates membrane fusion. The M protein is the most abundant structural protein that defines the shape of the virus. The N protein is the most abundantly shed viral protein during infection and can be detected in serum and urine samples within

the first 2 weeks of infection. The smallest major structural protein, E protein, participates in viral assembly and pathogenesis (Wang et al., 2020).

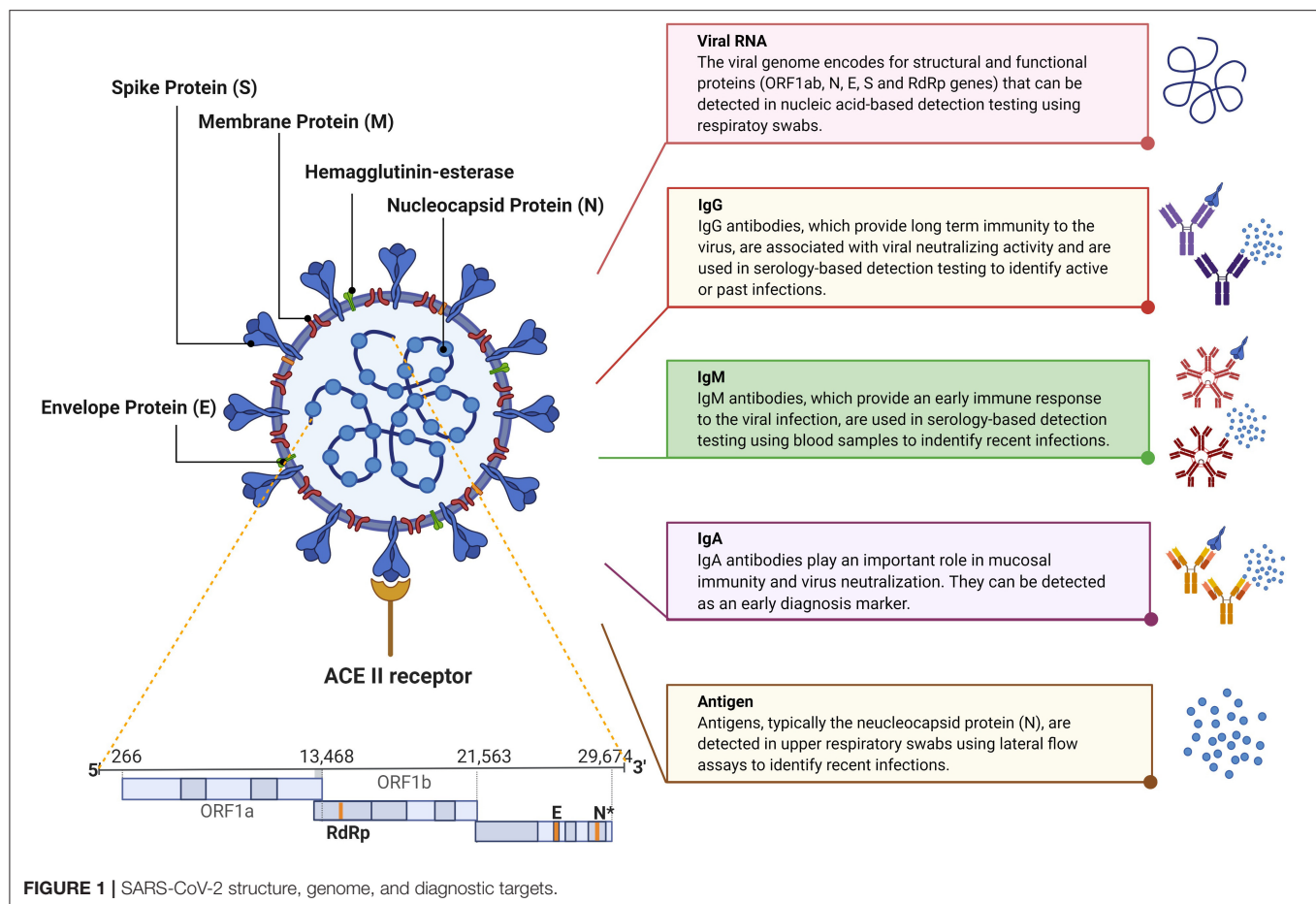
### SARS-CoV-2 Pathophysiology

Several studies have shown that SARS-CoV-2 infects cells with high expression of ACE2 receptors, such as type II pneumocytes in the upper and lower respiratory system, endothelium, myocardium, and gastrointestinal mucosa cells (Astuti and Ysrafil, 2020; Bobeck et al., 2020; Hoffmann et al., 2020). The virus enters the cell via endoplasmic uptake. Following fusion with the endosomal membrane, the viral RNA genome is released into the cytoplasm where replication of the virus genomes and production of its proteins take place. The newly synthesized nucleocapsid, made up of viral RNA and N protein, are imported into the endoplasmic reticulum-Golgi intermediate compartment (ERGIC) and the viral proteins are assembled with the rest of the proteins to form progeny viruses. The latter are then transferred in vesicles to the plasma membrane where they exit (Fehr and Perlman, 2015).

The clinical manifestations of COVID-19 patients range from mild (e.g., fever, non-productive cough, dyspnea, fatigue, sore throat, etc.) to severe complications, such as pneumonia and ARDS and may lead to death in chronic severe cases. Besides, infected individuals show high production of leukocytes, lymphopenia, and elevated levels of cytokines (e.g., IL-6) (Liu et al., 2020; Rothan and Byrareddy, 2020). The immune response triggered against this virus involves the secretion of three types of immunoglobulins, anti-SARS-CoV-2 immunoglobulins M (IgM), anti-SARS-CoV-2 immunoglobulins G (IgG), and anti-SARS-CoV-2 immunoglobulins A (IgA), which are essential biomarkers for identifying individuals affected by COVID-19, including those who may be asymptomatic or have recovered (Jacofsky et al., 2020).

## SARS-COV-2 BIOMARKERS FOR DIAGNOSIS

Current nucleic acid-based diagnostic assays target the E, S, RNA-dependent RNA polymerase (RdRp), N, and/or open reading frame (ORF1ab) genes (Chan et al., 2020; Chu et al., 2020; Corman et al., 2020). For these assays, upper and lower respiratory tracts samples are collected via nasopharyngeal (NP) or oropharyngeal (OP) swabs, sputum, endotracheal aspirate, bronchoalveolar lavage, or saliva where the SARS-CoV-2 RNA was found to be higher than in other samples, such as blood and stool. The latter two samples are only collected for research purposes (Vogels et al., 2020a; Zou et al., 2020). The analytical sensitivity of such assays is affected by the temporal profile of the viral load over the course of infection. Several studies suggest that the viral load peaks shortly around the time or even before symptoms onset then decreases quickly and monotonically within the first 7 days (Becherer et al., 2020; To et al., 2020b). Additionally, the virus remains detectable for 20 days or longer after symptom onset (**Figure 2**) (Zou et al., 2020). This means that false negatives may possibly be obtained early and late



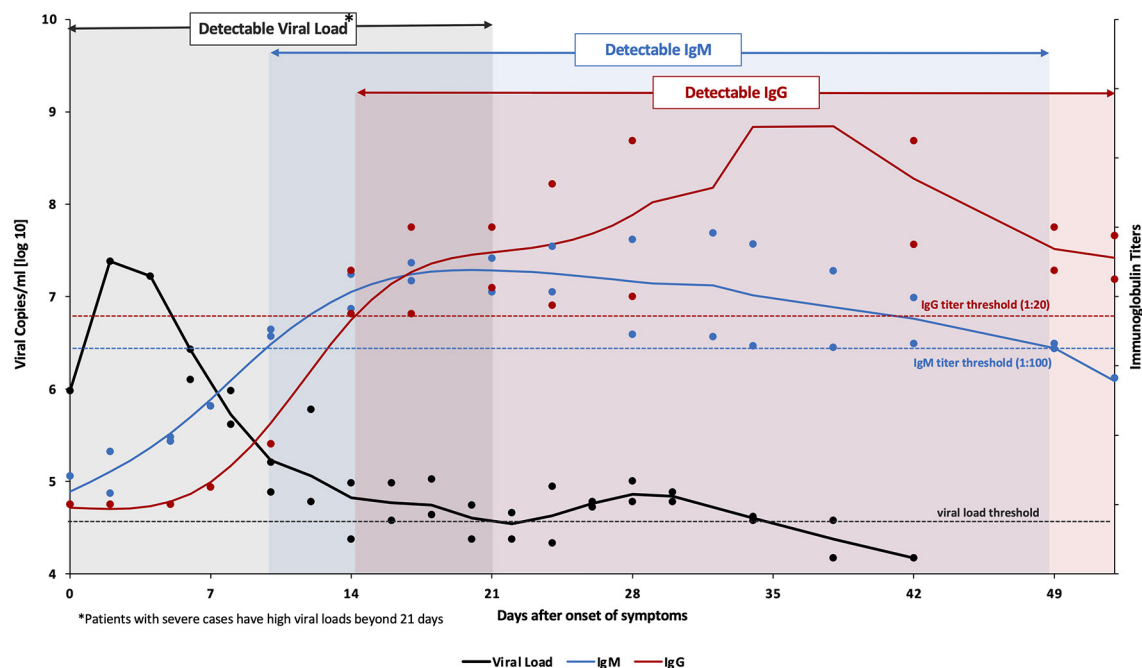
stages of the infection when using molecular diagnostic assays for testing. In addition, given the relatively short detection window of these assays, the true extent of exposure to the virus in a population may be underestimated.

Serology-based immunoassays have also been developed to detect antibodies for SARS-CoV-2 in the serum or plasma of patients, namely anti-S and anti-N IgM, IgG, and IgA (To et al., 2020a; Zou et al., 2020). IgM provides the first line of defense during a viral infection. Also, the IgM response to SARS-CoV-2 was reported to occur earlier than other immunoglobulins, at around 10 days after infection, but then decreases rapidly after 35 days and disappears (Figure 2). IgG on the other hand provides long-term immunity and immunological memory and is detectable starting 13–21 days after infection and persists for a longer time (Figure 2) (Tan et al., 2020). On the other hand, IgA levels in the blood and saliva specimens have been correlated with COVID-19 severity; therefore it can be used as a complementary biological marker for COVID-19 identification (Ma et al., 2020). Thus, antibodies indicate the true exposure to the virus in an individual since they can be detected long after the virus has disappeared (Demey et al., 2020). However, the lack of detectable antibodies at the early stages of the infection makes serology-based immunoassays unsuitable for the diagnosis of an active infection.

Although nucleic acid assays are rather vital for diagnostic purposes, especially in cases of mild to acute infection, serology-based testing is proving to be increasingly important in understanding the dynamics of the current pandemic as it continues to spread. Complementary to molecular-based assays and immunoassays, the FDA recently approved tests that can detect the viral antigens, mainly the N protein. Similar to the viral load, SARS-CoV-2 proteins are maximal during the first week of symptoms onset, and rapidly decline during the recovery phase. The diagnostic targets are highlighted in Figure 1 whereas the variation in the levels of SARS-CoV-2 viral load, IgM, and IgG post-infection are shown in Figure 2.

## MOLECULAR-BASED ASSAYS FOR SARS-COV-2 NUCLEIC ACID DETECTION

As soon as the genome sequence of SARS-CoV-2 was made publicly available on the Global Initiative on Sharing All Influenza Data (GISAID) (Udugama et al., 2020; Wu et al., 2020a), numerous molecular COVID-19 diagnostic kits were developed. This section is an analysis of the clinically conventional and novel methodologies for SARS-CoV-2 nucleic acid detection that received FDA EUA and/or European



**FIGURE 2 |** Variation levels of viral load, IgM and IgG post SARS-CoV-2 infection. Data collected from Tan et al. from 67 confirmed COVID-19 patients (both mild and severe cases) (Tan et al., 2020). Viral RNA (amplified ORF1ab gene) was detected in nasopharyngeal swabs using the Qiamp® viral RNA mini kit (QIAGEN, Hilden, Germany). The viral load threshold (black dashed line) indicates the detection limit of this kit corresponding to a cycle threshold value of 38 which is equivalent to 104.577 genomic copies/mL. On the other hand, IgM & IgG titers (anti-SARS-CoV-2 nucleocapsid immunoglobulins) were analyzed in serum samples using ELISA kits (Livzon Diagnostics Inc., Zhuhai, China). The blue and red dashed lines denote the cutoff value for a positive result. The bold lines represent the trends, fitted using smoothing splines in Matlab.

Conformity (CE Marking). The molecular detection kits are outlined in **Supplementary Table 1** [data obtained from (FDA, 2020b) and (FINDdx, 2020)], and their workflow is illustrated in **Figure 3**.

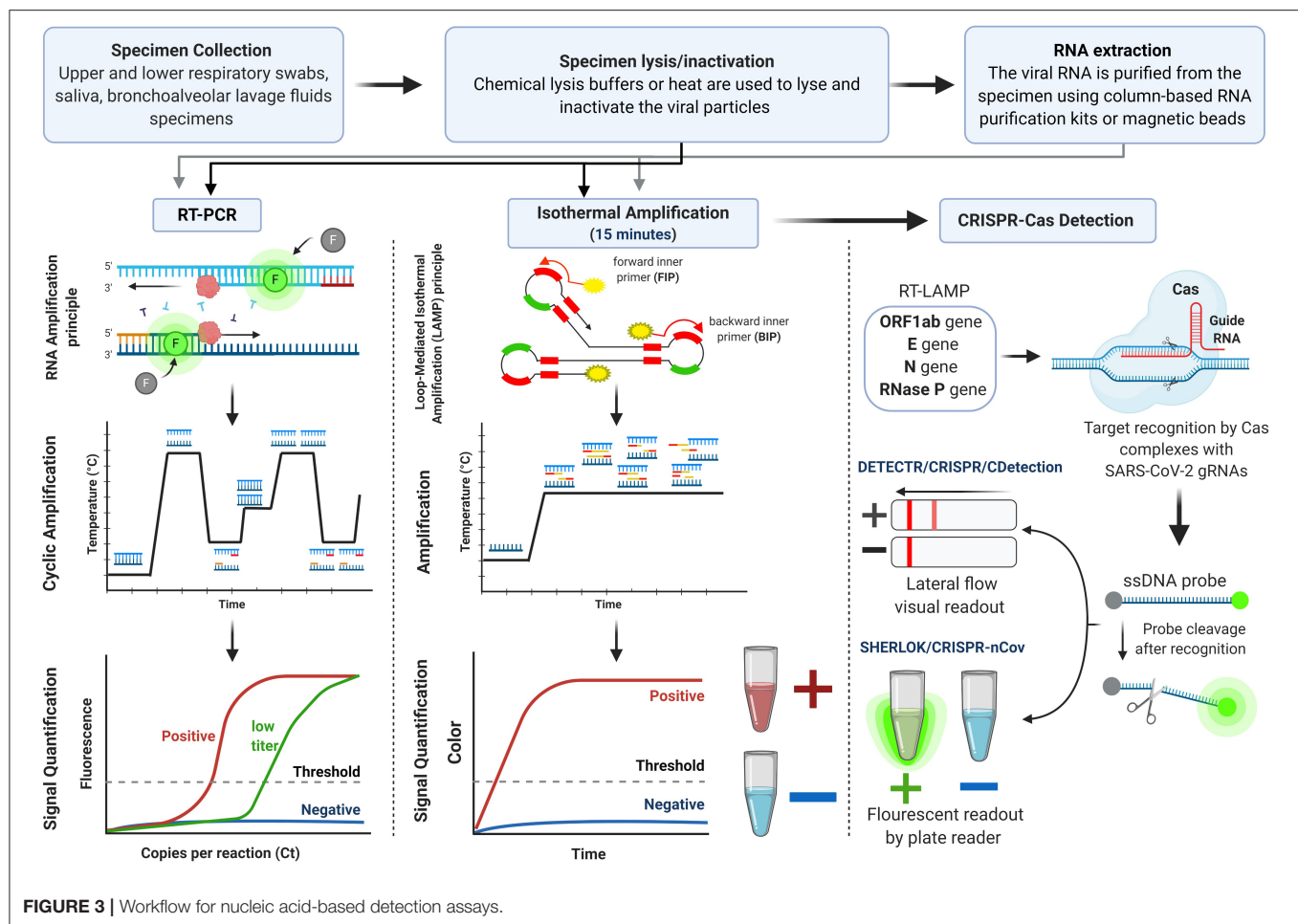
## Reverse Real-Time Polymerase Chain Reaction (RT-PCR) Assays for SARS-CoV-2 Detection

The current clinical standard molecular test for SARS-CoV-2 nucleic acid detection is the quantitative reverse RT-PCR assay. These assays were the first developed for COVID-19 diagnosis and remain the most used assays. More than one hundred RT-PCR kits have been designed and prototyped and have received FDA EUA approval for COVID-19 diagnosis genetically (presented in **Supplementary Table 1**). RT-PCR reaction involves the reverse transcription of SARS-CoV-2 genomic RNA into a complementary DNA (cDNA) followed by amplification of targeted sequences using a set of specific primers. A variety of gene targets with comparable sensitivities are used to recognize regions of the viral genes, such as structural proteins genes (N, E, S, M genes) and confirmatory genes (ORF1ab and RdRp genes). The latter genes are used to avoid potential cross-reactivity with other coronaviruses and any possibility of genetic drift in SARS-CoV-2. The Centers for Disease Control and Prevention (CDC) recommends screening

with nucleocapsid protein targets (N1 and N2) while the World Health Organization (WHO) recommends targeting the E gene followed by the confirmatory RdRp gene (Tang et al., 2020). The viral RNA is measured by the cycle threshold (Ct), which is the number of amplification cycles needed to produce a measurable fluorescent signal. The lower the Ct values, the higher the viral RNA load in a sample. The intensity of the fluorescent signal reflects the momentary amount of DNA amplicons; after 35–40 amplification cycles, the viral DNA is quantified and can be detected even if the starting viral RNA amount is small (reviewed in Kralik and Ricchi, 2017). The test typically takes 6–8 h on average, but with the need for clinical sample collection and transfer, the test requires 24 h at best. A positive PCR result reflects the presence of the viral RNA but does not necessarily indicate the presence of infectious viruses within the sample. In addition, PCR positivity is specimen dependent; it declines more slowly in sputum compared to fast declination in NP swabs (Wölfel et al., 2020).

Although RT-PCR is the gold standard with high specificity (~100%), sensitivity, and accuracy, the procedure is labor-intensive and relies on sophisticated instrumentation usually located at central laboratories and requires the use of biosafety level 2 cabinets (Younes et al., 2020). These assays are time-consuming and require technical expertise in specialized and controlled space making them unsuitable for deployment as point-of-care





**FIGURE 3 |** Workflow for nucleic acid-based detection assays.

rapid diagnostics but have the advantage of being high throughput.

To overcome the limitations of conventional real-time RT-PCR assays, fully automated high-quality molecular point-of-care diagnostic platforms have been developed. For example, Roche Molecular Systems, Inc. developed the automated Cobas<sup>®</sup> SARS-CoV-2 RT-PCR test which is intended for qualitative detection of the viral nucleic acid in NP and OP swabs. Roche Cobas<sup>®</sup> can deliver results within 3.5 h while running up to 96 tests simultaneously. Also, depending on the instrumentation used, it can process 384 specimens with the cobas 6800 System or 1,056 specimens with the cobas 8800 System in <8 h. Additionally, the Xpert<sup>®</sup> Xpress SARS-CoV-2 test developed by Cepheid (California, USA) integrates nucleic acid extraction, transcription and amplification in a single cartridge, and provides results within 45 min with 100% sensitivity and 99% specificity-agreement when compared to Roche Cobas<sup>®</sup> SARS-CoV-2 tests. Another forerunner in the field of testing is the BioFire Diagnostics, LLC, which developed the multiplexed BioFire Respiratory Panel 2.1 (RP2.1) closed system. The limit of detection (LoD) of the BioFire is 300 viral genomic copies/mL and gives results within 45 min as well.

## Reverse Transcription Loop-Mediated Isothermal Amplification (RT-LAMP) Assays for SARS-CoV-2 Detection

The limitations of RT-PCR, namely the complex and expensive instrumentation needed for thermal cycling, led to the development of isothermal nucleic acid amplification tests that overcome these issues (Huang et al., 2020). Currently, these point-of-care tests are becoming more appealing in clinical applications, mainly due to fast processing times and low-cost devices needed (Kashir and Yaqinuddin, 2020). They obviate the need for trained personnel, access to expensive laboratory equipment and high-tech facilities for sample processing, which is particularly important in developing countries with limited access to such resources. The most prominently used isothermal nucleic acid amplification test is the loop-mediated isothermal amplification (LAMP) (Nguyen et al., 2020). It was first described by Notomi et al. (in review), then further optimized for accelerated amplification by Nagamine et al. (Becherer et al., 2020). This technique uses four to six primers, inner and outer, which recognize six to eight different regions in the target DNA sequence, and a DNA polymerase with strand-displacement activity. The process is carried out at a constant

temperature ranging between 60 and 65°C, synthesizing target DNA up to  $10^9$  copies in less than an hour (Nguyen et al., 2020). The final products of LAMP are multiple inverted repeats of the target DNA with stem-loop structure (Becherer et al., 2020). LAMP combined with reverse transcription (RT-LAMP) allows for the direct detection of RNA and can thus be used for the rapid detection of SARS-CoV-2 (Kashir and Yaqinuddin, 2020; Park et al., 2020). Colorimetric or fluorescent read-out could be used for the visualization of the results (Becherer et al., 2020). This assay achieves a sample-to-result time of 1–2 h. This gives RT-LAMP a great advantage over RT-PCR that has a sample-to-result time of 6–8 h, ensuring a rapid response required in massive virus outbreaks. The diagnostic sensitivity and specificity of RT-LAMP assays designed for the detection of SARS-CoV-2 were found to be comparable to those of RT-PCR in various studies (Butt et al., 2020; Zhang et al., 2020b). These features suggest that RT-LAMP can be employed in the diagnosis of COVID-19 with high levels of precision, low levels of background signal and more tolerance to PCR-inhibitors (Becherer et al., 2020).

A few isothermal nucleic acid amplification assays have received FDA EUA approval and are currently available, including the Abbott ID NOW COVID-19 assay that utilizes isothermal amplification to detect the RdRp gene of SARS-CoV-2 RNA (Basu et al., 2020). This assay provides positive results within 5 min and negative results within 13 min with a LoD of 125 genome equivalents/mL and reported 100% sensitivity and specificity as claimed by its manufacturer (Harrington et al., 2020). However, on May 15, 2020, the FDA issued a public warning about Abbott ID NOW COVID-19 accuracy and performance. The test has reported negative results in one third of the samples tested positive by Cepheid Xpert Xpress when using NP swabs and in 45% of positive samples using dry nasal swab samples (Basu et al., 2020). Another assay that employs isothermal nucleic acid amplification is the iAMP<sup>®</sup> COVID-19 Detection Kit developed by Atila Biosystems Inc. which targets ORF1ab and N genes of SARS-CoV-2 RNA (Bulterys et al., 2020). It received FDA EUA in April 2020. The sample-to-result time is around 1 h and up to 94 samples per instrument can be run with a LoD of 4,000 copies/mL. The manufacturers reported 98% sensitivity and 93% specificity.

## CRISPR-Based Assays for SARS-CoV-2 Detection

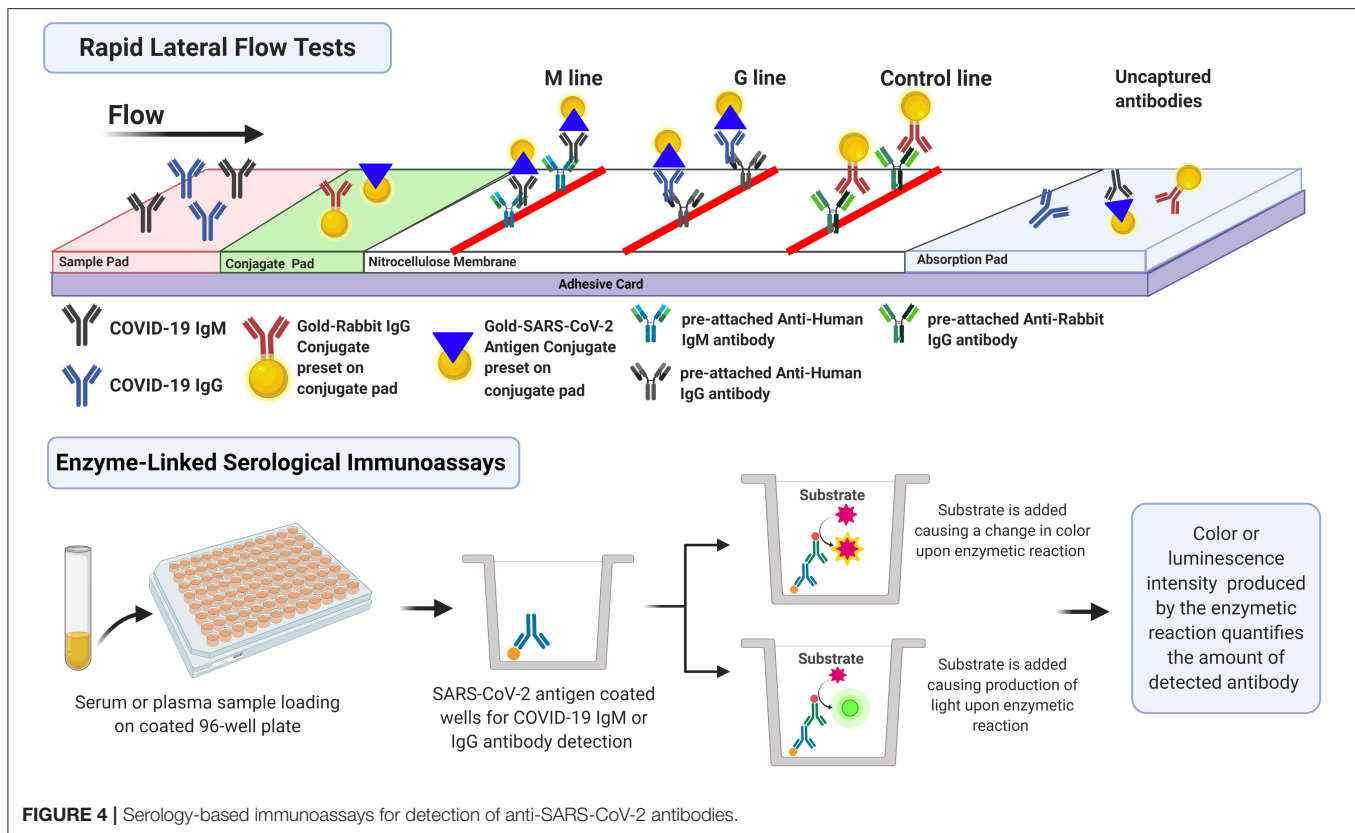
Over the past two years, the use of CRISPR in infectious diseases diagnostics has been gaining momentum (Bhattacharyya et al., 2018). CRISPR belongs to a family of palindromic nucleic acid repeats, found in bacteria, that can be recognized and cut by a unique set of effector enzymes known as the CRISPR-associated (Cas) proteins. The Cas enzymes display exceptionally sensitive and specific nucleic acid detection modalities as they can be programmed to identify and cut SARS-CoV-2 RNA sequences.

Mammoth Biosciences and Sherlock Biosciences have reconfigured their CRISPR-based platforms independently to rapidly and accurately detect SARS-CoV-2 nucleic acids

in respiratory specimens. Sherlock Biosciences developed the SHERLOCK method (specific high-sensitivity enzymatic reporter unlocking), which utilizes the Cas13a enzyme (Kellner et al., 2019). In contrast, Mammoth Biosciences developed the DETECTR method (DNA endonuclease targeted CRISPR trans reporter), which utilizes the Cas12a enzyme (Chen et al., 2018). Cas13a and Cas12a have a “collateral cleavage” activity triggered by a target-dependent binding between the Cas-guide RNA complex (CRISPR complex) and the targeted sequence. This event activates the nuclease enzyme activity of the Cas, followed by the cleavage of the nucleic acid reporter and the generation of a detectable signal. SHERLOCK-based detection method recently received FDA EUA. It combines Cepheid automated RT-PCR for SARS-CoV-2 nucleic acid amplification followed by collateral cleavage activity of the CRISPR complex programmed to target the SARS-CoV-2 sequences; the resultant fluorescent signal is then detected by a plate reader. The whole process takes less than an hour without elaborate instrumentation. It can detect targeted sequences at a concentration as low as 6.75 copies/ $\mu$ L; it also has 100% specificity and sensitivity with the absence of cross-reactivity with sequences of high homology (Zhang et al., 2020a). On the other hand, DETECTR-based detection uses an additional reporter dye (Fluorescein amidite, FAM), which produces color when cut. DETECTR combines RT-LAMP for SARS-CoV-2 targeted sequences amplification followed by lateral flow assay for visual read-out detection. The assay time is 30–40 min and has 95% sensitivity and 100% specificity (Broughton et al., 2020). According to the initial validation testing of the cutting-edge CRISPR-based detection platforms, these tests have great potential for diagnosis. They do not require heavy instrumentation, and the results can be read quickly by a paper strip or a plate reader with minimal cost and high sensitivity and specificity.

## SEROLOGY-BASED IMMUNOASSAYS (ANTIBODIES DETECTION)

Apart from molecular diagnostics and nucleic acid detection, various assays have been developed by several companies to test for antibodies produced in response to SARS-CoV-2 infection. Antibody-based tests are relatively cheap, easy to operate, and require less technical expertise compared to molecular-based assays. The dynamics of antibodies production may provide a larger window for detecting and monitoring current and past SARS-CoV-2 infections. Current serology-based tests include rapid lateral flow immunoassay tests also known as immunochromatographic assays (ICA), enzyme-linked immunosorbent assay (ELISA), automated chemiluminescence microparticle immunoassay (CMIA) among others. This section is a summary of two main approaches used to detect immunoglobulins produced against SARS-CoV-2 that received FDA EUA and/or CE Marking. These antibody detection tests are summarized in **Supplementary Table 1**, and the workflow is illustrated in **Figure 4**.



## Serology-Based Rapid Lateral Flow Immunoassay for Antibody Detection

Lateral flow assay allows for the qualitative detection (positive or negative) of antibodies found in a blood sample. This test is easy to perform, inexpensive to develop, and provides results within minutes. This gives lateral flow assays great advantage for rapid diagnostic testing of COVID-19 by testing for the presence of different isotypes of antibodies that target different SARS-CoV-2 proteins (N and S proteins among others). Several assays, referred to as total antibody assays, employed the detection of all isotypes (IgM, IgG, and IgA), while others targeted IgM and IgG exclusively. Both approaches were investigated by Lou et al. (2020) who compare the performance of 3 different lateral flow assays targeting IgG, IgM, and total antibody. They reported that the first detectable serological markers were total antibody, followed by IgM then IgG (9, 10, and 12 days after symptom onset). They also noted that the total antibody assay had the highest sensitivity among the others (98%) 2 weeks post-symptom onset.

The lateral flow assay requires a minimal sample volume of around 20  $\mu$ L of blood or 10  $\mu$ L of serum/plasma. It also does not require bulky instrumentation or trained personnel (Vashist, 2020). In this assay, the sample is placed on the absorbent sample pad of the lateral flow test strip and is allowed to migrate through the conjugate release pad which contains the SARS-CoV-2 antigen conjugated to colored or fluorescent particles, most commonly colloidal gold. The antigen is usually

the receptor-binding domain of SARS-CoV-2 spike protein or nucleocapsid protein. If the patient was infected with SARS-CoV-2 and had the specific antibodies, then the sample now containing IgG and/or IgM antibodies bound to the conjugated antigens migrates to the detection zone. This zone contains anti-human IgG and IgM lines (test lines) that capture the antigen-antibody complexes, in addition to a control line. The read-out, which appears as lines with varying intensities can be assessed using a dedicated reader or by eye (Koczula and Gallotta, 2016).

Several lateral flow assays for COVID-19 IgG and IgM antibodies have been FDA EUA approved, including qSARS-CoV-2 IgG/IgM Rapid Test developed by Cellex which targets the S and N proteins and gives qualitative results within 15–20 min with 93.8% positive percent agreement (PPA) and 96% negative percent agreement (NPA) (FDA, 2020c; Mathur and Mathur, 2020). AutoBio Diagnostics also developed anti-SARS-CoV-2 rapid test that tests for IgG only and targets the spike protein with reported 88.15% PPA and 99.04% NPA with previously PCR tested samples (Mathur and Mathur, 2020).

## Enzyme Linked Serology-Based Immunoassays for Antibody Detection

COVID-19 enzyme-linked serology-based immunoassays are rapidly emerging as tools for surveying exposed individuals, including those who are asymptomatic or have recovered. These tests are at increased demand to better quantify the number of COVID-19 cases for epidemiological and surveillance purposes.

Enzyme-linked immunoassays are usually performed in a laboratory setting and can be either qualitative or quantitative; specimens can be plasma or serum specimens. ELISA is the conventional platform for assessing SARS-CoV-2 exposure; it can detect antibodies at the lowest concentrations ( $\sim$ picogram/mL ranges). It is a microwell, plate-based assay used for the detection and quantification of antibodies produced against the viral infection. The well plate is coated with a deactivated virus or a recombinant viral antigen, typically, the S protein, (RBD) protein, or the N protein. Patient samples are then added to the well and the plate is incubated. If the patient has antibodies against the viral protein, an antibody-antigen complex is formed, and the complex can be detected by an enzyme-linked or a fluorescently tagged secondary antibody designed against the human antibodies (anti-human IgG/IgA/IgM). A colorimetric or a fluorescent signal is produced according to the type of secondary antibody used; the intensity of the signal reflects the quantity of the antibodies present within the sample after adjusting for the dilution factor. The whole process typically takes 2–5 h, but up to 96 samples can be tested at a time (Wild, 2013). It is worth noting that ELISA cannot tell if the detected antibodies are active or effective against the viral infection. Such information can be depicted by plaque reduction neutralization tests that involve cell culture, viral infection, and viral replication assessment. Several ELISA kits have been FDA approved for emergency use in COVID-19 diagnosis. For instance, Bio-Rad Laboratories Inc. designed the Platelia SARS-CoV-2 total Ab Assay which detects IgG, IgA, and IgM; it has 92% PPA and 99.5% NPA with previously PCR tested samples.

Another serology-based enzyme-linked platform is the CMIA (chemiluminescent microparticle immunoassay) that has low limits of antibody detection ( $\sim$ zeptomole  $10^{-12}$  mol) and involves chemiluminescence for signal read-out; it is a modified advanced form of ELISA. CMIA offers several advantages over ELISA in terms of cost, sensitivity, LOD, and reproducibility. Also, the testing time is reduced due to shorter incubation periods and reaction times, where both processes are fully automated by digital analyzers (Qin and Jin-Ming, 2015). On the contrary, similar to ELISA, the test is typically qualitative and quantitative; it is also laboratory-based, and the samples are either plasma or serum specimens. The test relies on magnetic protein-coated microparticles used as a solid support to coat the wells with the viral antigen of interest. The full assay takes 1–2 h to perform with incubation steps similar to the conventional ELISA. The substrate is added to the enzyme-linked secondary antibody, which is bound to the antibody-antigen complex, and produces a light (radiance) signal. The luminescence is used to quantify the amount of antibodies present in the sample. The use of streptavidin-coated magnetic beads with several biotinylated viral antigens allows high sensitivity multiplexing if several antibodies are needed to be detected at the same time within the same sample (Cinquanta et al., 2017). A very promising CMIA-based FDA approved assay is the SARS-CoV-2 IgG Assay by Abbott Laboratories Inc. It has more than 96% PPA and 99.63% NPA in samples taken 14 days post-symptoms onset. On the other hand, chemiluminescence-based assays can be coupled with electrical voltage instead of

enzyme-linked secondary antibodies for signal emission. Roche Diagnostics is a pioneer in this field with its Elecsys Anti-SARS-CoV-2 kit. Elecsys is an electrochemiluminescence microparticle immunoassay (ECMIA) that uses the Cobas immunoassay analyzer and takes only 18 min for the testing time. It uses the double antigen sandwich format to detect IgM, IgG, or IgA antibodies with high affinity. The first recombinant antigen is biotinylated while the second is coupled with ruthenium complex. When the double antigen-antibody sandwich complex is attained, streptavidin-coated microparticles are added to bind to the biotinylated antigen. The mixture is then aspirated to the measuring cell and microparticles are magnetically captured on the surface of the electrode. Application of voltage to the electrode induces radiance emission from the ruthenium and the light is measured by a photomultiplier. Elecsys Anti-SARS-CoV-2 has a high accuracy of targeting high affinity antibodies with 99.81% specificity and 100% sensitivity from samples taken 14 days post-symptoms onset; in addition, it is capable of running up to 300 serology tests/h depending on the type of the analyzer.

Currently, over 40 manufacturers have developed serology-based tests and received the FDA EUA. The FDA requires the laboratories to validate their assay as deemed appropriate (FDA, 2020a); thus, the absence of FDA oversight on these tests is a concern if we take into consideration the high variability of the proposed test formats (ICA, ELISA, CLIA, ECMIA) and the differences in the antibody class(es) detected. As such, along with the novelty of SARS-CoV-2 and our limited information regarding the human immune response to it, it is worth noting that serology-based immunoassays have not been fully evaluated and their true clinical performance is mostly unknown. In addition, according to the manufacturer's data sheets, the performance of serology immunoassays is frequently evaluated in comparison to results obtained by the RT-PCR molecular diagnostic assay; given the differences in both assays format along with the design and targets, serology negative results do not rule out the possibility of infection. Should mass testing and screening be recommended, it is vital for laboratories considering serology-based immunoassays to perform thorough verification studies to ensure the appropriate clinical performance of these tests and the accuracy of the obtained results.

## ANTIGEN-BASED ASSAYS FOR SARS-COV-2 DETECTION

Antigen-based diagnostics detect protein fragments on or within the virus rather than viral nucleic acids in specimens collected from NP swabs or nasal cavity. This type of testing is a rapid point-of-care platform that can detect active infections within 15 min compared to hours with RT-PCR diagnostics. These tests can be mass-produced at low cost and have a simpler setup compared to RT-PCR tests (Chen et al., 2015). Although antigen-based tests are very specific, they are not as sensitive as RT-PCR tests (CDC, 2020). This is attributed to the fact that rapid antigen testing sensitivity correlates directly with the viral load that is maximal during the first week of onset only. Thus, antigen-based testing has a relatively small window of detection during



the incubation period of infected individuals. RT-PCR is more sensitive because its LoD is as low as  $10^2$  genomic copies/mL, while that of rapid antigen tests is  $\sim 10^5$  genomic copies/mL when correlating the amount of viral proteins to viral nucleic acid quantity (Nash et al., 2020; Vogels et al., 2020b).

So far, EUA was issued to four antigen-based detection diagnostic tests: Sophia 2 SARS Antigen FIA (Quidel Corporation, USA), BD Veritor System for Rapid Detection of SARS-CoV-2 (Becton, Dickinson and Company (BD), USA), LumiraDx SARS-CoV-2 Ag Test (LumiraDx UK Ltd., UK) and BinaxNOW COVID-19 Ag Card (Abbott Diagnostics Scarborough, Inc.). These antigen-based detection tests are qualitative lateral flow immunoassays used to detect viral proteins, the N protein, in upper respiratory specimens during the acute phase of infection. A respiratory specimen is obtained (usually a NP or a nasal swab) and suspended in an extraction solution to liberate the viral antigens. The sample is then dispensed into the test cassette well where it migrates by capillary action to regions containing antibodies against the viral antigen. If SARS-CoV-2 antigens are present, a signal is produced and is detected. The signal can be colorimetric and read visually as in BD Veritor System for Rapid Detection of SARS-CoV-2 and BinaxNOW COVID-19 Ag Card tests, or it can be fluorescent (for higher sensitivity) and read by digital analyzers as in Sophia 2 SARS Antigen FIA and LumiraDx SARS-CoV-2 Ag Test. These tests are automated and are authorized for use in high and moderate complexity laboratories certified by CLIA, as well as for point-of-care testing by facilities operating under a CLIA Certificate of Waiver.

Among the tens of different tools developed and proposed for COVID-19 detection, by the time this review has been written, only tests belonging to five approaches received the FDA, and all are presented and discussed in this review paper. These approaches differ on various levels starting with the technology itself, specimen collection and targets, as well as sample processing. These differences are presented and compared in **Table 1**.

## TESTING SENSITIVITY VS. RAPIDITY

The current reliance on high accuracy detection of COVID-19 cases for community surveillance and safe reopening of societies has put testing sensitivity and rapidness under the spotlight. The gold standard for COVID-19 detection is the molecular RT-PCR which has low LoD and high sensitivity, but at the same time, it is expensive, laboratory-based and often takes at least 24–48 h for sample-to-answer-reporting time.

New developments in COVID-19 diagnostic technology are focused on reducing test cost and sample-to-result time to expand testing frequency and lessen testing turnaround time from days to minutes. However, the sensitivity of these tests is not comparable to that of RT-PCR making it almost impossible to get the FDA EUA/CE marking approval. However, such restrictions should be reconsidered when taking into account both viral kinetics and RT-PCR sensitivity. As discussed earlier, patients undergo a period of peak in viral load and infectiousness followed

by a rapid decline in viral levels and clearance. Given RT-PCR amplification is exponential, it can detect viral RNA at extremely low levels yielding high Ct values. Nevertheless, detection of low RNA levels may not hold much value as Singanayagam et al. (2020) showed. They demonstrated that the odds of recovering an infectious virus from patients decreased by 0.67 for each unit increase in Ct value. Additionally, only 8% of the samples with Ct > 35 yielded culturable virus (Singanayagam et al., 2020). These data were consistent with other studies by Bullard et al. (2020) and La Scola et al. (2020). Accordingly, a cheap, rapid, and robust test with acceptable sensitivity would be able to detect the viral infection at least at the contagious period of illness when the viral load is the highest and would help in halting and controlling the coronavirus pandemic.

Current attempts to improving testing accessibility and scalability in the Yale-NBA study [Surveillance **with** Improved Screening and Health (SWISH) study] have led to the development of the SalivaDirect test. SalivaDirect uses a conventional quantitative nucleic acid-based detection technique (RT-PCR or RT-LAMP) but replaces the nucleic acid extraction step with a simple proteinase K and heat treatment step. Bypassing the conventional intricate RNA extraction method minimizes sample processing time and reagents usage. Thus, it lowers the sample processing cost and alleviates the testing demands. The SalivaDirect kit recently received the FDA EUA approval and has shown more than 94% sensitivity agreement with the CDC RT-qPCR assay as claimed in their preprint (Vogels et al., 2020a). Nonetheless, using saliva as a specimen and enzymes for RNA extraction does not make this test a “rapid” one because of the amplification and detection steps required.

To meet the needs of COVID-19 mass testing, a true rapid test must be done outside laboratory settings with minimal machinery and technical expertise is needed. Also, given these tests are required around the world with different geographies and related economical constraints, it is vital for these rapid diagnostic tests to be affordable and cheap so that people can use them more frequently. In addition, these tests must possess acceptable sensitivity to detect SARS-CoV-2 infection in its contagious stage to stem the spread of the virus via individual screening. These challenges are clear when examining RT-PCR's sensitivity compared to its rapidity. By the time the RT-PCR results are reported, infected patients may no longer be in their contagious state while they were in contact with other individuals in their contagious period. Thus, RT-PCR is not suitable for daily and weekly surveillance due to its high testing turnaround time. In fact, a team has modeled surveillance effectiveness, taking into consideration testing sensitivity, testing frequency, and sample-to-answer reporting time. Their model, published in a preprint, indicates that controlling the COVID-19 outbreak depends largely on the frequency and rapidness of testing, and is marginally enhanced by high testing sensitivity (Larremore et al., 2020).

In response to the COVID-19 pandemic and the shortage of laboratory-based testing capacity and reagents, various rapid and sensitive tests are currently in development, many of which are the antigen-based diagnostics. The viral proteins are detected in the sample if present in sufficient concentrations without

**TABLE 1** | Comparisons of different COVID-19 diagnostic assays.

	RT-PCR assay	Isothermal amplification assay	CRISPR-based assay	Lateral flow assay	Enzyme linked tests
Target	ORF1ab, RdRp, E, S, and N genes	ORF1ab, RdRp, and N genes	ORF1ab, E, and N gene (Broughton et al., 2020)	-IgG and IgM antibodies -N protein (antigen)	IgG, IgM, and IgA antibodies
Specimen	Upper and lower respiratory specimens, saliva, bronchoalveolar lavage fluids	Upper and lower respiratory specimens, nasal, and throat swabs	Nasopharyngeal or oropharyngeal swabs and bronchoalveolar lavage fluids	-Serum, Saliva or Nasal swab fluids (antibodies)  -Nasopharyngeal or oropharyngeal swabs (antigen)	Plasma or serum samples
Day post-symptoms where the target is max	First week after symptom onset (Tan et al., 2020)	First week after symptom onset (Tan et al., 2020)	First week after symptom onset (Tan et al., 2020)	-IgM: 10–35 days after onset -IgG: 10 days after onset (Ma et al., 2020) -Antigen: before or at symptoms onset	-IgM: 10–35 days after onset -IgG: 10 days after onset (Ma et al., 2020)
Sample preparation	-RNA extraction -Target gene amplification -Fluorescent signal readout of the amplification signals	-15-min RNA sample preparation in sample buffer -Target gene isothermal amplification -Fluorescent readout signal of the amplification signals	-RNA extraction -Target gene isothermal amplification -Target recognition and cleavage -Lateral flow visual readout or fluorescent readout by a plate reader	Plasma or serum separation from specimen by centrifugation and transfer to the test cassette for lateral flow capillary movement (antibodies) Extraction of viral antigen from swabs by special media and loading to test cassette for lateral flow capillary movement (antigen) Lateral flow visual readout or fluorescent readout	-Plasma or serum separation from specimen by centrifugation or sampling tubes with separation gel -sample processing and coating with magnetic particles -Signal readout by a plate reader or a photomultiplier
Control Sample	Human RNase P gene (internal control)	N.A.	RNase P gene (positive control) (Broughton et al., 2020)	C line positive control band	N.A.
Number of samples per run	Device dependent (1 sample per run—tens-hundreds of samples per run)	1 sample/13 min	N.A.	1 sample per run	100–170 results/h
Assay-to-result time	120 min (excluding RNA extraction)	15–60 min 5–13 min	30–40 min (DETECTR) ~60 min (SHERLOCK)	15–20 min	35 min
Sample-to-result time	8 h	h	45 min–1 h	20–30 min	1–5 h
Result type	Quantitative	Qualitative	Qualitative	Qualitative	Quantitative
Sensitivity	94.34–100%	100%	95%	82–93.8% (antibodies) 80% (antigen)	87.5–100%
Specificity	94.87–100%	100%	100%	90.63–100% (antibodies) 100% (antigen)	95–100%
Instrumentation	High	Moderate	Low	Low	Low
Automation	Possible automation	Automated	Automated	Possible automation	-ELISA: semiautomated -CLIA: Automated
Point-of-care	Possible	Yes	Yes	Yes	No
Scale of production (easy, hard)	Hard	Hard	Easy	Easy	Easy
Cost (high, low)	High	Moderate-low (Cantera et al., 2019)	Low	Low	High-moderate

the need for amplification. The currently FDA EUA approved antigen-based tests detect the presence of the N protein in the sample, thus the virus must be permeated first for antigen extraction. In addition, some tests use fluorescent signal readout for improved sensitivity, making them more expensive and dependent on digital analyzers, thus they cannot be performed outside laboratory settings. Yet, a better rapid antigen-based diagnosis is a test that detects the S protein directly, without the need for antigen extraction, in a lateral flow immunoassay platform with a colorimetric readout. E25Bio Company has developed such a test and submitted its work for the FDA EUA approval, but has not received it yet. If we accept rapid tests with moderate sensitivity that can detect viral antigens in their peak (active phase of infection), then we might be able to manage the coronavirus transmission and halt its pandemic.

## DISCUSSION: UNMET NEEDS AND OTHER CONSIDERATIONS OF COVID-19 DIAGNOSTIC PLATFORMS

The large deployment of various SARS-CoV-2 diagnostics in several countries has aided in curbing the spread and transmission of the COVID-19 pandemic. In fact, mass daily testing is required to slowdown the crisis by identifying active cases. Hence, this will aid in isolating active cases and their contacts, reducing the pressure on intensive care units and allowing containment of possible new outbreaks at the earliest of time. Despite the relatively large number of SARS-CoV-2 diagnostic tests and the remarkable speed of evolving new ones, the performance of currently available tools is still unclear and requires further verification and confirmation. The utility of these diagnostic testing is contingent on several factors mainly the type of testing, the resources required, the cost of the test, the sensitivity and specificity as well as the time needed to obtain results.

RT-PCR is the primary molecular armamentarium for the etiological diagnosis of COVID-19. This nucleic acid-based approach is inherently quantitative, but current SARS-CoV-2 tests are being promoted by manufacturers as qualitative (either positive or negative). The obtained results are only indicative of whether the virus or its genetic material is present at the time of the testing, but do not rule out the probability of past infection. Positive results indicate the presence of the viral genome but do not infer the infection status of the patient. The latter should be determined by clinical testing combined with clinical history and complementary diagnostic tools, such as cell culture or antigen-based tests.

An ideal genetic target would include at least one conserved region and one SARS-CoV-2 specific region. To date, the choice of the genetic sequence in the various RT-PCRs kits has not offered a unique advantage to diagnostics, but detecting only one viral gene instead of two, when two sequences are tested, has been conflicting. In addition, negative results in suspects do not rule out the possibility of infection. In fact, several factors could lead to false negatives, such as poor sample quality, improper sample handling and storage, or inappropriate sample collection timing

(too early or too late) (To et al., 2020b; Williams et al., 2020). It is important to point out that viral shedding is related to the stage of illness and severity (Becherer et al., 2020). Besides, the lack of a standard sample control, a standard reference test, and the use of different sample collection and preparation protocols with the different LoD have hampered our understanding of the virus dynamics and the accuracy of the newly introduced molecular-based detection assays. These various molecular-based detection assays have been yielding different positive or negative agreement results when used in comparison to various RT-PCR due to the lack of a standard confirmatory RT-PCR kit for direct COVID-19 detection (Tahamtan and Ardebili, 2020). These differences are related to assay performance influenced by the specimen itself, the reagents and the primers used. In fact, several studies have documented that SARS-CoV-2 has been showing genetic diversity and evolution which might affect the RT-PCR results (Phan, 2020; Shen et al., 2020).

Similar to sample collection location and timing, sample storage, sample handling and sample viral inactivation tend to influence the diagnostic results and may yield false negatives in many cases. The collected clinical specimen should be stored promptly at 2–8°C, then processed immediately when shipped for RNA extraction to avoid RNA degradation. In addition, the specimen, if not used immediately, should be frozen in the transport media at –20 or ideally –70°C if a delay in sample processing is expected. Moreover, heat treatment of samples before RNA extraction at temperatures above 56°C for 30 min is not recommended; this may lead to sample inactivation and loss of detectable viruses in a sample. The latter would give false negatives especially in a weakly positive sample (Chen et al., 2020).

Given the aforementioned limitations, various integrated automated point-of-care molecular diagnostics are currently under development with some receiving EUA and aim to deliver rapid accurate results with low processing complexity. The enclosed system combining RNA extraction, amplification and detection within a sealed cartridge is suitable for testing without the need of biosafety cabinets and can be used to scale up testing with high throughput, such systems include ID Now by Abbott and Xpert Xpress SARS-CoV-2 test by Cepheid. In contrast to RT-PCR, some point-of-care tests do not use a positive human gene control. Thus, they can't determine whether a given sample contains sufficient viral RNA and may yield false negatives. In addition, isothermal amplification-based detection technology has low throughput but does not require sample transport, RNA extraction, or batching with other samples.

Complementary to molecular assays are immunoassays for COVID-19 epidemiological surveillance. They are good alternatives, especially in community clinics and small hospitals that do not have access to molecular diagnostics equipment and expertise. Immunoassays provide a cheap and rapid indirect measure of infection, confirming positive cases obtained by molecular testing. The detected IgM and IgG antibodies in clinical specimens are likely limited around the time of symptoms onset when the viral shedding is the highest and transmission rate is the maximal. The antibody responses to infection take several days or weeks to be detected, therefore negative results

do not exclude infection especially if the person has been recently exposed to the virus. The issue lies with patients having low viral load and poor immune response; therefore, such assays might miss capturing the antibody or the antigen in the sample and provide false negative results. On the contrary, immunoassays cross-reactivity with other coronaviruses proteins or antibodies has been very common and yielded false-positive results in many cases (CDC, 2020). The assessment of immunoassays has been done in comparison to the gold standard RT-PCR and therefore understanding the performance and the sensitivity of such tests has not been straightforward. Instead, the comparison must include the evaluation of antibody profiles at the different infection stages (early infection vs. late infection vs. convalescent period) and among asymptomatic cases.

Although WHO recommended immunoassays when molecular diagnostic testing is not available, these tests may be useful for determining the immune status of exposed individuals and the overall spread of COVID-19. However, immunoassays are unlikely to be useful for screening or early diagnosis. As such, these diagnostic tests can be essential tools for risk management and public health. Quantitative immunological tests are also critical for identifying recovered individuals with enough antibody titers who could donate their convalescent plasma to current COVID-19 patients. All in all, rapid low-cost point-of-care diagnostics are currently in high demand to rapidly discover active cases, limit viral transmission between the individuals and predict epidemiological outcomes for disease surveillance.

## CONCLUSION

Lessons learned from the challenges presented by the COVID-19 testing will remain relevant for potential future management and mitigation of new viral outbreaks. This is especially true as new and innovative screening technologies were developed and deployed in record time. It has become evident that high

accuracy, scalability, and rapid testing is essential in the fight against outbreaks, especially respiratory viral diseases that can be transmitted easily from person to person. Also, understanding the viral load over the course of the infection can have an impact on reducing false negatives. The same can be said for serological biomarkers. In addition, the deployment and frequency of testing across the globe can be influenced by the geographical and economic constraints in each country given the complicated workflow and price of some testing technologies, such as that of RT-PCR. Finally, managing the data for contact tracing in every country as few of these systems are connected to a global data base can be very challenging. Shared data can aid in understanding level of infections within populations locally and across the world enabling improved resource management and better understanding of the rate of transmission.

## AUTHOR CONTRIBUTIONS

MK, ZH, and SS developed the review outline, drafted and wrote the manuscript, and developed the figures. MK conceived the idea and supervised the content and writing. HZ critically contributed to the content and reviewed the manuscript to ensure accuracy and completeness. All authors contributed to the article and approved the submitted version.

## FUNDING

The authors acknowledged funding from the Maroun Semaan research initiative and AUB President's Innovation Challenge 2020.

## SUPPLEMENTARY MATERIAL

The Supplementary Material for this article can be found online at: <https://www.frontiersin.org/articles/10.3389/fbioe.2020.605702/full#supplementary-material>

## REFERENCES

- Astuti, I., and Ysrafil (2020). Severe acute respiratory syndrome coronavirus 2 (SARS-CoV-2): an overview of viral structure and host response. *Diabetes Metab. Syndr.* 14, 407–412. doi: 10.1016/j.dsx.2020.04.020
- Basu, A., Zinger, T., Inglima, K., Woo, K. M., Atie, O., Yurasits, L., et al. (2020). Performance of Abbott ID Now COVID-19 rapid nucleic acid amplification test using nasopharyngeal swabs transported in viral transport media and dry nasal swabs in a New York City academic institution. *J. Clin. Microbiol.* 58:e01136–20. doi: 10.1128/JCM.01136-20
- Becherer, L., Borst, N., Bakheit, M., Frischmann, S., Zengerle, R., and von Stetten, F. (2020). Loop-mediated isothermal amplification (LAMP)—review and classification of methods for sequence-specific detection. *Anal. Methods* 12, 717–746. doi: 10.1039/C9AY02246E
- Bhattacharyya, R. P., Thakku, S. G., and Hung, D. T. (2018). Harnessing CRISPR effectors for infectious disease diagnostics. *ACS Infect. Dis.* 4, 1278–1282. doi: 10.1021/acsinfecdis.8b00170
- Boback, K. A., Holtzclaw, A. W., Brown, T. E., and Clark, P. A. (2020). Effective use of angiotensin II in coronavirus disease 19-associated mixed shock state: a case report. *AcA Pract.* 14:e01221. doi: 10.1213/XAA.0000000000001221
- Broughton, J. P., Deng, X., Yu, G., Fasching, C. L., Servellita, V., Singh, J., et al. (2020). CRISPR-Cas12-based detection of SARS-CoV-2. *Nat. Biotechnol.* 38, 870–874. doi: 10.1038/s41587-020-0513-4
- Bullard, J., Dust, K., Funk, D., Strong, J. E., Alexander, D., Garnett, L., et al. (2020). Predicting infectious SARS-CoV-2 from diagnostic samples. *Clin. Infect. Dis.* doi: 10.1093/cid/ciaa638. [Epub ahead of print].
- Bulterys, P. L., Garamani, N., Stevens, B., Sahoo, M. K., Huang, C., Hogan, C. A., et al. (2020). Comparison of a laboratory-developed test targeting the envelope gene with three nucleic acid amplification tests for detection of SARS-CoV-2. *J. Clin. Virol.* 129:104427. doi: 10.1016/j.jcv.2020.104427
- Butt, A. M., Siddique, S., An, X., and Tong, Y. (2020). Development of a dual-gene loop-mediated isothermal amplification (LAMP) detection assay for SARS-CoV-2: a preliminary study. *medRxiv*. doi: 10.1101/2020.04.08.20056986
- Cantera, J. L., White, H., Diaz, M. H., Beall, S. G., Winchell, J. M., Lillis, L., et al. (2019). Assessment of eight nucleic acid amplification technologies for potential use to detect infectious agents in low-resource settings. *PLoS ONE* 14:e0215756. doi: 10.1371/journal.pone.0215756
- Cascella, M., Rajnik, M., Cuomo, A., Dulebohn, S. C., and Di Napoli, R. (2020). “Features, evaluation, and treatment of coronavirus,” in *StatPearls* (Treasure Island, FL: StatPearls Publishing).



- CDC (2020). *Interim Guidance for Rapid Antigen Testing for SARS-CoV-2*. Available online at: <https://www.cdc.gov/coronavirus/2019-ncov/lab/resources/antigen-tests-guidelines.html> (accessed September 8, 2020).
- Chan, J. F., Yip, C. C., To, K. K., Tang, T. H., Wong, S. C., Leung, K. H., et al. (2020). Improved molecular diagnosis of COVID-19 by the novel, highly sensitive and specific COVID-19-RdRp/HeL real-time reverse transcription-PCR assay validated *in vitro* and with clinical specimens. *J. Clin. Microbiol.* 58:e00310-20. doi: 10.1128/JCM.00310-20
- Chen, H., Wu, R., Xing, Y., Du, Q., Xue, Z., Xi, Y., et al. (2020). Influence of different inactivation methods on severe acute respiratory syndrome coronavirus 2 RNA copy number. *J. Clin. Microbiol.* 58:e00958-20. doi: 10.1128/JCM.00958-20
- Chen, J. S., Ma, E., Harrington, L. B., Da Costa, M., Tian, X., Palefsky, J. M., et al. (2018). CRISPR-Cas12a target binding unleashes indiscriminate single-stranded DNase activity. *Science* 360, 436–439. doi: 10.1126/science.aa.r6245
- Chen, Y., Chan, K.-H., Kang, Y., Chen, H., Luk, H. K., Poon, R. W., et al. (2015). A sensitive and specific antigen detection assay for Middle East respiratory syndrome coronavirus. *Emerg. Microbes Infect.* 4, 1–5. doi: 10.1038/emi.2015.67
- Chu, D. K. W., Pan, Y., Cheng, S. M. S., Hui, K. P. Y., Krishnan, P., Liu, Y., et al. (2020). Molecular diagnosis of a novel coronavirus (2019-nCoV) causing an outbreak of pneumonia. *Clin. Chem.* 66, 549–555. doi: 10.1093/clinchem/hvaa029
- Cinquanta, L., Fontana, D. E., and Bizzaro, N. (2017). Chemiluminescent immunoassay technology: what does it change in autoantibody detection? *Autoimmun. Highlights* 8:9. doi: 10.1007/s13317-017-0097-2
- Corman, V. M., Landt, O., Kaiser, M., Molenkamp, R., Meijer, A., Chu, D. K., et al. (2020). Detection of 2019 novel coronavirus (2019-nCoV) by real-time RT-PCR. *Euro Surveill.* 25:2000045. doi: 10.2807/1560-7917.ES.2020.25.3.2000045
- Demey, B., Daher, N., François, C., Lanoix, J. P., Duverlie, G., Castelain, S., et al. (2020). Dynamic profile for the detection of anti-SARS-CoV-2 antibodies using four immunochromatographic assays. *J. Infect.* 81, e6–e10. doi: 10.1016/j.jinf.2020.04.033
- FDA (2020a). *FAQs on Testing for SARS-CoV-2*. Available online at: <https://www.fda.gov/medical-devices/coronavirus-covid-19-and-medical-devices/faqs-testing-sars-cov-2> (accessed September 8, 2020).
- FDA (2020b). *In vitro Diagnostics EUAs*. Available online at: <https://www.fda.gov/medical-devices/coronavirus-disease-2019-covid-19-emergency-use-authorizations-medical-devices/in-vitro-diagnostics-euas> (accessed September 10, 2020).
- FDA (2020c). *Approval of Cellex, Inc. qSARS-CoV-2 IgG/IgM Rapid Test*. Available online at: <https://www.fda.gov/media/136622/download> (accessed August 20, 2020).
- Fehr, A. R., and Perlman, S. (2015). Coronaviruses: an overview of their replication and pathogenesis. *Methods Mol. Biol.* 1282, 1–23. doi: 10.1007/978-1-4939-2438-7\_1
- FINDdx (2020). *SARS-CoV-2 Diagnostic Pipeline*. Available online at: [https://www.finddx.org/covid-19/pipeline/?avance=Commercialized&type=all&test\\_target=all&status=CE-IVD&section=show-all&action=default](https://www.finddx.org/covid-19/pipeline/?avance=Commercialized&type=all&test_target=all&status=CE-IVD&section=show-all&action=default) (accessed September 10, 2020).
- Gottlieb, S., Rivers, C., McClellan, M. B., Silvis, L., and Watson, C. (2020). *National Coronavirus Response: A Road Map to Reopening*. Washington, DC: American Enterprise Institute. Available online at: <https://www.aei.org/wp-content/uploads/2020/03/National-Coronavirus-Response-a-Road-Map-to-Recovering-2.pdf>
- Harrington, A., Cox, B., Snowdon, J., Bakst, J., Ley, E., Grajales, P., et al. (2020). Comparison of Abbott ID now and Abbott m2000 methods for the detection of SARS-CoV-2 from nasopharyngeal and nasal swabs from symptomatic patients. *J. Clin. Microbiol.* 58:e00798-20. doi: 10.1128/JCM.00798-20
- Hoffmann, M., Kleine-Weber, H., Schroeder, S., Krüger, N., Herrler, T., Erichsen, S., et al. (2020). SARS-CoV-2 cell entry depends on ACE2 and TMPRSS2 and is blocked by a clinically proven protease inhibitor. *Cell* 181, 271–280.e278. doi: 10.1016/j.cell.2020.02.052
- Huang, W. E., Lim, B., Hsu, C. C., Xiong, D., Wu, W., Yu, Y., et al. (2020). RT-LAMP for rapid diagnosis of coronavirus SARS-CoV-2. *Microb. Biotechnol.* 13, 950–961. doi: 10.1111/1751-7915.13586
- Jacofsky, D., Jacofsky, E. M., and Jacofsky, M. (2020). Understanding antibody testing for COVID-19. *J. Arthroplasty* 35, S74–S81. doi: 10.1016/j.arth.2020.04.055
- Kaddoura, M., AlIbrahim, M., Hijazi, G., Soudani, N., Audi, A., Alkalamouni, H., et al. (2020). COVID-19 therapeutic options under investigation. *Front. Pharmacol.* 11:1196. doi: 10.3389/fphar.2020.01196
- Kashir, J., and Yaqinuddin, A. (2020). Loop mediated isothermal amplification (LAMP) assays as a rapid diagnostic for COVID-19. *Med. Hypotheses* 141:109786. doi: 10.1016/j.mehy.2020.109786
- Kellner, M. J., Koob, J. G., Gootenberg, J. S., Abudayyeh, O. O., and Zhang, F. (2019). SHERLOCK: nucleic acid detection with CRISPR nucleases. *Nat. Protoc.* 14, 2986–3012. doi: 10.1038/s41596-019-0210-2
- Koczula, K. M., and Gallotta, A. (2016). Lateral flow assays. *Essays Biochem.* 60, 111–120. doi: 10.1042/EBC20150012
- Kralik, P., and Ricchi, M. (2017). A basic guide to real time PCR in microbial diagnostics: definitions, parameters, and everything. *Front. Microbiol.* 8:108. doi: 10.3389/fmicb.2017.00108
- La Scola, B., Le Bideau, M., Andreani, J., Hoang, V. T., Grimaldier, C., Colson, P., et al. (2020). Viral RNA load as determined by cell culture as a management tool for discharge of SARS-CoV-2 patients from infectious disease wards. *Eur. J. Clin. Microbiol. Infect. Dis.* 39, 1059–1061. doi: 10.1007/s10096-020-03913-9
- Larremore, D. B., Wilder, B., Lester, E., Shehata, S., Burke, J. M., Hay, J. A., et al. (2020). Test sensitivity is secondary to frequency and turnaround time for COVID-19 surveillance. *medRxiv*. doi: 10.1101/2020.06.22.20136309
- Liu, B., Li, M., Zhou, Z., Guan, X., and Xiang, Y. (2020). Can we use interleukin-6 (IL-6) blockade for coronavirus disease 2019 (COVID-19)-induced cytokine release syndrome (CRS)? *J. Autoimmun.* 111:102452. doi: 10.1016/j.jaut.2020.102452
- Lou, B., Li, T. D., Zheng, S. F., Su, Y. Y., Li, Z. Y., Liu, W., et al. (2020). Serology characteristics of SARS-CoV-2 infection after exposure and post-symptom onset. *Eur. Respir. J.* 56:2000763. doi: 10.1183/13993003.00763-2020
- Ma, H., Zeng, W., He, H., Zhao, D., Yang, Y., Jiang, D., et al. (2020). COVID-19 diagnosis and study of serum SARS-CoV-2 specific IgA, IgM and IgG by chemiluminescence immunoanalysis. *medRxiv*. doi: 10.1101/2020.04.17.20064907
- Mathur, G., and Mathur, S. (2020). Antibody testing for COVID-19. *Am. J. Clin. Pathol.* 154, 1–3. doi: 10.1093/ajcp/aqaa082
- Nash, B., Badea, A., Reddy, A., Bosch, M., Salcedo, N., Gomez, A., et al. (2020). The impact of high frequency rapid viral antigen screening on COVID-19 spread and outcomes: a validation and modeling study. *medRxiv*. doi: 10.21203/rs.3.rs-104765/v1
- Nguyen, T., Duong Bang, D., and Wolff, A. (2020). 2019 novel coronavirus disease (COVID-19): paving the road for rapid detection and point-of-care diagnostics. *Micromachines* 11:306. doi: 10.3390/mi11030306
- Park, G. S., Ku, K., Baek, S. H., Kim, S. J., Kim, S. I., Kim, B. T., et al. (2020). Development of reverse transcription loop-mediated isothermal amplification assays targeting severe acute respiratory syndrome coronavirus 2 (SARS-CoV-2). *J. Mol. Diagn.* 22, 729–735. doi: 10.1016/j.jmoldx.2020.03.006
- Phan, T. (2020). Genetic diversity and evolution of SARS-CoV-2. *Infect. Genet. Evol.* 81:104260. doi: 10.1016/j.meegid.2020.104260
- Qin, X., and Jin-Ming, L. (2015). Advances and applications of chemiluminescence immunoassay in clinical diagnosis and foods safety. *Chinese J. Anal. Chem.* 43, 929–938. doi: 10.1016/S1872-2040(15)60831-3
- Rothan, H. A., and Byrareddy, S. N. (2020). The epidemiology and pathogenesis of coronavirus disease (COVID-19) outbreak. *J. Autoimmun.* 109:102433. doi: 10.1016/j.jaut.2020.102433
- Shen, Z., Xiao, Y., Kang, L., Ma, W., Shi, L., Zhang, L., et al. (2020). Genomic diversity of severe acute respiratory syndrome-coronavirus 2 in patients with coronavirus disease 2019. *Clin. Infect. Dis.* 71, 713–720. doi: 10.1093/cid/ciaa203
- Singanayagam, A., Patel, M., Charlett, A., Lopez Bernal, J., Saliba, V., Ellis, J., et al. (2020). Duration of infectiousness and correlation with RT-PCR cycle threshold values in cases of COVID-19, England, January to May 2020. *Euro Surveill.* 25:2001483. doi: 10.2807/1560-7917.ES.2020.25.32.2001483

- Tahamtan, A., and Ardebili, A. (2020). Real-time RT-PCR in COVID-19 detection: issues affecting the results. *Expert Rev. Mol. Diagn.* 20, 453–454. doi: 10.1080/14737159.2020.1757437
- Tan, W., Lu, Y., Zhang, J., Wang, J., Dan, Y., Tan, Z., et al. (2020). Viral kinetics and antibody responses in patients with COVID-19. *medRxiv*. doi: 10.1101/2020.03.24.20042382
- Tang, Y. W., Schmitz, J. E., Persing, D. H., and Stratton, C. W. (2020). Laboratory diagnosis of COVID-19: current issues and challenges. *J. Clin. Microbiol.* 58:e00512–20. doi: 10.1128/JCM.00512–20
- To, K. K., Tsang, O. T., Leung, W. S., Tam, A. R., Wu, T. C., Lung, D. C., et al. (2020a). Temporal profiles of viral load in posterior oropharyngeal saliva samples and serum antibody responses during infection by SARS-CoV-2: an observational cohort study. *Lancet Infect. Dis.* 20, 565–574. doi: 10.1016/s1473-3099(20)30196-1
- To, K. K., Tsang, O. T., Yip, C. C., Chan, K. H., Wu, T. C., Chan, J. M., et al. (2020b). Consistent detection of 2019 novel coronavirus in saliva. *Clin. Infect. Dis.* 71, 841–843. doi: 10.1093/cid/ciaa149
- Udugama, B., Kadhiresan, P., Kozlowski, H. N., Malekjahani, A., Osborne, M., Li, V. Y. C., et al. (2020). Diagnosing COVID-19: the disease and tools for detection. *ACS Nano* 14, 3822–3835. doi: 10.1021/acsnano.0c02624
- Vashist, S. K. (2020). In vitro diagnostic assays for COVID-19: recent advances and emerging trends. *Diagnostics* 10:202. doi: 10.3390/diagnostics10040202
- Vogels, C. B., Brackney, D., Wang, J., Kalinich, C. C., Ott, I., Kudo, E., et al. (2020a). SalivaDirect: simple and sensitive molecular diagnostic test for SARS-CoV-2 surveillance. *medRxiv*.
- Vogels, C. B., Brito, A. F., Wyllie, A. L., Fauver, J. R., Ott, I. M., Kalinich, C. C., et al. (2020b). Analytical sensitivity and efficiency comparisons of SARS-CoV-2 qRT-PCR assays. *medRxiv*.
- Wang, Q., Zhang, Y., Wu, L., Niu, S., Song, C., Zhang, Z., et al. (2020). Structural and functional basis of SARS-CoV-2 entry by using human ACE2. *Cell* 181, 894–904.e899. doi: 10.1016/j.cell.2020.03.045
- Wild, D. (2013). *The Immunoassay Handbook: Theory and Applications of Ligand Binding, ELISA and Related Techniques*. New York, NY: Elsevier.
- Williams, E., Bond, K., Zhang, B., Putland, M., and Williamson, D. A. (2020). Saliva as a noninvasive specimen for detection of SARS-CoV-2. *J. Clin. Microbiol.* 58:e00776–20. doi: 10.1128/JCM.00776–20
- Wölfel, R., Corman, V. M., Guggemos, W., Seilmaier, M., Zange, S., Müller, M. A., et al. (2020). Virological assessment of hospitalized patients with COVID-2019. *Nature* 581, 465–469. doi: 10.1038/s41586-020-2196-x
- Wu, F., Zhao, S., Yu, B., Chen, Y.-M., Wang, W., Song, Z.-G., et al. (2020a). A new coronavirus associated with human respiratory disease in China. *Nature* 579, 265–269. doi: 10.1038/s41586-020-2008-3
- Wu, J. T., Leung, K., and Leung, G. M. (2020b). Nowcasting and forecasting the potential domestic and international spread of the 2019-nCoV outbreak originating in Wuhan, China: a modelling study. *Lancet* 395, 689–697. doi: 10.1016/S0140-6736(20)30260-9
- Yeasmin, M., Tasnim, J., Akram, A., Yusuf, M. A., Shamsuzzaman, A., Molla, M. M. A., et al. (2020). Routes of transmission of newly emerging SARS-CoV-2: a systematic review. *Bangladesh J. Infect. Dis.* 7, S18–S31. doi: 10.3329/bjid.v7i0.46797
- Younes, N., Al-Sadeq, D. W., Al-Jighefee, H., Younes, S., Al-Jamal, O., Daas, H. I., et al. (2020). Challenges in laboratory diagnosis of the novel coronavirus SARS-CoV-2. *Viruses* 12:582. doi: 10.3390/v12060582
- Zhang, F., Abudayyeh, O. O., and Gootenberg, J. S. (2020a). A Protocol for Detection of COVID-19 Using CRISPR Diagnostics. Available online at: [https://www.broadinstitute.org/files/publications/special/COVID-19%20detection%20\(updated\).pdf](https://www.broadinstitute.org/files/publications/special/COVID-19%20detection%20(updated).pdf)
- Zhang, Y., Odiwuor, N., Xiong, J., Sun, L., Nyaruaba, R. O., Wei, H., et al. (2020b). Rapid molecular detection of SARS-CoV-2 (COVID-19) virus RNA using colorimetric LAMP. *medRxiv*. doi: 10.1101/2020.02.26.20028373
- Zhou, P., Yang, X. L., Wang, X. G., Hu, B., Zhang, L., Zhang, W., et al. (2020). A pneumonia outbreak associated with a new coronavirus of probable bat origin. *Nature* 579, 270–273. doi: 10.1038/s41586-020-2012-7
- Zou, L., Ruan, F., Huang, M., Liang, L., Huang, H., Hong, Z., et al. (2020). SARS-CoV-2 viral load in upper respiratory specimens of infected patients. *N. Engl. J. Med.* 382, 1177–1179. doi: 10.1056/NEJMc2001737

**Conflict of Interest:** The authors declare that the research was conducted in the absence of any commercial or financial relationships that could be construed as a potential conflict of interest.

Copyright © 2021 Habli, Saleh, Zaraket and Khraiche. This is an open-access article distributed under the terms of the Creative Commons Attribution License (CC BY). The use, distribution or reproduction in other forums is permitted, provided the original author(s) and the copyright owner(s) are credited and that the original publication in this journal is cited, in accordance with accepted academic practice. No use, distribution or reproduction is permitted which does not comply with these terms.



# Air Curtains Equipped With Hydroalcoholic Aerosol Sprayers for Massive COVID-19 Disinfection

Judit Raventós<sup>1</sup> and Raimon Sabate<sup>2,3\*</sup>

<sup>1</sup> Service of Psychiatry, Psychology and Psychosomatic Medicine, Dexeus University Hospital, Barcelona, Spain,

<sup>2</sup> Department of Pharmacy and Pharmaceutical Technology and Physical-Chemistry, School of Pharmacy and Food Sciences, University of Barcelona, Barcelona, Spain, <sup>3</sup> Institute of Nanoscience and Nanotechnology (IN2UB), Barcelona, Spain

**Keywords:** COVID-19, SARS-CoV2, coronaviral infections, viral outbreak investigation, pandemic (COVID-19), SARS-CoV2 infection

## OPEN ACCESS

### Edited by:

Jianming Qiu,  
University of Kansas Medical Center,  
United States

### Reviewed by:

Yi Zhang,  
Temple University, United States  
Baoming Liu,  
Johns Hopkins University,  
United States

### \*Correspondence:

Raimon Sabate  
rsabate@ub.edu

### Specialty section:

This article was submitted to  
Infectious Diseases - Surveillance,  
Prevention and Treatment,  
a section of the journal  
Frontiers in Public Health

**Received:** 13 July 2020

**Accepted:** 28 August 2020

**Published:** 28 January 2021

### Citation:

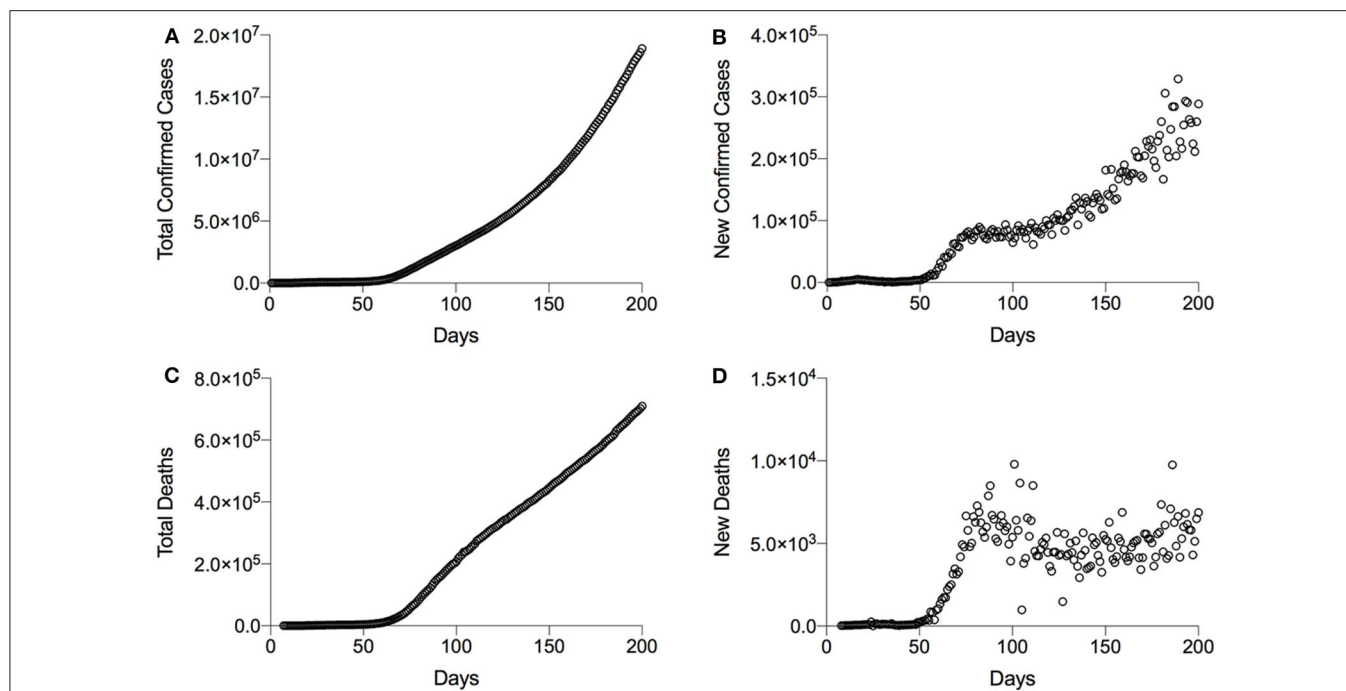
Raventós J and Sabate R (2021) Air  
Curtains Equipped With  
Hydroalcoholic Aerosol Sprayers for  
Massive COVID-19 Disinfection.  
*Front. Public Health* 8:582782.  
doi: 10.3389/fpubh.2020.582782

Coronavirus disease 2019 (COVID-19) affects thousands of healthcare workers in Europe. Latest figures show that healthcare workers represent up to 9 and 14% of Italy's and Spain's COVID-19 cases, respectively. In China, more than 3,300 healthcare workers have been contaminated (1, 2). Better protection for healthcare workers is clearly required. High levels of COVID-19 contamination in specialist wards and intensive care units and of equipment (from keyboards to gel hand sanitizers) indicate that the measures currently taken to control COVID-19 are insufficient, especially in hospital centers where a large number of infections occur and where the most vulnerable population is found.

COVID-19 incubation after a person-to-person transmission is stated to be of 2–10 days (about 5 days in average). The virus can spread *via* droplets falling on surfaces, e.g., clothing, and subsequent transfer *via* people's hands. It has been shown that coronaviruses such as severe acute respiratory syndrome (SARS), Middle East respiratory syndrome (MERS), or endemic human coronavirus (HCoV) can persist on inanimate surfaces for up to 9 days (3). Remarkably, surface disinfection with 0.1% sodium hypochlorite or 62–71% ethanol significantly reduces coronaviruses' infectivity after only 1 min of exposure. Since the stability of COVID-19 is similar to that of SARS-CoV-1 under analogous experimental circumstances (4), a potentially similar effect of these disinfectants against COVID-19 can be expected (3, 5). Hence, the implementation of hydroalcoholic disinfection firewalls as complementary disinfection systems for areas prone to having high viral loads, such as waiting rooms, entrances of hospital centers, etc., would minimize potential transmissions.

Due to the current lack of an efficient therapy or vaccine against COVID-19, the early containment to prevent the spread and the use of palliative/symptomatic treatments represent the two key options to slow down both the transmission (total confirmed cases) and mortality (total deaths) (6, 7). Most affected countries have opted, to a greater or lesser extent, for a combined system of global population confinement and treatment of the most serious cases (6, 9). In contrast, the UK has chosen not to confine the entire population and protect populations at risk (8). South Korea preferred the massive use of tests to control the spread (9).

The containment measures recommended by the WHO are aimed at avoiding person-to-person transmission; protective measures such as wearing masks and hand washing are meant to reduce the spread of coronaviruses through droplets (7). It should be taken into account that not all people will clean their hands correctly or will simply not do it. Furthermore, COVID-19 is stable in aerosols for hours and for days on surfaces, persisting for up to 9 days in the air (4), and on inanimate surfaces like metal, wood, paper, glass, plastic, ceramic, Teflon, polyvinyl chloride (PVC), silicon rubber, surgical gloves (latex), clothing (3), as well as on skin (such as face or hands). Considering these facts, current disinfection protocols are most likely insufficient to effectively eliminate viral presence in the air and on clothing and surfaces. The need to settle an effective massive disinfection system is evident.



**FIGURE 1** | Graphical representation of the global evolution of coronavirus disease 2019 (COVID-19) transmission and mortality. **(A)** Representation of the transmission as a function of total confirmed cases per day. **(B)** New cases per day. **(C)** Representation of the mortality as a function of total deaths per day. **(D)** New deaths per day. \*Data are obtained from WHO situation reports; the first situation report was published on January 20, 2020. \*\*WHO situation report number 28 gives all confirmed cases including both laboratory-confirmed and clinically diagnosed cases. To normalize the data, the total number of confirmed cases obtained from WHO reports 1 and 27 has been mathematically predicted, taking into account the clinically diagnosed cases. This adjustment has only been necessary in the case of China.

As evidenced in **Figure 1**, both the total confirmed cases and total deaths augment linearly, indicating that the control of the COVID-19 outbreak will need some time. The number of new deaths per day appears to be stabilized around WHO situation report 70; comparison of the data between March 30, 2020, and August 7, 2020 (**Figures 1B,D**), suggests that early containment/prevention of further spread and palliative/symptomatic treatments are effective measures. Importantly, new clinical treatments using potential drugs like dexamethasone have allowed stabilizing the number of new deaths per day. In contrast, the increase of new confirmed cases per day worldwide suggests that the current (local) containment/prevention practices to contain COVID-19 spreading are completely insufficient. New and complementary methods for the disinfection/decontamination of COVID-19-infested environments are definitively required. For instance, recent data have revealed an exponential increase of new cases in territories where exceptional confinement measures have been relaxed, such as Japan or Hong Kong (7).

In summary, there is an urgent need to find a highly efficient procedure to disinfect exposed body parts, clothing, and surfaces, which should be inexpensive and easy to implement. Since 62–71% hydroethanolic solutions significantly reduce COVID-19 infectivity within 1 min of exposure (3), we propose to equip air curtains with hydroalcoholic (70% ethanol) aerosol sprayers (or directly installing hydroalcoholic aerosol sprayers) in hospitals and healthcare centers. Nebulizers of hydroalcoholic aerosols

may also be installed in supermarkets, malls, and restaurants and in any other overcrowded place such as stadiums, concert halls, etc. It has been shown that the contact of 70% hydroalcoholic mixtures with the skin is not detrimental to health, and that such solutions do not cause damages on inert surfaces or tissues. Importantly, it has recently been demonstrated that the lifetimes at 25°C of hydroalcoholic droplets containing 0:100, 50:50, and 100:0 ethanol:water mixtures are 1,488, 1,035, and 183 s, respectively; hence, a theoretical lifetime of ~641 s for 70% hydroalcoholic droplets can be calculated by lineal regression with  $r^2 = 0.9698$  (10). Thus, the lifetime of hydroalcoholic droplets, which is 10 times longer than the active infectious period of the coronavirus, should be enough to remove all traces of COVID-19. The evaporation of the droplets is crucial regarding the effectiveness of the treatment and could be a handicap for the implementation of this disinfection system. The humidity level and the ambient temperature are key factors for the maintenance of the hydroalcoholic drops over time. Therefore, this might be a limiting factor in warm climates and/or under low relative humidity. However, the high versatility and adaptability of the system would allow these handicaps to be successfully addressed; for example, a simple change of the type of spray nozzles can modify the size of the droplets and thus modify their lifetime.

Potential over-decontamination and low environmental impact or toxicity to people or animals would be minimal because the hydroalcoholic solutions will be applied in very



specific and limited areas (*viz.* the passage areas of the air curtains) and for very short periods of time. Furthermore, it has been shown that the quantity of ethanol absorbed after intensive hand disinfection using commercially available hand rubs is minimal and below human toxic levels (11). Thus, 60–95% ethanol solutions are considered safe and effective for topical use on hands (11, 12). Whereas spraying individuals with disinfectants such as formaldehyde, chlorine-based agents, quaternary ammonium compounds, or other toxic chemicals is not recommended and may cause eye and skin irritation, bronchospasm, and gastrointestinal effects (7, 13–15), sprays containing hydroalcoholic solutions are widely used in cosmetics (e.g., deodorants) and are considered safe even at the respiratory level since it depends on the respiratory minute volume (16); in the case of hand washing, respiratory levels are very low.

Air curtains equipped with sprayers would effectively distribute hydroalcoholic droplets to surfaces, e.g., clothing, exposed body parts, equipment, etc., passing through, hence reducing the virus load. The systematic installation of hydroalcoholic nebulizers to the existing air curtains can help, in addition to the WHO recommendations, to prevent the spread of the virus (1, 7); this would represent an additional and nondisruptive measure to rapidly and economically reduce the propagation of the virus. Although the application of the

proposed system will not avoid in any case the spread of the virus by an infected person through droplets or contact, and that it will be impossible to access all potentially contaminated regions, the possibility to substantially reduce viral loads on clothing and visible parts of the body can be considered as a real and hopeful advance in COVID-19 disinfection.

## AUTHOR CONTRIBUTIONS

JR and RS contributed to the conceptualization, writing the original draft, and reviewing and editing. RS contributed to the supervision, project administration, and funding acquisition. Both authors have read and agreed to the published version of the manuscript.

## FUNDING

This work was supported by the Spanish Ministerio de Ciencia e Innovación (grant number CTQ2017-88446-R).

## ACKNOWLEDGMENTS

RS thanks the Spanish Ministerio de Ciencia e Innovación (grant number CTQ2017-88446-R).

## REFERENCES

1. The Lancet. COVID-19: protecting health-care workers. *Lancet*. (2020) 395:922. doi: 10.1016/S0140-6736(20)30644-9
2. Remuzzi A, Remuzzi G. COVID-19 and Italy: what next? *Lancet*. (2020) 395:1225–8. doi: 10.1016/S0140-6736(20)30627-9
3. Bedford J, Enria D, Giesecke J, Heymann DL, Ihekweazu C, Kobinger G, et al. COVID-19: towards controlling of a pandemic. *Lancet*. (2020) 395:1015–8. doi: 10.1016/S0140-6736(20)30673-5
4. Kampf G, Todt D, Pfaender S, Steinmann E. Persistence of coronaviruses on inanimate surfaces and their inactivation with biocidal agents. *J Hosp Infect*. (2020) 104:246–51. doi: 10.1016/j.jhin.2020.01.022
5. Henwood AF. Coronavirus disinfection in histopathology. *J Histotechnol*. (2020) 1:1–3. doi: 10.1080/01478885.2020.1734718
6. van Doremalen N, Bushmaker T, Morris DH, Holbrook MG, Gamble A, Williamson BN, et al. Aerosol and surface stability of SARS-CoV-2 as compared with SARS-CoV-1. *N Engl J Med*. (2020) 382:1564–67. doi: 10.1056/NEJMc2004973
7. Coronavirus disease (COVID-2019) situation reports. *Clinical Management of Severe Acute Respiratory Infection When Novel Coronavirus (nCoV) Infection is Suspected. Coronavirus Disease (COVID-19) Advice for the Public. Cleaning and Disinfection of Environmental Surfaces in the Context of COVID-19*. Geneva: World Health Organization. (2020). Available online at: <https://www.who.int/emergencies/diseases/novel-coronavirus-2019> (accessed May 4, 2020).
8. Hunter DJ. Covid-19 and the stiff upper lip - the pandemic response in the United Kingdom. *N Engl J Med*. (2020) 382:e31. doi: 10.1056/NEJMp2005755
9. Cohen J, Kupferschmidt K. Countries test tactics in 'war' against COVID-19. *Science*. (2020) 367:1287–8. doi: 10.1126/science.367.6484.1287
10. Gurrall P, Katreb P, Balusamy S, Banerjee S, Sahu KC. Evaporation of ethanol-water sessile droplet of different compositions at an elevated substrate temperature. *Int J Heat Mass Transfer*. (2019) 145:118770–805. doi: 10.1016/j.ijheatmasstransfer.2019.118770
11. Kramer A, Below H, Bieber N, Kampf G, Toma CD, et al. Quantity of ethanol absorption after excessive hand disinfection using three commercially available hand rubs is minimal and below toxic levels for humans. *BMC Infect Dis*. (2007) 7:117. doi: 10.1186/1471-2334-7-117
12. Food and Drug Administration. *Tentative Final Monograph for Healthcare Antiseptic Drug Products; Proposed Rule*. Food and Drug Administration Report. Vol. 59 (1994). p. 31441–52.
13. Mehtar S, Bulubula A N H, Nyandemoh H, Jambawai S. Deliberate exposure of humans to chlorine – the aftermath of Ebola in West Africa. *Antimicrob Resist Infect Control*. (2016) 5:45. doi: 10.1186/s13756-016-0144-1
14. Zock JP, Plana E, Jarvis D, Antó JM, Kromhout H, Kennedy SM, et al. The use of household cleaning sprays and adult asthma: an international longitudinal study. *Am J Respir Crit Care Med*. (2007) 176:735–41. doi: 10.1164/rccm.200612-1793OC
15. Weinmann T, Gerlich J, Heinrich S, Nowak D, von Mutius E, Vogelberg C, et al. Association of household cleaning agents and disinfectants with asthma in young German adults. *Occup Environ Med*. (2017) 74:684–90. doi: 10.1136/oemed-2016-104086
16. Rothe H, Fautz R, Gerber E, Neumann L, Rettinger K, et al. Special aspects of cosmetic spray safety evaluations: principles on inhalation risk assessment. *Toxicol Lett*. (2011) 205:97–104. doi: 10.1016/j.toxlet.2011.05.1038

**Conflict of Interest:** The authors declare that the research was conducted in the absence of any commercial or financial relationships that could be construed as a potential conflict of interest.

Copyright © 2021 Raventós and Sabate. This is an open-access article distributed under the terms of the Creative Commons Attribution License (CC BY). The use, distribution or reproduction in other forums is permitted, provided the original author(s) and the copyright owner(s) are credited and that the original publication in this journal is cited, in accordance with accepted academic practice. No use, distribution or reproduction is permitted which does not comply with these terms.



## OPEN ACCESS

## Edited by:

Jianming Qiu,  
University of Kansas Medical Center,  
United States

## Reviewed by:

Rodolfo Cordeiro Giunchetti,  
Federal University of Minas  
Gerais, Brazil  
Xiaoxia Dai,  
Xi'an Jiaotong University, China  
Natasha N. Gaudreault,  
Kansas State University, United States

## \*Correspondence:

Amador Goodridge  
agoodridge@indicat.org.pa  
Chong Li  
lichong@ilbp.ac.cn

†These authors have contributed  
equally to this work and share first  
authorship

## Specialty section:

This article was submitted to  
Infectious Diseases - Surveillance,  
Prevention and Treatment,  
a section of the journal  
Frontiers in Medicine

Received: 11 October 2020

Accepted: 28 January 2021

Published: 02 March 2021

## Citation:

Villarreal A, Rangel G, Zhang X,  
Wong D, Britton G, Fernandez PL,  
Pérez A, Oviedo D, Restrepo C,  
Carreira MB, Sambrano D,  
Eskildsen GA, De La Guardia C,  
Flores-Cuadra J, Carrera J-P,  
Zaldivar Y, Franco D, López-Vergès S,  
Zhang D, Fan F, Wang B,  
Sáez-Llorens X, DeAntonio R,  
Torres-Atencio I, Blanco I, Subía FD,  
Mudarra L, Benzadon A, Valverde W,  
López L, Hurtado N, Rivas N,  
Jurado J, Carvallo A, Rodríguez J,  
Pérez Y, Morris J, Luque O, Cortez D,  
Ortega-Barria E, Kosagisharaf R,  
Leonart R, Li C and Goodridge A  
(2021) Performance of a Point of Care  
Test for Detecting IgM and IgG  
Antibodies Against SARS-CoV-2 and  
Seroprevalence in Blood Donors and  
Health Care Workers in Panama.  
Front. Med. 8:616106.  
doi: 10.3389/fmed.2021.616106

# Performance of a Point of Care Test for Detecting IgM and IgG Antibodies Against SARS-CoV-2 and Seroprevalence in Blood Donors and Health Care Workers in Panama

Alcibiades Villarreal<sup>1†</sup>, Giselle Rangel<sup>1†</sup>, Xu Zhang<sup>2,3,4†</sup>, Digna Wong<sup>1</sup>, Gabrielle Britton<sup>1</sup>, Patricia L. Fernandez<sup>1</sup>, Ambar Pérez<sup>1</sup>, Diana Oviedo<sup>1,5</sup>, Carlos Restrepo<sup>1</sup>, María B. Carreira<sup>1</sup>, Dilcia Sambrano<sup>1</sup>, Gilberto A. Eskildsen<sup>1,6</sup>, Carolina De La Guardia<sup>1</sup>, Julio Flores-Cuadra<sup>7</sup>, Jean-Paul Carrera<sup>8</sup>, Yamitzel Zaldivar<sup>9</sup>, Danilo Franco<sup>8</sup>, Sandra López-Vergès<sup>8</sup>, Dexi Zhang<sup>2,3,4</sup>, Fangjing Fan<sup>2,3,4</sup>, Baojun Wang<sup>10</sup>, Xavier Sáez-Llorens<sup>11</sup>, Rodrigo DeAntonio<sup>11</sup>, Ivonne Torres-Atencio<sup>6</sup>, Isabel Blanco<sup>12</sup>, Fernando Díaz Subía<sup>12</sup>, Laiss Mudarra<sup>13</sup>, Aron Benzadon<sup>14</sup>, Walter Valverde<sup>15</sup>, Lineth López<sup>16</sup>, Nicolás Hurtado<sup>17</sup>, Neyla Rivas<sup>17</sup>, Julio Jurado<sup>17</sup>, Aixa Carvallo<sup>17</sup>, Juan Rodríguez<sup>17</sup>, Yaseikiry Perez<sup>18</sup>, Johanna Morris<sup>16</sup>, Odemaris Luque<sup>17</sup>, David Cortez<sup>19</sup>, Eduardo Ortega-Barria<sup>20</sup>, Rao Kosagisharaf<sup>1</sup>, Ricardo Leonart<sup>1</sup>, Chong Li<sup>2,3,4\*</sup> and Amador Goodridge<sup>1\*</sup>

<sup>1</sup> Centro de Biología Celular y Molecular de las Enfermedades, City of Knowledge, Instituto de Investigaciones Científicas y Servicios de Alta Tecnología (INDICASAT-AIP), Panama City, Panama, <sup>2</sup> Institute of Biophysics, Chinese Academy of Sciences, Beijing, China, <sup>3</sup> Beijing Zhongke Jianlan Biotechnology Co. Ltd., Beijing, China, <sup>4</sup> Zhongke Jianlan International Medical Research Institute, Melbourne, VIC, Australia, <sup>5</sup> Escuela de Psicología, Universidad Santa María La Antigua, Panama City, Panama, <sup>6</sup> Facultad de Medicina, Universidad de Panamá, Panama City, Panama, <sup>7</sup> Centro de Neurociencia, Instituto de Investigaciones Científicas y Servicios de Alta Tecnología, AIP (INDICASAT AIP), Panama City, Panama, <sup>8</sup> Department of Research in Virology and Biotechnology, Gorgas Memorial Institute of Health Studies, Panama City, Panama, <sup>9</sup> Department of Research in Surveillance and Biologic Risk 3, Gorgas Memorial Institute of Health Studies, Panama City, Panama, <sup>10</sup> Beijing Kewei Clinical Diagnostic Reagent Inc., Beijing, China, <sup>11</sup> Centro de Vacunación e Investigación, Centro de Vacunación e Investigación Panama Clinic, Panama City, Panama, <sup>12</sup> Medical Research Center, Pacífica Salud, Hospital Punta Pacífica, Panama City, Panama, <sup>13</sup> Departamento de Microbiología Humana/Inmunología, Facultad de Medicina, Universidad de Panamá, Panama City, Panama, <sup>14</sup> Servicio de Neurología. Complejo Hospitalario Dr. AAM, Universidad Nacional de Panamá, Panama City, Panama, <sup>15</sup> Complejo Hospitalario Metropolitano Dr. Arnulfo Arias Madrid, Caja de Seguro Social, Panama City, Panama, <sup>16</sup> Servicio de Hematología. Complejo Hospitalario Metropolitano Dr. Arnulfo Arias Madrid, Caja de Seguro Social, Panama City, Panama, <sup>17</sup> Complejo Hospitalario Manuel Amador Guerrero, Caja de Seguro Social, Colón, Panama, <sup>18</sup> Servicio de Hematología, Banco de Sangre. Complejo Hospitalario Metropolitano Dr. Arnulfo Arias Madrid, Caja de Seguro Social, Panama City, Panama, <sup>19</sup> Dirección Nacional de Laboratorios Clínicos, Ministerio de Salud, Panama City, Panama, <sup>20</sup> GlaxoSmithKline Vaccines, City of Knowledge, Panama City, Panama

Novel severe acute respiratory syndrome coronavirus 2 (SARS-CoV-2) is the etiologic agent of the ongoing coronavirus disease 2019 (COVID-19) pandemic, which has reached 28 million cases worldwide in 1 year. The serological detection of antibodies against the virus will play a pivotal role in complementing molecular tests to improve diagnostic accuracy, contact tracing, vaccine efficacy testing, and seroprevalence surveillance. Here, we aimed first to evaluate a lateral flow assay's ability to identify specific IgM and IgG antibodies against SARS-CoV-2 and second, to report the seroprevalence estimates of these antibodies among health care workers and healthy volunteer blood donors in Panama. We recruited study participants between April 30th and July 7th, 2020. For the test validation and performance evaluation, we analyzed serum samples from participants with clinical symptoms and confirmed positive RT-PCR

for SARS-CoV-2, and a set of pre-pandemic serum samples. We used two by two table analysis to determine the test positive and negative percentage agreement as well as the Kappa agreement value with a 95% confidence interval. Then, we used the lateral flow assay to determine seroprevalence among serum samples from COVID-19 patients, potentially exposed health care workers, and healthy volunteer donors. Our results show this assay reached a positive percent agreement of 97.2% (95% CI 84.2–100.0%) for detecting both IgM and IgG. The assay showed a Kappa of 0.898 (95%CI 0.811–0.985) and 0.918 (95% CI 0.839–0.997) for IgM and IgG, respectively. The evaluation of serum samples from hospitalized COVID-19 patients indicates a correlation between test sensitivity and the number of days since symptom onset; the highest positive percent agreement [87% (95% CI 67.0–96.3%)] was observed at  $\geq 15$  days post-symptom onset (PSO). We found an overall antibody seroprevalence of 11.6% (95% CI 8.5–15.8%) among both health care workers and healthy blood donors. Our findings suggest this lateral flow assay could contribute significantly to implementing seroprevalence testing in locations with active community transmission of SARS-CoV-2.

**Keywords:** COVID-19, Panama, serology, biomarker, immunochromatographic assay, diagnosis

## INTRODUCTION

Coronavirus disease 2019 (COVID-19) is a viral pneumonia and multi-systemic disease caused by severe acute respiratory syndrome coronavirus 2 (SARS-CoV-2), which first appeared in Wuhan, China in December 2019 (1, 2). Since then, the virus has spread rapidly with an explosive increase in cases across the globe. As of 12 January 2021, there have been over 95 million confirmed cases of COVID-19, including 911,877 deaths reported to WHO (3). According to the Pan American Health Organization (PAHO), by August 2020, Panama had a rate of 1,618 infected persons per 100,000 inhabitants (4, 5), placing it as the country with the second highest rate of infection in the Americas. This high rate is in part related to the fact that Panama is among the countries in the region that have conducted the highest number of tests. More than 1.5 million molecular tests have been conducted since early March 2020, and daily positivity rates in January 2021 have consistently been in the 20% range; there have been nearly 300,000 confirmed cases. In Panama, the majority of reported cases (93.2%) demonstrate mild symptoms, while 6.8% have required hospitalization. To date, there have been 4,738 (1.6%) deaths and over 240,000 (80%) patients have recovered (6).

Until a vaccine becomes available, most countries' containment efforts have relied heavily on non-pharmacological interventions to mitigate and suppress the disease. These include, but are not limited to, movement restrictions and reduced individual contact to decrease community transmission (7). As a result, the COVID-19 pandemic, in addition to being a public health emergency, has become a financial and sociopolitical crisis. Consequently, public health strategies are urgently needed in order to ease lock-down restrictions (8). One of the most effective strategies includes prompt and accurate diagnosis. The development of a diagnostic test that can be scaled-up to allow for mass screening among specific high-risk groups, such as health care workers (HCW), remains a key step

(9, 10). Such a test would aid with diagnosis, contact tracing, and vaccine evaluation, while also allowing serological surveillance at the local, regional, and national level (11).

More than 150 diagnostics tests have been developed since the beginning of the COVID-19 pandemic (12). The most-used platforms are enzyme-linked immunosorbent assays (ELISA) and rapid lateral flow immunoassays (LFIA) (13). In general, serological tests based on an LFIA platform are cost- and time-efficient, do not require sophisticated equipment or highly trained personnel, and can be used to assess population exposure. The cost of manufacturing these assays is  $<1$  dollar per test, with the market cost ranging from 15–20 USD; in contrast, an antigen test costs 45–50 USD and an RT-PCR test in Panamá costs up to 95–110 USD. LFIA platforms have generated substantial interest not only because they are cheaper to manufacture, but also because the tests are easier to store, distribute, and implement as a point-of-care test in remote areas. Unfortunately, some countries have rushed into large-scale deployment of rapid tests but have found that the clinical sensitivities are low and of poor value due to inadequate performance assessment (14, 15). The performance of rapid tests provided by manufacturers might show variations. Consequently, rapid tests should be rigorously validated in a large target population before being used as a stand-alone screening test (16).

Our study aimed to evaluate the performance of an LFIA for the detection of IgM and IgG anti-SARS antibodies in COVID-19-positive individuals (17). We hypothesize that the LFIA test would perform adequately for screening anti-SARS-CoV-2 antibodies among healthy blood donors (HD) and health care workers (HCW). First, we determined the test performance of the LFIA as a rapid serology test, using a standard panel of sera from COVID-19 patients and pre-pandemic donors. Second, we conducted a field evaluation of the LFIA test to determine the seroprevalence of anti-SARS-CoV-2 antibodies among HD and HCW. We found this test to be suitable for conducting seroprevalence studies, assessing population

exposure to the virus, and for evaluating the effects of lock-down flexibilization strategies.

## MATERIALS AND METHODS

### Lateral Flow Immunoassay Overview

We obtained an LFIA test developed by Dr. Chong Li's group from Institute of Biophysics, Chinese Academy of Science. The qualitative test (referred to as CAST—*Chinese Academy of Science Test*, from this point) detects and is capable of differentiating between specific IgM and IgG antibodies against SARS-CoV-2. The CAST uses a colored conjugate pad containing a recombinant SARS-CoV-2 nucleocapsid protein conjugated with colloid gold as the antigen. The CAST manufacturer's calculated analytical sensitivity and specificity for both IgM and IgG anti-SARS-CoV-2 antibodies at development were 87.01 and 98.89%, respectively, according to the kit insert literature. During development in China, no cross-reactivity was reported with specimens from patients infected with Human Immunodeficiency Virus (HIV), Hepatitis A Virus (HAV), Hepatitis B soluble Antigen, Hepatitis C Virus, *Treponema pallidum*, Human T Lymphocyte Virus (HTLV), Cytomegalovirus, Influenza Virus type A and B, Respiratory Syncytial Virus, Human Papilloma Virus, *Chlamydomphila pneumoniae*, *Legionella pneumophila*, *Mycoplasma pneumoniae*, or Human Parainfluenza viruses. Moreover, no cross-reactivity or interference was observed with endogenous substances, including common serum components, such as lipids, hemoglobin, bilirubin, albumin, uric acid, and glucose, or other common biological analytes, such as acetaminophen, acetoacetic acid, benzoylecgonine, caffeine, EDTA, ethanol, gentisic acid,  $\beta$ -Hydroxybutyrate, methanol, phenothiazine, phenylpropanolamine, and salicylic acid.

### Test Performance Evaluation by National Reference Laboratory

In Panama, the CAST was evaluated independently by the Gorgas Memorial Institute of Health Studies (GMI), the National Reference Public Health laboratory responsible for COVID-19 diagnostic test validation, as well as for national molecular SARS-CoV-2 diagnoses. The real-time reverse-transcription-polymerase chain-reaction (RT-qPCR) assay for detecting SARS-CoV-2 was used as a non-reference standard (18). We included 36 SARS-CoV-2 RT-qPCR-positive and 17 RT-qPCR-negative samples. We also tested 55 pre-pandemic samples that included sera from 10 patients with a known Dengue infection, 15 with pulmonary tuberculosis, 15 with latent tuberculosis infection, and 15 healthy blood donors. A total of 108 samples were used for performance evaluation. All RT-qPCR assays were performed at GMI by two trained technicians following best clinical laboratory practices and quality control assurance programs. The two technicians were trained on the safe handling of potentially infectious samples, the use of basic laboratory equipment and biosafety cabinets, and the correct use of personal protective equipment. Both technicians received specific training and demonstrated understanding of the test principles and kit components as well as the test procedure and interpretation

of results. To standardize the results, the same two technicians performed all the tests and set parameters such as the number of samples processed simultaneously, and the reading time. The technicians also took pictures of each of the results. No accidents or contamination were reported during the study. Both technicians were blinded to patient groups. The diagnostic accuracy of the CAST was evaluated as indicated below in the statistical analysis section.

### Field Evaluation of CAST: Study Participants and Sample Distribution

This study was conducted between April 30th and July 7th, 2020 in four private and public hospitals and two donation centers located in Panama and Colon cities (**Figure 1**). The sample size was calculated using an estimated sensitivity of at least 80% and a specificity of at least 90% for the CAST. Based on the target population of the study, which included positive cases and contacts, we assumed a prevalence of at least 15%. Thus, the sample size was estimated at a minimum of 650 participants, aiming for a 95% level of accuracy. The inclusion criteria were being an adult over 18 years old and providing written informed consent. All study participants completed a clinical screening survey for COVID-19-related symptoms and consented to submit samples for screening of other infections. Only healthy blood donors (HD) that tested negative for other infectious diseases, including Chagas disease, HIV, HBV, HAV, and HTLV1, were invited to participate in our study. The exclusion criteria comprised those with missing data and patients in intensive and semi-intensive care units. Health care workers (HCW) were asked to provide an additional blood sample 15 days after the first sample was taken. All HCW in contact with confirmed COVID-19 cases were considered high risk. Low-risk HCW were those who perform functions within medical facilities but do not have direct contact with COVID-19-positive patients.

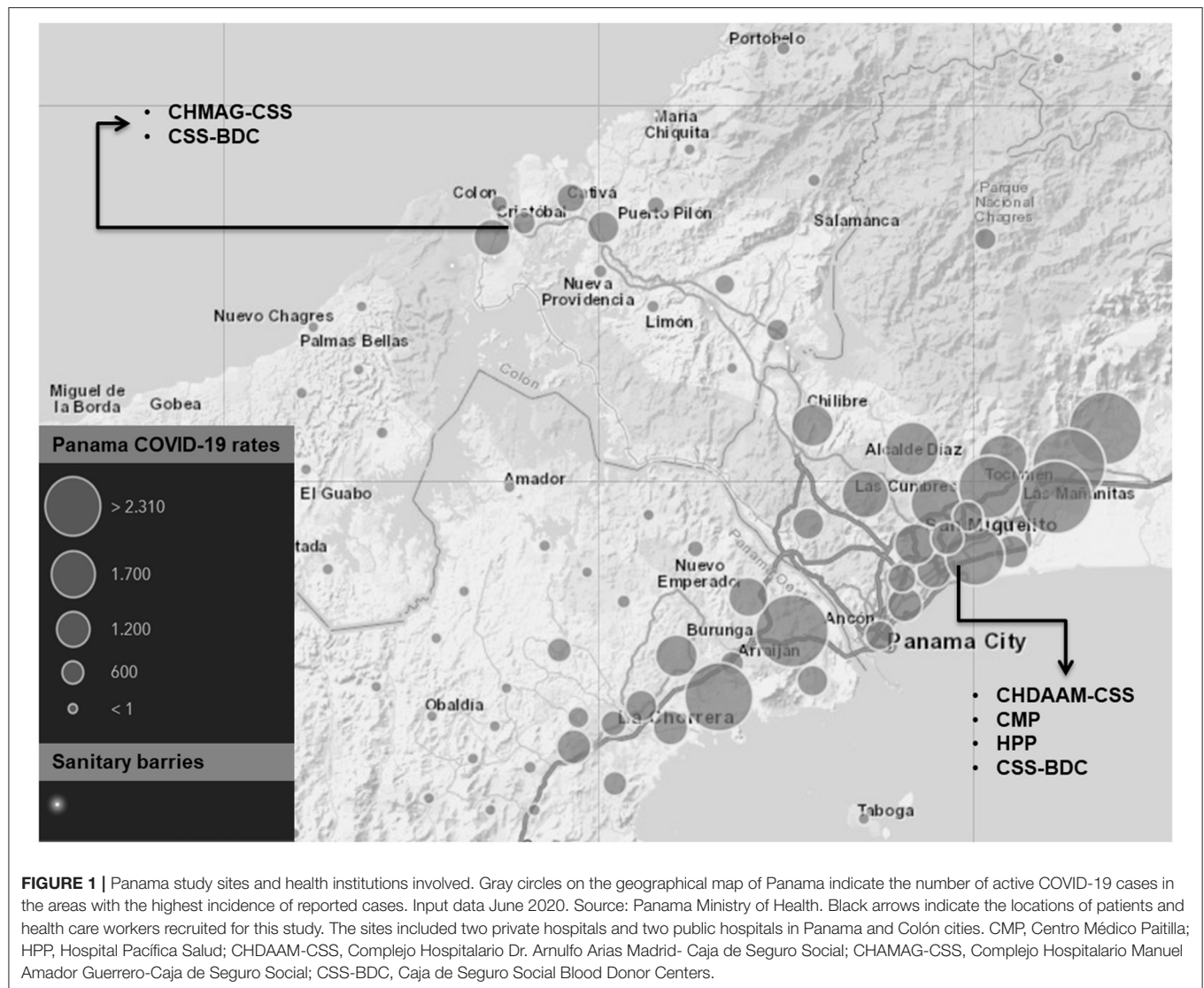
The recruitment staff for this study adhered to standard biosecurity and institutional safety procedures. According to country regulations, only medical technologists extracted blood samples. We recruited participants in COVID-19 Hospitals and in blood donation centers. All the staff used adequate personal protection equipment and followed the biosecurity protocols. They also received training on the handling of potentially infectious samples and their proper delivery to the laboratory. No accidents or contamination were reported during the study.

This study was registered with the Panama Ministry of Health (No. 1,462) and was approved by the National Research Bioethics Committee (CNBI; No. EC-CNBI-2020-03-43).

### Specimen Collection, Demographic and Clinical Data

Predesigned questionnaires related to COVID-19 from the World Health Organization (WHO) were completed by trained interviewers. The questionnaire was adapted from the Population-based age-stratified seroepidemiological investigation protocol for coronavirus 2019 (COVID-19) infection (19). This questionnaire was given to all study participants. Epidemiological data regarding sociodemographic





factors, medical history, current COVID-19 symptoms, and contacts were collected through personal interviews. Questions related to anosmia and ageusia symptoms were not included in the interview. Venous blood samples were collected from all the study participants for CAST analysis. The blood collection tubes were kept at room temperature to allow clot formation and then centrifuged for 10 min at 250g to obtain serum specimens. All rapid test analyses were conducted with fresh serum samples.

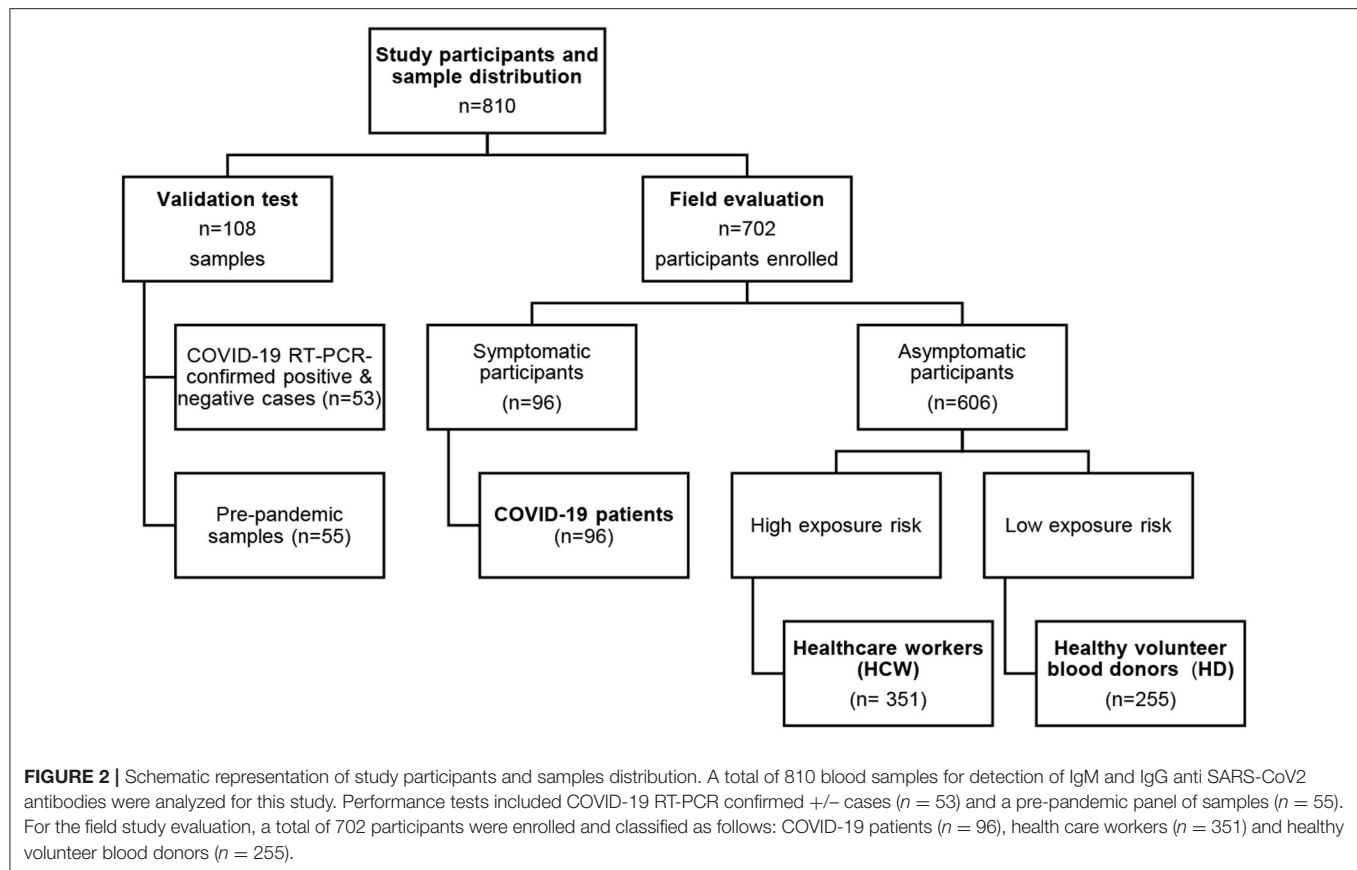
### IgM and IgG Antibody Detection by LFIA

We followed a step-wise protocol for conducting the CAST. Briefly, we added one drop of serum (~20–25  $\mu$ L) into the cassette sample well, followed by two drops of the developing buffer (~70  $\mu$ L). If IgM and/or IgG anti-SARS-CoV-2 antibodies are present in the sample, they will bind to the colloidal gold conjugate, forming an immunocomplex. This immunocomplex is then captured by the respective pre-coated band containing either anti-IgM or anti-IgG antibodies, forming a red colored

IgM and/or IgG line. The presence of one red line indicates the sample is positive for specific IgM or IgG anti SARS-CoV-2 antibodies, while the presence of two lines indicates the sample is positive for both IgM and IgG antibodies (**Supplementary Figure 1**). A third line functions as a positive control, indicating that the kit is working properly. All analyses were interpreted by two independent technicians at 15 min after the serum was added. If there were disagreements, a third trained technician evaluated the result and provided the final decision.

### Statistical Analysis

Data were analyzed with SPSS version 25.0 (Armonk, NY: IBM Corp.). A descriptive analysis was performed to calculate the frequencies and percentages for categorical variables. Continuous variables were presented as the mean  $\pm$  standard deviation (SD). For the groups evaluated with and without COVID-19 disease, the rapid test results were compared against the non-reference standard RT-qPCR. Estimations of Kappa and



positive percentage agreement (PPA) were calculated with a 95% confidence interval (20).  $P$ -values  $<0.05$  were considered statistically significant.

## RESULTS

### Study Site and Study Participants

This study was conducted between April 30th and July 7th, 2020 in four private and public hospitals located in Panama and Colon cities, as well as the blood donation center in Panama City (Figure 1). A total of 702 participants were recruited for the field study: 255 (36.3%) were HD, while the remaining 63.7% of the sample comprised 351 HCW and 96 COVID-19 patients (confirmed by RT-qPCR) (Figure 2). Table 1 summarizes the age, sex, COVID-19 exposure, and presence of comorbidities across participants in the COVID-19 patient, HCW, and HD groups. Among participants from the COVID-19 group, 67 (69.9%) reported a pre-existing chronic disease; whereas 90 (25.6%) HCW and 28 (11.0%) HD reported a pre-existing chronic disease.

### CAST Test Diagnostic Performance Using Panel of Reference Sera

Samples including positive and negative COVID-19 cases confirmed by RT-PCR, and a set of pre-pandemic panel samples were analyzed with the CAST platform. A comparison of the CAST and RT-PCR results and the analytical performance results

are shown in Table 2. For both IgM and IgG antibodies, the test demonstrated a negative predictive value (NPV) of 0.985% (95% C.I. 0.915–1). An evaluation of the negative percent agreement indicated that of the cases with negative RT-PCR test results, only five showed positive CAST results for IgM and four showed positive CAST results for IgG. Two of these cases that were positive for both IgM and IgG were later determined to be false RT-PCR negatives based on two additional commercial lateral flow immunoassays (data not shown). Virus clearance may explain the other cases that showed negative RT-PCR results but positive antibody results with the CAST. Of the pre-pandemic samples tested ( $n = 55$ ), only one from a patient who tested positive for Dengue showed a positive IgM result on the CAST platform (data not shown).

We proceeded to evaluate the CAST's performance in the field during the current COVID-19 pandemic in Panama. We recruited 96 COVID-19 ward patients (Figure 2). All participants from this group were RT-PCR-confirmed positive cases and developed moderate COVID-19 symptoms. Analysis of the COVID-19-confirmed patient group showed a PPA of 67.7% (95% CI 57.8–76.2%) for IgM and IgG anti-SARS-CoV-2 antibodies (Data not shown). In order to investigate seroconversion over the course of COVID-19 evolution in patients, the data from 66 sera samples were divided into three groups according to the time of sample collection after illness onset. The CAST results showed a PPA of 36.4% (95% CI

**TABLE 1 |** Sociodemographic and comorbid information of study groups according to positive CAST results.

Variables	COVID-19 patients Mean (SD) or # (%)		Healthcare workers (HCW) Mean (SD) or # (%)		Healthy voluntary donors (HD) Median (SD) or # (%)	
	Total participants (n = 96)	CAST Positive (n = 65)	Total participants (n = 351)	CAST Positive (n = 45)	Total participants (n = 255)	CAST Positive (n = 34)
Age	54.9 (15.7)	53.1 (14.5)	39.5 (11.5)	41.1 (11.3)	73.2 (11.1)	35.5 (10.3)
<20	0 (0%)	0 (0%)	0 (0%)	0 (0%)	7 (2.7%)	1 (2.9%)
20–39	16 (16.7%)	10 (15.4%)	198 (56.4%)	22 (48.9%)	141 (55.3%)	22 (64.7%)
40–59	44 (45.8%)	35 (53.8%)	137 (39.0%)	19 (42.2%)	100 (39.2%)	11 (32.3%)
60–79	31 (32.3%)	17 (26.1%)	19 (5.4%)	4 (8.9%)	7 (2.7%)	0 (0%)
>80	5 (5.2%)	3 (4.6%)	0 (0%)	0 (0%)	0 (0%)	0 (0%)
Sex						
Male	64 (66.7%)	46 (70.8%)	113 (32.3%)	10 (22.2%)	181 (71.0%)	23 (67.6%)
Female	32 (33.3%)	19 (29.2%)	238 (67.8%)	35 (77.7%)	74 (29.0%)	11 (32.4%)
COVID-19 contact						
No contact	27 (29.0%)	15 (23.1%)	52 (14.8%)	5 (11.1%)	222 (87.0%)	24 (70.6%)
Contact	34 (36.6%)	26 (40.0%)	256 (72.9%)	34 (75.6%)	20 (7.8%)	7 (20.6%)
Doesn't know	32 (34.4%)	23 (35.4%)	43 (12.2%)	6 (13.3%)	13 (5.1%)	3 (8.8%)
Chronic diseases						
Hypertension	46 (47.9%)	33 (50.8%)	55 (15.7%)	6 (13.3%)	15 (5.9%)	1 (2.9%)
Renal failure	13 (13.5%)	6 (9.2%)	1 (0.3%)	1 (2.2%)	0 (0%)	0 (0%)
Respiratory insufficiency	3 (3.1%)	1 (1.5%)	0 (0%)	0 (0%)	0 (0%)	0 (0%)
Cardiac insufficiency	3 (3.1%)	2 (3.1%)	0 (0%)	0 (0%)	0 (0%)	0 (0%)
Cancer	5 (5.2%)	2 (3.1%)	0 (0%)	0 (0%)	0 (0%)	0 (0%)
Diabetes	29 (30.2%)	21 (32.3%)	18 (5.1%)	2 (4.4%)	0 (0%)	0 (0%)
Asthma	1 (1.0%)	1 (1.5%)	11 (3.1%)	4 (8.9%)	7 (0%)	1 (2.9%)
Other <sup>a</sup>	7 (7.3%)	6 (9.2%)	23 (6.5%)	3 (6.7%)	5 (0%)	2 (5.8%)

<sup>a</sup>other chronic diseases reported by participants were dyslipidemia and thyroid disease. COVID-19 contact refers to those participants that had contact with a confirmed COVID-19 case in their household and/or during daily activities at work in a healthcare facility.

**TABLE 2 |** Diagnostic performance and diagnostic certainty of CAST using a panel of reference sera.

CAST device		RT-PCR SARS-CoV-2			Positive percent agreement (PPA) (95% CI)	Negative percent agreement (NPA) (95% CI)	Overall percent agreement (95% CI)	Kappa (95% CI)
		Positive	Negative	Total				
CAST IgM	Positive	35	4	39	97.2% (84.6–100.0)	94.4% (86.2–98.2)	95.4% (89.3–98.3)	0.898 (0.811–0.985)
	Negative	1	68	69				
	Total	36	72	108				
CAST IgG	Positive	34	4	38	97.2% (84.6–100.0)	95.8% (88.0–99.1)	96.3% (90.6–98.9)	0.918 (0.839–0.997)
	Negative	0	70	70				
	Total	34	74	108				

19.6–57.1%) for either or both IgM and IgG in patients whose samples were collected from 0 to 7 days after RT-PCR diagnosis (Table 3). PPA scores of 76.2% (95% CI 54.5–89.8%) and 71.4% (95% CI 49.8–86.4%) for IgM and IgG, respectively, were found for patients whose samples were collected from 8 to 14 days after positive RT-PCR results. The highest PPA score of 87.0% (95% CI 67.0–96.3%) for both IgM and IgG antibodies was found for samples collected more than 15 days after diagnosis (Table 3). We later analyzed the CAST's performance using fingerstick blood samples from 32 additional patients who had a positive RT-PCR

test for SARS-CoV-2. All 32 samples were positive for IgG and IgM antibodies (data not shown).

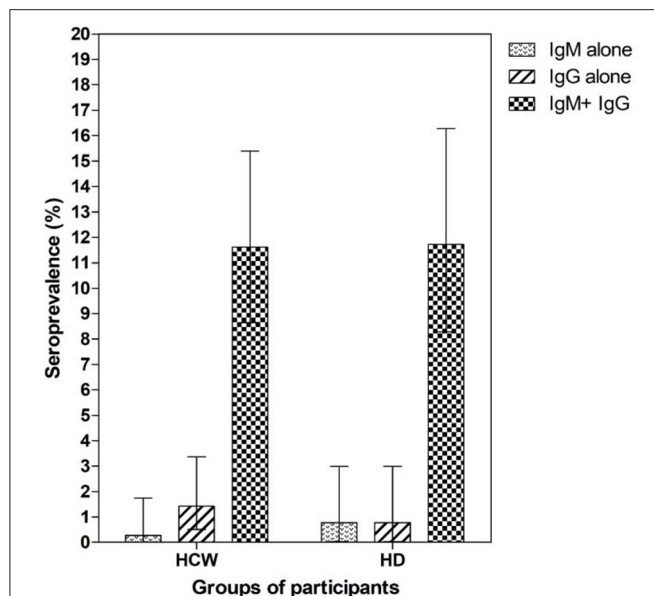
## Field Evaluation of CAST Among Health Care Workers and Healthy Blood Donors

To determine seroprevalence among a potentially exposed population and a population of healthy donors, we applied the CAST to participants with a high (HCW) and low (HD) risk of exposure to the virus. We found that 45 out of 351 HCW

**TABLE 3** | CAST SARS-CoV-2 IgM and IgG PPA by days post symptom onset in COVID-19 patients.

Time from symptom onset, days <sup>a</sup>	Positive /total samples tested	PPA (%)	95% CI
0–7	8/22	36.4	19.6–57.1
8–14	15/21	76.2	54.5–89.8
≥15	20/23	87.0	67.0–96.3

<sup>a</sup> Considering RT-PCR confirmed SARS-CoV-2 cases. PPA, Positive Percent Agreement.



**FIGURE 3** | Seroprevalence of SARS-CoV2 IgM and IgG in health care workers and healthy volunteer blood donors. A total of 351 healthcare workers (HCW) and 255 healthy volunteer donors (HD) were analyzed by rapid test for detection of anti SARS-CoV2 IgM and IgG antibodies. Each bar represents seroprevalence (%) according to the detection of IgM, IgG, or both IgM and IgG antibodies. Error bars represent the 95% CI.

tested positive for both IgM and IgG SARS CoV-2 antibodies, which corresponds to a prevalence of 11.61% (95% CI 8.6–15.4%) (Figure 3). In contrast, 86.97% (95% CI 83.0–90.1%) of the HCW samples were non-reactive, while 0.28% (95% CI 0–1.7%) and 1.42% (95% CI 0.5–3.4%) of the HCW samples were positive for only IgM or only IgG, respectively (data not shown). Next, we determined the seroprevalence among a group of HD and found that 11.72% (95% CI 8.3–16.3%) of the samples from this group were positive for both IgM and IgG anti-SARS-CoV-2 antibodies (Figure 3). Thus, 85.94% (95% CI 81.1–89.7%) of the HD samples were non-reactive, while 0.78% (95% CI 0–3.0%) of the HD samples were positive for only IgM or only IgG antibodies. We also found that there were no significant seroprevalence differences among HCW with clinical responsibilities (nurses and physicians) compared to those without clinical responsibilities (administrators, laboratory technicians, etc.) (12.9 vs. 14.1%, respectively,  $Chi\ square = 0.002$  with 1 degrees of freedom). In order to determine the risk of exposure during interactions with hospitalized COVID-19 patients, we asked HCW if they had been

in contact with those patients. We found that those HCW that reported having close contact with confirmed COVID-19 cases demonstrated a not significant higher seroprevalence than HCW that did not report close contact (12.4 vs. 1.8%, respectively,  $Chi\ square = 0.045$  with 1 degrees of freedom, data not shown).

We also analyzed differences in the age and gender of seropositive participants. In both the HCW and HD groups, we found a no significant higher seropositivity among participants in the age range of 20–39 years (48.9 and 64.7%, respectively,  $Chi\ square = 1.067$  and 0.002, respectively, with 1 degrees of freedom). Among seropositive HCW, 77.8% were female and 22.2% male (Table 1). The majority of HCW (75.6%) reported having contact with a confirmed COVID-19 case, while most of the HD participants reported no contact (70.6%).

## DISCUSSION AND CONCLUSION

Here we report COVID-19 antibody seroprevalence in HCW and HD among a convenience sample in Panama. We also report the performance of a rapid test kit for detecting anti-SARS-CoV-2 IgM/IgG antibodies with an LFIA. We tested serum samples from confirmed positive and negative COVID-19 patients and pre-pandemic samples collected in 2019. Our analysis showed a high Kappa correlation, indicating very close agreement between the RT-PCR and CAST. Based on our results, we conclude that the CAST is suitable for seroprevalence studies.

Our study estimates the seroprevalence of anti-SARS-CoV-2 IgM/IgG antibodies among a representative sample set of HCW and HD. Specifically, we investigated the seroprevalence in a group of hospitalized COVID-19 patients and a group of participants with a high risk of infection (health care workers) and another group with a low risk of contagion (healthy donors).

When we stratified the COVID-19 patient samples according to when they were collected in terms of number of days after symptom onset, we observed differences in the prevalence of positive results. A positivity rate of 87.0% (95% CI 67.0–96.3%) for both IgM and IgG antibodies was found in samples collected 15 days or more after a positive RT-PCR result. Similar to our findings, Pan et al. reported rapid test positivity rates of 11.1, 92.9, and 96.8% at the early convalescent (1–7 days after onset), intermediate (8–14 days after onset), and late convalescent stages (more than 15 days) of infection, respectively (21). High sensitivity of serological testing 2 weeks after symptom onset has been shown in other studies (22). In a study by Severance et al., 100% sensitivity was seen at ≥15 days post-PCR diagnosis, and Tang et al. reported 93.8% sensitivity (95% CI; 82.80–98.69) at ≥14 days PSO (23, 24). Based on our data, the usefulness of the CAST increased significantly 2 weeks post symptom onset. This observation indicates that the CAST could be used to evaluate the anti-SARS-CoV-2 antibody response 14 days after symptom onset, when the positivity rates are highest.

We found a seroprevalence of IgM and IgG antibodies of 11.61% (95% CI 8.6–15.4%) and 11.72% (95% CI 8.3–16.3%) in the HCW and HD groups, respectively. Given that HCW are a high-risk population (25, 26), it was quite surprising to find that the seroprevalence was nearly equal between the two groups,



similar to a previous report (27). It is worth mentioning that special precautions for blood donations are under investigation. To date, previous reports suggest no direct threat to blood safety itself (28–30). Likewise, it is important to highlight the ability of this rapid test to detect antibodies in mild or asymptomatic COVID-19 populations since there are indications that less severe illness is associated with lower antibody titers (31–34). As none of the members of this group reported being hospitalized or having symptoms clearly indicating recent infection, it is tempting to conclude that these represent asymptomatic cases that were infected while exposed to COVID-19 patients or in the community.

Theoretically, positive IgM and IgG tests for SARS-CoV-2 antibodies detected in patient blood samples indicate that it is likely that the individual is in the early convalescent stage of infection. Indeed, serology testing provides an important complement to RNA testing in the later stages of COVID-19 (35). If only IgG antibodies are detected, then it is probable that the person had an infection sometime in the past or the patient is in the convalescent stage of infection. Our study reveals the positivity rates for IgM and IgG between 0 and 15 days after symptom onset. Several scientists have reported that the detectable serology markers IgG and IgM have similar seroconversion in COVID-19 patients, with antibody levels increasing rapidly starting from 4 to 6 days after the appearance of symptoms (21, 35–37). Comprehensive studies looking at anti-SARS-CoV-2 antibody dynamics are warranted to fully describe their dynamics in the short and long term after infection.

In antibody-based testing, the window period depends on the seroconversion timeline. Antibodies to SARS-CoV-2 are typically detected 7–10 days post-illness onset. Several reports indicate patients seroconverting for IgM and IgG antibodies simultaneously within 2–3 weeks after illness onset; this can vary depending on factors including the patient's immune status and disease severity. Thus, detection of IgM without IgG is uncommon.

For example, Siracusano et al. reported that seroconversion appeared sequentially for total antibodies, IgM, and IgG, within a median time of 11, 12, and 14 days, respectively (38). Similarly, the median “window period” from illness onset to appearance of antibodies (range) was estimated at 10.2 (5.8–14.4) days post symptom initiation (39). Guo et al. profiled the early antibody response to NP protein in two cohorts of SARS-CoV-2-infected patients. The median time for IgM and IgA detection was at day 5 PSO (IQR 3–6) and day 14 PSO (IQR 10–18) for IgG. In yet another study, the median times of seroconversion for IgG, IgM, and IgA detected by an indirect immunofluorescence assay were 17 days after disease onset (40). Consequently, we similarly conclude that our CAST test would be more efficient if utilized 15 days after symptom onset.

Our study has several limitations. First, we were not able to use samples from individuals with other respiratory tract infections to rule out cross reactivity with human coronaviruses causing common seasonal colds. However, a set of 55 pre-pandemic samples was used to validate the test, and all but one tested

negative for anti-SARS-CoV-2 antibodies. Second, this rapid test is based on a colorimetric evaluation of the IgG and IgM bands determined by an operator, which implies the limitations that a qualitative inter-intra-operator evaluation might produce in terms of variability. In our study, this limitation was addressed by resorting to double operator evaluation and taking photographs of all test results to be re-analyzed by a third party in the case of first level evaluation disagreement. Third, the CAST is a qualitative detection method; thus, the antibody levels in COVID-19 patients were not measured in this study. Also, the sample size was calculated for the minimum sample required to validate the test. It is yet to be determined if the CAST produces the same results in a point-of-care setting using fresh blood samples since we used serum after centrifugation. Moreover, we have not evaluated if the CAST produces comparative results with ELISA or immunochemiluminescent tests. Ongoing work by our research team will allow us to establish the CAST's limits of detection by comparing results with an ELISA test.

The CAST (rapid test) has some advantages compared to other more complex laboratory-based tests. Compared to automated ELISA and immunochemiluminescent assays, CAST is economical and time efficient, does not require advanced equipment, is simple to perform, and requires minimal training. The CAST can be used for seroprevalence studies in primary health care settings as well as in specific contexts outside of hospitals, such as high-prevalence areas. Due to its low cost and short turnaround time, CAST is suitable for large-scale sample screening. In addition, using blood samples as opposed to nasal swabs could eliminate the need for operational steps that may produce aerosols and place technicians at higher risk. Some groups have attempted to compare serological tests with RT-PCR platforms. These tests have different targets and applications. The RT-PCR is intended for acute phase diagnosis, while the serology tests are intended for antibody seroprevalence studies.

In conclusion, the findings of this cross-sectional study demonstrate the value of the CAST for the detection of specific IgM and IgG antibodies at the population level, including among health care personnel, healthy blood donors, and other community members. The use of a rapid test among both healthy individuals and patients to conduct surveillance in outbreak areas could provide critical information about the status of the COVID-19 pandemic. Such a rapid test would allow the characterization of the pandemic's behavior at the community level and the identification of transmission hot spots in the community, which, in turn, would help us to better understand the situation and establish optimal strategies within quickly changing epidemic scenarios (15). In addition, it will facilitate the massification of diagnostic methods allowing us to determine the seroprevalence of the Panamanian population and the true extent of SARS-CoV-2 community spread.

## DATA AVAILABILITY STATEMENT

The raw data supporting the conclusions of this article will be made available by the authors, without undue reservation.

## ETHICS STATEMENT

The studies involving human participants were reviewed and approved by Comité Nacional de Bioética de la Investigación en Panamá. The patients/participants provided their written informed consent to participate in this study.

## AUTHOR CONTRIBUTIONS

All authors contributed to the conception, execution, data collection, analysis and writing of the manuscript.

## FUNDING

This research was supported by Panama's Secretaría Nacional de Ciencia Tecnología e Innovación (SENACYT) Rapid Grant No. COVID19-233 and Sistema Nacional de Investigación (SNI) for the following authors: AV, GB, PF, DO, CR, MC, RK, and AG. Laboratory equipment was previously acquired from National Institute of Health-NIH grant No. 5U01TW001021-05 awarded to EO-B. Additional support for personnel and field personnel was obtained from INDICASAT-AIP; the rapid test was donated by the Chinese Academy of Science; and supported by the National Natural Science Foundation of China (81672956 and 81972390), Beijing Science and Technology Projects (Z181100003818003), Beijing-Tianjin-Hebei Basic Research Cooperation Special Project (19JCZDJC65800(Z)),

China Children and Teenagers' Fund (Y1803001), Key Clinical Projects of Peking University Third Hospital (BYSY2017001), and Key Research and Development Plan Project of Hebei Province (20277705D).

## ACKNOWLEDGMENTS

We thank all the patients affected by COVID-19 for their participation in our study. We also thank the health care workers from all participating hospitals for their contributions to sampling and providing key information on the case distribution network. Special thanks to Dr. Victor Sanchez from SENACYT for his support of the collaboration network with the Ministry of Health and the National COVID-19 response. Lastly, we thank Colleen Goodridge for her critical review of the manuscript and valuable suggestions. This manuscript has been released as a pre-print at MedRxiv [Villarreal et al. (17)].

## SUPPLEMENTARY MATERIAL

The Supplementary Material for this article can be found online at: <https://www.frontiersin.org/articles/10.3389/fmed.2021.616106/full#supplementary-material>

**Supplementary Figure 1** | Representative picture of CAST IgM and IgG antibody test results. (A) Only IgM; (B) Only IgG; (C) Both IgM and IgG; (D) No IgM or IgG.

**Supplementary Table 1** | Symptoms among COVID-19 patients.

## REFERENCES

- Lu H, Stratton CW, Tang YW. Outbreak of pneumonia of unknown etiology in Wuhan, China: the mystery and the miracle. *J Med Virol.* (2020) 92:401–2. doi: 10.1002/jmv.25678
- Temgoua MN, Endomba FT, Nkeck JR, Kenfack GU, Tochie JN, Essouma M. Coronavirus Disease 2019 (COVID-19) as a multi-systemic disease and its impact in Low- and Middle-Income Countries (LMICs). *SN Compr Clin Med.* (2020) 2:1377–87. doi: 10.1007/s42399-020-00417-7
- WHO Coronavirus Disease (COVID-19) Dashboard. Available online at: [https://covid19.who.int/?gclid=CjwKCAjw4\\_H6BRALEiwAvgfzq34TfRvRSv7OVn2CVGz\\_VeWP3xHD7KU0LeyAR8ANCoXsSo5\\_s26whoC33gQAvD\\_BwE](https://covid19.who.int/?gclid=CjwKCAjw4_H6BRALEiwAvgfzq34TfRvRSv7OVn2CVGz_VeWP3xHD7KU0LeyAR8ANCoXsSo5_s26whoC33gQAvD_BwE) (accessed January 12, 2021).
- Organization PAH. COVID-19 - PAHO/WHO Response, Report 20. In: *Book COVID-19 - PAHO/WHO Response, Report 20*. Panama city: Pan American Health Organization (2020).
- Loaiza JR, Rao K, Eskildsen GA, Ortega-Barria E, Miller MJ, Gittens RA. COVID-19 pandemic in Panama: lessons of the unique risks and research opportunities for Latin America. *Rev Panam Salud Publica.* (2020) 44:e86. doi: 10.26633/RPSP.2020.86
- Li X, Zai J, Wang X, Li Y. Potential of large “first generation” human-to-human transmission of 2019-nCoV. *J Med Virol.* (2020) 92:448–54. doi: 10.1002/jmv.25693
- Wilder-Smith A, Chiew CJ, Lee VJ. Can we contain the COVID-19 outbreak with the same measures as for SARS? *Lancet Infect Dis.* (2020) 20:e102–7. doi: 10.1016/S1473-3099(20)30129-8
- Miller JM, Binnicker MJ, Campbell S, Carroll KC, Chapin KC, Gilligan PH, et al. A guide to utilization of the microbiology laboratory for diagnosis of infectious diseases: 2018 update by the infectious diseases society of America and the American society for microbiology. *Clin Infect Dis.* (2018) 67:813–6. doi: 10.1093/cid/ciy584
- Santiago I. Trends and innovations in biosensors for COVID-19 mass testing. *Chembiochem.* (2020) 21:2880–9. doi: 10.1002/cbic.202000250
- Younes N, Al-Sadeq DW, Al-Jighefee H, Younes S, Al-Jamal O, Daas HI, et al. Challenges in laboratory diagnosis of the novel coronavirus SARS-CoV-2. *Viruses.* (2020) 12:582. doi: 10.3390/v12060582
- Madore DV, Meade BD, Rubin F, Deal C, Lynn F, Meeting Contributors. Utilization of serologic assays to support efficacy of vaccines in nonclinical and clinical trials: meeting at the crossroads. *Vaccine.* (2010) 28:4539–47. doi: 10.1016/j.vaccine.2010.04.094
- COVID-19 Test Analysis. Available online at: <https://www.resiliencehealth.com/tests/data.html> (accessed January 12, 2021).
- Caini S, Bellerba F, Corso F, Diaz-Basabe A, Natoli G, Paget J, et al. Meta-analysis of diagnostic performance of serological tests for SARS-CoV-2 antibodies up to 25 April 2020 and public health implications. *Euro Surveill.* (2020) 25:2000980. doi: 10.2807/1560-7917.ES.2020.25.23.2000980
- Andersson M, Low N, French N, Greenhalgh T, Jeffery K, Brent A, et al. Rapid roll out of SARS-CoV-2 antibody testing-a concern. *BMJ.* (2020) 369:m2420. doi: 10.1136/bmj.m2420
- Lisboa Bastos M, Tavaziva G, Abidi SK, Campbell JR, Haraoui L-P, Johnston JC, et al. Diagnostic accuracy of serological tests for covid-19: systematic review and meta-analysis. *BMJ.* (2020) 370:m2516. doi: 10.1136/bmj.m2516
- Özçürümez MK, Ambrosch A, Frey O, Haselmann V, Holdenrieder S, Kiehnopf M, et al. SARS-CoV-2 antibody testing-questions to be asked. *J Allergy Clin Immunol.* (2020) 146:35–43. doi: 10.1016/j.jaci.2020.05.020
- Villarreal A, Rangel G, Zhang X, Wong D, De La Guardia C, Britton G, et al. Performance of a point of care test for detecting IgM and IgG antibodies against SARS-CoV-2 and seroprevalence in blood donors and health care workers in Panama. *medRxiv [preprint].* (2020). doi: 10.1101/2020.09.25.20201459
- Corman VM, Landt O, Kaiser M, Molenkamp R, Meijer A, Chu DK, et al. Detection of 2019 novel coronavirus (2019-nCoV) by real-time RT-PCR. *Euro Surveill.* (2020) 25:2000045. doi: 10.2807/1560-7917.ES.2020.25.3.2000045

19. WHO. Population-based age-stratified seroepidemiological investigation protocol for coronavirus 2019 (COVID-19) infection. In: *Book Population-Based Age-Stratified Seroepidemiological Investigation Protocol for Coronavirus 2019 (COVID-19) Infection* (Editor ed.<sup>^</sup>eds.). (2020).
20. Shen B, Zheng Y, Zhang X, Zhang W, Wang D, Jin J, et al. Clinical evaluation of a rapid colloidal gold immunochromatography assay for SARS-CoV-2 IgM/IgG. *Am J Transl Res.* (2020) 12:1348–54.
21. Pan Y, Li X, Yang G, Fan J, Tang Y, Zhao J, et al. Serological immunochromatographic approach in diagnosis with SARS-CoV-2 infected COVID-19 patients. *J Infect.* (2020) 81:e28–32. doi: 10.1016/j.jinf.2020.03.051
22. Deeks JJ, Dinnes J, Takwoingi Y, Davenport C, Spijker R, Taylor-Phillips S, et al. Antibody tests for identification of current and past infection with SARS-CoV-2. *Cochrane Database Syst Rev.* (2020) 6:Cd013652. doi: 10.1002/14651858.CD013652
23. Severance EG, Bossis I, Dickerson FB, Stallings CR, Origoni AE, Sullens A, et al. Development of a nucleocapsid-based human coronavirus immunoassay and estimates of individuals exposed to coronavirus in a U.S. metropolitan population. *Clin Vaccine Immunol.* (2008) 15:1805–10. doi: 10.1128/CVI.00124-08
24. Tang MS, Hock KG, Logsdon NM, Hayes JE, Gronowski AM, Anderson NW, et al. Clinical performance of two SARS-CoV-2 serologic assays. *Clin Chem.* (2020) 66:1055–62. doi: 10.1093/clinchem/hvaa120
25. Folgueira MD, Munoz-Ruiperez C, Alonso-Lopez MA, Delgado R. SARS-CoV-2 infection in Health Care Workers in a large public hospital in Madrid, Spain, during March 2020. *medRxiv [preprint].* (2020). doi: 10.1101/2020.04.07.20055723
26. Garcia-Basteiro AL, Moncunill G, Tortajada M, Vidal M, Guinovart C, Jiménez A, et al. Seroprevalence of antibodies against SARS-CoV-2 among health care workers in a large Spanish reference hospital. *Nat Commun.* (2020) 11:3500. doi: 10.1038/s41467-020-17318-x
27. Barrett ES, Horton DB, Roy J, Gennaro ML, Brooks A, Tischfield J, et al. Prevalence of SARS-CoV-2 infection in previously undiagnosed health care workers at the onset of the U.S. COVID-19 epidemic. *medRxiv [preprint].* (2020). doi: 10.1101/2020.04.20.20072470
28. Chang L, Yan Y, Zhao L, Hu G, Deng L, Su D, et al. No evidence of SARS-CoV-2 RNA among blood donors: a multicenter study in Hubei, China. *Transfusion.* (2020) 60:2038–46. doi: 10.1111/trf.15943
29. Dodd RY, Stramer SL. COVID-19 and blood safety: help with a dilemma. *Transfus Med Rev.* (2020) 34:73–4. doi: 10.1016/j.tmr.2020.02.004
30. Kwon SY, Kim EJ, Jung YS, Jang JS, Cho NS. Post-donation COVID-19 identification in blood donors. *Vox Sang.* (2020) 115:601–2. doi: 10.1111/vox.12925
31. Tang YW, Schmitz JE, Persing DH, Stratton CW. Laboratory diagnosis of COVID-19: current issues and challenges. *J Clin Microbiol.* (2020) 58:e00512–20. doi: 10.1128/JCM.00512-20
32. Wu F, Wang A, Liu M, Wang Q, Chen J, Xia S, et al. Neutralizing antibody responses to SARS-CoV-2 in a COVID-19 recovered patient cohort and their implications. *medRxiv [preprint].* (2020). doi: 10.2139/ssrn.3566211
33. Ma H, Zeng W, He H, Zhao D, Jiang D, Zhou P, et al. Serum IgA, IgM, and IgG responses in COVID-19. *Cell Mol Immunol.* (2020) 17:773–5. doi: 10.1038/s41423-020-0474-z
34. Okba NMA, Müller MA, Li W, Wang C, GeurtsvanKessel CH, Corman VM, et al. Severe acute respiratory syndrome coronavirus 2-specific antibody responses in coronavirus disease patients. *Emerg Infect Dis.* (2020) 26:1478–88. doi: 10.3201/eid2607.200841
35. Lou B, Li TD, Zheng SF, Su YY, Li ZY, Liu W, et al. Serology characteristics of SARS-CoV-2 infection after exposure and post-symptom onset. *Eur Respir J.* (2020) 56:2000763. doi: 10.1183/13993003.00763-2020
36. Adams ER, Ainsworth M, Anand R, Andersson MI, Auckland K, Baillie JK, et al. Antibody testing for COVID-19: a report from the National COVID Scientific Advisory Panel. *medRxiv [preprint].* (2020).
37. Zhang JJ, Dong X, Cao YY, Yuan YD, Yang YB, Yan YQ, et al. Clinical characteristics of 140 patients infected with SARS-CoV-2 in Wuhan, China. *Allergy.* (2020) 75:1730–41. doi: 10.1111/all.14238
38. Siracusano G, Pastori C, Lopalco L. Humoral immune responses in COVID-19 patients: a window on the state of the art. *Front Immunol.* (2020) 11:1049. doi: 10.3389/fimmu.2020.01049
39. Hueston L, Kok J, Guibone A, McDonald D, Hone G, Goodwin J, et al. The antibody response to SARS-CoV-2 infection. *Open Forum Infect Dis.* (2020) 7:ofaa387. doi: 10.1093/ofid/ofaa387
40. Woo PC, Lau SK, Wong BH, Chan KH, Chu CM, Tsoi HW, et al. Longitudinal profile of immunoglobulin G (IgG), IgM, and IgA antibodies against the severe acute respiratory syndrome (SARS) coronavirus nucleocapsid protein in patients with pneumonia due to the SARS coronavirus. *Clin Diagn Lab Immunol.* (2004) 11:665–8. doi: 10.1128/CDLI.11.4.665-668.2004

**Conflict of Interest:** EO-B was employed by the GlaxoSmithKline. CL, XZ, DZ, and FF were employed by company Beijing Zhongke Jianlan Biotechnology Co., Ltd., and BW was employed by company Beijing Kewei Clinical Diagnostic Reagent Inc.

The remaining authors declare that the research was conducted in the absence of any commercial or financial relationships that could be construed as a potential conflict of interest.

Copyright © 2021 Villarreal, Rangel, Zhang, Wong, Britton, Fernandez, Pérez, Oviedo, Restrepo, Carreira, Sambrano, Eskildsen, De La Guardia, Flores-Cuadra, Carrera, Zaldivar, Franco, López-Vergès, Zhang, Fan, Wang, Sáez-Llorens, DeAntonio, Torres-Atencio, Blanco, Subía, Mudarra, Benzaón, Valverde, López, Hurtado, Rivas, Jurado, Carvallo, Rodríguez, Perez, Morris, Luque, Cortez, Ortega-Barria, Kosagisharaf, Lleonart, Li and Goodridge. This is an open-access article distributed under the terms of the Creative Commons Attribution License (CC BY). The use, distribution or reproduction in other forums is permitted, provided the original author(s) and the copyright owner(s) are credited and that the original publication in this journal is cited, in accordance with accepted academic practice. No use, distribution or reproduction is permitted which does not comply with these terms.



# Time Till Viral Clearance of Severe Acute Respiratory Syndrome Coronavirus 2 Is Similar for Asymptomatic and Non-critically Symptomatic Individuals

Nitya Kumar<sup>1\*</sup>, AbdulKarim AbdulRahman<sup>2</sup>, Salman AlAli<sup>2</sup>, Sameer Ootom<sup>1</sup>, Stephen L. Atkin<sup>1</sup> and Manaf AlQahtani<sup>1,2</sup>

<sup>1</sup> Royal College of Surgeons in Ireland, Manama, Bahrain, <sup>2</sup> Bahrain Defense Force Hospital, Manama, Bahrain

## OPEN ACCESS

### Edited by:

Segaran P. Pillai,  
United States Department of  
Homeland Security, United States

### Reviewed by:

Takafira Mdluluza,  
University of Zimbabwe, Zimbabwe  
Jan Gerstoft,  
University of Copenhagen, Denmark

### \*Correspondence:

Nitya Kumar  
nkumar@rcsi-mub.com

### Specialty section:

This article was submitted to  
Infectious Diseases - Surveillance,  
Prevention and Treatment,  
a section of the journal  
Frontiers in Medicine

**Received:** 13 October 2020

**Accepted:** 17 February 2021

**Published:** 26 March 2021

### Citation:

Kumar N, AbdulRahman A, AlAli S,  
Ootom S, Atkin SL and AlQahtani M  
(2021) Time Till Viral Clearance of  
Severe Acute Respiratory Syndrome  
Coronavirus 2 Is Similar for  
Asymptomatic and Non-critically  
Symptomatic Individuals.  
Front. Med. 8:616927.  
doi: 10.3389/fmed.2021.616927

Despite the modeled estimations of the burden of asymptomatic spread, the duration of viral positivity and infectiousness of severe acute respiratory syndrome coronavirus 2 (SARS-CoV-2) remains understudied. The objective of the present study was to estimate and compare the time till viral clearance of SARS-CoV-2 in asymptomatic and non-critical symptomatic individuals. We studied 184 SARS-CoV-2-positive participants, of whom 145 were asymptomatic. Our analysis uncovered that time till viral negativity is similar for subclinical [median time till viral clearance: 11 days, interquartile range (IQR): 8, 14] and overt infections (median: 11 days, IQR: 9, 14) after controlling for age and sex. This has implications in understanding the period of infectivity for SARS-CoV-2 in order to plan adequate public health measures to control the community spread.

**Keywords:** SARS-CoV-2, asymptomatic, viral clearance, COVID-19, viral convergence

## INTRODUCTION

Asymptomatic severe acute respiratory syndrome coronavirus 2 (SARS-CoV-2) infections remain highly under-diagnosed (1) and are partly responsible for the recent uptick in coronavirus disease 2019 (COVID-19) cases following the reopening of business, universities, and schools around the globe, especially in the United States (2, 3) and the United Kingdom (4). Initial studies on asymptomatic spread report that it accounts for 6% to 30% of SARS-CoV-2 infections in various settings (5, 6). Although median time till viral clearance in symptomatic individuals has been reported to be between 10 and 14 days (7, 8), time kinetics of viral clearance and the duration of infectiousness in asymptomatic individuals remains poorly understood. The present analysis aimed to estimate time till viral clearance in asymptomatic individuals and see how it compares with that of non-critically symptomatic ones.

## METHODS

### Study Population

Study population consisted of individuals who arrived in Bahrain from Iran and Egypt between 25 February 2020 and 14 March 2020 and tested positive for SARS-CoV-2 upon mandatory COVID-19 screening prior to entering the country.



## Screening Procedure and Outcome Assessment

Information on reported COVID-19 symptoms was gathered from the study subjects who underwent nasopharyngeal swab testing for SARS-CoV-2 using reverse transcriptase–polymerase chain reaction (RT-PCR) test. After screening, all of the study subjects served mandatory quarantine in isolation wards (or hospitals, when symptomatic), until viral clearance occurred—defined as two consecutive negative RT-PCR test results 24 h apart. We used Thermo Fisher Scientific (Waltham, MA) TaqPath 1-Step RT-qPCR Master Mix, CG on the Applied Biosystems (Foster City, CA) 7500 Fast Dx RealTime PCR Instrument for conducting the PCR assay. The E gene was used and targeted for the assay, and when detected, the test was confirmed by RdRP and N genes. E gene Ct values > 40 were considered negative. For quality control, both positive and negative controls were used. Time until viral clearance was ascertained by testing the individuals every 2 days till viral clearance occurred. Any individuals who developed symptoms while undergoing quarantine were counted as symptomatic.

## Statistical Analyses

Age, sex, and presence of symptoms in the participants have been reported as proportions. Odds of being symptomatic were estimated using a logistic regression model, which was adjusted for categories of age and sex. Time till viral clearance has been reported as medians and interquartile ranges (IQRs) (computed from Kaplan–Meier analysis), and difference across categories of covariates was tested using a log rank test. Hazards of viral clearance were estimated using a Cox proportional hazards model.

## RESULTS

The total number of participants in the study was 184, which included 132 subjects who tested positive at screening and 52 out of 2,526 people who tested negative upon screening and went on to test positive at the end of quarantine. Most of the subjects had asymptomatic infection ( $n = 145$ , 78.8%) and were females ( $n = 115$ , 62.5%). The number of subjects progressively increased across increasing age categories, with 22.3% ( $n = 41$ ) of the subjects being in the  $\geq 60$  years category.

We did not find age categories or sex to significantly affect the odds of being symptomatic in the study sample, although people in the category of 50–59 years of age seemed to be more likely to be symptomatic (OR = 1.5, 95% CI = 0.4–5.3) after adjusting for differences in sex (Table 1).

Median time until viral clearance was similar for males and females (Table 2) and showed an increasing, though nonsignificant, trend across increasing age categories from 11 days in individuals of 0–29 years to 13 days in individuals of  $\geq 60$  years. Symptomatic and asymptomatic individuals had the same median time till viral clearance of 11 ( $p = 0.491$ ) days. To adjust for effects of age and sex, we computed hazards of viral clearance among the study subjects (Table 2) and did not see any difference between symptomatic and asymptomatic individuals (hazard

**TABLE 1 |** Subject characteristics and odds of being symptomatic.

	N (184)	%	Odds of being symptomatic [OR (95% CI)]
<b>Sex</b>			
Males	69	37.5	1.1 (0.5–2.4) <sup>a</sup>
Females	115	62.5	Reference group
<b>Age group</b>			
0–29	25	13.6	Reference group
30–39	23	12.5	0.4 (0.1–1.5) <sup>b</sup>
40–49	39	21.2	1.2 (0.3–4.3) <sup>b</sup>
50–59	56	30.4	1.5 (0.4–5.3) <sup>b</sup>
60+	41	22.3	0.8 (0.2–2.6) <sup>b</sup>
<b>Symptoms</b>			
Asymptomatic	145	78.8	NA
Symptomatic	39	21.2	NA

NA, not applicable.

<sup>a</sup>Adjusted for age group.

<sup>b</sup>Adjusted for sex.

**TABLE 2 |** Median time till viral clearance.

	<i>N</i> (184)	Hazards of viral clearance <sup>a</sup> [HR (95% CI)]	Time till viral clearance [median (IQR)]	<i>p</i> -value—log rank test
<b>Sex</b>				
Males	69	1.1 (0.7–1.5)	11 (8–14)	0.622
Females	115	Reference group	12 (10–14)	
<b>Age group</b>				
0–29	25	Reference group	11 (8–13)	0.265
30–39	23	0.7 (0.4–1.3)	11 (8–13)	
40–49	39	0.8 (0.5–1.4)	11 (8–13)	
50–59	56	0.7 (0.4–1.2)	12 (9–14.5)	
60+	41	0.6 (0.4–1.0)	13 (9–14)	
<b>Symptoms</b>				
Asymptomatic	145	Reference group	11 (8–14)	0.491
Symptomatic	39	1.08 (0.7–1.5)	11 (9–14)	

<sup>a</sup>Adjusted for all predictor variables.

ratio for symptomatic individuals compared with asymptomatic ones = 1.08, 85% CI = 0.7–1.5).

These results indicate that after age and sex were controlled for, time till viral negativity of subclinical infection is similar to that of a non-critically overt one.

## DISCUSSION AND CONCLUSION

To our knowledge, this is the first study reporting time till viral clearance of SARS-CoV-2 RNA in asymptomatic individuals and is the first of its kind analysis to uncover the finding that duration of viral positivity is similar for subclinical and overt infections after controlling for age and sex. Chang et al. (7) have reported the median time till viral in symptomatic patients to be 10.5

days, which is similar to our finding of 11 days in symptomatic individuals and not too different from that of asymptomatic individuals (10 days). Hu et al. (8) have reported the median time till negative convergence in symptomatic patients to be 14 days, which makes sense given the study participants were all highly symptomatic hospitalized patients. The authors also reported age of more than 45 years to be significantly associated with longer duration of viral clearance (HR: 0.37) in these patients. Although the present study saw an increasing trend in time till viral negativity with increasing age categories (HR = 0.8 for age category 40–50 years, HR = 0.7 for 50–60 years, HR = 0.6 for >60 years category), the trend was not statistically significant. This could be partly explained by the difference in severity between participants in our study and those studied by Hu et al., our study sample consisted of non-critical symptomatic and asymptomatic individuals, whereas participants of Hu et al. were symptomatic to the point of being hospitalized. When viewed in conjunction with the finding that asymptomatic and symptomatic individuals have similar viral loads as reported by Zou et al. (9), our results raise questions on similarities in duration of infectiousness between symptomatic and asymptomatic subjects. However, recent reports suggest that viral nucleic acids are still present in patient samples; therefore, asymptomatic patients may shed non-viable virus (especially those with low viral loads/high CT values threshold) that may culture negative though persistently test RT-PCR positive (10). One of the limitations in the present study is that in individuals who were symptomatic upon arrival, it was not possible to ascertain how long they would have been presymptomatic before they landed in Bahrain. This could

have affected the estimates of duration of viral positivity in symptomatic patients and warrants further research. Aside from this, these insights shed light on why asymptomatic spread is still very much a substantial risk and underscore the importance of not easing public health preventative measures as yet, such as restrictions on mass gathering, social distancing, and especially opening of businesses that would make population adherence to these measures difficult.

## DATA AVAILABILITY STATEMENT

The raw data supporting the conclusions of this article will be made available by the authors, without undue reservation.

## ETHICS STATEMENT

The studies involving human participants were reviewed and approved by Bahrain National Covid-19 Taskforce Ethics Committee. The patients/participants provided their written informed consent to participate in this study.

## AUTHOR CONTRIBUTIONS

NK: data analysis, interpretation, and preparation of the manuscript. AA and SA: conception and design, data collection, and manuscript review. SO and SLA: writing and manuscript review. MA: conception and design of the study and manuscript review. All authors contributed to the article and approved the submitted version.

## REFERENCES

1. Nishiura H, Kobayashi T, Miyama T, Suzuki A, Jung SM, Hayashi K, et al. Estimation of the asymptomatic ratio of novel coronavirus infections (COVID-19). *Int J Infect Dis.* (2020) 94:154–5. doi: 10.1016/j.ijid.2020.03.020
2. Levenson, E. UNC-Chapel Hill Reverses Plans for in-Person Classes after 130 Students Test Positive for Covid-19. *CNN, Cable News Network* (2020, August 18). Available online at: [edition.cnn.com/2020/08/17/us/coronavirus-college-university/index.html](https://edition.cnn.com/2020/08/17/us/coronavirus-college-university/index.html).
3. Cai W, Ivory D, Semple, K, Smith M, Lemonides A, Higgins L, et al. Tracking Coronavirus Cases at U.S. Colleges and Universities. *The New York Times* (2020, August 26). Available online at: [www.nytimes.com/interactive/2020/us/covid-college-cases-tracker.html](https://www.nytimes.com/interactive/2020/us/covid-college-cases-tracker.html).
4. Kumar S. Eat Out to Help Out' policy failed United Kingdom. *The Daily Targum.* (2020). Available online at: <https://www.dailytargum.com/article/2020/09/kumar-eat-out-to-help-out-policy-failed-united-kingdom>. (accessed September 15, 2020).
5. Arons MM, Hatfield KM, Reddy SC, Kimball A, James A, Jacobs JR, et al. Presymptomatic SARS-CoV-2 infections and transmission in a skilled nursing facility. *N Engl J Med.* (2020) 382:2081–90. doi: 10.1056/NEJMoa2008457
6. Mizumoto K, Kagaya K, Zarebski A, Chowell, G. Estimating the asymptomatic proportion of coronavirus disease 2019 (COVID-19) cases on board the Diamond Princess cruise ship, Yokohama, Japan, 2020. *Euro Surveill.* (2020). 25:2000180. doi: 10.2807/1560-7917.ES.2020.25.10.2000180
7. Chang D, Mo G, Yuan X, Tao Y, Peng X, Wang FS, et al. Time kinetics of viral clearance and resolution of symptoms in novel coronavirus infection. *Am J Respir Crit Care Med.* (2020) 201:1150–2. doi: 10.1164/rccm.202003-0524LE
8. Hu X, Xing Y, Jia J, Ni W, Liang J, Zhao D, et al. Factors associated with negative conversion of viral RNA in patients hospitalized with COVID-19. *Sci Total Environ.* (2020) 728:138812. doi: 10.1016/j.scitotenv.2020.138812
9. Zou L, Ruan F, Huang M, Liang L, Huang H, Hong Z, et al. SARS-CoV-2 viral load in upper respiratory specimens of infected patients. *N Engl J Med.* (2020) 382:1177–9. doi: 10.1056/NEJMc2001737
10. Xiao AT, Tong YX, Zhang S. False negative of RT-PCR and prolonged nucleic acid conversion in COVID-19: rather than recurrence. *J Med Virol.* (2020) 92:1755–6. doi: 10.1002/jmv.25855

**Conflict of Interest:** The authors declare that the research was conducted in the absence of any commercial or financial relationships that could be construed as a potential conflict of interest.

Copyright © 2021 Kumar, AbdulRahman, AlAli, Ootom, Atkin and AlQahtani. This is an open-access article distributed under the terms of the Creative Commons Attribution License (CC BY). The use, distribution or reproduction in other forums is permitted, provided the original author(s) and the copyright owner(s) are credited and that the original publication in this journal is cited, in accordance with accepted academic practice. No use, distribution or reproduction is permitted which does not comply with these terms.



# Comparison Between a Standard and SalivaDirect RNA Extraction Protocol for Molecular Diagnosis of SARS-CoV-2 Using Nasopharyngeal Swab and Saliva Clinical Samples

Sofía N. Rodríguez Flores<sup>1†</sup>, Luis Mario Rodríguez-Martínez<sup>1†</sup>,  
Bernardita L. Reyes-Berrones<sup>2</sup>, Nadia A. Fernández-Santos<sup>1</sup>, Elthon J. Sierra-Moncada<sup>3</sup>  
and Mario A. Rodríguez-Pérez<sup>1\*</sup>

## OPEN ACCESS

### Edited by:

Segaran P. Pillai,  
United States Department  
of Homeland Security, United States

### Reviewed by:

Malaya Sahoo,  
Stanford University, United States  
Bruno Jorge Antunes Colaço,  
University of Trás-os-Montes and Alto  
Douro, Portugal

### \*Correspondence:

Mario A. Rodríguez-Pérez  
drmarodriguez@hotmail.com;  
drmarodriguez1@hotmail.com

<sup>†</sup> These authors have contributed  
equally to this work

### Specialty section:

This article was submitted to  
Biosafety and Biosecurity,  
a section of the journal  
Frontiers in Bioengineering and  
Biotechnology

**Received:** 07 December 2020

**Accepted:** 23 February 2021

**Published:** 29 March 2021

### Citation:

Rodríguez Flores SN,  
Rodríguez-Martínez LM,  
Reyes-Berrones BL,  
Fernández-Santos NA,  
Sierra-Moncada EJ and  
Rodríguez-Pérez MA (2021)  
Comparison Between a Standard  
and SalivaDirect RNA Extraction  
Protocol for Molecular Diagnosis  
of SARS-CoV-2 Using  
Nasopharyngeal Swab and Saliva  
Clinical Samples.  
Front. Bioeng. Biotechnol. 9:638902.  
doi: 10.3389/fbioe.2021.638902

<sup>1</sup> Instituto Politécnico Nacional, Centro de Biotecnología Genómica, Reynosa, Mexico, <sup>2</sup> Laboratorio Estatal de Salud Pública de Tamaulipas, Secretaría de Salud de Tamaulipas, Ciudad Victoria, Mexico, <sup>3</sup> Universidad Autónoma de Nuevo León, Facultad de Ingeniería Mecánica y Eléctrica, San Nicolás de los Garza, Mexico

During the COVID-19 pandemic, a certified laboratory of Tamaulipas, Mexico has processed over 100,000 samples of COVID-19 suspected patients, working a minimum of 100 tests daily. Thus, it would be beneficial for such certified laboratories nationwide to reduce the time and cost involved in performing the diagnosis of COVID-19, from sample collection, transportation to local lab, processing of samples, and data acquisition. Here, 30 nasopharyngeal swab and saliva samples from the same COVID-19 individuals were assessed by a standard nucleic acid extraction protocol, including protein lysis with proteinase K followed by binding to column, washing, and elution, and by the SalivaDirect protocol based on protein lysis, skipping the other steps to reduce processing time and costs. The genomic RNA was amplified using a SARS-CoV-2 Real-Time PCR kit. A variation ( $P > 0.05$ ) in the 95% CIs = 72.6%–96.7% was noted by using the SalivaDirect protocol and saliva samples (sensitivity of 88.2%) in comparison to those of standard protocol with oropharyngeal swab samples (95% CIs = 97.5%–100%; sensitivity of 100%) as reported elsewhere. However, when using nasopharyngeal swab samples in the SalivaDirect protocol (sensitivity of 93.6%; 95% CIs = 79.2%–99.2%), it was in concordance ( $P < 0.05$ ) with those of the standard one. The logical explanation to this was that two samples with Ct values of 38, and 40 cycles for gene E produced two false negatives in the SalivaDirect protocol in relation to the standard one; thus, there was a reduction of the sensitivity of 6.4% in the overall assay performance.

**Keywords:** molecular diagnosis, RNA extraction protocol, clinical samples, COVID-19, SARS-CoV-2

## INTRODUCTION

Rapid and precise detection of COVID-19 is necessary for surveillance and control of the pandemic. qRT-PCR and nasopharyngeal swabs are the recommended test and sample to be used (Azzi et al., 2020). The sensitivity of qRT-PCR depends on the protocol, the sample analyzed, the number of clinical samples, and other factors (Yam et al., 2003). However, the collection of

nasopharyngeal or oropharyngeal samples causes discomfort to patients and may cause bleeding, especially in patients with thrombocytopenia (Chan et al., 2020). Collection of samples requires close contact between healthcare workers and patients, representing a risk factor of transmission of the virus because samples collected may contain live viruses (To et al., 2020b). These findings reinforce the use of barrier protection equipment as a control measure for all healthcare workers (Fakheran et al., 2020).

The two main components of a SARS-CoV-2 nucleic acid extraction kit are proteinase K and silica columns. Proteinase K is widely used in scientific research and industries mainly because only few proteins resist to it. It has potent activity to denature proteins, even in the presence of strong detergents, and it can be used to isolate viral genomic material (Yang et al., 2016). Thus, proteinase K is massively used in COVID-19 laboratories. Moreover, RNA purification based on silica columns is used mainly because it allows fast extractions with good yields of high-quality nucleic acids. However, silica columns are expensive, especially for non-developed countries (Nicosia et al., 2010).

Nowadays, qRT-PCR assays have enabled the diagnosis of COVID-19 from saliva (To et al., 2020a,b). On April 14, 2020, the United States-Food and Drug Administration (US-FDA) authorized the first saliva-based nucleic acid test for emergency use in COVID-19 diagnosis (Rutgers, 2020); namely, a saliva test in which the sample can be collected at home and mailed in for testing (Food and Drug Administration [FDA], 2020a). On August 15, 2020, the US-FDA authorized the SalivaDirect protocol, based on reduced times by skipping silica column wash in acid nucleic extraction protocol (Food and Drug Administration [FDA], 2020b; Vogels et al., 2020).

It has been shown that saliva sample collection for diagnosis and viral load monitoring of SARS-CoV-2 has many advantages. It requires less stringent conditions and can be used as a screening tool that highly minimize the chance of exposing healthcare workers in comparison to nasopharyngeal swabs (To et al., 2020a). Therefore, this sample collection can decrease the risk of nosocomial SARS-CoV-2 transmission, and it is not necessary the presence of trained personnel (Fakheran et al., 2020).

Previously, it was demonstrated that saliva has a high concordance rate with nasopharyngeal aspirate in the detection of respiratory viruses, including coronaviruses such as SARS-CoV-2 (To et al., 2019b, 2020a,b; Williams et al., 2020; Zheng et al., 2020). It has been reported that the use of saliva for coronaviruses detection such as SARS-CoV-2 is more sensitive and reliable than the use of nasopharyngeal swabs (To et al., 2017; Chan et al., 2020; Wyllie et al., 2020). Therefore, saliva has been used to screen respiratory viruses on patients without respiratory symptoms (To et al., 2019a).

Because of the ease of sample collection, self-collected saliva has been used in Hong Kong for diagnostic test, at the hospital accident and emergency department, at the airport, and in contact tracing for COVID-19 cases (Hong Kong SAR Government, 2020).

However, we notice that saliva collection had several problems that can be common when doing it daily. Also, we demonstrate the utility of the nucleic acid extraction SalivaDirect protocol

for RNA extraction of SARS-CoV-2 and the assessment of nasopharyngeal swabs and saliva clinical samples using a standard protocol and the SalivaDirect protocols.

## MATERIALS AND METHODS

### Clinical Samples and SARS-CoV-2 Nucleic Acid Extraction Protocols

Thirty nasopharyngeal swab clinical samples were examined using a standard protocol following the manufacturer's instructions (QIAamp Viral RNA Mini, Qiagen, MD, United States) at a certified laboratory. Briefly, 140  $\mu$ l of homogeneous (vortexed) nasopharyngeal swab clinical sample with 560  $\mu$ l of AVL buffer was mixed and incubated at room temperature (RT) for 10 min for lysing proteins. Ethanol (560  $\mu$ l) was added followed by nucleic acid binding to the column containing the filter and collector tube. It was centrifuged at 6000 $\times$ g, and the liquid was discarded through the filter tube. Then, 750  $\mu$ l of AW1 buffer was added and drowned by centrifugation followed by the same procedure but using AW2 buffer. A brief spin (1 min) removed the remaining buffers. The nucleic acids were eluted into a sterile 1.5-ml tube by adding 60  $\mu$ l of elution AVE buffer, incubated at RT for 1 min, centrifuged at 8,000  $\times$  g for 1 min, and stored at  $-80^{\circ}\text{C}$  for further analysis.

The same nasopharyngeal swab clinical samples of the same COVID-19 patients were also examined by using the SalivaDirect nucleic acids extraction protocol (Vogels et al., 2020). The main distinction between both protocols is that in the SalivaDirect protocol, the wash, column binding, and elution steps were skipped. Briefly, 50  $\mu$ l of the homogeneous (vortexed) nasopharyngeal swab clinical sample was added to 2.5  $\mu$ l of proteinase K (50 mg/ml) for lysing proteins. To inactivate proteinase K, the homogenate was incubated at  $95^{\circ}\text{C}$  for 5 min and stored at  $-80^{\circ}\text{C}$  for further analysis. The SalivaDirect assay was performed using saliva clinical sample from the same COVID-19 individuals.

### SARS-CoV-2 Nucleic Acid Amplification Protocol

The RNA amplification of SARS-CoV-2 was performed following the manufacturer's instructions of the SARS-CoV-2 Real-Time PCR kit (Vircell, Granada, Spain). Positive and negative controls were tested in parallel to validate the reaction.

A sample was considered positive if the cycle threshold (Ct) value obtained in E gene was less than 40 and the internal control, RdRp gene, showed amplification. A sample was considered negative if the assay did not show amplification for gene E but it did for the RdRp gene. If the assay did not show an amplification signal for the RdRp gene, the acid nucleic extraction protocol was repeated. The acid nucleic amplification assay was done all over again if the Ct value for gene E was over 40. As the gold protocols (from Qiagen and Vircell) used here have a sensitivity of 100% as reported elsewhere (World Health Organization [WHO], 2020),



it was used as reference to decide whether or not an individual was truly positive or negative to the tests.

## Statistical Analysis

The 95% exact Clopper-Pearson confidence intervals (CIs) surrounding the point estimate of the SalivaDirect protocol were calculated using the diagnostic test evaluation calculator (MedCalc software<sup>1</sup>; February 17, 2021) in relation to the gold standard protocol with nasopharyngeal swab clinical samples. Estimates for which the 95% CIs did not overlap were considered to be significantly different at the  $P < 0.05$  level.

## RESULTS

A variation ( $P > 0.05$ ) was noted when 30 saliva clinical samples were assessed by the SalivaDirect protocol (sensitivity of 88.2%; 95% CIs = 72.6%–96.7%) in relation to the gold standard protocol (95% CIs = 97.5%–100%; sensitivity of 100%) as reported elsewhere (World Health Organization [WHO], 2020; **Table 1**). This was because four out of 30 saliva clinical samples had late Ct values (ranging from 34 to 38 amplification cycles) for gene E, which are associated with low viral loads in the samples. However, the standard protocol with nasopharyngeal clinical samples was able to detect the virus in those samples with Ct values of up to 40 cycles.

The same 30 nasopharyngeal swab clinical samples from same COVID-19 individuals were assessed by the SalivaDirect protocol (**Table 1**). Only two out of 30 nasopharyngeal swab clinical samples were found to be false negatives (sensitivity of 93.7%; 95% CIs = 79.2%–99.2%), indicating that saliva clinical samples are less sensitive than nasopharyngeal swab samples. Thus, no significant difference ( $P > 0.05$ ) was seen between the two assays using nasopharyngeal swab clinical samples. In addition, eight saliva clinical samples in the standard protocol showed Ct values over 36, and these samples also showed positive results using the SalivaDirect protocol. Interestingly, there was concordance in the positive result using one nasopharyngeal swab sample with a Ct value of 40 for both assays (i.e., standard and SalivaDirect protocols).

## DISCUSSION

Saliva used as diagnostic sample provides an opportunity for simpler and more efficient tools for virus diagnosis, especially during the critical episodes of viral disease outbreaks (Khurshid et al., 2019). Furthermore, literature mentions that the screening times will be reduced by instructing patients to spit into a sterile bottle (Fakheran et al., 2020). However, in our gathering of samples with trained personnel, collection of nasopharyngeal swabs took less than 3 min, but getting saliva lengthened the process due to the wait for the patients to be able to salivate.

On several occasions, the patients produced largely sputum instead of saliva. In other studies, patients were asked to cough

out saliva and samples were mainly sputum (Cheng et al., 2020; To et al., 2020b; Zheng et al., 2020). Also, other patients cannot generate saliva.

Variation in viral load between saliva and sputum samples has not yet been reported (Chen L. et al., 2020; Zheng et al., 2020), but it is complicated to manipulate sputum in the laboratory due to its viscosity, in addition to containing higher concentrations of degrading enzymes that can interfere with detection processes.

In the clinical setting, we have observed that during the saliva collection, many patients contaminated the outside of the container with their saliva. This puts staff at risk, or it can lead to cross-sample contamination. Due to this and because saliva may allow transmission of virus (To et al., 2020b), we consider that it is necessary to use personal protection equipment and to follow all the established safety measures as with that of the nasopharyngeal swab collection. Saliva self-collection gives the possibility of collecting samples outside the hospitals, but it could damage the sample during patient handling or transportation. For these reasons, we do not consider viable the option of self-collection outside hospitals.

Here, the saliva samples were taken, stored in a cooler, and transported directly to the laboratory. Usually, the samples are collected, then sent out to the clinic, and later on the samples are sent to the laboratory (the next day if they are in another town). Thus, keeping the sample in a transportation medium should be considered. Lippi et al. (2020) suggested that sample collection errors and transportation factors also have an impact on assay detection accuracy. It has shown that liquid Amies medium, PBS, or maintenance medium can be used for homogenization of saliva samples (Williams et al., 2020; Wong et al., 2020).

To solve the logistic problems associated with sample collection, it is necessary to develop an easily and standardized method to collect the samples as well as for keeping the samples: Namely, putting the saliva sample into a sterile container and then viral transport medium (To et al., 2017), putting the saliva direct into a sterile container with viral transport medium (To et al., 2019a) or without viral transport medium (Moreno et al., 2020).

In the laboratory, the only drawback, as aforementioned, was the difficulty of working with viscous samples. It has been shown that the processing of nasopharyngeal swabs with proteinase K and without silica column washes was as effective as the standard protocol, indicating that this methodology can reduce time and costs. It was also demonstrated that nasopharyngeal swabs should be recommended as the sample to be used (Azzi et al., 2020).

Thirty patients were confirmed to harbor SARS-CoV2 nucleic acids using a standard protocol with nasopharyngeal swab clinical samples. When saliva clinical samples from the same patients were assessed with the SalivaDirect protocol (Vogels et al., 2020), four were found to be false negatives (sensitivity of 88.2%; 95% CIs = 72.6%–96.7%). A sensitivity of detection of the virus using gold standard protocols with oropharyngeal clinical samples was documented to be 100% (95% CIs = 97.5%–100%) (World Health Organization [WHO], 2020), indicating a significant variation ( $P > 0.05$ ) in the assays.

<sup>1</sup>[https://www.medcalc.org/calc/diagnostic\\_test.php](https://www.medcalc.org/calc/diagnostic_test.php)

**TABLE 1** | Comparison of three protocols for acid nucleic extraction of SARS-CoV-2 ( $n = 30$ ) individuals diagnosed with COVID-19 from nasopharyngeal swab and saliva clinical samples.

Protocol	Gene E	Gene Rp	No. of positive samples/ $n$	Sensitivity <sup>§</sup> %	95% Confidence intervals <sup>§</sup> %
	Ct-values <sup>§</sup> cycles	Ct-values <sup>§</sup> cycles			
Nucleic acid extraction standard protocol with nasopharyngeal exudate <sup>§</sup> (QIAamp Viral RNA Mini, Qiagen, MD, United States)	16–40	23–34	30/30	100	97.5–100 (World Health Organization [WHO], 2020)
Nucleic acid extraction SalivaDirect protocol with saliva <sup>§</sup> (Vogels et al., 2020)	9–39	12–40	26/30	88.2	72.6–96.7
Nucleic acid extraction SalivaDirect protocol with nasopharyngeal exudate <sup>§</sup> (Vogels et al., 2020)	17–38	18–39	28/30	93.7	79.2–99.2

<sup>§</sup>Proteinase K of unknown concentration.

<sup>§</sup>2.5  $\mu$ l (50 mg/ml) Proteinase K.

<sup>§</sup>Range.

<sup>§</sup>Calculated using MedCalc Software Ltd (2021).

The consequence for the decrease of the sensitivity was noted in samples with late Ct values (Ct values = 34–38 cycles) for gene E. In qRT-PCR, Ct scan is suggested as an auxiliary diagnostic method to avoid reporting false results and to increase sensitivity (Li et al., 2020). Chen J.H. et al. (2020) reported significant differences in the median Ct values for nasopharyngeal swabs in comparison to that on saliva samples (26.8 vs 29.7,  $p = 0.0002$ ), indicating that COVID-19 detection assay is less sensitive with saliva samples than nasopharyngeal swabs, which is in concordance with our findings.

Regarding the concordance between detection results of SARS-CoV-2 using nasopharyngeal swabs and saliva clinical samples, different sensitivity rates have been reported (Table 2). Here, the 30 nasopharyngeal swab clinical samples from same COVID-19 patients using the SalivaDirect protocol had a sensitivity of 93.7% (95% CIs = 79.2%–99.2%) which was not different ( $P > 0.05$ ) of that when saliva clinical samples were used (sensitivity of 80.2%; 95% CIs = 72.6%–96.7%). This is consistent as reported elsewhere (Azzi et al., 2020). Also, concordance ( $P > 0.05$ ) in nasopharyngeal swab samples using the SalivaDirect protocol (95% CIs = 79.2%–99.2%) and the gold standard protocol (95% CIs = 97.5%–100%) as reported by World Health Organization [WHO] (2020) was noted (Supplementary Table 1).

Infections by SARS-CoV-2 can be detected at high titers with tests based on saliva samples. It has been reported to be  $3.3 \times 10^6$  and  $10^{11}$  copies per  $\text{cm}^3$  (Cheng et al., 2020; Pan et al., 2020). In sputum, it has been reported to be  $10^9$  and  $1.34 \times 10^{11}$  copies per  $\text{cm}^3$  (Pan et al., 2020; To et al., 2020a).

However, an observational cohort showed that viral load in saliva was highest following symptom onset in the first week and then subsequently declined with time (To et al., 2020a). However, in one of these studies, viral RNA could still be detected from a third of patients for 20 days or longer, and in one patient, it was detected 25 days after symptom onset (To et al., 2020a). Wang et al. (2020) reported that the median duration of viral shedding in sputum was 34 days (24–40) and 19 days

(14–25) in nasopharyngeal swabs. Similarly, Park et al. (2020) reported that the median duration of SARS-CoV-2 viral detection after hospitalization was 34 days (22–67). After resolution of symptoms, SARS-CoV-2 was detected for a median of 26 days (9–48). For this, unlike nasopharyngeal swabs, saliva only can be used for early detection and subsequent viral load monitoring (To et al., 2020a,b; Wyllie et al., 2020).

Also, consideration should be the detection of SARS-CoV-2 in saliva by rapid antigen-based tests. In Mexico, the Institute for Epidemiological Diagnosis and Reference has approved rapid antigen-based kits from swab samples. The Panbio™ COVID-19 Ag rapid test device and Sofia 2 SARS antigen FIA kit can give results in 15 min; however, they showed a sensitivity of 85 and 80%, respectively, in patients who were in the first week of onset of symptoms. Probably, as the disease stage progresses, those rapid testing protocols will present less sensitivity by the decrease in viral load (Zhao et al., 2020), as well as a higher rate of

**TABLE 2** | Number of positive/individuals examined (percentage) when using either nasopharyngeal swabs or saliva clinical samples assessed by qRT-PCR for SARS-CoV-2.

Nasopharyngeal swab samples	Saliva samples	References
Positive/Individuals examined (%)	Positive/Individuals examined (%)	
12/12 (100)	11/12 (91.7)	To et al., 2020b*
23/23 (100)	20/23 (87.0)	To et al., 2020a
13/13 (100)	4/13 (30.76)	Chen J.H. et al., 2020
39/39 (100)	33/39 (84.0)	Williams et al., 2020
25/25 (100)	25/25 (100)	Azzi et al., 2020
47/65 (72.3)	37/42 (88.0)	Zheng et al., 2020*
55/58 (94.8)	52/58 (89.7)	Chen L. et al., 2020
47/53 (89)	41/53 (77)	Jamal et al., 2020

\*Saliva samples including saliva and sputum samples.

false negatives due to the low viral load in saliva (Chen J.H. et al., 2020).

For increasing the sensitivity of saliva tests to detect SARS-CoV-2, the instructions should clearly explain the saliva spitting procedure into a container to the individuals, in a “how-to” pamphlet, for example.

## Limitation of the Study

We are aware that our study has limitations as we only have tested a small sample size of individuals, but this is a common problem in studies on emerging infections, making most studies not conclusive. Furthermore, false negatives may occur due to the uncertainty of the first appearance of the symptoms or by technical deficiencies in sampling methodology (Sethuraman et al., 2020).

## DATA AVAILABILITY STATEMENT

The original contributions presented in the study are included in the article/**Supplementary Material**, further inquiries can be directed to the corresponding author.

## ETHICS STATEMENT

The studies involving human participants were reviewed and approved by The Ethical Committee of the Health Secretariat of México, given that the studies were conducted as part of the national COVID-19 surveillance program and were, therefore, part of a routine public health monitoring program conducted by the Mexican government. Written informed consent was not obtained from the individual(s) for the publication of any potentially identifiable images or data included in this article. However, it was explained the right to each individual to decide to participate or not voluntarily. Likewise, before each examination, the present research procedures were explained to the individuals, and a capsule summary of the project and its

process were provided. They were informed that the results of the tests would be available if requested.

## AUTHOR CONTRIBUTIONS

MR-P: conceptualization. MR-P and SRF: methodology, formal analysis, investigation, and writing–review, and editing. LR-M: writing–conceptualization, methodology. MR-P, SRF, LR-M, and ES-M: writing–original draft preparation. BR-B, NF-S, and ES-M: supervision. BR-B: funding acquisition. NF-S: project administration. All authors contributed to the article and approved the submitted version.

## FUNDING

The present work was performed under the auspices of the Laboratorio Estatal de Salud Pública de Tamaulipas (Secretaría de Salud-México) in collaboration with the Consejo Nacional de Ciencia y Tecnología (CONACYT), México (Grant No. 314311) where Dr. Lihua Wei was PI. SRF holds a M.Sc. scholarship from CONACYT, México (1004818). The funder had no role in study design, data collection and analysis, decision to publish, or preparation of the manuscript.

## ACKNOWLEDGMENTS

We are grateful to the individuals of the municipalities of Ciudad Victoria, Tamaulipas who granted us permission to obtain their clinical samples for COVID-19 testing.

## SUPPLEMENTARY MATERIAL

The Supplementary Material for this article can be found online at: <https://www.frontiersin.org/articles/10.3389/fbioe.2021.638902/full#supplementary-material>

## REFERENCES

- Azzi, L., Carcano, G., Gianfagna, F., Grossi, P., Gasperina, D. D., Genoni, A., et al. (2020). Saliva is a reliable tool to detect SARS-CoV-2. *J. Infect.* 81, e45–e50. doi: 10.1016/j.jinf.2020.04.005
- Chan, J. F., Yuan, S., Kok, K. H., To, K. K., Chu, H., Yang, J., et al. (2020). A familial cluster of pneumonia associated with the 2019 novel coronavirus indicating person-to-person transmission: a study of a family cluster. *Lancet* 395:10223. doi: 10.1016/S0140-6736(20)30154-9
- Chen, L., Zhao, J., Peng, J., Li, X., Deng, X., Zhi, J., et al. (2020). Detection of 2019-nCoV in saliva and characterization of oral symptoms in COVID-19 patients. *SSRN J.* 53:e12923. doi: 10.2139/ssrn.3556665
- Chen, J. H., Yip, C. C., Poon, R. W., Chan, K. H., Cheng, V. C., Hung, V. C. G., et al. (2020). Evaluating the use of posterior oropharyngeal saliva in a point-of-care assay for the detection of SARS-CoV-2. *Emerg. Microb. Infect.* 9, 1356–1359. doi: 10.1080/22221751.2020.1775133
- Cheng, V., Wong, S. C., Chen, J., Yip, C., Chuang, V., Ho, P. L., et al. (2020). Escalating infection control response to the rapidly evolving epidemiology of the coronavirus disease 2019 (COVID-19) due to SARS-CoV-2 in Hong Kong. *Infect. Control. Hosp. Epidemiol.* 4, 493–498. doi: 10.1017/ice.2020.58
- Fakheran, O., Dehghannejad, M., and Khademi, A. (2020). Saliva as a diagnostic specimen for detection of SARS-CoV-2 in suspected patients: a scoping review. *Infect. Dis. Pover.* 9:100. doi: 10.1186/s40249-020-00728-w
- Food and Drug Administration [FDA] (2020a). Accelerated Emergency Use Authorization (EUA) Summary SARS-CoV-2 Assay (Rutgers Clinical Genomics Laboratory). Available online at: <https://www.fda.gov/media/136875/download> (accessed September 28, 2020).
- Food and Drug Administration [FDA] (2020b). *Coronavirus (COVID-19) Update: FDA Issues Emergency use Authorization to Yale School of Public Health for SalivaDirect, which uses a New Method of Saliva Sample Processing*. Available online at: <https://www.fda.gov/news-events/press-announcements/coronavirus-covid-19-update-fda-issues-emergency-use-authorization-yale-school-public-health> (accessed November 7, 2020).
- Hong Kong SAR Government (2020). *COVID-19 Testing Extended*. Available online at: [https://www.news.gov.hk/eng/2020/03/20200319/20200319\\_174452\\_136.html](https://www.news.gov.hk/eng/2020/03/20200319/20200319_174452_136.html) (accessed November 19, 2020).
- Jamal, A. J., Mohammad, M., Coomes, E., Powis, J., Li, A., Paterson, A., et al. (2020). Sensitivity of nasopharyngeal swabs and saliva for the detection of severe acute respiratory syndrome coronavirus 2 (SARS-CoV-2). *MedRxiv* 72, 1064–1066. doi: 10.1101/2020.05.01.20081026

- Khurshid, Z., Zafar, M., Khan, E., Mali, M., and Latif, M. (2019). Human saliva can be a diagnostic tool for Zika virus detection. *J. Infect. Public Health* 12, 601–604. doi: 10.1016/j.jiph.2019.05.004
- Li, X., Geng, M., Peng, Y., Meng, L., and Lu, S. (2020). Molecular immune pathogenesis and diagnosis of COVID-19. *J. Pharm. Anal.* 10, 102–108. doi: 10.1016/j.jpha.2020.03.001
- Lippi, G., Simundic, A. M., and Plebani, M. (2020). Potential preanalytical and analytical vulnerabilities in the laboratory diagnosis of coronavirus disease 2019 (COVID-19). *Clin. Chem. Lab. Med.* 58, 1070–1076. doi: 10.1515/cclm-2020-0285
- MedCalc Software Ltd (2021). Available online at: [https://www.medcalc.org/calc/diagnostic\\_test.php](https://www.medcalc.org/calc/diagnostic_test.php) (accessed February 16, 2021).
- Moreno, C. J., Espinoza, M. A., Sandoval, J. C., Cantú, C. M., Barón, O. H., Ho, L., et al. (2020). Saliva sampling and its direct lysis, an excellent option to increase the number of SARS-CoV-2 diagnostic tests in settings with supply shortages. *J. Clin. Microbiol.* 58:e01659-20. doi: 10.1128/JCM.01659-20
- Nicosia, A., Tagliavia, M., and Costa, S. (2010). Regeneration of total RNA purification silica-based columns. *Biomed. Chromatogr.* 24, 1418–1422. doi: 10.1002/bmc.1418
- Pan, Y., Zhang, D., Yang, P., Poon, L., and Wang, Q. (2020). Viral load of SARS-CoV-2 in clinical samples. *Lancet Infect. Dis.* 20, 411–412. doi: 10.1016/S1473-3099(20)30113-4
- Park, S. Y., Yun, S. G., Shin, J. W., Lee, B. Y., Son, H., Lee, S., et al. (2020). Persistent severe acute respiratory syndrome coronavirus 2 detection after resolution of coronavirus disease 2019-associated symptoms/signs. *Korean J. Intern. Med.* 35:203. doi: 10.3904/kjim.2020.203
- Rutgers (2020). *New Rutgers Saliva Test for Coronavirus Gets FDA Approval*. Available online at: <https://www.rutgers.edu/news/new-rutgers-saliva-test-coronavirus-gets-fda-approval>
- Sethuraman, N., Jeremiah, S. S., and Ryo, A. (2020). Interpreting diagnostic tests for SARS-CoV-2. *JAMA* 323, 2249–2251. doi: 10.1001/jama.2020.8259
- To, K. K., Lu, L., Yip, C. C., Poon, R. W., Fung, A. M., Cheng, A., et al. (2017). Additional molecular testing of saliva specimens improves the detection of respiratory viruses. *Emerg. Microb. Infect.* 6:e49. doi: 10.1038/emi.2017.35
- To, K. K., Tsang, O. T., Leung, W. S., Tam, A. R., Wu, T. C., Lung, D. C., et al. (2020a). Temporal profiles of viral load in posterior oropharyngeal saliva samples and serum antibody responses during infection by SARS-CoV-2: an observational cohort study. *Lancet Infect. Dis.* 20, 565–574. doi: 10.1016/S1473-3099(20)30196-1
- To, K. K., Tsang, O. T., Yip, C. C., Chan, K. H., Wu, T. C., Chan, J. M.-C., et al. (2020b). Consistent detection of 2019 novel Coronavirus in Saliva. *Clin. Infect. Dis.* 71, 841–843. doi: 10.1093/cid/ciaa149
- To, K. K., Chan, K. H., Ho, J., Pang, P., Ho, D., Chang, A. C. H., et al. (2019a). Respiratory virus infection among hospitalized adult patients with or without clinically apparent respiratory infection: a prospective cohort study. *Clin. Microbiol. Infect.* 25, 1539–1545. doi: 10.1016/j.cmi.2019.04.012
- To, K. K., Yip, C. C., Lai, C. Y., Wong, C. K., Ho, D. T., Pang, P. K. P., et al. (2019b). Saliva as a diagnostic specimen for testing respiratory virus by a point-of-care molecular assay: a diagnostic validity study. *Clin. Microbiol. Infect.* 25, 372–378. doi: 10.1016/j.cmi.2018.06.009
- Vogels, C., Brackney, D., Kalinich, C. C., Ott, I. M., Grubaugh, N., and Wyllie, A. (2020). SalivaDirect<sup>TM</sup>: RNA extraction-free SARS-CoV-2 diagnostics. *Protocols* 5 doi: 10.17504/protocols.io.bkjgkujw
- Wang, K., Zhang, X., Sun, J., Ye, J., Wang, F., Hua, J., et al. (2020). Differences of Severe Acute respiratory syndrome Coronavirus 2 shedding duration in sputum and nasopharyngeal swab specimens among adult inpatients with Coronavirus disease 2019. *Chest* 158, 1876–1884. doi: 10.1016/j.chest.2020.06.015
- Williams, E., Bond, K., Zhang, B., Putland, M., and Williamson, D. A. (2020). Saliva as a noninvasive specimen for detection of SARS-CoV-2. *J. Clin. Microbiol.* 58:e0776-20. doi: 10.1128/JCM.00776-20
- Wong, R. C., Wong, A. H., Ho, Y. I., Leung, E. C., and Lai, R. W. (2020). Evaluation on testing of deep throat saliva and lower respiratory tract specimens with Xpert Xpress SARS-CoV-2 assay. *J. Clin. Virol.* 131:104593. doi: 10.1016/j.jcv.2020.104593
- World Health Organization [WHO] (2020). *Multiple Real-Time PCR Kit for Detection of 2019-CoV User Manual*. Available online at: [https://www.who.int/diagnostics\\_laboratory/eual/eul\\_0491\\_187\\_00\\_multiple\\_real\\_time\\_pcr\\_kit\\_for\\_detection\\_of\\_2019\\_ncov\\_ifu.pdf](https://www.who.int/diagnostics_laboratory/eual/eul_0491_187_00_multiple_real_time_pcr_kit_for_detection_of_2019_ncov_ifu.pdf) (accessed February 16, 2021).
- Wyllie, A. L., Fournier, J., Casanovas, A., Campbell, M., Tokuyama, M., Vijayakumar, P., et al. (2020). Saliva is more sensitive for SARS-CoV-2 detection in COVID-19 patients than nasopharyngeal swabs. *medRxiv* [Preprint], doi: 10.1101/2020.04.16.20067835
- Yam, W. C., Chan, K. H., Poon, L. L., Guan, Y., Yuen, K. Y., Seto, W. H., et al. (2003). Evaluation of reverse transcription-PCR assays for rapid diagnosis of severe acute respiratory syndrome associated with a novel coronavirus. *J. Clin. Microbiol.* 41, 4521–4524. doi: 10.1128/jcm.41.10.4521-4524.2003
- Yang, H., Zhai, C., Yu, X., Li, Z., Tang, W., Liu, Y., et al. (2016). High-level expression of Proteinase K from *Tritirachium album* Limber in *Pichia pastoris* using multi-copy expression strains. *Protein Expr. Purif.* 122, 38–44. doi: 10.1016/j.pep.2016.02.006
- Zhao, J., Yuan, Q., Wang, H., Liu, W., Liao, X., Su, Y., et al. (2020). Antibody responses to SARS-CoV-2 in patients of novel coronavirus disease 2019. *Clin. Infect. Dis.* 71, 2027–2034. doi: 10.1093/cid/ciaa344
- Zheng, S., Yu, F., Fan, J., Zou, Q., Xie, G., Yang, X., et al. (2020). Saliva as a diagnostic specimen for SARS-CoV-2 by a PCR-based assay: a diagnostic validity study. *SSRN J.* doi: 10.2139/ssrn.3543605

**Conflict of Interest:** The authors declare that the research was conducted in the absence of any commercial or financial relationships that could be construed as a potential conflict of interest.

Copyright © 2021 Rodríguez Flores, Rodríguez-Martínez, Reyes-Berrones, Fernández-Santos, Sierra-Moncada and Rodríguez-Pérez. This is an open-access article distributed under the terms of the Creative Commons Attribution License (CC BY). The use, distribution or reproduction in other forums is permitted, provided the original author(s) and the copyright owner(s) are credited and that the original publication in this journal is cited, in accordance with accepted academic practice. No use, distribution or reproduction is permitted which does not comply with these terms.





# Management of SARS-CoV-2 Infection: Key Focus in Macrolides Efficacy for COVID-19

Gaber El-Saber Batiha<sup>1\*</sup>, Marwa A. Zayed<sup>1</sup>, Aya A. Awad<sup>1</sup>, Hazem M. Shaheen<sup>1</sup>, Suleiman Mustapha<sup>2</sup>, Oscar Herrera-Calderon<sup>3</sup>, Jorge Pamplona Pagnossa<sup>4</sup>, Abdelazeem M. Algammal<sup>5</sup>, Muhammad Zahoor<sup>6</sup>, Achyut Adhikari<sup>7</sup>, Ishan Pandey<sup>8</sup>, Sara T. Elazab<sup>9</sup>, Kannan R. R. Rengasamy<sup>10</sup>, Natália Cruz-Martins<sup>11,12,13\*</sup> and Helal F. Hetta<sup>14</sup>

## OPEN ACCESS

### Edited by:

Segaran P. Pillai,  
United States Department of  
Homeland Security, United States

### Reviewed by:

Armelia Sari Widyarman,  
Trisakti University, Indonesia  
Imad Omar Al Kassaa,  
Lebanese University, Lebanon

### \*Correspondence:

Gaber El-Saber Batiha  
gaberbatiha@gmail.com  
Natália Cruz-Martins  
ncmartins@med.up.pt

### Specialty section:

This article was submitted to  
Infectious Diseases - Surveillance,  
Prevention and Treatment,  
a section of the journal  
Frontiers in Medicine

**Received:** 15 December 2020

**Accepted:** 23 February 2021

**Published:** 14 April 2021

### Citation:

Batiha G-S, Zayed MA, Awad AA,  
Shaheen HM, Mustapha S,  
Herrera-Calderon O, Pagnossa JP,  
Algammal AM, Zahoor M, Adhikari A,  
Pandey I, Elazab ST, Rengasamy KRR,  
Cruz-Martins N and Hetta HF (2021)  
Management of SARS-CoV-2  
Infection: Key Focus in Macrolides  
Efficacy for COVID-19.  
Front. Med. 8:642313.  
doi: 10.3389/fmed.2021.642313

<sup>1</sup> Department of Pharmacology and Therapeutics, Faculty of Veterinary Medicine, Damanhour University, Damanhour, Egypt, <sup>2</sup> Department of Crop Protection, University of Ilorin, Ilorin, Nigeria, <sup>3</sup> Department of Pharmacology, Bromatology and Toxicology, Faculty of Pharmacy and Biochemistry, Universidad Nacional Mayor de San Marcos, Lima, Peru, <sup>4</sup> Biological Sciences Department, Federal University of Lavras (UFLA), Lavras, Brazil, <sup>5</sup> Department of Bacteriology, Immunology, and Mycology, Faculty of Veterinary Medicine, Suez Canal University, Ismailia, Egypt, <sup>6</sup> Department of Biochemistry, University of Malakand, Chakdara, Pakistan, <sup>7</sup> Central Department of Chemistry, Tribhuvan University, Kirtipur, Nepal, <sup>8</sup> Department of Pathology, Motilal Nehru Medical College, Prayagraj, India, <sup>9</sup> Department of Pharmacology, Faculty of Veterinary Medicine, Mansoura University, Mansoura, Egypt, <sup>10</sup> Green Biotechnologies Research Centre of Excellence, University of Limpopo, Polokwane, South Africa, <sup>11</sup> Faculty of Medicine, University of Porto, Porto, Portugal, <sup>12</sup> Institute for Research and Innovation in Health (i3S), University of Porto, Porto, Portugal, <sup>13</sup> Laboratory of Neuropsychophysiology, Faculty of Psychology and Education Sciences, University of Porto, Porto, Portugal, <sup>14</sup> Department of Medical Microbiology and Immunology, Faculty of Medicine, Assiut University, Assiut, Egypt

Macrolides (e.g., erythromycin, fidaxomicin, clarithromycin, and azithromycin) are a class of bacteriostatic antibiotics commonly employed in medicine against various gram-positive and atypical bacterial species mostly related to respiratory tract infections, besides they possess anti-inflammatory and immunomodulatory effects. Coronavirus Disease 2019 (COVID-19) is an infectious disease caused by the severe acute respiratory syndrome of coronavirus 2 (SARS-CoV-2). It was first detected in Wuhan, Hubei, China, in December 2019 and resulted in a continuing pandemic. Macrolides have been extensively researched as broad adjunctive therapy for COVID-19 due to its immunostimulant abilities. Among such class of drugs, azithromycin is described as azalide and is well-known for its ability to decrease the production of pro-inflammatory cytokines, including matrix metalloproteinases, tumor necrosis factor- $\alpha$ , interleukin (IL)-6, and IL-8. In fact, a report recently published highlighted the effectiveness of combining azithromycin and hydroxychloroquine for COVID-19 treatment. Indeed, it has been underlined that azithromycin quickly prevents SARS-CoV-2 infection by raising the levels of both interferons and interferon-stimulated proteins at the same time which reduces the virus replication and release. In this sense, the current review aims to evaluate the applications of macrolides for the treatment of COVID-19.

**Keywords:** COVID-19, SARS-CoV-2 infection, macrolides, azithromycin, efficacy

## INTRODUCTION

Humanity is currently facing a deadly threat, a severe acute respiratory syndrome coronavirus 2 (SARS-CoV-2) pandemic, which is due to the novel 2019 coronavirus outbreak, also known as Coronavirus Disease (COVID-19) (1). As of November 22, 2020, COVID-19 was confirmed in 57,882,183 people worldwide, resulting in the premature deaths of more than 1,377,395 individuals. According to the World Health Organization (WHO), more than 220 countries have reported cases of the deadly virus (2). The continually increasing figures of diagnosed cases and the rise in mortality rate call for immediate, accessible treatment that is effective against the deadly virus (1). As a consequence, the use of macrolides for therapeutic applications is gaining much attention.

Macrolides (for example, erythromycin, fidaxomicin, clarithromycin, and azithromycin) are a class of bacteriostatic antibiotics commonly employed in medical practice against various gram-positive and atypical bacterial species mostly related to respiratory tract infections. Besides their antibacterial properties, macrolides are reported to also have anti-inflammatory and immunomodulatory effects (3–5). The infected host typically links viral respiratory infections, such as COVID-19, to an intense inflammatory response, characterized by hyperproduction of cytokine. Past preclinical and clinical studies have shown that macrolides control the susceptibility to inflammation, increase the buildup of anti-inflammatory cytokines, and also promote the antibody-building cycle. Due to its immunomodulating activities, macrolides have been researched to a great extent as a broad adjunctive therapy against viral respiratory infections, influenza inclusive (6). In this sense, this review seeks to evaluate the applications of macrolides in the possible treatment of COVID-19, with primary considerations on the most relevant macrolide, i.e., azithromycin, in a plausible curative mixture.

## RESEARCH METHODOLOGY

A MEDLINE literature search was performed using the following keywords: azithromycin and severe acute respiratory syndrome-coronavirus 2 (SARS-CoV2); COVID-19 and azithromycin; viral infections and azithromycin; azithromycin and chloroquine; Qt prolongation; and Qt prolongation and azithromycin. Here, we provided information on the most recent shreds of evidence investigated and on those essential in the synthesis and usage of macrolides as a possible effective treatment of COVID-19.

## AZITHROMYCIN: AN OVERVIEW

### Description

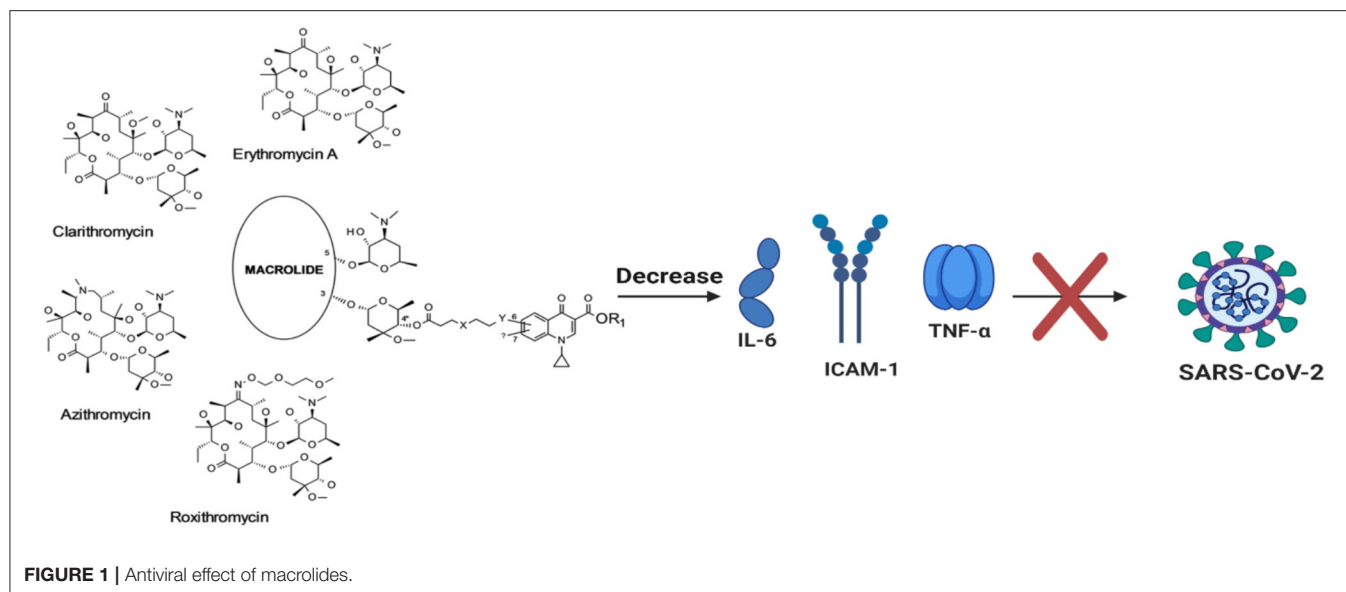
Azithromycin is described as an azalide that is structurally associated with the macrolide family of antibiotics. Macrolides are known to possess immunomodulating and anti-inflammatory activities apart from its antibiotic properties, with such components being able to proffer some effectiveness in a broad range of viral infections respiratory in nature (7).

## Pharmacokinetics

Azithromycin has a bioavailability of ~37%. However, it has been observed that the concomitant oral introduction of azithromycin in combination with food could significantly reduce the drug bioavailability by 50%. Subsequently, a one-time dosage (oral) of 500 mg with a plasma peak concentration within the range of 0.35 to 0.45 mg/L could be reached nearly within 2 h (8). Considering the concentration of 500 mg administered orally on a day followed by 250 mg on days 2 to 5, the mean and peak plasma concentrations would be, respectively, close to 0.25 and 0.05 mg/L. Such low concentrations are due to the effect of substantial and fast spread from plasma to tissues. The binding protein of the associated plasma is considered to be in a small amount of about 50% less at a plasma concentration with the normal treatment dose. The noticeable circulation volume is substantially high at a volume of 25–35 mg/kg (9).

Azithromycin, naturally eradicated by biliary and trans-intestinal excretion discharges, is not involved in stools, with urine excretion being considered a limited route for its removal. Approximately 6% of the oral and 12% of the intravenous doses are recovered without urinary changes. It takes the mean period of about 2–4 days for azithromycin to reach terminal elimination half-life (8). For aged patients, and even in cases of mild-to-moderate kidney or hepatic inadequacy, azithromycin pharmacokinetics is not substantially altered. The azithromycin dose and its dosage regimen agree with marketing authorization for superinfections of acute bronchitis. Indeed, the pharmacology of azithromycin was previously addressed in humans (10), finding that 37% of an individual oral dosage of 500 mg was bio-accessible and able to produce a serum concentration peak of 4 mg/L. Several concentration treatments (i.e., 500 mg in 2 doses with a 12 h separation followed by 500 mg for 5 days, or double doses of 250 mg with a 12 h separation, followed up by a quantity of 250 mg for 9 days) led to a minor serum concentration peak increase. Moreover, the protein serum binding of azithromycin decreased from 0.02 mg/L, which is at 50% to 0.5 mg/L at 12%. The tissue concentrations of this macrolide-type antibiotic were indicated to be amply increased than what is attainable in serum. For example, after administering dual concentrations of 250 mg each, 12 h apart, peak concentrations of azithromycin were stated in tonsil, prostate, and various other tissues (exceeding 3 mg/kg). However, the amount present in tissues weakened, with noticeable half-lives of ~55.2 h in prostate and 76.8 h in tonsil. In fact, the increased concentrations in such associated tissues indicate that the proposed standard treatment doses of 500 mg in a day followed consecutively by 250 mg for 4 days, or 500 mg for 3 days, would result in tissue concentrations above 3 mg/kg. This evidenced as the concentrations in tissues surpassed that of the associated pathogens' minimum inhibitory concentrations (MICs), with treatment doses proving to be effective in antagonizing soft-tissue and/or respiratory tract infections. Also, a one-time 1 g dose was suggested to be effectual in treating various sexually transmitted infections (11).

Antibacterial agents, such as azalide, particularly, azithromycin, were initially shown to possess several pharmacological effects from other antibacterials that are presently being used. As above mentioned, the drug has an



approximate bioavailability of 37%, where a quick dispensation accompanies the fast and substantial spread from serum to the intracellular fluid compartments to tissues. Tissue concentrations surpass the concentrations of serum by 100-fold in line with a 1-time dosage of azithromycin (500 mg), with drug concentrations in macrophage assisting in its ability to fight diseases. As referred, high azithromycin amounts are usually observed in prostate, tonsil, lymph nodes, lungs, and liver, with only minor concentrations being noticed in muscles and fat. For example, a 500 mg dose given on the 1st day, followed by 250 mg daily for 2–5 days, has previously been shown to maintain the azithromycin amount at sites where infections could be indicated and continues to be effective for many days even after cessation of administration. At the pharmacokinetic level, data have indicated that azithromycin has various therapeutic applications and effects (12).

## Toxicity

In a study conducted in rats, it was observed that the use of azithromycin leads to its hepatic accumulation and elevated azithromycin demethylase activity (13), due to interactivity with the cytochrome P450 system of liver cells' smooth endoplasmic reticulum. However, any significant clinical connections of the drug with theophylline or warfarin are yet to be detected, so that these agents should be clinically monitored. Furthermore, some macrolides have been observed to weaken digoxin metabolism, and such a relationship might occur with azalides (13).

The administration of cimetidine, along with azithromycin, has not been properly investigated, so that their significant effect on drugs pharmacokinetics needs to be addressed (13). Nevertheless, administering the drugs with some antacids (for example, Maalox) has shown to decrease the plasma concentrations of azithromycin down to 25%, even though there has been no observation in the reduction of absorption level (13).

## MACROLIDES' EFFECT AGAINST VIRAL INFECTION

In critical cases, the capability of the antibiotic (azithromycin) to decrease the production of matrix metalloproteinases (MMPs), tumor necrosis factor- $\alpha$  (TNF- $\alpha$ ), interleukin (IL)-6, and IL-8 has been addressed (14). Previously, such macrolide has shown the rise of neutrophil apoptosis and also the oxidative stress linked to inflammation in the resolution phase. Likewise, bafilomycin A<sub>1</sub>, erythromycin, and clarithromycin were studied to impede the making of IL-1 $\beta$ , IL-6, IL-8, TNF- $\alpha$ , and intercellular adhesion molecule (ICAM)-1 in influenza and rhinovirus-modeled infections (**Figure 1**) (15–18). To study the potency of bafilomycin A<sub>1</sub>, an inhibitor of vacuolar H<sup>+</sup>-ATPase, on rhinovirus (RV) airway epithelial tissue infections, primary tracheal epithelial cell cultures from human subjects were exposed to type 14 RV infection (RV14). The investigators involved confirmed RV infections by demonstrating that the viral titers in the supernatants of diseased cells and viral ribonucleic acid (RNA) in cells increased over time. The RV14 infection stimulated the cytokine production and also of messenger RNA (mRNA) of ICAM-1 in epithelial cells. Interestingly, bafilomycin A<sub>1</sub> repressed the ICAM-1 production and decreased the viral titers of RV14 before and after its confirmed infection. Furthermore, the susceptibility of the epithelial cells to RV14 was decreased by the macrolide antibiotic-bafilomycin A<sub>1</sub>.

Observations also revealed that RV14 enhanced the activation of nuclear factor- $\kappa$ B (NF- $\kappa$ B) in cells whereby bafilomycin A<sub>1</sub> lowered it. Also, the number of acidic endosomes present in the epithelial cells was observed to be reduced by bafilomycin A<sub>1</sub>. Such reactions were indicative of the bafilomycin A<sub>1</sub> potential to hinder RV14 infection by obstructing the RV RNA entrance into endosomes and also by decreasing the ICAM-1 expression in the associated epithelial cells. Thus, the use of bafilomycin A<sub>1</sub> could regulate respiratory tract inflammation after RV infection (15).

Influenza viruses that affect humans are also linked to the sialic acid  $\alpha$ -2,6-galactose sialyloligosaccharides (SA $\alpha$ 2,6Gal) present in the respiratory epithelial cells, the uncoating of this virus, and also their passages into the epithelial cells need a low endosome pH level to complete.

In addition, bafilomycin A<sub>1</sub> is able to restrain the growth of both type A and B influenza viruses in humans as indicated in Madin–Darby canine kidney cells (MDCK). Nevertheless, the repressive potential of this macrolide, clinically used to treat human influenza virus infections in respiratory tract, is yet to be thoroughly investigated. On the other hand, to evaluate the potency of clarithromycin in human influenza virus infection, epithelial cell samples from human windpipes (tracheal) were cultured and then subjected to infection by Influenza A virus subtype H<sub>3</sub>N<sub>2</sub>. The observed infection augmented the cytokine level and also the viral load, as well as IL-1 $\beta$  and IL-6 in supernatant liquids and also in viral RNA within cells. In addition, the cytokine contents in the supernatant liquid, the viral loads, the viral RNA within cells, and the infection vulnerability were generally decreased following clarithromycin use. Also, the expression of sialic acid  $\alpha$ -2,6-galactose sialyloligosaccharides (SA $\alpha$ 2,6Gal), a receptor for influenza virus in man, was reduced by clarithromycin on the mucous membrane surface of the tracheae. Clarithromycin was also observed to reduce the amount and intensity of acidic endosome fluorescence in cells where viral ribonucleoproteins (RNP) pass into the cytoplasm. Clarithromycin was stated to have, in nuclear extracts, decreased the NF- $\kappa$ B proteins, as also p50 and p65. These outcomes indicate that seasonal human influenza virus could be successfully constrained after clarithromycin use, reducing the sialic acid  $\alpha$ 2,6-galactose sialyloligosaccharides (SA $\alpha$ 2,6Gal), partially inhibiting NF- $\kappa$ B and raising the endosome pH level in respiratory epithelial cells. Thus, viral respiratory tract inflammatory infections could positively be controlled by clarithromycin (18). In addition, some data have also indicated that clarithromycin is able to inhibit IL-6, IL-8, and ICAM-1 and might thus be beneficial on the pathophysiological variations associated with RV infections. For example, the effects of clarithromycin on RV infections in adenocarcinomic human alveolar basal epithelial cells (A549) were thus examined. The procedure used was to treat cells with respect for 1, 10, and 100  $\mu$ m of clarithromycin, beginning at 3 days before laboratory infections or using clarithromycin at the time of infection. RV titers, according to the measurement by culture on Medical Research Council cell strain 5 (MRC-5), were decreased by clarithromycin, with this decrease being higher when treatment was applied 3 days before infection compared to when it was performed at the time of infection. Besides RV-induced development of IL-1 $\beta$ , IL-6, and IL-8, clarithromycin therapy was found to inhibit RV, with elicited increment in ICAM-1 mRNA and protein. The maximal treatment effect was detected at the post-infection period (after 3 days). Conversely, the IL-8 production is not significantly repressed following clarithromycin administration at the time of infection. Associated findings further suggest that treatment with clarithromycin may hinder the raise in cytokines, the induction of ICAM-1 expression, and viral

infection in adenocarcinomic human alveolar basal epithelial cells (A549) (17).

On the other side, Murphy et al. (19) found that azithromycin connected to T-helper (T<sub>H</sub>) phenotype led to a shift in both types one and two, also supporting the repairs of damaged tissues due to inflammation. Furthermore, azithromycin has been reported to attenuate the reactions of endotoxin-lipopolysaccharide on lung allogeneic graft bronchial epithelium cells (20–24). In another study, the use of azithromycin and midecamycin in respiratory epithelial cells of many human patients suppressed the raise in mucin and TNF- $\alpha$  levels (24). Indeed, it was stated that midecamycin and azithromycin lessened the phorbol myristate acetate (PMA)-induced MUC2 and MUC5AC mucin gene and protein expression in NCI-H292 cells while repressing the phorbol myristate acetate-mediated TNF- $\alpha$ . Also, azithromycin was revealed to be effective in reducing biofilm formation and in restraining the quorum sensing and bacterial protein synthesis. Effective azithromycin aggregation in cells, mostly phagocytes, is usually carried over places with infections, as expressed in the extensive distribution of tissue and plasma clearance. Additionally, azithromycin has been recommended for the treatment of bacterial infections, including dermal, genitourinary, and respiratory infections. It has also shown immunoregulatory efficacy in persistent and inflammatory diseases, including rosacea, diffuse panbronchiolitis (DPB), and transplant-related complications, including post-transplant bronchiolitis. Host-response modulation accelerates the long-lasting medicinal effectiveness in non-eosinophilic asthma (NEA), chronic obstructive pulmonary disease (COPD) exacerbations, and both cystic and non-cystic fibrosis bronchiectasis. Azithromycin also exerts stimulative activities on epithelial and immune cells linked to extracellular signal-regulated kinases (ERK) 1 and 2 and phospholipids, accompanied by the late modulation of NF- $\kappa$ B and activator protein-1 (AP-1) transcription factor, mucin release, and cytokine-related inflammation (25). It also exerts late repressive effects on cells' smooth function and also increase lysosomal buildup as a consequence of the disturbance in both intracellular lipid and protein transportation, while also exerting surface receptor expression modulation of autophagy and macrophage phenotype. Such alterations underlie several immunomodulatory activities, adding to the timely resolution of severe infections while mitigating aggravations in chronic respiratory tract diseases. Previously analyzed were groups of people with post-transplant bronchiolitis, who revealed to be responsive to azithromycin treatment, as well as some people with acute sepsis (26), periodontitis, and prostatitis; notwithstanding, a weakened effect is not likely to be critical in malaria. Anyway, given data currently available, the continual application of azithromycin needs to be well-adjusted against the possibility of bacterial resistivity. Indeed, despite that some reports have stated rare situations of torsades de pointes (TDP) in people who are at risk, the use of azithromycin has continued to show an encouraging track record of safety in its usage (23). An experiment was performed to study the function of human neutrophils and to circulate inflammatory mediators on 12 volunteers each receiving a different dose of 500 mg of



azithromycin per day (p.o.) for 3 days (20). Blood was drawn from volunteers in the following order: 1 h before treatment, 2 and a half h, 24 h, and also 28 days after administration. Neutrophil-degranulating activities following azithromycin use were stated to quickly decrease the activities of azurophilic granule enzymes in cells and to increase their serum level. Also, oxidation responses to the particulate stimulus were indicated to be highly improved. The activities observed were connected to an increase in neutrophil and plasma drug concentrations (20). The constant decrease in IL-6 serum and chemokine concentrations within ranges that were non-pathological followed a rise in apoptosis, and a slowing downregulation of the oxidative burst of neutrophils up to 28 days after administration of the final treatment dosage of azithromycin was also reported. The isolated blood neutrophils at this time still had identifiable amounts of the drug. Indeed, severe neutrophil stimulation may positively enhance azithromycin microbicidal effectiveness while the slowing down of possibly anti-inflammatory activities could restrain detrimental inflammations (20).

On the other hand, most asthma aggravations are due to RV infections (27). Currently available therapy for such exacerbation is believed to be insufficient. Preceding indications suggested that macrolide antibacterias possess both antiviral and anti-inflammatory capabilities even though the procedure directly involved is yet to be known. Furthermore, a study was carried out to investigate the anti-RV effects of macrolides (telithromycin, erythromycin, and azithromycin) by the induction of protein and antiviral messenger RNA (mRNA) in primary human bronchial epithelial cells (HBEpC), subjected to major group RV-6 and minor group RV-1B infection. The antiviral gene mRNA expression, IL-6 and IL-8 levels, RV release and replications, interferon- $\lambda$ 2/3, type I interferon- $\beta$  and type III interferon- $\lambda$ 1, and interferon-stimulated genes (oligoadenylate synthase, melanoma differentiation-associated gene 5, retinoic acid-inducible gene I, viperin, and MxA) were carefully addressed (22). Azithromycin treatment led to a significant increase in protein production and interferon and gene mRNA expression enhanced by RV-1B and RV-16, whereby erythromycin and telithromycin treatments were not significant enough. Moreover, azithromycin treatment further decreased the release of RV and its replication significantly. Observation also revealed that the RV-stimulated IL-6 and IL-8 protein and mRNA expressions were not indicated to be significantly decreased with azithromycin use (22). Indeed, there is a lot of evidence underlining that azithromycin has good anti-inflammatory potency (28). For instance, in acquired and innate immunity, macrophages are essential and enhance the pro-inflammatory cytokine production, such as IL-12, which comprises both p35 and p40 subunits. The primary aim of IL-12 is to boost type 1 T-helper ( $T_H1$ ) production and response. Thus, the effect of azithromycin on IL-12 p40 production in macrophages following stimulation of interferon- $\gamma$  and lipopolysaccharide were investigated. Azithromycin was used to pretreat the RAW264.7 macrophage cell line, which was followed by the production of lipopolysaccharide and interferon- $\gamma$  (21). Real-time polymerase chain reaction (RT-PCR) and enzyme-linked immunosorbent assay (ELISA) were

employed to evaluate the IL-12 production. Furthermore, reporter assay and electrophoretic mobility shift assay were also used to assess the IL-12 transcriptional regulation (29). Interferon consensus sequence-binding protein (ICSBP) and phosphorylation of activator protein-1 were evaluated by both immunoblotting (using specified antibodies against ICSBP and Jun-B) and immunoprecipitation (using phosphotyrosine), whereby azithromycin application decreased the induction of the IL-12 p40 promoter by lipopolysaccharide/interferon- $\gamma$  in a dosage-dependent way. The nuclear factor-mediated T-cells, activator protein-1, and interferon consensus sequence-binding protein to the DNA-binding site in the IL-12 p40 promoter were also indicated as being inhibited by azithromycin (21). Observations further revealed that azithromycin minimized the activities of the lipopolysaccharide/interferon- $\gamma$ -induced IL-12 p40 promoter. Stimulated cells that had been treated with azithromycin inhibited both JunB and ICSBP phosphorylation. Finally, the activities of IL-12 p40 transcription were decreased by azithromycin through inhibition of AP-1, ICSBP, and nuclear factor-activated T-cells in the promoter site. Such could be representative of a key procedure for the regulation of azithromycin anti-inflammatory activities in macrophages (21).

## AZITHROMYCIN EFFECTIVENESS IN COVID-19 MANAGEMENT

In a France-based clinical study, hydroxychloroquine was administered to 20 patients and compared to 16 patients who served as controls (not treated with hydroxychloroquine). Six patients were given a mixture of 200 mg of hydroxychloroquine administered three times a day for a period of 10 days and 500 mg of azithromycin on the first day (30). The investigating scientists concluded that 100% of patients administered the mixture were virologically attenuated during the 6th day as opposed to about 57.1% of patients who were treated with only hydroxychloroquine and 12.5% of those in the control groups (30). Contrary to this striking finding, in another study, 11 patients received a mixture of azithromycin and hydroxychloroquine [using the same dose described by Gautret et al. (30) and Molina et al. (31)]. It is also interesting to note that in the stated instance by Molina et al. (31), the patients incurred comorbidities significantly, related to conditions that were poor such as hematological cancer, human immunodeficiency virus infection, and obesity. Treatment had to be stopped for one patient just after 4 days due to Qt prolongation. Furthermore, on an updated report, Gautret et al. (30) stated a promising situation (which denotes patients that were no more given treatment and also required no oxygen treatment) in which out of 80 patients (81.3%) observed, 65 of them treated with azithromycin and hydroxychloroquine had a negative viral load test at 6 days in 83% of those treated with the mixture. Fifteen percent needed oxygen treatment, three patients required intensive care unit admission but later got better, while unfortunately, one patient died (30).

Two critical studies on the effectiveness of combining azithromycin and hydroxychloroquine as a treatment combination for the deadly virus were recently published.

Rosenberg et al. (32) described a retrospective multicenter cohort analysis on one thousand four hundred and thirty-eight patients with COVID-19 which were hospitalized. As a possible treatment for the virus, 735 patients received azithromycin and hydroxychloroquine. In a combined therapy (azithromycin + hydroxychloroquine), no significant variations were stated when compared to control patients (31). In addition, Mehra et al. (33) stated a situation in contradiction of the advantages of applying the treatment combination of chloroquine or hydroxychloroquine with clarithromycin or azithromycin to a total number of 96,032 COVID-19 patients. Having compared the patients' mortalities (in-hospital) that were given the mixture of quinoline and macrolide derivatives with those who received no treatment for the virus, the authors detected that the treatment combinations were linked to a high risk of death (32, 33). Presently, various trials are still ongoing in evaluating the potency of azithromycin in COVID-19 treatment. Placebo against azithromycin, in mixed form or against hydroxychloroquine or in triple combination with tocilizumab, is the most usual pattern studied (such as NCT04341870, NCT04329832, NCT04334382, NCT04332107, NCT04348474, NCT04341207, NCT04329572, NCT04339426, NCT04336332, NCT04335552, NCT04332094, NCT04339816, NCT04328272, NCT04338698, NCT04347512, NCT04345861, NCT04349592, NCT04321278, NCT04322396, NCT04344444, NCT04322123, NCT04334512, NCT04324463, NCT04351919, NCT04345419, NCT04341727, NCT04332835, NCT04349410, NCT04347031). The other research conducted by a French group also aimed to assess the efficacy, in particular by medical and other health workers who associate patients with the virus and those exposed to it (NCT 04344379) as well as to those at high risk of contracting the virus, using azithromycin and hydroxychloroquine as a way to prevent SARS-CoV-2 infection. The macrolide azithromycin is considered to be one of the drugs that have been included in the large adaptive RECOVERY test and also in the United Kingdom Medicines and Healthcare products Regulatory Agency study jointly sponsored by the University of Oxford with the European Union Clinical Trial (EudraCT) number: 2020-001113-21. In previous *in vitro* screen tests by the Food and Drug Administration (FDA)-approved chemical libraries, azithromycin has been shown to have the half-maximal inhibitory concentration ( $IC_{50}$ ) of  $2.12 \mu M$  in antagonism to SARS-CoV-2 (34). In connection to the aforementioned inflammatory reactions and effects, macrolides could plausibly exert a prophylactical function in staphylococcal and pneumococcal difficulties that come on with a particular incidence as complications of respiratory tract viral infection.

## CLUSTER OF DIFFERENTIATION 147 (CD147) AND COVID-2019 TREATMENT: POSSIBLE EFFECTS OF AZITHROMYCIN AND STEM CELL ENGAGEMENT

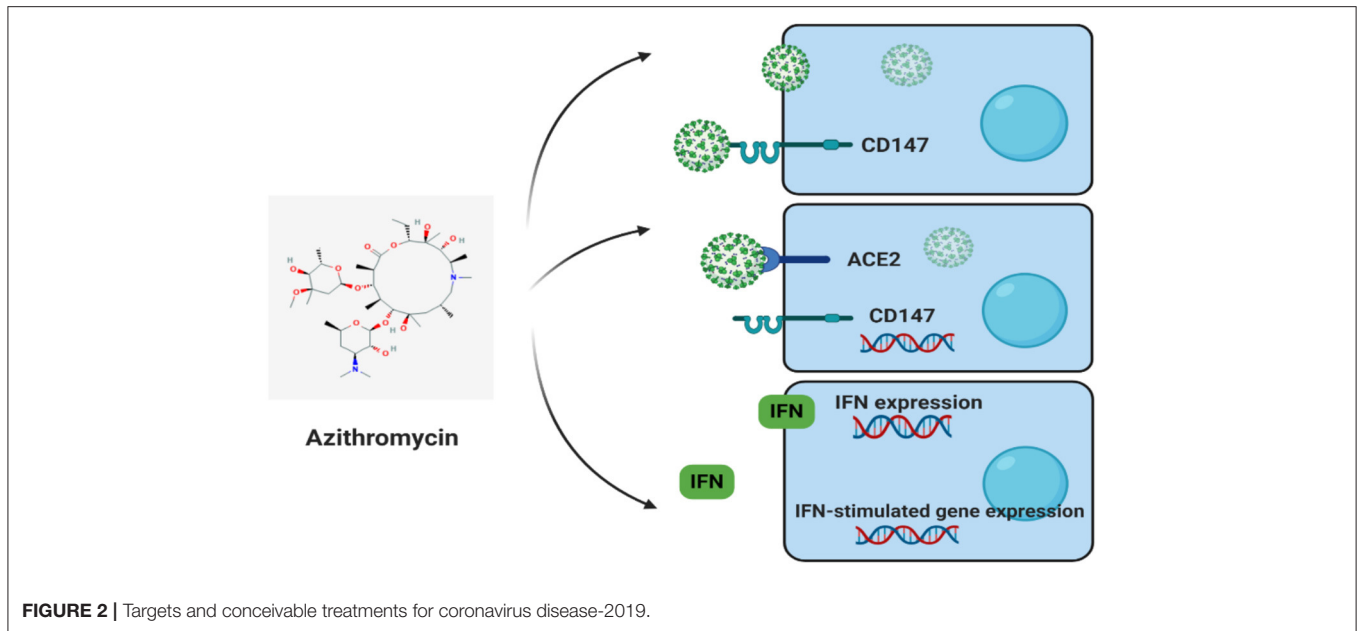
Angiotensin-converting enzyme 2 (ACE2) and cluster differentiation 147 (CD147) (also known as EMMPRIN or

Basigin) are host cell receptors and novel routes for SARS-CoV-2 invasion (**Figure 2**) (35). In host cells, ACE2 or CD147 binds to virus spike protein (S-protein), disseminating virus, and mediating viral invasion within other cells. The SARS-CoV-2-S-protein is similar to SARS-CoV S-protein, with both binding to ACE2, attacking host cells (35). Apart from ACE2, Wang et al. recently showed that CD147 could also bind to SARS-CoV-2-S-protein (35). Their investigation employed the use of an anti-CD147-Meplazumab, co-immunoprecipitation, ELISA, and immuno-electron microscopy to reveal the new CD147-S-protein route of viral invasion. As main statements, the study underlined a significant focus on the application and development of specified anti-SARS-CoV-2 medications. Furthermore, another medical trial by the Chinese in its second phase with the title: "Clinical Study of Anti-Cluster of Differentiation 147 Humanized Meplazumab for Injection to Treat with 2019-nCoV Pneumonia" (ClinicalTrials.gov Identifier: NCT04275245) is presently being conducted with the chief aim of restricting the CD147 protein by monoclonal antibodies to impede SARS-CoV-2-S-protein binding and further infections. The experiment is currently supervised by virologic clearance rate by using a RT-PCR of airway tract samples to evaluate the activities of Meplazumab. The drug is viewed as a very exact molecule against CD147. Despite such a distinction, it is not exempted from the facts that other medication affecting CD147 expression could also possess advantageous effectiveness in the treatment of COVID-19.

Also worth noting is that CD147 acts as a receptor for *Plasmodium falciparum* (protozoan that causes Malaria) invasion on red blood cells (RBCs). CD147, in addition to ACE2, also acts as a host cell receptor for SARS-CoV-2 invasion. Indeed, host cell invasion by SARS-CoV-2 (*in vitro* and phase II clinical trial) and *P. falciparum* is prevented by using treatment with anti-CD147. Azithromycin also quickly prevents SARS-CoV-2 infection and *P. falciparum* invasion, probably interfering with vital ligand/receptor interactions. However, azithromycin effectiveness in SARS-CoV-2 is soon to be assessed. As a matter of fact, antiviral responses in epithelial cells are induced by azithromycin by raising the levels of interferons and interferon-stimulated proteins and also reducing the virus replication and release. In addition, it also reduces MMP expression, a molecule nearly associated with CD147. *In vitro*, high glucose levels and influenza A virus in cells of patients with asthma increase CD147 expression, thus indicating plausible relationships with diabetes mellitus, asthma, and CD147 levels in medical complications due to SARS-CoV-2 infection.

## HYDROXYCHLOROQUINE AND AZITHROMYCIN ON SARS-COV-2 INFECTION: RECENT TRENDS

As referred above, azithromycin is a well-known drug and considered to be generally safe. In the United States of America, it has been extensively prescribed, e.g., with 12 million azithromycin prescriptions dispensed to children under 19 years old (36). Recent investigations placed both hydroxychloroquine



and azithromycin as among 97 possible effective drugs for COVID-19 management (37). In a preliminary clinical study, the use of hydroxychloroquine and/or with the combination of azithromycin to boost the drug potency was discovered to have positive effects in the mitigation of SARS-CoV-2 viral load in certain infected patients (30). Since the start of the worldwide pandemic, numerous strains have been isolated, of which one was SARS-CoV-2 IHUMI-3 which was examined by mixing different concentrations of both hydroxychloroquine and azithromycin with Vero E6 cells. Chloroquine has a reputation for both its immunomodulatory and anti-malaria effects and is also widely accepted and used worldwide (38–42). A new study (*in vitro*) indicated that the use of chloroquine inhibited the growth rate of SARS-CoV-2 (43). Such discovery is in line with other investigations conducted in ~100 admitted people with the virus (44, 45).

An analog of chloroquine is hydroxychloroquine, which has little concern on the drug-to-drug interactions. In an earlier SARS-CoV outbreak, hydroxychloroquine has been described to possess anti-SARS-CoV action in *in vitro* investigations (46). This indicates the possible pharmacological role that hydroxychloroquine could play in COVID-19 treatment and management. However, there is currently no medical proof to support the drug administration as a confirmed cure for SARS-CoV-2 infection. Nonetheless, the mechanism of action of both hydroxychloroquine and chloroquine molecules has not been extensively studied, as previous investigations had only hinted on the drug inhibitory potential through a sequence of steps against coronavirus. The treatments could alter the pH level of cell membrane surfaces and therefore could restrain the viral union to the cell membrane. Furthermore, this treatment could also hinder the following: the replication of nucleic acid, virus assembly, glycosylation of viral proteins, new virus particle transport, virus release, and other processes to attain antiviral reaction (47).

A consistent and dependable estimate of the amount of both chloroquine and hydroxychloroquine in lungs and other related tissues could thus be employed for treatment doses recommendation. A physiologically based pharmacokinetic (PBPK) model may be depended on for this estimate. PBPK is a technique that uses mathematical modeling to predict the drugs' concentration in tissues of humans *in silico* by integrating physiological and drug disposition parameters. PBPK are extensively required for the development of medicine in order to assist in identifying if a clinical trial is justified and validated in addition to aiding guidance on the use of such drugs based on appropriate authorized prediction models (48, 49).

Despite the efforts of innumerable researchers focusing on finding a therapeutic agent targeting directly SARS-CoV-2, a very incipient progress has been achieved in identifying curative therapies. By October 2020, many of the potential drugs/vaccines still figured as possible COVID-19 therapeutic agents and extensive clinical studies were warranted to verify their safety and efficacy (50). Regarding that containing the spread of the infection is the best way to control the COVID-19 pandemic, a vaccine that prevents future infections must be considered as a key priority. Also, the prevention of contamination and identification of clinical symptoms via diagnostics that rapidly and accurately detect SARS-CoV-2 infection are extremely important (51).

Hence, vaccines are the primary and most promising solution to mitigate new viral strains. The genome sequence and protein structure of SARS-CoV-2 were made accessible in record time, allowing the production of inactivated or attenuated viral vaccines. Nanotechnology also improves modern vaccines since they are ideal for antigen delivery, as adjuvants, and as mimics of viral structures (52). According to Iyer et al. (53), containing the spread of SARS-CoV-2 infection will potentially reduce the stress and pressure on the health-care professionals, as well as on the

researchers/scientists, capacitating them to deliver better effort on the development of specific vaccines for COVID-19.

## **AZITHROMYCIN, HYDROXYCHLOROQUINE, AND CHLOROQUINE: POTENTIALLY UNFAVORABLE OUTCOMES**

Besides the usual unpleasant effects, like headache, nausea, and itching, the utilization of hydroxychloroquine and chloroquine could lead some patients to severe arrhythmias, a reaction that the concomitant use of azithromycin could facilitate. Some severe but unusual possible dangers that could also occur comprise drug-to-drug interactions, idiosyncratic hypersensitivity reactions, neuropsychiatric effects, and hypoglycemia, with genetic variability which might also have a vital part in them. Not to mention, hydroxychloroquine and chloroquine are highly toxic when taken in excessive amounts (54).

### **QTc Interval Prolongation**

It is important to note that hydroxychloroquine and chloroquine interfere with ventricular repolarization, which leads to QTc interval prolongation and also heightened threats of torsades de pointes (TdP). This reaction is reliant on the kind of concentration of drug administered. Previous investigations observed that the mean QTc level of some volunteers increased to about 6.1 ms after administering a concentrated dose of 600 mg, and 28 ms after a dose of 1,200 mg (55, 56). Notwithstanding, such effects differed from person-to-person and were usually pronounced. Out of 30 children who received small concentrations of chloroquine to treat malaria, 1 had a rise of about 64 ms in QTc interval 1 day after taking the drug (57). The use of azithromycin alone is not known to significantly cause any QTc interval prolongation in clinical trials (58); however, in theory, when azithromycin is used together with hydroxychloroquine or with chloroquine, it may increase the TdP threat. Interestingly, no indication of such risk was reported when an animal model was used (59). Furthermore, the combined drugs have been safely and successfully used in the treatment of patients with malaria (60, 61). Nonetheless, with not much experience in treating patients with COVID-2019 and also the possible use of these medicines to treat cardiac disease or patients under the influence of drugs that delay repolarization, it is highly recommended to daily monitor the QTc interval at baseline throughout treatment, particularly if azithromycin has been prescribed. During prophylactic treatment, day-to-day monitoring may not be feasible; however, the baseline assessment of the QTc interval is highly recommended, specifically for patients diagnosed with cardiac disease. Where possible, it is well-advised to treat any electrolyte disorders and to limit or avoid the use of any medication with the ability to prolong the QT interval.

### **Microbiota Affection With Macrolides**

Regarding the difficulty of differentiating COVID-19 from bacterial pneumonia as stated by clinicians (62), many

considerations about the use of antibiotics should be taken such as the following: the uncertainty of the presence of bacterial superinfections; the absence of specific antiviral agents with proven efficacy; the relative high mortality; and the antimicrobial resistance caused by selective pressure on natural microbiota of individuals. The natural microbiota reduction can be considered a serious concern especially for individuals suffering mild symptoms of COVID-19. Still, even with the negative side effects, antibiotics should be considered as an alternative for treatment method for the most severe suspected or confirmed COVID-19 cases (e.g., patients presenting hypoxic respiratory failure demanding mechanical ventilation) (63).

Stricker and Fesler (64) state in their study that treatments using antibiotics somehow protect patients against SARS-CoV-2 and severe COVID-19 disease. Besides, in normal times, the medical practices do not recommend using antibacterial medications to treat viral infections in order to avoid overuse of antibiotics. Yet, the arrival of SARS-CoV-2 has forced a major review in the extensive medical literature in which some studies demonstrate potential antiviral and anti-inflammatory effects of numerous antibacterial agents such as azithromycin (65), ciprofloxacin (66), spiramycin (67), clarithromycin (68), nitazoxanide (69), metronidazole (70), doxycycline (71, 72), and other tetracyclines (73).

## **AZITHROMYCIN FOR COVID-19 MANAGEMENT: A FURTHER CONSIDERATION FOR SAFE USE**

A recent report by Juurlink (54) on hydroxychloroquine, chloroquine, and azithromycin did not address a safety concern in azithromycin application, which is imperative to recipients of allogeneic blood and marrow transplantation, in which the use of azithromycin could be advised for treating or preventing transplant-related lung diseases (i.e., bronchiolitis obliterans) (54). In a 2017 controlled randomized study involving participants who were receiving blood and marrow transplant, individuals assigned to receive prophylactic azithromycin were found to have significantly higher relapse rates for their underlying hematologic malignant disease, in addition to a rise in death rate generally (74).

## **CONCLUSION**

Azithromycin is a well-known antibiotic with good anti-inflammatory and immunomodulatory effects and considered to be generally safe, besides being reported as useful for the treatment of COVID-19. The combination treatment of hydroxychloroquine and azithromycin was documented to have positive effects to mitigate SARS-CoV-2 viral load in certain patients. Azithromycin and other macrolides, like bafilomycin A1, erythromycin, and clarithromycin were found to impede the making of IL-1 $\beta$ , IL-6, IL-8, TNF- $\alpha$ , and ICAM-1 in influenza- and RV-modeled infections.



## AUTHOR CONTRIBUTIONS

All authors listed have made a substantial, direct and intellectual contribution to the work, and approved it for publication.

## REFERENCES

- Ulrich, H, Pillat MM. CD147 as a target for COVID-19 treatment: suggested effects of azithromycin and stem cell engagement. *Stem Cell Rev Rep.* (2020) 16:434–40. doi: 10.1007/s12015-020-09976-7
- World Health Organization. Coronavirus disease (COVID-19) pandemic. World Health Organization (2020).
- Amsden G. Anti-inflammatory effects of macrolides—an underappreciated benefit in the treatment of community-acquired respiratory tract infections and chronic inflammatory pulmonary conditions? *J Antimicrobial Chemother.* (2005) 55:10–21. doi: 10.1093/jac/dkh519
- Zarogoulidis P, Papanas N, Kioumis I, Chatzaki E, Maltezos E, Zarogoulidis K. Macrolides: from in vitro anti-inflammatory and immunomodulatory properties to clinical practice in respiratory diseases. *Eur J Clin Pharmacol.* (2012) 68:479–503. doi: 10.1007/s00228-011-1161-x
- Kanoh S, Rubin BK. Mechanisms of action and clinical application of macrolides as immunomodulatory medications. *Clin Microbiol Rev.* (2010) 23:590–615. doi: 10.1128/CMR.00078-09
- Pani A, Lauriola M, Romandini A, Scaglione F. Macrolides and viral infections: focus on azithromycin in COVID-19 pathology. *Int J Antimicrobial Agents.* (2020) 56:106053. doi: 10.1016/j.ijantimicag.2020.106053
- Min J-Y, Jang YJ. Macrolide therapy in respiratory viral infections. *Med Inflam.* (2012) 2012:649570. doi: 10.1155/2012/649570
- Singlas E. Pharmacocinétique clinique de l'azithromycine. *Pathol Biol.* (1995) 43:505–11
- Matzneller P, Krasniqi S, Kinzig M, Sörgel F, Hüttner S, Lackner E, et al. Blood, tissue, and intracellular concentrations of azithromycin during and after end of therapy. *Antimicrobial Agents Chemother.* (2013) 57:1736–42. doi: 10.1128/AAC.02011-12
- Ma TKW, Chow KM, Choy ASM, Kwan BCH, Szeto CC, Li PKT. Clinical manifestation of macrolide antibiotic toxicity in CKD and dialysis patients. *Clin Kidney J.* (2014) 7:507–12. doi: 10.1093/ckj/sfu098
- Foulds G, Shepard R, Johnson R. The pharmacokinetics of azithromycin in human serum and tissues. *J Antimicrobial Chemother.* (1990) 25(suppl\_A):73–82. doi: 10.1093/jac/25.suppl\_A.73
- Lalak NJ, Morris DL. Azithromycin clinical pharmacokinetics. *Clin Pharmacokinet.* (1993) 25:370–4. doi: 10.2165/00003088-199325050-00003
- Lode H. The pharmacokinetics of azithromycin and their clinical significance. *Eur J Clin Microbiol Infect Dis.* (1991) 10:807–12. doi: 10.1007/BF01975832
- Lin SJ, Kuo ML, Hsiao HS, Lee PT. Azithromycin modulates immune response of human monocyte-derived dendritic cells and CD4+ T cells. *Int Immunopharmacol.* (2016) 40:318–26. doi: 10.1016/j.intimp.2016.09.012
- Suzuki T, Yamaya M, Sekizawa K, Hosoda M, Yamada N, Ishizuka S, et al. Bafilomycin A1 inhibits rhinovirus infection in human airway epithelium: effects on endosome and ICAM-1. *Am J Physiol Lung Cell Mol Physiol.* (2001) 280:L1115–27. doi: 10.1152/ajplung.2001.280.6.L1115
- Suzuki T, Yamaya M, Sekizawa K, Hosoda M, Yamada N, Ishizuka S, et al. Erythromycin inhibits rhinovirus infection in cultured human tracheal epithelial cells. *Am J Respir Crit Care Med.* (2002) 165:1113–8. doi: 10.1164/ajrccm.165.8.2103094
- Jang Y, Kwon H, Lee B. Effect of clarithromycin on rhinovirus-16 infection in A549 cells. *Eur Respiratory J.* (2006) 27:12–9. doi: 10.1183/09031936.06.00008005
- Yamaya M, Shinya K, Hatachi Y, Kubo H, Asada M, Yasuda H, et al. Clarithromycin inhibits type a seasonal influenza virus infection in human airway epithelial cells. *J Pharmacol Exp Therapeutics.* (2010) 333:81–90. doi: 10.1124/jpet.109.162149
- Murphy BS, Sundareshan V, Cory TJ, Hayes D Jr, Anstead M, Feola DJ. Azithromycin alters macrophage phenotype. *J Antimicrobial Chemother.* (2008) 61:554–60. doi: 10.1093/jac/dkn007
- Culić O, Eraković V, Cepelak I, Barišić K, Brajša KŽ, Ferencic Ž, et al. Azithromycin modulates neutrophil function and circulating inflammatory mediators in healthy human subjects. *Eur J Pharmacol.* (2002) 450:277–89. doi: 10.1016/S0014-2999(02)02042-3
- Yamauchi K, Shibata Y, Kimura T, Abe S, Inoue S, Osaka D, et al. Azithromycin suppresses interleukin-12p40 expression in lipopolysaccharide and interferon- $\gamma$  stimulated macrophages. *Int J Biol Sci.* (2009) 5:667. doi: 10.7150/ijbs.5667
- Gielen V, Johnston SL, Edwards MR. Azithromycin induces anti-viral responses in bronchial epithelial cells. *Eur Respiratory J.* (2010) 36:646–54. doi: 10.1183/09031936.00095809
- Parnham MJ, Haber VE, Giamarellos-Bourboulis EJ, Perletti G, Verleden GM, Vos R. Azithromycin: mechanisms of action and their relevance for clinical applications. *Pharmacol Ther.* (2014) 143:225–45. doi: 10.1016/j.pharmthera.2014.03.003
- Poachanukoon O, Koontongkaew S, Monthanapisit P, Pattanacharoenchai N. Macrolides attenuate phorbol ester-induced tumor necrosis factor- $\alpha$  and mucin production from human airway epithelial cells. *Pharmacology.* (2014) 93:92–9. doi: 10.1159/000358366
- Li, D-Q, Zhou N, Zhang L, Ma P, Pflugfelder SC. Suppressive effects of azithromycin on zymosan-induced production of proinflammatory mediators by human corneal epithelial cells. *Invest Ophthalmol Vis Sci.* (2010) 51:5623–9. doi: 10.1167/jovs.09-4992
- Afshar M, Foster CL, Layden JE, Burnham E. Azithromycin use and outcomes in severe sepsis patients with and without pneumonia. *J Crit Care.* (2016) 32:120–5. doi: 10.1016/j.jccr.2015.12.010
- Gibson PG, Yang IA, Upham JW, Reynolds P, Hodge S, James AL, et al. Effect of azithromycin on asthma exacerbations and quality of life in adults with persistent uncontrolled asthma (AMAZES): a randomised, double-blind, placebo-controlled trial. *Lancet.* (2017) 390:659–68. doi: 10.1016/S0140-6736(17)31281-3
- Zimmermann P, Ziesenis VC, Curtis N, Ritz N. The immunomodulatory effects of macrolides - a systematic review of the underlying mechanisms. *Front Immunol.* (2018) 9:302. doi: 10.3389/fimmu.2018.00302
- Hsu YH, Chang M S. Interleukin-20 antibody is a potential therapeutic agent for experimental arthritis. *Arthritis Rheumatism.* (2010) 62:3311–321. doi: 10.1002/art.27689
- Gautret P, Lagier JC, Parola P, Hoang VT, Meddeb L, Mailhe M, et al. Hydroxychloroquine and azithromycin as a treatment of COVID-19: results of an open-label non-randomized clinical trial. *Int J Antimicrob Agents.* (2020) 56:105949. doi: 10.1016/j.ijantimicag.2020.105949
- Molina JM, Delaugerre C, Le Goff J, Mela-Lima B, Ponscarne D, Goldwirt L, et al. No evidence of rapid antiviral clearance or clinical benefit with the combination of hydroxychloroquine and azithromycin in patients with severe COVID-19 infection. *Med Mal Infect.* (2020) 50:30085–8. doi: 10.1016/j.medmal.2020.03.006
- Rosenberg ES, Dufort EM, Udo T, Wilberschied LA, Kumar J, Tesoriero J, et al. Association of treatment with hydroxychloroquine or azithromycin with in-hospital mortality in patients with COVID-19 in New York state. *JAMA.* (2020) 323:2493–502. doi: 10.1001/jama.2020.8630
- Mehra MR, Desai SS, Ruschitzka F, Patel AN. RETRACTED: Hydroxychloroquine or chloroquine with or without a macrolide for treatment of COVID-19: a multinational registry analysis [published online ahead of print, 2020 May 22] [retracted in: *Lancet.* 2020 Jun 5;null]. *Lancet.* (2020). doi: 10.1016/S0140-6736(20)31180-6

## ACKNOWLEDGMENTS

NC-M acknowledges the Portuguese Foundation for Science and Technology under the Horizon 2020 Program (PTDC/PSI-GER/28076/2017).

34. Touret F, Gilles M, Barral K, Nougairède A, Decroly E, de Lamballerie X, et al. *In vitro* screening of a FDA approved chemical library reveals potential inhibitors of SARS-CoV-2 replication. *BioRxiv*. (2020) doi: 10.1038/s41598-020-70143-6
35. Wang K, Chen W, Zhou YS, Lian JQ, Zhang Z, Du P, et al. SARS-CoV-2 invades host cells via a novel route: CD147-spike protein. *BioRxiv*. (2020). doi: 10.1101/2020.03.14.988345
36. Fleming-Dutra KE, Demirjian A, Bartoces M, Roberts RM, Taylor T Jr, et al. Variations in antibiotic and azithromycin prescribing for children by geography and specialty—United States, 2013. *Pediatr Infect Dis J*. (2018) 37:52. doi: 10.1097/INF.0000000000001708
37. Nabirotkhin S, Peluffo A, E, Bouaziz J, Cohen D. Focusing on the unfolded protein response and autophagy related pathways to reposition common approved drugs against COVID-19. (2020). doi: 10.20944/preprints202003.0302.v1
38. Keyaerts E, Vijgen L, Maes P, Neyts J, Van Ranst M. In vitro inhibition of severe acute respiratory syndrome coronavirus by chloroquine. *Biochem Biophys Res Commun*. (2004) 323:264–8. doi: 10.1016/j.bbrc.2004.08.085
39. Romanelli F, Smith KM, Hoven AD. Chloroquine and hydroxychloroquine as inhibitors of human immunodeficiency virus (HIV-1) activity. *Curr Pharm Des*. (2004) 10:2643–8. doi: 10.2174/1381612043383791
40. Vincent MJ, Bergeron E, Benjannet S, Erickson BR, Rollin P, et al. Chloroquine is a potent inhibitor of SARS coronavirus infection and spread. *Virology*. (2005) 2:1–10. doi: 10.1186/1743-422X-2-69
41. Ooi EE, Chew JS W, Loh J, P, Chua R, et al. *In vitro* inhibition of human influenza A virus replication by chloroquine. *Virology*. (2006) 3:39. doi: 10.1186/1743-422X-3-39
42. Li C, Zhu X, Ji X, Quanqin N, Deng YQ, Tian M, et al. Chloroquine, a FDA-approved drug, prevents Zika virus infection and its associated congenital microcephaly in mice. *EBioMedicine*. (2017) 24:189–94. doi: 10.1016/j.ebiom.2017.09.034
43. Wang M, Cao R, Zhang L, Yang X, Liu J, Xu M, et al. Remdesivir and chloroquine effectively inhibit the recently emerged novel coronavirus (2019-nCoV) *in vitro*. *Cell Res*. (2020) 30:269–71. doi: 10.1038/s41422-020-0282-0
44. Sun X, Li S, Li K, Hu X. Pharmaceutical care of chloroquine phosphate in elderly patients with coronavirus pneumonia (COVID-19). *Aging Medicine*. (2020) 3:98. doi: 10.1002/agm2.12104
45. Xia J, Liu X, Chen H, Shang Y, Zhu H, Chen G, et al. Efficacy of Chloroquine and Lopinavir/Ritonavir in mild/general COVID-2019: a prospective, open-label, multicenter randomized controlled clinical study. *Trials*. (2020) 21:622. doi: 10.1186/s13063-020-04478-w
46. Biot C, Daher W, Chavain N, Fandeur T, Khalife J, Dive D, et al. Design and synthesis of hydroxyferroquine derivatives with antimalarial and antiviral activities. *J Med Chem*. (2006) 49:2845–9. doi: 10.1021/jm0601856
47. Fox RI. Mechanism of action of hydroxychloroquine as an antirheumatic drug. *Semin Arthritis Rheum*. (1993) 23(2 Suppl. 1):82–91. doi: 10.1016/S0049-0172(10)80012-5
48. Food U, Administration D. *Physiologically Based Pharmacokinetic Analyses—Format and Content Guidance for Industry*. Silver Spring, MD: Center for Drug Evaluation and Research, (2018).
49. Li M, Zhao P, Pan Y, Wagner C. Predictive performance of physiologically based pharmacokinetic models for the effect of food on oral drug absorption: current status. *CPT*. (2018) 7:82–9. doi: 10.1002/psp4.12260
50. Dube T, Ghosh A, Mishra J, Kompella UB, Panda JJ. Repurposed drugs, molecular vaccines, immune-modulators, and nanotherapeutics to treat and prevent COVID-19 associated with SARS-CoV-2, a deadly nanovector. *Adv Therap*. (2021) 4:2000172. doi: 10.1002/adtp.202000172
51. Singh VK, Mishra A, Singh S, Kumar P, Singh M, Jagannath C, et al. Emerging prevention and treatment strategies to control COVID-19. *Pathogens*. (2020) 9:501. doi: 10.3390/pathogens9060501
52. Shin MD, Shukla S, Chung YH, Beiss V, Chan SK, Ortega-Rivera OA, et al. COVID-19 vaccine development and a potential nanomaterial path forward. *Nat Nanotechnol*. (2020) 15:646–55. doi: 10.1038/s41565-020-0737-y
53. Iyer M, Jayaramayya K, Subramaniam MD, Lee SB, Dayem AA, Cho SG, et al. COVID-19: an update on diagnostic and therapeutic approaches. *BMB Rep*. (2020) 53:191. doi: 10.5483/BMBRep.2020.53.4.080
54. Juurink DN. Safety considerations with chloroquine, hydroxychloroquine azithromycin in the management of SARS-CoV-2 infection. *CMAJ*. (2020) 192:E450–3. doi: 10.1503/cmaj.200528
55. Mzayek F, Deng H, Mather FJ, Wasilevich EC, Liu H, Hadi CM, et al. Randomized dose-ranging controlled trial of AQ-13, a candidate antimalarial, and chloroquine in healthy volunteers. *PLoS Clin Trials*. (2007) 2:e6. doi: 10.1371/journal.pctr.0020006
56. Pukrittayakamee S, Tarning J, Jittamala P, Charunwatthana P, Lawpoolsri S, Lee S, et al. Pharmacokinetic interactions between primaquine and chloroquine. *Antimicrobial Agents Chemother*. (2014) 58:3354–9. doi: 10.1128/AAC.02794-13
57. Ursing J, Rombo L, Eksborg S, Larson L, Bruvoll A, Tarning J, et al. High-dose chloroquine for uncomplicated plasmodium falciparum malaria is well tolerated and causes similar QT interval prolongation as standard-dose chloroquine in children. *Antimicrob Agents Chemother*. (2020) 64:e01846-19. doi: 10.1128/AAC.01846-19
58. Juurink DN. The cardiovascular safety of azithromycin. *CMAJ*. (2014) 186:1127–8. doi: 10.1503/cmaj.140572
59. Fossa AA, Wisialowski T, Duncan JN, Deng S, Dunne M. Azithromycin/chloroquine combination does not increase cardiac instability despite an increase in monophasic action potential duration in the anesthetized guinea pig. *Am J Trop Med Hyg*. (2007) 77:929–38. doi: 10.4269/ajtmh.2007.77.929
60. Sagara I, Oduro AR, Mulenga M, Dieng Y, Ogutu B, Tiono AB, et al. Efficacy and safety of a combination of azithromycin and chloroquine for the treatment of uncomplicated *Plasmodium falciparum* malaria in two multi-country randomised clinical trials in African adults. *Malar J*. (2014) 13:458. doi: 10.1186/1475-2875-13-458
61. Chandramohan D, Dicko A, Zongo I, Sagara I, Cairns M, Kuepfer I, et al. Effect of adding azithromycin to seasonal malaria chemoprevention. *N Engl J Med*. (2019) 380:2197–206. doi: 10.1056/NEJMoa1811400
62. Bai HX, Hsieh B, Xiong Z, Halsey K, Choi JW, Tran TML, et al. Performance of radiologists in differentiating COVID-19 from non-COVID-19 viral pneumonia at chest CT. *Radiology*. (2020) 296:E46–54. doi: 10.1148/radiol.20200823
63. Huttner BD, Catho G, Pano-Pardo JR, Pulcini C, Schouten J. COVID-19: don't neglect antimicrobial stewardship principles!. *Clin Microbiol Infect*. (2020) 26:808–10. doi: 10.1016/j.cmi.2020.04.024
64. Stricker RB, Fesler MC. A novel plan to deal with SARS-CoV-2 and COVID-19 disease. *J Med Virol*. (2020) 92:1394–5. doi: 10.1002/jmv.25945
65. Menzel M, Akbarshahi H, Bjermer L, Uller L. Azithromycin induces antiviral effects in cultured bronchial epithelial cells from COPD patients. *Sci Rep*. (2016) 6:1–11. doi: 10.1038/srep28698
66. Poschet JF, Perkett EA, Timmins GS, Deretic V. Azithromycin ciprofloxacin have a chloroquine-like effect on respiratory epithelial cells. *BioRxiv*. (2020). doi: 10.1101/2020.03.29.008631
67. Zeng S, Meng X, Huang Q, Lei N, Zeng L, Jiang X, et al. Spiramycin and azithromycin, safe for administration to children, exert antiviral activity against enterovirus A71 in vitro and in vivo. *Int J Antimicrob Agents*. (2019) 53:362–9. doi: 10.1016/j.ijantimicag.2018.12.009
68. Arikata M, Itoh Y, Shichinohe S, Nakayama M, Ishigaki H, Kinoshita T, et al. Efficacy of clarithromycin against H5N1 and H7N9 avian influenza A virus infection in cynomolgus monkeys. *Antiviral Res*. (2019) 171:104591. doi: 10.1016/j.antiviral.2019.104591
69. Rossignol JF. Nitazoxanide: a first-in-class broad-spectrum antiviral agent. *Antiviral Res*. (2014) 110:94–103. doi: 10.1016/j.antiviral.2014.07.014
70. Gharebaghi R, Heidary F, Moradi M, Parvizi M. Metronidazole; a potential novel addition to the COVID-19 treatment regimen. *Arch Acad Emerg Med*. (2020) 8:e40. doi: 10.22037/aaem.v8i1.645
71. Rothan HA, Mohamed Z, Paydar M, Abd Rahman N, Yusof R. Inhibitory effect of doxycycline against dengue virus replication *in vitro*. *Arch Virol*. (2014) 159:711–8. doi: 10.1007/s00705-013-1880-7
72. Wu ZC, Wang X, Wei JC, Li B-B, Shao D-H, Li Y-M, et al. Antiviral activity of doxycycline against vesicular stomatitis virus *in vitro*. *FEMS Microbiol Lett*. (2015) 362:fnv195. doi: 10.1093/femsle/fnv195
73. Sodhi M, Etminan M. Therapeutic potential for tetracyclines in the treatment of COVID-19. *Pharmacotherapy*. (2020) 40:487–8. doi: 10.1002/phar.2395

74. Bergeron A, Chevret S, Granata A, Chevallier P, Vincent L, Huynh A, et al. Effect of azithromycin on airflow decline-free survival after allogeneic hematopoietic stem cell transplant: the allozithro randomized clinical trial. *JAMA*. (2017) 318:557–66. doi: 10.1001/jama.2017.9938

**Conflict of Interest:** The authors declare that the research was conducted in the absence of any commercial or financial relationships that could be construed as a potential conflict of interest.

Copyright © 2021 Batiha, Zayed, Awad, Shaheen, Mustapha, Herrera-Calderon, Pagnossa, Alghammal, Zahoor, Adhikari, Pandey, Elazab, Rengasamy, Cruz-Martins and Hetta. This is an open-access article distributed under the terms of the Creative Commons Attribution License (CC BY). The use, distribution or reproduction in other forums is permitted, provided the original author(s) and the copyright owner(s) are credited and that the original publication in this journal is cited, in accordance with accepted academic practice. No use, distribution or reproduction is permitted which does not comply with these terms.



# Advances in Synthetic Biology and Biosafety Governance

Jing Li<sup>††</sup>, Huimiao Zhao<sup>2\*</sup>, Lanxin Zheng<sup>1</sup> and Wenlin An<sup>1\*†</sup>

<sup>1</sup> College of Life Science and Technology, Beijing University of Chemical Technology, Beijing, China, <sup>2</sup> College of Humanities and Law, Beijing University of Chemical Technology, Beijing, China

## OPEN ACCESS

### Edited by:

Stephen Allen Morse,  
Centers for Disease Control  
and Prevention (CDC), United States

### Reviewed by:

Gerald Epstein,  
National Defense University,  
United States  
Siguna Mueller,  
Independent Researcher, Kaernten,  
Austria

### \*Correspondence:

Wenlin An  
wenlin.an@mail.buct.edu.cn;  
anwlin@163.com  
Huimiao Zhao  
zhaohuimiao@mail.buct.edu.cn

<sup>†</sup> These authors have contributed  
equally to this work

### Specialty section:

This article was submitted to  
Biosafety and Biosecurity,  
a section of the journal  
Frontiers in Bioengineering and  
Biotechnology

**Received:** 23 August 2020

**Accepted:** 17 February 2021

**Published:** 30 April 2021

### Citation:

Li J, Zhao H, Zheng L and An W  
(2021) Advances in Synthetic Biology  
and Biosafety Governance.  
Front. Bioeng. Biotechnol. 9:598087.  
doi: 10.3389/fbioe.2021.598087

Tremendous advances in the field of synthetic biology have been witnessed in multiple areas including life sciences, industrial development, and environmental bio-remediation. However, due to the limitations of human understanding in the code of life, any possible intended or unintended uses of synthetic biology, and other unknown reasons, the development and application of this technology has raised concerns over biosafety, biosecurity, and even cyberbiosecurity that they may expose public health and the environment to unknown hazards. Over the past decades, some countries in Europe, America, and Asia have enacted laws and regulations to control the application of synthetic biology techniques in basic and applied research and this has resulted in some benefits. The outbreak of the COVID-19 caused by novel coronavirus SARS-CoV-2 and various speculations about the origin of this virus have attracted more attention on bio-risk concerns of synthetic biology because of its potential power and uncertainty in the synthesis and engineering of living organisms. Therefore, it is crucial to scrutinize the control measures put in place to ensure appropriate use, promote the development of synthetic biology, and strengthen the governance of pathogen-related research, although the true origin of coronavirus remains hotly debated and unresolved. This article reviews the recent progress made in the field of synthetic biology and combs laws and regulations in governing bio-risk issues. We emphasize the urgent need for legislative and regulatory constraints and oversight to address the biological risks of synthetic biology.

**Keywords:** synthetic biology, artificial life, biosafety, regulation and legislation, public health emergency response system, pandemic control strategies

## INTRODUCTION

Synthetic biology emerged at the beginning of the 21st century and has demonstrated huge potentials for basic research and application. Meanwhile, many issues related to synthetic biology's biosafety and biosecurity need to be deliberated. Over the past decades, the United States, the European Union, and some Asian countries have made great efforts to formulate and implement relevant laws, regulations, and other approaches regarding govern synthetic biology research (Rager-Zisman, 2012; Buhk, 2014). The abrupt outbreak of the COVID-19 caused by the novel coronavirus SARS-CoV-2 at the end of 2019 swept around the world. In the past 1 year, 70.7 million people were infected with SARS-CoV-2 and 1.58 million people died from COVID-19, imposing huge impact on the international community. Although the precise origin of the novel coronavirus remains unresolved, in terms of the fast development of synthetic biology techniques, the outbreak



of COVID-19 has raised a lot of concerns. This is because these techniques allow researchers to quickly reconstruct or engineer/modify viruses based on available viral sequences (Chen et al., 2019). This article reviews the progress of synthetic biology in several fields, discusses the challenges and bio-risk concerns faced by synthetic biology, compares the current strategies in different countries, and offers suggestions to effectively prevent and curb the pandemic like COVID-19.

## OVERVIEW OF PROGRESS IN SYNTHETIC BIOLOGY

### Synthetic Biology

Synthetic biology is an emerging interdisciplinary research field that can broadly be described as the design and construction of novel artificial biological pathways, organisms or devices, or the redesign of existing natural biological systems, aiming to address important issues such as energy, materials, health, and environmental issues. With its rapid development, synthetic biology is becoming a leading third biotechnology revolution since the discovery of DNA double helix and the Human Genome Project. In 2014, the US Department of Defense listed it as one of its six major priority disruptive technologies for development in the 21st century (U.S. Department of Defense, 2014). Advances in biotechnology have promoted the rapid development of synthetic biology. Based on the third-generation genome sequencing, bioinformatics, and gene editing technologies, one can carry out a variety of research tasks using synthetic biology.

This can include genetically engineered life forms thus expanding the fields of genetics and genomics from systems biology to synthetic applications. Rewarding progress on solving medical problems, energy and metabolic engineering, environmental restoration, materials science, and plant science has been made by synthetic biology (Anderson et al., 2012; Liu and Stewart, 2015; Wang L. et al., 2018). In recent years, the in-depth development of cell-free systems has been changing the pattern of synthetic biology and eliminating some of the limitations of working with living cells (Tinafar et al., 2019).

The combination of synthetic biology and engineering improves people's understanding of the mechanism of action of biological components and the regulatory mechanism of the complex network in organisms (Bashor and Collins, 2018; Ozdemir et al., 2018). Tremendous breakthroughs have been witnessed in genetically engineered living organisms (including pathogens), but this increases potential bio-risks including biosafety, biosecurity, and even cyberbiosecurity.

### Potential Bio-Risks of Synthetic Biology

The potential bio-risks of synthetic biology include biosafety, biosecurity, and cyberbiosecurity. Biosafety initially appeared in the field of microbiology as an abbreviation of safety in biological containment. Thus, the original biosafety definition referred to the safety issue of microbial biocontainment. Later, in the field of transgenic biotechnology associated with genetically modified organisms (GMOs), biosafety emerged as an acronym for "safety in biotechnology," referring to the safety issues

associated with releasing GMOs into the open environment. The term "laboratory biosafety" is often used to refer specifically to safety issues related to the biological laboratory protection of pathogens, GMOs, or genetically modified pathogens. In general, biosafety refers to the safety with respect to the effects of biological research on humans and the environment (Merriam-Webster, 2021). Biosafety emphasizes the prevention of unintentional biotechnological and microbial bio-hazards (World Health Organization [WHO], 2018).

Biosecurity refers to taking proactive measures to avoid intentional biohazards, such as theft and misuse of biotechnology and microbiologically hazardous substances, aiming to reduce the risks associated with the misuse of synthetic biology which could cause harm to humans, animals, plants, and environment through the creation, production, and deliberate or accidental release of infectious disease agents or their byproducts (e.g., toxins). It involves disease control (e.g., vaccination management), exotic species, or access to safe and adequate food supply chains (World Health Organization [WHO], 2010).

Cyberbiosecurity has been proposed as an emerging hybridized discipline which encompasses cybersecurity, cyber-physical security, and biosecurity as applied to biological and biomedical-based systems, and was defined as "understanding the vulnerabilities to unwanted surveillance, intrusions, and malicious and harmful activities which can occur within or at the interfaces of comingled life and medical sciences, cyber, cyber-physical, supply chain and infrastructure systems, and developing and instituting measures to prevent, protect against, mitigate, investigate and attribute such threats as it pertains to security, competitiveness and resilience" (Murch et al., 2018). A more comprehensive definition of cyberbiosecurity is given by Peccoud et al. (2018), who consider that any unforeseeable adverse consequences fostered by the cyber-physical interface can be regarded as a kind of cyberbiosecurity, not merely behaviors related to intentional forms of misuse (Mueller, 2021).

### Bottlenecks in Synthetic Biology Development

Synthetic biology has undergone breakthroughs, but it is still in its early stages, and many of the challenging biological engineering and *de novo* synthesis of life forms are far from perfect due to limitations in knowledge and technology. The use of synthetic biology to reconstruct and synthesize life forms from scratch is currently limited to the following techniques including gene editing or synthesis based on known sequences and functions of already existing life forms, screening libraries for biological components, building regulatory modules and systems, and synthesizing life forms. Synthetic biology techniques need to be closely integrated with comprehensive knowledge of systems biology to enable the precise design, construction, and creation of new life forms. Unfortunately, our current understanding of the fine structure and regulatory mechanisms of life forms is very limited, making the task of designing and synthesizing entirely new life forms from scratch almost impossible.

However, with the development of systems biology, precision gene editing technology, bioengineering technology,

bioinformatics including multidimensional genomics, big data analysis, and artificial intelligence, the modification and synthesis of life forms might be helpful in breaking through the technical and cognitive bottlenecks currently faced by current synthetic biology. Unfortunately, at present, there is no evidence to prove that one can design and synthesize entirely new life forms, including viruses and other pathogens, without designing them based on known genome sequences and functions. The engineered life forms (including plants, animals, microorganisms, etc.) mentioned in this review are either limited modifications of existing life forms based on known gene sequences or *de novo* designed and chemically synthesized based on known genome sequences.

As mentioned above, it is almost impossible to synthesize an entirely new life form using current synthetic biology techniques. However, it has long been a debated concept over whether a GMO can be considered as a new organism. It is not very convincing to infer the origin of a new virus on the basis that one cannot currently synthesize a lifeform from scratch. Nevertheless, the public (and everyone else) is concerned about the actual biological risks of synthetic biology and whether Dual Use Research of Concern (DURC)/GoF research will lead to evolutionary acceleration and recombination, with unintended/undesirable consequences. The crucial bottleneck in synthetic biology is lacking full knowledge of the code of life and the limitations of technology.

Due to the importance of synthetic biology and general supports and endorsements from governments, breakthroughs in synthetic biology bottlenecks require innovative and comprehensive development of cross-disciplines. Therefore, for bio-risks concerns, it is necessary to enhance the implementation of laws and regulations to regulate synthetic biology researching activities and the applications of synthetic biology.

## BENEFITS AND POTENTIAL CONCERNS OF SYNTHETIC BIOLOGY TO HUMAN SOCIETY

### Medical Research

The in-depth intersection of synthetic biology and medical fields has created a variety of diagnostic and therapeutic approaches. It provides a new research direction for timely and treatment of diseases in the future. Engineered cells or bacteria are used for diagnosis and therapeutic purposes (Danino et al., 2015; Xie et al., 2016). The use of *Salmonella*, which carries genes for synthetic antitumor drugs, to control tumor growth by sensing the tumor hypoxic microenvironment and releasing drugs in a time-dependent manner is an innovative idea for cancer therapy (Din et al., 2016). Engineered phages could be used to kill antibiotic-resistant pathogens (Yehl et al., 2019). Researchers have developed a new type of tumor-attacking virus that not only kills tumor cells in the brain, but also blocks the growth of blood vessels in tumors, suggesting that the tumor-killing oncolytic viruses may be more effective in treating aggressive brain tumors if they carry vasculostatin, a protein that inhibits

the growth of blood vessels (Hardcastle et al., 2010). Synthetic circuits could be integrated into host cells and function as bio-sensors and regulators for cellular homeostasis or disease progression manipulation (Bai et al., 2016; Saxena et al., 2016). Application of engineered T cell by synthetic biology techniques, for example, Chimeric Antigen Receptor T-Cell Immunotherapy (CAR-T) could be used to treat leukemia (Fraietta et al., 2018). In addition, the idea of controlling engineered cells through external electronic system has been realized with the combination of synthetic biology and computer science (Shao et al., 2017).

Although synthetic biology has been developing rapidly in the medical field and has achieved several breakthroughs, rushed attempts to perform without adequate consideration of bio-risks issues at synthetic biology have also resulted in unintended deaths of patients, and unintended side effects due to individual differences in the use of synthetic biology in therapy still need to be taken seriously (Morgan et al., 2010).

As a novel gene editor, CRISPR/Cas makes it easier to edit sequence-specific genes, which has enabled the development of genetic models of disease and the study of therapeutic measures for human genetic diseases. However, the application of this gene-editing technology and its potential to cause genetic manipulation of humans and human embryos, CRISPR-modified cells and organisms have drawn focused attention to the implications for human biology and society (DiEuliis and Giordano, 2017). Therefore, the premature clinical applications may have erroneous effects.

In addition, gene-editing tools or synthetic biology could be used to enhance (*in vivo* or *in vitro*) production of traditional or novel neurotoxins or infectious agents or to modify existing agents that are known to act on the nervous system and brain to alter neural phenotypes that influence cognition, emotion, and behavior, which raise biosecurity concerns. Gene editing techniques are categorized as a potential vector or even an element of bioweapons of mass destruction (Servick, 2016), and it may be a potential game-changer for neuroweapons (DiEuliis and Giordano, 2017).

### Metabolism of Engineered Organisms

Synthetic biology has made new progress in the field of metabolism of organisms including bacteria, yeast, and mammalian cells through the integration of artificial metabolic networks into engineered strains. To reduce redundant metabolic pathways for better product conversion rates, some researchers have proposed the deletion of unnecessary genes in cells to build smaller genome organisms. Consequently, these organisms are customized to design and produce the desired products (Sung et al., 2016).

*Escherichia coli* has become an important research object in synthetic biology due to its fast growth rate and high conversion rate. The yield of target products increases dramatically in *E. coli* with engineered metabolic networks (Bogorad et al., 2013; Lin et al., 2015; Mahr et al., 2016). By now, a large number of engineered strains have been developed through the introduction of a metabolic network to produce biochemicals, biomaterials, biomedicine, and bioenergy (Saïda et al., 2006; Atsumi et al., 2008; Steen et al., 2010; Huo et al., 2011; Choi and Lee, 2013;

Yao et al., 2013; Studier, 2014; Baeshen et al., 2015; Hadadi et al., 2016; Gileadi, 2017).

As the first eukaryote to complete genome sequencing, *Saccharomyces cerevisiae* is a model organism widely used in industry. With the application of novel gene editing technologies such as CRISPR/Cas, engineered *S. cerevisiae* could be used to produce a variety of chemicals. A representative success case is the manufacturing of artemisinin precursor, artemisinin acid (Ro et al., 2006; Heidari et al., 2017). Moreover, researchers have been able to fully synthesize opioids in yeast (Galanie et al., 2016). The production of some rare medicinal extracts can also be synthesized through basic raw materials in engineered *S. cerevisiae* as a factory (Yan et al., 2014; Wang et al., 2015; Wei et al., 2015), significantly reducing the cost of extracting compounds from medicinal reservoirs. This method can replace large-scale cultivation of medicinal plants, hence, an important application of synthetic biology in the field of compound production (Zhao et al., 2019).

Synthetic biology plays a significant role in the pharmaceutical industry, food additives, cosmetics, and energy industries with renewable production methods, driving the development of human industry. The benefits of advances in genetic engineering technology, however, do not allay concerns about the development of synthetic biology, as the products of genetic engineering have significantly altered the life characteristics of engineered living organisms. In particular, the bio-risk aspects and any unexpected effects have not been fully analyzed in the strains which have been engineered by reducing metabolic pathways or deletion of unnecessary genes because of the uncertain consequence of the deletion of “necessary gene,” which might turn out to be necessary in some unrecognized context (Schumacher et al., 2020).

There are two types of biomolecular-based products being developed, including GMOs (e.g., organisms expressing bio-pesticides) and topical chemical or physical formulations for use in medicine, agriculture, and food production or preservation (e.g., antibiotics and biopesticides). Vectors harboring nucleic acids (DNA and RNA) and proteins that destroy or repair DNA for engineering can be applied to penetrate living cells, tissues, and organisms. Adequate assessment of the potential for these technologies to unintentionally cause harm to human health or the environment may be lacking, or may be reassigned to cause harm. Biologically active substances and vectors may escape risk assessment and regulatory review because they are often excluded from the hazardous chemical category and are explicitly excluded from the category of “genetically modified agents.” This emerging oversight loophole could lead to dual-use allocations or unintended harm to human health or the environment (Heinemann and Walker, 2019).

In addition, their environmental invasion capabilities and evolutionary potential are difficult to determine. Under the pressure of natural evolutionary and natural force, back-mutations and the entire spectrum of unintended effects are also inevitable, leading to loss of function of the engineered organism or unexpected consequences. Furthermore, the escape of engineered strains from the laboratory that produce harmful organic matter might cause ecosystem disruptions, and the

escape of strains carrying man-made removable elements might even amplify the resulting cascade of harm, disrupting the ecological balance in unforeseen ways. Besides, inhalation or contact ingestion caused by the application of these substances to insecticides or sprays may cause uncertain hazards, such as off-target effects of active ingredient concentration or gene silencing.

According to an American report, no known harmful effect from eating genetically modified foods (National Academies of Sciences and Medicine, 2016) has been affirmed. While the Russian Federation launched the GMOs of plant origin safety assessment system. This system accumulates all national and international experience and the latest scientific approaches and achievements to provide the most complete and reliable information on the potential genotoxic, immunotoxin, and allergenic effects of GMOs and be able to reveal the possible unintended effects of genetic modification (Tyshko and Sadykova, 2016). However, the long-term effects of genetically modified animal and plant products on human genetics and health are also unknown (Engdahl, 2013).

Recently, Bauer-Panskus et al. (2020) summarized the new challenges that arise in risk assessment when genetically engineered (GE) plants can persist and propagate in the environment as well as produce viable offspring, and pointed out that next generation effects may be influenced by heterogeneous genetic backgrounds that may trigger unexpected effects in interaction with environmental conditions. The biological characteristics of the original event cannot be considered sufficient to conclude the possible hazards of the next generation. Potential hazards identified by the European Food Safety Authority (EFSA) include exacerbation of weed problems, displacement, and even extinction of native plant species, resulting in a reasonable concern that might escape environmental risk assessment (ERA) because EFSA considers only the characteristics of the original events, leaving aside unexpected or unintended next-generation effects emerging from spontaneous propagation and gene flow. Therefore, the risk assessment of GE organisms capable of persistent and spontaneous propagation in the environment is in fact highly spatiotemporally complex, causing many uncertainties (Bauer-Panskus et al., 2020). In addition, biological activities used in technologies that allows DNA, RNA, and proteins to be delivered to cells, tissues, and organisms in the open environment may evade risk assessment and regulatory review because they are often excluded from the category of hazardous chemicals and are actively being excluded as agents of genetic modification. This emerging oversight vulnerability could lead to dual use or unintended harm to human health or the environment (Heinemann and Walker, 2019). As we cannot get an affirmative answer on the question whether all possible genetically modified foods are safe, we could not foresee what it would bring about if artificial life was released in nature.

## Environmental Monitoring and Bio-Remediation

With extensive use of antibiotics and organic pesticides, the treatment of refractory pollutants has attracted great attention.

Taking synthetic biology as a technical basis, diverse cell factories have shown great potentials in dealing with these severe environmental pollution issues, which is mainly in environmental monitoring and bio-remediation.

In terms of environmental monitoring, engineered cells are used as pollutant monitors. They are sensitive to specific substrates (pollutants) and convert them into human-recognizable signal outputs so that the degree of environmental pollution can be detected. Engineered *Pseudomonas putida* has been used to monitor the concentration of naphthalene in water and gas phases (Werlen et al., 2004). Through continuous optimization of *E. coli* strains, the detectable concentration of parathion, the main substance of organophosphorus pesticides by the engineered biosensor, has reached 10  $\mu\text{mol/L}$  (Chong and Ching, 2016). Concerning environmental bio-remediation, the engineered bacteria through synthetic biology can attain a complete degradation of organochlorine pesticide hexachlorophenol (Yan et al., 2006). DDT pollutants can also be degraded by engineered bacterial strains to stable 4-chlorobenzoic acid metabolites (Kamanavalli and Ninnekar, 2004).

Most bacteria rapidly reproduce in large numbers, and their ability to evolve and mutate allows them to survive in many artificially imposed or naturally occurring environmental stresses. It is difficult to predict how an engineered strain that escapes from the laboratory or is released into the environment will evolve and mutate under the selective pressures of the external environment. Therefore, the biosafety and biosecurity of engineered bacteria or other organisms modified by synthetic biology is currently a matter of great concern in many countries.

Commonly used methods to control of engineered bacteria include implanting a biosafety module in the engineered bacteria, which can trigger the death of the engineered bacteria or prevent the bacteria from self-replication after an escape (Jia et al., 2017). For engineered bacteria that are truly used in the environment, biological control methods, and efficiency need to be evaluated in a timely manner to avoid irreversible consequences.

## De novo Synthesis of Living Organisms

Well-established techniques such as gene sequencing and gene synthesis have promoted the rapid development of synthetic biology. Scientists have begun attempts to synthesize living organisms from scratch instead of solely modifying the genome of a living organism. Recent progress shows that scientists have achieved a leap from the synthesis of prokaryotes to eukaryotes.

On May 20, 2010, Gibson et al. (2010) published a paper in the journal *Science* on the first artificial synthetic cell named “Synthia,” which is a synthetic filamentous mycoplasma, and this artificial cell exhibited the expected characteristics and was capable of self-replication. On May 16, 2019, Chin’s team (Fredens et al., 2019) synthesized a four-mega base *E. coli* genome, and then transformed it into a bacterium called “Syn61” that uses only 61 codons. The synthetic bacteria exhibited a complete viability. Qin’s team (Shao et al., 2018) connected the 16 natural chromosomes of *S. cerevisiae* one by one and deleted redundant repeats, creating a simple yeast SY14 with only a single chromosome, which is different from normal forms of

yeast genome. A complete chemical synthesis of 4 *S. cerevisiae* autosomes was achieved in 2017, establishing a rapid customized synthesis technology for long eukaryotic chromosomes (Wu et al., 2017; Xie et al., 2017).

The application of synthetic biology techniques to synthetic life forms is extremely attractive for people to explore and trace the world of life. We may speculate that in the future, it might be possible to synthesize animal and plant varieties with full consideration of any associated bio-risks, which will greatly facilitate people’s understanding of the mysteries of life. However, at current development stage of synthetic biology without a complete understanding of the possible modes of operation and evolution of life, the impact of synthetic life forms on humans, society, and the environment are largely unknown, especially the potential concerns involving those artificially life forms themselves and other life forms. Therefore, the healthy development of synthetic biology still needs to consider a broader range of biosafety and biosecurity issues.

## Modification and Artificial Synthesis of Pathogens

With the development of synthetic biology, the modification and synthesis of pathogens based on the published pathogen’s gene sequence have become a reality. Cello et al. (2002) used chemical methods to synthesize a full-length poliovirus cDNA, which was transcribed into RNA by ordinary RNA polymerase. They successfully obtained the infectious virus by incubating transcribed RNA from poliovirus cDNA with cytoplasmic extracts of Hela cells. Tumpey et al. (2005) successfully synthesized the Spanish influenza virus. The team integrated all the eight coding gene segments of the virus into the genomic DNA of a common influenza virus based on a publication of the 1918 Spanish influenza virus genome sequence. The virus particles were then obtained from human kidney cells injected with the influenza virus containing eight gene fragments (Tumpey et al., 2005).

To study the mechanism of viruses, Menachery et al. (2015) applied reverse genetics approaches to insert bat coronavirus SHC014 spike protein into mouse adaptive SARS-CoV skeleton, so that the virus skeleton can recognize the ACE2 receptor via SHC014 spike protein and be successfully replicated in human airway cells. Virologist David Evans synthesized horsepox virus (an orthopox virus related to variola, but not variola), which was obtained by inserting the DNA into cells using recombinase (Noyce et al., 2018). Recently, scientists from Switzerland, Germany, and Russia reported the use of public available SARS-CoV-2 sequences to rapidly reconstruct the novel coronavirus in yeast (Thao et al., 2020).

As mentioned above, the current synthetic biology technology has not been able to achieve a complete *de novo* design and synthesis of a brand new virus. Nevertheless, *de novo* synthesis of viruses based on the existing viral genome sequences, or modification of the existing viral genome by splicing, varying toxicity, enhancing immune escape, changing incubation period, and target, as well as creating virus mutation libraries can be achieved within a short period of time. Nevertheless, the synthesis



of pathogens based on existing or modified genome sequences alone has its inherent limits as it ignores all the vast other steps and mechanisms life uses for plasticity and diversification.

Although synthesis of pathogens can facilitate scientific research on viral pathogenesis and drug development, modification or synthesis of pathogens is a dangerous endeavor, and any report of virus synthesis is accompanied by a great deal of discussion and controversy about biosafety and biosecurity issues (Couzin, 2002; Sharp, 2005; Thiel, 2018). Biosafety and biosecurity and even cyberbiosecurity during pathogen synthesis are big issues that need to be considered in any case. Avoiding any misuse, abuse, and accidental release of pathogens is of paramount importance in the conduct of pathogen research.

## CHALLENGES AND OPPORTUNITIES FOR SYNTHETIC BIOLOGY

Over the past two decades, synthetic biology has changed radically, due to its reliance on digitization and automation, offering powerful tools to engineer and even synthesize life forms. There have been quite some efforts to highlight the resulting dangers in this aspect. These concerns including biosafety, biosecurity, and cyberbiosecurity can no longer be ignored as this is how synthetic biology has been carried out.

Considering the unprecedented positive contributions of synthetic biology to people's lives, health and the environment, and the concerns raised by its application, we should take proper measures to embrace the opportunities and challenges presented by synthetic biology. The healthy development of synthetic biology will ultimately depend on resolving actual and perceived concerns regarding its biosafety and biosecurity, as well as the potential consequences of the accidental or deliberate release of synthetic biology-derived organisms.

Firstly, synthetic biology does not always achieve the desired results. Synthetic lifeforms are normally made according to human preferences or purposes, and to some extent, it might be also an accelerated process of natural evolution. However, due to our limits of life-code knowledge, the process and outcome of synthetic lifeforms will not always proceed as we designed. Allowing nature to unfold under the evolutionary accelerated pressure is an experiment where it is not clear exactly what will happen. A typical example is the gene editing event in human babies. It is true that the original intent of the technology was to solve the problem of human genetic diseases, but gene editing of human embryos carried out without proper ethical and biosafety evaluation raises serious biosafety concerns. According to the 2020 report "Heritable Human Genome Editing" from an international commission (Medicine, and Sciences., 2020), and the earlier 2017 report "Human Genome Editing: Science, Ethics, and Governance" (National Academies of Sciences et al., 2017), strict ethical evaluations and steps should be taken before proceeding to clinical human germ-line editing. Family, ethical, moral, and religious dimensions are all factors that should be taken into consideration, in addition to essential factors like scientific and medical safety assessments and regulatory frameworks (Medicine, and Sciences., 2020).

Secondly, the explosive growth of sequence information and the sharing mode of a large amount of genetic information have made the synthesis of pathogens much easier. The accessibility and openness nature of the web offers opportunities to anyone who wants to access a dangerous organism. At the same time, intentional data-information errors in information technology have the potential to cause major security problems in biology. With the increased automation of life sciences, the convergence of new biotechnology and information technology may have even more serious consequences (Dunlap and Pauwels, 2017; George, 2019; Murch and DiEuliis, 2019; Mueller, 2021). In the fourth industrial revolution, the intelligent and its connections to bio-labs open the risks of nefarious use to engineer or edit biological agents or toxins. With the combination of synthetic biology with artificial intelligence and automation, the bio-risks of synthetic biology do not only include intended attacks, but also unintended consequences due to the cyber-overlap and automation. Given advances in DNA synthesis techniques and the advent of robotic cloud laboratories, one may find ways to circumvent current governance barriers to enhance the virulence and transmissibility of pathogens (Dunlap and Pauwels, 2017).

Thirdly, the synthesis of live viruses can help people understand the pathogenic mechanism of pathogens and conduct targeted vaccine and drug development to deal with potential outbreaks. However, the synthetic technology of pathogens could aid bio-terrorism. Furthermore, we cannot guarantee that the pathogen sequences synthesized using pathogen synthesis techniques will be identical to the designed pathogen sequences, as any errors in the synthesis process and in the cyber/physical/natural interface could lead to unexpected mutations and unknown consequences.

A slight modification of the virus genome may result in a mutant virus with increased virus latency, increased pathogenicity, increased number of receptor recognition sites, more serious immune escape, and random mutations creating a mutant virus library, thus a serious consequence. Simplification of synthetic biology techniques creates additional safety risks, but the exposure of the problem can guide the elaboration of legislation and help promote further development of synthetic biology.

Finally, the mutation and gene recombination of pathogens are inevitable. Genome mutations and genetic recombination that occur between different pathogens are active to survive and adapt to the environment. Scientists use synthetic biology techniques to directly mutate the pathogens' genome to accelerate their evolution for scientific purposes, but sometimes the consequence of pathogen engineering is unpredictable because of the limits of individual knowledge about life code.

No matter whether it is the natural recombination of the pathogen genome, virus engineering, or even artificial synthesis in the laboratory, new pathogenic organisms could be produced. Therefore, biosafety and biosecurity are issues that must be highly evaluated for the healthy development of synthetic biology. Restrictions on pathogens and the parallel development of real-time detection technologies are equally urgent. Synthetic biology's development and imbalance of restrictions will have more impacts on industry, and more regulations and discussions

are necessary. There is an urgent need to curb bio-risks by laws and regulations.

## BIOSAFETY GOVERNANCE OF SYNTHETIC BIOLOGY IN DIFFERENT COUNTRIES

It is difficult to have precise definitions and legislations over synthetic biology because it is intertwined with various disciplines. Nevertheless, the legislation of synthetic biology in various countries are managed to be issued according to the research and application fields of synthetic biology.

### Status of Laws and Regulations on Synthetic Biology in the United States

The United States government has promulgated policies, regulations, and laws governing different biological products. For example, pathogens are classified based on their virulence levels and the availability of vaccines and/or effective anti-pathogen drugs. Various levels of physical containment have been mandated depending on pathogen classifications. In terms of laboratory managements, the US Centers for Disease Control and Prevention (CDC) and the National Institutes of Health (NIH) have published a manual on recommendations for the physical containment of pathogens entitled “Biosafety in Microbiology and Biomedical Laboratories” (Berns, 2014).

All medicines in the United States are governed by the Federal Food, Drug, and Cosmetic Act (FDCA). Specifically, Chapter 5 of the FDCA outlines the regulatory approval and testing of pharmaceuticals including specifications, labeling, safe handling, and directions for the safe use of such drugs, as well as requirements for clinical trials. Others such as Toxic Substance Control Law, Plant Insect Law, etc., oversee relevant departments (Trump, 2017).

After the anthrax attacks in 2001, the United States has introduced a series of laws and regulations covering many areas such as biosecurity threat prevention, biosafety drug development, and dual-use technology regulation. These laws and regulations include the Public Health Security and Bioterrorism Preparedness Response Act of 2002, the Bioshield Act, the Biological Defense and Pandemic Vaccine and Drug Development Act, the National Bioengineered Food Information Disclosure Standard, the U.S. Government’s Regulatory Policy for Life Sciences Dual-Use Research, and other laws and regulations.

Concerning the supervision of scientific life research, the United States government issued the policy of DURC. Life science is a research that, based on current knowledge, can reasonably be expected to provide knowledge, information, products, or technologies that could be directly misapplied to pose a significant threat, with a wide range of potential consequences, to public health and safety, crops and other plants, animals, the environment, materials, or national security.

There are two United States policies on dual-use research of concern. One is the United States Government Policy for

Oversight of Life Sciences DURC (U.S. Department of Health & Human Services, 2015). Being released on March 29, 2012, it established a United States Government policy for DURC as applied to a well-defined subset of life sciences research that involves 15 agents and toxins and seven categories of experiments and established regular review by Federal agencies of United States. The other is United States Government Policy for Institutional Oversight of Life Sciences DURC, which was released by the United States government on September 24, 2014. Institutional oversight of DURC is critical for a comprehensive oversight system. This policy ascertains the responsibility of institutions to oversight life sciences DURC, because institutions are most familiar with the life sciences research conducted in their facilities. Also, they are the most proper agencies to shoulder the responsibilities of promoting and strengthening research and communication in the field of life sciences.

These two DURC Policies are complementary to strengthen review and oversight of life sciences research to identify potential DURC, and to develop and implement risk mitigation where appropriate and as required by federal regulation. It supplements the existing regulations and policies of the United States government on the possession and handling of pathogenic microorganisms, and provides guidance to related individuals, including researchers, national security officials and global health experts. They emphasize a culture of responsibility by reminding all involved parties of the shared duty to uphold the integrity of science and prevent the misuse of synthetic biology.

### Status of Laws and Regulations on Synthetic Biology in the European Countries

According to the current EU legislation on GMOs, most of the research conducted in the field of synthetic biology is genetic engineering. This law regulates how organisms are genetically modified and how GMOs are used, including the marketing of GMOs and their products (Buhk, 2014). To limit the scope of application of the law, the EU has set up a special working group for considering applications of new biotechnology in plant breeding and other biological modifications. The European Union has formulated a series of directives for GMOs and emerging biotechnology covering labels, proper containment, trans-shipment, and safe use in research environments (Keiper and Atanassova, 2020).

The European Union’s legislation on the use and regulation of GMOs is mainly based on Directive 90/219/EC, which regulates the genetic modification activities of microorganisms and their cultivation, storage, transport, destruction and disposal, and Directive 2001/18/EC, which regulates the intentional release of GMOs. Although the EU legislation on synthetic biology has been continuously updated over the last two decades, the EU legal framework has been criticized as not being sufficiently comprehensive in scope, and proposals have been made to modify it to suit the rapid development of biotechnology and the new era of synthetic biology (Eriksson et al., 2018; Bratlie et al., 2019; Eriksson et al., 2020).

## Status of Laws and Regulations on Synthetic Biology in China

Synthetic biology is developing very fast in China, especially in the fields of advanced bio-manufacturing, microbial genome breeding, industrial enzyme engineering, and biomedicine. Considering the bio-risk concerns, China has promulgated laws and regulations on biosafety governance of synthetic biology for laboratory practice to secure biosafety and biosecurity (Table 1). The Standing Committee of the National People's Congress, the representative of China's supreme legislature, promulgated the Biosafety Law of the People's Republic of China in 2020. Chapters 4 and 5 of the Biosafety Law generally stipulate the security management of biotechnology research, development, and application activities, and of pathogenic microbe laboratories and formulate unified laboratory biosecurity standards. Any administrative regulations, local regulations and department rules cannot contravene this Biosafety Law. The Ministry of Science and Technology drafted the Regulations for the Safety Management of Biotechnology Research and Development (Biotechnology Research Regulations) right after the gene-edited baby event caused by a Chinese scientist to promote and guarantee the healthy and orderly development of China's biotechnology research and development activities and maintain national biosecurity. The gene-editing experiment seriously violated academic ethics and standards. The Procuratorate found that it was in a dilemma that there was no suitable law to convict Jiankui He guilty as no such a law existed to prohibit scientists from conducting gene-editing experiments on humans back then. The draft of the Biotechnology Research Regulations will fill this legal gap. In addition, a series of policies have been issued on the prevention and control of infectious diseases and laboratory management. Accordingly, various studies are supervised and managed per the grade standards; adequate risk assessments should be conducted during the transformation of research into practical applications to avoid major biosafety and biosecurity risks.

## Requirement of International Cooperation in the Prevention and Control of Bio-Risks

As globalization proceeds, the international cooperation regarding biosafety governance is necessary. To respond to the possible risks and threats from synthetic biology, countries are highly recommended to strengthen various measures such as strengthening the top-level design of biosafety, stepping up the formulation and improvement of national laws and policies. In addition, they are urged to focus on the overall biosafety and biosecurity education layout such as talent training and discipline creation to achieve a profound contribution to technology governance around the world.

The administration departments including government regulatory agencies, government funding agencies, and research institutions should improve the review system of scientific research projects, conduct potential risk analysis, and focus on engineering pathogenic microorganisms and biological research

that may have a negative impact on the natural environment, as well as research with ethical issues. The development of any project related to pathogens has potential biosafety risk. The corresponding review of the research proposal should be carried out before starting a project, in the process of implementation and during the translation of research results into practical applications. It is necessary to comprehensively evaluate the impact of bio-risks on natural environment and human society and take positive actions to guarantee national security and public interest whilst promoting the development of synthetic biology.

The Center for Biological Safety Strategic Research of Tianjin University in China and the Johns Hopkins Center for Health and Safety of the United States co-sponsored the "Track II dialogue" entitled "The Challenges Facing China and the United States in the Era of Synthetic Biology" in 2019 in Washington DC (Johns Hopkins Center for Health Security, 2019). Experts in technology, policy, law, and management from China and the United States discussed strategies for dealing with the potential biosafety risks of synthetic biology. The experts at the meeting pointed out that synthetic biology concerns stem from the biosafety risks due to the misuse of synthetic biological techniques by researchers and the potential biosecurity risk of abusing these techniques for terrorism (Johns Hopkins Center for Health Security, 2019). In addition, it is equally important to train and assess the biosafety awareness of researchers working with synthetic biology. The release of experimental products and experimental pathogens, intentional or unintentional, should be identified as a potential biosafety risk, which should be governed under strict regulation. Nevertheless, as a research technology that breaks through the laws of natural evolution, synthetic biology may have many unpredictable potential risks and its sustainable development necessitates a relatively complete and comprehensive governance system. Therefore, a more comprehensive and detailed regulatory system is required to control the development direction of the industry. In addition, although laws and regulations on biosafety and biosecurity concerns have been promulgated by many governments, more efforts are still needed to strengthen the exchange and sharing of knowledge on how to effectively respond to global epidemics like the COVID-19.

## SYNTHETIC BIOLOGY, PANDEMICS, AND ITS CONTROL STRATEGIES

Synthetic biology is a "double-edged sword." It can bring more knowledge about microorganisms and diseases for the benefit of humanity. As described in a report on DURC drafted by the National Science Advisory Board for Biosecurity (NSABB), synthetic biology has the potential to raise bio-risk concerns, either intentionally or unintentionally. As mentioned earlier, the concerns of synthetic biology come from the biosafety risks caused by the misuse of synthetic biology techniques by researchers, and potential biosecurity issues resulting from abuse of synthetic biotechnology for bioterrorism or warfare, or by accidental leaks.

**TABLE 1** | List of the regulations on biosafety governance of synthetic biology.

Laws and regulations	Issuing authority	Date of enactment
Biosafety Law of the People's Republic of China	The Standing Committee of the National People's Congress	Issued on October 17, 2020.
Regulations on Administration of Agricultural Genetically Modified Organisms Safety	State Council	Issued on May 23, 2001, amended in 2011 and 2017.
Regulations on the Biosafety Management of Pathogenic Microbiological Laboratories	State Council	Issued on November 12, 2004, amended in 2016 and 2018.
Measures for the Administration of the Safety Evaluation of Agricultural Genetically Modified Organisms	Ministry of Agriculture (dissolved, with its authorities having been assumed by Ministry of Agriculture and Rural Affairs)	Issued on January 5, 2002.
Working Rules of the Agricultural Genetically Modified Organisms (GMO) Safety Committee	Ministry of Agriculture (dissolved, with its authorities having been assumed by Ministry of Agriculture and Rural Affairs)	Issued on May 17, 2013.
Guidelines for Veterinary Laboratory Biosafety	Ministry of Agriculture (dissolved, with its authorities having been assumed by Ministry of Agriculture and Rural Affairs)	Issued on October 15, 2003.
Measures for the Biosafety Environmental Management of Pathogenic Microbe Laboratories	State Administration of Environmental Protection (dissolved, with its authorities having been assumed by Ministry of Ecology and Environment)	Issued on March 08, 2006.
Measures for the Safety Management of Biotechnology Research and Development	Ministry of Science and Technology	Issued on July 12, 2017.
Biosafety Guidelines on the Biosafety Governance of Novel Coronavirus High-grade Viral Microbiology Laboratory	Ministry of Science and Technology	Issued on January 23, 2020.

The recent outbreak of the novel coronavirus and various speculations about the origin of the virus have attracted more attention on biosafety of synthetic biology and its prevention as well as control of pandemics. Although the source of the virus is not yet known, and there is a lack of convincing proof that the novel coronavirus epidemic is related to biosafety concerns of synthetic biology, the global pandemic caused by the virus has already manifested itself and has caused enormous damage worldwide, including human lives, national economies, and social and moral aspects.

## Synthetic Biology and the Novel Coronavirus SARS-CoV-2

The novel coronavirus pandemic has swept across the world in just a few months and has made a quite big impact on the international community. Various hypotheses about the origin of the novel coronavirus SARS-CoV-2, especially the one which states that it was made and leaked out from a laboratory, have aroused great concerns globally. Although scientists have made considerable efforts to explore the origin of SARS-CoV-2, so far it remains an unsolved mystery.

### The Origin of Novel Coronavirus Remains Hotly Debated and Unresolved

After an outbreak of an epidemic, the search for the origin of the pathogen and the route of transmission has always been of interest to scientists and the public. The origin of the novel coronavirus SARS-CoV-2 is no exception. However, there are no persuasive data on the real onset of SARS-CoV-2 infection and spread in the pre-pandemic period worldwide since there are too many controversies and doubts about the origin of SARS-CoV-2.

Based on the genomic analysis of different strains of SARS-CoV-2 (Andersen et al., 2020; Benvenuto et al., 2020; Centers for Disease Control and Prevention, 2020; Lu et al., 2020; Paraskevis et al., 2020; Ren et al., 2020; Wan et al., 2020; Zhou P. et al., 2020; Zhu et al., 2020), 27 scientists, on February 19,

2020, issued a joint statement that the novel coronavirus might originate from wild animals (Calisher et al., 2020). In a review article published on February 26, 2020 in the journal "Emerging Microbes & Infections," Shan-Lu Liu and others speculated that the novel coronavirus might be a new virus formed by the recombination of bat coronavirus with other viruses in an intermediate host rather than been artificially engineered (Liu et al., 2020), although there lacks direct evidence to supporting their speculation. Internationally renowned viral evolutionists Kristian Andersen and Andrew Rambaut co-published a review article in *Nature Medicine* entitled "The Proximal Origin of SARS-CoV-2," indicating that this novel coronavirus is of wildlife origin (Andersen et al., 2020). Nevertheless, the above arguments did little to concerns that SARS-CoV-2 was the result of a laboratory accident or was intentionally engineered (Rasmussen, 2021).

One version of the laboratory origin story relies on the fact that SARS-CoV-2 was engineered for gain-of-function research and has been previously studied with bat SARS-like coronaviruses to understand the risk of cross-species transmission (Menachery et al., 2015; Rasmussen, 2021). Ironically, these gain-of-function research have provided valuable information about the biology of SARS-CoV-2.

From scientific point of view, before we would have obtained solid and convincing evidence to prove its true origin, we could not rule out the following possibilities (1) naturally occurring, (2) unintentionally made and leaked out of the lab, and (3) a combination/extension of (1) and (2), including under-appreciated or unassessed interactions between the man-made and the natural world. Ms. Angela L. Rasmussen recently published a short comment titled "On the origins of SARS-CoV-2" to appeal to the stakeholders in public health—scientists, clinicians and, most importantly, members of the public to understand or study the origins of SARS-CoV-2 using an evidence-driven approach (Rasmussen, 2021). Unfortunately, there is insufficient evidence to prove that it came from natural



evolution, neither is there sufficient evidence to prove that it was intentionally made and leaked out of a laboratory. SARS-CoV-2 is different enough from the closest published natural strain that it is very unlikely to have been engineered from that strain, but it cannot exclude the possibility that the immediate precursor is an unpublished and unacknowledged natural strain that was in the possession of a laboratory, and we cannot rule out the possibility that some strains could naturally evolved further in an environment of artificially imposed evolutionary pressure or under some unknown extreme natural evolutionary conditions. Compelling evidence of natural origin would be the discovery in nature of the immediate precursors, which has not been done.

There is an extensive history of pathogen emergence by natural routes: most novel viral pathogens that have caused epidemics or pandemics in humans have emerged naturally from wildlife reservoirs. Therefore, prevailing view among many scientists is that this virus could found its way into the human host through a series of unpleasant and unexpected encounters with animals (Rasmussen, 2021) although the true origin of SARS-CoV-2 is still hotly debated and unresolved.

### The Host of the Novel Coronavirus Remains a Mystery

Some researchers have conducted in-depth research on bat viruses and accumulated a lot of viral genome data. Sequence alignment showed that some viruses carried by bats, such as RaTG13 and RmYN02 have a high degree of similarity with the novel coronavirus, respectively (Zhou H. et al., 2020; Zhou P. et al., 2020). The high correlation between different bat coronaviruses and SARS-CoV-2 suggests that bats are likely hosts for SARS-CoV-2. However, based on the similarity and evolutionary analysis, the differences between SARS-CoV-2 and related bat coronaviruses may represent more than 20 years of natural sequence evolution, suggesting that these bat coronaviruses can be considered as either possible evolutionary precursors of SARS-CoV-2, but not as direct sources of SARS-CoV-2, or the immediate precursors of SARS-CoV-2 that could naturally evolve under some unknown extreme evolutionary conditions. Although there are many well-established bacterial or yeast-based gene combination platforms which make it possible to synthesize a living organism, there is lack of convincing evidence to prove or disprove that these platforms could have played some part in the missing intermediate host of SARS-CoV-2.

Since bats and humans have very low possibility of contact chances, one might argue that it is unlikely for bat to be an intermediate host to pass these viruses to humans. An additional argument for a non-bat intermediary is that the spike protein appears to include sequences from non-bat coronaviruses. But even though contact chances between bats and humans are low, they appear to have happened: according to Wang N. et al. (2018), “Serological Evidence of Bat SARS-Related Coronavirus Infection in Humans” 3% of people surveyed in seropositivity study had antibodies to bat coronaviruses. This is not a high ratio but it is certainly not zero. That is, notwithstanding the low contact

chances of bats and humans, we still can't rule out the possibility that bat is an intermediate host.

In addition to bats, pangolin is another wildlife possible host that may be related to SARS-CoV-2 since the receptor binding domain (RBD) on pangolin-borne virus – that part of the virus that binds directly to the receptor by which it gains entry into cells – matches the corresponding part of the SARS-CoV-2 virus better than any other virus (Lam et al., 2020; Xiao et al., 2020). Multiple SARS-CoV-2 related viruses were found in the tissues of Malayan pangolin smuggled from Southeast Asia to Southern China from 2017 to 2019. Different research groups isolated and sequenced coronaviruses from the smuggled pangolin intercepted by Guangdong Customs and found 99.8% sequence identity of the viral strains, and their sequence similarity with SARS-CoV-2 was 92.4%. Their RBDs were highly similar to SARS-CoV-2, and only one amino acid difference was found between the receptor binding motifs (RBM) of these viruses and SARS-CoV-2. Unlike healthy bats carrying coronaviruses, coronavirus-infected pangolins showed clinical signs and histopathological changes, including interstitial pneumonia and inflammatory cell infiltration, suggesting that pangolins are unlikely hosts for these coronaviruses and may be infected after spillover from their natural hosts, i.e., they may be intermediate hosts for the virus to humans, but the available data are also insufficient to explain pangolins as intermediate hosts for SARS-CoV-2.

Studies have also reported infection of dogs and cats with SARS-CoV-2, but the possibility of transmission of SARS-CoV-2 from cats to humans is uncertain. For the same reason, we need direct and convincing evidence to confirm the intermediate host relationship between humans and animals.

### Artificial Synthesis of Novel Coronavirus SARS-CoV-2

On May 4, 2020, scientists from Switzerland, Germany, and Russia reported that they had successfully pieced together synthetic viral gene fragments using the published SARS-CoV-2 sequence. They reconstructed the active novel coronavirus harboring green fluorescent signal in the sequence by using a well-established yeast-based gene combination platform (Thao et al., 2020). By artificially synthesizing the novel coronavirus, it can promote research on viral pathogenic mechanism, drug screening, and vaccine development. However, it also increases the chances of virus leakage or criminals using the information to create more infectious and toxic viruses.

### Synthetic Biology Involved in Pathogen Identification and Vaccine Development

Some countries take COVID-19 as an influenza, but extensive disease characterization data and research have shown that COVID-19 is not comparable to pandemic influenza, either in terms of its health hazards or its potential harm to society (Latreille and Lee, 2021). Evidence indicated that synthetic biology techniques play an important role in developing sensitive and specific diagnostic kits, vaccines and therapeutic drugs during the fighting against COVID-19.

Synthetic biology can facilitate the detection of SARS-CoV-2. The application of CRISPR-Cas technology in pathogen

identification has significantly reduced the cost of SARS-CoV-2 detection, with its total cost much lower than that of conventional RT-PCR assay. In scenarios where on-site testing is required, the CRISPR-Cas method offers additional advantages, particularly in terms of time savings (Clyde, 2021; Palaz et al., 2021; Rahimi et al., 2021). Furthermore, the CRISPR-Cas13-based detection technique can distinguish SARS-CoV-2 and its mutants (Wang et al., 2021). Recently, Wang et al. (2020) developed a highly sensitive, much more specific and accurate PfAgo-based detection of SARS-CoV-2, which can also distinguish mutants of coronavirus by combining the programmable nuclease PfAgo with RT-PCR technology (Wang et al., 2020).

With synthetic biology, significant progress has been made in SARS-CoV-2 vaccine development. Currently, most vaccines that have been or are being developed, such as inactivated vaccines, subunit vaccines, viral vector-based vaccines, etc., are based on synthetic biology (Strizova et al., 2021). However, it is of great importance to develop effective vaccines under the strict bio-risk assessment and governance (Haynes et al., 2020; Belete, 2021) as serious incidents have been witnessed in the development of vaccines in the past (Haynes et al., 2020). For example, the formalin-inactivated vaccine for Respiratory Syncytial Virus (FI-RSV) was discontinued because of vaccine-associated enhanced disease (VAED). In the current development of the COVID-19 vaccine, serious adverse events have previously triggered the suspension of trials while a comprehensive assessment of causality associated with vaccination was completed by an independent review committee, as was done in the chimpanzee adenovirus vector vaccine study (Phillips et al., 2020; Zimmer et al., 2020).

Biosafety of vaccine permeates the entire vaccine development and use process. In order to be able to implement an effective COVID-19 vaccine as widely, rapidly, and safely as possible, it is necessary to ensure that safety risks (e.g., VAED) are identified, quantified and weighed against potential benefits.

## CONCLUSION

The rapid development of synthetic biology has led to breakthroughs in biomedical, environmental science, energy, and food industries. However, due to limitations in the understanding of the code of life, as well as the possible intended or unintended uses of the technology, the development and application of synthetic biology has associated with bio-risks that may pose unknown hazards to public health and the environment. In order to manage the issue of bio-risk concerns, there is a great need for legislative and regulatory constraints and oversight when one is working with synthetic biology technologies, especially when dual-use biotechnology is involved. In the event of an outbreak, appropriate measures should be taken for the early prevention and control of epidemic regardless of the origin of the pathogens, and governance of pathogen-related research should be strengthened.

For biosafety and biosecurity concerns, synthetic biology may cause intentional or unintentional risks such as food security, ecological sustainability, despite its enormous economic

potential to provide society with more accessible, sustainable, and affordable materials. Thus, the industrialization process of synthetic biology may require some examination and development of existing economic and regulatory agencies. At the same time, the risk of unintended and unpredictable adverse effects on people's health and the environment should be taken into account when synthesizing organisms, because any negligence and mismanagement in such laboratories involving bio-risk concerns may lead to adverse consequences. In order to avoid such bio-risks pose by synthetic biology, actors working with pathogens should be limited to specially trained professionals, working under strict management and supervision.

Although there are bio-risk concerns with synthetic biology, it remains a powerful tool at our disposal in the face of threats to prevent the spread or recurrence of the same pandemic. Vaccines, pathogen specific antibodies and other drugs should be developed through synthetic biology techniques to reduce the loss of targets in case of pathogen mutations, and appropriated measures that improve the rapid response system for new infectious diseases should be put in place. The development of vaccines and effective drugs using synthetic biology techniques, under the governance of laws and regulations, may be the most practical way to ultimately control the epidemic. As John Glass addressed: "I believe that in my lifetime, we will see someone with nefarious intent use synthetic biology in a bad way to cause mayhem, terrorism, you name it. But I also believe that this same technology is going to save the world. I have faith in what we do and its potential" (Cell, 2018).

## AUTHOR CONTRIBUTIONS

WA conceived and supervised the study. JL and LZ wrote the initial manuscript, and WA rewrote the manuscript. HZ wrote the section "Biosafety Governance of Synthetic Biology in Different Countries." WA, HZ, and JL edited, corrected and proofread the full contents of the paper. All authors read and approved the final manuscript.

## FUNDING

National Key R&D Program "Synthetic Biology" key special project, 2018YFA0903000; National Natural Science Foundation General Project, 81672001; and Social Science Foundation of Beijing, China, Young Researchers Program "Improvement of Information Disclosure System on Public Health Emergencies," 20FXC029.

## ACKNOWLEDGMENTS

We acknowledge the funding by National Key R&D Program "Synthetic Biology" key special project and National Natural Science Foundation General Project, and HZ acknowledges the funding by Social Science Foundation of Beijing.

## REFERENCES

- Andersen, K. G., Rambaut, A., Lipkin, W. I., Holmes, E. C., and Garry, R. F. (2020). The proximal origin of SARS-CoV-2. *Nat. Med.* 26, 450–452. doi: 10.1038/s41591-020-0820-9
- Anderson, J., Strelkowa, N., Stan, G.-B., Douglas, T., Savulescu, J., Barahona, M., et al. (2012). Engineering and ethical perspectives in synthetic biology: rigorous, robust and predictable designs, public engagement and a modern ethical framework are vital to the continued success of synthetic biology. *EMBO Rep.* 13, 584–590. doi: 10.1038/embor.2012.81
- Atsumi, S., Hanai, T., and Liao, J. C. (2008). Non-fermentative pathways for synthesis of branched-chain higher alcohols as biofuels. *Nature* 451, 86–89. doi: 10.1038/nature06450
- Baeshen, M. N., Al-Hejin, A. M., Bora, R. S., Ahmed, M. M. M., Ramadan, H. A. I., Saini, K. S., et al. (2015). Production of Biopharmaceuticals in *E. coli*: current scenario and future perspectives. *J. Microbiol. Biotechnol.* 25, 953–962. doi: 10.4014/jmb.1412.12079
- Bai, P., Ye, H. F., Xie, M. Q., Saxena, P., Zulewski, H., Charpin-El Hamri, G., et al. (2016). A synthetic biology-based device prevents liver injury in mice. *J. Hepatol.* 65, 84–94. doi: 10.1016/j.jhep.2016.03.020
- Bashor, C. J., and Collins, J. J. (2018). Understanding biological regulation through synthetic biology. *Annu. Rev. Biophys.* 47, 399–423. doi: 10.1146/annurev-biophys-070816-033903
- Bauer-Panskus, A., Miyazaki, J., Kwall, K., and Then, C. (2020). Risk assessment of genetically engineered plants that can persist and propagate in the environment. *Environ. Sci. Eur.* 32:32.
- Belete, T. M. (2021). Review on up-to-date status of candidate vaccines for COVID-19 disease. *Infect. Drug Resist.* 14, 151–161. doi: 10.2147/idr.s288877
- Benvenuto, D., Giovanetti, M., Ciccozzi, A., Spoto, S., Angeletti, S., and Ciccozzi, M. (2020). The 2019-new coronavirus epidemic: evidence for virus evolution. *J. Med. Virol.* 92, 455–459. doi: 10.1002/jmv.25688
- Berns, K. I. (2014). Grand challenges for biosafety and biosecurity. *Front. Bioeng. Biotechnol.* 2:35.
- Bogorad, I. W., Lin, T.-S., and Liao, J. C. (2013). Synthetic non-oxidative glycolysis enables complete carbon conservation. *Nature* 502, 693–697. doi: 10.1038/nature12575
- Bratlie, S., Halvorsen, K., Myskja, B. K., Mellegård, H., Bjorvatn, C., Frost, P., et al. (2019). A novel governance framework for GMO: a tiered, more flexible regulation for GMOs would help to stimulate innovation and public debate. *EMBO Rep.* 20:e47812.
- Buhk, H. J. (2014). Synthetic biology and its regulation in the European Union. *N Biotechnol.* 31, 528–531. doi: 10.1016/j.nbt.2014.02.007
- Calisher, C., Carroll, D., Colwell, R., Corley, R. B., Daszak, P., Drosten, C., et al. (2020). Statement in support of the scientists, public health professionals, and medical professionals of China combatting COVID-19. *Lancet* 395, e42–e43.
- Cell. (2018). The future is synthetic biology. *Cell* 175, 895–897. doi: 10.1016/j.cell.2018.10.036
- Cello, J., Paul, A. V., and Wimmer, E. (2002). Chemical synthesis of poliovirus cDNA: generation of infectious virus in the absence of natural template. *Science* 297, 1016–1018. doi: 10.1126/science.1072266
- Centers for Disease Control and Prevention (2020). *CDC COVID Data Tracker*. Available online at: <https://www.cdc.gov/coronavirus/2019-nCoV/summary.html> (accessed February 8, 2020).
- Chen, M. Y., Butler, S. S., Chen, W., and Suh, J. (2019). Physical, chemical, and synthetic virology: reprogramming viruses as controllable nanodevices. *Wiley Interdiscip. Rev. Nanomed. Nanobiotechnol.* 11:e1545.
- Choi, Y. J., and Lee, S. Y. (2013). Microbial production of short-chain alkanes. *Nature* 502, 571–574. doi: 10.1038/nature12536
- Chong, H., and Ching, C. B. (2016). Development of colorimetric-based whole-cell biosensor for organophosphorus compounds by engineering transcription regulator DmpR. *ACS Synth. Biol.* 5, 1290–1298. doi: 10.1021/acssynbio.6b00061
- Clyde, D. (2021). SARS-CoV-2 detection goes mobile. *Nat. Rev. Genet.* 22:69. doi: 10.1038/s41576-020-00321-9
- Couzin, J. (2002). Virology: active poliovirus baked from scratch. *Science* 297, 174–175. doi: 10.1126/science.297.5579.174b
- Danino, T., Prindle, A., Kwong, G. A., Skalak, M., Li, H., Allen, K., et al. (2015). Programmable probiotics for detection of cancer in urine. *Sci. Transl. Med.* 7:289ra84. doi: 10.1126/scitranslmed.aaa3519
- DiEuliis, D., and Giordano, J. (2017). Why gene editors like CRISPR/cas may be a game-changer for neuroweapons. *Health Secur.* 15, 296–302. doi: 10.1089/hs.2016.0120
- Din, M. O., Danino, T., Prindle, A., Skalak, M., Selimkhanov, J., Allen, K., et al. (2016). Synchronized cycles of bacterial lysis for in vivo delivery. *Nature* 536, 81–85. doi: 10.1038/nature18930
- Dunlap, G., and Pauwels, E. (2017). Available online at: <https://www.weforum.org/agenda/2017/10/intelligent-and-connected-bio-labs-promise-and-peril-in-the-fourth-industrial-revolution> (accessed February 6, 2021).
- Engdahl, F. W. (2013). *GMO Scandal: the Long Term Effects of Genetically Modified Food on Humans*. Available online at: <https://www.globalresearch.ca/gmo-scandal-the-long-term-effects-of-genetically-modified-food-on-humans/14570> (accessed November 20, 2020).
- Eriksson, D., Custers, R., Edvardsson Björnberg, K., Hansson, S. O., Purnhagen, K., Qaim, M., et al. (2020). Options to reform the European Union legislation on GMOs: scope and definitions. *Trends Biotechnol.* 38, 231–234. doi: 10.1016/j.tibtech.2019.12.002
- Eriksson, D., Harwood, W., Hofvander, P., Jones, H., Rogowsky, P., Stöger, E., et al. (2018). A welcome proposal to amend the GMO legislation of the EU. *Trends Biotechnol.* 36, 1100–1103. doi: 10.1016/j.tibtech.2018.05.001
- Fraietta, J. A., Lacey, S. F., Orlando, E. J., Pruteanu-Malinici, I., Gohil, M., Lundh, S., et al. (2018). Determinants of response and resistance to CD19 chimeric antigen receptor (CAR) T cell therapy of chronic lymphocytic leukemia. *Nat. Med.* 24, 563–571.
- Fredens, J., Wang, K., de la Torre, D., Funke, L. F. H., Robertson, W. E., Christova, Y., et al. (2019). Total synthesis of *Escherichia coli* with a recoded genome. *Nature* 569, 514–518. doi: 10.1038/s41586-019-1192-5
- Galanie, S., Thodey, K., Trenchard, I., Interrante, M. F., and Smolke, C. (2016). Complete biosynthesis of opioids in yeast. *Abstr. Pap. Am. Chem. Soc.* 251, 1095–1100. doi: 10.1126/science.aac9373
- George, A. M. (2019). The national security implications of cyberbiosecurity. *Front. Bioeng. Biotechnol.* 7:51.
- Gibson, D. G., Glass, J. I., Lartigue, C., Noskov, V. N., Chuang, R.-Y., Algire, M. A., et al. (2010). Creation of a bacterial cell controlled by a chemically synthesized genome. *Science* 329, 52–56. doi: 10.1126/science.1190719
- Gileadi, O. (2017). Recombinant protein expression in *E. coli*: a historical perspective. *Methods Mol. Biol.* 1586, 3–10. doi: 10.1007/978-1-4939-6887-9\_1
- Hadadi, N., Hafner, J., Shajkofci, A., Zisaki, A., and Hatzimanikatis, V. (2016). ATLAS of biochemistry: a repository of all possible biochemical reactions for synthetic biology and metabolic engineering studies. *ACS Synth. Biol.* 5, 1155–1166. doi: 10.1021/acssynbio.6b00054
- Hardcastle, J., Kurozumi, K., Dmitrieva, N., Sayers, M. P., Ahmad, S., Waterman, P., et al. (2010). Enhanced antitumor efficacy of vasculostatin (Vstat120) expressing oncolytic HSV-1. *Mol. Ther.* 18, 285–294. doi: 10.1038/mt.2009.232
- Haynes, B. F., Corey, L., Fernandes, P., Gilbert, P. B., Hotez, P. J., Rao, S., et al. (2020). Prospects for a safe COVID-19 vaccine. *Sci. Transl. Med.* 12:eabe0948.
- Heidari, R., Shaw, D. M., and Elger, B. S. (2017). CRISPR and the rebirth of synthetic biology. *Sci. Eng. Ethics* 23, 351–363. doi: 10.1007/s11948-016-9768-z
- Heinemann, J. A., and Walker, S. (2019). Environmentally applied nucleic acids and proteins for purposes of engineering changes to genes and other genetic material. *Biosafety and Health* 1, 113–123. doi: 10.1016/j.bsheal.2019.09.003
- Huo, Y.-X., Cho, K. M., Rivera, J. G. L., Monte, E., Shen, C. R., Yan, Y., et al. (2011). Conversion of proteins into biofuels by engineering nitrogen flux. *Nat. Biotechnol.* 29, 346–351. doi: 10.1038/nbt.1789
- Jia, B., Qi, H., Li, B. Z., Pan, S., Liu, D., Liu, H., et al. (2017). Orthogonal ribosome biofirewall. *ACS Synth. Biol.* 6, 2108–2117. doi: 10.1021/acssynbio.7b00148
- Johns Hopkins Center for Health Security (2019). *Biosafety and Biosecurity in the Era of Synthetic Biology: Perspectives from the United States and China*. Available online at: [https://www.centerforhealthsecurity.org/our-work/pubs\\_archive/pubs-pdfs/2019/190916-ChinaUSmtgReport.pdf](https://www.centerforhealthsecurity.org/our-work/pubs_archive/pubs-pdfs/2019/190916-ChinaUSmtgReport.pdf) (accessed February 6, 2021).
- Kamanavalli, C. M., and Ninnekar, H. Z. (2004). Biodegradation of DDT by a *Pseudomonas* species. *Curr. Microbiol.* 48, 10–13. doi: 10.1007/s00284-003-4053-1



- Keiper, F., and Atanassova, A. (2020). Regulation of synthetic biology: developments under the convention on biological diversity and its protocols. *Front. Bioeng. Biotechnol.* 8:310.
- Lam, T. T., Shum, M. H., Zhu, H. C., Tong, Y. G., Ni, X. B., Liao, Y. S., et al. (2020). Identifying SARS-CoV-2 related coronaviruses in Malayan pangolins. *Nature* 583, 282–285.
- Latreille, E., and Lee, W. L. (2021). Interactions of influenza and SARS-CoV-2 with the lung endothelium: similarities, differences, and implications for therapy. *Viruses* 13:161. doi: 10.3390/v13020161
- Lin, Z., Zhang, Y., Yuan, Q., Liu, Q., Li, Y., Wang, Z., et al. (2015). Metabolic engineering of *Escherichia coli* for poly(3-hydroxybutyrate) production via threonine bypass. *Microbial. Cell Fact.* 14:185.
- Liu, S. L., Saif, L. J., Weiss, S. R., and Su, L. (2020). No credible evidence supporting claims of the laboratory engineering of SARS-CoV-2. *Emerg. Microbes Infect.* 9, 505–507. doi: 10.1080/22221751.2020.1733440
- Liu, W., and Stewart, C. N. Jr. (2015). Plant synthetic biology. *Trends Plant Sci.* 20, 309–317. doi: 10.1016/j.tplants.2015.02.004
- Lu, R., Zhao, X., Li, J., Niu, P., Yang, B., Wu, H., et al. (2020). Genomic characterisation and epidemiology of 2019 novel coronavirus: implications for virus origins and receptor binding. *Lancet* 395, 565–574. doi: 10.1016/s0140-6736(20)30251-8
- Mahr, R., von Boeselager, R. F., Wiechert, J., and Frunzke, J. (2016). Screening of an *Escherichia coli* promoter library for a phenylalanine biosensor. *Appl. Microbiol. Biotechnol.* 100, 6739–6753. doi: 10.1007/s00253-016-7575-8
- Medicine, and Sciences. (2020). *Heritable Human Genome Editing*. Washington, DC: The National Academies Press.
- Menachery, V. D., Yount, B. L. Jr., Debbink, K., Agnihothram, S., Gralinski, L. E., et al. (2015). A SARS-like cluster of circulating bat coronaviruses shows potential for human emergence. *Nat. Med.* 21, 1508–1513. doi: 10.1038/nm.3985
- Merriam-Webster (2021). *Biosafety*. in *Merriam-Webster.Com Dictionary*. Available online at: <https://www.merriam-webster.com/dictionary/biosafety> (accessed January 21, 2021).
- Morgan, R. A., Yang, J. C., Kitano, M., Dudley, M. E., Laurencot, C. M., and Rosenberg, S. A. (2010). Case report of a serious adverse event following the administration of T cells transduced with a chimeric antigen receptor recognizing ERBB2. *Mol. Ther.* 18, 843–851. doi: 10.1038/mt.2010.24
- Mueller, S. (2021). Facing the 2020 pandemic: what does cyberbiosafety want us to know to safeguard the future? *Biosafety and Health* 3, 11–21. doi: 10.1016/j.bshealth.2020.09.007
- Murch, R. S., So, W. K., Buchholz, W. G., Raman, S., and Peccoud, J. (2018). Cyberbiosafety: an emerging new discipline to help safeguard the bioeconomy. *Front. Bioeng. Biotechnol.* 6:39.
- Murch, R., and DiEuliis, D. (2019). Editorial: mapping the cyberbiosafety enterprise. *Front. Bioeng. Biotechnol.* 7:235.
- National Academies of Sciences, and Medicine (2016). *Genetically Engineered Crops: Experiences and Prospects*. Washington, DC: The National Academies Press.
- National Academies of Sciences, Engineering, and Medicine, National Academy of Medicine, and National Academy of Sciences. (2017). *Human Genome Editing: Science, Ethics, and Governance*. Washington, DC: The National Academies Press.
- Noyce, R. S., Lederman, S., and Evans, D. H. (2018). Construction of an infectious horsepox virus vaccine from chemically synthesized DNA fragments. *PLoS One* 13:e0188453. doi: 10.1371/journal.pone.0188453
- Ozdemir, T., Fedorec, A. J. H., Danino, T., and Barnes, C. P. (2018). Synthetic biology and engineered live biotherapeutics: toward increasing system complexity. *Cell Syst.* 7, 5–16. doi: 10.1016/j.cels.2018.06.008
- Palaz, F., Kalkan, A. K., Tozluyurt, A., and Ozsoz, M. (2021). CRISPR-based tools: alternative methods for the diagnosis of COVID-19. *Clin. Biochem.* 89, 1–13. doi: 10.1016/j.clinbiochem.2020.12.011
- Paraskevis, D., Kostaki, E. G., Magiorkinis, G., Panayiotakopoulos, G., Sourvinos, G., and Tsiodras, S. (2020). Full-genome evolutionary analysis of the novel corona virus (2019-nCoV) rejects the hypothesis of emergence as a result of a recent recombination event. *Infect. Genet. Evol.* 79:104212. doi: 10.1016/j.meegid.2020.104212
- Peccoud, J., Gallegos, J. E., Murch, R., Buchholz, W. G., and Raman, S. (2018). Cyberbiosafety: from naive trust to risk awareness. *Trends Biotechnol.* 36, 4–7. doi: 10.1016/j.tibtech.2017.10.012
- Phillips, N., Cyranoski, D., and Mallapaty, S. (2020). A leading coronavirus vaccine trial is on hold: scientists react. *Nature* doi: 10.1038/d41586-020-02594-w Online ahead of print.
- Rager-Zisman, B. (2012). Ethical and regulatory challenges posed by synthetic biology. *Perspect. Biol. Med.* 55, 590–607. doi: 10.1353/pbm.2012.0043
- Rahimi, H., Salehiabar, M., Barsbay, M., Ghaffarlou, M., Kavetsky, T., Sharafi, A., et al. (2021). CRISPR Systems for COVID-19 Diagnosis. *ACS Sens.* 10: 576875.
- Rasmussen, A. L. (2021). On the origins of SARS-CoV-2. *Nat. Med.* 27:1203.
- Ren, L. L., Wang, Y. M., Wu, Z. Q., Xiang, Z. C., Guo, L., Xu, T., et al. (2020). Identification of a novel coronavirus causing severe pneumonia in human: a descriptive study. *Chin. Med. J.* 133, 1015–1024.
- Ro, D. K., Paradise, E. M., Ouellet, M., Fisher, K. J., Newman, K. L., Ndungu, J. M., et al. (2006). Production of the antimalarial drug precursor artemisinic acid in engineered yeast. *Nature* 440, 940–943. doi: 10.1038/nature04640
- Saïda, F., Uzan, M., Odaert, B., and Bontems, F. (2006). Expression of highly toxic genes in *E. coli*: special strategies and genetic tools. *Curr. Protein Pept. Sci.* 7, 47–56. doi: 10.2174/138920306775474095
- Saxena, P., Charpin-El Hamri, G., Folcher, M., Zulewski, H., and Fussenegger, M. (2016). Synthetic gene network restoring endogenous pituitary-thyroid feedback control in experimental Graves' disease. *Proc. Natl. Acad. Sci. USA* 113, 1244–1249. doi: 10.1073/pnas.1514383113
- Schumacher, G. J., Sawaya, S., Nelson, D., and Hansen, A. J. (2020). Genetic information insecurity as state of the art. *Front. Bioeng. Biotechnol.* 8: 591980.
- Servick, K. (2016). *CRISPR—a Weapon of Mass Destruction?*. Available online at: <https://www.sciencemag.org/news/2016/02/crispr-weapon-mass-destruction> (accessed February 6, 2021).
- Shao, J., Xue, S., Yu, G., Yu, Y., Yang, X., Bai, Y., et al. (2017). Smartphone-controlled optogenetically engineered cells enable semiautomatic glucose homeostasis in diabetic mice. *Sci. Transl. Med.* 9:eal2298. doi: 10.1126/scitranslmed.aal2298
- Shao, Y., Lu, N., Wu, Z., Cai, C., Wang, S., Zhang, L.-L., et al. (2018). Creating a functional single-chromosome yeast. *Nature* 560, 331–335. doi: 10.1038/s41586-018-0382-x
- Sharp, P. A. (2005). 1918 flu and responsible science. *Science* 310:17. doi: 10.1126/science.310.5745.17
- Steen, E. J., Kang, Y., Bokinsky, G., Hu, Z., Schirmer, A., McClure, A., et al. (2010). Microbial production of fatty-acid-derived fuels and chemicals from plant biomass. *Nature* 463, 559–U182.
- Strizova, Z., Smetanova, J., Bartunkova, J., and Milota, T. (2021). Principles and challenges in anti-COVID-19 vaccine development. *Int. Arch. Allergy Immunol.* 1, 1–11.
- Studier, F. W. (2014). Stable expression clones and auto-induction for protein production in *E. coli*. *Methods Mol. Biol.* 1091, 17–32. doi: 10.1007/978-1-62703-691-7\_2
- Sung, B. H., Choe, D., Kim, S. C., and Cho, B.-K. (2016). Construction of a minimal genome as a chassis for synthetic biology. *Essays Biochem.* 60, 337–346. doi: 10.1042/ebc20160024
- Thao, T. T. N., Labrousse, F., Ebert, N., V'Kovski, P., Stalder, H., Portmann, J., et al. (2020). Rapid reconstruction of SARS-CoV-2 using a synthetic genomics platform. *Nature* 582, 561–565.
- Thiel, V. (2018). Synthetic viruses—anything new? *PLoS Pathog* 14:e1007019. doi: 10.1371/journal.ppat.1007019
- Tinafar, A., Jaenes, K., and Pardee, K. (2019). Synthetic biology goes cell-free. *BMC Biol.* 17:64.
- Trump, B. D. (2017). Synthetic biology regulation and governance: lessons from TAPIC for the United States, European Union, and Singapore. *Health Policy* 121, 1139–1146. doi: 10.1016/j.healthpol.2017.07.010
- Tumpey, T. M., Basler, C. F., Aguilar, P. V., Zeng, H., Solórzano, A., Swayne, D. E., et al. (2005). Characterization of the reconstructed 1918 Spanish influenza pandemic virus. *Science* 310, 77–80. doi: 10.1126/science.1119392



- Tyshko, N. V., and Sadykova, E. O. (2016). Regulation of genetically modified food Use in the Russian federation. *Food Nutr. Sci.* 7, 743–751. doi: 10.4236/fns.2016.79075
- U. S. Department of Defense (2014). *DoD Science & Technology Priorities*. Available online at: [https://community.apan.org/wg/afosr/m/alea\\_stewart/135113](https://community.apan.org/wg/afosr/m/alea_stewart/135113) (accessed June 2, 2020).
- U. S. Department of Health & Human Services (2015). *United States Government Policy for Oversight of Life Sciences DURC*. Available online at: <https://www.phe.gov/s3/dualuse/Pages/USGOversightPolicy.aspx> (accessed January 17, 2021).
- Wan, Y., Shang, J., Graham, R., Baric, R. S., and Li, F. (2020). Receptor recognition by the novel coronavirus from wuhan: an analysis based on decade-long structural studies of SARS coronavirus. *J. Virol.* 94:e00127–20.
- Wang, F., Yang, J., He, R., Yu, X., Chen, S., Liu, Y., et al. (2020). PfAgo-based detection of SARS-CoV-2. *Biosens. Bioelectron.* 177:112932. doi: 10.1016/j.bios.2020.112932
- Wang, L., Jiang, S., Chen, C., He, W., Wu, X., Wang, F., et al. (2018). Synthetic genomics: from DNA synthesis to genome design. *Angew. Chem. Int. Ed.* 57, 1748–1756. doi: 10.1002/anie.201708741
- Wang, N., Li, S. Y., Yang, X. L., Huang, H. M., Zhang, Y. J., Guo, H., et al. (2018). Serological evidence of bat SARS-related coronavirus infection in humans. *China. Virol. Sin.* 33, 104–107. doi: 10.1007/s12250-018-0012-7
- Wang, P., Wei, Y., Fan, Y., Liu, Q., Wei, W., Yang, C., et al. (2015). Production of bioactive ginsenosides Rh2 and Rg3 by metabolically engineered yeasts. *Metab. Eng.* 29, 97–105. doi: 10.1016/j.ymben.2015.03.003
- Wang, Y., Zhang, Y., Chen, J., Wang, M., Zhang, T., Luo, W., et al. (2021). Detection of SARS-CoV-2 and its mutated variants via CRISPR-Cas13-based transcription amplification. *Anal. Chem.* doi: 10.1021/acs.analchem.0c04303 Online ahead of print.
- Wei, W., Wang, P., Wei, Y., Liu, Q., Yang, C., Zhao, G., et al. (2015). Characterization of *Panax ginseng* UDP-Glycosyltransferases catalyzing protopanaxatriol and biosyntheses of bioactive ginsenosides F1 and Rh1 in metabolically engineered yeasts. *Mol. Plant* 8, 1412–1424. doi: 10.1016/j.molp.2015.05.010
- Werlen, C., Jaspers, M. C., and van der Meer, J. R. (2004). Measurement of biologically available naphthalene in gas and aqueous phases by use of a *Pseudomonas putida* biosensor. *Appl. Environ. Microbiol.* 70, 43–51. doi: 10.1128/aem.70.1.43–51.2004
- World Health Organization [WHO] (2018). *Biosafety and Biosecurity*. Geneva: WHO.
- World Health Organization [WHO] (2010). *Biosecurity: an Integrated Approach to Manage Risk to Human, Animal and Plant Life and Health*. Geneva: WHO.
- Wu, Y., Li, B.-Z., Zhao, M., Mitchell, L. A., Xie, Z.-X., Lin, Q.-H., et al. (2017). Bug mapping and fitness testing of chemically synthesized chromosome X. *Science* 355:eaaf4706.
- Xiao, K., Zhai, J., Feng, Y., Zhou, N., Zhang, X., Zou, J.-J., et al. (2020). Isolation and characterization of 2019-nCoV-like coronavirus from malayan pangolins. *bioRxiv. [Preprint]* doi: 10.1101/2020.02.17.951335
- Xie, M., Ye, H., Wang, H., Hamri, G. C.-E., Lormeau, C., Saxena, P., et al. (2016). beta-cell-mimetic designer cells provide closed-loop glycemic control. *Science* 354, 1296–1301. doi: 10.1126/science.aaf4006
- Xie, Z.-X., Li, B.-Z., Mitchell, L. A., Wu, Y., Qi, X., Jin, Z., et al. (2017). “Perfect” designer chromosome V and behavior of a ring derivative. *Science* 355:eaaf4704.
- Yan, D. Z., Liu, H., and Zhou, N. Y. (2006). Conversion of *Sphingobium chlorophenolicum* ATCC 39723 to a hexachlorobenzene degrader by metabolic engineering. *Appl. Environ. Microbiol.* 72, 2283–2286. doi: 10.1128/aem.72.3.2283–2286.2006
- Yan, X., Fan, Y., Wei, W., Wang, P., Liu, Q., Wei, Y., et al. (2014). Production of bioactive ginsenoside compound K in metabolically engineered yeast. *Cell Res.* 24, 770–773. doi: 10.1038/cr.2014.28
- Yao, Y.-F., Wang, C.-S., Qiao, J., and Zhao, G.-R. (2013). Metabolic engineering of *Escherichia coli* for production of salivanic acid via an artificial biosynthetic pathway. *Metab. Eng.* 19, 79–87. doi: 10.1016/j.ymben.2013.06.001
- Yehl, K., Lemire, S., Yang, A. C., Ando, H., Mimeo, M., Torres, M. T., et al. (2019). Engineering phage host-range and suppressing bacterial resistance through phage tail fiber mutagenesis. *Cell* 179, 459–469.e9.
- Zhao, X., Park, S. Y., Yang, D., and Lee, S. Y. (2019). Synthetic biology for natural compounds. *Biochemistry* 58, 1454–1456. doi: 10.1021/acs.biochem.8b00569
- Zhou, H., Chen, X., Hu, T., Li, J., Song, H., Liu, Y., et al. (2020). A novel bat coronavirus reveals natural insertions at the S1/S2 cleavage site of the spike protein and a possible recombinant origin of HCoV-19. *bioRxiv [Preprint]* doi: 10.1101/2020.03.02.974139
- Zhou, P., Yang, X. L., Wang, X. G., Hu, B., Zhang, L., Zhang, W., et al. (2020). A pneumonia outbreak associated with a new coronavirus of probable bat origin. *Nature* 579, 270–273. doi: 10.1038/s41586-020-2012-7
- Zhu, N., Zhang, D., Wang, W., Li, X., Yang, B., Song, J., et al. (2020). A Novel Coronavirus from Patients with Pneumonia in China, 2019. *N. Engl. J. Med.* 382, 727–733.
- Zimmer, C., Thomas, K., and Mueller, B. (2020). *AstraZeneca Partly Resumes Coronavirus Vaccine Trial After Halting it for Safety*. Available online at: <https://www.nytimes.com/2020/09/12/health/astrazeneca-coronavirus-vaccine-trial-resumes.html> (accessed February 6, 2021).

**Conflict of Interest:** The authors declare that the research was conducted in the absence of any commercial or financial relationships that could be construed as a potential conflict of interest.

Copyright © 2021 Li, Zhao, Zheng and An. This is an open-access article distributed under the terms of the Creative Commons Attribution License (CC BY). The use, distribution or reproduction in other forums is permitted, provided the original author(s) and the copyright owner(s) are credited and that the original publication in this journal is cited, in accordance with accepted academic practice. No use, distribution or reproduction is permitted which does not comply with these terms.



# Early Warning Information for Severe and Critical Patients With COVID-19 Based on Quantitative CT Analysis of Lung Segments

Xu Yuyun<sup>1†</sup>, Yu Lexi<sup>2†</sup>, Wang Haochu<sup>1</sup>, Shu Zhenyu<sup>1\*</sup> and Gong Xiangyang<sup>1\*</sup>

<sup>1</sup> Department of Radiology, Zhejiang Provincial People's Hospital, Affiliated People's Hospital, Hangzhou Medical College, Hangzhou, China, <sup>2</sup> Wuhan Wuchang Hospital, Wuchang Hospital Affiliated to Wuhan University of Science and Technology, Wuhan, China

## OPEN ACCESS

### Edited by:

Segaran P. Pillai,  
United States Department of  
Homeland Security, United States

### Reviewed by:

Wenting Li,  
Anhui Provincial Hospital, China  
Xiaojiong Jia,  
Harvard Medical School,  
United States

### \*Correspondence:

Shu Zhenyu  
9798714@qq.com  
Gong Xiangyang  
cjr.gxy@hotmail.com

<sup>†</sup>These authors have contributed  
equally to this work

### Specialty section:

This article was submitted to  
Infectious Diseases – Surveillance,  
Prevention and Treatment,  
a section of the journal  
Frontiers in Public Health

**Received:** 20 August 2020

**Accepted:** 12 April 2021

**Published:** 13 May 2021

### Citation:

Yuyun X, Lexi Y, Haochu W, Zhenyu S  
and Xiangyang G (2021) Early Warning  
Information for Severe and Critical  
Patients With COVID-19 Based on  
Quantitative CT Analysis of Lung  
Segments.  
Front. Public Health 9:596938.  
doi: 10.3389/fpubh.2021.596938

**Background:** The coronavirus disease 2019 (COVID-19) outbreak is spreading rapidly around the world.

**Purpose:** We aimed to explore early warning information for patients with severe/critical COVID-19 based on quantitative analysis of chest CT images at the lung segment level.

**Materials and Methods:** A dataset of 81 patients with coronavirus disease 2019 (COVID-19) treated at Wuhan Wuchang hospital in Wuhan city from 21 January 2020 to 14 February 2020 was retrospectively analyzed, including ordinary and severe/critical cases. The time course of all subjects was divided into four stages. The differences in each lobe and lung segment between the two groups at each stage were quantitatively analyzed using the percentage of lung involvement (PLI) in order to investigate the most important segment of lung involvement in the severe/critical group and its corresponding time point.

**Results:** Lung involvement in the ordinary and severe/critical groups reached a peak on the 18th and 14th day, respectively. In the first stage, PLIs in the right middle lobe and the left superior lobe between the two groups were significantly different. In the second stage and the fourth stage, there were statistically significant differences between the two groups in the whole lung, right superior lobe, right inferior lobe and left superior lobe. The rapid progress of the lateral segment of the right middle lobe on the second day and the anterior segment of the right upper lobe on the 13th day may be a warning sign for severe/critical patients. Age was the most important demographic characteristic of the severe/critical group.

**Conclusion:** Quantitative assessment based on the lung segments of chest CT images provides early warning information for potentially severe/critical patients.

**Keywords:** coronavirus, COVID-19, lung, prognosis, severe acute respiratory syndrome

## INTRODUCTION

The coronavirus disease 2019 (COVID-19) outbreak was declared a global health emergency by the WHO on 30 January 2020. As the new coronavirus is far more transmissible than SARS and MERS, it has led to outbreaks in many countries and regions around the world. According to the latest report of the World Health Organization, more than twelve million people have been infected, and

about 2.8 million patients have died from COVID-19 pneumonia<sup>1</sup>, with a fatality rate of around 1–3% (1). Although the mortality rate of COVID-19 is much lower than the 9.6% of SARS and 34.4% of MERS, its strong pathogenicity is notable.

According to the Diagnosis and Treatment of Novel Coronavirus Pneumonia (trial version seven) of China, COVID-19 patients can be classified into mild, ordinary, severe, and critical cases (2). Among them, severe and critical patients are at a higher risk of acute respiratory distress syndrome, especially those with a severe onset and fast progression. If not treated in time, the ordinary cases may develop into severe/critical cases or even progress to death (3), so early warning of potentially severe/critical patients may further improve their prognosis. CT examination, as an essential method for the detection and assessment of COVID-19 pneumonia, provides essential information for clinical decision-making (4). Generally, CT imaging manifestations correspond to the severity of COVID-19 pneumonia (5); however, due to the potential radiation damage, CT scans should not be performed too often. Therefore, it is essential to optimize the timing of CT scans for early warning of disease deterioration with less radiation exposure, to help clinicians manage patients quickly and accurately (6).

Recent works have reported the characteristic imaging features of COVID-19 pneumonia, such as ground-glass opacities in the early stage, consolidation, and “crazy-paving” patterns in the peak stage, subpleural distribution, etc. (7, 8). However, due to the lack of accurate quantification tools, these radiological reports mainly used qualitative descriptions for lung involvement. Although there have been studies that used semi-quantitative methods such as a CT score to show the lung changes during the time course of COVID-19 pneumonia, it is very subjective, time-consuming, and it has low inter-rater reliability. In particular, Pan Fen described the imaging symptoms of the four stages of the lung in detail, but a method based on artificial visual assessment may not be able to mine additional potential information about the disease, and the assessment of the disease from the whole lung may not reveal the detailed progress of the disease (9). Therefore, it is necessary to introduce a fully automatic and quantitative method to provide clinicians with a method for accurate evaluation to guide efficient intervention and treatment. In addition, a quantification based on the segmental and lobar lung may help in understanding the precise development of COVID-19 pneumonia.

With growing global concerns about the COVID-19 outbreak, an accurate understanding of the evolution of chest imaging findings and the correlated timepoints are essential for effective patient management and treatment. Therefore, the purpose of our study is to explore the specific lung segments and possible transition times of progressive lesions and to identify potential severe/critical pneumonia patients early to further reduce the related mortality. We compared the differences in segmental distribution and longitudinal changes between severe/critical and ordinary COVID-19 patients based on a quantitative analysis at the lung segment level.

<sup>1</sup><https://covid19.who.int/>.

## MATERIALS AND METHODS

### Study Population

This study was approved by the institutional review board and the local ethics committee of Zhejiang Provincial People's Hospital and Wuhan Wuchang hospital. All investigations were conducted under the Declaration of Helsinki. Written informed consent was waived for this retrospective study, which involved no potential risk to the patients. The dataset in this study was collected from Wuhan Wuchang hospital for COVID-19 patients in Wuhan city. Patients with COVID-19 pneumonia were diagnosed by real-time reverse-transcriptase polymerase chain reaction of throat swabs or lower respiratory tract samples from 24 January 2020 to 14 February 2020. Their information was retrospectively analyzed, including demographic data, initial clinical symptoms, history of underlying diseases, CT imaging data, and laboratory test data. According to the Diagnosis and Treatment of Novel Coronavirus Pneumonia (seventh trial version) of China (2), all subjects were divided into ordinary patients ( $n = 45$ ) and severe/critical patients ( $n = 36$ ), including six critical cases. The starting point of the longitudinal study was defined as the time point of symptom onset, and the endpoint was set as discharge, transfer, or death. In addition, there were no patients with negative imaging findings and no pediatric patients in the dataset. Specific grouping details can be found in the **Supplementary Material**. The coinfection of bacterial or viral pneumonia during hospitalization were recorded including the Nine joint tests for respiratory pathogens (antibodies): influenza B virus, Q fever rickettsiae, influenza A virus, adenovirus, mycoplasma pneumoniae, Legionella pneumoniae, respiratory syncytial virus, Chlamydia pneumoniae, Parainfluenza virus.

### CT Scanning Parameters

All patients underwent multiple non-contrast chest CT scans using a single inspiratory phase on a multi-detector CT scanner (Philips Medical Systems, Cleveland). Patients were instructed about breath-holding. CT images were then acquired during a single breath-hold. The tube voltage was set at 120 kVp during the CT acquisition. The CT images were reconstructed on the raw data with a matrix size of  $512 \times 512$  as axial images (thickness of 2 mm and increment of 2 mm). The mean volume CT dose index range was 5.2–12.6 mGy. The scan range was from the apex of the lungs to the level of the costal angle of the base of the lungs.

### CT Image Assessment

Two chest radiologists (Y.L. and H.W., with ~20 years of experience in thoracic imaging), reviewed all of the CT scans independently and reached decisions by consensus. They were aware that the patients had COVID-19 pneumonia but were blinded to information concerning the patients' clinical conditions, such as laboratory results and the severity of symptoms and signs. Each of the five lung lobes was assessed for the degree of involvement and scored as 0 for 0%, 1 for 1–25%, 2 for 26–50%, 3 for 51–75%, or 4 for 76–100%. A total lung involvement severity score was reached by summing the five lobe scores (range of possible scores, 0–20) (8). All CT data were imported into AI software (care.ai<sup>®</sup> Intelligent Evaluation System, Version 6) for automatic lung involvement detection and

**TABLE 1** | Baseline clinical information of the study population.

Characteristic	Study Population (n = 81)	Ordinary group (n = 45)	Severe/ critical group (n = 36)	P-value
<b>Demographics</b>				
Age (y)	55 (46, 67)	50 (40, 58)	63 (52, 71)	<0.001
Male sex, n (%)	47 (58)	24 (53.3)	23 (63.9)	0.339
Heart rate, (n/minute)	80 (78, 96)	82 (78, 105)	80 (76, 91)	0.285
Respiratory frequency, (n/minute)	20 (20, 23)	20 (20, 23)	20 (20, 23)	0.282
Time between initial symptoms and hospitalization, (days)	6 (4, 8)	6 (4, 9)	6 (3, 8)	0.619
Time from initial symptom to first CT scan, (days)	9 (5, 31)	10 (5, 14)	7 (4, 11)	0.36
Days of hospitalization, (days)	19 (16, 24)	20 (16, 24)	18 (15, 24)	0.437
<b>Initial clinical symptoms, n (%)</b>				
Fever	80 (96.4)	44 (97.7)	36 (100)	0.368
Cough	71 (87.7)	40 (88.9)	31 (86.1)	0.706
Expectoration	27 (33.3)	12 (26.7)	15 (41.7)	0.155
Chest pain and tightness	18 (22.2)	8 (17.8)	10 (27.8)	0.282
Dizziness and headache	16 (19.8)	8 (17.8)	8 (22.2)	0.618
Nausea and vomiting	7 (8.6)	5 (11.1)	2 (5.6)	0.377
Myalgia	12 (14.8)	8 (17.8)	4 (11.1)	0.401
Weakness	49 (60.5)	31 (68.9)	18 (50)	0.084
Abdominal pain and diarrhea	5 (6.2)	3 (6.7)	2 (5.6)	0.836
Rhonchi (n/%)	57 (70.4)	29 (64.4)	28 (77.8)	0.192
Coinfection	12 (14.8)	5 (11.1)	7 (19.4)	0.294
<b>History of underlying diseases, n (%)</b>				
Hypertension	21 (25.9)	14 (31.1)	7 (19.4)	0.234
Diabetes	11 (13.6)	5 (11.1)	6 (16.7)	0.468
Liver injury	17 (21)	9 (20)	8 (22.2)	0.807
Nephropathy	5 (6.2)	1 (2.2)	4 (11.1)	0.099
<b>Laboratory test</b>				
C-reactive protein (mg/L)	34.95 (11.84, 48.22)	30.88 (10.7, 51.6)	26.69 (12.94, 45.6)	0.775
Leukocyte ratio (%)	3.51 (2.96, 4.88)	3.68 (2.86, 5.03)	3.49 (2.99, 4.48)	0.864
Neutrophil ratio (%)	77.7 (60.4, 84.1)	77.7 (62.2, 84.8)	77.25 (58.43, 81.98)	0.537
Lymphocyte ratio (%)	15.14 (10.05, 22.05)	15.5 (9.8, 22.1)	14.1 (10.43, 24.48)	0.977

quantitative analysis. The parameter of the percentage of lung involvement (PLI) was selected, which is defined as the ratio of pneumonia volume to the whole/segmental lung, as it is close to the CT score due to their similarity in assessing lung involvement by ratio to analyse the lung condition of five lung lobes and the corresponding 18 subordinate lung segments. Details about the 18 lung segments and the pneumonia assessment software can

be found in the **Supplementary Material**. Finally, a correlation analysis was performed between the CT scores and the parameter of PLI for their reliability.

## Longitudinal Assessment of Lung Involvement

We divided the time course into four stages according to the quartiles of the CT scans of the two groups of patients. All CT duration times were sorted orderly first, and then we took the quartiles (25%, median, 75%, 100%) as the corresponding stage. The lung involvement of the lung lobes and segments of the ordinary and severe/critical groups at each stage were compared to identify the specific segment location of significant differences. Then, the specific segment that contributed most to the corresponding lung lobe involvement of each stage was selected using the ROC curve. Finally, a longitudinal analysis was performed on the PLIs of the specific segments. Thus, the specific lung involvement segment and its corresponding progression time point for severe/critical cases were identified.

## Statistical Analysis

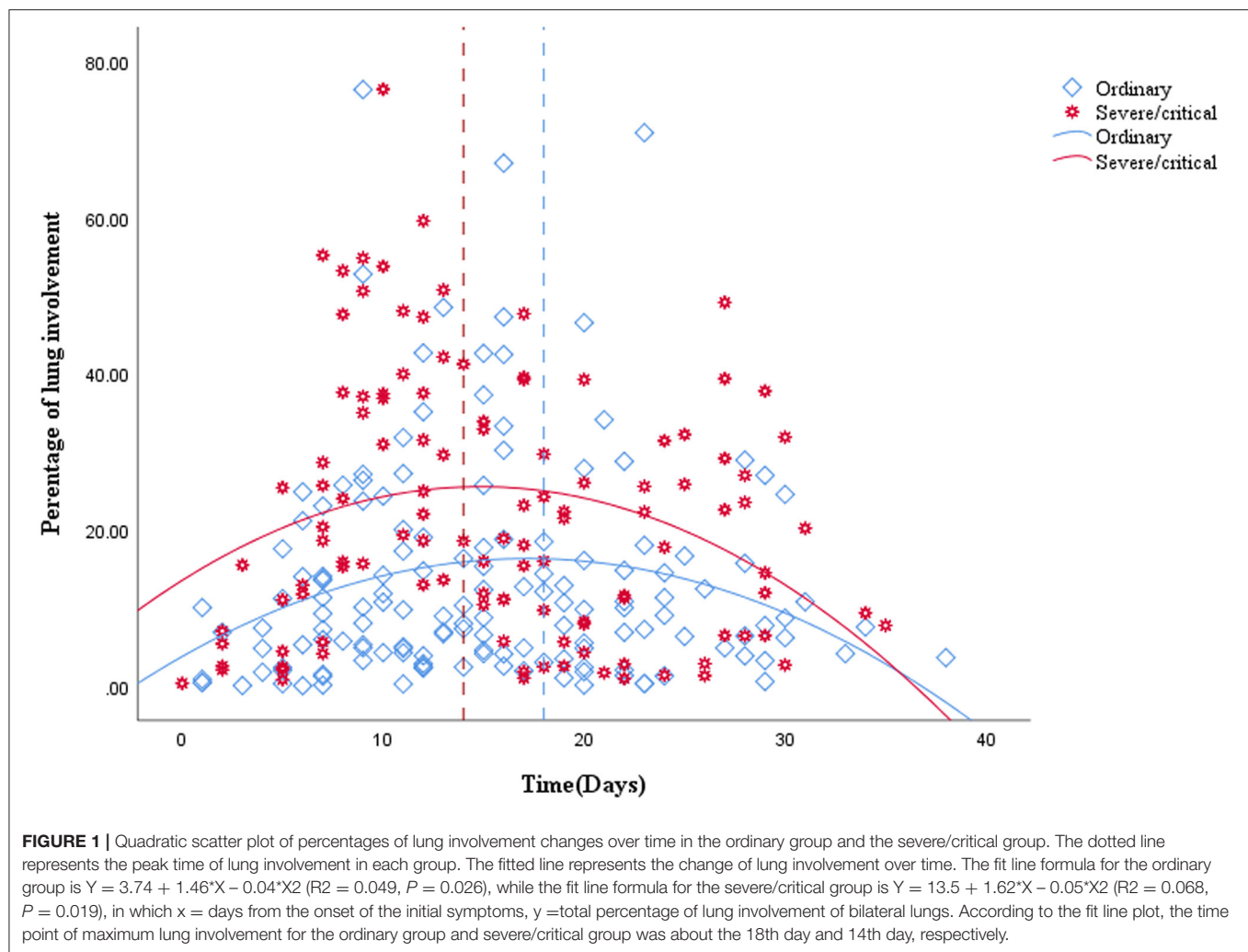
The Statistical Package for Social Sciences (SPSS) version 25.0 (SPSS, Inc., Chicago, IL, USA) software package was used for statistical analysis. The Kolmogorov–Smirnov test was used for normality testing of the measurement data. The normally distributed data were evaluated using the independent sample *t*-test, whereas the non-normally distributed data were evaluated using the Mann–Whitney U test. The differences between categorical variables were tested by the chi-square test. Continuous variables from the clinical information were described using mean, median, and interquartile range (IR), and continuous variables from the CT image dataset were described using mean  $\pm$  standard deviation. The results with a two-tailed *P* < 0.05 were considered significant.

## RESULTS

### Demographic Data

Of the 81 patients with COVID, 55 (58%) were male, and their average age was 55 (IR, 46, 67; range, 21–93). The median time from initial symptoms to admission was 6 days (IR, 4, 8; range, 1–20 days), the average time from initial symptoms to the first CT scan was 9 days (IR, 5, 13; range, 0–25 days), and the average hospitalization time was 20 days (IR, 16, 25; range, 8–33). The main symptom among the initial symptoms was a fever in 80 (96.4%) cases, followed by a cough in 71 (87.7%) cases, then fatigue in 49 (60.5%) cases. Among all the patients, 12 cases were confirmed with other infections, including one *Legionella pneumophila* pneumonia, one *Klebsiella pneumoniae*, one multiple bacterial pneumonia, one *Mycoplasma pneumoniae*, one *Mycoplasma pneumoniae* with adenovirus infection, two adenovirus infections, two parainfluenza virus infections, one respiratory syncytial virus infection, and two influenza B virus infections. There was no significant difference in the number of coinfection cases between ordinary patients and severe/critical patients.





The most common underlying disease was hypertension, with a total of 21 (25.9%) cases. The number with wet and dry rales on clinical physical examinations of the lung were 57 (70.4%). The C-reactive protein on laboratory tests was increased with an average of 34.95 (IR, 11.84–48.22). The white blood cell count was slightly lower, with a median of 3.51 (IR, 2.96, 4.88), and the percentages of neutrophils and lymphocytes were low, with median values of 77.7 (IR, 60.4–84.1) and 15.14 (IR, 10.05–22.05), respectively. There was a statistically significant difference in age between ordinary patients and severe/critical patients [50 (IR, 40–58; range 28–72 vs. 63 (IR, 52–71; range, 34–93 years old),  $P < 0.05$ ], while the other clinical data were not significantly different ( $P > 0.05$ ). Six of the patients died eventually, and the other 75 patients were cured and discharged. See **Table 1** for details.

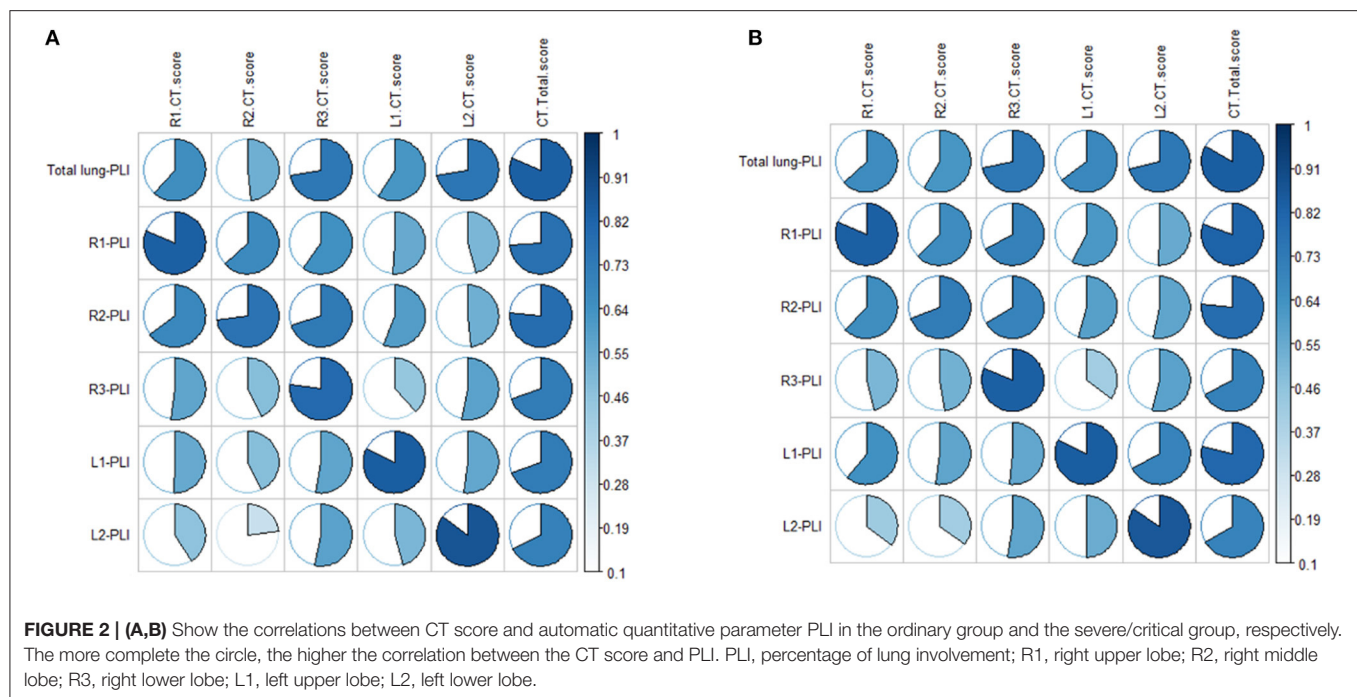
## The Stages and Dynamic Changes of Lung Involvement

A total of 265 CT scans were performed in 81 patients during their hospitalization. According to the quartile of all of the ordinary patients' 149 CT scans, the stages for the ordinary cases were as follows: the first stage on days 0–9, the second stage

on days 10–14, the third stage on days 15–20, and the fourth stage from day 21 to the endpoint. By the quartile of all of the severe/critical patients' 116 CT scans, the first stage for the severe/critical group was on days 0–9, the second stage on days 10–15, the third stage on days 16–22, and the fourth stage from day 23 to the endpoint. The fitted curve of the PLI shows that pulmonary lesions reached their maximum severity on the 18th day for the ordinary group, while it was the 14th day for the severe/critical group. See **Figure 1** for details.

## CT Quantitative Evaluation of Lung Lobes

Correlation analysis between the CT score and the PLI value showed a high correlation in both the ordinary group and the severe/critical group, with the correlation coefficient of each lung lobe  $>0.8$ , as shown in **Figure 2**. In the first stage, there was a statistically significant difference in PLI between the right middle lobe and the left superior lobe of the two groups ( $6.2 \pm 13.3$  vs.  $12.8 \pm 16.7$ ,  $7.1 \pm 14.2$  vs.  $10.5 \pm 13.9$ ,  $P < 0.05$ ). In the second stage, there was a statistically significant difference in the whole lung, right superior lobe, right inferior lobe and left superior lobe ( $13.3 \pm 12.3$  vs.  $25.4 \pm 19.8$ ,  $9.9 \pm 16.1$  vs.  $25.3 \pm 23.4$ ,  $20 \pm 19.3$



vs.  $36.6 \pm 25.2$ ,  $8.3 \pm 10$  vs.  $17.9 \pm 17.9$ ,  $P < 0.05$ ). The lung lobes with significant differences in the fourth stage were the same as those in the second stage ( $12.2 \pm 13.4$  vs.  $21 \pm 15.2$ ,  $9 \pm 14.9$  vs.  $23.1 \pm 21.7$ ,  $17.7 \pm 17.7$  vs.  $28.8 \pm 22.7$ ,  $9.9 \pm 13.3$  vs.  $17.9 \pm 13$ ,  $P < 0.05$ ). There was no significant difference in PLI in all lobes of the lung in the third stage ( $P > 0.05$ ), as shown in Table 2 and Figure 3.

## CT Quantitative Evaluation of Lung Segments

In the first stage, there was a statistically significant difference in the PLIs in the lateral and medial segments of the right middle lobe and the inferior lingular segment in the left upper lobe ( $P < 0.05$ ) in the two groups. In the second stage, the PLIs of the ordinary and severe/critical groups were significantly different in the apical, posterior, and anterior segments of the superior lobe of the right lung, all five segments in the right inferior lung, and the superior lingular segment of the left superior lung. In the fourth stage, PLIs between the two groups in the apical, anterior, and posterior segment of the right superior lobe and superior and the medial basal segment of the right inferior lobe were significantly different. See details in Figure 4.

The ROC curve shows the greatest diagnostic power in the lateral segment of R2 in the first stage, anterior segment of R1 in the second stage, and posterior segment of the right upper lobe in the fourth stage with AUC, sensitivity, and specificity respectively of 0.721, 0.755, 0.734; 0.937, 0.556, 0.577; and 0.5, 0.906, 0.889. See Table 3 for details.

The scatter graph shows that the progress of the lateral segment of the right middle lobe was faster in the severe/critical group than that of the ordinary group from the second day in the first stage. In the second stage, the progress of the anterior

segment of the right upper lobe was faster in the severe/critical group than that of the ordinary group on the 13th day, as shown in Figure 5. The fitted line of the fourth stage did not show statistical significance. Examples of the lung involvement evolution of two patients on CT images detected by AI software are shown in Figure 6.

## DISCUSSION

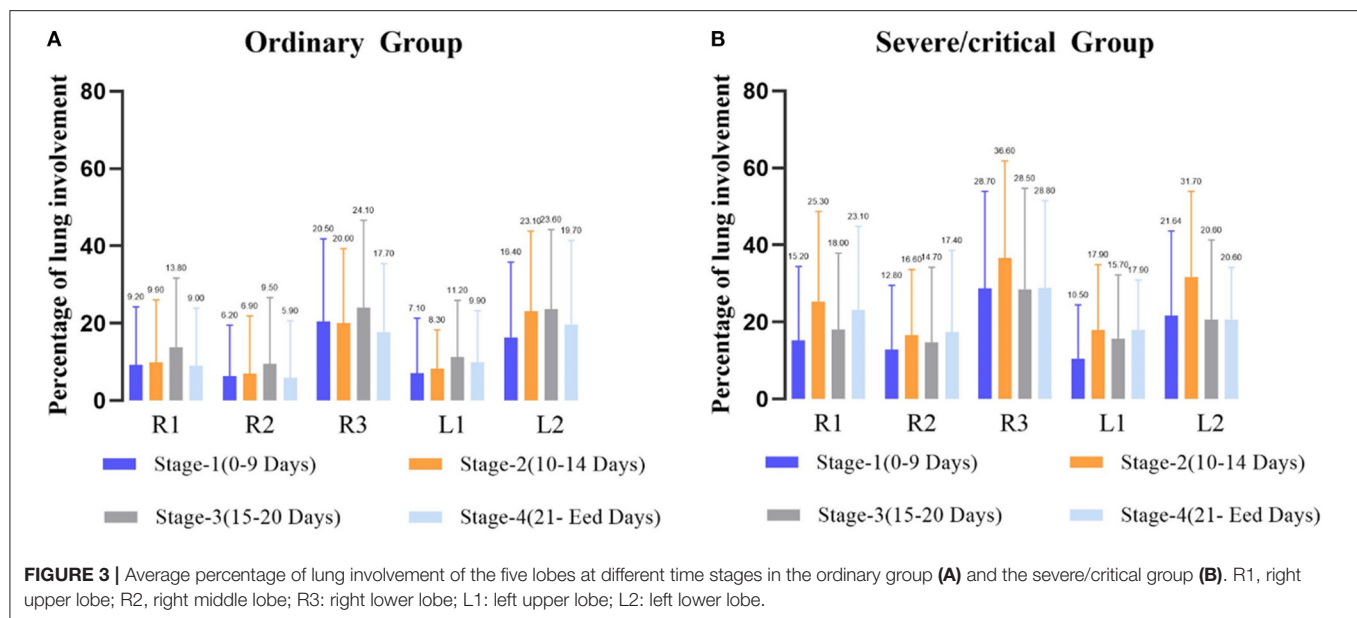
Our study showed that age is the most important factor in differentiating the ordinary and severe/critical patients by demographics and clinical characteristics, which further supports previous research showing that older adults with COVID-19 are more likely to suffer from severe disease and have a poor prognosis (10). In addition, we found that the time to the lung involvement peak of the severe/critical patients is earlier than that of ordinary patients, which indicates that the severe/critical patients progress more swiftly, maybe due to the existence of a cytokine storm syndrome (11). Finally, we identified two major meaningful lung segments and timepoints in severe/critical patients. The lung involvement in the lateral segment of the right middle lobe on the second day and anterior segment in the right upper lobe on the 13th day after onset may suggest the possibility of potentially severe patients. Of note, the percentage of lung involvement had a high correlation with CT score, which suggested that the AI system we applied is highly reliable, which is consistent with other studies that the AI system can be a supplementary diagnostic method for clinicians (12).

This study showed that although age is an important indicator, it can only act as a risk factor during follow-up and was unable to predict short-term disease development. CT imaging can be

**TABLE 2** | Percentages of lung involvement in different stages of the ordinary and severe/critical groups.

	Stage-1		Stage-2		Stage-3		Stage-4	
	Ordinary group (n = 42)	Severe/critical group (n = 32)	Ordinary group (n = 32)	Severe/critical group (n = 27)	Ordinary group (n = 39)	Severe/critical group (n = 31)	Ordinary group (n = 36)	Severe/critical group (n = 26)
PLI of bilateral lungs (%)	11.9 ± 14.7	17.3 ± 17.2	13.3 ± 12.3	25.4 ± 19.8	16.4 ± 16.1	19.4 ± 17.4	12.2 ± 13.4	21 ± 15.2
P-value	0.131		0.011*		0.582		0.015*	
PLI of R1 (%)	9.2 ± 15	15.2 ± 19.2	9.9 ± 16.1	25.3 ± 23.4	13.8 ± 17.9	18 ± 19.9	9 ± 14.9	23.1 ± 21.7
P-value	0.058		0.003*		0.566		0.005*	
PLI of R2 (%)	6.2 ± 13.3	12.8 ± 16.7	6.9 ± 15	16.6 ± 17	9.5 ± 17.1	14.7 ± 19.5	5.9 ± 14.7	17.4 ± 21.2
P-value	0.003*		0.011		0.442		0.051	
PLI of R3 (%)	20.5 ± 21.3	28.7 ± 25.2	20 ± 19.3	36.6 ± 25.2	24.1 ± 22.5	28.5 ± 26.2	17.7 ± 17.7	28.8 ± 22.7
P-value	0.114		0.008*		0.425		0.046*	
PLI of L1 (%)	7.1 ± 14.2	10.5 ± 13.9	8.3 ± 10	17.9 ± 17.9	11.2 ± 14.7	15.7 ± 16.5	9.9 ± 13.3	17.9 ± 13
P-value	0.047*		0.013*		0.135		0.005*	
PLI of L2 (%)	16.4 ± 19.4	21.64 ± 22	23.1 ± 20.7	31.7 ± 22.2	23.6 ± 21.1	20.6 ± 20.7	19.7 ± 21.7	20.6 ± 13.5
P-value	0.27		0.153		0.591		0.185	

PLI, percentage of lung involvement; R1, right upper lobe; R2, right middle lobe; R3, right lower lobe; L1, left upper lobe; L2, left lower lobe. \* $p < 0.05$ .

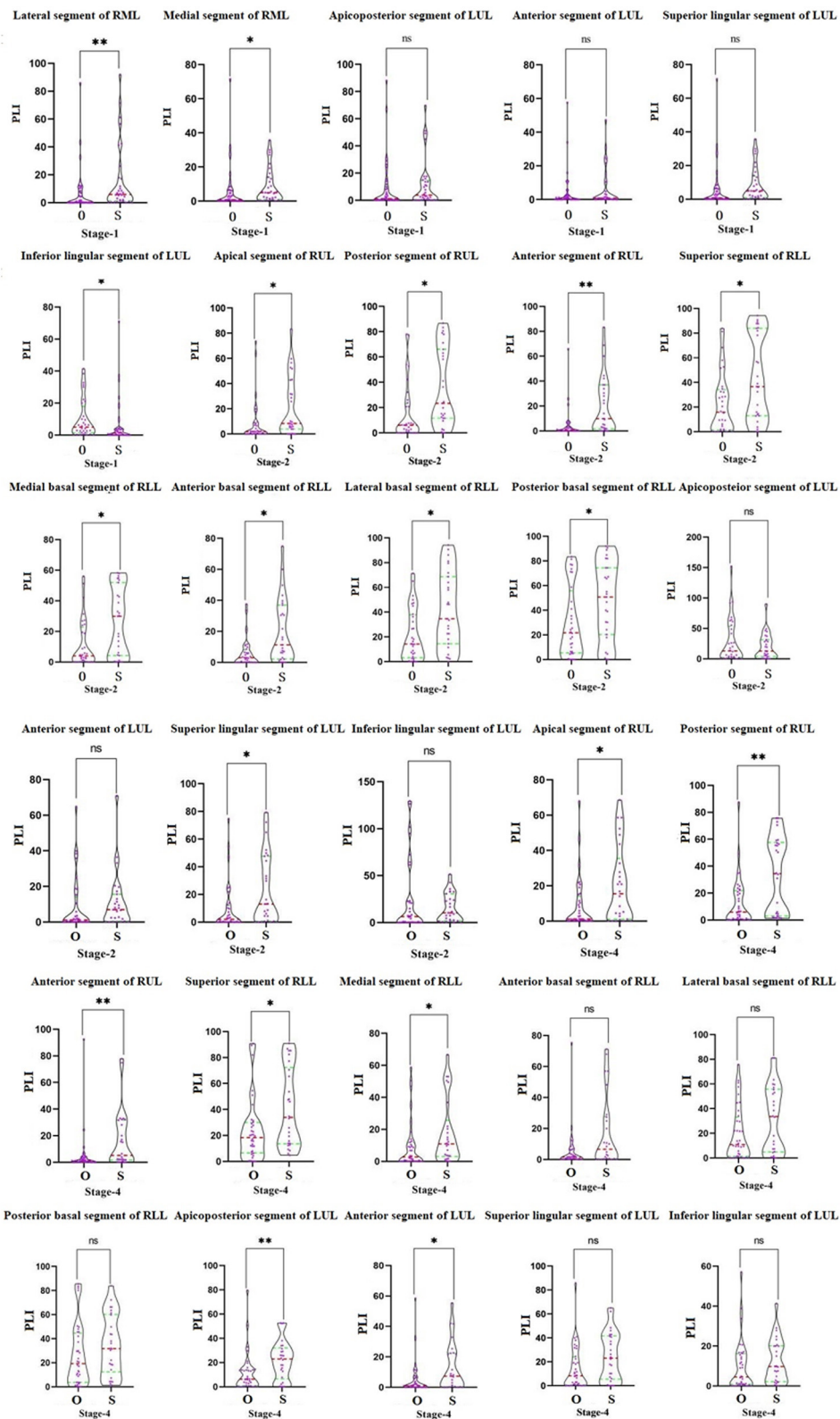


used as a powerful predictive tool for early warning of short-term disease progression during follow-up. However, it needs to be emphasized that CT is a monitoring method for use only during a special period, and it is still necessary to consider the radiation damage of CT. Therefore, it is significant to identify the key timepoints of the disease for optimizing the frequency of CT examinations.

In this study, we first used the traditional visual CT score to analyse the entire treatment timeline and it showed that the peak time of lung involvement in the ordinary and severe/critical groups were 18 and 14 days, respectively. The time to the peak of severe/critical disease is obviously shorter, which may be related to the existence of a cytokine storm syndrome. The peak time of bilateral lower lung involvement of severe/critical patients was in

the second stage (10–15 days), which is consistent with the results of the study by Heshui et al. (13), who found that the disease reached a peak within 2 weeks after onset and was mainly in the lower lobe. This may be because viral pneumonia mainly involves the lower lobes (14).

Furthermore, our study based on average PLIs at each stage further confirmed our results, that is, whether in the ordinary group or the severe group, the lung involvement of the bilateral lower lobes was greater than of the other lobes. In the severe group, we found the lung involvement peaks were during the second stage, and they were significantly higher than that of the ordinary patients at the same stage, which further shows that the severely ill patients had experienced rapid development in the second stage. However, lung involvement in the right middle lobe



**FIGURE 4 |** The comparison of the percentage of lung involvement of 18 lung segments in five lung lobes between the ordinary group and the severe/critical group. The red dotted line represents the median, and the green dotted line represents the quartile. O means ordinary group and S means severe/critical group. PLI, percentage of lung involvement; RML, right middle lobe; LUL, left upper lobe; RUL, right upper lobe; RLL, right lower lobe. \* $P < 0.05$ , \*\* $P < 0.01$ .



reached its highest in the fourth stage, and we speculate that this may be related to the lateral segment of the right middle lobe progressing rapidly in the first stage, staying stable during the

**TABLE 3 |** Diagnostic efficacy of percentage of lung involvement in the lung segments in different stages.

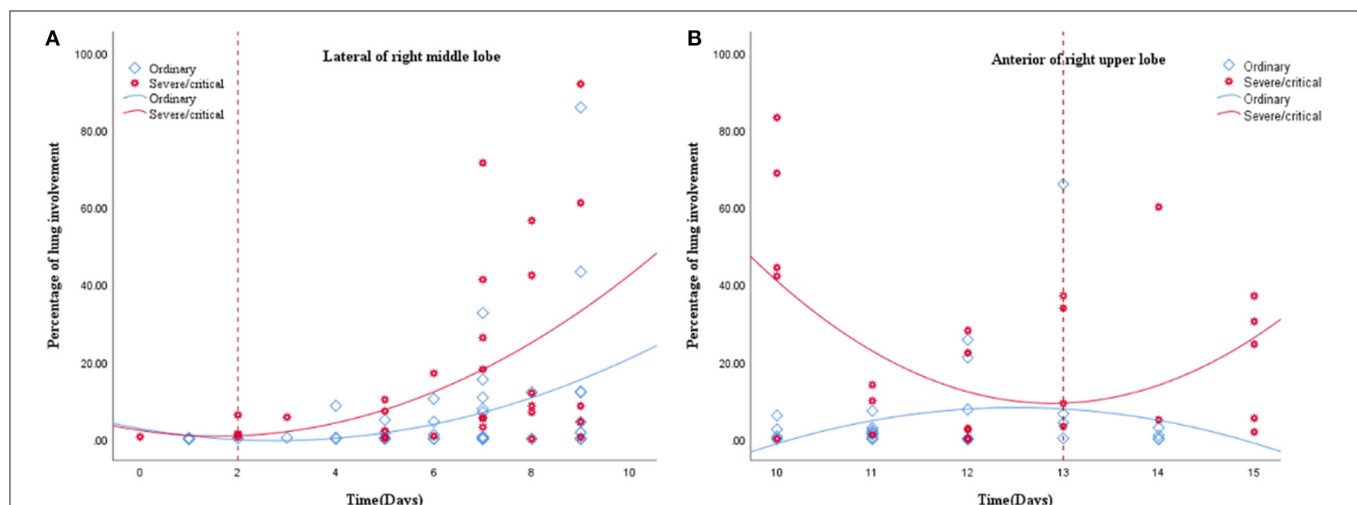
	Name of lung segment	AUC	Sensitivity	Specificity
Stage-1	Inferior lingular segment of L1	0.683	0.562	0.786
	Lateral segment of R2	0.721*	0.937	0.5
	Medial segment of R2	0.662	0.781	0.524
Stage-2	Apical segment of R1	0.662	0.778	0.625
	Posterior segment of R1	0.729	0.815	0.687
	Anterior segment of R1	0.755*	0.556	0.906
	Superior segment of R3	0.689	0.556	0.781
	Anterior basal segment of R3	0.72	0.704	0.719
	Medial basal segment of R3	0.69	0.519	0.875
	Lateral basal segment of R3	0.699	0.741	0.594
	Posterior basal segment of R3	0.659	0.704	0.625
Stage-4	Superior lingular segment of L1	0.634	0.407	0.875
	Anterior segment of R1	0.705	0.769	0.639
	Apical segment of R1	0.669	0.462	0.861
	Posterior segment of R1	0.734*	0.577	0.889
	Superior segment of R3	0.674	0.538	0.833
	Medial Basal segment of R3	0.678	0.885	0.417
	Apicoposterior segment of L1	0.707	0.692	0.778
	Anterior segment of L1	0.657	0.5	0.833

\*Represents the lung segment that contributes the most to lung involvement at each stage. R1, right upper lobe; R2, right middle lobe; R3, right lower lobe; L1, left upper lobe; L2, left lower lobe.

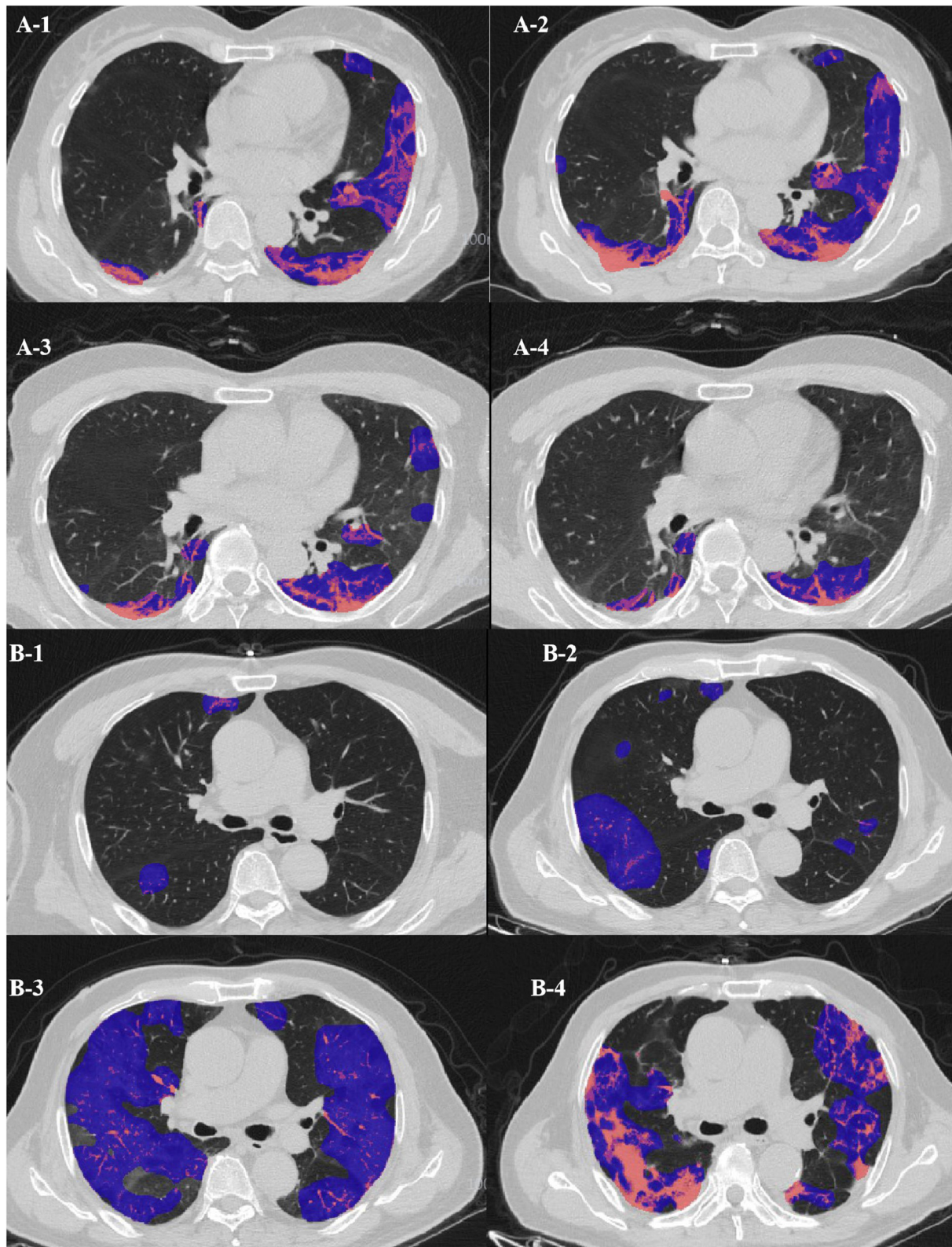
later stage and then being absorbed slowly. A systematic review by Sana et al. (15) demonstrated that the greatest severity of CT findings was visible around day 10 after symptom onset, which is similar to the peak in our severe/critical group but a little earlier than that of our ordinary group. They showed that the imaging signs resolved after week 2 of the disease, which is also consistent with our results for the severe/critical group progressing earlier than the ordinary group.

In addition, we found a strange phenomenon. Among the five lobes, the peaks of the right upper, middle, and left upper lungs all occurred in the fourth stage, while the two lower lung involvement peaks occurred in the second stage. During the development of the disease, we speculate that the infection route of COVID-19 may develop from the bottom of the lung to the tip of the lung. This is significantly different from the lung involvement progression of ordinary patients, which occurs at the third stage peak. This may also be an early warning of the development of severe patients.

To further clarify the progress of severe patients in different precise anatomical locations in the lung lobes, it is necessary to evaluate the segmental lung involvement. Recent studies on COVID-19 have shown that the superior and posterior basal segments of the lower lobe of the lungs are the main locations affected by COVID-19 (16). However, due to the small range of lung segments, the use of traditional semi-quantitative and descriptive assessments of the evolution of the lesions in the corresponding small lung segments may have large deviations, especially for severe patients, and thus subjective evaluation may not reveal the dynamic relationship between development of the disease and time. Therefore, quantitative research using an AI system may be more accurate in revealing small-scale longitudinal lesion changes such as in the lung segments.



**FIGURE 5 | (A,B)** show the fitted line of the lung involvement of the lateral segment of the right middle lobe and anterior segment of the right superior lobe in the first and second stages, respectively. The fit line formula of the first stage is  $Y = 2.23 - 1.88 * x + 0.59 * x^2$  ( $R^2 = 0.213$ ,  $P = 0.031$ ), and the formula of the second stage is  $Y = 6.42E2 - 98.18 * x + 3.81 * x^2$  ( $R^2 = 0.238$ ,  $P = 0.038$ ), in which  $x$  = days from the onset of the initial symptoms,  $y$  = percentages of lung involvement of lateral segment of right middle lobe and anterior segment of right upper lobe, respectively. The fit line plot shows that lung involvement accelerated on days 2 and 13 for the ordinary group and severe/critical group, respectively.



**FIGURE 6 | (A)** Evolution of CT findings in a 51-year-old female patient of the clinically ordinary type presenting with persistent fever ( $37.8^{\circ}\text{C}$ ) for 5 days. **(A-1)** At the presentation (stage 1, day 5), with a PLI of 18.11%, showing a small region of subpleural GGO with partial consolidation mainly in the left upper lobe; **(A-2)** stage 2  
(Continued)

**FIGURE 6** | day 10, with a PLI of 25.48%, a region of GGO enlarged while the density decreased; **(A-3)** stage 3 day 16, the density of the GGO further resolved, with a PLI of 14.71%; **(A-4)** stage 4 day 28, with a PLI of 8.93%, resolution with minimal residual GGO and parenchymal bands. **(B)** Evolution of CT findings in a 68-year-old male patient of the clinically severe type presenting with persistent fever (38.3°C) for 3 days, and with coronary heart disease for 5 years. **(B-1)** At presentation (stage 1, day 2), with a PLI of 2.7%, only small patchy GGO was visible; **(B-2)** stage 2 day 11, with a PLI of 12.7%, progressed into large patchy region of GGO; **(B-3)** stage 3 day 18, with a PLI of 57.75%, bilateral “white lung”; **(B-4)** stage 4 day 23, with a PLI of 48.87%, the “white lung” resolved obviously.

Although AI cannot replace expert assessment at this stage, AI can provide considerable information to help clinicians perform rapid and complex decision-making. In this study, our results show a correlation between the percentage of lesions extracted by AI and the percentage of lesion involvement manually evaluated exceeds 0.8, which proves the reliability of the AI intelligent recognition system in identifying the lesions of COVID-19 pneumonia patients in this study. The AI-based quantitative analysis results show that the lesions in the anterior segment of the right upper lobe of the severe type in the second stage were significantly accelerated compared with the ordinary type.

Another result of this study is that the peak of the percentage of lung lesions in severe patients appeared in the second stage, and during the entire lesion change of right upper lobe over time, the peak of the second stage was already close to the peak of the fourth stage, so we speculate the lesions in the upper lobe of the right lung, especially the changes in the anterior segment lesions, may be an important sign of the accelerated progression of severe patients in the advanced stage. The mechanism that causes the rapid progression of the lesion may also be related to the anatomical structure of the upper lung lobe. An earlier study showed that when the lung is full of secretions, due to the anatomical position of the upper lung lobe, the vertical gradient of lung blood flow will affect the upper lobe ventilation or asymmetric perfusion, which leads to repeated infections and scars more likely to occur in the lower ventilated upper lobe (17). The pathological autopsies of patients who died from COVID-19 showed that there is a large amount of mucus secreted between the alveoli (18), so the progression of the lesions in the upper right lobe, especially the anterior segment, may further reflect this pathological mechanism. The peak of pneumonia in severe patients at 14 days also further supports this pathological mechanism, which may indicate the short-term effect of an inflammatory storm.

In addition, we found that the lateral segment of the right middle lobe in the first stage is also a typical anatomical site for severe pneumonia. Studies have shown that bronchiectasis caused by atypical infection is more serious in the right middle lobe, usually manifesting as bronchiectasis and atelectasis. It has also been shown that bronchiectasis has a greater impact on the middle lobe of the right lung (19, 20). Existing COVID-19 research has shown that traction bronchiectasis may reflect the viral load and virulence of COVID-19, and it is more common in emergency patients (21). The time curve shows that the lesions of the right middle lobe of the right lung in the first stage of severe patients progressed significantly faster than in ordinary patients, so we speculate that bronchiectasis in the early stage, especially on the second day, may be an early warning message for potentially severe patients.

Another study performed at the lung segment level also showed that COVID had a predominance of bilateral lower distribution, which is consistent with the previous descriptive studies (9, 21) and may be due to the physiologic characteristics of the lung caused by regional inhomogeneity as a result of the influence of gravity (22). However, the anterior segment in severe cases also progresses rapidly, and this may be attributed to many severe patients needing to lie down due to insufficiency of effective oxygen from their severe pneumonia, which then aggravates the lung involvement. This study further explored lung segment involvement and identified the most suggestive lung segments and their corresponding time for potentially severe/critical patients. Another explanation for this finding could be the fact that viral infections are prone to involve the lower lungs (13). A previous study showed CT signs of aggravation and repair coexisted in advanced-phase disease. Our graph of this study showed the lung involvement in all lobes in the ordinary group in the last stage resolved more obviously than those in the severe/critical group, which may be due to the weaker organ function in the elderly patients in the severe/critical group (23).

Our study has some limitations. First, the sample size is small, and pediatric patients are not included. Therefore, the results may only represent a specific age group of COVID-19 patients. Second, we do not have any treatment information about these patients, which may affect the patients' time course and CT quantification results. Finally, severe and critical cases were studied as one whole group. We may consider an independent study of critical cases in the future.

In conclusion, lung involvement in the lateral segment of the right middle lobe in the early stage or the rapid progression of the anterior segment of the right superior lobe in the middle stage is highly suspicious for a poor conversion, which can be used as a warning message for severe/critical patients.

## DATA AVAILABILITY STATEMENT

The original contributions presented in the study are included in the article/**Supplementary Material**, further inquiries can be directed to the corresponding author/s.

## ETHICS STATEMENT

The studies involving human participants were reviewed and approved by Ethics committee of Wuhan Wuchang Hospital. Written informed consent for participation was not required for this study in accordance with the



national legislation and the institutional requirements. Written informed consent was waived for this was a retrospective study, which involved no potential risk to the patients.

## AUTHOR CONTRIBUTIONS

XY, GX, and SZ designed the study. YL, SZ, and XY performed the data acquisition and analysis. XY and SZ drafted and wrote the manuscript. All authors contributed to the article and approved the submitted version.

## REFERENCES

- Asselah T, Duranetel D, Pasmant E, Lau G, Schinazi RF. COVID-19: discovery, diagnostics and drug development. *J Hepatol.* (2021) 74:168–84. doi: 10.1016/j.jhep.2020.09.031
- National Health Commission of the People's Republic of China. *Diagnosis and Treatment Protocols of Pneumonia Caused by a Novel Coronavirus (Trial Version 7).*
- Li K, Wu J, Wu F, Guo D, Chen L, Fang Z, et al. The clinical and chest CT features associated with severe and critical COVID-19 pneumonia. *Invest Radiol.* (2020) 55:327–31. doi: 10.1097/RLI.0000000000000672
- Ai T, Yang Z, Hou H, Zhan C, Chen C, Lv W, et al. Correlation of chest CT and RT-PCR testing for coronavirus disease 2019 (COVID-19) in China: a report of 1014 cases. *Radiology.* (2020) 296:E32–40. doi: 10.1148/radiol.20200642
- Chung M, Bernheim A, Mei X, Zhang N, Huang M, Zeng X, et al. CT imaging features of 2019 novel coronavirus (2019-nCoV). *Radiology.* (2020) 295:202–7. doi: 10.1148/radiol.20200230
- Pan Y, Guan H, Zhou S, Wang Y, Li Q, Zhu T, et al. Initial CT findings and temporal changes in patients with the novel coronavirus pneumonia (2019-nCoV): a study of 63 patients in Wuhan, China. *Eur Radiol.* (2020) 30:3306–9. doi: 10.1007/s00330-020-06731-x
- Xie X, Zhong Z, Zhao W, Zheng C, Wang F, Liu J. Chest CT for typical 2019-nCoV pneumonia: relationship to negative RT-PCR testing. *Radiology.* (2020) 296:E41–5. doi: 10.1148/radiol.20200343
- Bernheim A, Mei X, Huang M, Yang Y, Fayad ZA, Zhang N, et al. Chest CT findings in coronavirus disease-19 (COVID-19): relationship to duration of infection. *Radiology.* (2020) 295:200463. doi: 10.1148/radiol.20200463
- Pan F, Ye T, Sun P, Gui S, Liang B, Li L, et al. Time course of lung changes on chest CT during recovery from 2019 novel coronavirus (COVID-19) pneumonia. *Radiology.* (2020) 295:715–21. doi: 10.1148/radiol.20200370
- Wang W, Tang J, Wei F. Updated understanding of the outbreak of 2019 novel coronavirus (2019-nCoV) in Wuhan, China. *J Med Virol.* (2020) 92:441–7. doi: 10.1002/jmv.25689
- Huang C, Wang Y, Li X, Ren L, Zhao J, Hu Y, et al. Clinical features of patients infected with 2019 novel coronavirus in Wuhan, China. *Lancet.* (2020) 395:497–506. doi: 10.1016/S0140-6736(20)30183-5
- Li L, Qin L, Xu Z, Yin Y, Wang X, Kong B, et al. Artificial intelligence distinguishes covid-19 from community acquired pneumonia on chest ct. *Radiology.* (2020) 296:E65–71. doi: 10.1148/radiol.20200905
- Wang Q, Zhang Z, Shi Y, Jiang Y. Emerging H7N9 influenza A (novel reassortant avian-origin) pneumonia: radiologic findings. *Radiology.* (2013) 268:882–9. doi: 10.1148/radiol.13130988
- Shi H, Han X, Jiang N, Cao Y, Alwalid O, Gu J, et al. Radiological findings from 81 patients with COVID-19 pneumonia in Wuhan, China: a descriptive study. *Lancet Infect Dis.* (2020) 20:425–34. doi: 10.1016/S1473-3099(20)30086-4
- Salehi S, Abedi A, Balakrishnan S, Gholamrezanezhad A. Coronavirus disease 2019 (COVID-19): a systematic review of imaging findings in 919 patients. *Am J Roentgenol.* (2020) 215:87–93. doi: 10.2214/AJR.20.23034
- Yang W, Cao Q, Qin L, Wang X, Cheng Z, Pan A, et al. Clinical characteristics and imaging manifestations of the 2019 novel coronavirus disease (COVID-19): a multi-center study in Wenzhou city, Zhejiang, China. *J Infect.* (2020) 80:388–93. doi: 10.1016/j.jinf.2020.02.016
- Friedman PJ, Harwood IR, Ellenbogen PH. Pulmonary cystic fibrosis in the adult: early and late radiologic findings with pathologic correlations. *AJR Am J Roentgenol.* (1981) 136:1131–44. doi: 10.2214/ajr.136.6.1131
- Xu Z, Shi L, Wang Y, Zhang J, Huang L, Zhang C, et al. Pathological findings of COVID-19 associated with acute respiratory distress syndrome. *Lancet Respir Med.* (2020) 8:420–2. doi: 10.1016/S2213-2600(20)30076-X
- Lee Y, Song JW, Chae EJ, Lee HJ, Lee CW, Do KH, et al. CT findings of pulmonary non-tuberculous mycobacterial infection in non-AIDS immunocompromised patients: a case-controlled comparison with immunocompetent patients. *Br J Radiol.* (2013) 86:20120209. doi: 10.1259/bjr.20120209
- Lynch DA, Simone PM, Fox MA, Bucher BL, Heinig MJ. CT features of pulmonary *Mycobacterium avium* complex infection. *J Comput Assist Tomogr.* (1995) 19:353–60. doi: 10.1097/00004728-199505000-00003
- Zhao W, Zhong Z, Xie X, Yu Q, Liu J. Relation between chest CT findings and clinical conditions of coronavirus disease (COVID-19) pneumonia: a multicenter study. *Am J Roentgenol.* (2020) 214:1072–7. doi: 10.2214/AJR.20.22976
- Gurney J, Schroeder B. Upper lobe lung disease: physiologic correlates. *Rev Radiol.* (1988) 167:359–66. doi: 10.1148/radiology.167.2.3282257
- Zhou S, Wang Y, Zhu T, Xia L. CT features of coronavirus disease 2019 (COVID-19) pneumonia in 62 patients in Wuhan, China. *Am J Roentgenol.* (2020) 214:1287–94. doi: 10.2214/AJR.20.22975

## FUNDING

This work was supported by National Key Research and Development Projects (2017YFC0114103) and Key Research and Development Projects in Zhejiang Province (2020C01058).

## SUPPLEMENTARY MATERIAL

The Supplementary Material for this article can be found online at: <https://www.frontiersin.org/articles/10.3389/fpubh.2021.596938/full#supplementary-material>

**Conflict of Interest:** The authors declare that the research was conducted in the absence of any commercial or financial relationships that could be construed as a potential conflict of interest.

Copyright © 2021 Yuyun, Lexi, Haochu, Zhenyu and Xiangyang. This is an open-access article distributed under the terms of the Creative Commons Attribution License (CC BY). The use, distribution or reproduction in other forums is permitted, provided the original author(s) and the copyright owner(s) are credited and that the original publication in this journal is cited, in accordance with accepted academic practice. No use, distribution or reproduction is permitted which does not comply with these terms.





# COVID-19 Score for Testing Symptomatic Low Risk Children: “STUDY SAFE”

Gavriela Feketea<sup>1,2\*</sup> and Vasiliki Vlachas<sup>2,3\*</sup>

<sup>1</sup> “Iuliu Hatieganu” University of Medicine and Pharmacy, Cluj-Napoca, Romania, <sup>2</sup> Paediatric Department, Karamandaneio Children's Hospital of Patras, Patras, Greece, <sup>3</sup> Department of Early Years Learning and Care, University of Ioannina, Ioannina, Greece

**Keywords:** RT-PCR—polymerase chain reaction with reverse transcription, SARS-CoV-2, COVID-19, scoring—algorithm, safety

## OPEN ACCESS

### Edited by:

Stephen Allen Morse,  
Centers for Disease Control and  
Prevention (CDC), United States

### Reviewed by:

Mark Graham,  
King's College London,  
United Kingdom  
Silvia Garazzino,  
University Hospital of the City of  
Health and Science of Turin, Italy

### \*Correspondence:

Gavriela Feketea  
gabychni@otenet.gr;  
feketea.gabriela@umfcluj.ro  
Vasiliki Vlachas  
vasovlaha@gmail.com

### Specialty section:

This article was submitted to  
Infectious Diseases - Surveillance,  
Prevention and Treatment,  
a section of the journal  
Frontiers in Medicine

**Received:** 21 December 2020

**Accepted:** 19 May 2021

**Published:** 15 June 2021

### Citation:

Feketea G and Vlachas V (2021)  
COVID-19 Score for Testing  
Symptomatic Low Risk Children:  
“STUDY SAFE”.  
Front. Med. 8:644813.  
doi: 10.3389/fmed.2021.644813










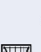







Telemedicine has undergone remarkable expansion since the beginning the COVID-19 pandemic (1), for visits related not only to COVID-19, but also other acute and chronic illnesses. The major advantage of telemedicine is the opportunity for patients to receive medical advice in their own home, without the risk of exposure to SARS-CoV-2. It has been shown that virtual medical visits significantly decrease the mortality of some medical conditions such as cardiac diseases (2). The use of algorithms appears to facilitate the practice of telemedicine.

SARS-CoV-2 has expanded rapidly over the world. The vaccines against COVID-19 have been implemented extensively by many countries but herd immunity is, as yet, far from being achieved. Currently, only one vaccine has been authorized to be used for adolescents above the age of 16 years. However, according to the recommendations of the US Centers for Disease Control and Prevention (CDC), even if a youngster has been immunized, testing should be done in the case of symptoms related to COVID-19 (3). Most of the children infected with SARS-CoV-2 are asymptomatic or develop mild symptoms, but even in the presymptomatic or asymptomatic state, school-age children and adolescents can transmit the infection to vulnerable individuals.



During the past winter, 2020–2021, a significant decrease in the prevalence of respiratory viral infections was noted, which is attributed to the preventive measures instituted against COVID-19 (4). As a result, children with viral symptoms are regarded as having a high suspicion of COVID-19 infection. Both the CDC and the European Centre for Disease Prevention and Control (ECDC) recommend the testing by RT-PCR for SARS-CoV-2 of all patients presenting to the health care system with symptoms compatible with COVID-19 infection, as part of active case finding for SARS-CoV-2 (5, 6), wherever testing capacity is sufficient. Testing all children with fever and/or cough will be difficult for several countries with limited test supplies and/or when the health system is overwhelmed. In an attempt to conserve resources and to formulate the means of evaluation via telemedicine, taking into consideration the evidence that children usually suffer from mild COVID-19 infection, we developed the current “STUDY SAFE” algorithm.

This scoring system is straightforward and is based on epidemiological data concerning the child's exposure risk for COVID-19 (Figure 1). It can be easily implemented in telemedicine consultations, and can guide primary care physicians in making a decision about when a diagnostic RT-PCR test for COVID-19 needs to be performed in symptomatic school age children. The diagnostic tests for COVID-19 can be conducted at home by the caregiver, under the virtual guidance of the primary care doctor.

The patients at high-risk for severe COVID-19, such as children with comorbidities, and those with known exposure, will undergo testing without the need for scoring according to the algorithm. In addition, the children with moderate or severe symptoms should be advised to seek medical care immediately in an emergency department or an ambulatory health care setting,

	0	1	2	3
School (number of pupils) 	<15	15-20	>25	
Transport to/from school    	Car, cycle, walking	Carpooling with the same persons	School bus (same classmates)	Metro, train, bus (>15 minutes)
Urbanism (size of city) 	Small town	Big town	City	Capital of state or region
Disease (confirmed cases in community) 	No cases	Low	Medium	High
Youth disease (confirmed cases at school) 	No cases	1	>1 Cases only in one class	>1 Cases in different classes
Sports   	Outdoor, no body contact	Outdoor, team sports with minimal contact	Indoor no body contact	Indoor team sports, Common changing rooms, team-competitions
Activities (ex-school)  	With the same classmate	1 activity with other persons	>1 activity with other persons	Theater, acting, choir, wind instruments
Family  	0	Persons with risk for severe COVID-19	Parents – jobs with high exposure	Low economical status
Eating  	Only snacks from home	Catering lunch in classroom	Catering lunch in common area	

Score	Testing SARS-CoV-2 rapid test	Needed actions if testing is not possible	When to go back to school
<8	Negative test	Isolation at home as during a common viral infection	at least 24 hours after they no longer have symptoms <u>without</u> taking antipyretics
<8	Positive test	Isolation at home for 10 days	at least 24 hours after they no longer have symptoms <u>without</u> taking antipyretics
>8	Negative/Positive	Isolation at home for 10 days	at least 24 hours after they no longer have symptoms <u>without</u> taking antipyretics

  sample to be taken at home or at the nearest Centre - after telemedicine consultation

Testing with RT-PCR without scoring: children with a known exposure to a confirmed COVID-19 case, high-risk and medium-risk patients for severe COVID-19.

The high-risk for severe COVID-19 patients should be advised to immediately seek care in an emergency department, the medium-risk patients to visit an ambulatory setting and the low-risk patients to stay home with close follow-up by telemedicine.

**FIGURE 1** | COVID-19 score "STUDY SAFE" for testing low-risk school-age children with symptoms compatible with COVID-19.

according to the severity of the symptoms (7); prior notification of the health care department is highly recommended.

The score provided by the algorithm is calculated based on the risk of contracting and/or transmitting SARS-CoV-2. Various factors are taken into consideration, including the socioeconomic status, the risk of exposure, based on the nature of the child's activities, the practice of social distancing and the spread of SARS-CoV-2 in the local community.

The criteria for scoring stratification were determined based on the current knowledge and recommendations of public health authorities with regard to the risk for SARS-CoV-2 transmission in nine contexts, including the population density of the area, confirmed cases in the community and at school, the child's age, the number of pupils per school class, mode of transport, sports, extracurricular activities, family setting, dining conditions.

All the children with symptoms related to COVID-19 should remain at home and be tested with the SARS-CoV-2 rapid test. The children with a low score ( $< 8$ ) remain at home until their symptoms are improved and they have been fever free for 24 h without antipyretics. They can come out of confinement 24 h after they become afebrile without antipyretics and the rest of the symptoms have improved, according to CDC guidelines (8). The children with a positive rapid test should remain in isolation at home for 10 days. The children with a score of above 8 should remain in isolation for 10 days, even in the case of a negative rapid test. We came to that decision based on fact that this group of children have extensive social interactions, and the sensitivity of the SARS-CoV-2 rapid test has been reported to be between 34 and 88% (9). In order to avoid the diverse outcome of false negative results in those children with many possible contacts, we suggested that they remain at home for 10 days. They can come out of isolation when they have been afebrile for 24 h without antipyretics and the rest of their symptoms are improved.

The World Health Organization (WHO) recommends that schoolchildren maintain a physical distance of at least 1 m inside the classrooms and in areas with community transmission. In the case of cluster-transmission, WHO recommends a risk-based approach, and in areas with sporadic cases/no cases of COVID-19, only the children aged above 12 years should keep the physical distance of 1 m (10). According to the CDC, children in larger in-person activities and events have a medium risk for SARS-CoV-2 transmission (5). We consider low risk for COVID-19 transmission those classrooms with  $< 15$  pupils and high risk those with more than 25 pupils.

There is increasing evidence that indoor sports and sports with intensive body contact pose a higher risk of transmission than outdoor athletics and non-contact sports. CDC categorize team-based practice as increased risk, and as higher risk full competition between teams (5).

It has been shown up to the present, that the older children are responsible for higher transmission rate of SARS-CoV-2. The infection rate among family members in Southern Korea from index cases aged 0–9 years and 10–19 years was 5.3 and 18.6%, respectively (11). Based on that evidence we placed children aged above 10 years in a higher risk group for transmission.

With regard to dining at school, the CDC recommends the children to have meals outdoors as much as possible. When this is not feasible, they advise maintenance of a distance of 6 feet (2 m) while eating or in the food service line (5). In the

present risk assessment, we assigned higher points when the children were eating in the cafeteria compared with having lunch in the classroom.

During school transit, CDC recommends preferring forms of transport with minimal contact (5). In this algorithm we placed the children at higher risk for transmission when they were using public transport or the school bus for a trip of longer than 15 min.

The confirmed cases in the community are considered as "Low" when  $< 20$  new cases have been diagnosed per 100,000 people, "Medium" when 20–59.9/100,000 people have been diagnosed and "High" when  $> 60/100,000$  have been diagnosed in the past 2 weeks (12).

Every child with symptoms related to COVID-19 should have a SARS-CoV-2 rapid self-test performed by their parents. In Greece, the self-tests were introduced for surveillance in school-age children on a weekly basis in April 2021. In other countries, including the UK and Germany, such tests have been available for school children since February 2021.

The scoring system presented here could be a useful tool for screening school age children without comorbidities, presenting with mild symptoms, for performing RT-PCR test for SARS-CoV-2. The goal is to prevent COVID-19 transmission in the community. After the successful "stay home, stay safe" policy, as the schools are reopened, the school children will still need to stay at home when they are sick, preventing the viral spread, and return to school and their other activities when the risk of transmission has passed. As more information becomes available about COVID-19, this "STUDY SAFE" score may need revisions, but it is a starting point for clinicians to manage children without comorbidities in COVID-19 era. The diagnostic test for COVID-19 can be done at home by the parent under the virtual guidance of the clinician. The algorithm presented is a simple tool to guide the physicians and can be easily performed via telemedicine.

## AUTHOR CONTRIBUTIONS

GF and VV contributed equally to the design and implementation of the research, to the analysis of the results, to assemble the figure, and to the writing of the manuscript. All authors contributed to the article and approved the submitted version.

## REFERENCES

- Ye S, Kronish I, Fleck E, Fleischut P, Homma S, Masini D, et al. Telemedicine expansion during the COVID-19 pandemic and the potential for technology-driven disparities. *J Gen Intern Med.* (2021) 36:256–8. doi: 10.1007/s11606-020-06322-y
- Lange SJ, Ritchey MD, Goodman AB, Dias T, Twentyman E, Fuld J, et al. Potential indirect effects of the COVID-19 pandemic on use of emergency departments for acute life-threatening conditions — United States, January–May 2020. *MMWR Morb Mortal Wkly Rep.* (2020) 69:795–800. doi: 10.15585/mmwr.mm6925e2
- Christie A, Mbaeyi SA, Walensky RP. CDC Interim Recommendations for fully vaccinated people: an important first step. *JAMA.* (2021) 325:1501–2. doi: 10.1001/jama.2021.4367
- Chiu NC, Chi H, Tai YL, Peng CC, Tseng CY, Chen CC, et al. Impact of wearing masks, hand hygiene, and social distancing on influenza, enterovirus, and all-cause pneumonia during the coronavirus pandemic: retrospective national epidemiological surveillance study. *J Med Internet Res.* (2020) 22:e21257. doi: 10.2196/21257
- US Centers for Disease Control and Prevention. *Coronavirus Disease 2019 (COVID-19).* Available online at: <https://www.cdc.gov/coronavirus/>

- 2019-ncov/community/schools-childcare/index.html (accessed September 25, 2020).
6. European Centre for Disease Prevention and Control. *COVID-19 Testing Strategies and Objectives*. Available online at: <https://www.ecdc.europa.eu/en/publications-data/covid-19-testing-strategies-and-objectives> (accessed September 25, 2020).
  7. Feketea GM, Vlach V. A decision-making algorithm for children with suspected coronavirus disease 2019. *JAMA Pediatrics*. (2020) 174:1220–2. doi: 10.1001/jamapediatrics.2020.2999
  8. US Centers for Disease Control and Prevention. *When You Can be Around Others After You Had or Likely Had COVID-19*. Available online at: <https://www.cdc.gov/coronavirus/2019-ncov/if-you-are-sick/end-home-isolation.html> (accessed May 7, 2021).
  9. Griffin S. Covid-19: Lateral flow tests are better at identifying people with symptoms, finds Cochrane review. *BMJ*. (2021) 372:n823. doi: 10.1136/bmj.n823
  10. World Health Organization. *Q&A: Schools and COVID-19*. Available online at: <https://www.who.int/emergencies/diseases/novel-coronavirus-2019/question-and-answers-hub/q-a-detail/q-a-schools-and-covid-19> (accessed September 25, 2020).
  11. Park YJ, Choe YJ, Park O, Park S, Kim YM, Kim J, et al. Contact tracing during coronavirus disease outbreak, South Korea, 2020. *Emerg Infect Dis*. (2020) 26:2465–8. doi: 10.3201/eid2610.201315
  12. European Centre for Disease Prevention and Control. *Coronavirus Disease 2019 (COVID-19) in the EU/EEA and the UK—eleventh update: Resurgence of Cases*. Available online at: <https://www.ecdc.europa.eu/sites/default/files/documents/covid-19-rapid-risk-assessment-20200810.pdf> (accessed May 7, 2021).

**Conflict of Interest:** The authors declare that the research was conducted in the absence of any commercial or financial relationships that could be construed as a potential conflict of interest.

Copyright © 2021 Feketea and Vlach. This is an open-access article distributed under the terms of the Creative Commons Attribution License (CC BY). The use, distribution or reproduction in other forums is permitted, provided the original author(s) and the copyright owner(s) are credited and that the original publication in this journal is cited, in accordance with accepted academic practice. No use, distribution or reproduction is permitted which does not comply with these terms.





# Oropharyngeal Probiotic ENT-K12 Prevents Respiratory Tract Infections Among Frontline Medical Staff Fighting Against COVID-19: A Pilot Study

## OPEN ACCESS

### Edited by:

Stephen Allen Morse,  
Centers for Disease Control  
and Prevention (CDC), United States

### Reviewed by:

Dorothee Von Laer,  
Innsbruck Medical University, Austria  
Sumit Ghosh,  
The Research Institute at Nationwide  
Children's Hospital, United States

### \*Correspondence:

Qiang Wang  
wangqiang@wust.edu.cn  
Qingming Wu  
wuhe9224@sina.com  
Baoli Zhu  
zhubaoli@im.ac.cn  
Junbo Xia  
xjb47@126.com

† These authors have contributed  
equally to this work and share first  
authorship

### Specialty section:

This article was submitted to  
Biosafety and Biosecurity,  
a section of the journal  
Frontiers in Bioengineering and  
Biotechnology

Received: 04 January 2021

Accepted: 11 May 2021

Published: 24 June 2021

### Citation:

Wang Q, Lin X, Xiang X, Liu W,  
Fang Y, Chen H, Tang F, Guo H,  
Chen D, Hu X, Wu Q, Zhu B and Xia J  
(2021) Oropharyngeal Probiotic  
ENT-K12 Prevents Respiratory Tract  
Infections Among Frontline Medical  
Staff Fighting Against COVID-19:  
A Pilot Study.  
Front. Bioeng. Biotechnol. 9:646184.  
doi: 10.3389/fbioe.2021.646184

Qiang Wang<sup>1\*†</sup>, Xuan Lin<sup>2†</sup>, Xiaochen Xiang<sup>1</sup>, Wanxin Liu<sup>1</sup>, Ying Fang<sup>2</sup>, Haiping Chen<sup>2</sup>,  
Fang Tang<sup>2</sup>, Hongyan Guo<sup>2</sup>, Di Chen<sup>2</sup>, Xiafen Hu<sup>1</sup>, Qingming Wu<sup>1\*</sup>, Baoli Zhu<sup>3,4,5,6\*</sup> and  
Junbo Xia<sup>7\*</sup>

<sup>1</sup> Institute of Infection, Immunology and Tumor Microenvironment, Hubei Province Key Laboratory of Occupational Hazard Identification and Control, Medical College, Wuhan University of Science and Technology, Wuhan, China, <sup>2</sup> Huarun WISCO General Hospital Affiliated to Wuhan University of Science and Technology, Wuhan, China, <sup>3</sup> CAS Key Laboratory of Pathogenic Microbiology and Immunology, Institute of Microbiology, Chinese Academy of Sciences, Beijing, China, <sup>4</sup> Savaid Medical School, University of Chinese Academy of Sciences, Beijing, China, <sup>5</sup> Beijing Key Laboratory of Antimicrobial Resistance and Pathogen Genomics, Beijing, China, <sup>6</sup> Department of Pathogenic Biology, School of Basic Medical Sciences, Southwest Medical University, Luzhou, China, <sup>7</sup> Department of Pulmonary Medicine, Affiliated Hangzhou First People's Hospital, Zhejiang University School of Medicine, Hangzhou, China

Healthcare workers at the frontline are facing a substantial risk of respiratory tract infection during the COVID-19 outbreak due to an extremely stressful work schedule and public health event. A well-established first-line defense on oropharyngeal microbiome could be a promising strategy to protect individuals from respiratory tract infections including COVID-19. The most thoroughly studied oropharyngeal probiotic product which creates a stable upper respiratory tract microbiota capable of preventing upper respiratory tract infections was chosen to evaluate the safety and efficacy on reducing episodes of upper respiratory tract infections for COVID-19 healthcare workers. To our knowledge to date, this is the very first study describing the beneficial effects of oropharyngeal probiotic been administered by healthcare workers during the COVID-19 pandemic. In this randomized controlled trial, we provided the probiotics to frontline medical staff who work in the hospitals in Wuhan and had been in close contact with hospitalized COVID-19 patients for prophylactic use on a daily basis. Our finding suggests that oropharyngeal probiotic administration significantly reduced the incidence of respiratory tract infections by 64.8%, reduced the time experiencing respiratory tract infections and oral ulcer symptoms by 78%, shortened the days absent from work by 95.5%, and reduced the time under medication where there is no record of antibiotic and anti-viral drug intake in the probiotic group. Furthermore, medical staff treated with Bactoblis experienced sustained protection from respiratory tract infections since the 10th day of oropharyngeal probiotic administration resulting in an extremely low incidence rate of respiratory tract infections.

**Keywords: oropharyngeal probiotic ENT-K12, respiratory tract infections, healthcare workers, COVID-19, group A  $\beta$ -hemolytic streptococcus**

## INTRODUCTION

Frontline medical staff fighting against COVID-19 are facing a substantial risk of respiratory tract infection during the COVID-19 outbreak due to an extremely stressful work schedule and public health event. During January 20, 2020 and February 5, 2020, it has been observed that the case infection rate of healthcare workers (2.10%) was dramatically higher than that of non-healthcare workers (0.43%) in a tertiary hospital during the early stage of COVID-19 outbreak in Wuhan (Lichun et al., 2020). Not only the COVID-19, but the general respiratory tract infection risk of healthcare workers is clearly higher than that of non-healthcare workers (Yaowen et al., 2016). Healthcare workers play an essential role in fighting the unexpected pandemic. Providing effective protection for healthcare workers from respiratory infections is essential.

Recent studies have shown that the microbiota in the lung contributes to immunological homeostasis and can potentially, when affected by dysbiosis, alter susceptibility to viral infection, and with respect to COVID-19, a highly significant difference in the lung microbiota composition has been observed between patients with COVID-19 pneumonia and healthy subjects, implying a dysbiosis occurred in the lung microbiota of patients who had a pathogen-enriched microbiota; not only can lung microbiota dysbiosis create a more fertile ground for viral aggression, but it can also promote a worsening of the patient condition (Zijie et al., 2020). A half-year prospective cohort study showed that nasopharyngeal microecological imbalance was caused by trans-colonization of oral microbiota, leading to upper respiratory tract infections (Lirong et al., 2020). An earlier study also demonstrated that inducing immune responses that were localized to the airway were more protective against challenge with pathogenic human coronaviruses, and that the strategy of inducing innate and specific immune responses at airway epithelium cells could also be useful in the context of protecting human host from other pathogenic respiratory viruses (Jincun et al., 2016).

Apparently, as in many other respiratory pathogens, the coronavirus is transmitted from an infected person's mouth or nose through small liquid particles when they cough, sneeze, speak, or breathe heavily. Hence, the protection from these liquid particles of different sizes, ranging from larger "respiratory droplets" to smaller "aerosols," become a key target for protection. Specifically, for healthcare workers who are in close contact with hospitalized COVID-19 patients, it is extremely important to make sure that the healthcare workers are fully equipped with proper protection, e.g., secondary and tertiary prevention. One possible additional way to protect human host from respiratory tract infections is to boost the immunity and maintain a healthy and balanced microflora at oropharyngeal environment of individuals via probiotics administration (Olga et al., 2014; Clark et al., 2016; Martens et al., 2018). Probiotics are live, non-pathogenic bacteria that may have an effect on both viral and bacterial infection. Recent trials have demonstrated that probiotics may impact the immune system, but only the commensal oral probiotic strain *Streptococcus thermophilus* ENT-K12 has been shown to successfully colonize the oral cavity

and to modulate the nasopharyngeal microbiota (Ilchenko et al., 2019a,b). In fact, a slow-dissolved oropharyngeal probiotic formula containing ENT-K12 has been clinically demonstrated to improve the upper respiratory tract microbiota protecting the host from pathogenic bacteria, fungi, and viruses thereby reducing the incidence of viral respiratory tract infections and bacterial co-infections (Wilcox et al., 2019). With several clinical studies providing the safety and effectiveness (Wilcox et al., 2019), the said probiotic formula appears to be a promising agent to be administered for prophylactic or probiotic treatments to protect individuals during the outbreak of seasonal or emerging respiratory infection diseases.

## MATERIALS AND METHODS

The trial was conducted according to the criteria set by the Declaration of Helsinki and with the approval of the local ethics committee, the Ethics Committee of Medical school of Wuhan University of Science and Technology (registration number 202003). All the medical staff who participated in the trial were informed of the trial methods and signed the consent. The study product, Bactoblis oropharyngeal probiotic formula, is formulated in the form of slowly dissolving oral lozenges by Probiotet GmbH (Herisau, Switzerland); the preparation of this formula used in the clinical trial contained no less than 1 billion colony-forming units (cfu)/lozenge of *S. thermophilus* ENT-K12 over shelf-life.

The multicenter, open, randomized controlled clinical trial was conducted on 200 frontline medical staff enrolled in Wuhan, China, and treated between March 5, 2020 and April 5, 2020. All the enrolled individuals were healthy doctors and nurses 20–65 years of age and work in close contact with hospitalized COVID-19 patients; while taking care of the hospitalized COVID-19 patients, the subjects are fully equipped with proper protection, e.g., secondary and tertiary prevention. The following exclusion criteria were used: individuals who had an acute respiratory tract infection or have been diagnosed as COVID-19 infection, underwent antibiotic treatment at the time of enrolling, known allergy against milk proteins, and were immunocompromised or immunodeficient.

The enrolled medical staff were provided with a 1-month supply of study product and instructed to take 2 lozenges a day, taking a single lozenge after breakfast every morning and before bedtime after brushing their teeth every evening, respectively. The subjects were required to suck the lozenge until it is fully dissolved (approximately 4–5 min) and to make sure that the lozenge is not chewed or directly swallowed. They were instructed not to drink or swallow any substance for at least 1 h after the administration of the study product.

The study involved at least two visits over a 1-month period, screening visit (visit 1) and final visit (visit 2). Additional visits took place if the enrolled medical staff experienced symptoms of respiratory tract infections, so a diagnosis could be confirmed and if necessary, a prescription provided. At the screening visit (visit 1), the overall details of the study were explained to the enrolled medical staff and informed consent was obtained from

the said individuals. The medical history of the individuals was reviewed and inclusion and exclusion criteria were confirmed. The medical staff was asked to maintain their standard diet and exercise routine.

The participated subjects were required to return for final visits after 30 days and return any unused study product. Compliance will be assessed by counting unused lozenges at the final visit; compliance criteria judged at  $\geq 90\%$  of dispensed lozenges consumed.

The subjects were instructed to contact the study physician at any time during the study in case of symptoms of respiratory tract infection or pneumonia, such as sore throat, fever more than  $38^{\circ}\text{C}$ , dyspnea, enlarged lymph nodes, and/or the appearance of abscesses (pus) or white patches on tonsils. At each visit, any adverse events were recorded.

## Objectives

The primary objective of this study is to investigate the benefits of oropharyngeal probiotic in preventing respiratory tract infections in frontline medical staff who are in close contact with COVID-19 hospitalized patients during the COVID-19 outbreak that causes an extremely stressful work schedule. The secondary objective is to investigate the incidence rate of COVID-19 in hospital pneumonia infection, resorting to antibiotic therapy, treatment with antipyretics, anti-viral drugs, and steroids, and working days lost during the episodes of respiratory infections. The onset of side effects while the product was being administered has also been observed.

## Statistical Analysis

SPSS version 25.0 software is used for statistical analysis. For baseline characteristics of participants,  $M \pm SD$  was used to describe the variation degree of samples between groups, and  $M (P_{25}-P_{75})$  was used to describe if the data did not follow normal distribution. For the quantitative data of normal distribution, the difference between populations was inferred by the two independent samples *t*-test (Wilcoxon's rank sum test was used for the non-normal distribution data), and  $\chi^2$  test or Fisher's exact test was used for the qualitative data. The Kaplan-Meier statistic was used to estimate the level of protection of respiratory tract infection by administration of oropharyngeal probiotic over time. Survival analysis was used to determine the difference in cumulative morbidity among patients under different conditions during clinical observation.

## RESULTS

One-hundred medical staff were treated with two lozenges of study product daily for 30 consecutive days. The other 100 medical staff served as the control group in the same period. As shown in **Table 1**, the two groups did not differ in their baseline characteristics. Seven subjects dropped out of the study on the first few days after enrollment for personal reasons. Deducting the seven subjects dropping out from the study, 98 medical staff were treated for 30 days with probiotic, while 95 did not receive probiotic and were considered to be the control group.

**TABLE 1 |** The baseline characteristics of participants.

	Probiotic group	Control group	P value
Age	36.13 $\pm$ 8.62	35.74 $\pm$ 8.88	0.754 <sup>c</sup>
Gender			0.620 <sup>b</sup>
Male	30 (30/98)	26 (26/95)	
Female	68 (68/98)	69 (69/95)	
Professional category			0.522 <sup>b</sup>
Resident Doctor	10	11	
Attending Doctor	20	17	
Associate Chief Doctor	23	18	
Chief Doctor	7	3	
Nurse	38	46	
Daily working hours	7.09 $\pm$ 1.17	7.02 $\pm$ 1.09	0.664 <sup>c</sup>
Beds to attend	9 (7–15)	9 (6–12)	0.276 <sup>a</sup>
Pneumococcal vaccine			0.982 <sup>b</sup>
No	97	94	
Yes	1	1	
Influenza vaccine			0.964 <sup>b</sup>
No	94	91	
Yes	4	4	

*X  $\pm$  S is used to describe the average level and variability of the data.*

<sup>a</sup>Wilcoxon's rank sum test.

<sup>b</sup>Chi-square test.

<sup>c</sup>Student's *t*-test.

Compliance with the probiotic treatment was very good and well tolerated by the subjects with no side effects reported. The probiotic group consisted of 30 males and 68 females, mean age  $36.13 \pm 8.62$  years. The control group consisted of 26 males and 69 females, mean age  $35.74 \pm 8.88$  years. The two groups had no statistically significant differences in age and gender. As per the professional category of enrolled medical staff, the probiotic group consisted of 10 resident doctors, 20 attending doctors, 23 associate chief doctors, 7 chief doctors, and 38 nurses, with mean daily working hours  $7.09 \pm 1.17$  and average 9 beds to attend. The control group consisted of 11 resident doctors, 17 attending doctors, 18 associate chief doctors, 3 chief doctors, and 46 nurses, with mean daily working hours  $7.02 \pm 1.09$  and average 9 beds to attend. The two groups had no statistically significant differences in the constituent ratio of positions they hold, daily working hours, and beds to attend. Regarding the vaccination status of the enrolled medical staff, only 1 out of 98 in the probiotic group had pneumococcal vaccine and 4 out of 98 had influenza vaccine, while 1 out of 95 in the control group had pneumococcal vaccine and 4 out of 95 had influenza vaccine. The two groups had no statistically significant differences in the vaccination status.

**Table 2** shows the data on the prevalence of respiratory tract infection episodes during March 5, 2020 and April 5, 2020. Prophylaxis with oropharyngeal probiotic significantly reduced the incidence of respiratory tract infections by 64.8% ( $p < 0.005$ ) comparing with the control group, of which 8 episodes of respiratory tract infections were observed in the group of 98 probiotic-treated medical staff and 22 episodes were observed in the group of 95 non-treated medical staff, with none of the episodes having been confirmed to be COVID-19 infection verified by SARS-CoV-2 nucleic acid test (data not shown). Key

**TABLE 2 |** The difference analysis of each factor between two groups.

	Probiotic group	Control group	Total	P value
Incidence of respiratory tract infections	8/98 (8.16%)	22/95 (23.16%)	30/193 (15.54%)	0.004 <sup>b</sup>
Sore throat	4/98 (4.08%)	10/95 (10.53%)	14/193	0.084 <sup>b</sup>
Cough/itchy throat	3/98 (3.06%)	3/95 (3.16%)	6/193	0.969 <sup>b</sup>
Low fever	1/98 (1.02%)	5/95 (5.26%)	6/193	0.090 <sup>b</sup>
Nasal congestion/dizziness	0	2/95 (2.11%)	2/193	0.149 <sup>b</sup>
Acute otitis media	0	1/95 (1.05%)	1/193	0.492 <sup>c</sup>
Oral ulcer	0	1/95 (1.05%)	1/193	0.492 <sup>c</sup>
Sick days (days/person)	0.23 ± 0.961	1.05 ± 2.317	0.64 ± 1.807	0.004 <sup>a</sup>
Duration of each episode (days/episode)	2.88 ± 2.031	4.67 ± 2.652	4.17 ± 2.592	0.025 <sup>a</sup>
Days of absence from work (days/person)	0.03 ± 0.225	0.67 ± 2.322	0.35 ± 1.664	0.002 <sup>a</sup>
Taking Chinese medicine (days/person)	0.16 ± 0.905	0.72 ± 1.939	0.44 ± 1.527	0.006 <sup>a</sup>
Taking antibiotics (days/person)	0	0.54 ± 1.827	0.26 ± 1.306	0.001 <sup>a</sup>
Taking anti-viral drug (days/person)	0	0.48 ± 1.884	0.24 ± 1.341	0.006 <sup>a</sup>
Taking anti-inflammatory drug (days/person)	0	0.11 ± 0.778	0.05 ± 0.547	0.150 <sup>a</sup>

The quantitative variables in this table are non-normally distributed because there are plenty of 0 values that appeared in the raw data; the  $M \pm SD$  is used to describe the average level and the degree of variability instead of using the form of median ( $P_{25}$ – $P_{75}$ ).

<sup>a</sup>Wilcoxon's rank sum test.

<sup>b</sup>Chi-square test.

<sup>c</sup>Fisher's exact test.

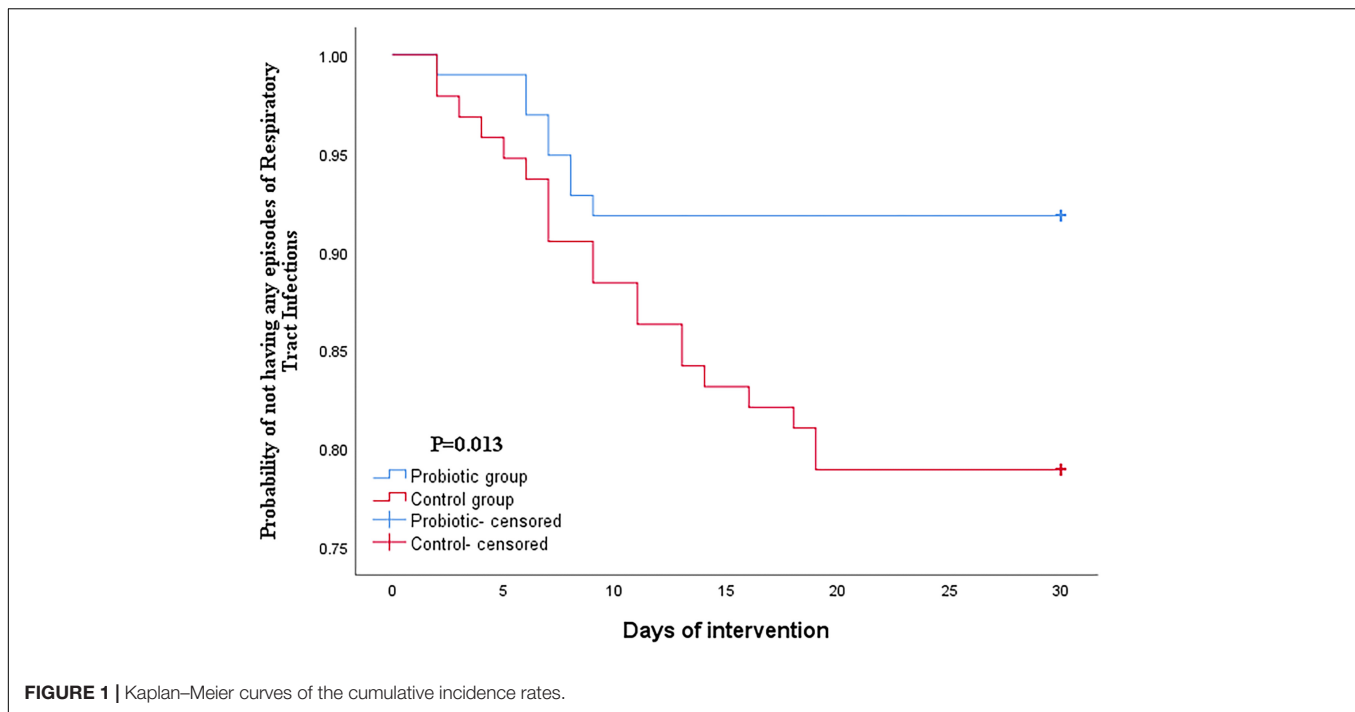
symptoms of the respiratory tract infections observed during this study include sore throat, cough and itchy throat, low fever, nasal congestion and dizziness, acute otitis media, and oral ulcer. Serological diagnosis including blood cytokine detection were not conducted due to the highly occupied workload for the frontline medical staff during the study period. However, the subjects having professional medical skills have been able to express and diagnose their symptoms accurately, hence, confirming the episodes of upper respiratory tract infections accurately. Among the eight episodes observed in the probiotic group, four showed symptoms of mainly sore throat, three showed symptoms of mainly cough and itchy throat, and one subject experienced low fever. As for the 22 episodes observed in the control group, 10 showed symptoms of mainly sore throat, 3 showed symptoms of mainly cough and itchy throat, 5 subjects experienced low fever, 2 subjects had nasal congestion and dizziness or headache, 1 subject reported acute otitis media along with sore throat, and 1 subject had oral ulcer. Comparing the key symptoms of upper respiratory tract infections, a trend of decreased incidence of key symptoms was observed during the prophylaxis with oropharyngeal probiotics, of which the incidence of sore throat was reduced by 61.3% and the incidence of low fever was reduced by 80.6% ( $p < 0.1$ ). By comparison with the control group, the frontline medical staff in the probiotic group experienced a significantly lower number of days experiencing respiratory tract infection (RTi) symptoms (78%,  $p < 0.005$ ). In fact, 23 days (0.23 days/person) of experiencing RTi symptoms were observed in the probiotic group whereas a total of 100 days (1.05 days/person) was observed in the control group. Meanwhile, treatment with oropharyngeal probiotic resulted in a significantly shorter (by 38%,  $p < 0.05$ ) average duration of infection episodes (2.88 days/episode) compared with the control group (4.67 days/episode). Due to the reduction in total episodes, sick days, and duration of each episodes, the subjects treated with

probiotic had significantly less days absent from work by 95.5% ( $p < 0.005$ ); in other words, totally 3 days (0.03 days/person) of absence from work were reported in the probiotic group whereas totally 63 days (0.67 days/person) were reported in the control group.

During the study period, when there was evidence of a respiratory tract infection, the enrolled medical staff in both groups were asked to record the variety and duration of drug treatment, and continue taking probiotic throughout the study period, including in case of antibiotic treatment required. Our data reveal that the frontline medical staff in the probiotic group took significantly less medication compared with the control group. The number of days taking Chinese herbal medicine was observed to be reduced by 77.8% ( $p < 0.01$ ); it is reported that totally 16 days (0.16 days/person) of medication history on Chinese herbal medicine was observed in the probiotic group compared with totally 68 days (0.72 days/person) observed in the control group. Further, during the randomized controlled trial, participants in the probiotic group had no record of antibiotic and anti-viral drug intake compared with 51 and 46 days of antibiotic and anti-viral drug intake in the control group ( $p = 0.001$  and  $p < 0.01$ ), respectively. No intake of steroid/anti-inflammatory drug was also observed in the probiotic group compared with 10 days of intake of steroid/anti-inflammatory drugs in the control group.

Furthermore, the Kaplan–Meier statistic was used to estimate the level of protection of respiratory tract infection by administration of oropharyngeal probiotic over time. As shown in **Figure 1**, the Kaplan–Meier curve of probability not having any episodes of respiratory tract infections decreased gradually from 1 on the first day of this trial. Notably, the cumulative incidence of respiratory tract infection stopped increasing on day 10 in the probiotic group. This implicates that frontline medical staff in the probiotic group experienced sustained



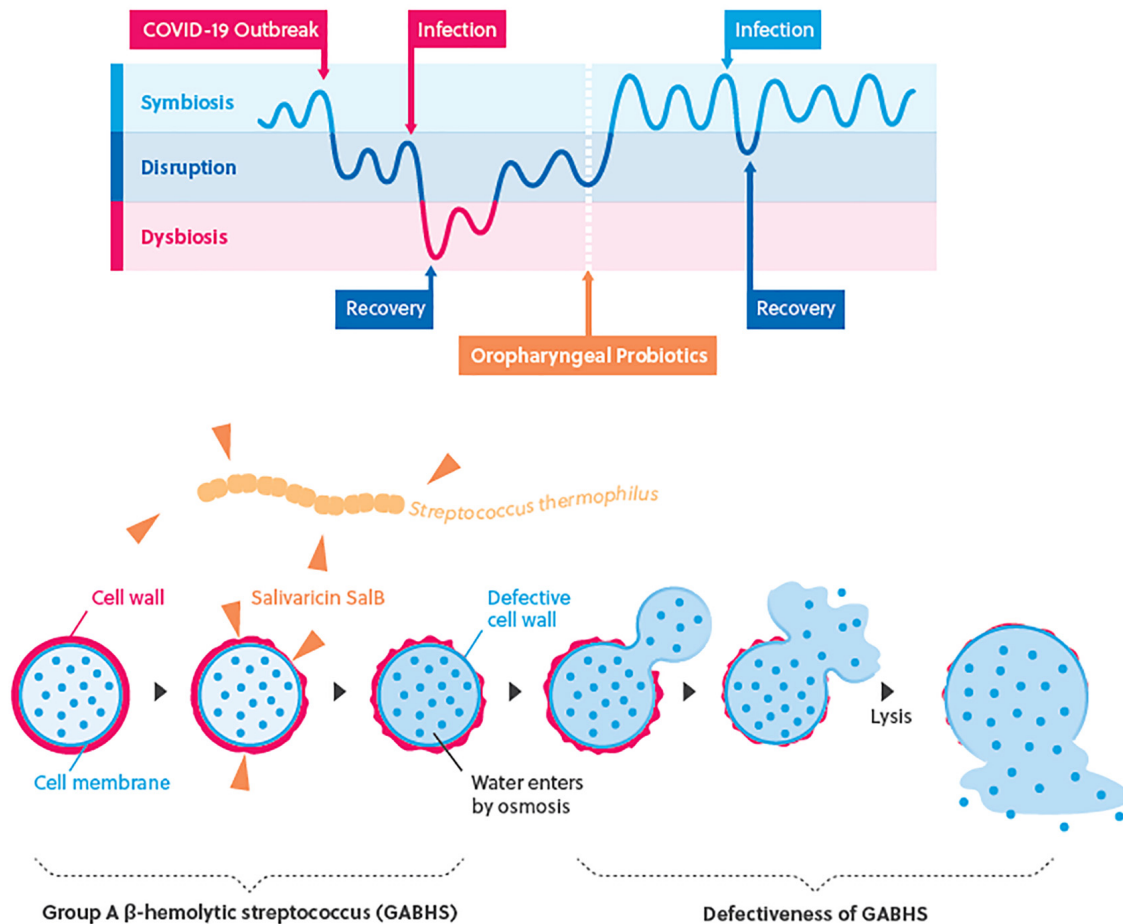


protection from respiratory tract infections after a certain time of oropharyngeal probiotic administration resulting in an extremely lower incidence rate of respiratory tract infections comparing with control group ( $p = 0.013$ ).

## DISCUSSION

Oral commensal microorganism has a central role in the homeostasis of airway mucosa and programming of the immune system (Harald et al., 2012). The said respiratory microbiota is sensitive to multiple factors, such as lifestyle, aging, environment, and disease (Mikari et al., 2018; Hongcheng et al., 2020). A cohort study has demonstrated that nasopharyngeal microecological imbalance was caused by trans-colonization of oral microbiota, leading to upper respiratory tract infections (Wing et al., 2019). Longitudinal observations have also found that psychological stress, mood states, or life events are associated with susceptibility of viral and intracellular bacterial infections and reduced lung function due to decreased cellular immune processes, such as those initiated by NK cells (Trueba and Ritz, 2012). Besides, SARS-CoV-2 mainly infect human angiotensin-converting enzyme 2 (ACE2), which is mainly expressed in tongue epithelial cells, while the viral load of SARS-CoV-2 in posterior oropharyngeal saliva samples was highest during the first week of symptom onset (Lirong et al., 2020), which further reveals that homeostasis of oropharyngeal mucosa that has an impact on the programming of the innate immune system could play an important role as a frontline defense and protect human host from respiratory tract infections including SARS-CoV-2. The results of this study indicate that oropharyngeal probiotic formula containing *S. thermophilus*

ENT-K12 can reduce susceptibility to respiratory tract infections for frontline medical staff fighting against COVID-19. The mechanisms that underlie these effects have been described in previous studies, which includes colonization of the probiotics in oropharynx having the ability to locally release the two antibiotics, salivaricin A2 and B, to reduce the risk of colonization by group A  $\beta$ -hemolytic streptococcus including *S. pyogenes*; a common pathogen persists in the pharynx in a carrier state in approximately 10% of the population, which is a common cause of pharyngeal infections and a common bacterial pathogen that causes co-infection during viral infection (Upton et al., 2001). The salivaricin-producing probiotic strains has been proven to be of great value in the development of new and novel antibacterial therapies in this era of emerging antibiotic resistance via curing multi-resistant infections or reshaping the endogenous microbiota for prophylaxis purposes (Piewngam et al., 2018; Khan et al., 2019; Pascal et al., 2019; Barbour et al., 2020). As shown in **Figure 2**, the hypothetical graph indicates the host oropharyngeal microflora interactions which are divided into three states, symbiosis, disruption, and dysbiosis; when the host oropharyngeal microflora remains in the symbiosis state, the host is relatively more tolerant to the infections or environment factors which may disrupt the host's immune responses. When frontline medical staff fighting COVID-19 switched to an unregulated and stressed work schedule during the pandemic outbreak, the disruption of symbiosis state could be induced and made the individuals more susceptible to the infections which further altered the host oropharyngeal microflora to become a dysbiosis state. Administration of oropharyngeal probiotics was able to establish a more balanced homeostatic relationship between the oropharyngeal microflora and the cells of the immune system responding to the infections and surrounding



**FIGURE 2 |** The hypothetical graph of interactions of host oropharyngeal microflora and immune responses.

environment that shapes the oropharyngeal microflora, the said symbiosis state may provide more protections for the frontline medical staff fighting against COVID-19 from respiratory tract infections including COVID-19. The salivaricin, SalB, produced by oropharyngeal probiotics further protects the frontline medical staff from bacterial coinfections via disabling the reproduction of pathogenic bacteria on the oropharyngeal mucus surfaces (Barbour et al., 2016).

These results can be supported by our findings that prophylaxis with oropharyngeal probiotic formula containing ENT-K12 strain among COVID-19 frontline medical staff reduced the prevalence of respiratory tract infections by approximately 65%, sick days by approximately 80%, and no record of antibiotic, anti-viral drug and steroid/anti-inflammatory drug intake during this trial.

The proposed anti-viral capability of oropharyngeal probiotic has been attributed to the observed development of an innate immune response as revealed by detection of enhanced sufficient amount of IFN- $\gamma$  in human saliva 10 h after oral lozenge administration (Di Pierro, 2020).

The administration of the ENT-K12 dose used in the present study has been shown to result in successful colonization of the

oral cavity (Burton et al., 2010). Further, both the antibacterial as well as the anti-viral activity demonstrated in previous studies with the oropharyngeal probiotic may have contributed to the observed clinical benefits in the present study and may explain both the reduced incidence and duration of respiratory infections in the probiotic group of frontline medical staff.

According to our knowledge to date, this is the very first study describing the beneficial effects of oropharyngeal probiotic strain that has been administered by medical staff during an emerging disease outbreak. The Kaplan–Meier curve indicates that frontline medical staff treated with oropharyngeal probiotic experienced an extremely low incidence rate of respiratory tract infections after only 10 days of probiotic administration, suggesting that a healthier and more balanced oropharynx microflora homeostasis can be achieved by probiotic administration of 2 lozenges a day for about 10 days; this finding suggested that the colonization of ENT-K12 strain can be implemented by taking slow-dissolved probiotic formula 2 lozenges per day over about 10 days, which can be supported by a previous study demonstrating that K12 strain colonization can be achieved over 14 days while taking 1 lozenge per day or 3 days while taking 4 lozenges per day, defined by the sufficient

amount of salivarin A2 and B that had been detected in the saliva or on site, and the target habitat sites are pharynx, tongue, and buccal membranes which are also the habitats of agents causing pharyngitis (Horz et al., 2007). Besides the action mode of salivarin described previously, a well-maintained oropharynx homeostasis status also helps keeping the human host tolerant of respiratory tract infections. Previous studies have demonstrated that the use of oropharyngeal probiotic as part of the complex therapy of recurrent tonsillitis for 30 days was characterized by a rapid relief of both local and general manifestations of recurrent tonsillitis, as well as a significant improvement in the microflora of the upper respiratory tract (Ilchenko et al., 2020; Kramarev et al., 2020). It is noted that in the control group, the incidence rate of respiratory tract infections increased linearly until the 20th day and seemed to slow down in the last 10 days during this trial, which may be explained by the fact that the number of hospitalized COVID-19 patients gradually decreased after they were cured and left the hospitals and the relief of COVID-19 pandemic in Wuhan area, thus relieved the shortage of medical resources during the emergence of the outbreak which caused extremely stressful work schedule and which also made the medical staff experience a lower immunity during the period of medical resource shortage.

Considering that the clinical benefit of oropharyngeal probiotic plays a role in creating a stable upper respiratory tract microbiota capable of protecting the host from respiratory tract infections, and its anti-viral capability to build a well-established first-line defense on the upper respiratory tract and oropharyngeal microbiome to protect individuals from respiratory tract infection could be a promising strategy to prevent respiratory tract infections, including COVID-19 infections.

Another public health crisis is that the number of pathogenic bacterial strains resistant to antibiotics has dramatically increased during the past decades so that some pathogenic microbes are totally insensitive to current antibiotics (De Francesco et al., 2010; Jakobsson et al., 2010; Beata and Anna, 2015); the new trends of research on antibacterial peptides produced by probiotics known as bacteriocins could provide beneficial features to substitute antibiotics or reduce the emergence of resistant strains. Fortunately, many human commensal bacterial species are able to be mobilized to produce bacteriocins and prevent bacterial infection at the external surface of human epithelia, which gives a great opportunity to cure multi-resistant infections or finely reshape the endogenous microbiota for prophylaxis purposes (Cotter et al., 2013; Sarah et al., 2019). According to the finding of this study and previous studies conducted with the same oropharyngeal probiotic formula, demonstrating a significant reduction by more than 90% of antibiotic use among subjects taking probiotics, administration of the slow-dissolved oropharyngeal probiotic could be a promising strategy to reduce the worldwide public health crisis related to the development of pathogenic antibiotic-resistant strains that caused respiratory tract infections, especially those that cause recurrent respiratory tract infections such as *Streptococcus pneumoniae*.

## CONCLUSION

This study evaluated the oropharyngeal probiotic in frontline medical staff in Wuhan fighting against COVID-19, and the results provide further support that administration of oropharyngeal probiotic which creates a stable upper respiratory tract microbiota can at least, for a short period of 20 days, protect frontline medical staff from upper respiratory tract infections, capable of reducing the duration of sick days, days absent from work, and days taking antibiotics and anti-viral drugs. This study certainly exhibits some limits: the absence of blind conditions, the small size of the sample which is not sufficient enough to detect the prevention effect of COVID-19 infections, not able to be involved in checking viral or streptococcal infection during the extremely busy work schedule, an inability to follow up the enrolled medical staff in the next subsequent month to assess further trends in infective oropharyngeal events due to that the number of hospitalized COVID-19 patients on the study sites gradually decreased when they are cured and leave hospital after April and May 2020, and an inability to analyze the composition of oropharyngeal microflora before and after oropharyngeal probiotic treatment, thus not able to directly prove the better homeostasis after a certain time of probiotic administration. Nevertheless, the findings of this study together with the beneficial clinical effects and improved oropharyngeal microbiota discovered from previous human clinical studies, and excellent tolerability and compliance, as well as the absence of side effects, demonstrated that the slow-dissolved oropharyngeal probiotic formula can be a valid solution in the prevention of respiratory tract infections.

## DATA AVAILABILITY STATEMENT

The data analyzed in this study is subject to the following licenses/restrictions: The datasets used and/or analyzed during the current study are available from the corresponding author on reasonable request. Requests to access these datasets should be directed to QWa, wangqiang@wust.edu.cn.

## ETHICS STATEMENT

The studies involving human participants were reviewed and approved by Ethics Committee of Medical school of Wuhan University of Science and Technology (registration number 202003). The patients/participants provided their written informed consent to participate in this study.

## AUTHOR CONTRIBUTIONS

BZ and QWu guided and completed the whole experimental design. FT, HG, and DC involved in the data collection. JX and XH were responsible for the arrangement of data. XX

and WL were responsible for analyzing the data. YF and HC participated in the interpretation of the results. QWa and XL wrote the initial draft with all authors providing critical feedback and edits to subsequent revisions. QWa, JX, BZ, and QWu reviewed and revised the manuscript before submission, they are co-corresponding authors.

## FUNDING

This work was supported by funding from Qingdao Amchem International Co. Ltd.; 2020 General Planning Fund Project for Humanities and Social Sciences of the Ministry of

Education, China, Project reference number 20YJA880053; WUST National Defense Pre-research Foundation, China, Project reference number GF202003; and the Strategic Priority Research Program of Chinese Academy of Sciences, Project reference number XDB29020203.

## ACKNOWLEDGMENTS

We thank all the frontline medical staff in Wuhan whose participation during the battle of fighting COVID-19 made this study possible.

## REFERENCES

- Barbour, A., Tagg, J., and Abou-Zied, O. (2016). New insights into the mode of action of the lantibiotic salivaricin B. *Sci. Rep.* 6:31749. doi: 10.1038/srep31749
- Barbour, A., Wescombe, P., and Smith, L. (2020). Evolution of lantibiotic salivaricins: new weapons to fight infectious diseases. *Trends Microbiol.* 28, 578–593. doi: 10.1016/j.tim.2020.03.001
- Beata, Z. J., and Anna, B. (2015). Antibiotic resistance of *Streptococcus pneumoniae* in children with acute otitis media treatment failure. *Int. J. Pediatric Otorhinolaryngol.* 79, 2129–2133. doi: 10.1016/j.ijporl.2015.09.030
- Burton, J. P., Chilcott, C. N., Wescombe, P. A., and Tagg, J. R. (2010). Extended safety data for the oral cavity probiotic *Streptococcus salivarius* K12. *Probiotics Antimicro. Prot.* 2, 135–144. doi: 10.1007/s12602-010-9045-4
- Clark, A. S., Nabeetha, A. N., Ali, A. F., Gregory, P. D., James, E. G., Ellen, R. W., et al. (2016). Nasopharyngeal microbiota composition of children is related to the frequency of upper respiratory infection and acute sinusitis. *Microbiome* 4:34. doi: 10.1186/s40168-016-0179-9
- Cotter, P., Ross, R., and Hill, C. (2013). Bacteriocins — a viable alternative to antibiotics? *Nat. Rev. Microbiol.* 11, 95–105. doi: 10.1038/nrmicro2937
- De Francesco, V., Giorgio, F., Hassan, C., Manes, G., Vannella, L., Panella, C., et al. (2010). Worldwide *H. pylori* antibiotic resistance: a systematic review. *J. Gastrointest. Liver Dis.* 19, 409–414.
- Di Pierro, F. (2020). A possible probiotic (*S. salivarius* K12) approach to improve oral and lung microbiotas and raise defenses against SARS-CoV-2. *Minerva Med.* 111, 281–283. doi: 10.23736/S0026-4806.20.06570-2
- Harald, R., Per, B., and Mathias, H. (2012). The impact of perinatal immune development on mucosal homeostasis and chronic inflammation. *Nat. Rev. Immunol.* 12, 9–23. doi: 10.1038/nri3112
- Hongcheng, Z., Shuaiyin, C., and Fan, Y. (2020). Alternation of nasopharyngeal microbiota in healthy youth is associated with environmental factors: implication for respiratory diseases. *Int. J. Environ. Health Res.* 1:11. doi: 10.1080/09603123.2020.1810209
- Horz, H. P., Meinelt, A., Houben, B., and Conrads, G. (2007). Distribution and persistence of probiotic *Streptococcus salivarius* K12 in the human oral cavity as determined by real-time quantitative polymerase chain reaction. *Oral. Microbiol. Immunol.* 22, 126–130. doi: 10.1111/j.1399-302X.2007.00334.x
- Ilchenko, S. I., Fialkovska, A. A., and Ivanus, S. G. (2019a). The effectiveness application of the respiratory probiotic *Streptococcus salivarius* K12 for the correction of dysbiotic oral cavity disorders in children with juvenile rheumatoid arthritis. *Clin. Pediatr.* 3:116.
- Ilchenko, S. I., Fialkovska, A. A., and Ivanus, S. H. (2020). The effectiveness of using respiratory probiotic *Streptococcus salivarius* K12 in children with recurrent tonsillitis. *Actual Infectol.* 8, 25–29. doi: 10.22141/2312-413x.8.2.2020.199732
- Ilchenko, S. I., Fialkovska, A. A., and Mozheiko, T. V. (2019b). Modern possibilities of correcting dysbiotic disorders of the mucous membranes of the upper respiratory tract in infants. *Clin. Pediatr.* 14:7.
- Jakobsson, H. E., Jernberg, C., and Andersson, A. F. (2010). Short-term antibiotic treatment has differing long-term impacts on the human throat and gut microbiome. *PLoS One* 24:e9836. doi: 10.1371/journal.pone.0009836
- Jincun, Z., Jingxian, Z., Ashutosh, K. M., Rudragouda, C., Craig, F., David, K. M., et al. (2016). Airway memory CD4+ T cells mediate protective immunity against emerging respiratory coronaviruses. *Immunity* 44, 1379–1391. doi: 10.1016/j.immuni.2016.05.006
- Khan, R., Petersen, F. C., and Shekhar, S. (2019). Commensal bacteria: an emerging player in defense against respiratory pathogens. *Front. Immunol.* 10:1203. doi: 10.3389/fimmu.2019.01203
- Kramarev, S. O., Yevtushenko, V. V., Seryakova, I. Y., and Kaminskaya, T. N. (2020). Application of *Streptococcus salivarius* K12 probiotic strain in the treatment of acute tonsillopharyngitis in children. *Actual Infectol.* 8, 29–34. doi: 10.22141/2312-413x.8.3-4.2020.212657
- Lichun, Z., Xiang, W., Chongchong, Z., Qin, L., Shuang, L., Qin, S., et al. (2020). Analysis of the infection status of the medical staff in Wuhan during the COVID-19 outbreak: a cross-sectional study. *Clin. Infect. Dis.* 71, 2109–2113. doi: 10.1093/cid/cia588
- Lirong, B., Cheng, Z., Jiajia, D., Lei, Z., Yan, L., and Jianxun, S. (2020). Oral Microbiome and SARS-CoV-2: beware of lung co-infection. *Front. Microbiol.* 11:1840. doi: 10.3389/fmicb.2020.01840
- Martens, K., Pugin, B., De Boeck, I., Spacova, B., Steelant, S. F., Seys, S., et al. (2018). Probiotics for the airways: potential to improve epithelial and immune homeostasis. *Allergy* 73, 1954–1963. doi: 10.1111/all.13495
- Mikari, A., Toru, T., and Michiko, F. (2018). Tongue microbiota and oral health status in community-dwelling elderly adults. *Clin. Sci. Epidemiol.* 3, e00332–e00418. doi: 10.1128/mSphere.00332-18
- Olga, S., Viktoria, B. S., Bernard, B., Anne, B., Kristina, K., Mélissa, L., et al. (2014). Nasopharyngeal microbiota in healthy children and Pneumonia patients. *J. Clin. Microbiol.* 52, 1590–1594. doi: 10.1128/JCM.03280-13
- Pascal, H., Laura, L. G., Philippe, G., and Mignolet, J. (2019). Mobilization of Microbiota commensals and their bacteriocins for therapeutics. *Trends Microbiol.* 27, 690–702. doi: 10.1016/j.tim.2019.03.007
- Piewngam, P., Zheng, Y., Nguyen, T. H., Dickey, S. W., Joo, H. S., Villaruz, A. E., et al. (2018). Pathogen elimination by probiotic *Bacillus* via signalling interference. *Nature* 562, 532–537. doi: 10.1038/s41586-018-0616-y
- Sarah, K., Daniel, T., and Irene, L. W. (2019). Does probiotic consumption reduce antibiotic utilization for common acute infections? A systematic review and meta-analysis. *Eur. J. Public Health* 29, 494–499. doi: 10.1093/eurpub/cky185
- Trueba, A. F., and Ritz, T. (2012). Stress, asthma, and respiratory infections: pathways involving airway immunology and microbial endocrinology. *Brain Behav. Immun.* 29, 11–27. doi: 10.1016/j.bbi.2012.09.012
- Upton, M., Tagg, J. R., Wescombe, P., and Jenkinson, H. F. (2001). Intra- and Interspecies signaling between *Streptococcus salivarius* and *Streptococcus pyogenes* mediated by SalA and SalA1 lantibiotic peptides. *J. Bacteriol.* 183, 3931–3938. doi: 10.1128/jb.183.13.3931-3938.2001
- Wilcox, C. R., Stuart, B., Leaver, H., Lown, M., Willcox, M., Moore, M., et al. (2019). Effectiveness of the probiotic *Streptococcus salivarius* K12 for the treatment and/or prevention of sore throat: a systematic review. *Clin. Microbiol. Infect.* 25, 673–680. doi: 10.1016/j.cmi.2018.12.031



- Wing, H. M., Melanie, C., and Wouter, D. S. P. (2019). Loss of microbial topography between oral and nasopharyngeal microbiota and development of respiratory infections early in life. *Eur. Respiratory J.* 54(Suppl. 63):A4995. doi: 10.1183/13993003
- Yaowen, Z., Jing, Z., Dong, W., Zhirong, Y., Yanyan, W., and Zhiyuan, Y. (2016). Annual surveys for point-prevalence of healthcare-associated infection in a tertiary hospital in Beijing, China, 2012-2014. *BMC Infect. Dis.* 16:161. doi: 10.1186/s12879-016-1504-4
- Zijie, S., Yan, X., Lu, K., Wentai, M., Leisheng, S., Li, Z., et al. (2020). Genomic diversity of SARS-CoV-2 in Coronavirus Disease 2019 patients. *Clin. Infect. Dis.* 9:ciaa203. doi: 10.1093/cid/ciaa203

**Conflict of Interest:** The authors declare that the research was conducted in the absence of any commercial or financial relationships that could be construed as a potential conflict of interest.

Copyright © 2021 Wang, Lin, Xiang, Liu, Fang, Chen, Tang, Guo, Chen, Hu, Wu, Zhu and Xia. This is an open-access article distributed under the terms of the Creative Commons Attribution License (CC BY). The use, distribution or reproduction in other forums is permitted, provided the original author(s) and the copyright owner(s) are credited and that the original publication in this journal is cited, in accordance with accepted academic practice. No use, distribution or reproduction is permitted which does not comply with these terms.



## OPEN ACCESS

### Edited by:

Stephen Allen Morse,  
Centers for Disease Control and Prevention  
(CDC), United States

### Reviewed by:

Xiaoxia Dai,  
Xi'an Jiaotong University, China  
Sumit Ghosh,  
The Research Institute at Nationwide  
Children's Hospital, United States

### \*Correspondence:

Nicole R. LeBoeuf  
nleboeuf@bwh.harvard.edu  
Peter K. Sorger  
peter\_sorger@hms.harvard.edu  
sorger\_admin@hms.harvard.edu

### <sup>†</sup>ORCID:

Akshay Kothakonda  
0000-0001-5424-4228  
Lyla Atta  
0000-0002-6113-0082  
Deborah Plana  
0000-0002-4218-1693  
Avilash Cramer  
0000-0003-0014-8921  
Jacob Freake  
0000-0002-5198-835X  
Enze Tian  
0000-0001-6410-5360  
Christopher Van  
0000-0003-3262-964X  
Christopher Hansen  
0000-0002-6640-2745  
Helen Yang  
0000-0002-9455-5300  
Michael S. Sinha  
0000-0002-9165-8611  
Ju Li  
0000-0002-7841-8058  
Sherry H. Yu  
0000-0002-1432-9128  
Nicole R. LeBoeuf  
0000-0002-8264-834X  
Peter Sorger  
0000-0002-3364-1838

<sup>†</sup>These authors have contributed equally to  
this work

### Specialty section:

This article was submitted to  
Biosafety and Biosecurity,  
a section of the journal  
Frontiers in Bioengineering and  
Biotechnology

Received: 04 April 2021

Accepted: 31 July 2021

Published: 06 September 2021

### Citation:

Kothakonda A, Atta L, Plana D, Ward F,  
Davis C, Cramer A, Moran R, Freake J, Tian E,  
Mazor O, Gorelik P, Van C, Hansen C,  
Yang H, Li Y, Sinha MS, Li J, Yu SH,  
LeBoeuf NR and Sorger PK (2021) De Novo  
Powered Air-Purifying Respirator Design and  
Fabrication for Pandemic Response.  
Front. Bioeng. Biotechnol. 9:690905.

# De Novo Powered Air-Purifying Respirator Design and Fabrication for Pandemic Response

Akshay Kothakonda<sup>1,2†</sup>, Lyla Atta<sup>1,3†</sup>, Deborah Plana<sup>1,4,5†</sup>, Ferrous Ward<sup>1,2†</sup>, Chris Davis<sup>1,6</sup>,  
Avilash Cramer<sup>1,5†</sup>, Robert Moran<sup>1,7</sup>, Jacob Freake<sup>1,8†</sup>, Enze Tian<sup>1,9†</sup>, Ofer Mazor<sup>1,10</sup>,  
Pavel Gorelik<sup>1,10</sup>, Christopher Van<sup>1,11†</sup>, Christopher Hansen<sup>1,12†</sup>, Helen Yang<sup>1,13†</sup>, Yao Li<sup>1,14</sup>,  
Michael S. Sinha<sup>1,13†</sup>, Ju Li<sup>1,14†</sup>, Sherry H. Yu<sup>1,15†</sup>, Nicole R. LeBoeuf<sup>1,16\*†</sup> and  
Peter K. Sorger<sup>1,4\*†</sup>

<sup>1</sup>Greater Boston Pandemic Fabrication Team (PanFab) c/o Harvard-MIT Center for Regulatory Science, Harvard Medical School, Boston, MA, United States, <sup>2</sup>Department of Aeronautics and Astronautics, MIT, Cambridge, MA, United States, <sup>3</sup>Department of Biological Engineering, Johns Hopkins University School of Medicine, Baltimore, MD, United States, <sup>4</sup>Harvard Ludwig Cancer Research Center and Department of Systems Biology, Harvard Medical School, Boston, MA, United States, <sup>5</sup>Harvard-MIT Division of Health Sciences and Technology, Cambridge, MA, United States, <sup>6</sup>GenOne Technologies, Cambridge, MA, United States, <sup>7</sup>Mine Survival Inc., Panama City Beach, FL, United States, <sup>8</sup>Fikst Product Development, Woburn, MA, United States, <sup>9</sup>Beijing Key Laboratory of Indoor Air Quality Evaluation and Control, Department of Building Science, Tsinghua University, Beijing, China, <sup>10</sup>Research Instrumentation Core Facility, Harvard Medical School, Boston, MA, United States, <sup>11</sup>Borobot, Middleborough, MA, United States, <sup>12</sup>Harvard Graduate School of Design, Cambridge, MA, United States, <sup>13</sup>Harvard-MIT Center for Regulatory Science, Harvard Medical School, Boston MA, United States, <sup>14</sup>Department of Nuclear Science and Engineering and Department of Materials Science and Engineering, MIT, Cambridge, MA, United States, <sup>15</sup>Department of Dermatology, Yale School of Medicine, New Haven, CT, United States, <sup>16</sup>Department of Dermatology, Center for Cutaneous Oncology, Brigham and Women's Hospital and Dana-Farber Cancer Institute, Boston, MA, United States

The rapid spread of COVID-19 and disruption of normal supply chains has resulted in severe shortages of personal protective equipment (PPE), particularly devices with few suppliers such as powered air-purifying respirators (PAPRs). A scarcity of information describing design and performance criteria for PAPRs represents a substantial barrier to mitigating shortages. We sought to apply open-source product development (OSPD) to PAPRs to enable alternative sources of supply and further innovation. We describe the design, prototyping, validation, and user testing of locally manufactured, modular, PAPR components, including filter cartridges and blower units, developed by the Greater Boston Pandemic Fabrication Team (PanFab). Two designs, one with a fully custom-made filter and blower unit housing, and the other with commercially available variants (the "Custom" and "Commercial" designs, respectively) were developed; the components in the Custom design are interchangeable with those in Commercial design, although the form factor differs. The engineering performance of the prototypes was measured and safety validated using National Institutes for Occupational Safety and Health (NIOSH)-equivalent tests on apparatus available under pandemic conditions at university laboratories. Feedback was obtained from four individuals; two clinicians working in ambulatory clinical care and two research technical staff for whom PAPR use is standard occupational PPE; these individuals were asked to compare PanFab prototypes to commercial PAPRs from the perspective of usability and suggest areas for improvement. Respondents rated the PanFab Custom PAPR a 4 to 5 on a 5 Likert-scale 1) as compared to current PPE options, 2) for the sense of security with use in a clinical setting, and 3) for comfort

compared to standard, commercially available PAPRs. The three other versions of the designs (with a Commercial blower unit, filter, or both) performed favorably, with survey responses consisting of scores ranging from 3 to 5. Engineering testing and clinical feedback demonstrate that the PanFab designs represent favorable alternatives to traditional PAPRs in terms of user comfort, mobility, and sense of security. A nonrestrictive license promotes innovation in respiratory protection for current and future medical emergencies.

**Keywords:** COVID-19, pandemic response, 3D-printing, powered air-purifying respirators, personal protective equipment, open source product development, injection molding, medical device design

## INTRODUCTION

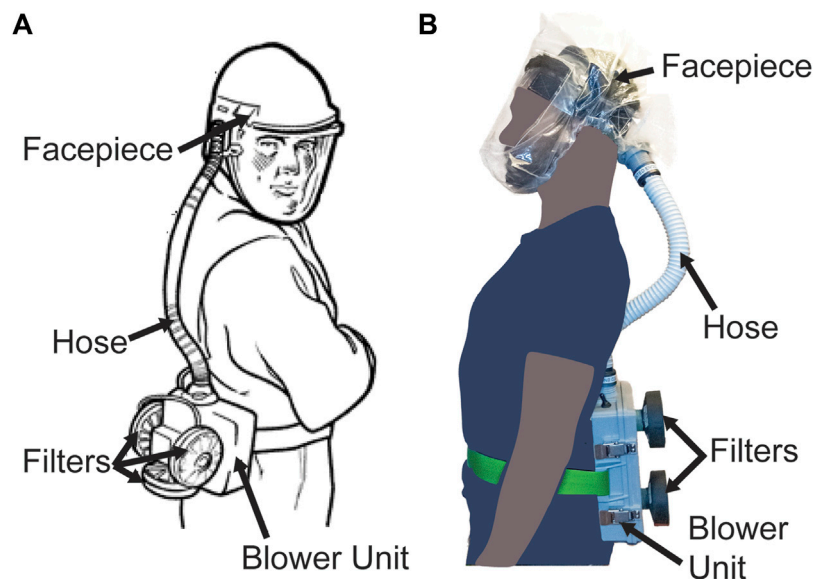
The rapid and global spread of COVID-19 has led to dramatic increases in demand for personal protective equipment (PPE) for healthcare workers as well as significant disruption of supply chains and distribution networks for these products. As a consequence, the availability of high-quality respiratory protection has been problematic, causing healthcare institutions to reuse normally disposable filtering facepiece respirators (FFRs; N95-type masks) and turn to non-traditional devices as substitutes (Hack the Pandemic, 2020; Thingiverse.com, 2020; COVID-19 Response, 2020; Get Us PPE, 2021; Open Mask, 2021). Non-traditional supply chains commonly involve community-based collaborations among independent engineers, scientists, hobbyists, and volunteers in partnership with healthcare and academic institutions (McCue, 2020; Westervelt, 2020; NIH 3D Print Exchange, 2020; Sinha et al., 2020; Clark, 2020). While multiple non-traditional designs for simple PPE products such as face shields have emerged (Mostaghimi et al., 2020), and multiple commercial and non-traditional technologies have been developed to decontaminate or reuse N95-type masks (N95 Decon, 2020; McAvoy et al., 2021), few alternative sources of supply exist for more complex products. This is particularly true of powered air-purifying respirators (PAPRs) which can be worn by individuals unable to fit N95-type masks, are more comfortable in many settings, and also provide a higher level of respiratory protection. Ongoing efforts to increase the supply of PAPRs have largely involved large manufacturing companies with government support (e.g., the 3M Ford Limited-Use Public Health Emergency PAPR) (CDC, 2020a; Limited-Use Public Health Emergency PAPR, 2021).

PAPRs typically cover the entire head with a loose-fitting headpiece or hood and provide a continuous supply of filtered air to a user from a blower worn on a belt or backpack. Like N95 masks, PAPRs are used in both healthcare and industrial settings, but under non-pandemic conditions, healthcare use of PAPRs is typically limited to situations in which a healthcare worker (HCW) is unable to wear a disposable N95 mask yet must care for a patient with a suspected or confirmed airborne infection, such as tuberculosis (Institute of Medicine, 2015). Common reasons for being unable to wear a N95 mask are the presence of facial hair and poor mask fit for individuals with small or narrow faces; the latter is often revealed by qualitative fit tests routinely performed on HCWs (Occupational Safety and

Health Administration, 2021). It is estimated that ~10% of HCWs fail fit testing (Institute of Medicine, 2015), and for these individuals PAPRs are the best, and in some instances the only, alternative form of respiratory protection. N95 masks are often reused in pandemic conditions due to supply shortages, leading to concerns about further loss of fit after multiple don-doff cycles (Bergman et al., 2012).

In addition, HCWs report that PAPRs are more comfortable than masks in situations in which continuous respiratory protection is required for many hours, especially for those who have respiratory symptoms under normal circumstances or who work in hot conditions. It has also been observed that many healthcare workers who must wear N95-type masks day after day (e.g., during a sustained pandemic) experience painful abrasions (Gheisari et al., 2020; Lan et al., 2020). Attempts to mitigate discomfort by using creams, tapes, or loosening the straps that hold masks against a user's face can decrease respiratory protection (Bui et al., 2021). PAPRs overcome this problem and provide better protection: commercial PAPRs certified by the National Institutes for Occupational Safety and Health (NIOSH) offer higher filtration efficiency as compared to N95 masks (99.97 vs. 95%) (Institute of Medicine, 2015) and have assigned protection factors substantially higher than those of N95-type masks (Tompkins and Kerchberger, 2010). PAPRs are also better suited to periods of very high demand: whereas N95 masks are designed for one-time use, commercially available PAPRs are designed to be sterilized and reused multiple times (Rebmann and Wagner, 2009).

PAPRs are generally in short supply in most US healthcare institutions, which typically seek the lowest cost approach to respiratory protection for HCWs. The acquisition costs for commercial PAPRs are ~100–1,000-fold higher than N95 masks: purchasing managers report that a low-cost PAPR retails for ~800.00 USD and a medium-priced device sells for ~2,000.00 USD (3M, 2021) whereas N95-type masks normally cost ~1.50 USD per unit in bulk (the cost of N95-type masks increased 5–10 fold during the COVID-19 pandemic, however) (Ivry and Kochkodin, 2020). PAPR filters must be replaced regularly and are also relatively expensive (Institute of Medicine, 2015). Thus, despite multiple Federal panels and reports spanning a period of two decades calling for innovations in respiratory protection (Sinha et al., 2020), there has been little concrete response. This is a setting in which open-



**FIGURE 1** | PAPR components. **(A)** Diagram of PAPR components, adapted from OSHA.gov (OSHA Technical Manual, 2006). **(B)** PanFab PAPR described in this work.

source product development (OSPD) (Huizingh, 2011) has the potential to make a substantial contribution.

PAPRs are composed of three primary functional components: the filter cartridge, the blower unit, and the facepiece, which is connected to the blower via a flexible hose. Additional components, such as low flow rate alarms, enhance user safety and usability (Figure 1). The blower unit and its associated power and control systems are enclosed inside an airtight housing. This housing couples to the filter cartridges and to the hose. The blower unit pulls room air through one or multiple high-efficiency particulate air/high-efficiency particulate absorbing (HEPA) filter cartridges, thereby removing aerosols and small particles. The blower then pushes the filtered air into the facepiece (also known as a hood) through the hose, and it is breathed in by the user. In the case of a loose-fitting facepiece, air also escapes through gaps between the facepiece material and the user's body. The presence of positive pressure in the facepiece ensures that unfiltered outside air does not enter the facepiece and is not inhaled by the user.

The current shortage of PAPRs likely reflects the complexity of these devices, which have multiple components, each requiring significant expertise to design, engineer, and test. Resources describing the design criteria for PAPRs used in healthcare settings are scarce because most designs are proprietary, making it challenging for new or local manufacturers to help address shortages. Additionally, the regulatory approval process for PAPRs via NIOSH is significantly more complex than regulatory approval processes for simpler devices such as face shields (Mostaghimi et al., 2020) that have already been produced in bulk by non-traditional suppliers. In the US, PAPRs are regulated by the Occupational Safety and Health Administration (OSHA) under the Respiratory Protection standard (29 CFR 1910.134). This requires that PAPRs be

approved by NIOSH but does not require 510(k) premarket notification or clearance by the Food and Drug Administration (FDA) (eCFR, 2021; CDC, 2014). One resulting challenge is that NIOSH testing standards are highly prescriptive, but the physical and engineering principles underlying these tests are not always obvious. The prescriptive approach may be appropriate under normal circumstances when it is important to maintain quality standards in the face of cost pressure, but it is problematic in emergency conditions in which approved testing apparatus are in short supply. In the current work we therefore rely on "NIOSH-equivalent" testing to assess performance.

We sought to create public domain PAPR designs with non-restrictive licensing that would help to address current and future shortages in respiratory protection. We also sought to use open source product development to address the broader problems of supply chain disruption caused by healthcare emergencies and shortages of medical supplies in resource-limited environments (e.g., developing nations). After consulting with clinicians and infection control specialists, we focused our efforts on designing filter cartridges and blower units (consisting of a housing, blower, battery, flow control system, and flow control alarm), the two PAPR components most commonly in shortage. NIOSH standard testing procedures (STPs) (CDC, 2020b), which specify the testing requirements needed for NIOSH approval of PAPRs, provided performance specifications for the filter cartridge and blower unit components (Supplementary Material S1); we used these specifications to guide PAPR design.

In this paper, we describe the design, validation, and user testing of modular PAPR components- the filter cartridges and the blower units, developed by the Greater Boston Pandemic Fabrication Team (PanFab) (PanFab, 2021). These components are intended to provide alternatives to standard commercially available PAPR



components and to be locally manufacturable in times of severe PAPR shortage. For both the filter cartridge and the blower unit components, we describe a “PanFab Custom Design” and a “PanFab Commercial Design” to accommodate different scenarios with respect to shortages of materials. The Custom design has less reliance on commercial products and supply chains and can be fabricated in large part using additive manufacturing (3D-printing) methods for low volume production or injection molding for high volume needs (Antonini et al., 2021). The Commercial design relies on commercially available parts made for other products and requires fewer custom fabrication steps, facilitating rapid introduction of new, locally fabricated units. The PanFab PAPR components are modular and interchangeable: any combination of components can be used together and also with traditional PAPR components from leading suppliers. For example, the PanFab Custom Filter can be used with the PanFab Commercial Blower Unit and vice-versa. The PanFab PAPR components are also compatible with the widely used ILC Dover Sentinel XL PAPR facepiece (ILC Dover, 2021) and filters. The blower unit can also be adapted to other commercially available PAPR facepieces by fabricating a slightly modified hose-to-facepiece connector. Under the provisions of a Creative Commons Attribution-ShareAlike 4.0 International Public License, other entities are free to use components of the PanFab PAPRs by themselves, in their own designs, or to innovate these designs further.

Initial prototype testing was conducted at academic laboratories using equipment and supplies that were available during the COVID-19 pandemic. User feedback on the functionality and comfort of the designs was then obtained at a major US academic medical center from four participants: two healthcare providers and two research technicians who used PAPRs regularly as part of standard PPE prior to the pandemic. User feedback was elicited to identify possible points of improvement for future PAPR designs and is intended to be part of an iterative process; insufficient testing was performed to achieve statistical significance or meet NIOSH certification standards. We intend for this to happen as part of scale-up prior to large scale manufacturing. Performance testing was conducted using alternative apparatus and methods than those prescribed by NIOSH, which are hard to replicate outside of a conventional certification laboratory. An additional limitation of our approach is that PAPR certification, like certification of most medical products, requires a manufacturing process controlled by a quality management system (e.g., one similar to ISO 9001 standards). Achieving this standard is only possible in a commercial setting, and we are therefore collaborating with an industrial partner to create a design amenable to NIOSH standards. Future users of the PanFab PAPRs must perform their own testing and confirm that fabricated products meet the requirements of FDA Emergency Use Authorizations and similar regulatory guidance. We return to this issue in the discussion section.

## METHODS

### Prototype Development

NIOSH requirements (NIOSH STP CVB-APR-STP-0081) specify that PAPRs have a minimum filtration efficiency of

99.97% for NaCl aerosols (this corresponds to the 100-N class of PAPRs). To reduce the power required to drive air through filters, they should also have as little pressure drop as possible at the minimum required flow rate of 170 L per minute (lpm; NIOSH STP RCT-APR-STP-0012). For the PanFab Commercial PAPR, we selected a commercially available HEPA filter that is used in consumer vacuum cleaners and widely available; we speculated that supply of these filters is unlikely to be significantly affected by disruption of medical device supply chains caused by COVID-19 or similar pandemics. For the PanFab Custom PAPR, a custom-designed filter cartridge was designed to be lighter in weight and have a lower form factor as compared to the Commercial version.

Design of the blower units focused on meeting the required flow rate of  $\geq 170$  lpm and overcoming pressure drops caused by the filters and tubing in the air flow path at this flow rate. In addition, blower units needed to be operational for at least 1 h, comfortable to wear, sterilizable, airtight, and relatively silent (NIOSH STP RCT-APR-STP-0030). For a full list of design requirements and NIOSH testing requirements, refer to **Table 1** and **Table 2**, respectively. **Supplementary Material S2** provides a full discussion of the design methodology and resulting prototype components.

### Prototype Testing

NIOSH has developed several STPs for testing the safety and functionality of PAPR components (CDC, 2020c). Third-party commercial laboratories typically test PAPRs to these STPs as means to establish compliance with NIOSH standards. However, high demand for testing during the COVID-19 pandemic made many of these test options either unavailable or considerably delayed. As an alternative, we devised apparatus intended to perform the physical, chemical, and engineering measurements described in NIOSH STPs but using materials readily available in university laboratories. Prototype testing was carried out across several university laboratories at MIT on the filters, blowers, power systems, control and warning systems, and the seals between components. The use of these “NIOSH-equivalent” tests allowed us to perform PAPR design and testing in an emergency setting, but does not obviate the need for testing to NIOSH STPs prior to large scale manufacturing. The type of testing needed for clinical implementation of our designs in an emergency setting remains to be determined; as the COVID-19 pandemic recedes we hope that regulatory agencies will provide better guidance on balancing risks under these circumstances.

A loose-fitting facepiece known as the VHA ADAPT PAPR Hood, developed by the Center for Limb Loss and MoBility (CLiMB) at the University of Washington (UW Mechanical Engineering Research Centers, 2012), was used for prototype testing. This facepiece was used in place of standard commercial PAPR facepieces such as the ILC Dover Sentinel XL PAPR facepiece both because these were in limited supply and because we sought to create an all open-source design (testing of the CLiMB facepiece is beyond the scope of the current work and expected to take place independently). However, the PanFab PAPR is compatible with ILC Dover facepieces.

**TABLE 1 |** PanFab PAPR design components, selection criteria, specifications, and commercial components.

Component	Design/Selection criteria	PanFab component specifications	Traditional commercial component
Filter	<ul style="list-style-type: none"> <li>High filtration efficiency under NIOSH filtration test conditions</li> <li>Minimal pressure drop at required flow rate</li> <li>Easy replaceability</li> </ul>	<ul style="list-style-type: none"> <li>Milwaukee HEPA rated filter, part number: 49-90-1900</li> <li>Custom Filters LLC 100-P rated filter</li> </ul>	<ul style="list-style-type: none"> <li>ILC Dover high efficiency particulate air filter, part number: S-4002</li> </ul>
Blower Unit	<ul style="list-style-type: none"> <li>Flow rate of over 170 lpm</li> <li>Static pressure rating sufficient to overcome pressure drops and provide required flow rate</li> <li>Power rating low enough to minimize battery size/weight</li> </ul>	<ul style="list-style-type: none"> <li>Delta electronics centrifugal blower, part number: 603-2093-ND               <ul style="list-style-type: none"> <li>Maximum flow rate: 518 lpm</li> <li>Maximum static pressure: 403.5 Pa</li> <li>Rated voltage: 12VDC</li> <li>Current rating: 0.58A</li> <li>Noise: 50.5 dBA at 1m</li> </ul> </li> </ul>	<ul style="list-style-type: none"> <li>ILC Dover sentinel XL PAPR blower unit, part number: S-2002</li> </ul>
Housing	<ul style="list-style-type: none"> <li>Non-porous, hard material</li> <li>Airtight sealing</li> <li>Easy opening/closing for battery charging</li> <li>Easy coupling/decoupling with filters</li> <li>Low weight and form factor</li> <li>Easily and cheaply 3D-printable and injection moldable</li> </ul>	<ul style="list-style-type: none"> <li>Custom housing:               <ul style="list-style-type: none"> <li>ABS 3D-printed or injection molded</li> <li>EPDM 1/4" thick cam and groove gasket for sealing at filter outlet and silicone 1/8" nominal diameter O-ring for housing lid sealing</li> <li>Draw latches for housing lid closure</li> </ul> </li> <li>Pelican case housing:               <ul style="list-style-type: none"> <li>Pelican V100 vault small pistol case</li> </ul> </li> </ul>	
Control system	<ul style="list-style-type: none"> <li>Regulate flow rate</li> <li>Measure flow rate</li> <li>Sound an alarm at least 80 dBA at ears if flow rate falls below 170 lpm</li> </ul>	<ul style="list-style-type: none"> <li>Arduino R3 controller</li> <li>OSH Park custom-printed shield</li> <li>Sensirion differential pressure sensor, part number: SDP810-500PA               <ul style="list-style-type: none"> <li>Range: -500 to 500 Pa</li> </ul> </li> <li>Precision Electronics Corporation potentiometer, part number: RV4NAYSD103A               <ul style="list-style-type: none"> <li>Response: linear</li> <li>Resistance: 10k-ohms</li> <li>Power Rating: 2W</li> </ul> </li> <li>Mallory Sonalert Products piezoelectric buzzer, part number PS-580Q               <ul style="list-style-type: none"> <li>Voltage rating: 5V-15V</li> <li>Current: 150mA</li> <li>Frequency: 2.8 kHz</li> <li>Sound Level: 100 dB at 12 V and 100 cm</li> </ul> </li> </ul>	
Battery	<ul style="list-style-type: none"> <li>Match blower power characteristics</li> <li>Capacity to run the PAPR for at least 1 h</li> <li>Lightweight and small form factor</li> <li>Safe for use in medical setting</li> </ul>	<ul style="list-style-type: none"> <li>Tenergy NiMH battery pack, Amazon Standard Identification Number: B077Y9HNTF               <ul style="list-style-type: none"> <li>Voltage: 12V</li> <li>Capacity: 2,000 mAh</li> <li>Maximum discharge current: 2A</li> </ul> </li> </ul>	<ul style="list-style-type: none"> <li>ILC Dover sentinel XL PAPR battery, part number: S-2003</li> </ul>
Facepiece	<ul style="list-style-type: none"> <li>Coverage of nose and mouth</li> <li>Conductive to communication</li> <li>Compatible with equipment such as stethoscope</li> <li>Compatible with eyewear</li> <li>Avoids fogging</li> </ul>	<ul style="list-style-type: none"> <li>University of Washington VHA ADAPT PAPR Hood</li> </ul>	<ul style="list-style-type: none"> <li>ILC Dover sentinel XL PAPR clear hood, part number: S-3101</li> </ul>

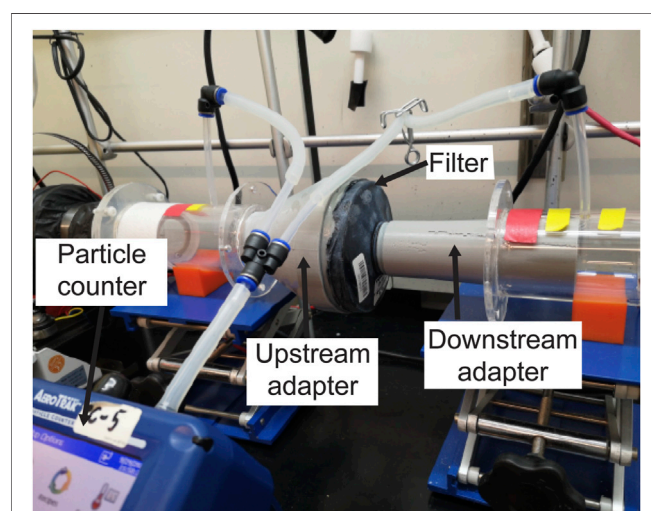
## Filter Testing

NIOSH performs two distinct filtration efficiency tests: a full loading test and an instantaneous (abbreviated) test, the latter of which estimates the lowest filtration efficiency expected at the start of a filter's service life. NIOSH performs the loading

filtration efficiency test of 100-N class of PAPR filters using 75 nm median diameter NaCl aerosols (NIOSH STP CVB-APR-STP-0081). To test the filtration efficiency for the PanFab PAPR filters, we modified a previously described university-based apparatus (Plana et al., 2021) originally used to assess the

**TABLE 2 |** PanFab PAPR component validation test type, regulatory guidance, and alternative test results. Full STPs available as **Supplementary Material 1**.

Test type	Relevant NIOSH STP	Result of NIOSH-alternative test
Filtration efficiency	Procedure No. CVB-APR-STP-0081 determination of particulate filter efficiency level against solid particulates (PAPR 100-N) Procedure No. TEB-APR-STP-0001 determination of particulate filter penetration (PAPR) test	Milwaukee filters: 99.99%, 100% at 300 nm and 230 lpm Custom filter: 99.99% at 300 nm and 230 lpm Milwaukee filters: 99.18% and 99.58% at 170 lpm Custom Filter: 99.98% at 170 lpm 240 lpm at 70% blower duty cycle
Flow rate	Procedure No. RCT-APR-STP-0012 determination of air flow for powered air-purifying respirators	Pass, n = 1
Qualitative fit	Procedure No. RCT-APR-STP-0067 Particulate respirator qualitative fit test utilizing saccharin or bitrex solutions	Pass, n = 1
Sealing	Procedure No. CVB-APR-STP-0010 determination of respirator fit, quantitatively using corn oil aerosol, for powered air-purifying respirators with loose-fitting respiratory inlet coverings	Pass, n = 1
Noise level	Procedure No. RCT-APR-STP-0030: determination of noise level test, power air-purifying respirator with hoods or helmets	58.1 to 59.2 dBA at full battery charge and maximum blower speed
Low flow rate alarm	Procedure No. CVB-APR-STP-0085 determination of low flow warning device sound level	Between 82.95 and 84.7 dBA at 230 lpm flow rate
Audibility test	Procedure No. CVB-APR-STP-0088 determination of low flow warning device activation Procedure No. CVB-APR-STP-0089 determination of communication performance test for speech conveyance and intelligibility	Pass, n = 1

**FIGURE 2 |** Loading filtration test setup, with filter cartridge in line with KCl-containing air stream. Other components of the apparatus have been previously described (Plana et al., 2020).

filtration efficiency of N95-type FFRs (**Figure 2**). Due to the unavailability of NaCl aerosol generators, KCl was used instead. A Collison Nebulizer (MRE 6-Jet, BGI Inc., Waltham, MA) generated aqueous KCl particle streams, a Handheld Particle Counter (TSI 9306-V2 AeroTrak, TEquipment, Long Branch, NJ) was used to count particles, and a differential pressure gauge (purchased from McMaster-Carr, Elmhurst, IL, part number 4125K21) measured the pressure drop across the filter.

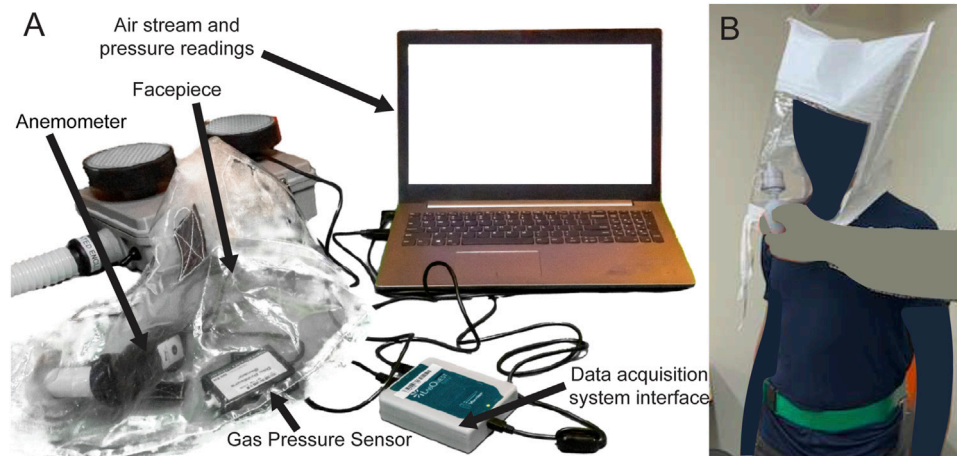
The AeroTrak Counter had a lower measurable limit of 300 nm particle size, which we expect to result in a more conservative estimate of filtration efficiency than particle sizes specified in NIOSH STPs (Stafford and Ettinger, 1967). Filter cartridges were placed within the apparatus in line with the flow of the KCl-containing particle stream. Special 3D-printed

adapters, sealed to the cartridges, were tightly coupled to upstream and downstream air ducts, ensuring no leakage. Filtration efficiency was computed from the measured KCl concentrations upstream and downstream of the cartridges.

The US Code of Federal Regulations (42 CFR § 84.175) specifies that PAPR performance should also be tested using dioctyl phthalate to assess its resistance to oil droplets (NIOSH STP TEB-APR-STP-0001). This is an instantaneous filtration test in which a filter cartridge is challenged with a dioctyl phthalate-containing aerosol for approximately 10 s. In lieu of dioctyl phthalate, which is a suspected carcinogen (National Biomonitoring Program, 2019), an aerosol containing the oil polyalphaolefin (PAO) was used. PAO is a chemical representative of the most widely used class of synthetic lubricants and a substitute for dioctyl phthalate accepted by the US military (Carlon et al., 1991). Filtration efficiency testing was then performed as described above.

### Air-Flow Testing

NIOSH requires a minimum flow rate of 170 lpm for PAPRs that have loose fitting facepieces (Approval Tests and Standards for Air-Purifying Particulate Respirators, 2020), as described in NIOSH STP RCT-APR-STP-0012. To measure flow rate, the STP describes connecting a vacuum chamber, evacuated with a vacuum pump, to a running PAPR blower unit and using a dry test meter to measure flow rate. In the absence of this setup, a conventional impeller type anemometer (Vernier Software and Technology, Beaverton, OR) was connected to the air inlet at the facepiece, with the neck opening sealed with tape (**Figure 3A**). An adapter was 3D-printed to couple the facepiece inlet to the anemometer flow area, such that all the flow into the facepiece passed through the cross-sectional area of the anemometer inlet. Flow rate was calculated by multiplying the air velocity recorded on the anemometer with the cross-sectional area. Additionally, a Vernier Gas Pressure Sensor placed inside the facepiece measured the positive pressure created in the facepiece. While not as precise as the procedure described in NIOSH STP RCT-APR-STP-0012,



**FIGURE 3 | (A)** Test setup to measure flow rate and the positive pressure inside the facepiece, using Vernier Anemometer and Gas Pressure Sensor. PAPR facepiece contains anemometer and gas pressure sensor. Tape covers the neck opening of the facepiece for testing. **(B)** Bitrex Fit Test setup.

we expect that the modified test provides a close approximation of the flow rate using equipment available in a standard laboratory.

### Facepiece Fit Testing

To determine if unfiltered air can enter the facepiece, we conducted a Bitrex (Edinburgh, Scotland) qualitative fit test as described in NIOSH STP RCT-APR-STP-0067 (Current Standard Testing Procedures for Air-Purifying Respirators, 2020) on one test subject (**Figure 3B**). This test evaluates whether flow rate into the facepiece is sufficient to prevent unfiltered ambient air from reaching the user; the unfiltered ambient air contains an aqueous aerosol of denatonium benzoate (a bitter chemical) and subjects are asked if they can taste it during the test. Under the NIOSH Interim Final Rule for PAPR testing, the fit test is to be performed as per NIOSH STP CVB-APR-STP-0010, wherein subjects donning the PAPR are sent into a room filled with corn oil aerosol. If the subject is able to taste the corn oil, the test is deemed to have failed. However, given the lack of a dedicated room in which to perform this test we adopted a Bitrex fit testing procedure which is commonly used in hospital settings to evaluate respirators of different types. The Bitrex test is a permissible substitute for corn oil testing according to pre-pandemic NIOSH testing requirements.

### Housing Sealing Testing

A modified Bitrex fit test was also used to evaluate the quality of seal created by the PAPR housing (we were unable to use the standard CVB-APR-STP-0010 testing protocol due to limitations in the availability of the necessary equipment). Bitrex was sprayed on the sealing surfaces of the blower units, including where the two parts of the blower unit join, the switch mount, and the filter connections. If a test subject can taste the Bitrex solution, the test was judged to have failed. Commercial Milwaukee vacuum cleaner filters sourced from a local home improvement store (or on-line) were connected to both blower units during these tests.

### Auditory, Communication, and Low Flow Rate Alarm Testing

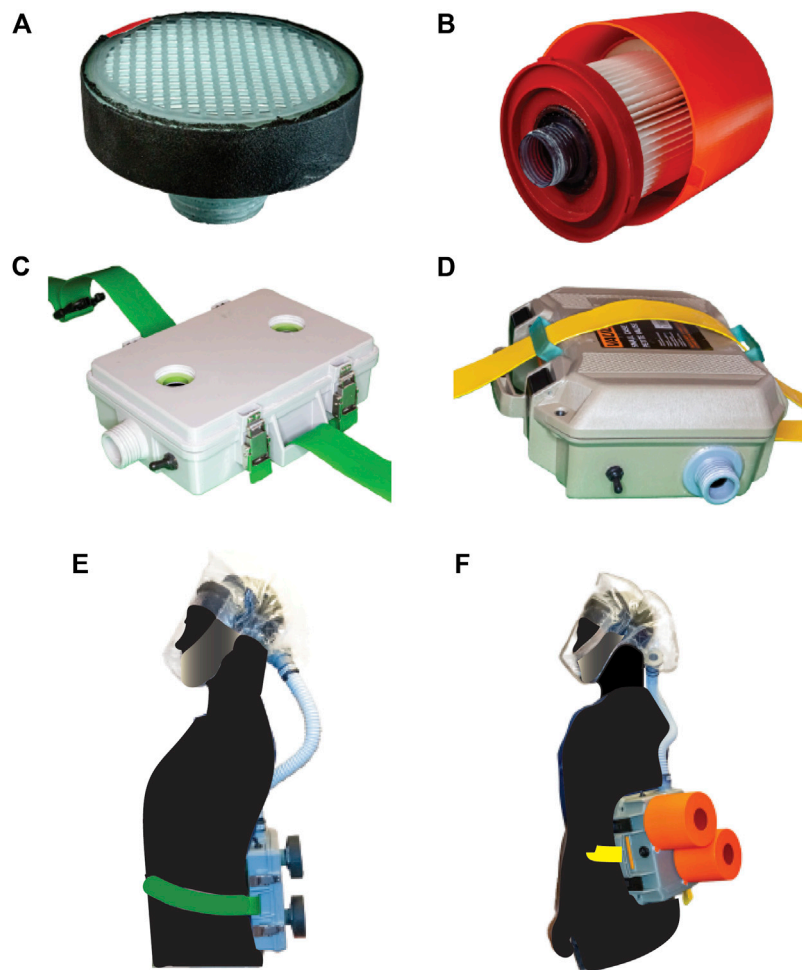
NIOSH STP RCT-APR-STP-0030 requires the noise level at each ear, with the blower unit running at maximum flow, not exceed 80 A-weighted decibels (dBA). We used a Vernier SLM-BTA Sound Level Meter to measure sound level. We also tested ease of communication following NIOSH STP CVB-APR-STP-0089. The subject was tasked with speaking and listening to a set of words. Ease of communication was evaluated by counting the number of words correctly transcribed in each task, normalized by baseline performance without the PAPR.

NIOSH STP CVB-APR-STP-0085 requires that PAPRs have an alarm to alert users when air flow rate falls below the minimum level of 170 lpm. Auditory alarms are required to be louder than 80 dBA. We used a Vernier SLM-BTA Sound Level Meter to measure the sound level of the low flow rate alarm after triggering the alarm by manually restricting the air flow at the facepiece inlet.

## RESULTS

PanFab Custom and Commercial Designs were developed for both filter cartridges and blower units (**Figure 4**). For a full description of the filter and blower unit designs, refer to **Table 1** and **Supplementary Material S2**. A Milwaukee Tool (Brookfield, WI) HEPA-rated vacuum cleaner filter (part number 49-90-1900) was selected as the PanFab Commercial Filter Cartridge. This filter model is readily available in North American home improvement stores and similar types of filters are available in other countries, driven by increasing concern about the health effects of exposure to silica dust in construction (Poinen-Rughooputh et al., 2016). Widespread innovation is occurring in this area (with many new tools having integrated HEPA filtration) and groups interested in other ways to develop respiratory protection devices for HCWs are encouraged to stay abreast of these developments. A custom 3D-printed





**FIGURE 4 |** PanFab PAPR components. **(A)** PanFab Custom filter cartridge. **(B)** PanFab Commercial filter cartridge. **(C)** PanFab Custom blower unit. **(D)** PanFab Commercial blower unit. **(E)** PanFab Custom Design (Custom filter cartridge plus Custom blower unit). **(F)** PanFab Commercial Design (Commercial filter cartridge plus Commercial blower unit).

adapter converts the outlet of the Milwaukee filter to standard NATO 40-millimeter threaded connection, allowing it to be used with the PanFab and other commercial blower units. With slight modification of the adapters, other commercial HEPA-rated vacuum cleaner filters could be used as alternatives. A custom 3D-printed filter cover protects the filter fabric. The Custom variant of the PanFab filter cartridge was designed in collaboration with Custom Filters LLC (Aurora, IL) to have the necessary 100-P rating while remaining small and light. Two filters were used in both variants of the PAPR as opposed to one, so as to minimize the pressure drop for a given flow rate and to provide redundancy.

A centrifugal blower (Delta Electronics, Neihu, Taiwan, Part Number BFB1012HD-04D4L) generates a 230 lpm flow rate, higher than the required 170 lpm, and a 12-volt (V) NiMH battery pack (Tenergy, Fremont, CA, Amazon Standard Identification Number: B077Y9HNTF) was used to power it; this battery pack was sufficient for ~4 h of continuous use. The battery can be charged in various ways, including with solar

power, as long as 12 Voltage Direct Current (VDC) < 1.8 A (Amp) can be supplied through an electrical connector compatible with that used in the battery. A wide variety of 12V NiMH and lithium ion battery packs are available at home improvement centers and could be used as substitutes following performance testing.

Control circuitry was based on a standard Arduino R3 board (Arduino LLC, Boston, MA) with a custom-fabricated shield (OSH Park, Portland, OR). Discrete components connected to the shield included a 10 kilohm potentiometer (Precision Electronics Corporation, North York, ON, Canada, part number RV4NAYS103A), differential pressure sensor (Sensirion AG, Staefa, Switzerland, part number SDP810-500PA), and piezoelectric buzzer (Mallory Sonalert Products Inc., Indianapolis, IN, part number PS-580Q). These components were used for control and alarm tasks such as regulating the air flow rate, measuring flow rate, and sounding the low-flow buzzer. All of the discrete components are readily substitutable with similar products made by multiple

manufacturers. We established that the Sonalert buzzer generated a sound of at least 80 dBA (as per CVB-APR-STP-0085) when the flow rate fell below a NIOSH specified threshold (as per CVB-APR-STP-0088). The shield circuit diagram, fabrication files, and Arduino code are all available in **Supplementary Material S4**.

The housings that enclose the blower, battery, and control components were designed to be airtight when closed, with the filters and hose attached. In the case of the Commercial Design, a Pelican V100 Vault Case (Pelican Products, Torrance, CA) was used with custom made “inserts” for connection to filters and hose via NATO 40mm connections. The Custom housing was designed to be smaller and lighter in weight, with integrated connections to the filters and hose. A hood coupler and a locking ring were designed to connect the hose to the facepieces, which use a NATO 40 mm threaded connection. Finally, a hose adapter was designed to form air-tight connections between the ends of the plastic hose, the housing outlet, and the facepiece inlet. While all custom-made parts, including the custom housing, were 3D printed for prototyping, these designs were also optimized for injection molding to facilitate future high volume production (Antonini et al., 2021). The CAD files for all custom and 3D printable/moldable parts, as well as printing instructions, are in **Supplementary Material S4**.

With their respective filters installed, the PanFab Custom and Commercial PAPRs weighed 1.87 and 3.36 kg, respectively. Both PanFab PAPRs are worn on the waist using a Skil-Care (Yonkers, NY) PathoShield Gait Belt. This 50 mm wide web belt is heat-sealed (rather than stitched), has a liquid-proof plastic coating covering the vinyl webbing (for easy cleaning) and a Delrin side-release buckle; it is widely available in healthcare settings and many functionally identical substitutes exist. The maximum enveloping cuboidal dimensions of the PanFab Custom and Commercial PAPRs (including their respective filters) along lateral, longitudinal, and sagittal axes are 21 cm × 25.8 cm × 12.4 cm and 30.6 cm × 33.6 cm × 25.4 cm respectively. Run time for the PanFab blower units was measured to be approximately 3 h and 55 min and charge time approximately 2 h and 53 min at 0.9 A charging current, with a variance on the order of 1–2 min for the runtime and charge time respectively. This compares favorably to the Ford-3M Limited-Use Public Health Emergency PAPR blower unit, which weighs 2.7 kg, runs for 4–6 h, and has a charge time of 1.5 h with a 3 Amp hour battery (Limited-Use Public Health Emergency PAPR, 2021). Alternative battery packs could easily be added to the PanFab design to increase run time; charge time is primarily a function of the charger.

The estimated cost in parts for a single unit of the PanFab Custom PAPR is 284 USD and for the PanFab Commercial PAPR is 328 USD. A detailed *Bill of Materials* for both PAPRs is provided in **Supplementary Material S4**. Consultation with industry experts in the area of respiratory protection, including a NIOSH certified manufacturer, allowed us to estimate the final cost for PanFab designs including commercialization and labor costs, and account for discounts for materials ordered in bulk. This yielded an estimated per-unit cost for the PanFab Custom PAPR of 310 USD. In comparison, the Ford-3M PAPR designed for pandemic response has been reported to sell for 715 USD (Cole, 2020). This compares with

low-cost commercial PAPR prices of ~800 USD per unit, a 3 M Versaflo PAPR price of ~1,775 USD per unit (3M, 2021), and N95 mask costs of ~1.50 USD per unit.

The development of functional PanFab PAPR prototypes took a total of eight months with initial product specification and prototyping completed in three months. Additional manufacturing modifications took an additional two months. The latter set of modifications readied the PAPRs for large-scale production via injection molding. While prototyping was underway, the design validation and testing procedure was established over a period of five months. Design validation was constrained by the availability of testing resources under pandemic conditions. This, together with a dearth of explanations for testing specifications, were the primary factors slowing completion of the project. We hope that our descriptions of testing approaches and regulatory documents will allow others to proceed more quickly.

## Testing and Validation

PanFab PAPR components underwent a series of rigorous testing and validation steps. As mentioned earlier, many traditional NIOSH tests were not readily available from commercial laboratories due to high demand associated with the COVID-19 pandemic. Moreover, tests are highly prescriptive and not easily set up in an academic research laboratory. A further compromise we were forced to make is that full NIOSH certification was simply not possible for the PanFab PAPRs, regardless of testing procedures, in the absence of documentation that they would be manufactured according to established quality-control criteria. Compliance with these manufacturing standards is important, but it is secondary to our goal of developing a functional PAPR design. We therefore established alternate test setups and protocols to replicate several NIOSH tests (**Table 2**). The ability of the final designs to pass these tests should increase the confidence of traditional and non-traditional manufacturers that PanFab designs are very likely to pass full NIOSH certification; we very strongly encourage formal certification testing prior to use of these designs in a healthcare setting.

## Filter Tests

Two filter cartridges were used in PanFab PAPRs. One was an off-the-shelf HEPA-rated vacuum cleaner filter manufactured by Milwaukee, and the other was a 100-P rated filter designed in collaboration with Custom Filters LLC. As part of loading test, two Milwaukee filter cartridges and one Custom Filters filter were challenged with KCl aerosol at an operationally equivalent flow rate of 230 lpm. Filtration efficiency with 300 nm aerosol size was found to be 99.99 and 100.00% for two replicate Milwaukee filters and 99.99% for the Custom Filters filter, thereby exceeding the NIOSH salt aerosol filtration efficiency criteria of 99.97%. Equipment was not available to measure filtration efficiency below 300 nm but it is generally observed that HEPA filtration efficiency is lowest at 300 nm and increases as particle size falls (US EPA, 2019). Results from our testing apparatus also correlate with prior testing done at ICS Laboratories, Inc. (Brunswick, OH) for N95-type respirators; ICS Laboratories, Inc. performs third

party testing to NIOSH standards using NIOSH STPs (for more information, visit [Cleanmask.org](https://www.cleankmask.org) (Clean Mask, 2021)).

In the PAO-based instantaneous filtration test carried out by Custom Filters LLC, two Milwaukee filter cartridges and one Custom Filters cartridge were challenged with 90.56 mg/m<sup>3</sup> PAO aerosols at 85 lpm. Filtration efficiency was 99.18 and 99.58% for the two Milwaukee filter replicates and 99.98% for the Custom Filters filter. While the Milwaukee filter does not pass the NIOSH requirement of efficiency higher than 99.97% for oil-based aerosol, consultation with experts on NIOSH certification and regulation led us to conclude that this would not necessarily preclude use in a healthcare setting, given the low concentration of oil aerosols found in this environment. Oil aerosols are primarily a concern in industrial settings in which PAPRs are also used.

### Air Flow Tests

Using the apparatus described in the Methods section, flow rate was calculated as the product of the measured velocity and the cross-sectional area of the anemometer. Flow rate with a 70% blower Pulse Width Modulation (PWM) duty cycle was measured to be close to 240 lpm for both filter types. A positive pressure of 40 Pa was recorded inside the facepiece.

### Facepiece Fit Tests

Qualitative fit testing, using Bitrex as the testing agent was performed repeatedly on one subject, as per RCT-APR-STP-0067. Tests were performed with all configurations of the Commercial and Custom PAPR designs (i.e., using Custom and Commercial blower units with Commercial and Custom filter cartridges). The University of Washington (CLIMB) (UW Mechanical Engineering Research Centers, 2012) facepiece was used in our tests. No Bitrex could be tasted by the subject in any of the test configurations, in any of the tasks prescribed in the facepiece fit test STP, indicating a successful result.

### Housing Sealing Tests

Bitrex was sprayed on the sealing surfaces of the PAPR blower units. No Bitrex was tasted when tests were performed with both of the PAPR housings, indicating successful seals for both PanFab PAPR designs.

### Auditory Communication Tests

Noise level in the facepiece at the ears was measured at between 58.1 and 59.2 dBA at full battery charge and maximum blower speed, which is lower than the 80 dBA limit set in RCT-APR-STP-0030. Low flow alarm sound level at the ears was found to be between 82.95 and 84.7 dBA at battery charge corresponding to the as-designed low flow condition of 230 lpm flow rate, which passes the 80dBA requirement in CVB-APR-STP-0085. The ability of PAPR wearers to communicate with other individuals was tested with one subject as per CVB-APR-STP-0089 with a 99.9% performance rating for listening and 74% for speaking tasks; both pass the required 70% threshold (see the STP for definition of performance rating). Full information regarding PanFab PAPR validation testing performed during pandemic conditions is summarized in **Table 2**.

**TABLE 3 |** Test subject demographic information.

Subject	Height (cm)	Weight (kg)	BMI	Sex	Regular PAPR Use
1	160	57	22.3	Female	No
2	175	70	22.9	Male	No
3	178	100	31.6	Male	Yes
4	175	136	42.9	Female	Yes

## End-User Feedback

To evaluate factors affecting usability in a clinical setting, we created a clinical feedback questionnaire and distributed it to four participants who used and rated the performance of the PanFab PAPRs. Two participants were clinicians, who had not used PAPRs regularly prior to the pandemic, and two were research technical staff for whom PAPR use is a standard part of occupational PPE (**Table 3**).

User testing of PanFab PAPRs focused on three main criteria: 1) comparison to current PPE options; 2) sense of security with use in a clinical setting; and 3) comfort as compared to standard commercially available PAPRs. Additional questions assessed the PAPR facepiece alone, as well as ease of donning and doffing. A full list of questions and results are available in **Supplementary Material S3**. Four versions of the PanFab PAPR were assessed using different types of filters and blower units: one with a commercial filter and blower unit (PanFab Commercial Design), one with a custom filter and blower unit (PanFab Custom Design), and two versions with mixed Custom and Commercial filters and housings. Of all PanFab PAPR versions, the PanFab Custom Design performed most favorably: all four respondents rated the PanFab Custom PAPR superior to current PPE options, with a score of 4–5 on a 5 Likert-scale across the three criteria listed below (**Table 4**).

The three other versions of the designs (with a Commercial blower unit, filter, or both) performed favorably, with survey responses consisting of scores ranging from 3–5. Participants experienced more issues with mobility as compared to the fully-custom PAPR, and comments on PAPR versions using commercial parts emphasized the need for better weight distribution to improve balance. Participant comments across all PAPR design versions focused on possible improvements regarding the sizing and comfort of the PAPR facepiece, which was not part of the current study and was instead provided by collaborators. In sum, the clinical feedback suggested that the PanFab PAPRs are favorable alternative forms of PPE in terms of user comfort, mobility, and sense of security with use. Additional testing with a larger number of participants will be required to formally compare the performance of different PAPR configurations.

## DISCUSSION

The successful design, prototyping, and testing of a PAPR by a volunteer team comprising medical professionals, scientists, student engineers, and concerned citizens (the PanFab team)

**TABLE 4 |** Clinical feedback survey results. Score averaged among four users.

Enclosure	Filter	Compare to available PPE, average user score <sup>a</sup> (n = 4)	Sense of security with use, average user score <sup>b</sup> (n = 4)	Comfort compared to standard PAPR, average user score <sup>c</sup> (n = 4)
Custom	Custom	4	4.75	5
Custom	Milwaukee	3.75	4.75	4.25
Pelican	Custom	3.25	4.5	3.75
Pelican	Milwaukee	3	4	3.25

<sup>a</sup>Score of 1 = PanFab PAPR much worse than current PPE options, 5 = PanFab PAPR much better than current PPE options.

<sup>b</sup>Score of 1 = Very uncomfortable, 5 = Very comfortable.

<sup>c</sup>Score of 1 = PanFab PAPR much worse than standard, 5 = PanFab PAPR much better than standard.

demonstrates the potential for addressing pandemic-related shortages of relatively complex types of PPE using a rapid and iterative approach to prototyping and design (Antonini et al., 2021). The process generated near-final PAPR designs with full-time effort by three graduate engineering students, support from a clinical specification and testing team, access to standard academic laboratories, and modest financial support provided in part by the MIT COVID-19 Emergency Fund and the decision of the US National Institutes of Health to allow individuals paid by Federal research grants to devote time and effort to pandemic mitigation. Testing required more time than design and fabrication, as discussed below.

## Design and Results

The PanFab Commercial Design used commercially available components with custom-fabricated modifications while the PanFab Custom Design used additive manufacturing (3D-printing) to create a fully customized, lighter weight, and smaller enclosure. Frequent feedback from clinicians who use PAPRs in a hospital setting strongly influenced design decisions, particularly with respect to PAPR comfort and usability. Key design decisions included determining size and orientation of the housing, the number and orientation of the filters, and the method of donning/doffing the blower unit. Feedback from manufacturing experts yielded a design that is amenable to large-scale production by injection molding of the blower housing. PanFab PAPR designs are modular and compatible with several standard commercial PAPR components, including facepieces and filters, allowing for substitution of components in limited supply. The PanFab Custom Design compares favorably to the 3 M Ford Limited-Use Public Health Emergency PAPR (Limited-Use Public Health Emergency PAPR, 2021) with respect to weight and size, although the 3 M Ford unit appears to use higher performance batteries. Both PanFab designs also compare favorably to commercial PAPRs with respect to cost.

The safety and functionality of PanFab PAPRs was evaluated using protocols that closely followed NIOSH STPs and aimed to meet or exceed the functional objectives of those tests. Given the limitations imposed by pandemic conditions, it was necessary to use substitute tests in university laboratories rather than use a NIOSH-specific apparatus at a commercial pre-certification laboratory. PanFab PAPRs passed all of the performed tests, in

various combinations of Commercial and Custom components. User feedback on the PAPRs was obtained from clinicians inexperienced in using PAPRs and technical research staff who routinely use PAPRs in a major Boston-area hospital. The PanFab Custom Design scored favorably as compared to the traditionally manufactured PAPRs (primarily from ILC Dover) available to hospital staff. This feedback also guided improvements that were made during iterative design of the prototype (e.g., using a different hood with the PAPR design to accommodate a greater diversity of user face shapes).

A limitation in the current study is that PanFab PAPRs were not tested in real-world settings, including for extended periods of time in a hospital. We are therefore unable to make claims about the durability of the designs in clinical use or the resistance of the units to damage. We were also unable to assess the efficacy of different methods for sterilizing PanFab PAPRs, but materials used in the designs are compatible with alcohol-based wipes (e.g., acrylonitrile butadiene styrene (Industrial Specialties Mfg and IS MED Specialties, 2019) allowing CDC recommendations for disinfecting PAPRs to be followed (CDC, 2020b). Previous research also suggests that ionized hydrogen peroxide techniques would be compatible with PAPR sterilization (Cramer et al., 2021). Additional usability, durability and sterilization testing await the availability of additional PAPR units assembled during production scale-up. However, the tests in this paper achieve the goal of PAPR design validation.

## Challenges in Design, Testing, and Regulatory Approval

During early specification and prototyping, we faced significant challenges in locating relevant design criteria for PAPRs. There also exists very limited information in the public domain on alternate testing equipment. Answers to questions such as the minimum time of continuous device operation required, relevant material characteristics for facepiece fabrics, and appropriate materials for the pathway for inhaled air were not readily available. We therefore sought out experts with relevant expertise. Substantial time and effort would have been saved had a centralized resource of information been available. To streamline the process for future crises, we have consolidated relevant information collected from US regulatory agencies in **Supplementary Material S1**. We encourage individuals from



other countries to contact us with information relevant to products in their markets and will provide this updated information on PANFAB.ORG.

When evaluating our designs, we found that it was difficult to use NIOSH standard testing procedures since the necessary equipment was not readily available. Informed substitution was made difficult by prescriptive procedures and opaque objectives in terms of fundamental mechanical or physical principles being assessed. Our use of third-party commercial labs that test to NIOSH standards was also limited by long lead times and a requirement for multiple samples of each prototype, which would require financial resources beyond those available to our group. Thus, testing equipment and protocols, as opposed to design and fabrication, emerged as the primary challenge in developing the PanFab PAPRs.

Despite our best efforts, regulatory hurdles remain for use PanFab PAPRs in a clinical setting. To receive NIOSH certification, a product must be manufactured and submitted by a NIOSH-approved manufacturer with a quality management system in place. Under normal circumstances, this requirement guarantees the safety of products made in volume. However, this restricts the development of new products to NIOSH-approved manufacturers, which has had the effect of creating near-monopolies for some types of PPE. To improve resilience in future emergencies, regulators might consider how to optimally balance the risk of non-traditional PPE against the risk of no protection at all. We propose that consideration be given to rules that allow non-NIOSH certified fabricators to respond to declared healthcare emergencies while still complying with the most critical aspects of functional testing. Under this process, critical “go or no-go” tests would be defined by clearly described physical principles and corresponding testing protocols that could be performed on generally available laboratory equipment. The modified standards would include an explicit description of the end goal of the test and suggest a range of alternative devices that can be used to measure airflow, filtration efficiency, audibility, user testing etc. Rational substitution of instruments would also be allowed. While we do not advocate for relaxing standards under non-crisis conditions, modifying and streamlining testing procedures for prototype devices would reduce barriers to the entry of new products and promote innovation.

## CONCLUSION

The current COVID-19 crisis has revealed major weaknesses and points of failure in our health care system and its supply chains, particularly for PPE. This does not come as a surprise. Multiple studies over a 15-year period have decried the absence of innovation in the design and provision of respiratory protection for health care and other essential workers (Sinha et al., 2020). For example, a 2006 report by the US Institute of Medicine (IOM) called for urgent research to inform the design and development of new medical masks and respirators (Institute of Medicine, 2006); a 2008 IOM report addressed the design and engineering of more effective PPE (Institute of Medicine, 2008); the 2009 Project B.R.E.A.T.H.E. report laid out a comprehensive action plan for a new generation of respirators (Department of Veterans Affairs, 2009); and a 2019 consensus report from the US

National Academies of Sciences echoed the same urgent needs (National Academies of Sciences, Engineering, and Medicine, 2019). Despite these repeated calls for action and greater innovation, there has been little response from the commercial sector or from government: in the COVID-19 pandemic, most innovation has come from volunteer groups of scientists and clinicians allied with maker communities with access to rapid prototyping and fabrication equipment, technology that is increasingly inexpensive and available to ordinary citizens (Sinha et al., 2020). Thus, open source product development (OSPD) (Huizingh, 2011) emerges as perhaps the only avenue to mitigating existing weaknesses while increasing product innovation under both normal and crisis conditions.

An OSPD approach is not a panacea and it is not free. As discussed above, it would be helpful for NIOSH and other regulatory agencies to develop less prescriptive testing procedures for products such as PAPRs. Funding is also essential. The work described here benefited from the generosity of many individuals but all attempts to fund it via competitive applications to foundations or universities were turned down because research into respiratory protection is not considered innovative by conventional academic criteria (salary support for grant-funded investigators was, however, temporarily available under relaxed grant guidelines from the US National Cancer Institute under NOT-CA-20-054). This speaks to a larger problem in matching acute healthcare needs to available expertise and necessary resources in academia, not just industry.

The production of a regulated medical product is difficult to achieve in the absence of commercial expertise. This is consistent with previous data showing that OSPD is most effective within the context of private-public partnerships (Bonvoisin et al., 2018). We are therefore working with an industry partner to develop PanFab PAPRs into commercial products. However, all the PanFab PAPR designs and software described here remain public domain resources and are available under non-restrictive Creative Commons Attribution-ShareAlike 4.0 International Public License; the design files, CAD files, and code are available on GitHub (<https://github.com/labsyspharm/PanFab-PAPR-2021>) and on the NIH 3D-Print exchange online repository (NIH 3D Print Exchange, 2020). Additionally, all materials needed for the construction and use of the design are also available in **Supplementary Material S2**, **Supplementary Material S4**. We hope that these materials serve as a resource for further development and innovation.

## DATA AVAILABILITY STATEMENT

The original contributions presented in the study are included in the article/**Supplementary Material** and can also be found on GitHub (<https://github.com/labsyspharm/PanFab-PAPR-2021>) and through the online NIH 3D Print Exchange (<https://3dprint.nih.gov/discover/3dpx-015673>; <https://3dprint.nih.gov/discover/3dpx-015672>; <https://3dprint.nih.gov/discover/3dpx-015671>; <https://3dprint.nih.gov/discover/3DPX-015674>).

## ETHICS STATEMENT

The studies involving human participants were reviewed and approved by The Partners Healthcare Institutional Review Board (protocol #2021P000727). Written informed consent for participation was not required for this study in accordance with the national legislation and the institutional requirements.

## AUTHOR CONTRIBUTIONS

PanFab PAPR design, prototyping, and production: AK, LA, DP, FW, CD, AC, RM, JF, OM, PG, CV, CH, YL, NL, and PS. PanFab PAPR filtration testing: ET and JL. PanFab PAPR prototype iteration and clinical feedback coordination: NL. Manuscript writing: AK, LA, DP, and PS. Manuscript review and editing: AK, LA, DP, FW, CD, AC, RM, JF, ET, OM, PG, CV, CH, HY, YL, MS, JL, SY, NL, and PS. Greater Boston Pandemic Fabrication Team (PanFab) Consortium Coordination: DP, HY, NL, and PS.

## FUNDING

This work was supported by the MIT COVID-19 Emergency Fund, by the Harvard-MIT Center for Regulatory Science, by NIH/NCI Grants P30-CA006516, U54-CA225088 (to PS, NL, and DP), and T32-GM007753 (to DP), and by the Harvard Ludwig Center. AC is supported by the Hugh Hampton Young Fellowship of MIT. LA is supported by T32-GM136577.

## REFERENCES

- 3M (2021). 3M™ Versaflo™ Heavy Industry PAPR Kit TR-300N+ HIK 1 EA/Case. Available at: [https://www.3m.com/3M/en\\_US/p/d/v100559008/](https://www.3m.com/3M/en_US/p/d/v100559008/) (Accessed April 4, 2021).
- Antonini, M.-J., Plana, D., Srinivasan, S., Atta, L., Achanta, A., Yang, H., et al. (2021). A Crisis-Responsive Framework for Medical Device Development Applied to the COVID-19 Pandemic. *Front. Digit. Health.* 3, 617106. doi:10.3389/fdgh.2021.617106
- Approval Tests and Standards for Air-Purifying Particulate Respirators (2020). Approval Tests and Standards for Air-Purifying Particulate Respirators. *Fed. Regist.* 85, 20601–20603. Available at: <https://www.federalregister.gov/documents/2020/04/14/2020-07804/approval-tests-and-standards-for-air-purifying-particulate-respirators>.
- Bergman, M. S., Viscusi, D. J., Zhuang, Z., Palmiero, A. J., Powell, J. B., and Shaffer, R. E. (2012). Impact of Multiple Consecutive Donnings on Filtering Facepiece Respirator Fit. *Am. J. Infect. Control.* 40, 375–380. doi:10.1016/j.jaicc.2011.05.003
- Bonvoisin, J., Buchert, T., Preidel, M., and Stark, R. (2018). How Participative Is Open Source Hardware? Insights From Online Repository Mining. *Des. Sci.* 4, 3–7. doi:10.1017/dsj.2018.15
- Bui, A.-T. N., Yu, Z., Lee, K., Li, S. J., Tsiaras, W. G., Yu, S. H., et al. (2021). A Pilot Study of the Impact of Facial Skin Protectants on Qualitative Fit Testing of N95 Masks. *J. Am. Acad. Dermatol.* 84, 554–556. doi:10.1016/j.jaad.2020.06.069
- Carlson, H. R., Guelta, M. A., and Gerber, B. V. (1991). Some Candidate Replacement Materials for Diethyl Phthalate in “Hot Smoke” Aerosol Penetrometer Machines. *Aerosol Sci. Technol.* 14, 233–246. doi:10.1080/02786829108959486
- CDC (2020a). Considerations for Optimizing the Supply of Powered Air-Purifying Respirators (PAPRs). *Centers Dis. Control. Prev.* Available at: <https://www.cdc.gov/coronavirus/2019-ncov/hcp/ppe-strategy/powering-air-purifying-respirators-strategy.html> (Accessed April 4, 2021).

## ACKNOWLEDGMENTS

We thank Jennifer Delaney (Washington University), Hunter Engineering Company (Bridgeton, MO), Joseph Iaquinto (University of Washington), Ben Linville-Engler (Manufacturing Emergency Response Team), Jinhan Mo (Tsinghua University), the MGB Full Body Protection Working Group, the Ju Li Group (MIT), the Rutledge Lab (MIT), Paul Nederhoed (Paul Nederhoed Photography, LLC), David Krikorian and Meghan Patterson (DFCI), Mike Copponi (DFCI), Brandon Beller (PanFab), Thomas Pouchot (NIOSH), Norman Wen (Emulate Inc), David Turner (DFCI Animal Research Facility), Myron Kassaraba (MIT Technology Licensing Office), and Grant Zimmermann (Harvard Office of Technology Development). Local citizens and engineers have generously donated their time and resources to PanFab and they are essential to program success.

## SUPPLEMENTARY MATERIAL

The Supplementary Material for this article can be found online at: <https://www.frontiersin.org/articles/10.3389/fbioe.2021.690905/full#supplementary-material>

**SUPPLEMENTARY MATERIAL S1** | NIOSH PAPR standard testing procedures.

**SUPPLEMENTARY MATERIAL S2** | Full description of PanFab PAPR design methodology and selected prototype components.

**SUPPLEMENTARY MATERIAL S3** | Full clinical survey questions and results.

**SUPPLEMENTARY MATERIAL S4** | PanFab PAPR design materials and instructions, including: 3D-printing instructions, Arduino code, assembly instructions, bill of materials, CAD design files, custom Arduino shield design, and use instructions.

- [gov/coronavirus/2019-ncov/hcp/ppe-strategy/powering-air-purifying-respirators-strategy.html](https://www.cdc.gov/coronavirus/2019-ncov/hcp/ppe-strategy/powering-air-purifying-respirators-strategy.html) (Accessed April 4, 2021).
- CDC (2020b). Powered Air Purifying Respirators (PAPRs). *Centers Dis. Control. Prev.* Available at: <https://www.cdc.gov/coronavirus/2019-ncov/hcp/ppe-strategy/powering-air-purifying-respirators-strategy.html> (Accessed April 4, 2021).
- CDC (2020c). Powered Air-Purifying Respirators (PAPR) Tests | NPPTL | NIOSH | CDC. Available at: <https://www.cdc.gov/niosh/npptl/stps/aprespInterim.html>.
- CDC (2014). Respiratory Protective Devices Used in Healthcare. Federal Register. Available at: <https://www.federalregister.gov/documents/2014/03/14/2014-05611/respiratory-protective-devices-used-in-healthcare>.
- Clark, P. A. (2020). Makers Are 3D Printing Ventilator Gear and Sewing Masks to Fight the Coronavirus. *Time*. Available at: <https://time.com/5811091/makers-3d-printing-coronavirus/>.
- Clean Mask (2021). Available at: <http://cleanmask.org/index> (Accessed April 4, 2021).
- Cole, C. (2020). We Try Ford's Respirator That's Protecting Health Care Workers From Coronavirus. *Roadshow*. Available at: <https://www.cnet.com/roadshow/news/ford-respirator-healthcare-workers-coronavirus/>.
- COVID-19 Response (2020). Lowell Makes. Available at: <https://lowellmakes.com/covid-19-response/> (Accessed April 4, 2021).
- Cramer, A. K., Plana, D., Yang, H., Carmack, M. M., Tian, E., Sinha, M. S., et al. (2021). Analysis of SteraMist Ionized Hydrogen Peroxide Technology in the Sterilization of N95 Respirators and Other PPE. *Sci. Rep.* 11, 2051. doi:10.1038/s41598-021-81365-7
- Current Standard Testing Procedures for Air-Purifying Respirators (2020). Current Standard Testing Procedures for Air-Purifying Respirators | NPPTL | NIOSH | CDC. Available at: <https://www.cdc.gov/niosh/npptl/stps/apresp.html> (Accessed April 4, 2021).

- Department of Veterans Affairs (2009). Project Better Respiratory Equipment Using Advanced Technologies for Healthcare Employees (B.R.E.A.T.H.E.). *Fed. Regist.* 66198–66200. Available at: <https://www.federalregister.gov/documents/2009/12/14/E9-29709/project-better-respiratory-equipment-using-advanced-technologies-for-healthcare-employees-breathe>.
- eCFR (2021). eCFR: Title 29. Available at: <https://ecfr.federalregister.gov/current/title-29/subtitle-B/chapter-XVII/part-1910/subpart-I/section-1910.134> (Accessed April 4, 2021).
- Get Us PPE (2021). Available at: <https://getusppe.org/> (Accessed April 4, 2021).
- Gheisari, M., Araghi, F., Moravvej, H., Tabary, M., and Dadkhahfar, S. (2020). Skin Reactions to Non-Glove Personal Protective Equipment: an Emerging Issue in the COVID-19 Pandemic. *J. Eur. Acad. Dermatol. Venereol.* 34, e297. doi:10.1111/jdv.16492
- Hack the Pandemic (2020). Hack the Pandemic – Copper 3D | Antibacterial 3D Printing. Available at: <https://copper3d.com/hackthepandemic/> (Accessed April 4, 2021).
- Huizingh, E. K. R. E. (2011). Open Innovation: State of the Art and Future Perspectives. *Technovation*. 31, 2–9. doi:10.1016/j.technovation.2010.10.002
- ILC Dover (2021). PAPRs to Protect against Infectious Diseases | ILC Dover. Available at: <https://www.ilcdover.com/catalog/infectious-disease-paprs/> (Accessed April 4, 2021).
- Industrial Specialties Mfg and IS MED Specialties (2019). Plastic Compatibility With Sterilization Methods.. Available at <https://www.industrialspec.com/resources/plastics-sterilization-compatibility/>.
- Institute of Medicine (2006). *Reusability of Facemasks during an Influenza Pandemic: Facing the Flu*. Washington: National Academies Press, 11637. doi:10.17226/11637
- Institute of Medicine (2008). *Preparing for an Influenza Pandemic: Personal Protective Equipment for Healthcare Workers*. Washington: National Academies Press, 11980. doi:10.17226/11980
- Institute of Medicine (2015). *The Use and Effectiveness of Powered Air Purifying Respirators in Health Care: Workshop Summary*. Washington: National Academies Press, 18990. doi:10.17226/18990
- Ivry, B., and Kochkodin, B. (2020). *For New York, 58-Cent Medical Masks Now Priced at \$7.50 Each*. New York, NY: Bloomberg.com.
- Lan, J., Song, Z., Miao, X., Li, H., Li, Y., Dong, L., et al. (2020). Skin Damage Among Health Care Workers Managing Coronavirus Disease-2019. *J. Am. Acad. Dermatol.* 82, 1215–1216. doi:10.1016/j.jaad.2020.03.014
- Limited-Use Public Health Emergency PAPR (2021). Limited-Use Public Health Emergency PAPR | 3M Personal Protective Equipment (PPE) Info. Available at: [https://www.3m.com/3M/en\\_US/worker-health-safety-us/covid19/ford-papr/](https://www.3m.com/3M/en_US/worker-health-safety-us/covid19/ford-papr/) (Accessed April 4, 2021).
- McAvoy, M., Bui, A.-T. N., Hansen, C., Plana, D., Said, J. T., Yu, Z., et al. (2021). 3D Printed Frames to Enable Reuse and Improve the Fit of N95 and KN95 Respirators. *BMC Biomed. Eng.* 3, 10. doi:10.1186/s42490-021-00055-7
- McCue, T. J. (2020). 3D Printer Groups Continue Working Round the Clock to Help 2020 PPE Shortage. *Forbes*. Available at: <https://www.forbes.com/sites/tjmccue/2020/03/30/protect-healthcare-workers-3d-printer-groups-race-to-help-2020-ppe-shortage-coronavirus-covid19/> (Accessed April 4, 2021).
- Mostaghimi, A., Antonini, M.-J., Plana, D., Anderson, P. D., Beller, B., Boyer, E. W., et al. (2020). Regulatory and Safety Considerations in Deploying a Locally Fabricated, Reusable Face Shield in a Hospital Responding to the COVID-19 Pandemic. *Med* 1, 139–151. doi:10.1016/j.medj.2020.06.003
- N95 Decon (2020). Available at: <https://www.n95decon.org/> (Accessed April 4, 2021).
- National Academies of Sciences, Engineering, and Medicine (2019). *Reusable Elastomeric Respirators in Health Care: Considerations for Routine and Surge Use*. Washington, DC: The National Academies Press, 25275. doi:10.17226/25275
- National Biomonitoring Program (2019). Phthalates Factsheet | National Biomonitoring Program | CDC. Available at: [https://www.cdc.gov/biomonitoring/Phthalates\\_FactSheet.html](https://www.cdc.gov/biomonitoring/Phthalates_FactSheet.html) (Accessed April 4, 2021).
- NIH 3D Print Exchange (2020). NIH 3D Print Exchange | A Collection of Biomedical 3D Printable Files and 3D Printing Resources Supported by the National Institutes of Health (NIH). *NIH 3D Print Exchange*. Available at: <https://3dprint.nih.gov/>.
- Occupational Safety and Health Administration (2021). Respirator Fit Testing | Occupational Safety and Health Administration. Available at: [https://www.osha.gov/video/respiratory\\_protection/fittesting\\_transcript.html](https://www.osha.gov/video/respiratory_protection/fittesting_transcript.html) (Accessed April 4, 2021).
- Open Mask (2021). Available at: <https://open-mask.org/> (Accessed April 4, 2021).
- OSHA Technical Manual (2006). OSHA Technical Manual (OTM) | Section VIII: Chapter 2: Respiratory Protection | Occupational Safety and Health Administration. Available at: [https://www.osha.gov/dts/osta/otm/otm\\_viii/otm\\_viii\\_2.html](https://www.osha.gov/dts/osta/otm/otm_viii/otm_viii_2.html) (Accessed April 4, 2021).
- PanFab (2021). Available at: <https://www.panfab.org/> (Accessed April 4, 2021).
- Plana, D., Tian, E., Cramer, A. K., Yang, H., Carmack, M. M., Sinha, M. S., et al. (2021). Assessing the Filtration Efficiency and Regulatory Status of N95s and Nontraditional Filtering Face-Piece Respirators Available During the COVID-19 Pandemic. *BMC Infect. Dis.* 21, 712. doi:10.1186/s12879-021-06008-8
- Poinen-Rughooputh, S., Rughooputh, M. S., Guo, Y., Rong, Y., and Chen, W. (2016). Occupational Exposure to Silica Dust and Risk of Lung Cancer: an Updated Meta-Analysis of Epidemiological Studies. *BMC Public Health*. 16, 1137. doi:10.1186/s12889-016-3791-5
- Rebmann, T., and Wagner, W. (2009). Infection Preventionists' Experience During the First Months of the 2009 Novel H1N1 Influenza A Pandemic. *Am. J. Infect. Control*. 37, e5–e16. doi:10.1016/j.ajic.2009.09.003
- Sinha, M. S., Bourgeois, F. T., and Sorger, P. K. (2020). Personal Protective Equipment for COVID-19: Distributed Fabrication and Additive Manufacturing. *Am. J. Public Health*. 110, 1162–1164. doi:10.2105/ajph.2020.305753
- Stafford, R. G., and Ettinger, H. J. (1967). Filter Efficiency as a Function of Particle Size and Velocity. *Atmos. Environ.* 6, 353–362. doi:10.1016/0004-6981(72)90201-6
- Thingiverse.com (2020). HEPA Covid Coronavirus Face Mask by Kvaththro. Available at: <https://www.thingiverse.com/thing:4222563> (Accessed April 4, 2021).
- Tompkins, B. M., and Kerchberger, J. P. (2010). Personal Protective Equipment for Care of Pandemic Influenza Patients: A Training Workshop for the Powered Air Purifying Respirator. *Anesth. Analgesia*. 1, 1. doi:10.1213/ANE.0b013e3181e780f8
- US EPA (2019). What Is a HEPA Filter? *US EPA*. Available at: <https://www.epa.gov/indoor-air-quality-iaq/what-hepa-filter-1>.
- UW Mechanical Engineering Research Centers (2012). Available at: <https://www.me.washington.edu/research/centers> (Accessed April 4, 2021).
- Westervelt, E. (2020). Can the U.S. Crowdfund its Way Out of a Mask Shortage? No, but it Still Helps. *NPR.Org*. Available at: <https://www.npr.org/2020/03/25/820795727/can-the-u-s-crowdfund-its-way-out-of-a-mask-shortage-no-but-it-still-helps> (Accessed April 4, 2021).

**Conflict of Interest:** PS is a member of the SAB or Board of Directors of Applied Biomath, Glencoe Software and RareCyt Inc and has equity in these companies; he is on the SAB of NanoString Inc. and Montai Helath. In the last 5 years the Sorger lab has received research funding from Novartis and Merck. PS declares that none of these relationships are directly or indirectly related to the content of this manuscript. NL is a consultant for or has received honoraria from the following companies: Seattle Genetics, Sanofi, and Bayer. CD, RM, and JF are employees of GenOne Technologies, Mine Survival Inc., and Fikst Product Development, respectively.

The remaining authors declare that the research was conducted in the absence of any commercial or financial relationships that could be construed as a potential conflict of interest.

**Publisher's Note:** All claims expressed in this article are solely those of the authors and do not necessarily represent those of their affiliated organizations, or those of the publisher, the editors and the reviewers. Any product that may be evaluated in this article, or claim that may be made by its manufacturer, is not guaranteed or endorsed by the publisher.

Copyright © 2021 Kothakonda, Atta, Plana, Ward, Davis, Cramer, Moran, Freake, Tian, Mazor, Gorelik, Van, Hansen, Yang, Li, Sinha, Li, Yu, LeBoeuf and Sorger. This is an open-access article distributed under the terms of the Creative Commons Attribution License (CC BY). The use, distribution or reproduction in other forums is permitted, provided the original author(s) and the copyright owner(s) are credited and that the original publication in this journal is cited, in accordance with accepted academic practice. No use, distribution or reproduction is permitted which does not comply with these terms.



# Critical Capability Needs for Reduction of Transmission of SARS-CoV-2 Indoors

Jayne B. Morrow<sup>1,2\*</sup>, Aaron I. Packman<sup>3</sup>, Kenneth F. Martinez<sup>2,4</sup>, Kevin Van Den Wymelenberg<sup>5</sup>, Darla Goeres<sup>1</sup>, Delphine K. Farmer<sup>6</sup>, Jade Mitchell<sup>7</sup>, Lisa Ng<sup>8</sup>, Yair Hazi<sup>4</sup>, Monica Schoch-Spana<sup>9</sup>, Sandra Quinn<sup>10</sup>, William Bahnfleth<sup>11</sup> and Paula Olsiewski<sup>9,12</sup>

## OPEN ACCESS

### Edited by:

Jianming Qiu,  
University of Kansas Medical Center,  
United States

### Reviewed by:

Jitendra Kumar Biswal,  
International Centre  
for Foot-and-Mouth Disease, India  
Segaran P. Pillai,  
United States Department  
of Homeland Security, United States

### \*Correspondence:

Jayne B. Morrow  
jayne.morrow@montana.edu

### Specialty section:

This article was submitted to  
Biosafety and Biosecurity,  
a section of the journal  
Frontiers in Bioengineering and  
Biotechnology

**Received:** 14 December 2020

**Accepted:** 29 April 2021

**Published:** 29 September 2021

### Citation:

Morrow JB, Packman AI,  
Martinez KF,  
Van Den Wymelenberg K, Goeres D,  
Farmer DK, Mitchell J, Ng L, Hazi Y,  
Schoch-Spana M, Quinn S,  
Bahnfleth W and Olsiewski P (2021)  
Critical Capability Needs  
for Reduction of Transmission  
of SARS-CoV-2 Indoors.  
Front. Bioeng. Biotechnol. 9:641599.  
doi: 10.3389/fbioe.2021.641599

<sup>1</sup> Center for Biofilm Engineering, Montana State University, Bozeman, MT, United States, <sup>2</sup> Integrated Bioscience and Built Environment Consortium (IBEC), Sanford, FL, United States, <sup>3</sup> Department of Civil and Environmental Engineering, Northwestern University, Evanston, IL, United States, <sup>4</sup> HWC Inc., Washington, DC, United States, <sup>5</sup> Biology and the Built Environment Center, College of Design, Institute for Health in the Built Environment, University of Oregon, Eugene, OR, United States, <sup>6</sup> Department of Chemistry, Colorado State University, Fort Collins, CO, United States, <sup>7</sup> Department of Biosystems Engineering, Michigan State University, East Lansing, MI, United States, <sup>8</sup> Engineering Laboratory, National Institute of Standards and Technology, Gaithersburg, MD, United States, <sup>9</sup> Johns Hopkins Center for Health Security, Johns Hopkins University Bloomberg School of Public Health, Baltimore, MD, United States, <sup>10</sup> Department of Family Science and Center for Health Equity, School of Public Health, University of Maryland, College Park, MD, United States, <sup>11</sup> Department of Architectural Engineering, The Pennsylvania State University, University Park, PA, United States, <sup>12</sup> Alfred P. Sloan Foundation, New York, NY, United States

Coordination of efforts to assess the challenges and pain points felt by industries from around the globe working to reduce COVID-19 transmission in the indoor environment as well as innovative solutions applied to meet these challenges is mandatory. Indoor infectious viral disease transmission (such as coronavirus, norovirus, influenza) is a complex problem that needs better integration of our current knowledge and intervention strategies. Critical to providing a reduction in transmission is to map the four core technical areas of environmental microbiology, transmission science, building science, and social science. To that end a three-stage science and innovation Summit was held to gather information on current standards, policies and procedures applied to reduce transmission in built spaces, as well as the technical challenges, science needs, and research priorities. The Summit elucidated steps that can be taken to reduce transmission of SARS-CoV-2 indoors and calls for significant investments in research to enhance our knowledge of viral pathogen persistence and transport in the built environment, risk assessment and mitigation strategy such as processes and procedures to reduce the risk of exposure and infection through building systems operations, biosurveillance capacity, communication form leadership, and stakeholder engagement for optimal response. These findings reflect the effective application of existing knowledge and standards, emerging science, and lessons-learned from current efforts to confront SARS-CoV-2.

**Keywords:** SARS-CoV-2, COVID-19, indoors, transmission, risk reduction and mitigation measures, biosurveillance, human factors, buildings



## INTRODUCTION

Although SARS-CoV-2 and the subsequent COVID-19 disease are unique, the foundation of knowledge to assess and mitigate the risk of viral transmission in the built environment is robust. In 2013, the US government published science and technology roadmaps (National Science and Technology Council [NSTC], 2013a,b) providing the foundations for biosurveillance and biological incident response and recovery capacities that are relevant to the COVID-19 pandemic. A National Academies of Sciences Engineering and Medicine [NASEM] (2017) consensus report summarized the state of knowledge, identified gaps, and outlined a multidisciplinary research agenda for achieving indoor environments that promote health and prevent disease (Engineering and National Academies of Sciences and Medicine [NASEM], 2017). Since 2004, the Alfred P. Sloan Foundation has funded some 230 projects totaling nearly \$80 million to help hundreds of microbiologists, chemists, engineers, architects and building scientists come together to study the ordinary indoor environments where people live, work and play (oral remarks at CLEAN 2020, 2020). A research agenda for viruses in the built environment published in 2020, just months before COVID-19 took hold, identified four priority areas, including identifying and evaluating interventions for controlling viruses indoors (Prussin et al., 2020). These reports provide a framework to understand knowledge gaps and opportunities to reduce transmission of COVID-19 in the indoor environment.

The purpose of this article is to present the findings from a virtual science and innovation summit, CLEAN 2020 (further referred to as “the Summit”), held throughout August, 2020 (CLEAN 2020, 2020). The goal of the Summit was to bring together leaders from business, policy, standards development, science and engineering to (1) understand the current state of the science and knowledge of the factors unique to SARS-CoV-2 transmission and control, and (2) identify opportunities to coordinate science and research to control viral transmission in the built environment. Critical to providing a reduction in transmission is to articulate the research and knowledge gaps to coordinate resources to address dynamic challenges in responding to the COVID-19 pandemic. The Summit is the first of its kind to assess current challenges and pain points felt by industries from around the globe working to safely reopen facilities to customers and employees and inspire innovative solutions to meet these challenges. Research, knowledge and standards development activities across environmental microbiology, building science and engineering, transmission and social sciences (see **Figure 1**) were discussed, and key findings are reported here.

## IDENTIFIED CAPACITY NEEDS AND OPPORTUNITIES FOR COORDINATED SCIENCE AND TECHNOLOGY INVESTMENT

### Viral Fate, Transport, and Persistence

Elucidation of transmission pathways and associated risks requires knowledge of viral shedding and persistence in the



**FIGURE 1 |** Science Communities Represented in the CLEAN 2020 Summit.

air, on surfaces and in water (Hermesch et al., 2020; Lednicky et al., 2020; Santarpia et al., 2020; van Doremalen et al., 2020). Knowledge of these factors are critical to mitigating viral transmission and enabling effective decision making. Understanding viral distribution and transmission in buildings, even of well-studied pathogens in buildings other than hospitals, has been lacking. This was clear early in the response to COVID-19 when guidance focused on transmission via direct person-to-person contact or indirect surface contact, which underestimated total exposure (particularly via aerosols) and overemphasized the potential for surface decontamination to reduce transmission (How Coronavirus Spreads | CDC, 2020). More information is needed on viral shedding from individuals, infectious dose response, how viruses are transferred from people to building surfaces and air/water systems (notably including bathrooms/toilets/sinks), the persistence of infectious viruses (virions) in these environments, and how people acquire microbes indoors. Experience with related pathogens, such as SARS-CoV-1, suggests that the virus persists in water and infections are transmitted through building air and water systems (Duan et al., 2003; Lee, 2003a,b; Bogler et al., 2020) and that highly localized outbreaks originating from a single resident can spread throughout high-density housing units to entire building complexes and urban neighborhoods (Lee, 2003b; Yu et al., 2014). Recent studies have suggested that persistence of SARS-CoV-2 is similar to SARS-CoV-1 (van Doremalen et al., 2020). SARS-CoV-2 is transmitted through droplets and/or aerosols contributing substantially to superspreader events (Dietz et al., 2020; Fang et al., 2020; Kang et al., 2020; Leclerc et al., 2020; Liu et al., 2020; Morawska et al., 2020; Moriarty et al., 2020; Qian et al., 2020; Rapid Expert Consultation, 2020; Meyerowitz et al., 2021). Most current knowledge of the redistribution of SARS-CoV-2 in the built environment is based on ribonucleic acid (RNA)

**TABLE 1** | Current and proposed definitions.

Current definitions	Infectious disease clinicians	Aerosol scientists
Aerosol	Particles less than 5 $\mu\text{m}$ in aerodynamic diameter CDC Environmental Guidelines, 2020.	Solid particles or liquid droplets that are suspended in air. Comprise a wide range of particle diameters (Adhikari et al., 2019).
Droplets	Liquid particles $\geq 5 \mu\text{m}$ which primarily fall out of the air quickly (within a few seconds) within 1–2 m from their generation point.	Not defined separately from aerosols. Nonetheless, only aerosol particles or droplets that are visible ( $> 100 \mu\text{m}$ ) deposit within a few seconds and a distance of 1–2 m.
<b>Proposed definitions:</b>		
Spray-borne transmission	Particles $> 100 \mu\text{m}$ that directly hit the eyes, nose, or mouth	

measurements. Detection and quantification of infective virus is not equivalent to viral RNA. Not all detected RNA is associated with infectious virus, and RNA is generally more persistent than infectious virus in the environment (Bivins et al., 2020; Widders et al., 2020). We need to understand the relationship between RNA detection and infectivity for all types of clinical and environmental matrices (e.g., swab, lavage, sputum, lung sample, feces, air, water, surfaces) as well as how the RNA signal decays in these matrices. Standard methods of testing for the presence of SARS-CoV-2 virions and viral RNA in all relevant media (e.g., saliva droplets, respiratory fluid, colonic fluid, and environmental samples) are still lacking.

The Summit provided a foundation to better understand the potential of airborne transmission of SARS-CoV-2 (Morawska and Milton, 2020) and the evidence supporting source control of other respiratory pathogens (Milton et al., 2013; Leung et al., 2020). The Summit suggested that discrepancies in definitions of aerosols and droplets has caused confusion in both the lay public, engineers and the scientific community. **Table 1** contrasts definitions from the infectious disease literature compared with those from aerosol scientists. The Summit discussions yielded proposed definitions for spray-borne transmission to be  $> 100 \mu\text{m}$  particles or droplets that directly inoculate the eyes, nose, or mouth; and aerosol transmission to include particles or droplets  $< 100 \mu\text{m}$  that can be inhaled into the lungs.

Performing routine environmental assessments at scale will require validated, standardized, specific, sensitive, and high-throughput methods, coordinated sample-collection workflows, and integration of multiple types of data. Variation in methods is known to result in uncertainty and create broad spreads in analytical results (Downey et al., 2012a,b). The Summit identified gaps in standard methods for (1) sample collection according to validated sampling strategies; (2) sample processing and analysis; (3) interpretation of analytical results; and (4) data integration needed to confidently assess transmission risks and identify the most likely environmental routes of exposure. The Summit reviewed current information on viral fate and transport, surveillance methods, and standards for building infection control. Data were presented on SARS-CoV-2 persistence as a function of temperature and relative

humidity (RH) and ultraviolet (UV) light exposure (Biryukov et al., 2020; Ratnesar-Shumate et al., 2020; Schuit et al., 2020). Results to date show inactivation on surfaces is highly dependent on temperature and RH with viral half-life on surfaces at roughly 18 h–1 week depending on surface type under low temperature and low RH, and only a few hours at high temperature and high RH (Biryukov et al., 2020). These data and other recent studies (e.g., Chin et al., 2020; Gormley et al., 2020; van Doremalen et al., 2020; Delikhoo et al., 2021; Harris-Lovett et al., 2021; Marquès and Domingo, 2021) are a start to understanding viral fate indoors; however, additional assessments of viral persistence on a broader range of surface types including porous surfaces and textiles of various composition and age are required. The Summit discussed the likelihood of fomite transfer rates to be consistent with infectious viruses between people and surfaces (Ansari et al., 1988; Mbithi et al., 1992; Thomas et al., 2014; Hirose et al., 2020). These data as well as recent decontamination studies (Kampf et al., 2020) will inform strategies to determine the extent of contamination and guide public health and safety actions such as cleaning, quarantine, isolation, and/or testing. Data integration that includes viral persistence in air, water and wastewater can be applied in real-time modeling tools to support biosurveillance operations to identify new outbreaks, emergence of new or mutated viral pathogens, and guide building and facility operations including air handling, air treatment and surface disinfection.

## Reducing the Risk of Exposure and/or Infection

Methods to reduce the risk of exposure or infection are essential for rapid recovery from a pandemic or other infectious disease transmission incident. Risk-reduction strategies include actions such as quarantine, social distancing, and other measures to mitigate the transmission of disease including cleaning, hygienic practices, decontamination and building air handling operations to mitigate contamination. Quantitative estimates of risk and characterization of the certainty of those risk estimates will inform decisions as to which risk-reduction strategies will be most effective. For example, current guidance on the use and application of existing decontamination methods and strategies is limited in application scenario and may not address or be appropriate for all exposure reduction measures needed (EPA, 2021). The Summit focused conversations on the hierarchy of controls approaches to reducing transmission, development, and integration of decontamination methods and understanding the process for technologies to demonstrate safety and efficacy, aerosol transmission reduction, and building operations.

## Engineering Controls for Reduction of Aerosol Transmission

Within the hierarchy of controls, the top level of exposure control is elimination of the infectious agent. Specific building design and engineering controls can be applied that contribute to elimination or reduction of exposure to viral particles such as filtration, transmission barriers (e.g., masks, plexiglass partitions), and inactivation and dilution with outside air.

Control banding can also be an effective tool for reducing exposure when there are uncertainties in exposure routes. Control banding involves a generic technique that determines a control measure based on a range or “band” of hazards and exposure levels; in essence, a qualitative assessment for determining the level of risk for a specific job and workplace. It applies a bands hierarchy to define the appropriate type or mix of control measures to put in place. Control banding can be appropriately applied to SARS-CoV-2 protection due to the lack of exposure limits or until there is a clear indication of minimal infectious dose (Van Damme et al., 2021). It can also be used to reduce exposure to agent-containing aerosols to increasingly lower levels by selecting additional control strategies such as engineering controls including air filtration and cleaning, and barrier protections, for example, from the source and pathway categories and thus reducing the reliance on personal protective equipment (PPE) (Centers for Disease Control and Prevention [CDC], 2021).

High Efficiency Particulate Air (HEPA) portable air cleaners can help to decrease the airborne concentration of small particles within a room, but they will not protect an individual that is in close proximity to someone who coughs or sneezes. Barrier protections such as plexiglass partitions can help decrease the transmission of large particles that have been disseminated through spray-borne mechanisms such as coughing or sneezing but for smaller particles, the impact becomes limiting and may interfere with designed airflow. The Summit provided information on the efficacy of face coverings as a combination of filtration and barrier controls to reduce the bioburden to the space. Studies have shown that face coverings (cloth and surgical masks) can effectively reduce particle emissions even at the small size range, this effectiveness assumes a good face fit (Asadi et al., 2020; Moghadas et al., 2020). The fabric captures particles exhaled by the wearer, but face seal leakage (e.g., gaps at the cheeks) may allow many of the smaller particles (those inhaled deeply into the lungs) to escape. The corollary to particle escape through gaps is preferential flow during inhalation through gaps. The discussion drew attention to the use of face coverings and a false sense of safety resulting in the wearer overly relying on face coverings and subsequently not applying other basic infectious disease control efforts such as social distancing and avoidance of high-risk environments.

Additionally, installation of disinfecting ultraviolet germicidal irradiation (UVGI) systems (either inside a room or embedded within the ventilation system) can help to reduce the concentration of active aerosolized pathogens (Jensen et al., 2005; Centers for Disease Control and Prevention [CDC], 2009), however, caution must be taken to reduce potential skin/eye exposure when utilizing UV systems. Increasing the supply of filtered outside air into a room by various means can also significantly reduce and dilute airborne particle concentration. Increasing the filtration efficiency of the HVAC system by switching to a higher Minimum Efficiency Reporting Value (MERV) filter will promote the reduction of indoor fine particles. Ventilation and filtration are potentially effective mechanisms to remove exhaled particles from indoor air that avoid the unintended chemical consequences of some of the biocidal

treatments described next. It must be noted that first the UVGI and MERV units need validation and careful consideration for application to real-world buildings and usage including impact on power consumption due to the increased energy needs of dense filters.

## Decontamination and Disinfection

A decontamination or disinfection method is evaluated for its potential to inactivate the pathogen or biocidal efficacy. Standard methods exist to validate the efficacy of biocides used in surface decontamination (ASTM International methods E1053-20, and E2721-16). Products that have met the performance guidelines for effective surface decontamination can be found on the U. S. Environmental Protection Agency's (EPA) List N (EPA, 2020). List N posting requires testing according to the chemical formulation of the biocide, application procedure and validation of label instructions. Biocidal efficacy is a function of both concentration and time; labels prescribe contact time for a certain kill rate and inadequate contact time may severely hamper the efficacy of the biocide and the kill of the microorganism (or destruction of the virus). Thus, not only must the efficacy be validated, but also the approach used to apply the biocide. The standard methods were originally designed for enveloped viruses—surrogates were used based on the understanding that they predict how the biocides will work against SARS-CoV-2. The Summit discussion considered issues and challenges with surrogate models for SARS-CoV-2 in determining biocide efficacy and differences between validated performance on non-porous surfaces, compared to porous surfaces such as textiles. Additionally, novel and emerging biocides were discussed for which application methods are inconsistent with the method used to qualify the biocide for inclusion in List N. These include the growing use of spray or fumigation techniques, novel air cleaning approaches, such as room fumigation with disinfectants and ozone or hydroxyl radical generators, now on the market. These products are not biocides and are not listed in List N as verification of disinfection chemistry performance is required and standard methods for air cleaning approaches are needed.

The Summit discussion included an assessment of the growing interest in using UVGI to deactivate viruses on either surfaces or airborne particles. Laboratory studies suggest that UV can be effective for hard surface disinfection (Raguse et al., 2016). However, organic materials (e.g., biofilms, phlegm or respiratory fluid, nasal secretions) reduce UV penetration, and thus lowers the efficacy of UV light (Nerandzic et al., 2014; Cadnum et al., 2016). Further, certain types of UV light can be dangerous to human health or potentially cause indoor photochemistry. UV efficacy is also a function of wavelength, distance from the surface, surface type and may be pathogen specific (Mitchell et al., 2019). Initial studies of persistence and sensitivity to disinfection have indicated SARS-CoV-2 behaves similar to other enveloped viruses (Morris et al., 2020; van Doremalen et al., 2020; Marquès and Domingo, 2021). However, studies of the efficacy of UV light against aerosolized microbes and SARS-CoV-2 in particular are limited and more data are required to better understand opportunities for broader application of germicidal UV.



EPA's List N provides critical information necessary for decision-makers for the appropriate and efficacious selection of biocides for surface decontamination strategies. However, other critical parameters to consider when selecting what biocide to use include impacts on human health, the environment, and materials. Biocides that are often the most effective are often the most toxic or damaging (Mattila et al., 2020a,b). Bleach and some of these other cleaning products can chemically react with material surfaces, potentially causing long-term damage which will result in increased operating costs and environmental consequences (Hora et al., 2020). Balancing the need for immediate and effective decontamination with the long-term unintended consequences from chemical exposure was a focus of discussion for the Summit. Further research into secondary reactions or chemical byproducts from decontamination are warranted, and regulatory agencies should consider these consequences as part of any product assessments and include this information on the product's label so that the consumer may make an informed decision on its optimal use.

The Summit recognized that initial urgency around surface decontamination was similar to an acute infection but responding to the SARS-CoV-2 pandemic aligns more as a chronic contaminant for which we need to develop long-term approaches to continually manage and contain this virus. The Summit uncovered several research needs focused around long-term cleaning strategies that balance effective decontamination with materials, environmental and health considerations. Specifically, we need:

- Clean-in-place validation: how often do surfaces actually need to be cleaned? Which material surfaces are more susceptible to damage with different disinfectants?
- Methods to validate new technologies to demonstrate their efficacy.
- Ways to test the impact of cleaners on materials, environment and health in real-world environments that consider the proper use of a disinfectant for the appropriate situation and the potential for secondary chemistry and other complex interactions, including potential interaction between disinfectants.

## Processes and Building Systems Operations

We can reduce viral transmission through a combination of engineering controls including ventilation, filtration, and other supplemental air cleaning applications. Buildings have been designed and operated for thermal comfort and indoor air quality since the energy crisis, for energy efficiency. Ventilation rates in many buildings are too low and filter efficiencies in recirculated airstreams is too low to properly control infectious aerosol concentrations. Indoor air quality standards for non-healthcare buildings focus on control of building-generated contaminants and human body odor with the goal of achieving acceptable perceived air quality and do not necessarily provide adequate filtration for preventing aerosol transmission and protection against infection. Furthermore, once a building is commissioned, if it was commissioned, there is often too little attention or resources to ensure ventilation systems are

operating properly. Going forward, there must be improvements in the design and operation of the built environment to minimize disease transmission, improve air quality, and ensure occupant health as much as reasonable. The Summit discussion referenced the basics of ventilation—delivering outdoor air to occupants and filtering recirculated air and the need for a renewed investment to ensure operational performance. The American Society of Heating, Refrigerating and Air-Conditioning Engineers, ASHRAE, has provided guidance for building system operations including a combination of: increase ventilation and reduce recirculation if feasible (meet code requirements at a minimum), employ higher filtration efficiencies (MERV 13 preferred), maintain design temperature, and RH% and use supplementary UV-C and portable HEPA air cleaners (ASHRAE, 2020; Persily and Ng, 2020).

Airborne transmission of SARS-CoV-2 has been generally accepted by scientists as a significant component of the COVID-19 pandemic (Morawska and Milton, 2020), and recent studies have implicated indoor transmission as a major factor in both local COVID-19 outbreaks and the global spread of the pandemic (Prather et al., 2020; Fang et al., 2020; Leclerc et al., 2020; Qian et al., 2020; Meyerowitz et al., 2021). However, limited information is available on SARS-CoV-2 transmission through building HVAC systems and infectivity via this pathway is unknown (Dietz et al., 2020; Fang et al., 2020; Horve et al., 2020; Meyerowitz et al., 2021). Nevertheless, dilution of indoor air via properly filtered outdoor air remains critical to reducing infectious disease transmission, particularly in settings such as hospitals (Allen and Marr, 2020; Dietz et al., 2020; Morawska et al., 2020). While the number of supply air changes (outdoor air plus any filtered recirculation air) present in many hospitals (typically 6 h<sup>-1</sup>–12 h<sup>-1</sup>) cannot be reached in many commercial buildings such as offices and schools, there are controls (e.g., masks, filtration) that can help increase the equivalent air changes in commercial buildings and thus reduce exposure to airborne aerosols (Dietz et al., 2020; Prather et al., 2020). When modifications to HVAC systems are contemplated in order to reduce pathogen transmission risk, it is important to consider a holistic approach. Applying any risk mitigation strategy (e.g., increased outside air, increased filter efficiency, increased air changes) in isolation may have unintended consequences. For example, increasing filter efficiency may reduce total air changes if the fan systems cannot overcome the increased pressure drop. Similarly, increasing outside air to reduce the fraction of recirculated air may result in a lower total airflow and increase energy consumption in order to maintain thermal comfort.

Currently vacant buildings will 1 day be re-occupied and many people are paying more attention to ventilation. Occupants may demand more information about the HVAC systems serving them. While accurate real-time monitoring of particulate matter smaller than 2.5  $\mu\text{m}$  (PM 2.5) and volatile organic compounds (VOC) are largely cost prohibitive now. Similarly, consumer grade PM 2.5 sensors PM 2.5 (Wang et al., 2020) may offer qualitative evidence of system performance. While these sensors do not monitor pathogens directly, integrating particle sensors into a building operational processes can be useful and begin to pave the way for the future of indoor biosurveillance.



## Establishing Biosurveillance Capacity

A clear recommendation from the Summit is the need to develop strategies for comprehensive surveillance of air, water, and surfaces to assess COVID-19 re-emergence as well as new pandemic and epidemic viruses. Surveillance for disease agents, or biosurveillance, is an active data-gathering effort that relates disease activity to threats to human or animal health in order to achieve situational awareness of disease activity and provide an early warning of emerging threats (National Science and Technology Council [NSTC], 2013b). Threat detection must be coordinated with decision-making bodies and communicated with the public in order to prevent, manage or mitigate disease (Planning Committee on Information-Sharing Models and Guidelines for Collaboration: Applications to an Integrated One Health Biosurveillance Strategy—A Workshop, Board on Health Sciences Policy, and Institute of Medicine, 2011). Traditional surveillance systems used by public health for detecting and responding to infectious disease outbreaks often operate with considerable delay (e.g., diagnostic testing delays are well documented), thus complementary biosurveillance of the built environment is needed to reduce the time to information and inform decisions and actions. The Summit identified a need for coordinated surveillance of schools, workplaces, and other high-risk facilities (e.g., hospitals, senior living facilities, and cruise ships). The Summit panel discussions reviewed current efforts to develop surveillance strategies that include monitoring humans, wastewater, building surfaces, and air handling systems. Current data streams for surveillance of SARS-CoV-2 include public health laboratory testing, public health contact tracing, rapid detection on building surfaces and in air systems, as well as building and municipal wastewater systems. However, these data streams are currently analyzed separately, which hinders threat assessment and response. The Summit discussed the needs for integrating these data streams, as well as other critical innovations to expedite information flow, increase accuracy and repeatability, and enhance situational awareness and confidence in reopening. There is a clear need for an integrated population-level biosurveillance program that includes human diagnostic testing, human screening, biosurveillance at multiple scales including indoor spaces (surfaces and air), building scale (air, wastewater and wastewater vent stacks), campus or neighborhood scale (wastewater from multiple buildings), and community/city-scale surveillance (sentinel locations). A strategy for coordinated and sustained surveillance of the built environment and people is needed in order to implement a real-time, data-driven decision-making platform that can quickly respond to disease outbreaks.

Currently, several public and private organizations are conducting building surface surveillance and developing data-driven action plans. During the COVID-19 pandemic, many academic institutions (Betancourt et al., 2020; Barich and Slonczewski, 2021; Gibas et al., 2021; Harris-Lovett et al., 2021) and jurisdictional authorities (Gonzalez et al., 2020; Larsen and Wigginton, 2020; Medema et al., 2020; Peccia et al., 2020) around the globe rapidly developed and deployed wastewater and building air HVAC surveillance tools (Hermesch et al., 2020; Horve et al., 2020). These data sets provide the opportunity to develop best practices and validate sample collection and

processing methods. While many surveillance methods have been deployed, integrated data-driven response protocols and risk mitigation strategies are still needed (Larsen and Wigginton, 2020; Thompson et al., 2020; Harris-Lovett et al., 2021). Critical to underpinning decision-making is to know how viral RNA concentration corresponds to concentration of infectious virus, how long viral RNA persists in the built environment and the understanding of how viral RNA persistence is related to infectiousness. Additionally, there are limited common requirements for surveillance programs and decisions made with surveillance data (Aguar-Oliveira et al., 2020; Centers for Disease Control and Prevention [CDC], 2020) and they are not well coordinated globally. To foster an integrated response, there is a clear need to develop standardized methods, a common data archive and metadata standards for all SARS-CoV-2 environmental results. Working to standardize these approaches will help establish monitoring tools that can be broadly and consistently deployed to facilitate both building/facility-level and community-level responses.

Furthermore, recognizing the role of ecosystem dynamics and the impact of ecosystem health on incidents of spillover events and overall fate and transport of zoonotic diseases is foundational to biosurveillance strategies. The Summit discussion introduced the role of ecosystem health and other enabling conditions pivotal to viral spillover from bat populations (Plowright et al., 2014). Plowright et al. (2017) proposed ecological changes including deforestation that result in stress in bat populations (e.g., scarce food resources) drives the redistribution of bat populations where spillover events can occur. The role of transmission of viruses from animals to humans requires exposure and susceptibility of recipient hosts (e.g., including livestock, wild animals and humans) as well as survival of the virus in the environment post bat shedding (Plowright et al., 2017). A key finding of the Summit discussion on biosurveillance is the need for ecosystem monitoring in order to elucidate the impact of ecosystem health on emergence of novel diseases like SARS-CoV-2.

## Risk Assessment and Mitigation Strategy

Risk and exposure reduction require data and information accumulated through a comprehensive risk assessment process. Quantitative microbial risk assessment (QMRA) is a computational method for integrating the hazard characteristics of infectious agents (e.g., viruses) in macro- and micro-environments with human activities that result in exposure (Quantitative Microbial Risk Assessment, 2020, 2nd Edition | Wiley). QMRA also predicts the risk of infection or illness outcomes associated with these exposures. Within the larger framework of risk analysis, risk assessment methods can be used to effectively design and evaluate risk management strategies based on their likely impact on risk reduction and lead to informed risk communication. Risk assessment is also used to prioritize exposure pathways within an environment and therefore inform decisions about which risk mitigation efforts are most appropriate based on an understanding of the fate and transport mechanisms of pathogens within and on various environmental matrices involved in the transmission pathway (i.e., air, surfaces, food, etc.) Hence, risk assessment requires

the integration of multiple data streams and models that describe biological (excretion rates, exhalation/inhalation rates, decay/persistence etc.), physical (aerosolization rates, transport, transfer rates, etc.) and chemical (cleaning, disinfection, etc.) processes leading to environmental concentrations when specific conditions are present at the point of exposure. An exposure dose is then calculated based on the magnitude or extent of contact, duration and frequency of human activities. The likelihood of an adverse health outcome (infection, illness or death) at given exposure levels also follows a quasi-mechanistic approach defined by a dose-response model. Such models account for the distribution of pathogens within the matrix and the probability that a pathogen can survive to initiate infection reaching a target receptor. While models have been developed for highly infectious viruses through the inhalation route previously (Watanabe et al., 2010; Mitchell et al., 2020), a SARS-CoV-2 specific model has not yet been developed. In the absence of a dose-response model, the Wells-Riley equation has been used for simple and quick assessments for airborne pathogens including SARS-CoV-2 (Sze To and Chao, 2010). However, the validity and generalizability of the underlying assumptions of this approach are unknown, and data are needed to establish the relationship between exposure dose and risk of infection for SARS-CoV-2 in order to move forward with less uncertainty in QMRA models. During the Summit, there was some discussion about models and several tools for exposure and risk quantification that allow for quick assessments in specific environments, under certain environmental conditions and social/behavioral components of exposure (population density/duration of time spent in the room) (Kasibhatla et al., 2020; Rocha-Melogni et al., 2020). Several others have emerged in the gray literature or situationally to address the need to assess risks quantitatively (and/or semi-quantitatively), but the full capacity of risk assessment approaches have yet to be brought to bear to address COVID-19 which was identified as a critical gap. Quantitative assessments of risk are needed to determine likely exposure doses of viral particles through each exposure pathway (air and surfaces) and to estimate actual risk reduction provided by a suite of technologies (e.g., disinfection) and operational practices (e.g., air handling, surface cleaning). These assessments would incorporate both inherent variability and uncertainty in order to lead to better decision making and communication as determining an acceptable level of risk is based on assessing both expected values and levels of certainty. Finally, these assessments are needed to provide more comprehensive information for specifying risk mitigation strategies, critical control points for multi-barrier approaches that can be used in concert with epidemiological-based models which focus on testing, isolation, quarantine and eventually vaccination strategies.

## Communication, Leadership, and Stakeholder Engagement

Critical to the success of any risk reduction strategy is insight from the social and behavioral sciences. Throughout the Summit opportunities for science communication and organizational

leadership to shape the understanding of the risk and risk perception, decision-making and collective actions to begin to safely resume normal activities were discussed. Engineering controls and management practices to reduce viral transmission in the built environment are more protective, and perceived as more protective, when the system's design accounts for the concerns, values, behaviors, and information needs of a building's occupants—whether workers, students, or patrons. Given that knowledge of human factors is essential to safe congregation, “people” experts (i.e., social, behavioral, and communication scientists) as well as epidemiologists, microbiologists, and building engineers/scientists are necessary to develop effective indoor air quality approaches. Summit panelists who addressed the human elements of safe indoor congregation spotlighted three main challenges and outlined some best practices:

- **Communication**—A growing reliance on social media and the nature of the COVID-19 threat (e.g., difficulty in seeing the cause-and-effect relationship between mitigation measures and health outcomes, binary thinking about public health and economic matters) has produced a complex communication environment. A clear need exists for better coordination and deployment of information resources. Federal strategy and guidance are important drivers for effective local and regional response; in the absence of effective governmental structures, individual companies, schools, and facilities have instituted *ad hoc* measures, and infection control managers have been left to share information via their own networks.
- **Stakeholder Engagement**—Top-down, one-sided conversations about issues regarding safe congregation have a limited capacity to achieve necessary behavior change or to engender public confidence in protective measures. Instead, it is important that end users of the built environment have an opportunity to provide feedback into mitigation planning and that they feel listened to and respected. Decision makers must be willing to understand users' values and beliefs. In doing so, they will be in a better position to understand and leverage group norms that shape adoption of personal protective measures like mask-wearing and physical distancing.
- **Leadership**—The delivery of factual information alone, including that regarding personal protective behaviors and system-level protections, will not create the desired change among building occupants. Emotions are present. Leaders, for instance, should express empathy for users' health and safety concerns. In addition, leaders and managers should positively model the behaviors that they want to see in their workforce, customer base, or other constituencies.

## CONCLUSION

The Summit was impactful because it brought disparate groups together that do not commonly work together to meet the changing needs of the community and incorporate

lessons-learned into best practices that are holistic. The research community has come together in unprecedented ways to respond to the pandemic. Such focused efforts can be used to guide basic research funding priorities and coordinate funding for identified capability gaps as well as serve as the foundation for future policy development. The research community will continue to benefit from coordinating what is known about buildings and viruses including the unique findings from studying SARS-CoV-2, and rapidly sharing the gaps in our collective knowledge using tools like virtual workshops.

## AUTHOR CONTRIBUTIONS

All authors listed have made a substantial, direct and intellectual contribution to the work, and approved it for publication.

## REFERENCES

- Adhikari, U., Chabrelie, A., Weir, M., Boehnke, K., McKenzie, E., Ikner, L., et al. (2019). A case study evaluating the risk of infection from middle eastern respiratory syndrome coronavirus (MERS-CoV) in a hospital setting through bioaerosols. *Risk Anal.* 39, 2608–2624. doi: 10.1111/risa.13389
- Aguiar-Oliveira, M. L., Campos, A., Matos, A. R., Rigotto, C., Sotero-Martins, A., Teixeira, P. F. P., et al. (2020). Wastewater-based epidemiology (Wbe) and viral detection in polluted surface water: a valuable tool for covid-19 surveillance—a brief review. *Int. J. Environ. Res. Public Health* 17, 1–19. doi: 10.3390/ijerph17249251
- Allen, J. G., and Marr, L. C. (2020). Recognizing and controlling airborne transmission of SARS-CoV-2 in indoor environments. *Indoor Air* 30, 557–558. doi: 10.1111/ina.12697
- Ansari, S. A., Sattar, S. A., Springthorpe, V. S., Wells, G. A., and Tostowaryk, W. (1988). Rotavirus survival on human hands and transfer of infectious virus to animate and nonporous inanimate surfaces. *J. Clin. Microbiol.* 26, 1513–1518. doi: 10.1128/jcm.26.8.1513-1518.1988
- Asadi, S., Cappa, C. D., Barreda, S., Wexler, A. S., Bouvier, N. M., and Ristenpart, W. D. (2020). Efficacy of masks and face coverings in controlling outward aerosol particle emission from expiratory activities. *Sci. Rep.* 10:15665. doi: 10.1038/s41598-020-72798-7
- ASHRAE (2020). *ASHRAE Resources Available to Address COVID-19 Concerns. COVID-19 Preparation. Resources.* Available online at: <https://www.ashrae.org/technical-resources/resources> (accessed November 16, 2020).
- Barich, D., and Slonczewski, J. L. (2021). Wastewater virus detection complements clinical COVID-19 testing to limit spread of infection at Kenyon College. *medRxiv [Preprint]* 2021.01.09.21249505. doi: 10.1101/2021.01.09.21249505
- Betancourt, W. W., Schmitz, B. W., Innes, G. K., Pogreba Brown, K. M., Prasek, S. M., Stark, E. R., et al. (2020). Wastewater-based epidemiology for averting COVID-19 outbreaks on the university of arizona campus. *medRxiv [Preprint]* 2020.11.13.20231340. doi: 10.1101/2020.11.13.20231340
- Biryukov, J., Boydston, J. A., Dunning, R. A., Yeager, J. J., Wood, S., Reese, A. L., et al. (2020). Increasing temperature and relative humidity accelerates inactivation of SARS-COV-2 on surfaces. *mSphere* 5, e00044–e00120. doi: 10.1128/mSphere.00441-20
- Bivins, A., Greaves, J., Fischer, R., Yinda, K. C., Ahmed, W., Kitajima, M., et al. (2020). Persistence of SARS-CoV-2 in water and wastewater. *Environ. Sci. Technol. Lett.* 7, 937–942. doi: 10.1021/acs.estlett.0c00730
- Bogler, A., Packman, A., Furman, A., Gross, A., Kushmaro, A., Ronen, A., et al. (2020). Rethinking wastewater risks and monitoring in light of the COVID-19 pandemic. *Nat. Sustain.* 3, 981–990. doi: 10.1038/s41893-020-00605-2
- Cadnum, J. L., Tomas, M. E., Sankar, T., Jencson, A., Mathew, J. I., Kundrapu, S., et al. (2016). Effect of variation in test methods on performance of Ultraviolet-C radiation room decontamination. *Infect. Control Hosp. Epidemiol.* 37, 555–560. doi: 10.1017/ice.2015.349

## ACKNOWLEDGMENTS

The authors acknowledge the contributions of Summit Steering Committee, participants, moderators, numerous speakers from industry, government and academic institutions that shared their experience and insights including Kesal Patel, Anthony Cowan, Edward Cowan, Destiny Aman, Ginger Chew, Bryon Marsh, Travis McLing, Shawn Ryan, Tod Companion, Matthew Moe, Kristen Omberg, Ajay Menon, Boris Lushniak, Andrew Persily, Jennifer Roberts, John Koerner, John Spengler, Justine Parker, Matthew Fields, Meghan Suter, Ramon Sanchez, Bill Adams, Lidia Morawska, Wendy Purcell, Keely Maxwell, Brett Cole, Claire Bird, Sonya Stokes, John Howard, Francis Padilla, Jennifer Lincoln, and David Michaels. Funding for Summit was provided by the Alfred P. Sloan Foundation, Cardno ChemRisk, AIHA, HWC, and Re-U-Zip.

- CDC Environmental Guidelines (2020). *CDC Environmental Guidelines | Guidelines Library | Infection Control | CDC.* Available online at: <https://www.cdc.gov/infectioncontrol/guidelines/environmental/index.html> (accessed November 25, 2020).
- Centers for Disease Control and Prevention [CDC] (2009). *Environmental Control for Tuberculosis: Basic Upper-Room Ultraviolet Germicidal Irradiation Guidelines for Healthcare Settings.* DHHS The National Institute for Occupational Safety and Health, Vol. 87. Available online at: <http://www.cdc.gov/niosh/docs/2009-105/> (accessed November 25, 2020).
- Centers for Disease Control and Prevention [CDC] (2020). *National Wastewater Surveillance System (NWSS) A New Public Health Tool to Understand COVID-19 Spread in a Community.* Available online at: <https://www.cdc.gov/coronavirus/2019-ncov/cases-updates/wastewater-surveillance.html> (accessed February 10, 2021).
- Centers for Disease Control and Prevention [CDC] (2021). *Centers for Disease Control and Prevention (CDC) Control Banding | NIOSH | CDC.* Available online at: <https://www.cdc.gov/niosh/topics/ctrlbanding/default.html> (accessed February 12, 2021).
- Chin, A. W. H., Chu, J. T. S., Perera, M. R. A., Hui, K. P. Y., Yen, H. L., Chan, M. C. W., et al. (2020). Stability of SARS-CoV-2 in different environmental conditions. *medRxiv [Preprint]* 2020.03.15.20036673. doi: 10.1101/2020.03.15.20036673
- CLEAN 2020 (2020). *CLEAN 2020 Summit.* Available at online: <http://www.clean2020summit.org/> (accessed December 01, 2020).
- Delikhoo, M., Guzman, M. I., Nabizadeh, R., and Baghani, A. N. (2021). Modes of transmission of severe acute respiratory syndrome-coronavirus-2 (Sars-cov-2) and factors influencing on the airborne transmission: a review. *Int. J. Environ. Res. Public Health* 18, 1–18. doi: 10.3390/ijerph18020395
- Dietz, L., Horve, P. F., Coil, D. A., Fretz, M., Eisen, J. A., and Van Den Wymelenberg, K. (2020). 2019 Novel Coronavirus (COVID-19) pandemic: built environment considerations to reduce transmission. *mSystems* 5, e00245–e00320. doi: 10.1128/msystems.00245-20
- Downey, A. S., Da Silva, S. M., Olson, N. D., Filliben, J. J., and Morrow, J. B. (2012a). Impact of processing method on recovery of bacteria from wipes used in biological surface sampling. *Appl. Environ. Microbiol.* 78, 5872–5881. doi: 10.1128/AEM.00873-12
- Downey, A. S., Delaney, L. J., and Morrow, J. B. (2012b). *Best Practices for Sample Collection and Transport During an Initial Response to Potential Biothreat Materials.* Gaithersburg, MD: National Institute of Standards and Technology.
- Duan, S. M., Zhao, X. S., Wen, R. F., Huang, J. J., Pi, G. H., Zhang, S. X., et al. (2003). Stability of SARS Coronavirus in Human Specimens and Environment and Its Sensitivity to Heating and UV Irradiation. *Biomed. Environ. Sci.* 16, 246–255.
- EPA (2020). *Disinfectants Pesticides. List N Tool COVID-19 Disinfect.* Washington, DC: United States Environmental Protection Agency.
- EPA (2021). *EPA Disinfectant Use and Coronavirus (COVID-19) | Coronavirus (COVID-19) | US EPA.* Available online at: <https://www.epa.gov/coronavirus/disinfectant-use-and-coronavirus-covid-19> (accessed April 23, 2021).



- Fang, F. C., Benson, C. A., del Rio, C., Edwards, K. M., Fowler, V. G., Fredricks, D. N., et al. (2020). COVID-19—Lessons Learned and Questions Remaining. *Clin. Infect. Dis* [Online ahead of print] doi: 10.1093/cid/ciaa1654
- Gibas, C., Lambirth, K., Mittal, N., Juel, M. A. I., Barua, V. B., Brazell, L. R., et al. (2021). Implementing building-level SARS-CoV-2 wastewater surveillance on a university campus. *Sci. Total Environ.* 782:146749. doi: 10.1101/2020.12.31.20248843
- Gonzalez, R., Curtis, K., Bivins, A., Bibby, K., Weir, M. H., Yetka, K., et al. (2020). COVID-19 surveillance in Southeastern Virginia using wastewater-based epidemiology. *Water Res.* 186:116296. doi: 10.1016/j.watres.2020.11.6296
- Gormley, M., Aspray, T. J., and Kelly, D. A. (2020). COVID-19: mitigating transmission via wastewater plumbing systems. *Lancet Glob. Heal.* 8:e643. doi: 10.1016/S2214-109X(20)30112-1
- Harris-Lovett, S., Nelson, K. L., Beamer, P., Bischel, H. N., Bivins, A., Bruder, A., et al. (2021). Wastewater surveillance for SARS-CoV-2 on college campuses: initial efforts, lessons learned, and research needs. *Int. J. Environ. Res. Public Heal.* 18:4455. doi: 10.3390/ijerph18094455
- Hermesch, A. C., Horve, P. F., Edelman, A., Dietz, L., Constant, D., Fretz, M., et al. (2020). Severe acute respiratory syndrome Coronavirus 2 (SARS-CoV-2) environmental contamination and childbirth. *Obstet. Gynecol.* 136, 827–829. doi: 10.1097/AOG.0000000000004112
- Hirose, R., Ikegaya, H., Naito, Y., Watanabe, N., Yoshida, T., Bandou, R., et al. (2020). Survival of severe acute respiratory syndrome Coronavirus 2 (SARS-CoV-2) and influenza virus on human skin: importance of hand hygiene in coronavirus disease 2019 (COVID-19). *Clin. Infect. Dis* [Online ahead of print] doi: 10.1093/cid/ciaa1517
- Hora, P. I., Pati, S. G., McNamara, P. J., and Arnold, W. A. (2020). Increased use of quaternary ammonium compounds during the SARS-CoV-2 pandemic and beyond: consideration of environmental implications. *Environ. Sci. Technol. Lett.* 7, 622–631. doi: 10.1021/acs.estlett.0c00437
- Horve, P. F., Dietz, L., Fretz, M., Constant, D. A., Wilkes, A., Townes, J. M., et al. (2020). Identification of SARS-CoV-2 RNA in healthcare heating, ventilation, and air conditioning units. *medRxiv [Preprint]* 2020.06.26.20141085. doi: 10.1101/2020.06.26.20141085
- How Coronavirus Spreads | CDC. (2020). *How Coronavirus Spreads | CDC*. Available online at: <https://www.cdc.gov/coronavirus/2019-ncov/prevent-getting-sick/how-covid-spreads.html> (accessed October 27, 2020).
- Jensen, P. A., Lambert, L. A., Iademarco, M. F., and Ridzon, R. (2005). Guidelines for preventing the transmission of mycobacterium tuberculosis in health-care settings, 2005. *Morb. Mortal. Wkly. Rep.* 54, 1–141.
- Kampf, G., Todt, D., Pfaender, S., and Steinmann, E. (2020). Persistence of coronaviruses on inanimate surfaces and their inactivation with biocidal agents. *J. Hosp. Infect.* 104, 246–251. doi: 10.1016/j.jhin.2020.01.022
- Kang, M., Wei, J., Yuan, J., Guo, J., Zhang, Y., Hang, J., et al. (2020). Probable evidence of fecal aerosol transmission of SARS-CoV-2 in a high-rise building. *Ann. Intern. Med.* 173, 974–980. doi: 10.7326/M20-0928
- Kasibhatla, P., Jimenez, J., Fay, J., Albright, E., and Pan, W. (2020). *Estimation of COVID-19 Infection Risk from Airborne Transmission During Classroom Teaching*. Available online at: <http://covid-exposure-modeler-data-devils.cloud.duke.edu/>
- Larsen, D. A., and Wigginton, K. R. (2020). Tracking COVID-19 with wastewater. *Nat. Biotechnol.* 38, 1151–1153. doi: 10.1038/s41587-020-0690-1
- Leclerc, Q. J., Fuller, N. M., Knight, L. E., Funk, S., and Knight, G. M. (2020). What settings have been linked to SARS-CoV-2 transmission clusters? *Wellcome Open Res.* 5:83. doi: 10.12688/wellcomeopenres.15889.2
- Lednický, J. A., Lauzardo, M., Fan, Z. H., Jutla, A. S., Tilly, T. B., Gangwar, M., et al. (2020). Viable SARS-CoV-2 in the air of a hospital room with COVID-19 patients. *medRxiv [Preprint]* 2020.08.03.20167395. doi: 10.1101/2020.08.03.20167395
- Lee, S. H. (2003a). The SARS epidemic in Hong Kong: what lessons have we learned? *J. R. Soc. Med.* 96, 374–378. doi: 10.1258/jrsm.96.8.374
- Lee, S. H. (2003b). The SARS epidemic in Hong Kong. *J. Epidemiol. Commun. Heal.* 57, 652–654. doi: 10.1136/jech.57.9.652
- Leung, N. H. L., Chu, D. K. W., Shiu, E. Y. C., Chan, K.-H., McDevitt, J. J., Hau, B. J. P., et al. (2020). Respiratory virus shedding in exhaled breath and efficacy of face masks. *Nat. Med.* 26, 676–680. doi: 10.1038/s41591-020-0843-2
- Liu, Y., Ning, Z., Chen, Y., Guo, M., Liu, Y., Gali, N. K., et al. (2020). Aerodynamic characteristics and RNA concentration of SARS-CoV-2 aerosol in Wuhan hospitals during COVID-19 outbreak. *bioRxiv [Preprint]* 2020.03.08.982637. doi: 10.1101/2020.03.08.982637
- Marquès, M., and Domingo, J. L. (2021). Contamination of inert surfaces by SARS-CoV-2: persistence, stability and infectivity. A review. *Environ. Res.* 193:110559. doi: 10.1016/j.envres.2020.110559
- Mattila, J. M., Arata, C., Wang, C., Katz, E. F., Abeleira, A., Zhou, Y., et al. (2020a). Dark chemistry during bleach cleaning enhances oxidation of organics and secondary organic aerosol production indoors. *Environ. Sci. Technol. Lett.* 7, 795–801. doi: 10.1021/acs.estlett.0c00573
- Mattila, J. M., Lakey, P. S. J., Shiraiwa, M., Wang, C., Abbott, J. P. D., Arata, C., et al. (2020b). Multiphase chemistry controls inorganic chlorinated and nitrogenated compounds in indoor air during bleach cleaning. *Environ. Sci. Technol.* 54, 1730–1739. doi: 10.1021/acs.est.9b05767
- Mbithi, J. N., Springthorpe, V. S., Boulet, J. R., and Sattar, S. A. (1992). Survival of hepatitis A virus on human hands and its transfer on contact with animate and inanimate surfaces. *J. Clin. Microbiol.* 30, 757–763. doi: 10.1128/jcm.30.4.757-763.1992
- Medema, G., Heijnen, L., Elsinga, G., Italiaander, R., and Brouwer, A. (2020). Presence of SARS-Coronavirus-2 RNA in sewage and correlation with reported COVID-19 prevalence in the early stage of the epidemic in the Netherlands. *Environ. Sci. Technol. Lett.* 7, 511–516. doi: 10.1021/acs.estlett.0c00357
- Meyerowitz, E. A., Richterman, A., Gandhi, R. T., and Sax, P. E. (2021). Transmission of SARS-CoV-2: a review of viral, host, and environmental factors. *Ann. Intern. Med.* 174, 69–79. doi: 10.7326/M20-5008
- Milton, D. K., Fabian, M. P., Cowling, B. J., Grantham, M. L., and McDevitt, J. J. (2013). Influenza virus aerosols in human exhaled breath: particle size, culturability, and effect of surgical masks. *PLoS Pathog.* 9:e1003205. doi: 10.1371/journal.ppat.1003205
- Mitchell, J., Dean, K., and Haas, C. (2020). Ebola virus dose response model for aerosolized exposures: insights from primate data. *Risk Anal.* 40, 2390–2398. doi: 10.1111/risa.13551
- Mitchell, J. B., Sifuentes, L. Y., Wissler, A., Abd-Elmaksoud, S., Lopez, G. U., and Gerba, C. P. (2019). Modelling of ultraviolet light inactivation kinetics of methicillin-resistant *Staphylococcus aureus*, vancomycin-resistant *Enterococcus*, *Clostridium difficile* spores and murine norovirus on fomite surfaces. *J. Appl. Microbiol.* 126, 58–67. doi: 10.1111/jam.14103
- Moghadas, S. M., Fitzpatrick, M. C., Sah, P., Pandey, A., Shoukat, A., Singer, B. H., et al. (2020). The implications of silent transmission for the control of COVID-19 outbreaks. *Proc. Natl. Acad. Sci. U.S.A.* 117, 17513–17515. doi: 10.1073/pnas.2008373117
- Morawska, L., and Milton, D. K. (2020). It is time to address airborne transmission of COVID-19. *Clin. Infect. Dis. Off. Publ. Infect. Dis. Soc. Am.* 71, 2311–2313. doi: 10.1093/cid/ciaa939
- Morawska, L., Tang, J. W., Bahnfleth, W., Bluyssen, P. M., Boerstra, A., Buonanno, G., et al. (2020). How can airborne transmission of COVID-19 indoors be minimised? *Environ. Int.* 142:105832. doi: 10.1016/j.envint.2020.105832
- Moriarty, L. F., Plucinski, M. M., Marston, B. J., Kurbatova, E. V., Knust, B., Murray, E. L., et al. (2020). Public health responses to COVID-19 outbreaks on cruise ships — Worldwide, February–March 2020. *Morb. Mortal. Wkly. Rep.* 69, 347–352. doi: 10.15585/mmwr.mm6912e3
- Morris, D. H., Yinda, K. C., Gamble, A., Rossine, F. W., Huang, Q., Bushmaker, T., et al. (2020). The effect of temperature and humidity on the stability of SARS-CoV-2 and other enveloped viruses. *bioRxiv Prepr. Serv. Biol. [Preprint]* doi: 10.1101/2020.10.16.341883
- National Academies of Sciences Engineering and Medicine [NASEM] (2017). *Microbiomes of the Built Environment: A Research Agenda for Indoor Microbiology, Human Health, and Buildings*. Washington, DC: The National Academies Press.
- National Science and Technology Council [NSTC] (2013a). *Biological Response and Recovery Science and Technology Roadmap*. Washington, DC. Available online at: [https://obamawhitehouse.archives.gov/sites/default/files/microsites/ostp/NSTC/brrst\\_roadmap\\_2013.pdf](https://obamawhitehouse.archives.gov/sites/default/files/microsites/ostp/NSTC/brrst_roadmap_2013.pdf) (accessed October 10, 2020).
- National Science and Technology Council [NSTC] (2013b). *National Biosurveillance Science and Technology Roadmap*. Washington, DC. Available



- online at: [https://obamawhitehouse.archives.gov/sites/default/files/microsites/ostp/biosurveillance\\_roadmap\\_2013.pdf](https://obamawhitehouse.archives.gov/sites/default/files/microsites/ostp/biosurveillance_roadmap_2013.pdf) (accessed October 10, 2020).
- Nerandzic, M. M., Fisher, C. W., and Donskey, C. J. (2014). Sorting through the Wealth of Options: comparative evaluation of two ultraviolet disinfection systems. *PLoS One* 9:e107444. doi: 10.1371/journal.pone.0107444
- Peccia, J., Zulli, A., Brackney, D. E., Grubaugh, N. D., Kaplan, E. H., Casanovas-Massana, A., et al. (2020). Measurement of SARS-CoV-2 RNA in wastewater tracks community infection dynamics. *Nat. Biotechnol.* 38, 1164–1167. doi: 10.1038/s41587-020-0684-z
- Persily, A. K., and Ng, L. C. (2020). *Ventilation Impacts on Indoor Aerosol Transport and Current HVAC Recommendations for Re-Opening Buildings*. Gaithersburg, MD: National Institute of Standards and Technology.
- Planning Committee on Information-Sharing Models and Guidelines for Collaboration: Applications to an Integrated One Health Biosurveillance Strategy—A Workshop, Board on Health Sciences Policy, and Institute of Medicine (2011). *Introduction and Overview*. Available online at: <https://www.ncbi.nlm.nih.gov/books/NBK189584/> (accessed November 15, 2020)
- Plowright, R. K., Eby, P., Hudson, P. J., Smith, I. L., Westcott, D., Bryden, W. L., et al. (2014). Ecological dynamics of emerging bat virus spillover. *Proc. R. Soc. B Biol. Sci.* 282:20142124. doi: 10.1098/rspb.2014.2124
- Plowright, R. K., Parrish, C. R., McCallum, H., Hudson, P. J., Ko, A. I., Graham, A. L., et al. (2017). Pathways to zoonotic spillover. *Nat. Rev. Microbiol.* 15, 502–510. doi: 10.1038/nrmicro.2017.45
- Prather, K. A., Wang, C. C., and Schooley, R. T. (2020). Reducing transmission of SARS-CoV-2: masks and testing are necessary to combat asymptomatic spread in aerosols and droplets. *Science* 368, 1422–1424. doi: 10.1126/science.abc6197
- Prussin, A. J., Belser, J. A., Bischoff, W., Kelley, S. T., Lin, K., Lindsley, W. G., et al. (2020). Viruses in the Built Environment (VIBE) meeting report. *Microbiome* 8:1. doi: 10.1186/s40168-019-0777-4
- Qian, H., Miao, T., Liu, L., Zheng, X., Luo, D., and Li, Y. (2020). Indoor transmission of SARS-CoV-2. *Indoor Air* 31, 639–645. doi: 10.1111/ina.12766
- Quantitative Microbial Risk Assessment. (2020). *Quantitative Microbial Risk Assessment*, 2nd Edn. Hoboken, NJ: Wiley.
- Raguse, M., Fiebrandt, M., Stapelmann, K., Madala, K., Laue, M., Lackmann, J. W., et al. (2016). Improvement of biological indicators by uniformly distributing *Bacillus subtilis* spores in monolayers to evaluate enhanced spore decontamination technologies. *Appl. Environ. Microbiol.* 82, 2031–2038. doi: 10.1128/AEM.03934-15
- Rapid Expert Consultation (2020). *Rapid Expert Consultation on the Possibility of Bioaerosol Spread of SARS-CoV-2 for the COVID-19 Pandemic (April 1, 2020)*. Washington, DC: National Academies Press.
- Ratnesar-Shumate, S., Williams, G., Green, B., Krause, M., Holland, B., Wood, S., et al. (2020). Simulated sunlight rapidly inactivates SARS-CoV-2 on surfaces. *J. Infect. Dis.* 222, 214–222. doi: 10.1093/infdis/jiaa274
- Rocha-Melogni, L., Crank, K., Bibby, K., Gray, G. C., and Deshusses, M. A. (2020). *Aerosol-Mediated Infectious Disease Risk Assessments*. Available online at: [https://rapidqmr.shinyapps.io/Rapid\\_QMRA/](https://rapidqmr.shinyapps.io/Rapid_QMRA/) (accessed November 10, 2020).
- Santarpia, J. L., Rivera, D. N., Herrera, V. L., Morwitzer, M. J., Creager, H. M., Santarpia, G. W., et al. (2020). Aerosol and surface contamination of SARS-CoV-2 observed in quarantine and isolation care. *Sci. Rep.* 10:12732. doi: 10.1038/s41598-020-69286-3
- Schuit, M., Ratnesar-Shumate, S., Yolitz, J., Williams, G., Weaver, W., Green, B., et al. (2020). Airborne SARS-CoV-2 is rapidly inactivated by simulated sunlight. *J. Infect. Dis.* 222, 564–571. doi: 10.1093/infdis/jiaa334
- Sze To, G. N., and Chao, C. Y. H. (2010). Review and comparison between the Wells-Riley and dose-response approaches to risk assessment of infectious respiratory diseases. *Indoor Air* 20, 2–16. doi: 10.1111/j.1600-0668.2009.00621.x
- Thomas, Y., Boquete-Suter, P., Koch, D., Pittet, D., and Kaiser, L. (2014). Survival of influenza virus on human fingers. *Clin. Microbiol. Infect.* 20, O58–O64. doi: 10.1111/1469-0691.12324
- Thompson, J. R., Nanchaiah, Y. V., Gu, X., Lee, W. L., Rajal, V. B., Haines, M. B., et al. (2020). Making waves: wastewater surveillance of SARS-CoV-2 for population-based health management. *Water Res.* 184:116181. doi: 10.1016/j.watres.2020.116181
- Van Damme, W., Dahake, R., van de Pas, R., Vanham, G., and Assefa, Y. (2021). COVID-19: does the infectious inoculum dose-response relationship contribute to understanding heterogeneity in disease severity and transmission dynamics? *Med. Hypotheses* 146:110431. doi: 10.1016/j.mehy.2020.110431
- van Doremalen, N., Bushmaker, T., Morris, D. H., Holbrook, M. G., Gamble, A., Williamson, B. N., et al. (2020). Aerosol and surface stability of SARS-CoV-2 as compared with SARS-CoV-1. *N. Engl. J. Med.* 382, 1564–1567. doi: 10.1056/nejmc2004973
- Wang, Z., Delp, W. W., and Singer, B. C. (2020). Performance of low-cost indoor air quality monitors for PM<sub>2.5</sub> and PM<sub>10</sub> from residential sources. *Build. Environ.* 171:106654. doi: 10.1016/j.buildenv.2020.106654
- Watanabe, T., Bartrand, T. A., Weir, M. H., Omura, T., and Haas, C. N. (2010). Development of a dose-response model for SARS coronavirus. *Risk Anal.* 30, 1129–1138. doi: 10.1111/j.1539-6924.2010.01427.x
- Widders, A., Broom, A., and Broom, J. (2020). SARS-CoV-2: the viral shedding vs infectivity dilemma. *Infect. Dis. Heal.* 25, 210–215. doi: 10.1016/j.idh.2020.05.002
- Yu, I. T. S., Qiu, H., Tse, L. A., and Wong, T. W. (2014). Severe acute respiratory syndrome beyond amoy gardens: completing the incomplete legacy. *Clin. Infect. Dis.* 58, 683–686. doi: 10.1093/cid/cit797

**Conflict of Interest:** KM and YH were affiliated to the commercial company HWC Inc.

The remaining authors declare that the research was conducted in the absence of any commercial or financial relationships that could be construed as a potential conflict of interest.

**Publisher's Note:** All claims expressed in this article are solely those of the authors and do not necessarily represent those of their affiliated organizations, or those of the publisher, the editors and the reviewers. Any product that may be evaluated in this article, or claim that may be made by its manufacturer, is not guaranteed or endorsed by the publisher.

Copyright © 2021 Morrow, Packman, Martinez, Van Den Wymelenberg, Goeres, Farmer, Mitchell, Ng, Hazi, Schoch-Spana, Quinn, Bahnfleth and Olsiewski. This is an open-access article distributed under the terms of the Creative Commons Attribution License (CC BY). The use, distribution or reproduction in other forums is permitted, provided the original author(s) and the copyright owner(s) are credited and that the original publication in this journal is cited, in accordance with accepted academic practice. No use, distribution or reproduction is permitted which does not comply with these terms.

# Advantages of publishing in Frontiers



## OPEN ACCESS

Articles are free to read  
for greatest visibility  
and readership



## FAST PUBLICATION

Around 90 days  
from submission  
to decision



## HIGH QUALITY PEER-REVIEW

Rigorous, collaborative,  
and constructive  
peer-review



## TRANSPARENT PEER-REVIEW

Editors and reviewers  
acknowledged by name  
on published articles

## Frontiers

Avenue du Tribunal-Fédéral 34  
1005 Lausanne | Switzerland

Visit us: [www.frontiersin.org](http://www.frontiersin.org)

Contact us: [frontiersin.org/about/contact](http://frontiersin.org/about/contact)



## REPRODUCIBILITY OF RESEARCH

Support open data  
and methods to enhance  
research reproducibility



## DIGITAL PUBLISHING

Articles designed  
for optimal readership  
across devices



## FOLLOW US

@frontiersin



## IMPACT METRICS

Advanced article metrics  
track visibility across  
digital media



## EXTENSIVE PROMOTION

Marketing  
and promotion  
of impactful research



## LOOP RESEARCH NETWORK

Our network  
increases your  
article's readership